CROSS METATHESIS APPROACHES FOR BROUSSONETINE C, G AND 12-*C*-GLYCOSYL-DODECANOIC ACIDS AND EXPLORATION OF CLICK REACTION IN CRYSTAL ENGINEERING

BY

KULBHUSHAN A. DURUGKAR

Dr. C. V. RAMANA

(RESEARCH GUIDE)

ORGANIC CHEMISTRY DIVISION

NATIONAL CHEMICAL LABORATORY

PUNE–411008

APRIL–2009

Cross Metathesis Approaches for Broussonetine C, G & 12-*C*-Glycosyl-dodecanoic Acids and Exploration of Click Reaction in Crystal Engineering

A THESIS
SUBMITTED FOR THE DEGREE OF
DOCTOR OF PHILOSOPHY
(IN CHEMISTRY)

TO

UNIVERSITY OF PUNE

BY

Mr. Kulbhushan A. Durugkar

Dr. C. V. Ramana

(Research Guide)

ORGANIC CHEMISTRY DIVISION
NATIONAL CHEMICAL LABORATORY
PUNE–411008

April–2009

DEDICATED
TO
MY PARENTS

DECLARATION

The research work embodied in this thesis has been carried out at National Chemical Laboratory, Pune under the supervision of **Dr. C. V. Ramana**, Organic Chemistry Division, National Chemical Laboratory, Pune – 411 008. This work is original and has not been submitted in part or full, for any degree or diploma of this or any other University.

Organic Chemistry Division
National Chemical Laboratory
Pune – 411008
April 2009 **(Kulbhushan A. Durugkar)**

राष्ट्रीय रासायनिक प्रयोगशाला
(वैज्ञानिक तथा औद्योगिक अनुसंधान परिषद)
डॉ. होमी भाभा मार्ग पुणे - 411 008. भारत
NATIONAL CHEMICAL LABORATORY
(Council of Scientific & Industrial Research)
Dr. Homi Bhabha Road, Pune - 411 008. India.

Dr. C. V. Ramana

Phone: +91–20–25902577
+91–20–25902455
E–mail: vr.chepuri@ncl.res.in

CERTIFICATE

The research work presented in thesis entitled **"Cross Metathesis Approaches for Broussonetine C, G & 12-*C*-Glycosyl-dodecanoic Acids and Exploration of Click Reaction in Crystal Engineering"** has been carried out under my supervision and is a bonafide work of **Mr. Kulbhushan A. Durugkar**. This work is original and has not been submitted for any other degree or diploma of this or any other University.

Pune – 411008
April 2009

Dr. C. V. Ramana
(Research **Guide**)

Communication Channels
NCL Level DID : 2590
NCL Board No. : +91-20-25902000
EPABX : +91-20-25893300
+91-20-25893400
FAX
Director's Office : +91-20-25902601
COA's Office : +91-20-25902660
COS&P's Office : +91-20-25902664
WEBSITE
www.ncl-india.org

Acknowledgements

It gives me immense pleasure to express my deep sense of gratitude to my teacher and research guide ***Dr. C. V. Ramana****, who has helped me a lot to learn and think more about chemistry. He has introduced me to the area of multistep synthesis, interdisciplinary areas like glyco-nanoparticle synthesis and crystal engineering. I thank him for an excellent and inspiring guidance, constant encouragement, sincere advice and unstinted support during all the times of my Ph.D. work. Working with him was a great pleasure and learning experience.*

I would like to thank our interdisciplinary collaborators Dr. B. L. V. Prasad and Dr. R. G. Gonnade for guidance and help. I am highly thankful to D. K. Mohapatra for his sincere efforts and patience in guiding me in my early days of research career.

I would like to thank Dr. M. K. Gurjar, Dr. Hotha, Dr. HV Thulasiram, Mr. I. Shivakumar, Dr. M. N. Deshmukh, Dr. H. B. Borate, Dr. S. P. Chavan, Dr. U. R. Kalkote, Dr. R. A Joshi, Dr. R. R. Joshi and Dr. Gajbhiye for timely help and discussions. I am thankful to my mentors at my school, college and University for their inspirational teaching, ethics and discipline.

I gratefully acknowledge the training and support extended by my senior colleagues Dr. Sankar, Dr. Krishnakanth, Dr. Arindam, Dr. Joseph, Dr. Sridhar, Dr. Srinivas, Dr. Sidharth, Dr. Nagaprasad, Dr. Ekambram, Dr. Mahesh, Dr. Smriti, Dr. Sukhen, Dr. Manjusha, and Dr. Dhananjoy during the tenure of my Ph.D life. I would like to express thanks all my colleagues Ramdas, Tushar, Bhagwat, Bhargava, Sahoo, Sumanth, Gorakh, Sabita, Seetaram, Hasibur, Rita, Ramesh, Raghupathi, Nageswar, Anuj, Susheel, Kiran, Soumitra, Pradip, Chinmoy, Bhaskar, Indu, Abhijit, Srinivas, Sharad, Ganesh, Rosy, Debabrata, Mohabul, Giri, Rambabu, Sunil, Rahul, Pitambar, yogesh, Sridhar, Sachin, Vilas, Ajay, Mangesh, shyam, chandrababu, Suneel, Yadagiri and Senthil for their cooperation and friendly attitude.

I am also thankful to my friends Nagendra, Vinod, Rameshwar, Shriram, Amol, Laxman, Namdev, Pandurang and Awadut for their continuous encouragement, help and whose companionship always kept my mood cheerful and with whom I shared golden moments. My sincere thanks to all other friends from NCL and SA for their co-operation specially Nilkant. A special thanks all "NCL-Chemistry" members for their cheerful company.

Help from the spectroscopy, mass and microanalysis group is gratefully acknowledged. I sincerely thank Dr. Rajmohan and Mrs. Shanthakumari for their helpful discussions and cooperation. My sincere thanks to Dr. G. Pandey, Head, Division of Organic Chemistry for his cooperation and support. My honest thanks to Mrs. Raphel, Mrs. Kulkarni, and all other OCD office staff for their cooperation.

It is impossible to express my sense of gratitude for my parents in mere words. Whatever I am and whatever I will be in future is because of their enormous blessings, commitments to my ambitions and their selfless sacrifices. Words fall short to thank my wife, Sphurti for her love and support at tough time.

Finally I thank Director, National Chemical Laboratory; Pune for providing infrastructural facilities to complete my work successfully. Financial assistance from CSIR, New Delhi in the form of fellowship is gratefully acknowledged.

Kulbhushan A. Durugkar

DEFINATIONS AND ABBREVIATIONS

Ac	–	Acetyl
AcOH	–	Acetic acid
Ac_2O	–	Acetic anhydride
AIBN	–	2,2'-Azobisisobutyronitrile
aq.	–	Aqueous
Bn	–	Benzyl
BnBr	–	Benzyl bromide
$BF_3{\cdot}Et_2O$	–	Boron trifluoride diethyl ether complex
Boc	–	*Tert*-Butoxy carbonyl
n-BuLi	–	*n*-Butyl lithium
Cat.	–	Catalytic/catalyst
Cbz	–	Benzyloxycarbonyl
CM	–	Cross metathesis
Conc.	–	Concentrated
$CuSO_4$	–	Copper sulphate
CSA	–	Camphor sulphonic acid
m-CPBA	–	*m*-Chloroperbenzoic acid
DCM	–	Dichloromethane
DFT	–	Density functional theory
DIBAL-H	–	Di-isobutly aluminium hydride
DMF	–	*N*,*N*-Dimethylformamide
DMAP	–	*N*,*N'*-Dimethylaminopyridine
DMP	–	2, 2-Dimethoxypropane
DMSO	–	Dimethyl sulfoxide
EtOH	–	Ethanol
Et_2O	–	Diethyl ether
EtOAc	–	Ethyl acetate
Et_3N	–	Triethylamine
IBX	–	Iodoxybenzoic acid
Im	–	Imidazole

K^tOBu	–	Potassium tertiary butoxide
LAH	–	Lithium aluminium hydride
LDA	–	Lithium diisopropylamide
LiN_3	–	Lithium azide
Na_2CO_3	-	Sodium carbonate
NaN_3	–	Sodium azide
NMR	–	Nuclear magnetic resonance
Ms/Mesyl	–	Methanesulfonyl
Me	–	Methyl
ORTEP	–	Oak Ridge Thermal Ellipsoid Plot
Pd/C	–	Palladium on Carbon
Ph	–	Phenyl
Py	–	Pyridine
PTSA	–	*Para*-Toluenesulfonic acid
RCM	–	Ring closing metathesis
rpm	–	Rotations per minute
rt	–	Room temperature
sat.	–	Saturated
TEMPO	–	2,2,6,6-tetramethyl-1-piperidinyloxy free radical
TFA	–	Trifluoro acetic acid
Tf_2O	–	Trifluoromethanesulphonic anhydride
THF	–	Tetrahydrofuran
TMSOTf	–	Trimethylsilyl trifluoromethanesulphonate
TPP/PPh_3	–	Triphenylphosphine
TsCl	–	*para*-Toluenesulphonyl chloride

GENERAL REMARKS

- ^{1}H NMR spectra were recorded on AV–200 MHz, AV–400 MHz, and DRX–500 MHz spectrometer using tetramethylsilane (TMS) as an internal standard. Chemical shifts have been expressed in ppm units downfield from TMS.
- ^{13}C NMR spectra were recorded on AV–50 MHz, AV–100 MHz, and DRX–125 MHz spectrometer.
- EI Mass spectra were recorded on Finngan MAT–1020 spectrometer at 70 *eV* using a direct inlet system.
- The X-Ray Crystal data were collected on *Bruker SMART APEX* CCD diffractometer using Mo K_{α} radiation with fine focus tube with 50 kV and 30 mA.
- Infrared spectra were scanned on Shimadzu IR 470 and Perkin-Elmer 683 or 1310 spectrometers with sodium chloride optics and are measured in cm^{-1}.
- Optical rotations were measured with a JASCO DIP 370 digital polarimeter.
- Melting points were recorded on Buchi 535 melting point apparatus and are uncorrected.
- All reactions are monitored by Thin Layer Chromatography (TLC) carried out on 0.25 mm E-Merck silica gel plates (60F–254) with UV light, I_2, and anisaldehyde in ethanol as developing agents.
- All reactions were carried out under nitrogen or argon atmosphere with dry, freshly distilled solvents under anhydrous conditions unless otherwise specified. Yields refer to chromatographically and spectroscopically homogeneous materials unless otherwise stated.
- All evaporations were carried out under reduced pressure on Buchi rotary evaporator below 45 °C unless otherwise specified.
- Silica gel (60–120), (100–200), and (230–400) mesh were used for column chromatography.

CONTENTS

ABSTRACT

ABSTRACT

The thesis entitled **"Cross Metathesis Approaches for Broussonetine C, G & 12-*C*-Glycosyl-dodecanoic Acids and Exploration of Click Reaction in Crystal Engineering"** consists of two chapters. Each chapter is again sub-divided in two sections. Chapter I, section I describes cross metathesis approaches for broussonetine C and G. Second section deals with the synthesis of *C*-glycosides of dodecanoic acid employing cross metathesis and their application as new capping/reducing agents for silver nanoparticles synthesis. Chapter II, Section I presents "Cu(I) Promoted One–pot "S_NAr–Click Reaction" of Fluoronitrobenzenes". Application of this methodology for the "Click" Synthesis of isomeric compounds for assessing the efficiency of bifurcated Cl···NO_2 synthon form the section II of chapter II.

Chapter 1

Section I: Cross metathesis approach for broussonetine C and G

The broussonetines are a class of polyhydroxylated alkaloids which have been isolated from the branches of Asian paper mulberry tree *Broussontia kazinoki* and comprise a new class of glycosidase inhibitors. The 29 unique broussonetines show very potent and selective glycosidase inhibitory activities and as such have enormous therapeutic potential as anti-tumor and anti-HIV agents. It is particularly interesting that the variation of the 13 carbon side chain functionality plays a key role in influencing the potency and enzyme specificity of glycosidase inhibitory activity. The promising biological activities and also the availability of a range of family members, this broussonetine natural products family provides an opportunity to synthetic chemists to explore flexible synthetic methods that can address the synthesis of any of these members with an ease. To embark in this direction, by invoking cross metathesis as the key transform, we have identified two potential key retrons **1.33** and **1.34** which can be advanced to both broussonetines A–D and broussonetines E–M respectively, by selecting an appropriate C_{12} or C_9 unit. In the following pages, we describe our efforts in this direction by taking the broussonetine C and G as the representatives from each type.

Figure 1 *Cross metathesis strategy for broussonetines*

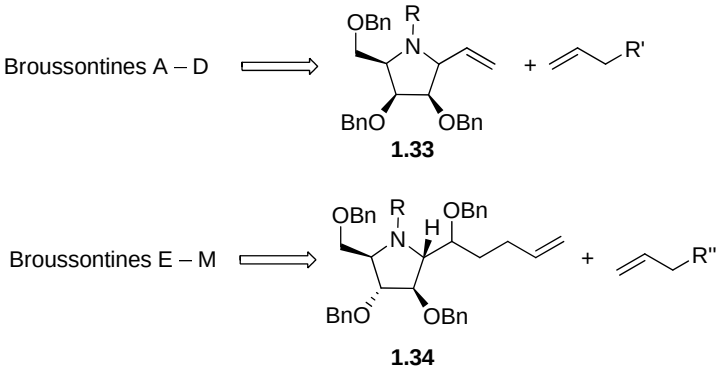

Considering the superior glycosidase inhibitory activities amongst the all other members of this family, broussonetine G (**1.28**, IC_{50}=3 nm, β-galactosidase; 24 nm, β-glucosidase, 760 nm, β-mannosidase) has been selected as the first target in our studies. Broussonetine G contains a structurally interesting 5,6-spiroketal at the end of alkane chain. Broussonetine C (**1.27**, IC_{50}=36 nm, β-galactosidase; 320 nm, β-mannosidase) selected as the representative of the first type broussonetines, has a 13 carbon side chain with a carbonyl group at C(10'). Despite their promising biological activities, there is only a single report (from Trost's group) on the synthesis of broussonetine G and a couple of reports for the synthesis of broussonetine C (Yoda and Perlmutter groups). A detailed retrosynthetic planning for broussonetine G and C is given in the figure 2.

Figure 2 *Retrosythesis for broussonetine G & C*

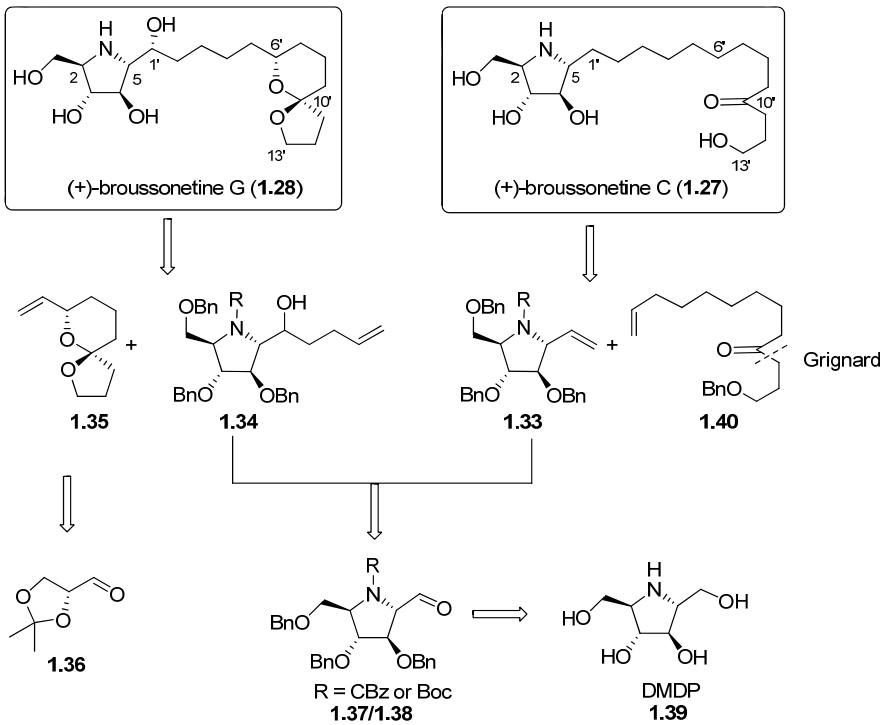

Cross metathesis approach for the synthesis of Broussonetine G

As shown in scheme 1, synthesis started with the commercially available L-sorbose, which was advanced to known pyrrolidine **1.39** according to the reported procedure, which was protected with triposgene under biphasic condition and the free hydroxyl groups were tribenzylated to give **1.49**. Carbamate functionality on saponification gave aminol and the ring nitrogen was protected as benzyl carbonate **1.51**. Primary alcohol at C_1 was oxidized with TEMPO radical and trichloroisocyanuric acid and the resulting aldehyde was subjected for a Grignard reaction with 3-butenylmagnesium bromide. Inseparable mixture of isomers in **1.52a/1.52b** were converted to corresponding acetate derivatives, from which one of the isomer (**1.34**) could be separated by flash column chromatography.

Scheme 1 *Synthesis of the chiral core subunit of* (+)*-broussonetine G*

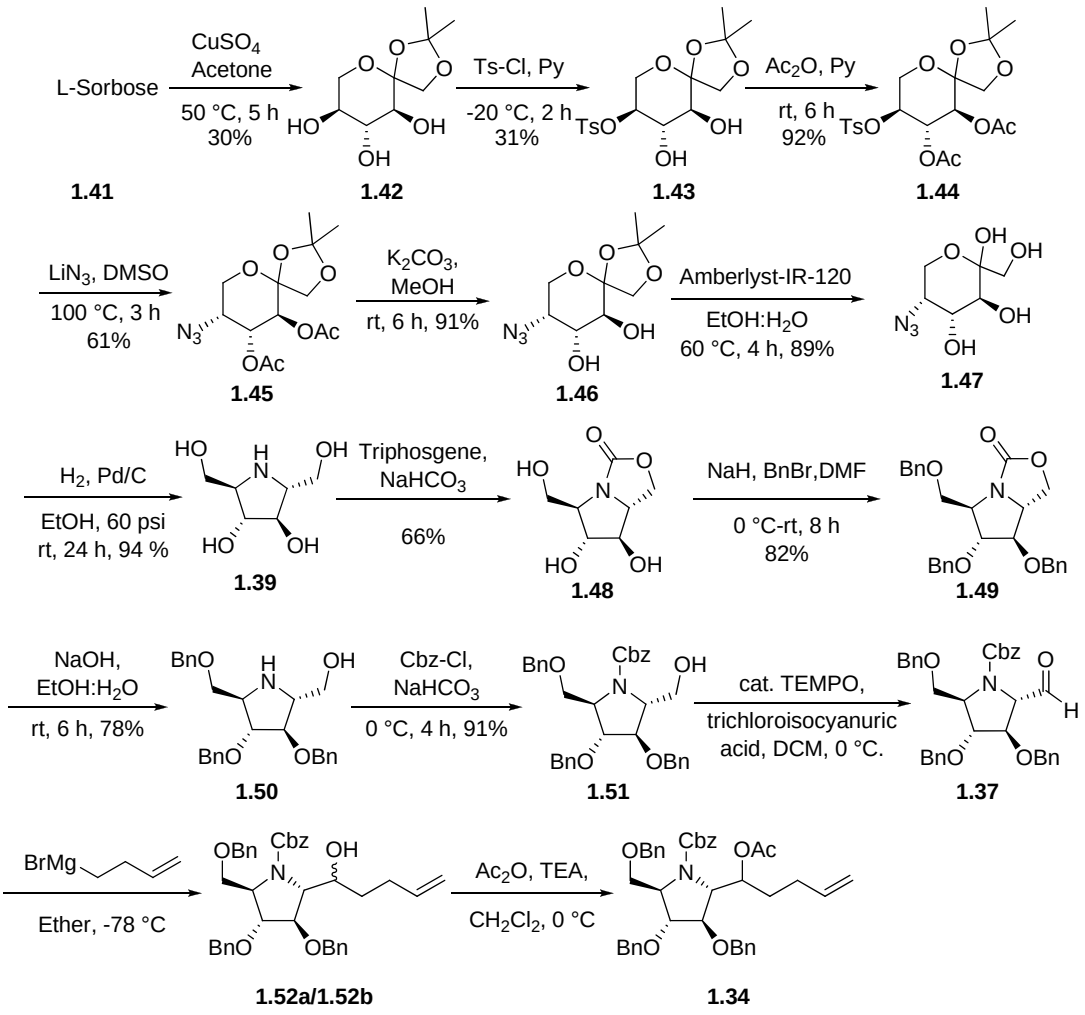

As shown in scheme 2, spiroketal side chain was synthesized from readily available D-mannitol. The known dicatetonide was cleaved to get (*R*)–glyceraldehyde **1.36** which on Wittig olefination, hydrogenation and controlled reduction with DIBAL-H yielded the aldehyde **1.57** which further underwent Wittig olefination. The acetonide was deprotected which *in situ* cyclised to give spiroketal alcohol **1.63**. This was subjected to routine oxidation and Wittig olefination sequence to get the low boiling, volatile spiroketal fragment **1.35**.

Scheme 2 *Synthesis of the spiroketal fragment of* (+)*-broussonetine G*

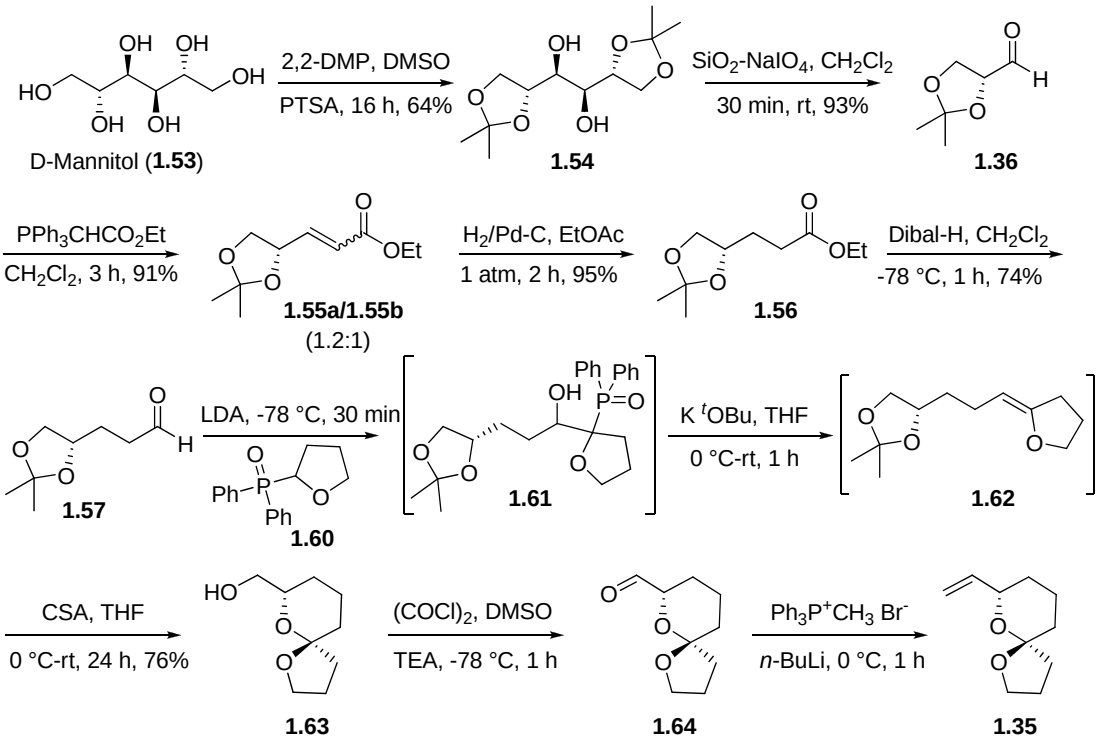

As shown in scheme 3, **1.34** was subjected to cross metathesis with the spiroketal side chain **1.35** employing 1st generation Grubbs' catalyst. The characterization of compound **1.65** was done extensively. First hydrogenation and then acetate deprotection did not work well to yield one of the pure isomer of broussonetine family. So acetate functionality was saponified by sodium methoxide and global deprotection of benzyl groups under hydrogenation condition was attempted in which reaction mixture shows compound peaks (analyzed by mass spectrum), but attempts to purify final compound **1.28** were unsuccessful.

Scheme 3 *Cross Metathesis approach for broussonetine G*

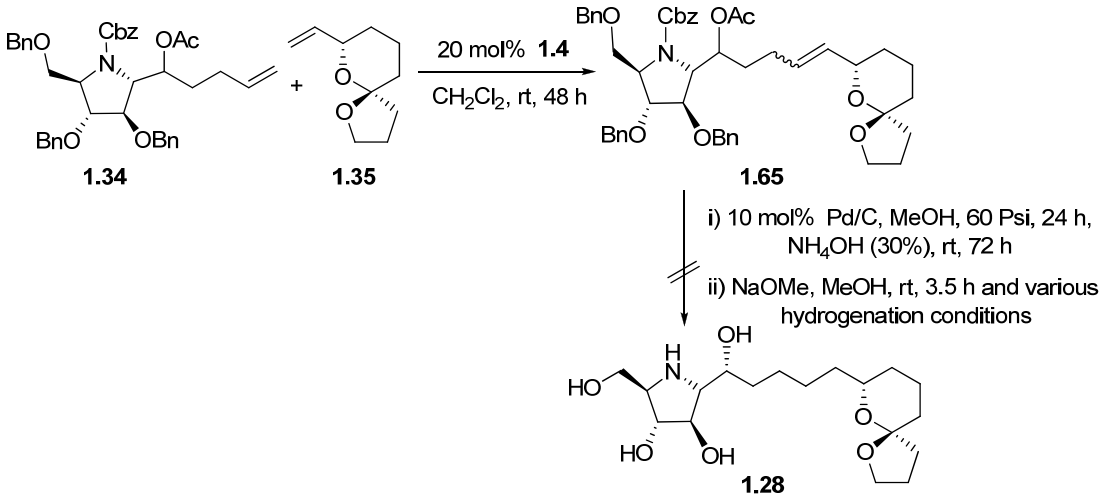

The α/β mixture **1.52a/52b** was treated with sodium hydride to get inseparable mixture of bicylic compounds **1.69a/1.69b**. The core molecule **1.69a/1.69b** and spiroketal fragment **1.35** was coupled together employing cross metathesis as a key reaction to yield **1.70a/1.70b**. Debenzylation using palladium hydroxide and carbamate deprotection using aq. NaOH was successful to get **1.28**, optical rotation and all other spectroscopic data were matching with the natural product as well as with the data provided by Trost *et al*. (scheme 4).

Scheme 4 *Synthesis of broussonetine-G*

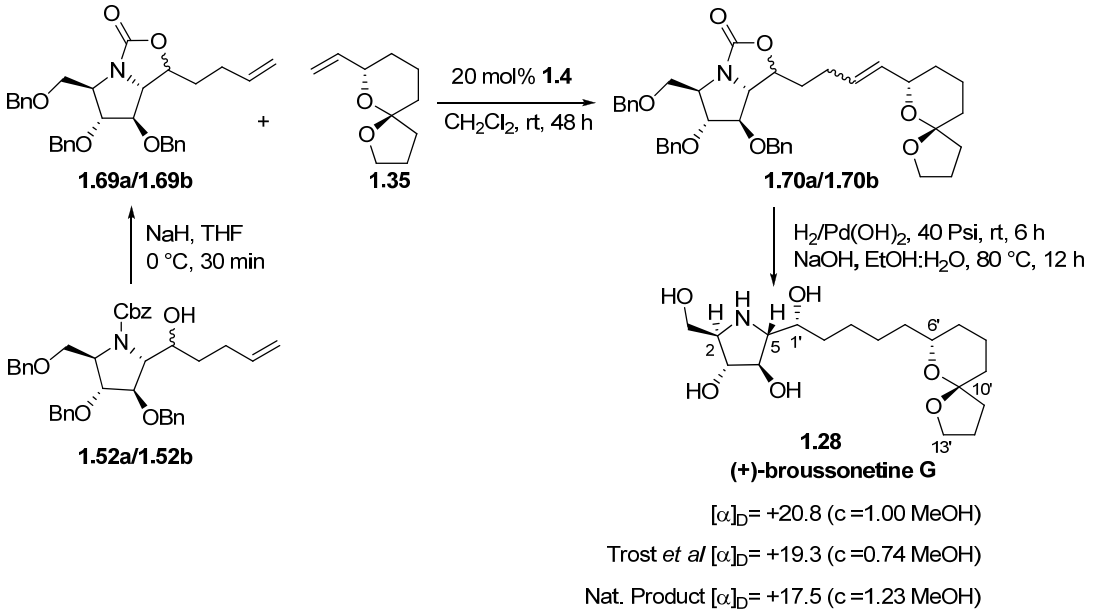

Cross metathesis approach for synthesis of Broussonetine C

As shown in scheme 5, aliphatic 13 carbon side chain was prepared starting from 9-decene-1-ol (**1.72**), which was oxidized using IBX to yield the aldehyde **1.73**. Treatment of **1.73** with 3-(benzyloxy)propyl magnesium bromide gave **1.74**. The obtained alcohol (**1.74**) was again oxidized using IBX to yield side chain **1.40**. The carbonyl group was masked using 1,3 propane diol to yield **1.75**.

Scheme 5 *Synthesis of 13-C sidechain of* (+)*-broussonetine C*

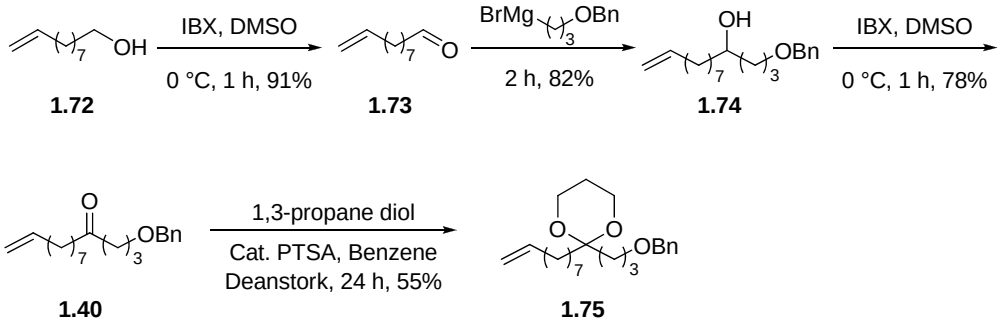

One carbon Wittig olefination of aldehyde **1.37** yielded the olefin **1.33**, the cross metathesis of which with **1.75** yielded only dimers. Gratifyingly, the cross metathesis of **1.33** with **1.40** yielded **1.78**, which was well characterized. The catalytic hydrogenation of protected (+)-broussonetine C (**1.78**) was attempted in different conditions but our attempts to get pure **1.27** were futile. (Scheme 6)

Scheme 6 *Cross metathesis approach for* (+)*-broussonetine C*

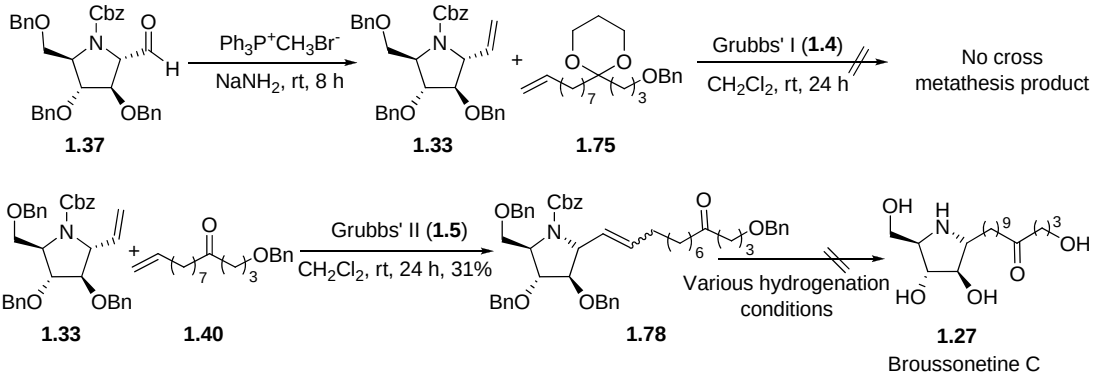

Next we opted for a Boc protecting group on ring nitrogen and planned to remove it after hydrogenolysis. **1.80** on TEMPO oxidation and Wittig olefination gave **1.81** which

underwent cross metathesis with keto side chain **1.40** to yield **1.83**. The deprotection of **1.83** was also found to be futile exercise by conducting the hydrogenation either first or after the Boc deprotection. (Scheme 7)

Scheme 7 *Cross Metathesis approach for broussonetine-C*

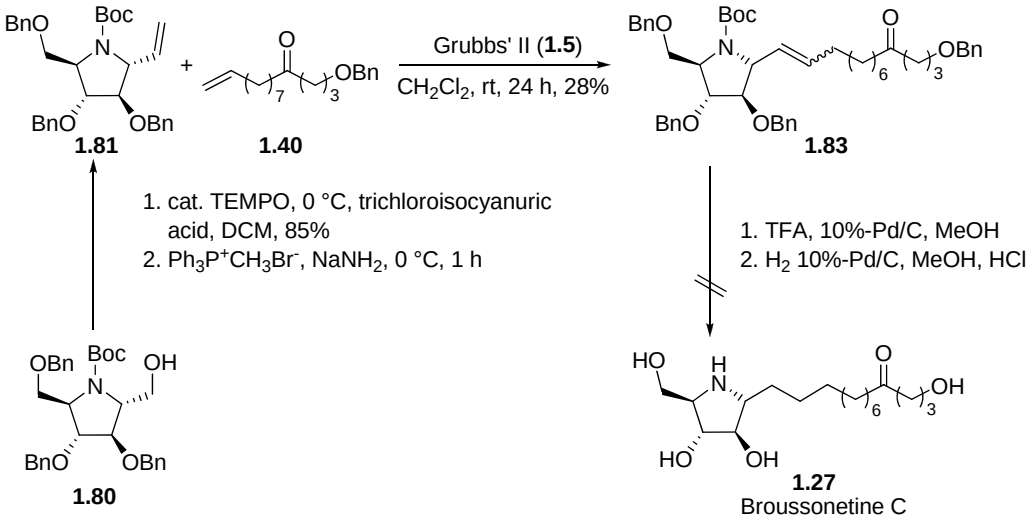

In summery employing cross metathesis as a key reaction, synthesis of (+)-broussonetine G and benzyl protected (+)-broussonetine C has been accomplished using chiral pool approach. Global deprotection of **1.78**, **1.83** was attempted, though the formation of the requisite products is noticed however, the isolation of the pure (+)-broussonetine C was found to be a difficult task.

Chapter 1

Section II: Synthesis of *C*-Glycosides of dodecanoic acid employing cross metathesis and their application as new capping/reducing agents for silver nanoparticles synthesis.

Over the last decade, the potential of noble metal nanoparticles has been explored in various fields such as optics, microelectronics, sensors, catalysis, and so on. The mutually advantageous conjugation of metal nanoparticles with biomolecules or biologically relevant ligands has gained much impetus because of their promising biomedicinal and bioanalytical applications in addition to hydrophilic rendition to surfaces and biocompatiblity. In this context, *glyconanoparticles* (GNPs), derived from the surface modification of metal nanoparticles by connecting with sugar residues through

O-glycoside linkages, have been recognized as novel tools to investigate carbohydrate recognition processes.

C-Glycosides, which entail methylene substitution for the anomeric oxygen, offer a great deal of stability without substantial conformational amendment. Considering the fact that simple monosaccharides in biological systems can exist either in furanose or pyranose forms, three compounds **1.101**–**1.103** were selected as representatives of pentoaldofuranose (D-*ribo*), pentoaldopyranose (D-*ribo*) and hexoaldopyranose (D-*gluco*), respectively. The *C*-allyl sugar derivatives were synthesized by allylation of corresponding peracylated glucocides using allyl trimethyl silane and BF_3 etharate. (Scheme 8)

Scheme 8 *Synthesis of the C-allyl sugar derivatives*

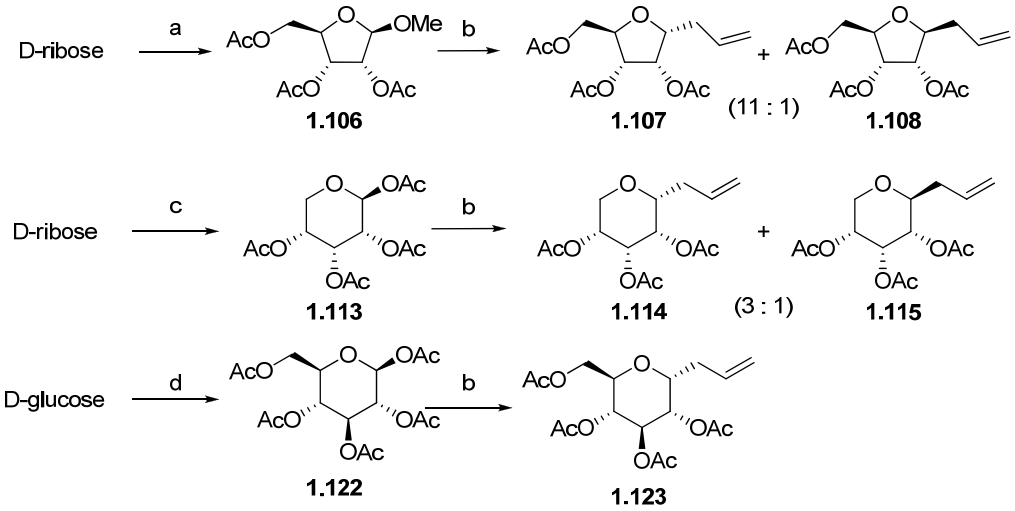

a) i. Cat. H_2SO_4, MeOH, 0 °C, 15 h; ii. Ac_2O, pyridine 0 °C–rt; b) Allyltrimethyl silane, $BF_3.Et_2O$, Cat TMSOTf, CH_3CN, 0 °C–rt, 8 h; c) Cat. HCl, Ac_2O, pyridine, 0 °C-rt; d) Cat. $HClO_4$, Ac_2O, pyridine 0 °C-rt.

Peracetylated *C*-allyl glycosides **1.107**, **1.114** and **1.123** which underwent cross metathesis with 10-undecene-1-ol using Grubbs' 2nd generation catalyst (5 mol%) to afford inseparable mixture of *E/Z* olefins **1.109**, **1.116**, **1.124**, along with the 10-undecene-1-ol dimmer (Scheme 9). The olefin mixture was hydrogenated to yield saturated alcohols **1.111**, **1.120**, **1.125**. Oxidation of the hydroxyl group with $RuCl_3.6H_2O$ and $NaIO_4$ followed by deacetylation completed the synthesis of 12-*C*-α-glycosyldodecanoic acids **1.101–1.103** in overall yields of 49%, 50% and 47%, respectively.

Scheme 9 *Synthesis of 12-α-C-glycosyl dodecanoic acids*

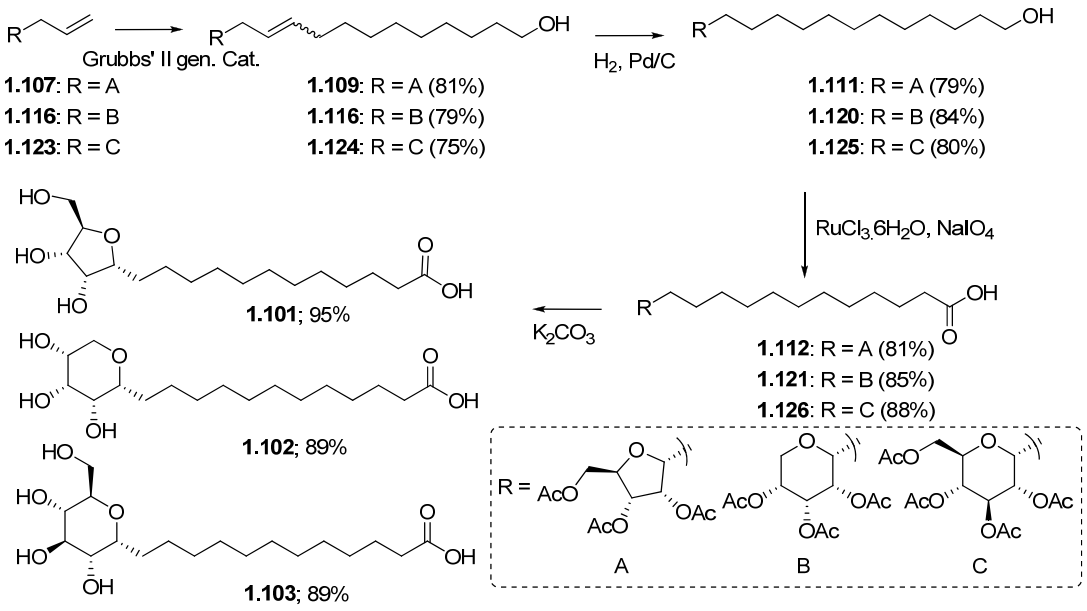

After synthesizing the requisite *C*-glycosyl acids **1.101**–**1.103**, the next objective was to use them as capping agents for metal nanoparticles. After a substantial optimization of the experimental parameters, a reductive synthesis of desired *C*-glycoside capped silver nano particles was concluded successfully by heating equimolar quantities silver nitrate and *C*-glycoside **1.101** or **1.102** in dilute alkaline solution (10^{-4} M). The reduction was instantaneous and the Ag NPs could be isolated as stable powders by simple centrifugation.

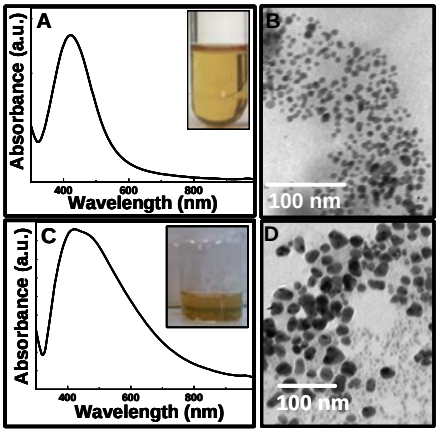

Figure 3 *Figures A and C showing the UV-vis spectra of AgNPs synthesized from* **1.101** *and* **1.102** *respectively. Figure B and D showing TEM image of AgNPs synthesized from* **1.101** *and* **1.102** *respectively. Insets (A) and (C) shows the colors of the AgNPs synthesized from* **1.101** *and* **1.102**, *respectively.*

With *C*-glucoside **1.103**, aggregation of the initially formed Ag NPs occured. Figures A and C (Inset, Figure 3) show UV-Vis spectra and recorded from alkaline solutions of silver nitrate and acids **1.101** and **1.102**, respectively. The strong absorption at *ca.* 410 nm clearly indicates the formation of Ag NPs. Transmission electron microscope (Figures 3B and 3D) images of synthesized Ag NPs revealed average particle size to be ~15 nm.

In summery a concise synthesis of 12-*C*-glycosylated dodecanoic acids employing an olefin cross metathesis reaction is developed. Examination of these acids as capping agents for the synthesis of metal nanoparticles reveal that they do not cap the Co-metal nanoparticles synthesized in aqueous phase, but that two of them (**1.101**, **1.102**) can reduce $AgNO_3$ and cap the resulting Ag nanoparticles in water without any aggregation.

Chapter 2

Section I: "Cu(I) Promoted One–pot "S_NAr–Click Reaction" of Fluoronitrobenzenes".

The nucleophilic substitution reaction (S_NAr) of activated aryl halides is an important transformation for C−C and C−hetero atom bond formation with aryl rings. These reactions are facilitated by the presence of –M groups like a nitro or a carbonyl ortho or para to the leaving group in general and with meta isomers in some rare cases. Various carbon and hetero atom nucleophiles have been employed in this context. Reports concerning the azide as a nucleophile in S_NAr were mainly limited to the mechanistic investigations.

Inspired with the broad spectrum application of Cu(I)–catalyzed 1,3-cycloaddition between an azide and an alkyne in the discovery of drugs and materials, and less reports concerning the azide as a nucleophile in S_NAr reaction, we have initiated a program to design a methodology in which these two reactions occur in one pot.

To this end, by screening various conditions we could conduct successfully the S_NAr of 2- & 4-fluoronitrobenzenes in presence of phenyl acetylene. The potential of this approach has been demonstrate by providing a rapid access for various 1,4-substituted triazoles. Control experiments revealed that both the steps are catalyzed by Cu(I) and also the course of reaction as S_NAr followed by [3+2]-cycloaddition (Scheme 10).

Scheme 10 *The one pot "S_NAr-click reaction" employing functionalized alkynes*

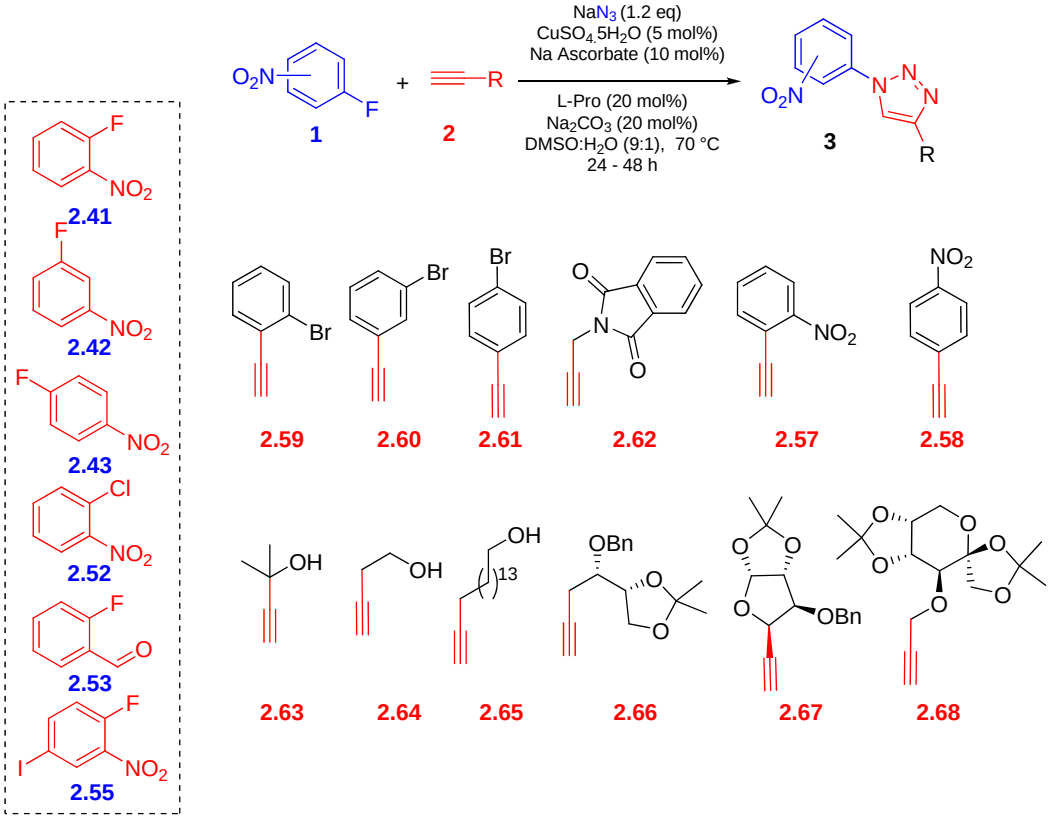

To conclude, a three component one–pot "S_NAr–click reaction" has been explored by employing *o*- and *p*-nitrofluorobenezenes and a diverse set of alkynes. Control experiments reveal the course of the reaction as S_NAr with azide nucleophile followed by the cycloaddition of the resulting nitroazidobenzene intermediate and both the reactions being catalyzed by Cu(I). The reactions are generally regioselective and various commonly employed protecting groups are found to be compatible with the conditions employed.

Chapter 2

Section II: the "Click" Synthesis of isomeric compounds for assessing the efficiency of bifurcated Cl···NO_2 synthon

After the disclosure of bifurcated three-centered NO_2…X (X=Cl, Br, I) supramolecular synthon by Desiraju and co-workers, the occurrence of these soft and weak three-center interactions was analyzed using Cambridge Crystal Structure Database searches. Allen *et al.* used a combination of systemic database analysis and high-level *ab*

initio molecular orbital calculations to provide significant insight into the geometry of NO_2…X interactions (figure 4). They classified NO_2…X interactions according to the close approach of X atom to NO_2 group into three different motifs; (I) symmetric bifurcated motif, (II) the asymmetric bifurcated motif and the (III) motif in which halogen (X) forms mono-coordinate interactions with one nitro O atom. In the first two categories the X atom approaches both nitro O atoms in a bifurcated manner (X…O trans to C–N); the tendency to form such bifurcated motifs increases in the order C1 < Br < I whereas in the last category X...O in a *cis* relationship to the nitro C substituent about the N–O bond. Though NO_2…X symmetric bifurcated motif has been regarded as a 'discriminator synthon' its predictability, when examined over a range of isomeric compounds revealed certain limitations. Focusing on the Cl…NO_2 synthon, we describe synthesis and the structural analysis of a collection of isomeric compounds with modular positioning of Cl and NO_2 on a flexible tricyclic template.

Figure 4 *Designed isomers and possible Cl···NO_2-synthon geometries*

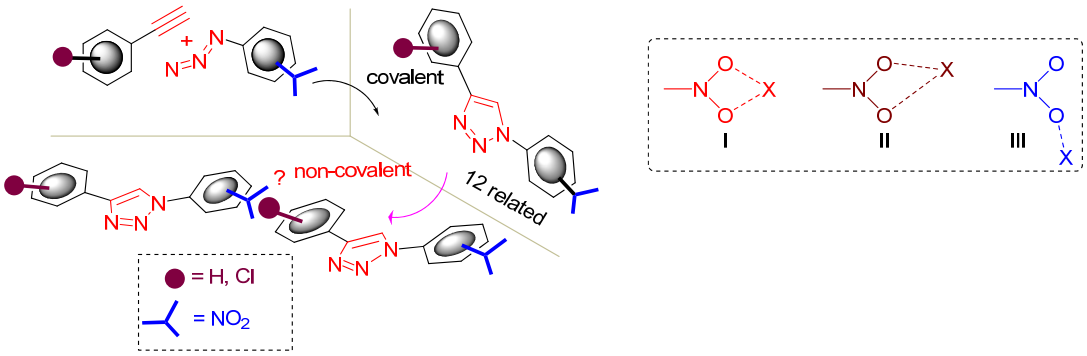

The Cu mediated Huisgen's azide-[3+2] cycloaddition [Fokin–Finn–Sharpless's ''click reaction''] has served as the flexible molecular construct in our synthesis employing either corresponding azide of SNAr of respective fluronitrobenzene with sodium azide (*in situ*) followed by the click reaction (Scheme 11). Having no motifs that form the conventional hydrogn bond, this selected scaffold offered an opportunity for understanding molecular association either via Cl …NO_2 or Cl... Cl interacting synthons and to study the interplay of other weak intermolecular interactions in molecular aggregation. The intramolecular association of all the 12 compounds synthesized in this context were analyzed with the help of the single crystal X-ray diffraction studies.

Scheme 11 *Hüisgen [3+2] cycloaddition reaction between fluoronitrobenzenes* ***2.40****,* ***2.42****, & 3-azidonitrobenzene (****2.95****), and alkynes* ***2.43****,* ***2.89****–****2.91.***

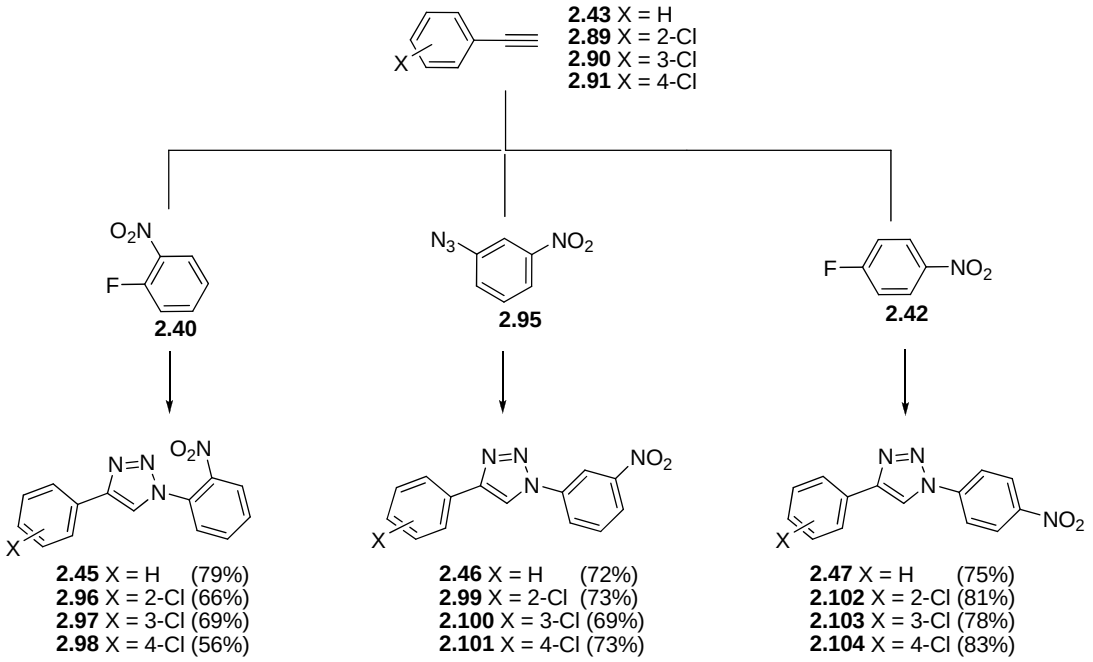

Interestingly in none of the nine isomers the bifurcated Cl …NO_2 synthon has been seen. A comprehensive compilation of various weaker interactions observed in crystal structures of all the compounds revealed that out of nine compounds, molecules in two compounds (**2.98** and **2.101**) have Cl···NO_2 association, in one compounds Cl···Cl short contact (**2.102**) and in four compound (**2.96**, **2.97**, **2.100** and **2.102**) C-H···Cl electrostatic interaction were present.

In conclusion, the potential of Cu(I) catalysed azide-alkyne "Click Reaction" as a simple synthetic tool to build a collection of crystalline isomeric compounds with modular positioning of Cl and NO_2 functional groups and evaluation of the occurrence of bifurcated Cl…NO_2 synthon was studied.

CHAPTER-I

Section I: Cross metathesis approach for broussonetines C & G

1.1 Introduction

1.1.1 Olefin metathesis:

The Nobel Prize in chemistry 2005 was equally shared by Dr. Yves Chauvin, Professor Robert H. Grubbs, and Professor Richard R. Schrock for their pioneering contribution in the "*development of the metathesis method in organic synthesis*".

The very foundation of organic synthesis consists of reactions that can reliably and efficiently form carbon-carbon bonds. In recent years, the olefin metathesis reaction has attracted widespread attention as a versatile carbon-carbon bond-forming method. Derived from the Greek words *meta* (change) and *thesis* (position), metathesis is the exchange of parts of two substances. The olefin metathesis reaction can be thought of as a reaction in which all the carbon-carbon double bonds in an olefin (alkene) are cut and then rearranged in a statistical fashion.

Scheme 1.1 *Olefin metathesis reactions*

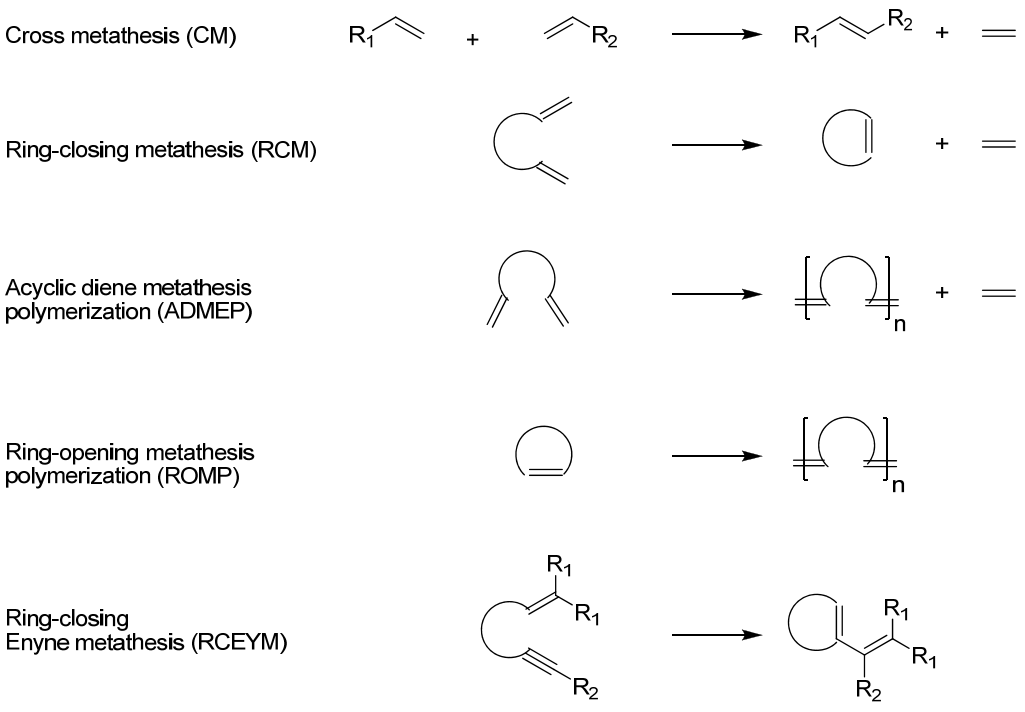

In 1950's the first metal catalyzed metathesis reaction was discovered by Ziegler (Nobel prize in chemistry 1963), i.e. polymerization of ethylene. Metathesis, with its multiple facets, has become one of the most important chemical transformations. The olefin metathesis has been broadly divided as cross metathesis (CM), ring closing metathesis (RCM), acyclic diene metathesis polymerization (ADMEP), ring opening metathesis polymerization (ROMP).(Scheme 1.1). Through these reactions, olefin metathesis provides a route to unsaturated molecules that are often challenging or impossible to prepare by any other means. Some of the most impressive achievements include the use of ROMP to make functionalized polymers, the synthesis of small to large heterocyclic systems by RCM, and the CM of olefins with pendant functional groups.[1] However until a few years ago, the scope of the reaction was quite limited because of insufficient catalyst performance. It is only through major advances in catalyst design that tremendously expanded applications have recently become possible. To a large extent, these efforts to improve catalyst performance have been motivated and inspired by the desire to apply olefin metathesis to new synthetic challenges.

1.1.2 Olefin Cross-Metathesis:

Olefin cross-metathesis[2] can be formally described as the intermolecular mutual exchange of alkylidene (or carbene) fragments between two olefins promoted by metal-carbene complexes. There are three main variations on this theme (Scheme 1.2): a) Cross metathesis (CM), b) Ring opening cross metathesis (ROCM), and c) Enyne cross metathesis (EYCM).

Scheme 1.2 *Olefin cross metathesis reactions*

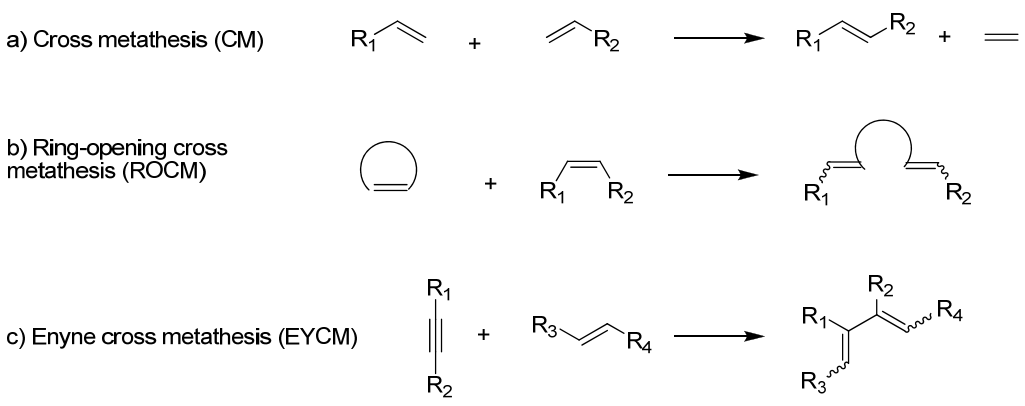

As an acyclic carbon-carbon bond forming tool, cross metathesis has numerous advantages typical of modern olefin-metathesis reactions:

1) The process is catalytic—typically 1–5 mol% of catalyst required.

2) High yields can be obtained under mild conditions in relatively short reaction times.

3) A wide range of functional groups are tolerated, with minimal substrate protection necessary.

4) The reaction is reversible, relatively atom-economic, and gaseous ethylene is usually the only byproduct, which is an important consideration in industrial applications.

5) The olefin substrates are generally easier and less expensive to prepare than those associated with other common catalytic C–C bond-forming reactions (e.g. unsaturated boranes, stannanes, halides, triflates).

6) The olefinic products are suitable for further structural elaboration (e.g. hydrogenation, epoxidation, halogenation, cycloaddition).

7) High levels of chemo-, regio-, and stereoselectivity can be attained.

Cross-metathesis (CM) has found numerous industrial uses, including the well known Shell Higher Olefin Process (SHOP),[3] the Further Exploitation of Advanced Shell Technology (FEAST) Process, and the Phillips Triolefin Process.[4] CM is not yet in such widespread laboratory use as the more entropically favorable ring-closing metathesis (RCM) reaction.

The early examples of olefin cross metathesis employed classical catalysts, which usually included a tungsten chloride or oxychloride and an alkyl metal species. These catalysts were less reactive to olefins due to their increased stability and yields were generally found to be low.[5] The other established catalyst is dichlorobis(2,6-dibromophenoxy)oxotungsten, $Cl_2(ArO)_2W{=}O$.[6] Although this system shows good functional group tolerance and has been used for many syntheses, it is considered to be unsuitable for industrial applications owing to its complexity and cost. Olefin metathesis began to receive more attention in 1993, when Basset and coworkers developed and applied the tungsten catalysts **1.1** and **1.2** for cross metathesis reactions.[7] One of the most useful catalysts for olefin metathesis reactions is the molybdenum catalyst (**1.3**) developed by Schrock *et al*.[8] Although the major advantage of **1.3** is its high reactivity towards a broad range of substrates having a variety of functional groups, this catalyst also has some limitations. Its major drawbacks are that it is air sensitive and has moderate to poor functional group tolerance.

Figure 1.1 *Catalysts for olefin cross metathesis*

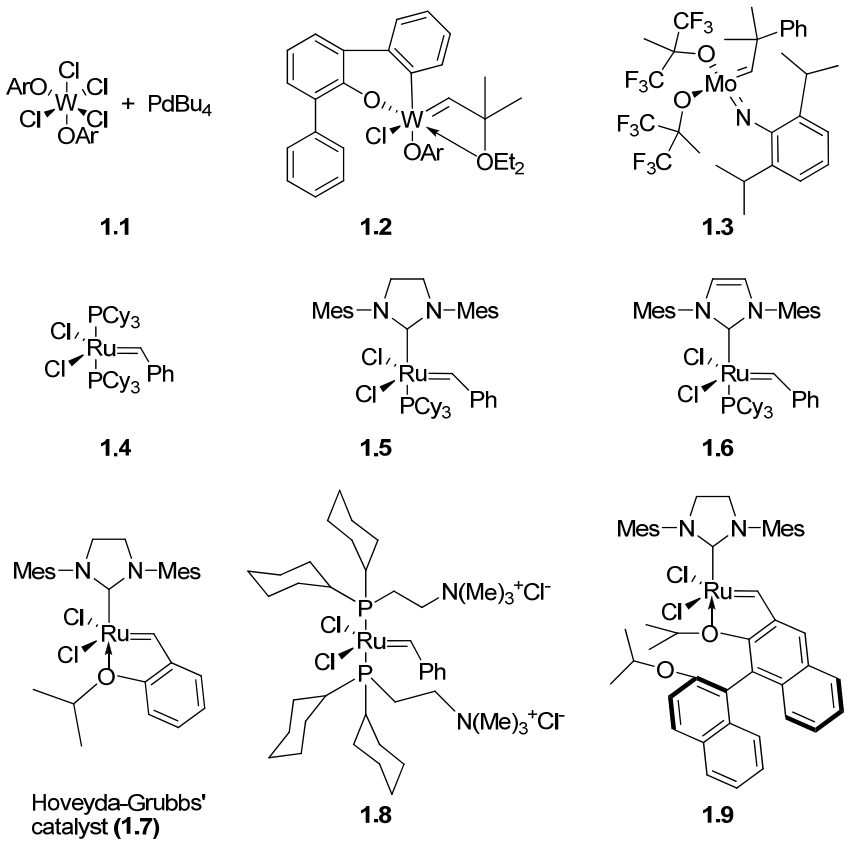

Much work on the development of catalytic systems has been done by Grubbs' and coworkers using four very important ruthenium based catalysts; **1.4–1.7**.[9] The Schrock catalyst is more active and is useful in the conversion of sterically demanding substrates, while the Grubbs' catalysts tolerate a wide variety of functional groups. The second generation Grubbs' catalysts are even more stable and more active than the original versions and have allowed many groups to breathe new life into what were previously in many cases little more than unselective mechanistic curiosities. Although all the four catalysts benefit from the same impressive tolerance to air, moisture and various functional groups, catalyst **1.4** (first generation Grubbs' catalysts) provides improved initiation rates and can be prepared easily. In addition to the catalytic systems discussed above, a few other transition metal catalysts have been prepared for olefin metathesis reactions. Among them, the water soluble ruthenium catalyst **1.8**,[10] also developed by Grubbs and coworkers. Blechert and coworkers reported the novel ruthenium-alkylidene BINOL-based catalyst **1.9**[11] as an addition to the growing list of

second generation catalysts. This catalyst is significant in that it display increased activity, relative to **1.6** and **1.7**, while retaining stability even after exposure to air for one week. The improved reactivity and stability of this catalyst has been attributed to the increased steric bulk of the ligands. (Figure 1.1).

1.1.3 Mechanism

A general mechanistic scheme[12] for the CM of two symmetrically substituted olefins (in practice, this is quite difficult) is presented in Figure 1.2. The first step in the catalytic cycle (after the first catalyst turnover to produce A) is a [2+2] cycloaddition reaction between olefin B and a transition metal carbene A to give a metallacyclobutane C. The latter undergoes subsequent collapse in a productive fashion to afford a new olefin product D and a new metal carbine (alkylidene) E, which carries the alkylidene fragment R_1. Similarly, E can react with a molecule of F via G to yield D and A, which then re-enters the catalytic cycle. The net result is that D is formed from B and F with A and E as catalytic intermediates.

Figure 1.2 *Mechanism of olefin metathesis*

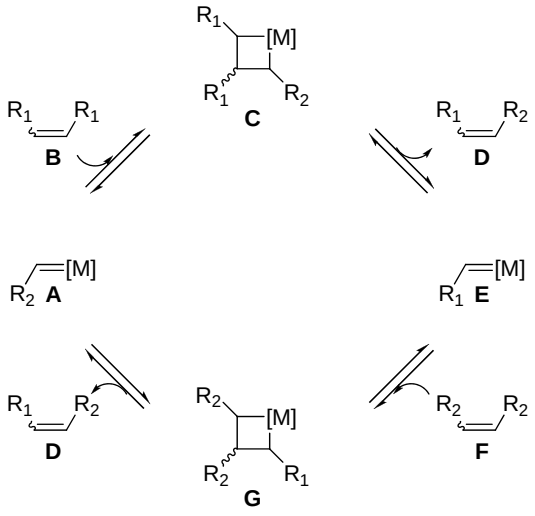

1.1.4 Synthesis of Biologically Important Molecules

From humble beginnings the evolution of CM into a flexible and powerful methodology for synthesis of biomolecules (and their analogues) and of natural products is steadily gaining momentum. Quite recently the volume of material published in this

area has increased as more and more chemists are turning to CM to achieve smooth high yielding transformations as key components of multistep selective syntheses.

Scheme 1.3 *Synthesis of "molecular asterisks" by CM*

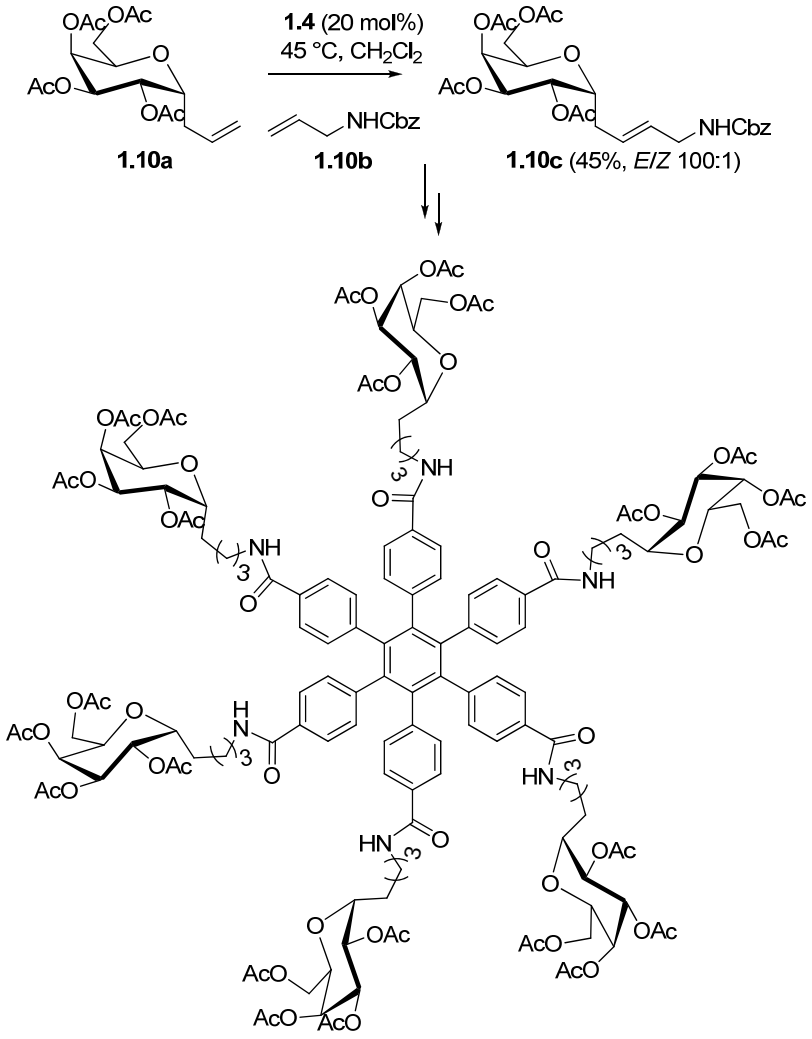

Roy and coworkers have used a selective CM reaction as a key C-C bond-forming step in the preparation of so-called "molecular asterisks."[13] An initial CM reaction between peracetylated α-D-allylgalactopyranoside **1.10a** with protected amine **1.10b** catalyzed by **1.4** afforded cross-product **1.10c** in moderate yield with complete *E* selectivity (Scheme 1.3). The predominance of the *E* isomer in this CM reaction remains to be explained; CM reactions involving various other sugar derivatives under identical conditions gave selectivity no better than 4:1 in favor of the *E* form. Glycoside **1.10a** then served as the template on which to build the necessary functionality to give the aryl glycoside cluster **1.10** after Sonogashira coupling and cyclotrimerization reactions.

Roy and Gan prepared divalent sialoside derivatives based on a CM reaction.[14] For example, the dimerization of sialosides **1.11a**–**1.11c** promoted by **1.4** allowed the isolation of dimers **1.11d**–**1.11f** (Scheme 1.4). Yields were good using *O*-α-sialosides, however thiosialoside **1.11b** was a considerably less efficacious CM partner as a result of the coordinating (and hence catalyst poisoning) proclivities of sulfides.

Scheme 1.4 *Synthesis of sialoside dimers*

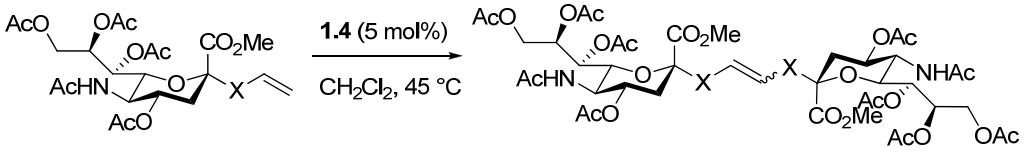

1.11a X = OCH_2
1.11b X = $O(CH_2)_3$
1.11c X = SCH_2 (10 mol% **1.4**)

1.11d X = OCH_2 (82%, *E*/*Z* 7:1)
1.11e X = $O(CH_2)_3$ (88%, *E*/*Z* 3:1)
1.11f X = SCH_2 (26%, *E*/*Z* 2.5:1)

The cross-metathesis of *O*- or *C*-allyl glycosides and *N*-alkenyl-containing oligosaccharide derivatives (peptoids) has been reported by Hu and Roy.[15]

Scheme 1.5 *Synthesis of peptoids*

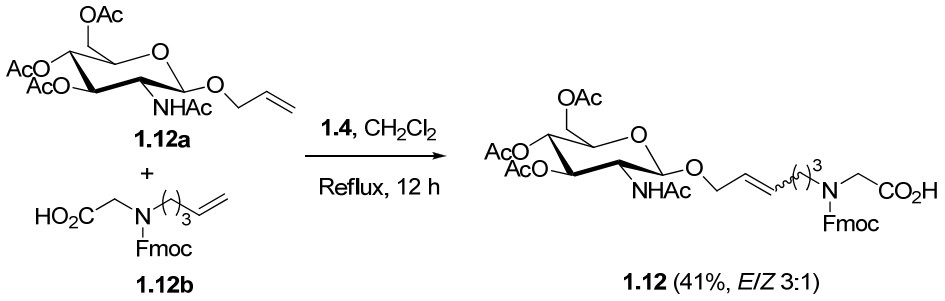

1.12 (41%, *E*/*Z* 3:1)

The treatment of a GlcNAc derivative (**1.12a**) with *N*-allylamine in the presence of Grubbs' catalyst (**1.4**) gave no cross-metathesis product, but dimerization of **1.12a** was achieved in 30% yield. Alternatively, the use of amine **1.12b** in the cross-metathesis reaction with **1.12a** gave **1.12** in 41% yield. This was a surprising result, since free carboxylic acids are not considered to be good substrates for olefin metathesis reactions (Scheme 1.5).

Blechert, S. and coworkers[16] constructed a small library of glycopeptides employing cross-metathesis in a posttranslational manner as a synthetic method for connecting sugar and peptide moieties. Catalyst **1.7** was shown to outperform catalyst **1.4**.

The unprotected glycoside **1.13a** gave variable yields, whereas acetate protected gave consistently good yields. The low yields obtained with vinylic **1.13c** are due to steric bulk of the α, β-branched olefin (Scheme 1.6).

Scheme 1.6 *Synthesis of glycopeptide library*

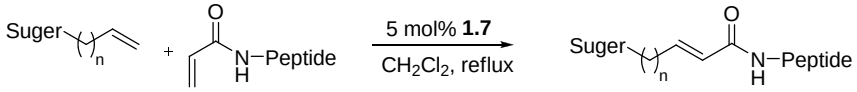

Entry	Peptide	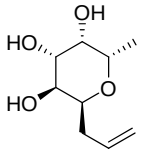 **1.13a**	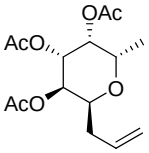 **1.13b**	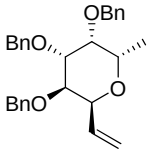 **1.13c**
1	GlyProOMe **1.13d**	65%	77%	65%
2	GlyGlyOMe **1.13e**	72%	65%	30%
3	AlaAlaOMe **1.13f**	15%	66%	35%
4	GlyglyAlaOMe **1.13g**	36%	58%	33%
5	LeuAlaProOMe **1.13h**	40%	62%	17%

In all cases *E*/*Z* ratio was > 19:1.

Scheme 1.7 *Synthesis of complex glycosyl amino acid from pentenyl glycoside*

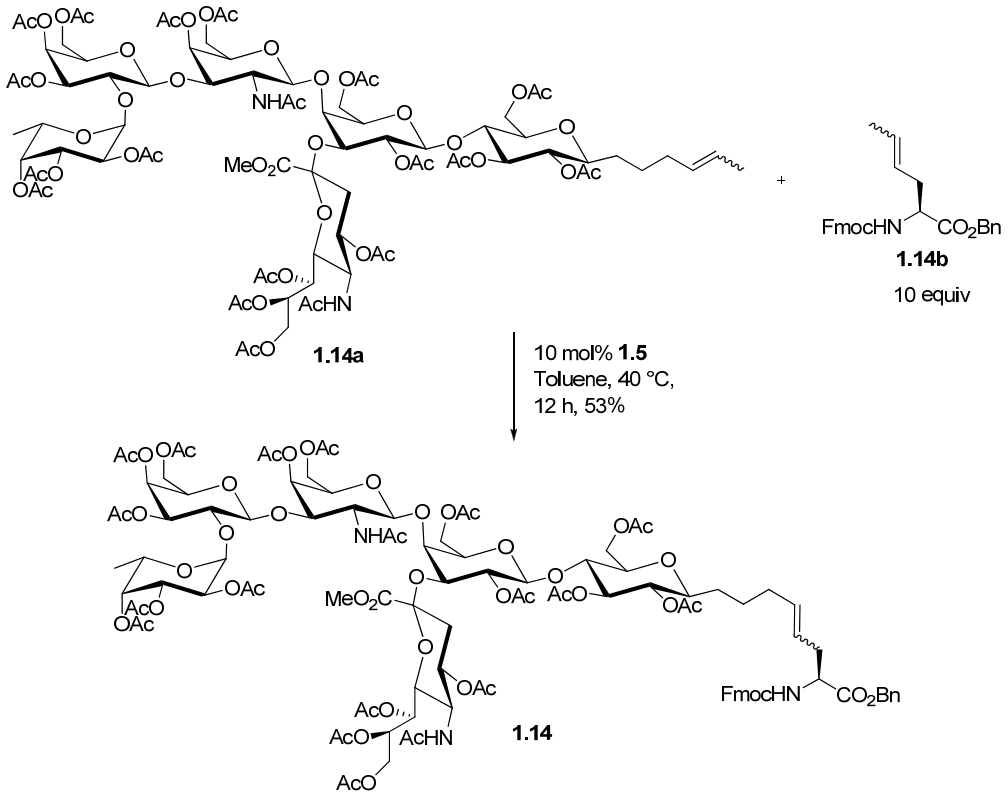

Danishefsky, S. J. and coworkers[17] have synthesized complex glycosyl amino acid (**1.14**) from pentenyl glycoside (**1.14a**) by a procedure of sequential cross metathesis followed by hydrogenation. The resulting N-protected amino acids were equipped for incorporation into multivalent or clustered manifestations of carbohydrate-based cancer vaccines. (Scheme 1.7)

Dondoni *et al.*[18] reported a successful CM between olefinated carbohydrates such as **1.15a** and vinyloxazolidenes such as **1.15b** catalyzed by the second-generation Grubbs catalyst **1.5** (20 mol%). After CM, the vinyloxazolidene protecting group can be cleaved with Jones reagent to unmask *C*-glycosyl amino acids such as **1.15** (Scheme 1.8). This methodology has also been extended to prepare a potential glycopeptide nephritogenoside mimetic.

Scheme 1.8 *C-glycosyl amino acid synthesis by CM*

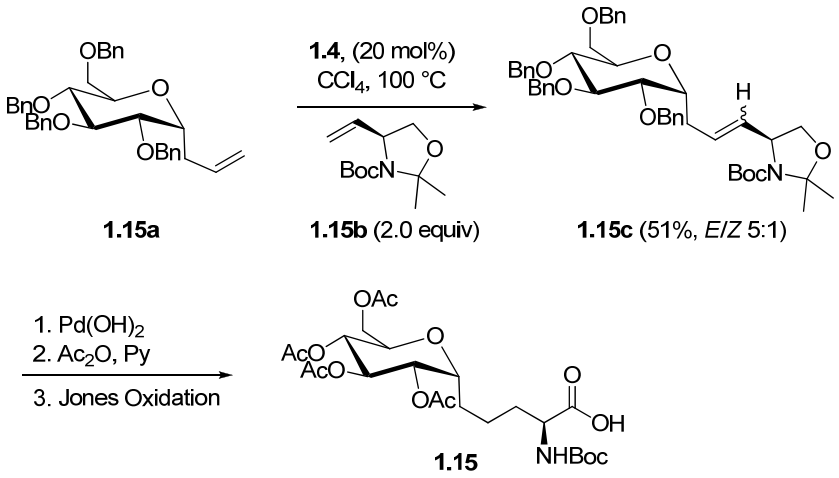

Dondoni *et al.* extended the earlier work of synthesizing *C*-glycosyl amino acid to *C*-Iminoglycosyl α-amino acid[19] by utilizing cross metathesis as a key reaction. They utilized various *N*-Cbz-protected allyl *C*-iminoglycosides with *N*-Boc-vinyl-oxazolidine as metathesis partners. The isolated yields of the CM products (mixtures of *E*- and *Z*-alkenes) varied in the range 40–70%. *β*-Linked *C*-allyl iminosugar **1.16a**, the *N*-Boc-vinyloxazolidine **1.15b** (2 equiv) and the Grubbs' catalyst 1,3-dimesityl-4,5-dihydroimidazol- 2-ylideneruthenium carbene **1.5** (0.2 equiv) in CCl_4 were heated at 100 °C (sealed vial) for 3.5 h. The results were quite disappointed as this condition was established by themselves. Hence, the above model reaction between **1.16a** and **1.15b** was performed under milder conditions in CH_2Cl_2 at 40 °C for 18 h with a higher excess

(3 equiv) of the vinyloxazolidine **1.15b** and 20 mol % of the Ru-carbene catalyst **1.5** (Scheme 1.9). This reaction afforded the desired CM olefin **1.16b** (*E*/*Z* mixture) in 50% isolated yield by column chromatography. In addition, the unchanged reactants **1.16a** and **1.15b** were partly recovered (15–20%) while the remaining material was composed of a complex mixture of products. The elaboration of **1.16b** was effectively carried out by first reducing the carbon-carbon double bond by *in situ* generated diimide from tosylhydrazine and sodium acetate and then by submitting the product **1.16c** to the oxidative cleavage of the oxazolidine ring by the Jones reagent. Similar results were obtained in case of α-linked *C*-allyl pyrrolidine iminosugar **1.16d**.

Scheme 1.9 *C-Iminoglycosyl α-amino acid synthesis by CM*

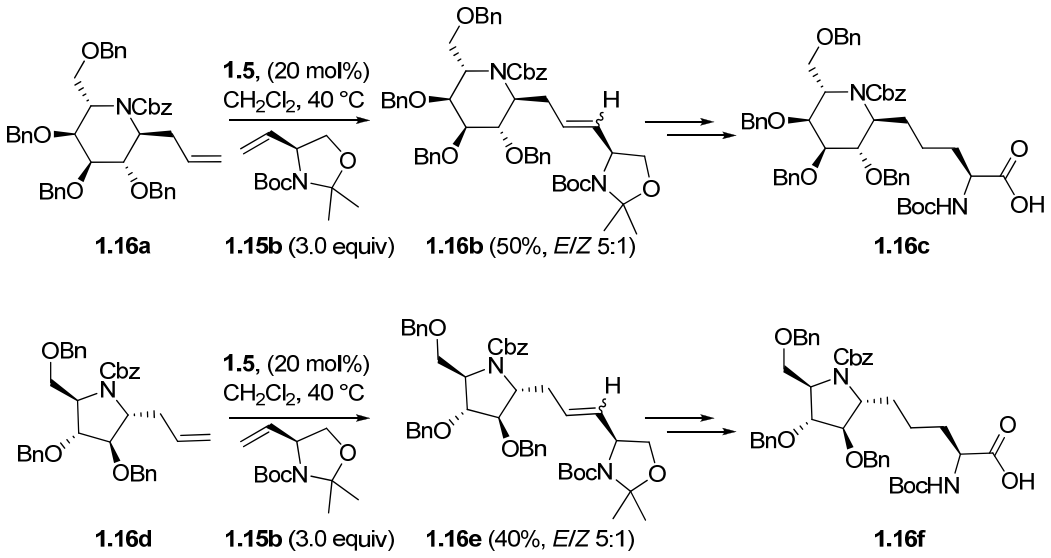

The studies by Davis *et al.* describe the conversion of a cysteine residue (Scheme 1.10, A) into dehydroalanine on protein surfaces (Scheme 1.10, B).[20] The α,β-unsaturated amide can undergo a conjugate addition reaction with a thiol to provide a functionalized protein (Scheme 1.10, C). Alternatively, reaction of the dehydroalanine with allylmercaptan affords an allylsulfide group (Scheme 1.10, D), which can undergo cross metathesis with an alkene in the presence of the Hoveyda-Grubbs metathesis catalyst (**1.7**) to obtain the functionalized protein E (Scheme 1.10). Davis and colleagues find that allylsulfides are superior substrates for the cross-metathesis reaction in water compared with other modified alkenes, including vinyl and homoallylsulfides, potentially owing to the optimum sulfur coordination to the ruthenium center. The two key developments

presented in these studies are generation of the dehydroalanine group as a Michael acceptor on protein surfaces and cross-metathesis of proteins under aqueous conditions, which makes a powerful reaction in organic and polymer chemistry potentially available for the elaboration of biopolymers. The authors successfully perform cross metathesis on an allyl substrate placed on a flexible loop of the serine protease subtilisin.

Scheme 1.10 *Cross-metathesis reactions in bioconjugate chemistry*

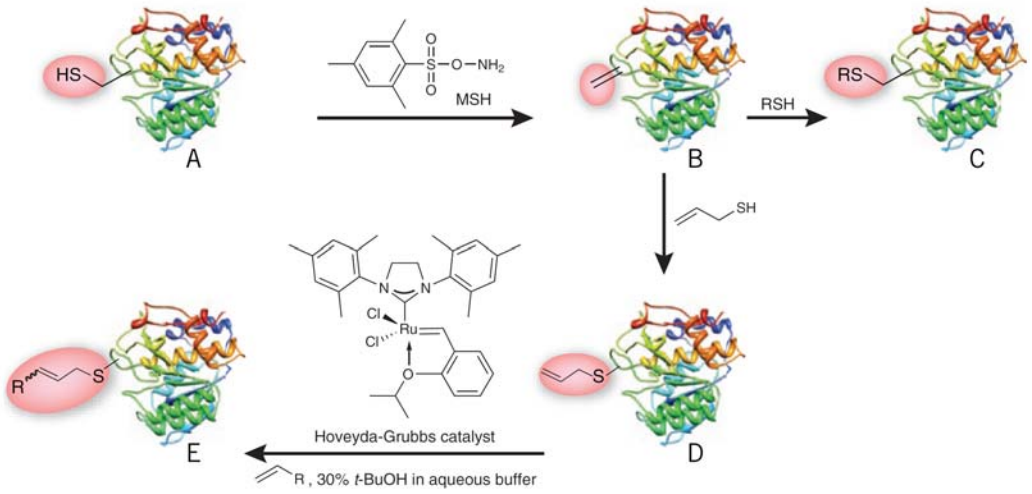

1.1.5 Applications in Total Synthesis

Although not nearly as successful as RCM in this area, CM is finding increasingly wide application in the synthesis of natural products as the chemo- and stereoselectivity of this process steadily improve. Some examples have already been noted: Verbicky and Zercher[21] have utilized a CM coupling strategy in the formal synthesis of the antifungal natural product (–)-FR-900848. Based on CM methodology initially proposed by Grubbs and coworkers[22] (i.e. selective CM by an initial self-metathesis of one olefin partner followed by CM coupling of the resulting dimer with a terminal olefin), self-metathesis of enantiopure cyclopropane **1.17a** with **1.4** (5 mol%) gave dimer **1.17b** in reasonable yield. CM coupling of **1.17b** with tetracyclopropane **1.17c** again promoted by **1.4** (5 mol%) furnished the key intermediate **1.17** (Scheme 1.11), which after selective cleavage of the benzoyl group is identical to an advanced intermediate in the synthesis of (–)-FR- 900848 by Barrett and Kasdorf.[23]

Scheme 1.11 *Formal synthesis of (–)-FR-900848*

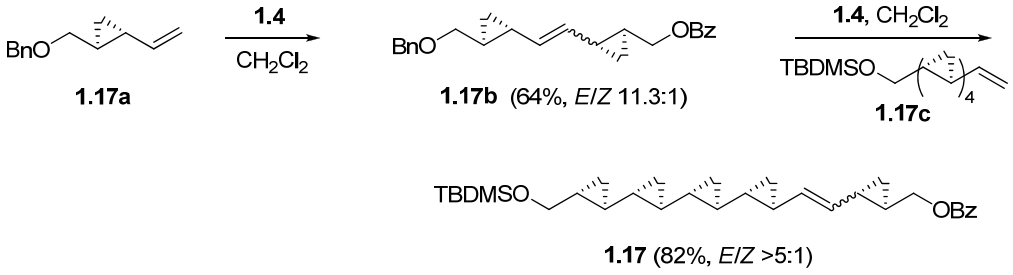

Koskinen *et al*. have applied CM to the synthesis of the cytotoxic natural product pachastrissamine (jaspine-B).[24] Coupling of the alkyl chain to the furan derivative **1.18a** was effected using Grubbs' cross-metathesis reaction. Reaction of **1.18a** with Grubbs' 2nd generation catalyst **1.5** and an excess of 1-tetradecene (**1.18b**) provided the desired alkene **1.18c** in excellent yield (87%). According to ^{1}H NMR the alkene was produced only in the *E*-configuration. Finally, hydrogenation and Boc group deprotection afforded pachastrissamine (jaspine B) **1.18** in 76% yield (Scheme 1.12).

Scheme 1.12 *CM in the synthesis of pachastrissamine (jaspine B)*

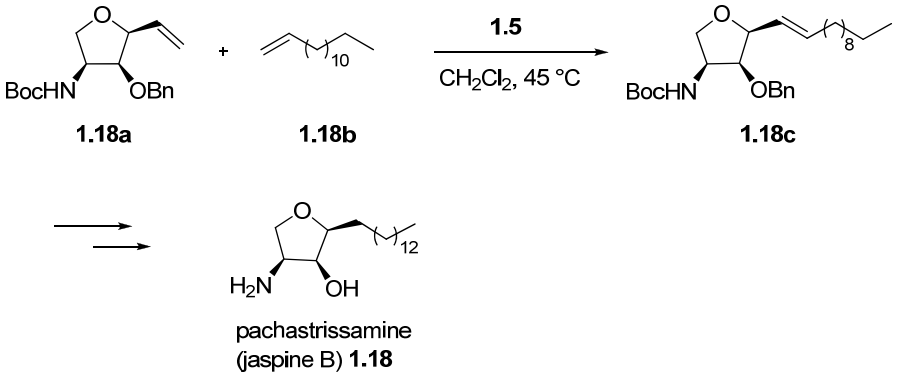

Cossy *et al*. have also applied CM to the synthesis of the piperidine alkaloid (–)-prosophylline.[25] Metathesis coupling of alkene (+)-**1.19a** with 2 equivalents of ketone **1.19b** in the presence of **1.5** (5 mol%) resulted in the formation of advanced intermediate (+)-**1.19c** in acceptable yields, which can be transformed into the natural product (–)-prosophylline (**1.19**) after a hydrogenation/deprotection sequence (Scheme 1.13).

Scheme 1.13 *CM in the synthesis of (–)-prosophylline*

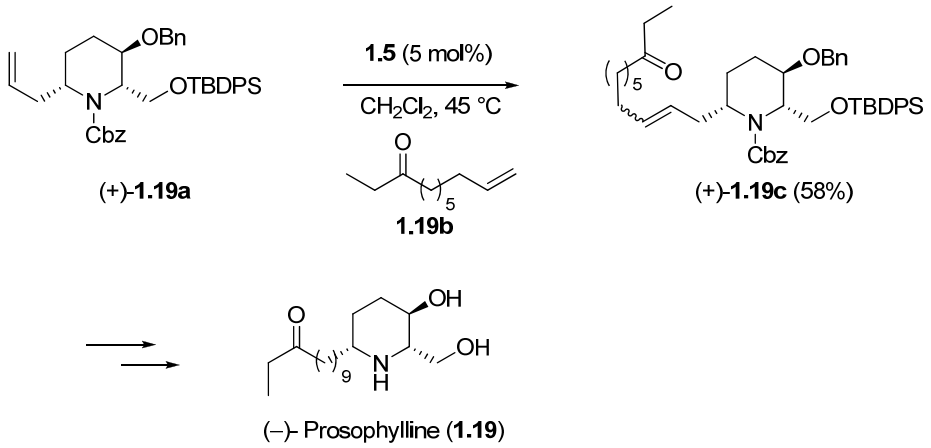

Radha Krishna *et al*. have applied CM to the synthesis of 2,6-disubstituted piperidine alkaloid, (–)-andrachcinidine.[26] In order to access the intermediate **1.20c** (Scheme 1.14) they adopted the olefin cross metathesis strategy through the coupling of fragments **1.20a** and **1.20b** using Grubbs' catalyst (**1.5**). Initially, the reaction was attempted in CH_2Cl_2 or toluene as the solvent in combination with Grubbs' 1st generation (**1.4**) or 2nd generation (**1.5**) catalysts. The best yield of **1.20c** (60%), was obtained when olefin cross metathesis was performed using **1.20a** and **1.20b** in 1:2 ratio with Grubbs' second generation catalyst in toluene along with the dimer **1.20d**. Further hydrogenation, intramolecular SN^2 cyclization and function groups manipulations led to the synthesis of natural product (–)-andrachcinidine (**1.20**).

Scheme 1.14 *CM in the synthesis of (–)-andrachcinidine*

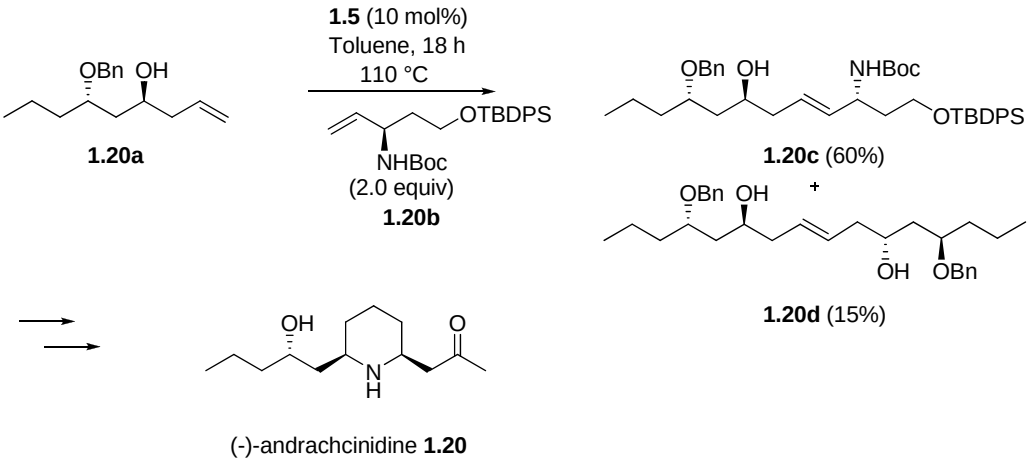

Arimoto *et al.* have applied CM to the synthesis of marine natural product containing impressive bioactivities and 6-aza-spiro[4.5]decane architectural structure of pinnaic acid.[27] Authors first examined the upper side-chain connection, with the less reactive ethyl methacrylate **1.21b** as solvent. Compound **1.21c** was obtained in 74% yield by mixing compound **1.21a** and 10 mol% Hoveyda-Grubbs second-generation catalyst **1.7** under reflux for 13 h. The trisubstituted alkene of **1.21c** was exclusively obtained in the desired *E* configuration. The homodimer of **1.21a** was also formed in the above metathesis (14% yield). When the isolated dimer **1.21d** was subjected again to the same reaction conditions, the dimer reached equilibrium with **1.21c**. TBDPS deprotection and Grieco elimination generated the terminal alkene **1.21e**. The next step was the cross-metathesis again. However, in the two precursors **1.21e** and **1.212f**, there are a total of four types of carbon-carbon double bonds which made the reaction even more challenging than the upper side-chain case. Fortunately, the two terminal double bonds proved to be more reactive, presumably for steric reasons, and led to the fully protected pinnaic acid **1.21g** as a single *E* isomer in 69% yield (based on 42% recovered starting material). Next, after successive deprotection of the two silyl protecting groups, the TFA amide, and ethyl ester by the usual method, the chiral pinnaic acid (**1.21**) was accomplished (Scheme 1.15).

Scheme 1.15 *CM in the synthesis of pinnaic acid*

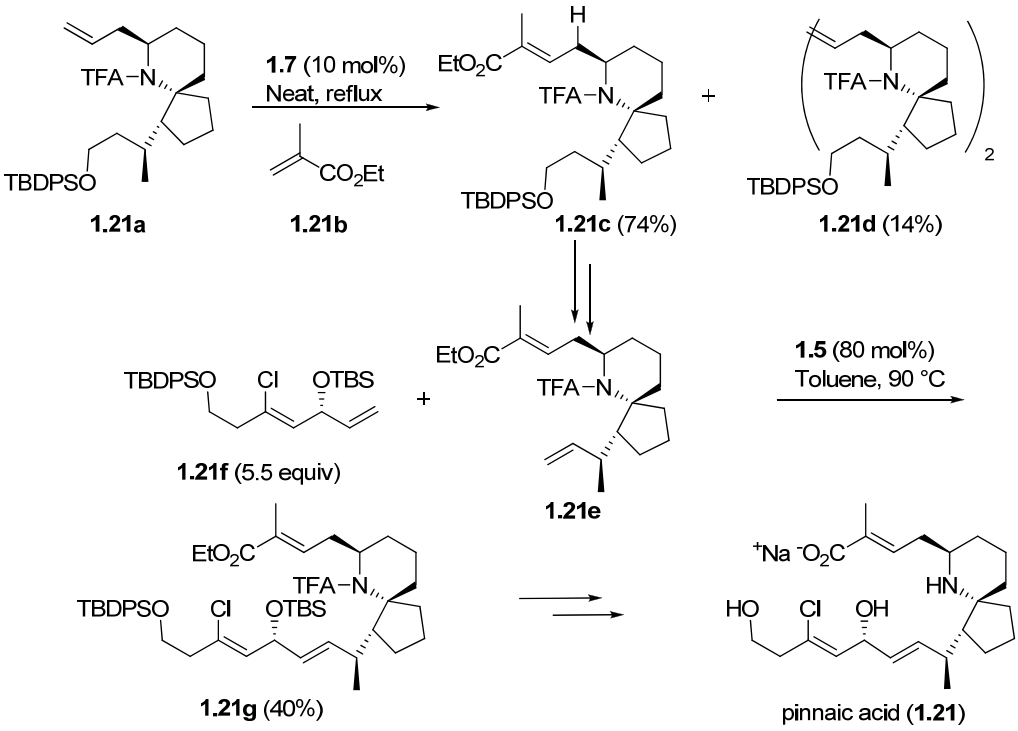

Hong *et al.* have applied an olefin cross-metathesis reaction for late installation of the thioester to the strained 16-membered depsipeptide core of macrocyclic natural product largazole.[28] With the 16-membered cyclic depsipeptide core **1.22a** and the thioester **1.22b** in hand, final olefin cross metathesis reaction of the macrocycle **1.22a** and the thioester **1.22b** was attempted under various conditions (Scheme 1.16)**.** After extensive optimization of reaction conditions, authors were delighted to find that olefin cross metathesis reaction of the macrocycle **1.22a** and the thioester **1.22b** in the presence of Grubbs' second-generation catalyst (50 mol %, toluene, reflux, 4 h) provided **1.5** in 41% (64% BRSM, (*E*)-isomer only) yield identical in all respects with authentic largazole. The olefin cross-metathesis reaction of **1.22a** and **1.22b** in toluene occurred in a higher yield than in CH_2Cl_2 or benzene. Hoveyda-Grubbs' catalyst was not as effective as Grubbs' second generation catalyst in the olefin cross metathesis reaction.

Scheme 1.16 *CM in the synthesis of largazole*

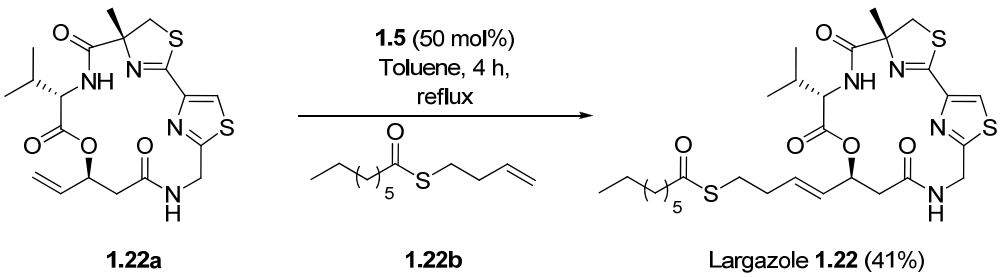

One of the inherent limitations of the CM reaction is that it can fail in cases involving strained olefins, for which ROM-CM pathways are preferable. An impressive example is the synthesis of the AB fragment of ciguatoxin by Hirama and co-workers.[29] A high catalyst loading CM reaction between seven membered ring substrate **1.23a** (itself formed by RCM) and acetate **1.23b** proceeded in poor yield and also gave a mixture of diastereomers, epimeric at the indicated carbon center **1.23** (Scheme 1.17).

Scheme 1.17 *Synthesis of AB-ring fragment of ciguatoxin by CM*

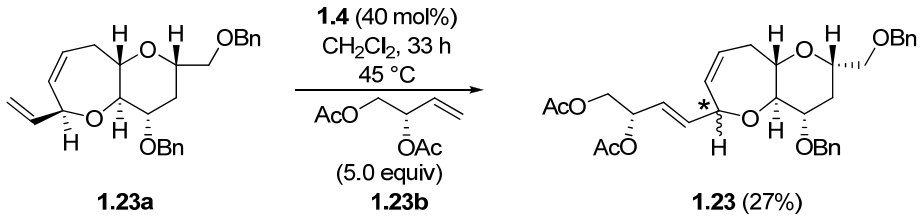

McDonald and Wei[30] reported the synthesis of the ABC tristetrahydropyran moiety common to the thyrsiferol and venustatriol natural products using a CM coupling step. Metathesis coupling of terminal olefin **1.24a** with 105 equivalents of chiral epoxide **1.24b** catalyzed by the second-generation Grubbs' catalyst **1.5** (10 mol%) gave a mixture of CM product **1.1.24** (44%), homodimer **1.24c**, and unreacted **1.24b** (Scheme 1.18). Taking advantage of the fact that both **1.24a** and **1.24c** can participate in further CM couplings, the recovered starting material and dimer were subjected to a further charge of **1.5** in the presence of additional **1.24b**, which led to another 20% yield of **1.24**.

Scheme 1.18 *Synthesis of ABC-ring fragment of thyrsiferol by CM*

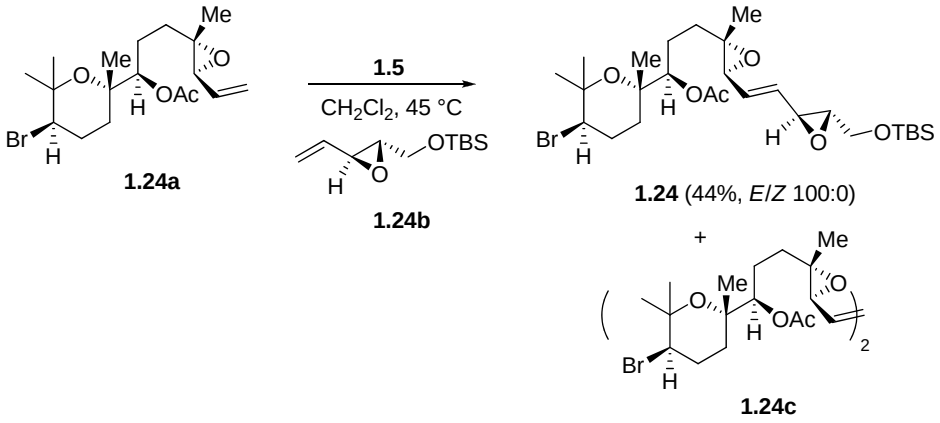

An elegant example of the coupling of two different fragments by means of alkene cross metathesis can be found in the total synthesis and structure revision of amphidinolide W (**1.25**, Scheme 1.19) by the Ghosh group.[31] The strategy adopted by the researchers for the formation of the macrocyclic ring system involved the coupling of the two advanced intermediates **1.25a** and **1.25b** through alkene cross metathesis followed by a late-stage macrolactonization. To their delight, the cross metathesis between **1.25a** and **1.25b** proceeded smoothly over the course of 15 h upon the addition of catalyst **1.5** (6 mol%) to a refluxing solution of the two components in CH_2Cl_2, affording the desired product **1.25c** in excellent yield (85%) and with good *E* selectivity (*E*/*Z* 11:1). An excess of alkene **1.25b** was required, as this substrate underwent competitive homodimerization to give compound **1.25d** (which was itself inert to secondary metathesis reactions). Furthermore, it was found that the specific employment of an acetate protecting group for the allylic secondary hydroxy group in coupling partner **1.25a** was required for optimum results. With an efficient, modular approach to compound **1.25c** now at their disposal, the

researchers were able to advance this key intermediate over a number of steps to complete the total synthesis of the revised structure **1.25** of the targeted natural product.

Scheme 1.19 *Fragment coupling through cross metathesis in the total synthesis of the revised structure of amphidinolide W* (**1.25**)

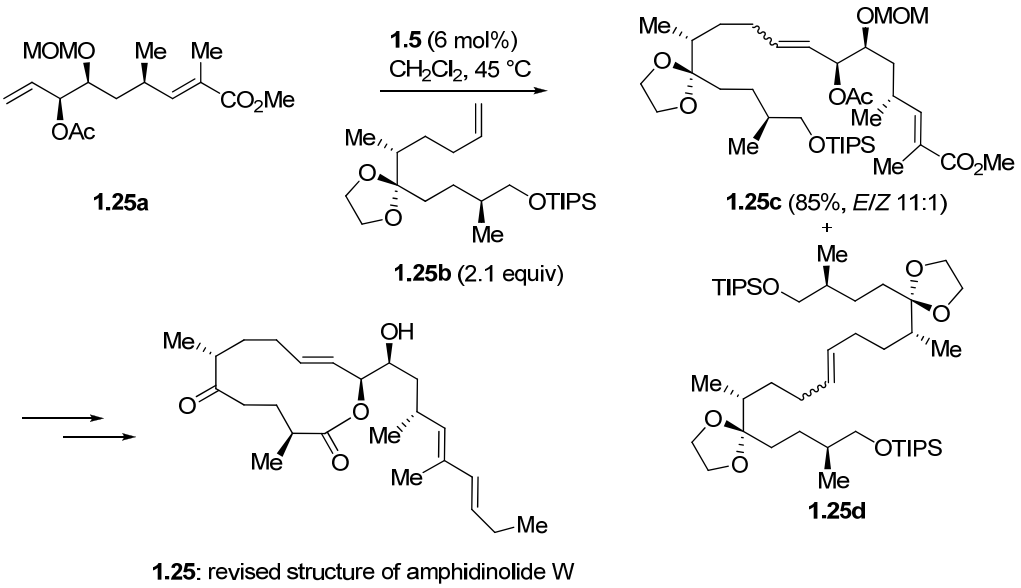

Dimerization based cross metathesis approach was employed by the Corey group in their quest to determine the correct structure of the polycyclic oxasqualenoid glabrescol.[32] The team had originally prepared compound **1.26a** (Scheme 1.20), corresponding to the structure first proposed for the natural product. However, much to their dismay, the spectroscopic data of their synthetic material did not match that reported for the natural product. The team was, therefore, faced with the task of having to synthesize a number of other possible stereoisomers, which could correspond to either the C_S or C_2-symmetric nature of the natural product, before they could clear the ambiguity regarding the actual structure of glabrescol. One of the targeted stereoisomers was compound **1.26d**, which, following their general polycyclization strategy, they hypothesized could be derived from bisepoxide **1.26c**, the symmetrical nature of which lends itself to its preparation through a dimerization protocol. Indeed, the team found that readily available epoxide **1.26b** underwent selective cross-metathesis upon treatment with initiator **1.4** (10 mol%) in CH_2Cl_2 at ambient temperature to afford the coupled product **1.26c**. Pleasingly, only the terminal alkene units participated in the metathesis event, with no interference from the more sterically hindered trisubstituted olefins. Furthermore, the

reaction was also superbly stereoselective, with the *E*-isomeric product being formed exclusively, although in this context the stereoselectivity was irrelevant as the newly formed double bond was immediately reduced in the next step. The resulting product **1.26c** was then elaborated to give the desired pentacyclic diol **1.26d**. Unfortunately, the new synthetic material the team now had in their hands still did not correspond to natural glabrescol, and it would be only after a great deal of further synthetic effort that the true structure of the natural product would be revealed as **1.26**.

Scheme 1.20 *Dimerization through cross metathesis in the total synthesis of a glabrescol diastereomer* (**1.26d**)

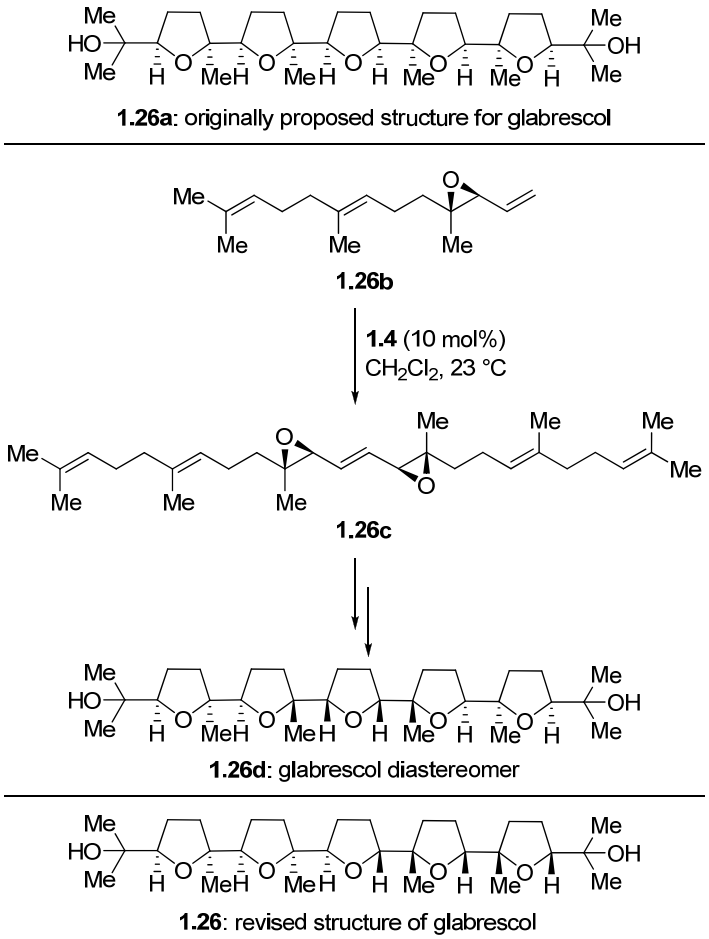

Schreiber and Diver[33] utilized CM to dimerize the immunosuppressant FK506. Treatment of the macrocycle with **1.4** (10 mol %) at room temperature furnished the corresponding dimer (FK1012) in moderate yield (Scheme 1.21). The high functional group tolerance of **1.4** allows this reaction to be carried out on the unprotected substrate,

despite the presence of several potential chelating groups in the molecule. FK1012 was found to activate signal-transduction pathways and gene transcription in mammalian cells.

Scheme 1.21 *Dimerization of FK506 by CM*

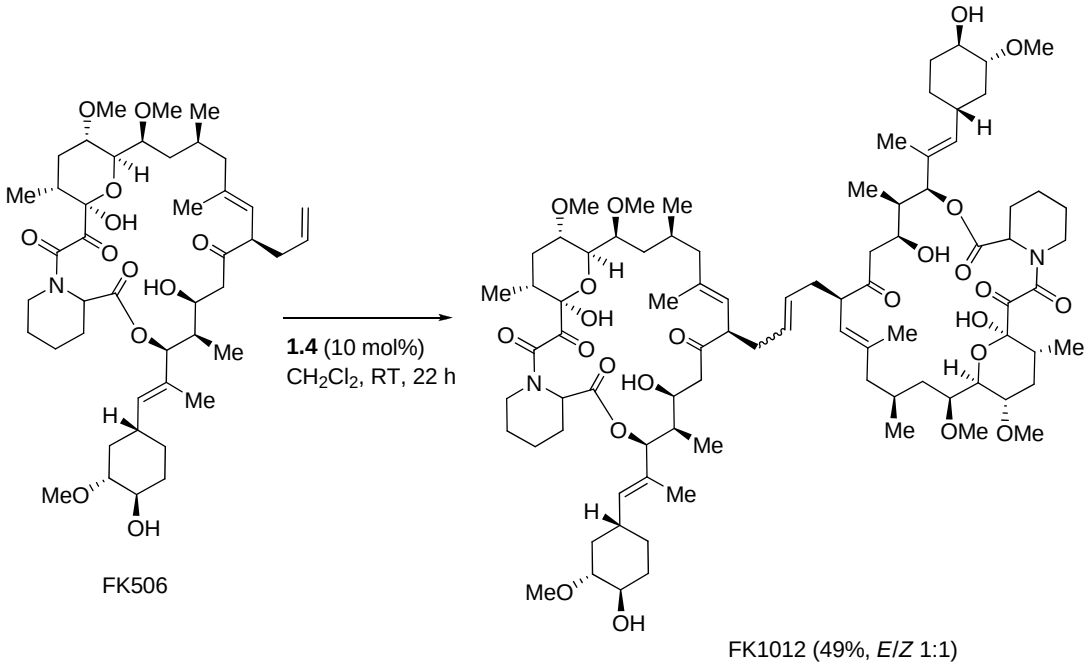

1.2 Introduction

Glycosides comprise a large class of biomolecules that include glycoproteins (antibodies, antigens), oligosaccharides (starch, chitin, and cellulose), and glycolipids (Figure 1.3). Glycoside biochemistry is a fundamental process for all living systems and the biological importance of glycosides in living systems is readily apparent from a basic understanding of molecular biology.

Figure 1.3 *The glycosidic bond and representative glycosides*

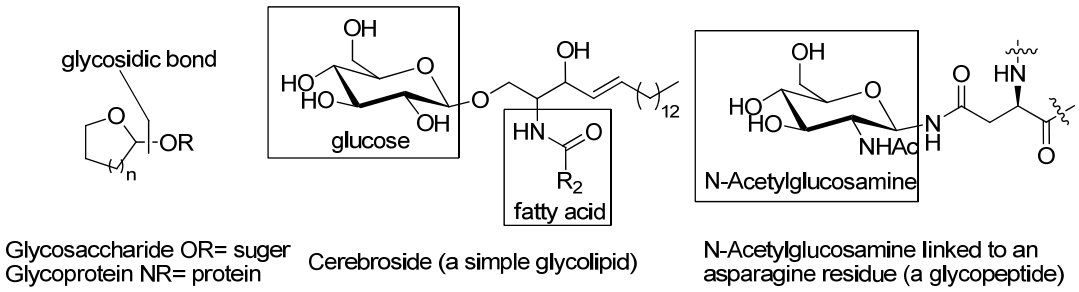

Carbohydrates play a crucial role in a variety of biochemical processes including molecular recognition, stimulation of the immune system and energy storage. Moreover, it has been shown that cell surface carbohydrates serve as points of attachment for bacteria, viruses and toxins, and as such are intrinsically involved in the genesis and spread of a number of life threatening diseases. The importance of carbohydrates as monomeric units hinges on the ability of glycosidase enzymes to cleave the glycosidic bonds in glycosides to release low molecular weight oligosaccharides and monomeric carbohydrates, a process which is of enormous significance in determining the biochemical pathways and life cycles of all organisms.

Generally, *in vivo* processing of glycosides is under rigorous enzymatic control. Without the kinetic acceleration provided by an enzyme, glycosides do not possess sufficient kinetic lability to hydrolyze on a biological time scale (Figure 1.4).

Figure 1.4 *Relative hydrolysis rates of pyranosides*

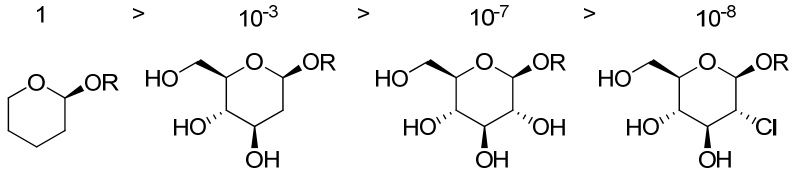

The relative kinetic stability of glycosides over simple pyranosides results from the electron withdrawing nature of the neighboring electronegative substituents which inhibit formation of the intermediate oxocarbenium ion (Scheme 1.22).[34] The class of enzymes which are responsible for the hydrolysis of glycosidic bonds in oligosaccharides and glycoconjugates are known as glycosidases, and more than 200 glycosidases have thus far been discovered.[35] To catalyze the reaction, glycosidase enzymes must stabilize the formation of the intermediate oxocarbenium ion and induce conformational changes that accelerate the rate by which hydrolysis occurs. The rate acceleration achieved by glycosidases is as much as a factor 10^{15} over the uncatalyzed reaction. The mechanism by which enzymatic glycolysis occurs is depicted below (Scheme 1.22).

Scheme 1.22 *Hydrolytic mechanism of a retaining β–glucosidase*

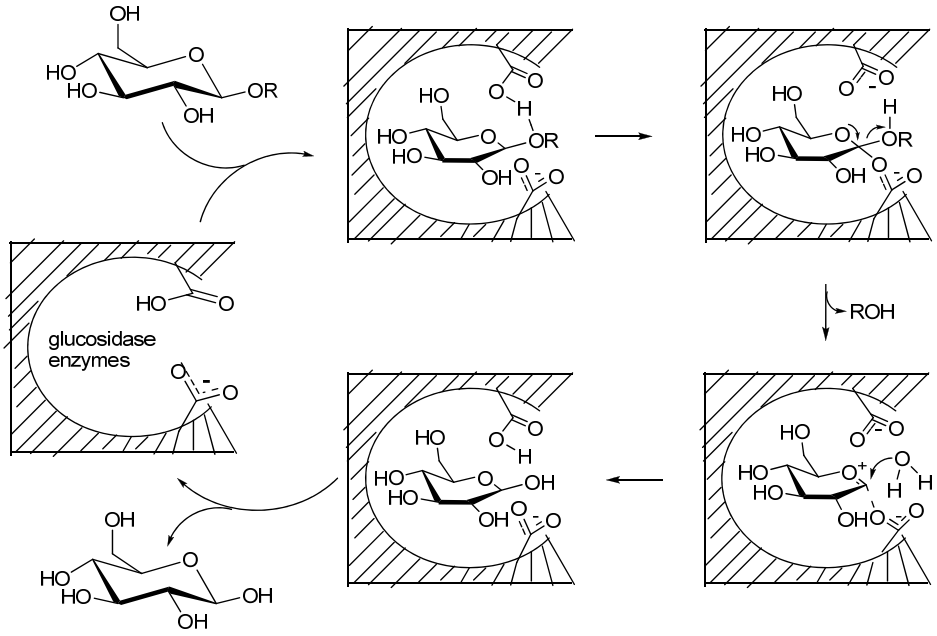

Since enzyme catalyzed carbohydrate hydrolysis is such a biologically widespread process, it is not particularly surprising that molecules which bind to glycosidases and inhibit their function, glycosidase inhibitors exhibit potent biological activity. The

resulting potential applications of glycosidase inhibitors as antiviral, antibacterial, antimetastatic, anti-diabetic or agrochemical agents have been the subject of copious research throughout the scientific community worldwide.[36]

Nojirimycin the first molecule to be recognized as a glycosidase inhibitor, was isolated in 1966 from the broth of *Streptomyces roseochromogenes*.[37] Although initially described as an antibiotic, nojirimycin was quickly established to be a potent inhibitor of α- and β-glucosidases.[38] Since then, over two hundred glycosidase inhibitors have been isolated from plants and micro-organisms (Figure 1.5).

Figure 1.5 *Several representative glycosidase inhibitor natural products*

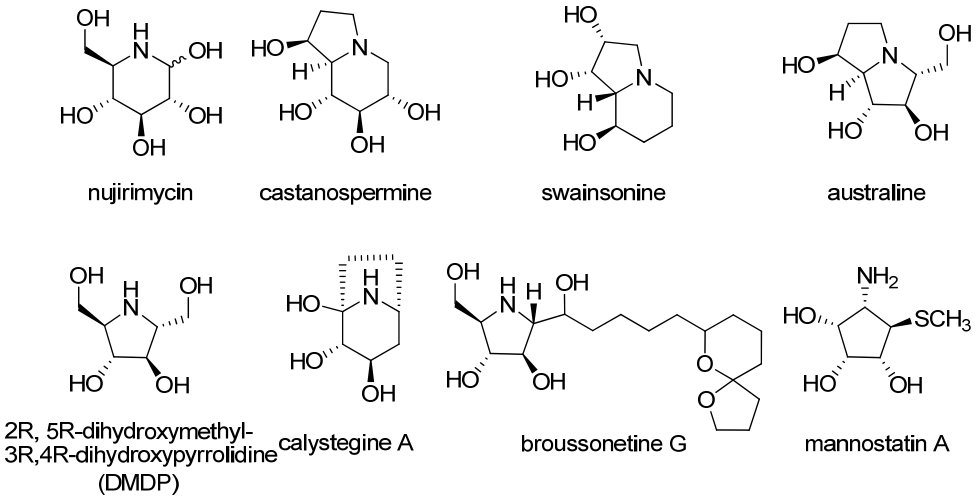

The glycosidase inhibitory properties of polyhydroxy alkaloid natural products stems from their structural resemblance to the cationic oxonium intermediate depicted above (Scheme 1.22).

Scheme 1.23 *Mechanism of glycosidase inhibition*

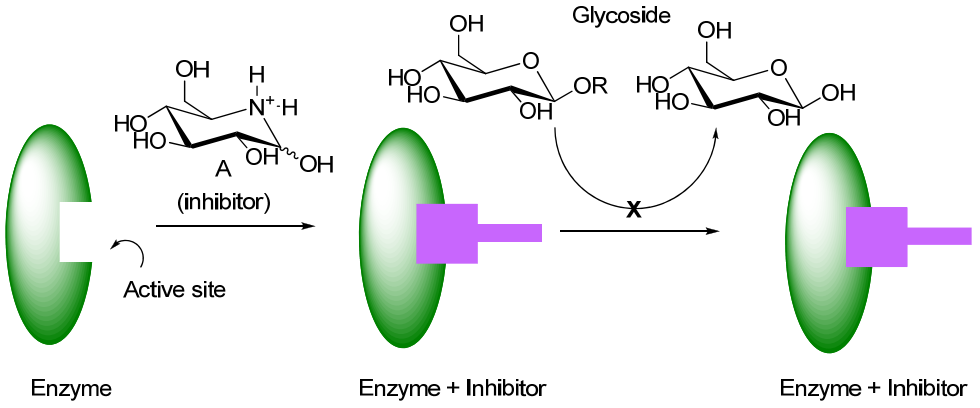

At biological pH, protonation of the amine moiety of the alkaloid occurs and results in a polyhydroxy ammonium complex A, which mimics the intermediate saccharide oxonium intermediate (Scheme 1.23). The glycoside inhibitor can thus selectively bind to the target enzyme and reduce the binding equilibrium for the particular glycoside, resulting in inhibition of the enzyme. The potential biological implications of this inhibition can be exploited to target particular therapeutic areas if the inhibition is selective for a particular cell type or biological process. The use of glycosidase inhibitors to combat various disease groups as well as insecticidal/agrochemical uses is described below.

1.2.2 Formation and Processing of Glycoproteins

Figure 1.6 *The dolichol-pyrophosphoryl oligosaccharide protein glycosylation precursor*

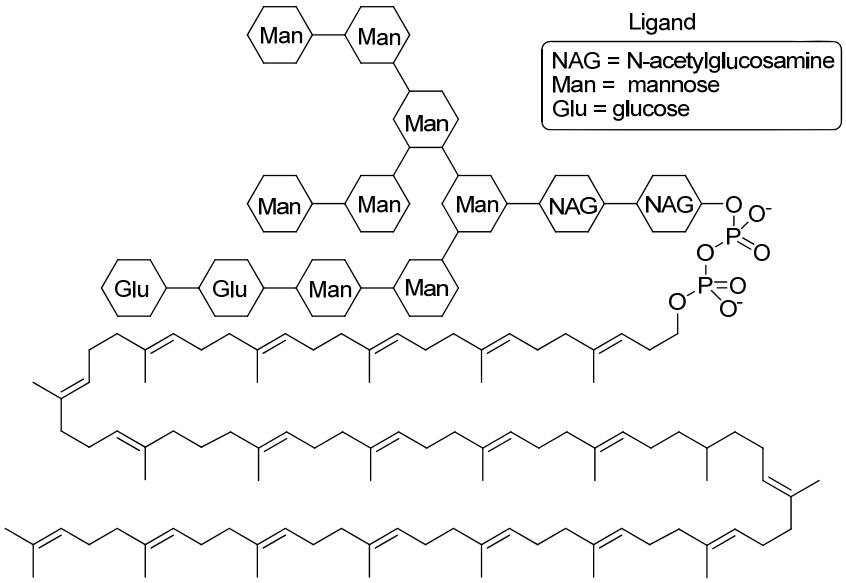

Glycoproteins can be found on cell and viral surfaces and are intimately responsible for cell-cell recognition, cell-cell adhesion, cell-virus recognition, and regulation. Since glycoproteins are so closely associated with viral infectivity and tumor metastasis, clinical therapies for many diseases have focused on the manipulation or destruction of these biomolecules. The biosynthesis of N-linked glycoproteins is performed by the cotranslational transfer of a common oligosaccharide precursor ($Glc_3Man_9GlcNAc_2$) from the dolicholpyrophosphoryl oligosaccharide protein (Figure

1.6) to the glycosylation site (Asn-X-Ser/ Thr) of newly synthesized polypeptides in the endoplasmic reticulum.[39]

Scheme 1.24 *Schematic pathway of oligosaccharide processing on glycoproteins*

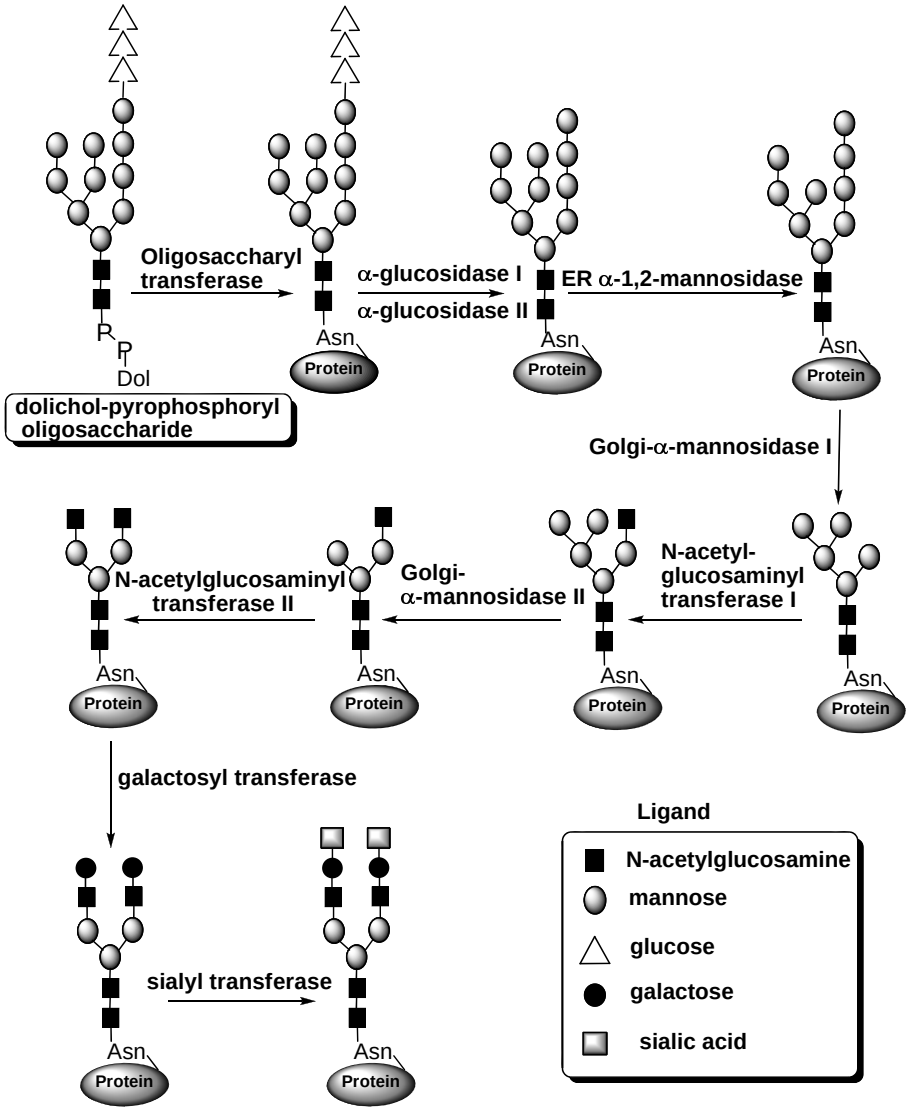

Scheme 1.24 depicts a typical pathway for glycoprotein processing. The N-glycan chain is modified by a series of enzyme catalyzed reactions within the endoplasmic reticulum and Golgi apparatus. The processes involve trimming (removal and replacement of the sugar constituents) by the action of specific processing α-glucosidases and α-mannosidases and elongation of the glycoproteins by the addition of fucose, galactose, N-acetylglucosamine and sialic acids catalyzed by glycosyl transferases and

sulfotransferases. In viruses, the viral envelope glycoproteins are often essential for viron assembly and secretion and/or infectivity; thus compounds that interfere with the glycoside and glycosylation process of viral glycoproteins can be expected to be antiviral agents.

1.2.3 Pharmacological Utilization of Glycosidase Inhibitors

1.2.3.1 Antiviral Agents

Enveloped viruses are covered in a membrane sheath derived from the host-cell that contains proteins known as envelope proteins. These envelope proteins have been shown to be central in virus assembly and entry. In many of the enveloped viruses, the envelope proteins are modified by N-linked glycosylation, and these proteins which are present on the surface of the virus have been shown to affect viral stability, antigenicity, and biological function of the virus. As such, the modification or removal of these proteins by interference with the biological cycle that produces them offers a potential therapeutic pathway.

The human immunodeficiency virus (HIV), the agent responsible for Acquired Immune Deficiency Syndrome (AIDS), contains two major envelope proteins on the viral surface, gpl20 and gp41. Glycoprotein gpl20 binds to the CD_4 antigen of T_4 lymphocytes and gp4l anchors the envelope to the viral membrane. These proteins play a crucial role in viral absorption, penetration, syncytium formation and viral propagation. Compounds which can interrupt the formation of these surface proteins offer a potential target against HIV infection. A particular pharmacological target has been the inhibition of the first two trimming steps, which utilize the α-glucosidase I and II. Disruption of the production of gpl20 and gp4l in the viral life cycle offers a potential strategy for the combat of the HIV virus.

Figure 1.7 *Anti-HIV agents*

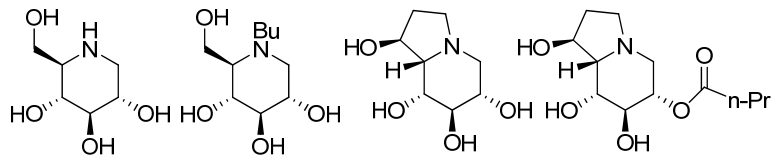

Several α-glucosidase inhibitors have been evaluated as potential anti-HIV agents (Figure 1.7).[40] These compounds are potent inhibitors towards processing α-glucosidase, and their *in vitro* antiviral activities correlate well with their inhibitory activity towards α-glucosidase I.[41] To date problems have been encountered in adapting these compounds into drug therapies for HIV patients as achieving therapeutic serum concentrations of inhibitors needed to inhibit α-glucosidase I sufficiently has proven difficult and side effects such as diarrhea have been shown to occur.[42]

1.2.3.2 Anti-diabetic Agents

Diabetes mellitus is a condition caused by disruption in the function and regulation of insulin, the hormone responsible for transport of glucose into cells. As a result of this insulin malfunction, a large quantity of glucose, the main source of cellular energy and growth, passes through the body unutilized. In the United States alone, 18.2 million people (or about 6.2%) of the population have been diagnosed with Type I (510% of cases) or Type II (90–95% of cases) diabetes.[43] In Type I diabetes, the body does not produce insulin; in Type II diabetes, the body produces insulin, but does not use it effectively. As management of blood glucose levels is critical, one strategy for treatment of Type II noninsulin dependent diabetes (NIDD) has been to delay the digestion of ingested carbohydrates by inhibition of glycosidases, thereby lowering blood glucose levels.

Figure 1.8 *Anti-diabetic agents*

Nojirimycin, the first glucose analogue recognized as a glucosidase inhibitor, was one 0f the first molecules to investigated a s an anti-diabetic agent. (Figure 1.8) The molecule shows potent α- and β-glucosidase inhibitory activity, but the molecule is unsuitable for drug therapies because of the instability of the compound resulting from the labile C-1 hydroxyl group. Therefore 1-deoxynojirimycin (DNJ) was investigated as an anti-diabetic.[44] Although DNJ showed potent *in vitro* α-glucosidase activity, its *in vivo*

activity was only average. After screening 0f many derivatives 0f DNJ, miglitol (G1yset®, Bayer) was selected for its potent *in vitro* and *in vivo* α-glucosidase activity and was granted FDA approval in 1999.

1.2.3.3 Anti-cancer Agents

The presence of oligosaccharides on the surface of tumor cells plays an important role in tumor growth and metastasis. The ability of iminosugars to inhibit glycosylation or the processing of asparagine linked oligosaccharides, offers a potential target for iminosugar derived cancer therapies. Swainsonine has perhaps achieved the most attention as an anti-tumor agent and immune system stimulant (Figure 1.9). Although the academic literature contains a multitude of descriptions of swainsonine as a potential anti-cancer drug, it has not been approved for biomedical use due to its variable and nonspecific biological activity. This has inspired copious research involved with synthetic preparation and biological assays of structural analogs of swainsonine. In addition to swainsonine, castanospermine has also been investigated as an anti-cancer compound. Although swainsonine and castanospermine have received the most attention as anticancer agents, any highly active glycosidase inhibitor can be a potential anti-tumor agent if specific biological activity against cancer cells can be attained.

Figure 1.9 *Anti-cancer agents*

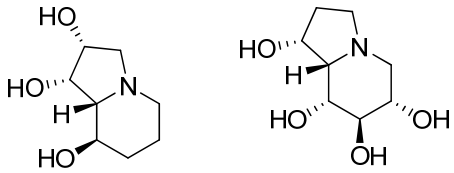

Swainsonine castanospermine

1.2.4.1 Broussonetines

The broussonetines are a class of polyhydroxylated alkaloids which have been isolated from the branches of the deciduous tree *Broussontia kazinoki*. Untill recently, about 29 unique compounds belonging to this family of natural products have isolated and characterized.[49] These compounds show striking glycosidase inhibitory properties, and as such have enormous therapeutic potential as anti-tumor and anti-HIV agents.[50] The members of the broussonetine family all share a polyhydroxylated pyrrolidine core and a

13 carbon side chain containing diverse functional groups. The structures of the broussonetine family are depicted below (Figure 1.10 and Figure 1.11).

Figure 1.10 *Broussonetines A-O*

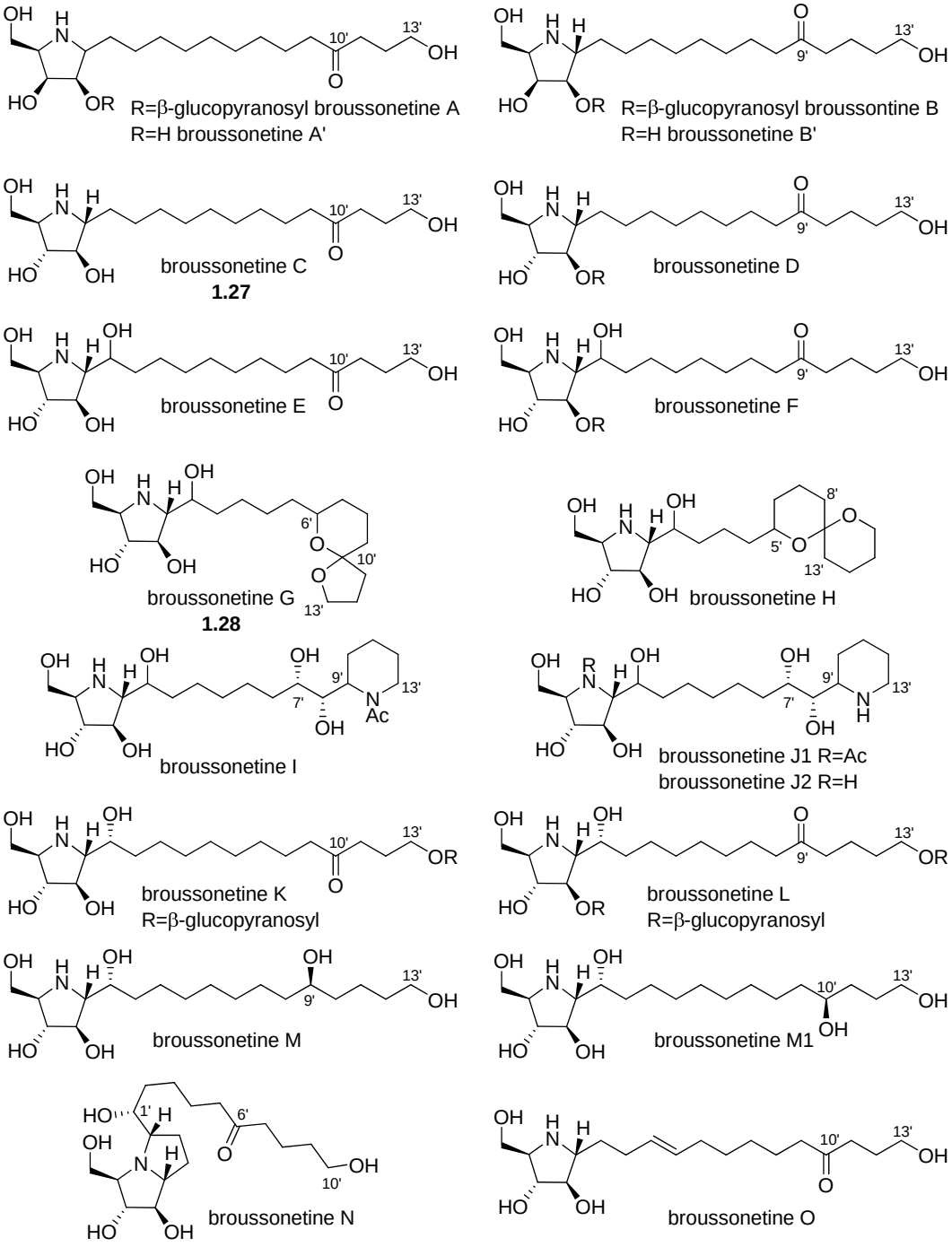

Figure 1.11 *Broussonetines P-X*

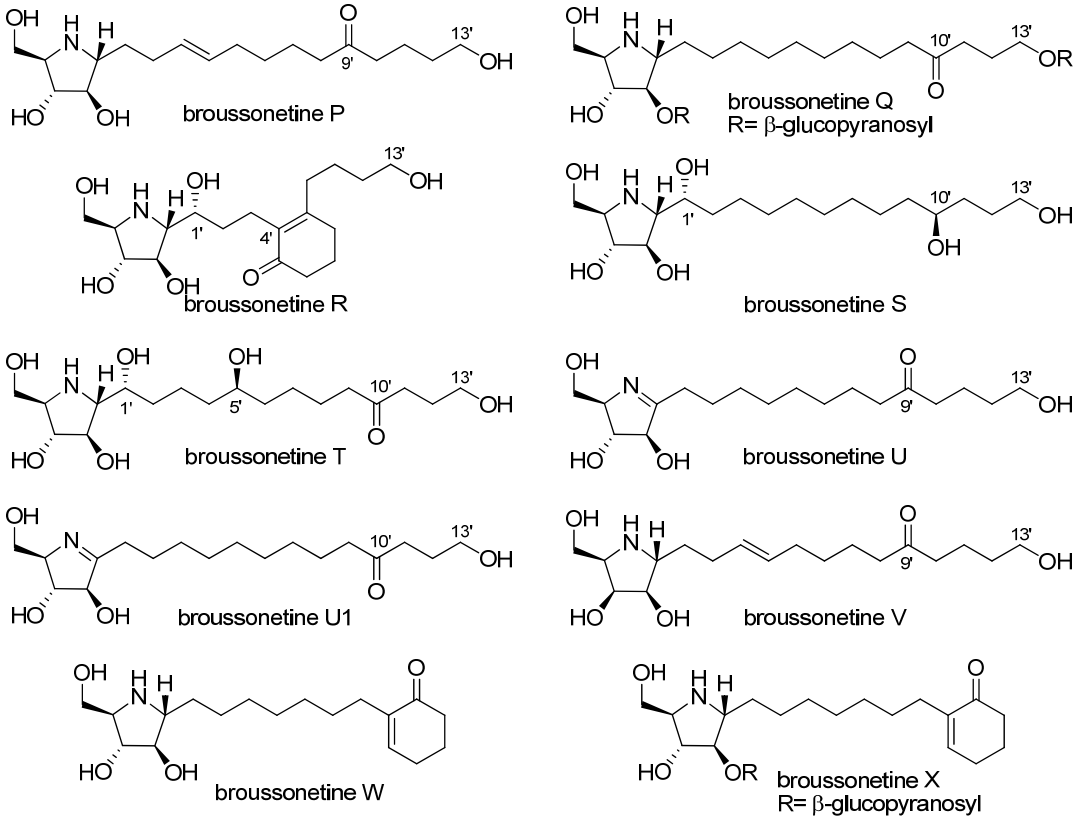

Despite the interesting structural features and biological activity of these compounds, only two members of this family of natural products have been synthesized so far. The total synthesis of broussonetine C has been reported by Yoda and coworkers in 1999 followed by Perlmutters' synthesis in 1997. The other member of this family which has been synthesized is broussonetine G by Trosts' group in 2003.

Yodas' group chiral pool based synthesis of broussonetine C (Scheme 1.25).[51] Imide **1.29a** was derived from D-tartaric acid in five steps, and is desymmetrized by first alkylating with undecenylmagnesium bromide, followed by Lewis acid promoted deoxygenation of a α-hydroxylactam intermediate giving exclusively the trans product, **1.29b**. Further functional group manipulations yield the natural product **1.27** (which was characterized as the triacetate derivative **1.29g**) in 10% overall yield from D-tartaric acid, and with the longest linear sequence of 26 steps.

Scheme 1.25 *Yoda's synthesis of* (+)*-broussonetine C*

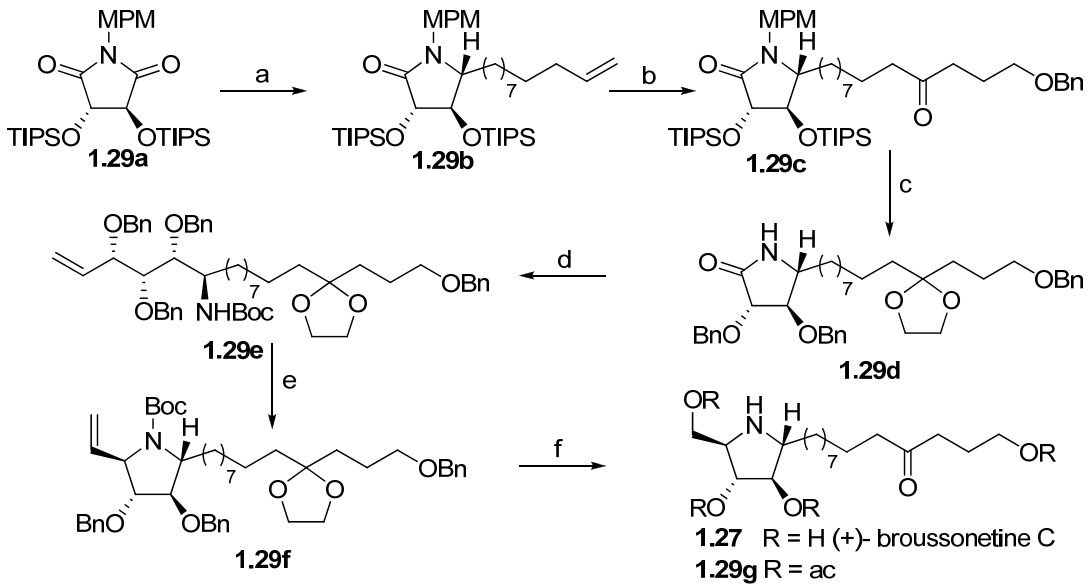

Conditions: (a) (i) undecenylmagnesium bromide, THF, rt; (ii) Et_3SiH, $BF_3.OEt_2$, CH_2Cl_2, –78 to –50 °C, 83% over 2 steps. (b) (i) OSO_4, NMO, acetone/H_2O, 99%; (ii) $NaIO_4$, Et_2O/H_2O, 99%; (iii) 3-benzyloxypropylmagnesium bromide, THF, 0 °C, 85% over 2 steps; (iv) PCC, CH_2Cl_2, 4 Å M.S., 90%. (c) (i) TBAF, THF, 92%; (ii) BnBr, Ag_2O, EtOAc, 100%; (iii) CAN, CH_3CN, 70%; (iv) ethylene glycol, *p*-TsOH, benzene, reflux, 96%. (d) (i) Boc_2O, NEt_3, DMAP, CH_2Cl_2, 100%; (ii) vinylmagnesium bromide, THF, –78 °C; (iii) $NaBH_4$, $CeCl_3$, MeOH, –45 °C, 78% over 2 steps. (e) (i) MsCl, NEt_3, CH_2Cl_2; (ii) ^{t}BuOK, THF, 92%; (f) (i) OSO_4, NMO, acetone/H_2O, 100%; (ii) $NaIO_4$, Et_2O/H_2O; (iii) $NaBH_4$, MeOH, 92% (iv) Pd, HCO_2H, MeOH, 83%; (v) HCl, EtOAc; (vi) Ac_2O, pyridine, DMAP, 67% over 2 steps.

Scheme 1.26 *Perlmutter's synthesis of* (+)*-broussonetine C*

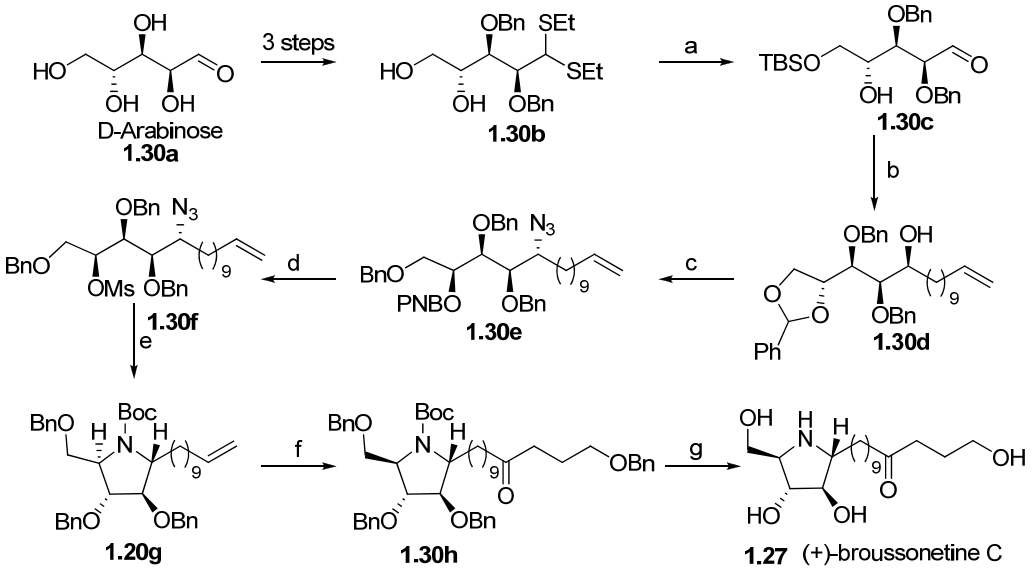

Conditions: (a) (i) TBSCI, imidazole, DMF, 87%; (ii) HgO, $HgCl_2$, acetone/H_2O, 60 °C. (b) (i) undecenylmagnesium bromide, THF, 80% over 2 steps, <95:5 dr; (ii) HCI, MeOH, 0 °C, 86%; (iii) benzaldehyde dimethyl acetal, *p*-TsOH, CH_2Cl_2, –20 °C to rt, 70%. (c) (i) MsCl, NEt_3, CH_2Cl_2, 0 °C to rt; (ii) NaN_3, DMF, 60 °C, 80% over 2 steps; (iii) $AlCl_3$, $BH_3.NMe_3$, THF, 0 °C to rt, 89%; (iv) DEAD, PPh_3, *p*-nitrobenzoic acid, THF, 88%. (d) (i) PPh_3:H_2O (1:1), THF, 60 °C, 85%; (ii) NaOH, MeOH, 76%; (iii) Boc_2O, NEt_3, THF, 80%; (iv) MsCl, NEt_3, CH_2Cl_2, 0 °C to rt. (e) K^{t}OBu, THF, 93% over 2 steps. (f) (i) $K_2OsO_4.2H_2O$, NMO, acetone:H_2O, rt; (ii) $NaIO_4$, Et_2O/H_2O, 88% over 2 steps; (ii) benzyloxypropylmagnesium bromide, THF, 0 °C to rt, 70%; (iv) Dess-Martin periodinane, CH_2Cl_2, 0 °C, 90%. (g) Pd/C, H_2 (1 atrn), EtOH, 70%; (ii) TFA, CH_2Cl_2, 0 °C, 60%.

A carbohydrate based synthesis of broussonetine C was also recently reported by Perlmutter and Vounatsos.[52] The synthesis starts with D-arabinose, which is transformed by standard methods over three steps into dithioacetal (Scheme 1.26). Diastereoselective Grignard addition with undecenylmagnesium bromide affords the *syn* alcohol diastereomer **1.30d** with >95:5 dr. Addition of azide under Mitsunobu conditions followed by subsequent functional group interconversion and mesylation of the C_2 hydroxyl group affords intermediate **1.30f**. The product is cyc1ized with ^{t}BuOK to provide the requisite pyrrolidine **1.30g** with the correct stereochemical configuration. Installation of the sidechain functionality by a method analogous to that of Yoda et. al provides the natural product in 19 steps from D-arabinose.

A paper from the Brimble group describes an approach towards a total synthesis of broussonetine H.[53] Thus far they have completed a 15 step synthesis of the spiroketal containing side chain **1.31** from L-glutamic acid and have not yet reported the synthesis of the core or the coupling of the two halves of the molecule. (Scheme 1.27)

Scheme 1.27 *Brimble's synthesis of the spiroketal fragment of* (+)*-broussonetine H*

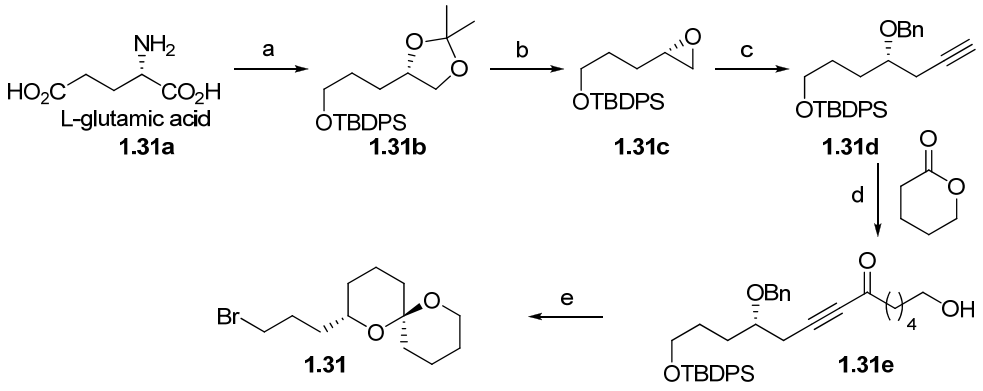

Conditions: (a) (i) $NaNO_2$, HCl, H_2O, 0 °C, 54%; (ii) $LiAlH_4$, THF, reflux, 47%; (iii) *p*-TsOH, acetone, 85%; (iv) TBDPSCI, imidazole, CH_2Cl_2, 87%, (b) (i) PPTS, MeOH, 72%; (ii) TsCl, DMAP, NEt_3, CH_2Cl_2, 95%; (iii) NaH, 18-crown-6, THF, 86%. (c) (i) trimethylsilylacetylene, *n*-BuLi, $BF_3.OEt_2$, THF, –78 °C; (ii) NaOMe, MeOH, 94% over 2

steps; (iii) NaH, BnBr, TBAI, DMF, 88%. (d) *n*-BuLi, $BF_3.OEt_2$, THF, –78 °C, 86%. (e) (i) H_2, Pd/C, EtOAc, 86%; (ii) TBAF, THF, 96%; (iii) MsCI, DMAP, pyridine, 78%; (iv) LiBr, acetone, reflux, 85%.

A recent paper from Trost's group describes the first total synthesis of (+)-broussonetine G.[54] Authors utilized palladium-catalyzed dynamic kinetic asymmetric transformation (DYKAT) as a key reaction, for constructing the chiral core subunit of (+)-broussonetine G. The synthesis began with the addition of nitrogen nucleophile phthalimide to butadiene monoxide to give **1.32b** in a highly regio- and enantioselective fashion (94% yield, 98%ee) (Scheme 1.28). After deprotection of the diimide to give a vinylglycinol, formation of the cyclic carbamate with triphosgene gave vinyloxazolidinone **1.32c.** Best results for the second palladium catalyzed DYKAT reaction were obtained with ligand **1.32f**, which gave the desired product **1.32d** in 91% yield with excellent diastereoselectivity (d.r. 93:7). After benzyl protection, RCM with Grubbs' catalyst **1.5**, functional group transformation they obtained the chiral core subunit **1.32e** of (+)-broussonetine G.

Scheme 1.28 *Synthesis of the chiral core subunit of* (+)*-broussonetine G*

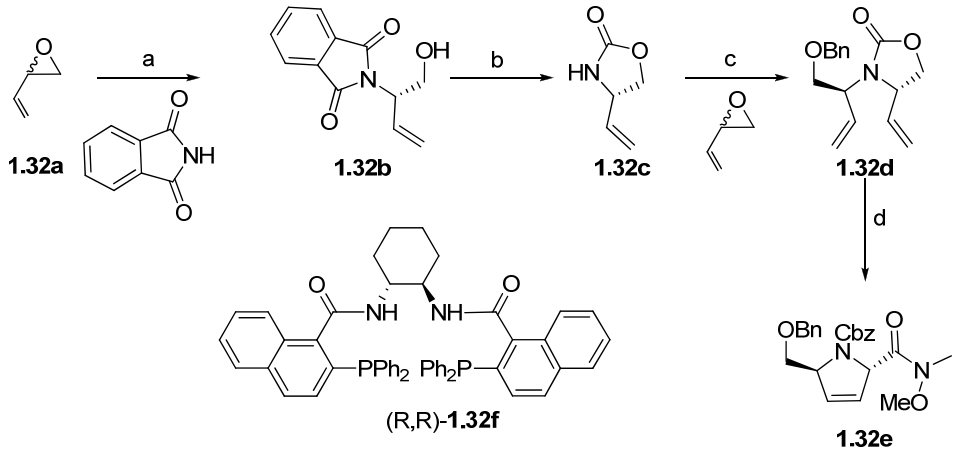

Conditions: (a) [{$(C_3H_5)PdCl\}_2$] (0.4 mol%), (R,R)-**1.32f** (1.2 mol%), Na_2CO_3, CH_2Cl_2, rt, 94%, 98% ee; (b) (i) ethylenediamine, EtOH, reflux, 84%; (ii) triphosgene, $NaHCO_3$, toluene/H_2O, 0 °C, 85%; (c) (i) $[Pd_2(dba)_3]\cdot CHCl_3$ (0.25 mol%), (R,R)-**1.32f** (0.75 mol%), DBU(1 mol%), CH_2Cl_2, rt, 91%, 93:7 d.r.; (ii) NaH; BnBr, TBAI, THF, rt, 84%; (d) (i) **1.5** (1.2 mol%), CH_2Cl_2, reflux, 87%; (ii) NaOH, EtOH/H_2O (3:1), reflux; (iii) BnOCOCl, $NaHCO_3$, Na_2CO_3, H_2O, 0 °C–rt, 99%; (iv) TEMPO, KBr, NaOCl, $NaHCO_3$, acetone/H_2O, 0 °C, 89%; (v) HNMe-(OMe)·HCl, pybop, iPr_2NEt, CH_2Cl_2, 81%.

The synthesis of the side chain began with the addition of 1-pentyne to δ-valerolactone, followed by protection of the primary alcohol with trityl chloride to give alkynone **1.32h** (Scheme 1.29). Reduction of **1.32h** by using Noyori's enantioselective

transfer hydrogenation protocol gave propargyl alcohol **1.32i** (97% ee). The alkyne zipper reaction was performed to give the desired terminal alkyne. Protection of the secondary alcohol followed by alkylation of the terminal alkyne with ethylene oxide provided the desired homopropargyl alcohol. After acid-catalyzed global deprotection, the resulting triol **1.32j** underwent the requisite regioselective palladium-catalyzed spiroketalization reaction to give the desired 5,6-spiroketal with excellent diastereoselectivity (d.r. 97:3) due to the anomeric affect. Subsequent bromination of the primary alcohol gave bromide **1.32k**.

Scheme 1.29 *Synthesis of the spiroketal fragment of* (+)*-broussonetine G*

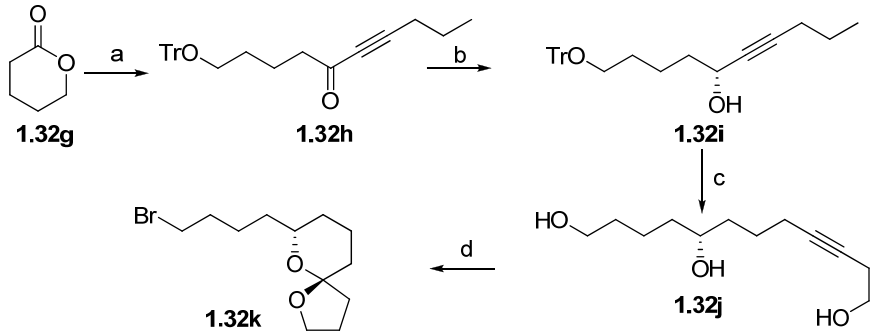

Conditions: (a) (i) *n*BuLi, 1-pentyne, THF, –78 °C-rt, 94%; (ii) TrCl, NEt_3, DMAP, DMF, rt, 77%; (b) [(η^6-*p*-cymene)Ru{(1*R*,2*R*)-*p*-TsNCH(Ph)CH(Ph)NH}] (3 mol%), *i*PrOH, rt, 95%, 97% ee; (c) (i) KH (10 equiv), 1,3-diaminopropane, THF, 79%; (ii) 3,4-dihydro-2*H*-pyran, PPTS, CH_2Cl_2, rt, 76%; (iii) *n*BuLi, $AlMe_3$, $BF_3{\cdot}OEt_2$, Et_2O, –78 °C; then ethylene oxide, –78 °C, rt, 76%; (iv) HCl/MeOH (1%), 95%; (d) (i) [$PdCl_2(PhCN)_2$] (2 mol%), CH_3CN/THF (3:2), 85%, 97:3 d.r.; (ii) PPh_3Br_2, imidazole, THF, 91%.

Scheme 1.30 *Completion of the synthesis of* (+)*-broussonetine G*

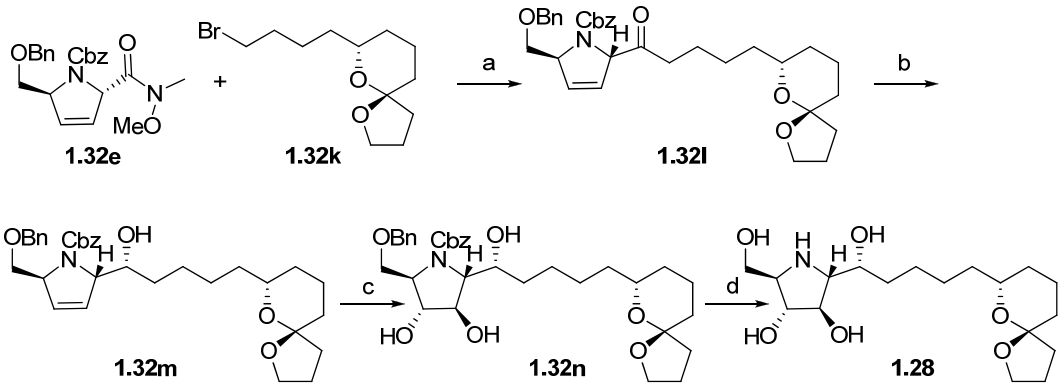

Conditions: (a) **1.32k** (1.2 equiv), Mg, THF, reflux-rt; **1.32e**, rt, 65%; (b) DIBAL-H, Et_2O, 0 °C, 76%, 4.3:1 d.r.; (c) $F_3CC(O)CH_3$, oxone, Na_2CO_3, CH_3CN/H_2O, 0 °C, 68%; (d) (i) TFA, THF/ H_2O, 65 °C, 73%; (ii) Pd/C, MeOH, HCl, H_2 (1 atm), rt, 95%;

Coupling of the two fragments via the alkyl magnesium reagent derived from alkyl bromide **1.32k** led to a ketone. Subsequent diastereoselective reduction of the ketone with DIBAL-H gave a 4.3:1 (R/S) diastereomeric mixture of secondary alcohols. Epoxidation of dihydropyrrole **1.32m** led to a mixture of epoxides, both of which gave the same triol **1.32e** as a single diastereomer upon hydrolysis with aqueous TFA. To complete the synthesis, removal of the protecting groups by hydrogenolysis gave the natural product **1.28**, (+)-broussonetine G. (Scheme 1.30)

Apart from the above four approaches, there were no reports documenting any efforts directed towards the total synthesis of this class of natural products. Considering their promising bioactivity and lack of a general approach to pure natural products, we have designed a program to construct the same in a modular way and thus form the main content of the present section.

1.3 Present Work

The broussonetines are a class of polyhydroxylated alkaloids which have been isolated from the branches of Asian paper mulberry tree *Broussontia kazinoki* and comprise a new class of glycosidase inhibitors.[49] The 29 unique broussonetines (see Figures 1.10 and 1.11) show very potent and selective glycosidase inhibitory activities and as such have enormous therapeutic potential as anti-tumor and anti-HIV agents.[50] It is particularly interesting that the variation of the 13 carbon side chain functionality plays a key role in influencing the potency and enzyme specificity of glycosidase inhibitory activity. The promising biological activities and also the availability of a range of family members, this broussonetine natural products family provides an opportunity to synthetic chemists to explore flexible synthetic methods that can address the synthesis of any of these members with an ease. To embark in this direction, by invoking cross metathesis as the key transform, we have identified two potential key retrons **1.33** and **1.34** which can be advanced to either broussonetines A–D and broussonetines E–M respectively, by selecting an appropriate C_{12} or C_9 unit. In the following pages, we describe our efforts in this direction by taking the broussonetines C and G as the representatives from each type. (Figure 1.12)

Figure 1.12 *Cross metathesis strategy for broussonetines*

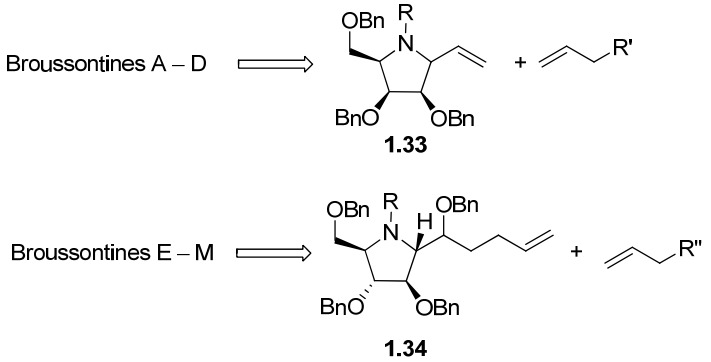

Considering the superior glycosidase inhibitory activities amongst the all other members of this family, broussonetine G (**1.28**, IC_{50}=3 nm, β-galactosidase; 24 nm, β-glucosidase, 760 nm, β-mannosidase) has been selected as the first target in our studies. Broussonetine G contains a structurally interesting 5,6-spiroketal at the end of alkane chain. Broussonetine C (**1.27**, IC_{50}=36 nm, β-galactosidase; 320 nm, β-mannosidase)

selected as the representative of the first type broussonetines, has a 13 carbon side chain with a carbonyl group at C (10'). (Figure 1.13)

Figure 1.13 (+)-*broussonetine G &* (+)-*broussonetine C*

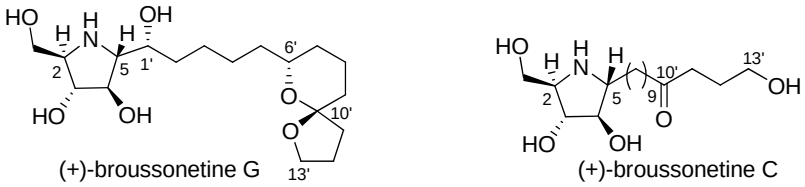

Isolated from Asian Mulberry Tree *Broussontia kazinoki,* Potential Anti-tumor,AIDS theraputic. Inhibitory Activity:

Enzyme	IC_{50} (μm) for **1.28**	IC_{50} (μm) for **1.27**	DNJ[a]
α-glucosidase	NI	NI	0.93
β-glucosidase	0.024	NI	0.58
β-galactosidase	0.003	0.036	NI
α-mannosidase	NI	NI	NI
β-mannosidase	0.76	0.32	NI

[a]DNJ: deoxynojirimycin; NI: upto 100μm or no inhibition

Despite their promising biological activities, there is only a single report (from Trost's group) on the synthesis of broussonetine G and a couple of reports for the synthesis of broussonetine C (Yoda and Perlmutter groups).[51,52] A detailed retrosynthetic planning for broussonetines G and C is given in the scheme 1.31.

Scheme 1.31 *Retrosythesis for broussonetine G & C*

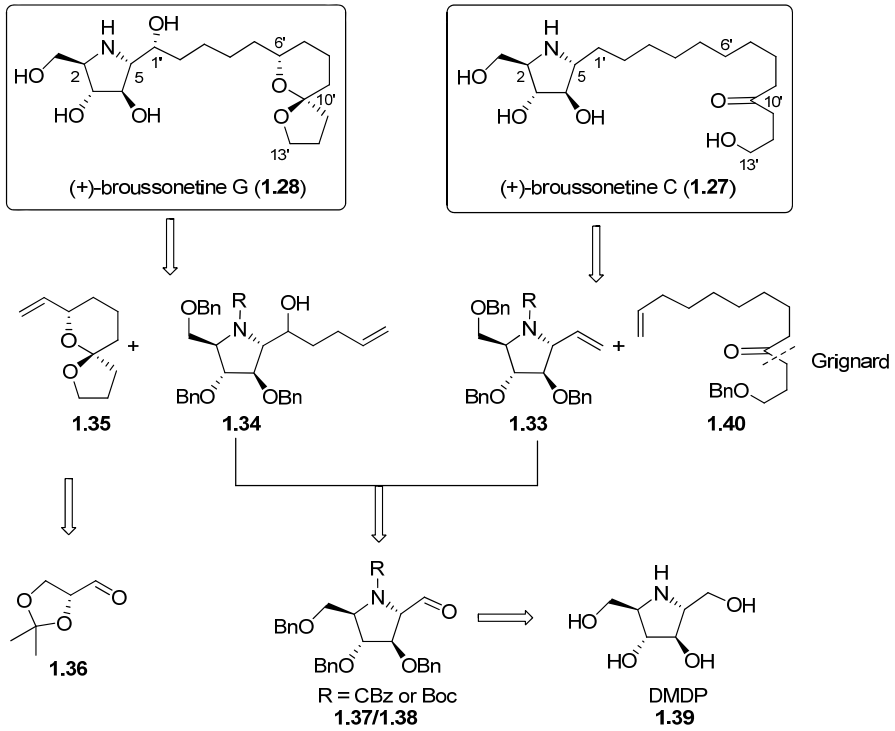

1.3 Cross metathesis approach for the synthesis of (+)-broussonetine G

1.3.1 Synthesis of the pyrrolidine subunit of (+)-broussonetine G

One of the advanced intermediate we identified for the synthesis either of the pyrrolidine coupling partners is DMDP (**1.39**). By virtue of being a natural product, several reports for the synthesis of the DMDP are documented and is available commercially. However, considering the cost limitations, we have followed one of the available protocol for its synthesis that starts with the easily available L-sorbose. The reported procedure involves about 7 steps and 7 operations. However, when performed on large scales, we have opted either for the purification by crystallization or advancing the crude intermediate for the next reaction without any further purification. The details of our preparation of DMDP will be described in the following paragraphs.

As shown in scheme 1.32, the synthetic sequence started with the commercially available L-sorbose (**1.41**), which was advanced to the known 5-*O*-tosly derivative **1.44** according to the reported procedure.[55]

Scheme 1.32 *Synthesis of 5-O-tosly derivative **1.44** from L-sorbose*

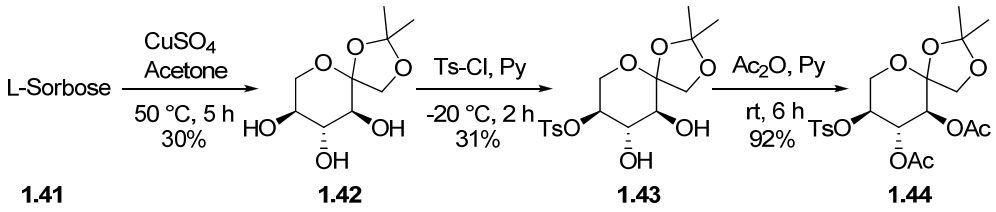

L-sorbose was subjected for the acetonide protection using anhydrous copper sulphate and dry acetone to prepare the 1,2-*O*-isopropylidine-L-sorbopyranose (**1.42**) in 30% isolated yield (after crystallization) along with the L-sorbofuranose 1,2:5,6-diacetaonide (27%). The less hindered equatorial hydroxy at C-5 was readily tosylated with an equimolar amount of tosyl chloride at 0 °C to produce the 5-*O*-tosly derivative (**1.43**) in 31% yield. It was acylated by acetic anhydride and pyridine to procure the 3,4-di-*O*-acetly-1,2-*O*-isopropylidine-5-*O*-tosyl-α-L-sorbose (**1.44**). The spectral data of compound **1.44** were in good agreement with the reported data.

Subsequently, tosylate **1.44** was subjected for the azide displacement using lithium azide (in DMSO at 100 °C for 3 h) to obtain the C-5 azide **1.45** with invertion (Scheme 1.33). IR spectra showed the characteristic N=N=N strech at 2107 $\tilde{\nu}$.

Deacetylation of **1.45** with K_2CO_3/MeOH gave the diol **1.46**, which was directly used for the acetonide deprotection by employing acidic ion-exchange resin Amberlyst IR-120 to prepared 5-azido-5-deoxy-D-fructose (**1.47**) as a crystalline solid.[56] Finally, the catalytic hydrogenation of azide **1.47** over 10% Pd/C (EtOH) gave a quantitative yield of pyrrolidine **1.39** without any trace of C-2 epimer. In the ^{13}C NMR spectrum of **1.39**, only three carbon resonances at δ 62.1 (d), 62.2 (d) and 78.1 (t) ppm, establishing the C_2 symmetry present in the DMDP.

Scheme 1.33 *Synthesis of DMDP **1.39***

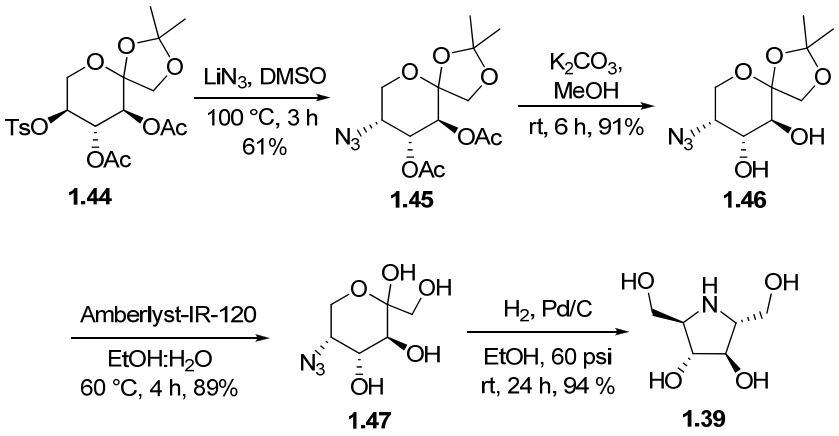

Scheme 1.34 *Synthesis of protected DMDP **1.51***

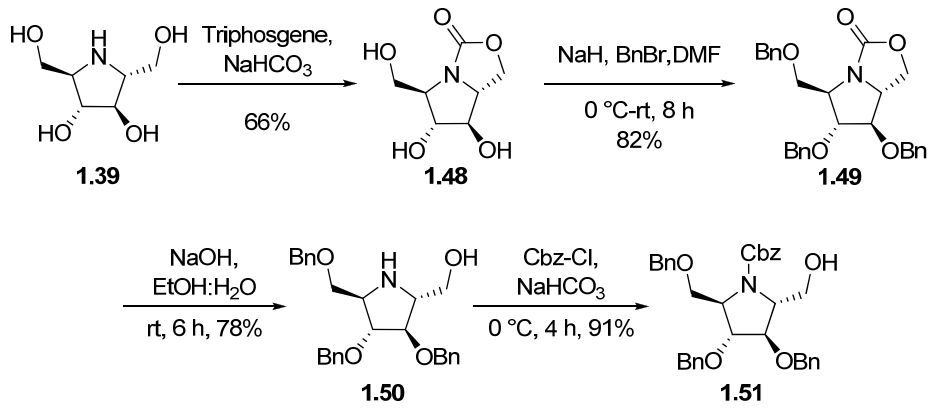

Thus synthesized DMDP (**1.39**) was treated with the triphosgene under biphasic conditions to afford the oxazolidinone **1.48**. The remaining free hydroxyl groups were protected as their benzyl ethers to prepare the fully protected DMDP derivative **1.49**. The ^{13}C NMR spectrum showed the carbamate functionality at δ 160.2 and benzyl CH_2 at

δ 71.3, 71.9, and 72.7 ppm. Further IR spectra show characteristic 1759 $\tilde{\nu}$. Rest of the analytical data was in full agreement with the assigned structure.

The cyclic carbamate functionality of the oxazolidinone **1.49** was deprotected by base-mediated hydrolysis to prepare the aminol (**1.50**). The ring nitrogen was protected as its benzyl carbamate **1.51** by treatment with CbzCl in the presence of potassium carbonate (Scheme 1.34). The C=O strech at 1701 $\tilde{\nu}$ confirmed the presence of Cbz group. The doubling of the many of the signals in ^{1}H as well as in ^{13}C NMR spectra was indicative of rotamers in solution due to the restricted rotation around the carbonyl group of the carbmate. Analytical data was in full agreement with the assigned structure.

Scheme 1.35 *Synthesis of aldehyde **1.37***

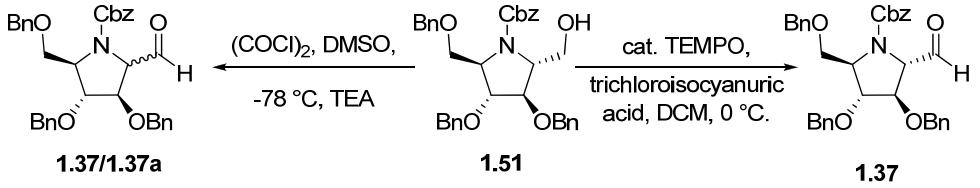

The primary alcohol at C-1 was oxidized under Swern conditions. However, due recemisation at C(2) under these conditions a mixture of epimers **1.37/1.37a** were obtained (Scheme 1.35). The ^{1}H NMR spectrum of **1.37** revealed the aldehyde proton resonated as two doublets at δ 9.34 and 9.44 whereas in **1.37a** it resonates at δ 9.41 and 9.47. After exploring a couple of oxidants under neutral conditions, finally the oxidation of **1.51** could be conducted successfully without any racemization by employing catalytic TEMPO radical and trichloroisocyanuric acid as a reoxidant in CH_2Cl_2 at 0 °C. The resulting aldehyde was subjected for the chain elongation without any further purification.

Scheme 1.36 *Synthesis of the chiral core subunit of* (+)*-broussonetine G*

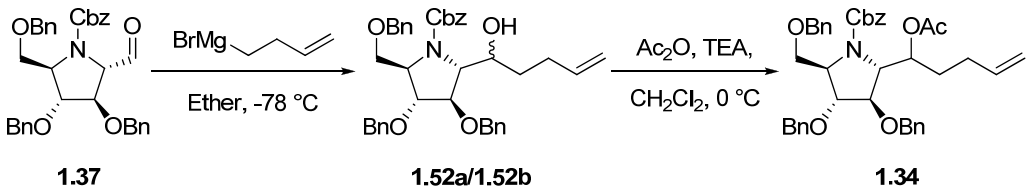

The addition of Grignard reagent prepared from 3-butenyl bromide was carried out at low temperature which yielded an inseparable epimeric mixture **1.52a/1.52b**. The ^{1}H NMR spectrum of it revealed the olefin proton resonated at δ 5.72 and 5.14 whereas

vinylic and allylic CH_2 resonated at δ 2.11 and 1.51 ppm respectively. Further mass spectra showed (*m/z*) at 644.3 $[M+Na]^+$. One of the isomer could be separated after the derivatization as acetate **1.34**, using flash column chromatography (Scheme 1.36). The appearance of singlet at δ 2.78 showed the presence of CH_3 of acetate group. The free rotation of C-N bond between carbonyl carbon of Cbz group and nitrogen of pyrrolidine core could be effected by recording ^1H spectra at 333 °K. The ^{13}C spectra showed the appearance of two peaks at 170.0 (s) and 20.8 (q) indicating the presence of acetate moiety. IR and mass spectral analysis further confirmed the assigned structures of **1.134.** Due to the problem with the rotamers population in solution, the fixing of the absolute stereochemistry of the newly generated center in the acetate **1.134** has been postponed till the completion of the synthesis.

1.3.2 Synthesis of spiroketal sidechain of (+)-broussonetine G

The synthetic started with D-mannitol, **1.53** (Scheme 1.37). D-mannitol was treated with 2,2-dimethoxy propane in dry DMSO in presence of catalytic PTSA to afford 1,2:5,6-*bis*-*O*-isopropylidine-D-mannitol (**1.54**) in 84% yield.[57] Oxidative cleavage of **1.54** using silica gel impregnated sodium metaperiodate[58] gave the three-carbon (*R*)-glyceraldehyde synthon **1.36** in 93% yield. The two carbon Wittig homologation of 1.149 with carboethoxymethylene triphenylphosphorane in CH_2Cl_2 at rt gave an inseparable *E/Z* mixture of olefins (**1.55a/1.55b**) in a 1.2:1 ratio. In the ^1H NMR spectrum of olefins, the characteristic signal of olefinic proton appeared at δ 6.08 (d, *J* = 16.0 Hz, 1H), 6.85 (dd, *J* = 6.5 and 16.0 Hz, 1H) ppm, indicating the presence of *E* olefin majorly. Whereas the characteristic signal of olefinic proton at δ 5.85 (d, *J* = 12.0 Hz, 1H), 6.35 (dd, *J* = 6.2 and 12.0 Hz, 1H) ppm, confirmed the presence of *Z* olefin as a minor isomer. The catalytic hydrogenation of **1.55a/1.55b** by using 5% Pd/C in ethyl acetate gave **1.56** in very good yields. In the ^1H NMR spectrum of **1.56**, the signals corresponding to the olefin protons were absent and two new multiplets at δ 1.86 and 2.42 integrating for 2H each were appeared. The carbonyl carbon of ester functionality resonated at δ 172.7 ppm in ^{13}C NMR spectra, also C=O strech at 1730 $\tilde{\nu}$ shows the presence of ester functionality. Other specroscopic data were in accordance with the assigned structure. Controlled reduction of the ester functionality to aldehyde was successfully carried out by using 1 equivelent of DIBAL-H at −78 °C to afford the intermediate aldehyde **1.57** in 74% isolated yield. Traces of over reduced product was also observed. After having an easy access for **1.57**

our next concern was the Wittig-Horner reaction with (2-tetrahydrofuranyl) diphenylphospine oxide (**1.60**).

Scheme 1.37 *Synthesis of aldehyde **1.57***

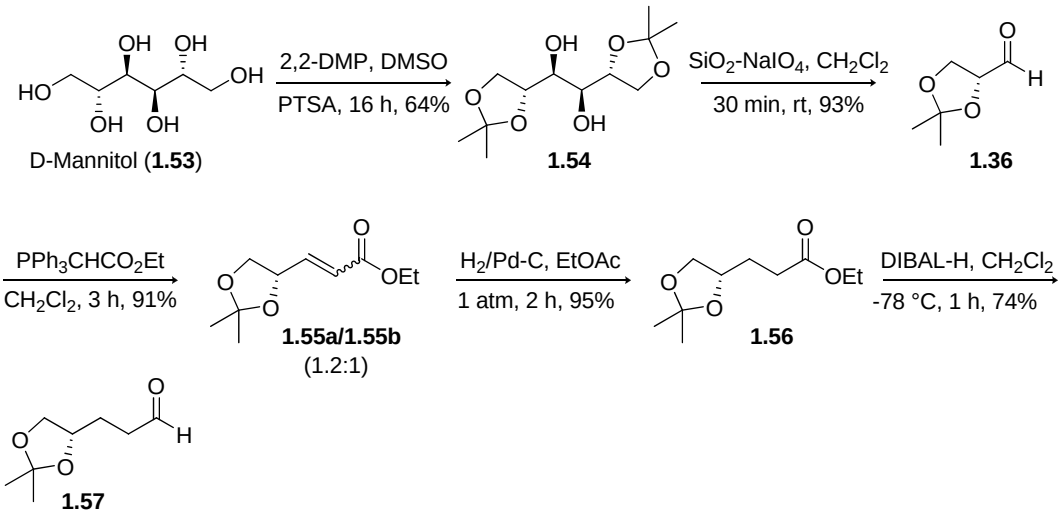

The synthesis of the (2-tetrahydrofuranyl) diphenylphospine oxide (**1.60**) was started with the treatment of a benzene solution of 3,4-dihydro-2-*H*-pyran (**1.58**) and triphenyl phospine with gaseous hydrogen chloride to provide the cyclic ether phosphonium salt (**1.59**). The phosponium salt was converted to the corresponding diphenylphosphine oxide (**1.60**) by brief (2 h) treatment with 1 N sodium hydroxide under reflux. (Scheme 1.38) IR data shows peaks at 3059, 2978 $\tilde{\nu}$ indicate the C-H stretch whereas peaks at 1591, 1484, and 1430 $\tilde{\nu}$ indicated the presence of aromatic ring. The characteristic peaks at 1180, 1050 $\tilde{\nu}$ indicated P=O stretch, and C-O stretch. ^{13}C NMR spectrum showed no of signals doubled due to multiplicity of phosporous.

Scheme 1.38 *Synthesis of* (*2-tetrahydrofuranyl*) *diphenylphospine Oxide **1.60***

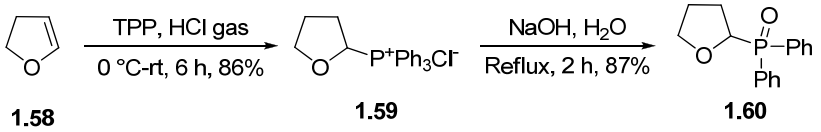

Stepwise Wittig-Horner reaction commenced with the genaration of anion of (2-tetrahydrofuranyl) diphenylphospine oxide (**1.60**) with LDA at −78 °C. Quenching the reaction mixture at low temperture with water and work up afforded the adduct **1.61** in almost quantitative yield. Subsequent treatment of this adduct in THF solution at rt with a

slight excess of potassium *t*-butoxide completed the Wittig-Horner reaction, the resuting intermediate exo-enol ether **1.62** was used for the next transformation with out any further purification.

Scheme 1.39 *Synthesis of the spiroketal fragment of* (+)*-broussonetine G*

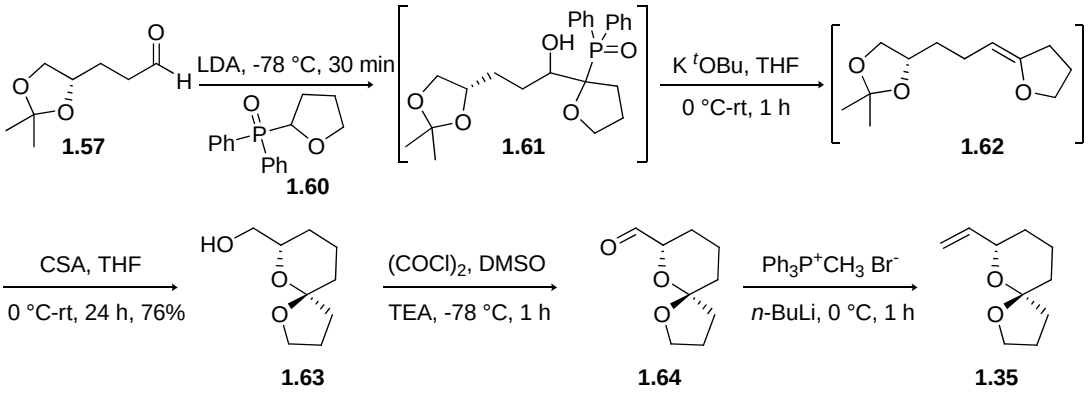

The acetonide of the enol ether **1.62** was deprotected which *in situ* cyclised to give spiroketal alcohol **1.63** using a trace of camphor sulphonic acid in THF; over a period of 24 h. Cyclisation resulted exclusively with **1.63** due to anomeric effect. The ^{13}C NMR spectra of **1.63** showed peak at δ 106 ppm indicating the quaternary carbon of the spirocyclic core. A presence of seven CH_2 and one CH confirmed the authentically spiro compound. Other specroscopic data matches with the assigned structure. The spirocyclic alcohol **1.63** was subjected to routine Swern oxidation and Wittig olefination sequence to get low boiling, volatile spiroketal fragment **1.35**. (Scheme 1.39)

1.3.3 Cross metathesis approach for the total synthesis of (+)-broussonetine G

As shown in scheme 1.40, cross metathesis was attempted between the chiral core subunit **1.34** and excess of (5 equivalents) spiroketal side chain **1.35** employing Grubbs' I catalyst (**1.4**) in different solvents and conditions. Initially cross metathesis was attempted in benzene and toluene solvents at rt and at elevated temperatures (Table 1, entries 1–4). The spiroketal side chain dimer (**1.66**) was isolated as the major product along with trace amounts of cross metathesis product (**1.65**). Chiral core subunit **1.34** was almost recovered in quantitative amounts. By changing solvent to dichloromethane (Table 1, entry 5) the yield improved to 41% by carrying out reaction with **1.4** (Grubbs' I catalyst, 20 mol %) at rt for 48 h. When reaction was carried out at reflux conditions, the dimer of

spiroketal side chain **1.66** formation was much faster as compared to the cross coupling product (Table 1, entry 6).

Scheme 1.40 *Cross metathesis approach for* (+)*-broussonetine G*

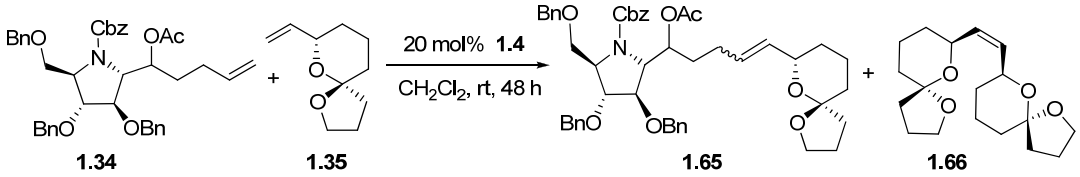

Table 1

Entry	Catalyst	Solvent	Condition	Time	Products (yields)*		
					1.65	**1.66**	Recovered **1.34**
1	1.4	Benzene	rt	48 h	0	40	95
2	1.4	Benzene	80 °C	48 h	9	82	80
3	1.4	Toluene	rt	48 h	6	56	95
4	1.4	Toluene	90 °C	48 h	13	75	76
5	**1.4**	**CH_2Cl_2**	**rt**	**48 h**	**41**	**27**	**22**
6	1.4	CH_2Cl_2	40 °C	8 h	5	90	80

* isolated yields

The characterization of compound **1.65** was done extensively. ^{1}H and ^{13}C NMR spectra were carried out at 343 °K and 333 °K respectively because of which the rotamers formed due to presence of N-Cbz group disappeared. A ^{13}C NMR spectrum has all characteristic peaks of both fragments. The peaks at δ 153.64 (s), 169.21 (s) ppm indicate the pressence of N-Cbz and O-Ac carbonyl carbon, peak at δ 105.21 (s) corresponds to the spirocyclic quarternary carbon also the peaks at δ 128.49 (d), 131.95 (d) ppm indicate the pressence of olefin. IR spectra shows characteristic speaks at υ 1736, 1698 cm^{-1} of acetate and the Cbz carbonyl stretch. Other spectroscopy data was in agreement with the assigned structure. After having the broussonetine G or its isomer in protected form in our hands, stage was set for the global deprotection. Initial attempts comprising the hydrogenation followed by deacetylation does not provide a pure sample of broussonetine G or its C-6 epimer. (Scheme 1.41)

Scheme 1.41 *Attempted removal of protecting groups in* ***1.65***

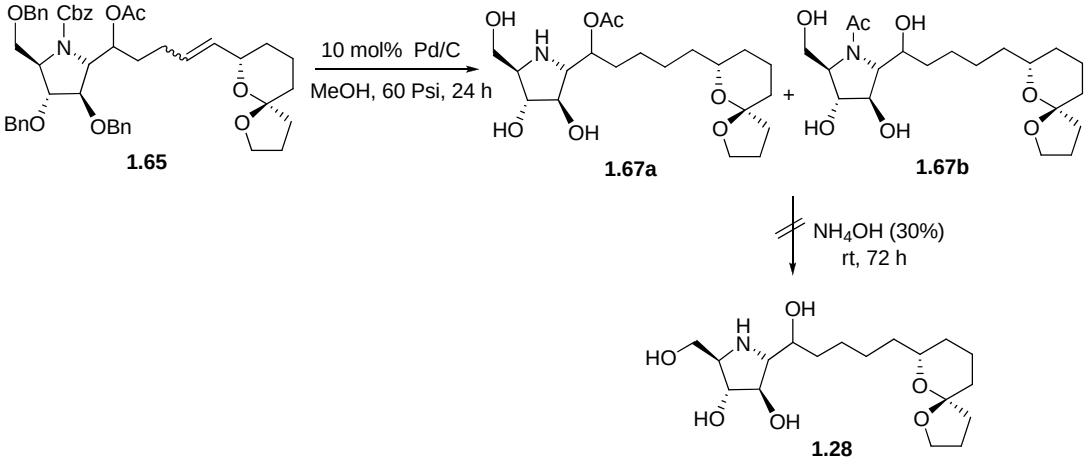

Alternatively, the acetate groups were removed by sodium methoxide and then global deprotection of benzyl groups under hydrogenation condition was attempted in which reaction mixture shows all the peaks corresponding to broussonetine G (**1.28**) however purification of the same was found to be difficult task. (Scheme 1.42)

Scheme 1.42 *Second attempt removal of protecting groups in* ***1.65***

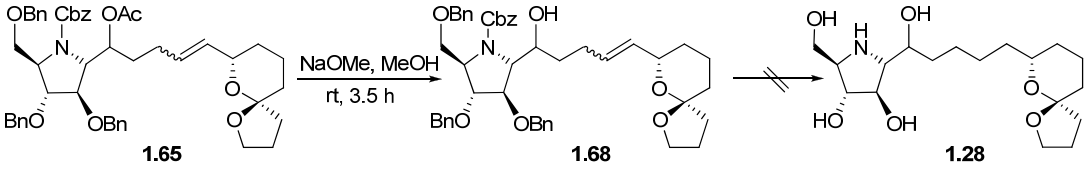

As an alternative approach, the epimeric mixture **1.52a/1.52b** was treated with sodium hydride to get inseparable mixture of bicylic compounds **1.69a/1.69b** and subjected for the cross metathesis reaction with the spiroketal fragment **1.35**. The reaction was successful with the use of 20 mol% of Grubbs' I gen. catalyst **1.4** at rt for 48 h to yield *E/Z* and bicyclic mixture **1.70a/1.70b** (Scheme 1.43). Subsequent hydrogenolysis using 10 mol% palladium hydroxide over hydrogen atmosphere at ballon pressure for 6 h resulted in with the debenzylation and double bond reduction. After purification the NMR data of the resulting product **1.71** has revealed mainly the presence of one isomer. A ^{13}C NMR spectrum has the characteristic peaks of both fragments. The peak at δ 161.6 (s) ppm indicated the presence of carbamate carbonyl carbon and a peak at δ 106.2 (s) ppm indicate the spirocyclic quarternary carbon. Absence of olefinic and aromatic peaks indicated the completion of hydrogenation. IR spectra showed the characteristic

carbamate peak at υ 1747 cm^{-1}. Further mass spectra shows (*m/z*) at 408.3 $[M+Na]^+$. Other spectroscopy data was in agreement with the assigned structure.

Scheme 1.43 *Another cross metathesis approach for* (+)*-broussonetine G*

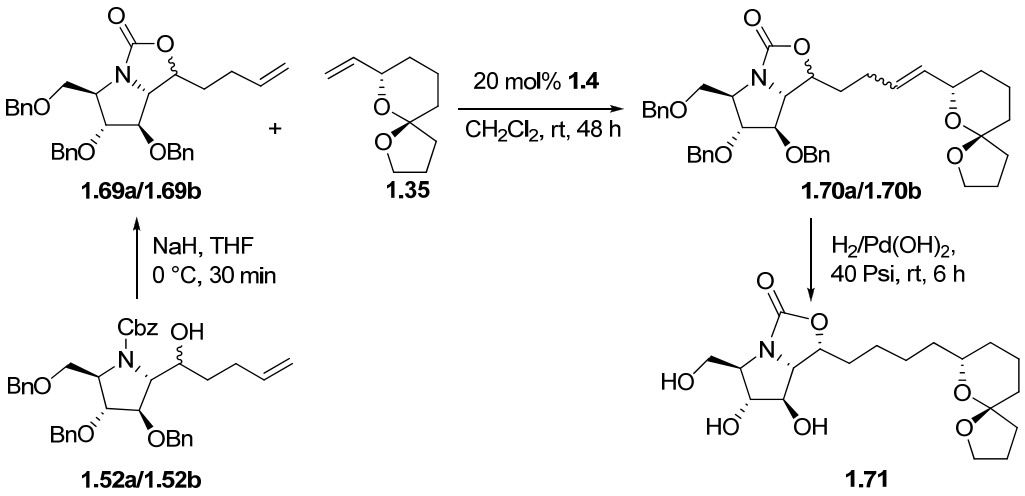

Finally, the carbamate deprotection using aq. NaOH was accomplished (Scheme 1.44). Fortunately the optical rotation and all other spectroscopic data were matching with the natural product as well as with the data provided by Trost *et al*.[54]

Scheme 1.44 *Carbamate deprotection of* ***1.71*** *& comparism of optical rotation data***.**

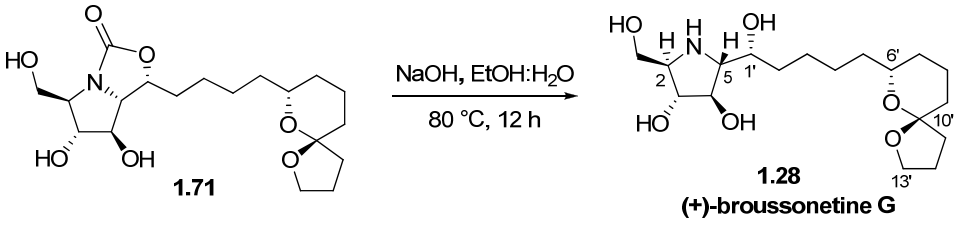

$[\alpha]_D$= +20.8 (c =1.00 MeOH)

Trost *et al*. $[\alpha]_D$= +19.3 (c =0.74 MeOH)

Nat. Product $[\alpha]_D$= +17.5 (c =1.23 MeOH)

The optical rotation of our synthesized diastereomer is +20.8 (*c* 1.0, MeOH) whereas the optical rotation of natural product reported is +17.5 (*c* 1.23, MeOH) and that of synthesized (+)-broussonetine G is +19.3 (*c* 0.74, MeOH).

1.4 Cross metathesis approach for the synthesis of (+)-broussonetine C

1.4.1. Synthesis of the pyrrolidine fragment

The synthesis started with exploring the one carbon Wittig homologation of the intermediate aldehyde **1.37** which indeed was problematic in the beginning. When the ylide was generated from the corresponding bromide salt by employing whether *n*-BuLi or potassium *tert*-butoxide as a base, no olefin product was observed. However, when sodamide was employed, the desired olefin product **1.33** could be obtained in moderate yields (22%). ^{1}H NMR spectra at 343 °K showed the olefinic protons at 5.06–5.14 (m, 2H) and 5.80 (ddd, J = 7.8, 10.0, 17.3 Hz, 1H) whereas ^{13}C NMR specra at 333 °K showed olefinic CH_2 at δ 115.9 ppm and CH at δ 136.5 ppm. Further mass spectra shows (*m/z*) at 586.6 $[M+Na]^+$. Other spectroscopic data were in agreement with the assigned structure. (Scheme 1.45)

Scheme 1.45 *Synthesis of the chiral core subunit of broussonetine C (**1.33**)*

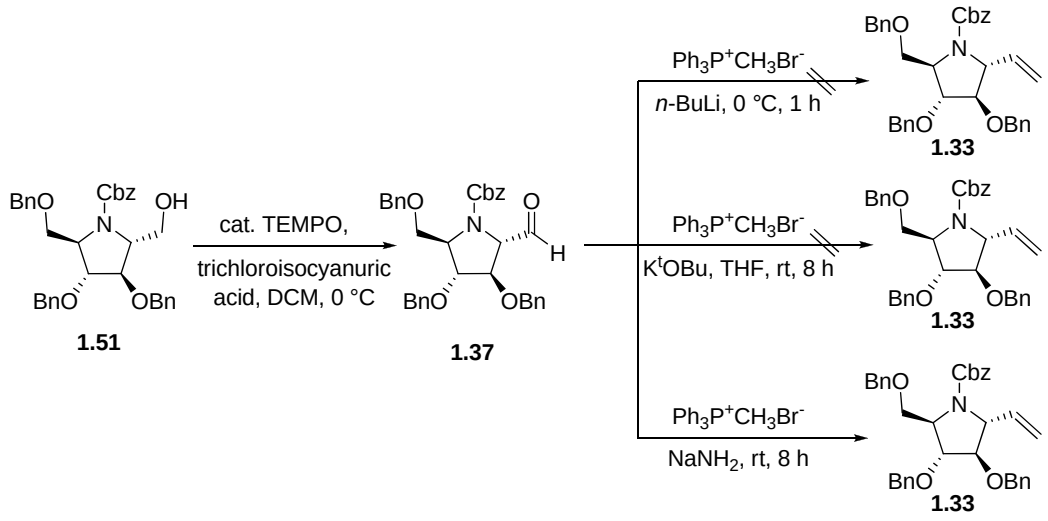

1.4.2 Synthesis of 13-C sidechain of (+)-broussonetine C

The synthetic sequences started with commercially available 9-decene-1-ol (**1.72**) (Scheme 1.46). It was oxidized using IBX to yield dec-9-enal (**1.73**) which was subjected for the Grignard reaction. The 3-(benzyloxy)-propylmagnesium bromide was prepared according to the established procedure and added to the 9-decen-1-al (**1.73**) to procure the alcohol **1.74** in 82% yield. The resulting alcohol was oxidized using IBX to yield the C_{10}-

keto fragment **1.40**. The carbonyl group was masked as its ketal derivative **1.75** in 55% yield, by acid-mediated ketalization using 1,3-propanediol.

Scheme 1.46 *Synthesis of 13-C sidechain of* (+)*-broussonetine C (**1.75**)*

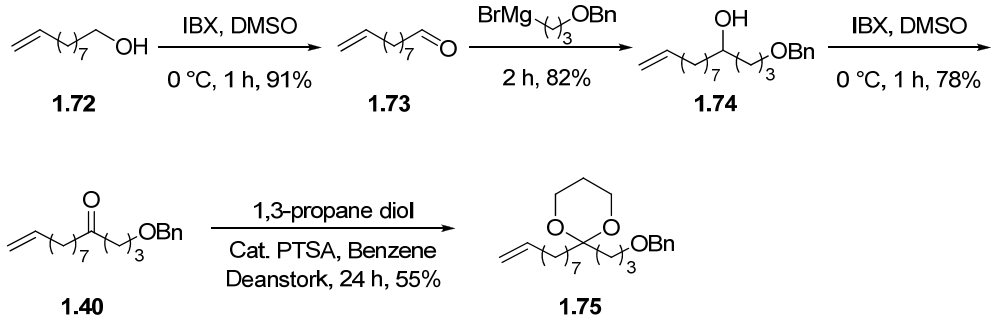

1.4.3 Cross metathesis approach for the synthesis of (+)-broussonetine C

After having the two requisite fragments **1.33** and **1.75** with suitable protecting groups, the stage was now set for the projected cross metathesis reaction. Discouragingly, under the conditions (20 mol% of Grubbs' I catalyst (**1.4**) in CH_2Cl_2 at rt for 24 h) that have employed in the broussoneting G synthesis, the cross metathesis of **1.33** and **1.75** yielded mainly the sidechain dimer (**1.76**), and unreacted sidechain (**1.75**) also two other products resulting from the hydrolysis of the ketal unit of **1.75** and its further self dimerization product. (Scheme 1.47) This indicated that the olefin of the chiral core subunit was unreactive probably due to the steric bulk around the olefin.

Scheme 1.47 *Cross metathesis approach for* (+)*-broussonetine C*

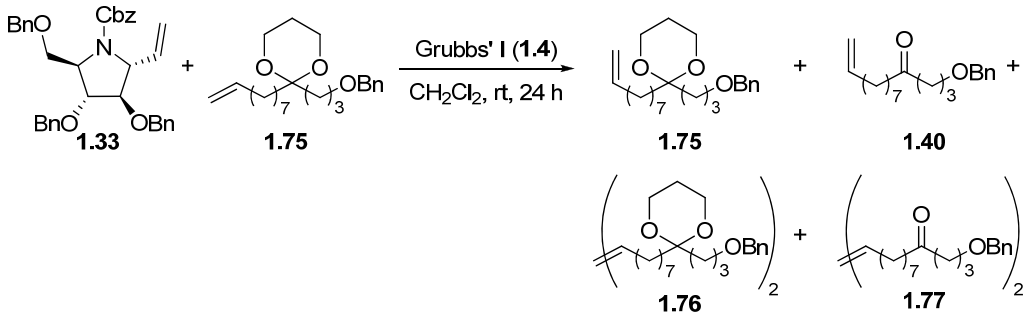

As ketal unit was succeptible for hydrolysis under the cross metathesis conditions, we have attempted the cross metathesis reaction of olefin with the free ketone derivative **1.40**. Various solvents were explored for the cross metathesis reaction employing Grubbs'

I (**1.4**) or II catalysts (**1.5**) at different temperatures (Table 2, Scheme 1.48). The formation of 13-C keto side chain dimer (**1.77**) was exclusive with Grubbs' I gen. catalyst (**1.4**) in benzene or toluene solvents (Table 2, entries 1–4) and only trace amounts of cross metathesis product (**1.78**) could be seen. The olefin subunit **1.33** was almost recovered in quantitative amounts from these reactions. By changing solvent to dichloromethane (Table 2, entry 5), the yield improved to 11 %. The yield of the reaction was increased to 31% by carrying out reaction with **1.5** (Grubbs' II catalyst, 20 mol %) at rt for 24 h, along with 13-C keto side chain dimer (**1.77**). (Table 2, entry 6)

Scheme 1.48 *Cross metathesis approach with keto sidechain for* (+)*-broussonetine C*

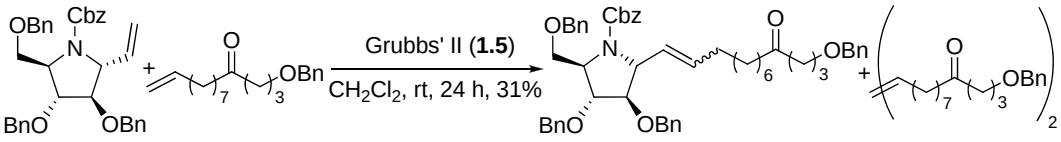

Table 2

Entry	Catalyst	Solvent	Condition	Time	Products (yields)*		
					1.78	**1.77**	Recovered **1.33**
1	1.4	Benzene	rt	48 h	0	29	94
2	1.4	Benzene	80 ^{o}C	24 h	0	84	85
3	1.4	Toluene	rt	48 h	0	47	95
4	1.4	Toluene	90 ^{o}C	24 h	0	77	87
5	1.4	CH_2Cl_2	rt	24 h	11	65	55
6	**1.5**	**CH_2Cl_2**	**rt**	**24 h**	**31**	**29**	**21**

* isolated yields

Characterization of the compound **1.78** was carried out by extensive spectral analyses. The ^{13}C NMR spectrum of **1.78** has showed the characteristic peaks of the both the fragment. Peaks at δ 155.0 (s) ppm indicated the presence of N-Cbz carbonyl carbon and peak at δ 210.5 (s) indicated the carbonyl carbon of the C_{13} keto side chain. The peaks at δ 133.0 (d), 127.7 (d) ppm indicated the pressence of an olefin unit. IR spectra showed characteristic speaks at υ 1734, 1699 cm^{-1} of Cbz and keto carbonyl stretch. Other spectroscopy data were in agreement with the assigned structure. After having the (+)-broussonetine C in protected form in our hand, the stage was set for the removal of protecting groups to complete the total synthesis of **1.27**.

Scheme 1.49 *Catalytic hydrogenation of protected* (+)*-broussonetine C* ***(1.78)***

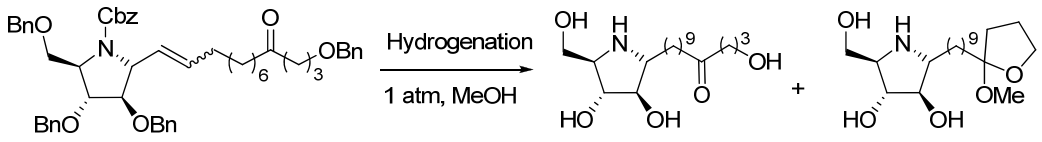

1.78 **1.27** **1.79**

Broussonetine C

Table 3

Entry	Condition	Time	Products*
1	H_2, 10%-Pd/C	24 h	**1.27** + **1.79** + partially hydrogenated products
2	H_2, 10%-Pd/C	72 h	**1.27** + **1.78**
3	H_2, 10%-Pd/C, HCl	48 h	Complex mixture
4	H_2, Pd Black, 5% AcOH	24 h	**1.27** + partially hydrogenated products
5	H_2, Pd Black, 5% AcOH	75 h	**1.27** + other peaks

* peaks detected in mass spectrum

Catalytic hydrogenation of protected (+)-broussonetine C (**1.78**) was attempted in different conditions and monitored by mass spectroscopy (Scheme 1.49). Catalytic hydrogenation with 10% Pd/C at 1 atm pressure for 24 h over hydrogen atmosphere yielded compound has a mass peaks at 346.7058, 360.7421 indicative of the M+1 peak of **1.27** and **1.79**, but it also yielded peaks at 436.8682, 450.8832, 541.0409 indicating the pressence of one or two benzyl groups in both compounds. Continued hydrogenation for 72 h yielded only peaks corresponding to **1.27** and **1.79** (Table 3, entry 1 & 2). Whereas addition of 1 drop of HCl to the reaction and hydrogenation for 24 h yielded complex mixture, the molecular ion peak disappeared but hydrochloride salt ion peak was also not observed (Table 3, entry 3). Catalytic hydrogenation over Pd black which is well known for global deprotection and 5% acetic acid in methanol for 24 h yielded peaks corresponding to **1.27** and partially hydrogenated products. Continuing the reaction for longer time i.e. 75 h has resulted mainly with the appearance of the peaks at 346.4628, 413.5209 in the MS indicative of the M+1 peak of **1.27** and other peak (Table 3, entry 4 & 5).

As our attempts to get the pure compound **1.27** following a hydrogenolyis for global deprotection at the end were futile, we next opted for a Boc protecting group on ring nitrogen and planned to remove it after hydrogenolysis. The synthesis of the corresponding Boc-protected olefin derivative was commenced with the treatment of

aminol **1.50** with Boc anhydride in presence of TEA to yield **1.80**. The primary alcohol at C-(1) was oxidized to **1.38** using TEMPO radical and trichloroisocyanuric acid. One carbon Wittig olefination on this substrate with potassium *tert*-butoxide as a base did not yield required olefin product, but it yielded aromatized product **1.82**. In case of $NaNH_2$, desired olefin product **1.81** was obtained in 39% yield. (Scheme 1.50).

Scheme 1.50 *Synthesis of the Boc protected chiral core subunit of broussonetine C*

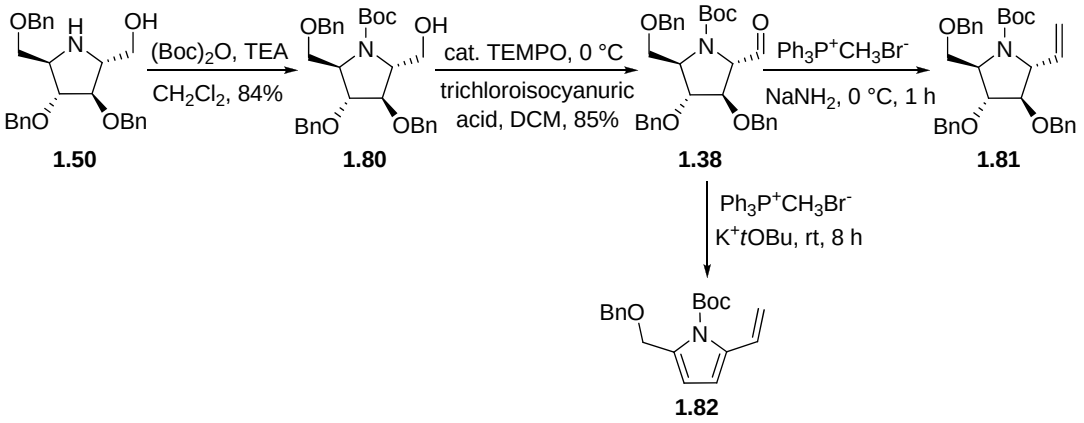

^{1}H NMR spectra at 343 °K showed the olefinic protons at 5.06 (d, J = 10.3 Hz, 1H), 5.11 (d, J = 7.3 Hz, 1H), 5.79 (ddd, J = 8.3, 10.0, 17.6 Hz, 1H) whereas ^{13}C NMR specra at 343 °K showed olefinic CH_2 at δ 115.5, ppm and CH at δ 136.8 ppm. Further mass spectra shows (*m/z*) at 530.2 $[M+Na]^+$. Other spectral data were in agreement with the assigned structure.

Scheme 1.51 *Cross metathesis approach with Boc protected chiral core subunit*

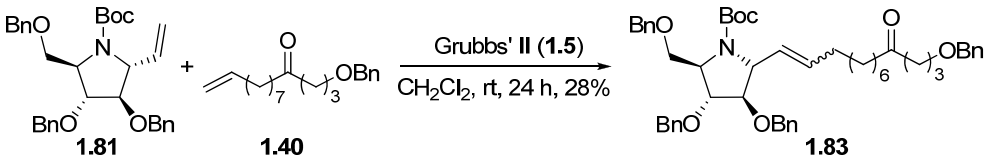

The crucial reaction, i.e. the cross metathesis of Boc protected chiral core subunit **1.81** and 13-C keto side chain **1.40** was carried out with Grubbs II catalyst (**1.5**, 20 mol%) in CH_2Cl_2 at rt for 24 h to afford the fully protected broussonetine C derivative **1.83**. (Scheme 1.51) The characterization of compound **1.83** was done extensively. The free rotation of C-N bond between carbonyl carbon of Boc group and nitrogen of pyrrolidine core was effected by recording ^{1}H and ^{13}C spectra at 343 ^{o}K. Both spectra showed the

peaks of two coupling partners. In ^{1}H NMR spectra olefin peaks were observed at δ 5.30–5.54 (m, 2H) whereas in ^{13}C NMR spectra they were observed at δ 127.5 and 131.6 ppm. Further mass spectra shows (*m/z*) at 804.5 $[M+1]^{+}$.

Scheme 1.52 *Catalytic hydrogenation of* (***1.83***)

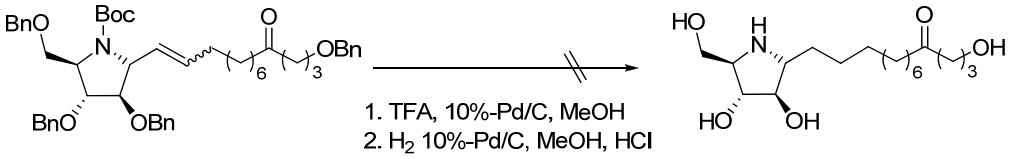

1.83 **1.27**

Broussonetine C

The deprotection of **1.83** was also found to be futile exercise by conducting the hydrogenation either first or after the Boc deprotection. Though, the formation requisite product was noticed when the crude reactions were analysed by MS, however the attempts to purify final compound **1.27** were unsuccessful (Scheme 1.52). After exploring various conditions and spending sufficient time, we have abandoned this scheme at this stage.

1.4.4 Conclusion

Employing cross metathesis as a key reaction, synthesis of (+)-broussonetine G and benzyl protected (+)-broussonetine C has been accomplished using chiral pool approach. Global deprotection of **1.78**, **1.83** was attempted, though the formation of the requisite products is noticed however, the isolation of the pure (+)-broussonetine C was found to be a difficult task.

1.4 Experimental

1,2-*O*-Isopropylidine- L-sorbopyranose (1.42)

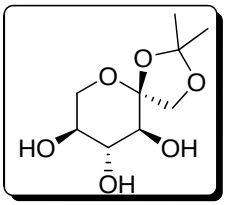

Anhydrous copper sulphate (100 g) was suspended in dry acetone (850 ml) in a three necked r.b. flask fitted with a paraffin-seal stirrer, thermometer, and a guard tube. Pure anhydrous sorbose (10 g, 55.5 mmol) was then added and the mixture heated to 50 °C under vigorous stirring for 5 h. The cooled reaction mixture was then filtered through two layers of filter paper and the residue washed with acetone. The slightly acidic filtrate was made alkaline by addition of 17.5% solution of NaOH (1 ml) and acetone removed at the ordinary temperature in a rotary evaporator. The resulting syrupy residue was treated with dry ether until turbid. After keeping in a refrigerator overnight, the crystals were filtered when the pure material (3.3 g) was obtained in clusters of colorless needles in 27% yield.

Mol. Formula	: $C_9H_{16}O_6$
M. P.	: 143–144 °C (lit 142 °C)
$[\alpha]_D$	: –85.0 (*c* 7.25, H_2O) (lit –88.7 (*c* 7.25, H_2O))
IR ($CHCl_3$) $\tilde{\nu}$	: 3404, 2924, 2854, 1460, 1374, 1059 cm^{-1}.
^{1}H NMR ($CDCl_3$, 200 MHz)	: δ 1.45 (s, 3H), 1.51 (s, 3H), 2.00–3.00 (br s, 3H), 3.38 (d, *J* = 8.0 Hz, 1H), 3.60–3.77 (m, 4H), 3.95 (d, *J* = 8.7 Hz, 1H), 4.15 (d, *J* = 8.7 Hz, 1H) ppm.
^{13}C NMR (DMSO-d_6, 50 MHz)	: δ 26.3 (q), 27.3 (q), 63.3 (t), 67.0 (d), 70.6 (d), 71.2 (t), 74.9 (d), 105.8 (s), 111.0 (s) ppm.
ESI-MS (*m/z*)	: 243.5 $[M+Na]^+$.

1,2-*O*-Isopropylidine-5-*O*-tosyl-α-L-sorbose (1.43)

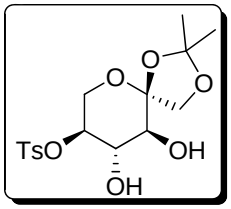

1,2-*O*-Isopropylidine-L-sorbopyranose (**1.42**) (30.0 g, 136.2 mmol) and tosyl chloride (27.0 g, 141.7 mmol) were added to dry pyridine (200 ml), and the solution was kept at 0 °C for 5 h. The reaction mixture was then poured into cold water and extracted with chloroform. The extract was dried and evaporated to dryness. The residue crystallized immediately and this mass was then cooled and stirred in absolute ether (50 ml). After further cooling, the crystalline product was removed by filtration: yield 15.9 g (31%).

Mol. Formula	: $C_{16}H_{22}O_8S$
M. P.	: 135 °C (lit 130 °C)
$[\alpha]_D$	: –61.1 (*c* = 1.1, $CHCl_3$). (lit –52.1 (*c* = 1.1, $CHCl_3$))
IR ($CHCl_3$) $\tilde{\nu}$	: 3505, 2983, 1402, 1364, 1189, 1174 cm^{-1}.
^{1}H NMR ($CDCl_3$, 200 MHz)	: δ 1.38 (s, 3H), 1.43 (s, 3H), 2.46 (s, 3H), 3.24 (d, *J* = 9.3 Hz, 1H), 3.60–3.71 (m, 3H), 3.79 (d, *J* = 8.6 Hz, 1H), 3.94 (br s, 2H), 4.10 (d, *J* = 8.6 Hz, 1H), 4.18 (ddd, *J* = 7.5, 9.1, 16.4 Hz, 1H), 7.37 (d, *J* = 8.1 Hz, 2H), 7.81 (d, *J* = 8.1 Hz, 2H) ppm.
^{13}C NMR ($DMSO-d_6$, 50 MHz)	: δ 21.3 (q), 26.1 (q), 27.2 (q), 60.1 (t), 70.3 (d), 71.0 (t), 71.4 (d), 79.0 (d), 105.5 (s), 111.6 (s), 128.0 (d, 2C), 130.2 (d, 2C), 133.3 (s), 145.1 (s) ppm.
ESI-MS (*m/z*)	: 397.2 $[M+Na]^+$.
Elemental Analysis	Calcd.: C, 51.33; H, 5.92; S, 8.56 Found: C, 51.29; H, 5.89; S, 8.51

1,2-*O*-Isopropylidine-3,4-di-*O*-acetyl-5-*O*-tosyl-α-L-sorbose (1.44)

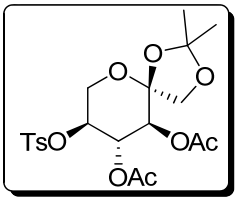

To a solution of (**1.43**) (10.0 g, 26.7 mmol) in dry pyridine (30 ml), acetic anhydride (6.82 ml, 66.8 mmol) was added slowly at 0 °C. The reaction mixture was stirred at rt for 6 h. Pyridine was evaporated at reduced pressure and crude was extracted with ethyl acetate. Purified by column chromatography to get pure **1.44** as white powder (11.32 g, 92% yield).

Mol. Formula	: $C_{20}H_{26}O_{10}S$
M. P.	: 115 °C (lit 109–110 °C)
$[\alpha]_D$	: −33.6 (*c* 1.1, $CHCl_3$), (lit –27.5 (*c* = 1.1, $CHCl_3$))
IR ($CHCl_3$) $\tilde{\nu}$	: 3020, 1752, 1374, 1216, 1190, 1178, 1057 cm^{-1}.
^{1}H NMR ($CDCl_3$, 200 MHz)	: δ 1.39 (s, 3H), 1.45 (s, 3H), 1.78 (s, 3H), 2.04 (s, 3H), 2.46 (s, 3H), 3.80 (d, *J* = 9.5 Hz, 1H), 3.87 (d, *J* = 8.6 Hz, 2H), 3.91 (d, *J* = 9.5 Hz, 1H), 4.54 (ddd, *J* = 8.2, 9.1, 16.4 Hz, 1H), 4.92 (d, *J* = 10.0 Hz, 1H), 5.37 (dd, *J* = 9.3, 10.0 Hz, 1H), 7.35 (d, *J* = 8.1 Hz, 2H), 7.76 (d, *J* = 8.1 Hz, 2H) ppm.
^{13}C NMR ($CDCl_3$, 50 MHz)	: δ 20.1 (q), 20.2 (q), 21.4 (q), 25.7 (q), 26.2 (q), 60.4 (t), 68.8 (d), 70.2 (d), 71.2 (t), 74.7 (d), 95.9 (s), 103.2 (s), 112.5 (s), 127.7 (d, 2C), 129.7 (d, 2C), 133.2 (s), 144.9 (s), 169.0 (s), 169.6 (s) ppm.
ESI-MS (*m/z*)	: 481.3 $[M+Na]^+$.
Elemental Analysis	Calcd.: C, 52.39; H, 5.72; S, 6.99 Found: C, 52.42; H, 5.68; S, 6.95

5-Azido-5-deoxy-3,4-di-*O*-acetyl-1,2-*O*-isopropylidene-β-D-fructopyranose (1.45)

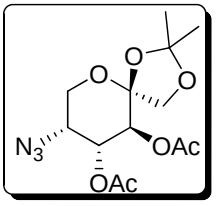

A solution of tosylate **1.44** (10 g, 21.8 mmol) and lithium azide (14.18 g, 218 mmol) in 200 ml of DMSO was heated at 100 °C for 3 h. The reaction mixture was poured into water and extracted with ethyl acetate. The organic layer was dried with sodium sulphate and concentrated under reduced pressure. The product was purified by column chromatography on silica gel (4:l hexane/ethyl acetate) to afford **1.45** (7.18 g, 61%) as a colorless syrup.

Mol. Formula	: $C_{13}H_{19}N_3O_7$
$[\alpha]_D$	: −117.7 (*c* 1.0, $CHCl_3$)
IR ($CHCl_3$) $\tilde{\nu}$	: 2991, 2107, 1754, 1373, 1223, 1092 cm^{-1}.
^{1}H NMR ($CDCl_3$, 200 MHz)	: δ 1.40 (s, 3H), 1.46 (s, 3H), 2.10 (s, 3H), 2.11 (s, 3H), 3.75 (dd, *J* = 1.8, 12.6 Hz, 1H), 3.93 (dd, *J* = 9.5, 14.7 Hz, 2H), 4.08 (dd, *J* = 1.8, 11.6 Hz, 1H), 4.11 (m, 1H), 5.30 (d, *J* = 3.5 Hz, 1H), 5.38 (d, *J* = 10.5 Hz, 1H) ppm.

^{13}C NMR ($CDCl_3$, 75 MHz)	: δ 20.0 (q), 20.2 (q), 25.8 (q), 26.0 (q), 59.7 (d), 61.7 (t), 66.6 (d), 71.0 (d), 71.6 (t), 104.3 (s), 112.0 (s), 169.5 (s, 2C) ppm.
ESI-MS (*m/z*)	: 352.1 $[M+Na]^+$.
Elemental Analysis	Calcd.: C, 47.41; H, 5.82; N, 12.76 Found: C, 47.37; H, 5.77; N, 12.71

5-Azido-5-deoxy-1,2-*O*-isopropylidene-β-D-fructopyranose (1.46)

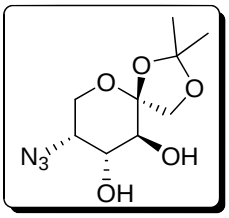

To a solution of **1.45** (6 g, 18.2 mmol) in methanol (100 ml), solid potassium carbonate (5.54 g, 40 mmol) was added at 0 °C and stirred at rt for 6 h. Methanol was evaporated at reduced pressure and then extracted with ethyl acetate. Purified by column chromatography on silica gel (2:1 hexane/ethyl acetate) to obtain **1.46** (4.08 g, 91%) as a colorless thick syrup.

Mol. Formula	: $C_9H_{15}N_3O_5$
$[\alpha]_D$	: −170.5 (*c* 1.0, $CHCl_3$)
IR ($CHCl_3$) $\tilde{\nu}$	: 3413, 3019, 2938, 2107, 1402, 1216, 1091 cm^{-1}.
^{1}H NMR ($CDCl_3$, 300 MHz)	: δ 1.45 (s, 3H), 1.49 (s, 3H), 2.44 (br s, 1H), 3.44 (br s, 1H), 3.72–3.79 (m, 2H), 3.94–4.00 (m, 3H), 4.01 (d, *J* = 8.8 Hz, 1H), 4.18 (d, *J* = 8.8 Hz, 1H) ppm.
^{13}C NMR ($CDCl_3$, 50 MHz)	: δ 25.9 (q), 26.2 (q), 61.77 (t), 62.0 (d), 68.8 (d), 71.3 (d), 71.6 (t), 105.5 (s), 112.0 (s) ppm.
ESI-MS (*m/z*)	: 268.5 $[M+Na]^+$.
Elemental Analysis	Calcd.: C, 44.08; H, 6.17; N, 17.13 Found: C, 44.13; H, 6.11; N, 17.08

5-Azido-5-deoxy-D-fructose (1.47)

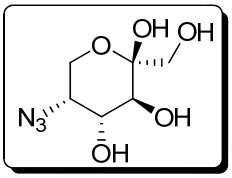

A solution of diol **1.46** (3.44 g, 14 mmol) in EtOH (14 ml) and water (45 ml) was treated with Amberlyst IR-120 (7 g**;** hydrogen form), and the mixture was heated at 60 °C for 4 h. The reaction mixture was filtered, decolorized, and then extracted with ether. The aqueous layer was concentrated at reduced pressure to afford **1.47** as a white solid (2.56 g, 89%).

Mol. Formula	: $C_6H_{11}N_3O_5$
M. P.	: 121 °C (lit 117 °C)
IR ($CHCl_3$) $\tilde{\nu}$	: 3370, 2110, 1090, 1065 cm^{-1}.
^{1}H NMR (D_2O, 200 MHz)	: δ 3.71–3.82 (m, 2H), 3.94–4.04 (m, 4H), 4.15 (d, *J* = 9.4 Hz, 1H) ppm.
^{13}C NMR (D_2O, 125 MHz)	: δ 61.0 (t), 62.7 (d), 63.8 (t), 67.9 (d), 69.9 (d), 98.3 (s) ppm.
ESI-MS (*m/z*)	: 228.5 $[M+Na]^+$.

(2*R*,3*R*,4*R*,5*R*)-2,5-Bis(hydroxymethyl)pyrrolidine-3,4-diol (1.39)

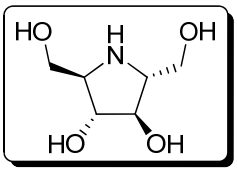

To a solution of 5-azidofructose **1.47** (2.0 g, 9.7 mmol) in 100 ml of EtOH, catalytic amount of 10% Pd/C (100 mg) was added and the resulting suspension was hydrogenated at 60 psi for 24 h. The crude were filtered trough celite pad and the filtrate was concentrated affording 1.50 g (94%) of **1.39** as a pale brown thick syrup.

Mol. Formula	: $C_6H_{13}NO_4$
$[\alpha]_D$	: +49.6 (*c* 1.0, H_2O), (lit +55.8 (*c* 1.0, H_2O))
IR (nujol) $\tilde{\nu}$	: 3346, 2923, 1462, 1376, 1149, 1048 cm^{-1}.
^{1}H NMR (D_2O, 300 MHz)	: δ 3.02–3.07 (m, 2H), 3.63 (dd, *J* = 6.6, 11.7 Hz, 2H), 3.71 (dd, *J* = 3.6, 11.7 Hz, 2H), 3.84 (dd, *J* = 2.2, 5.1 Hz, 2H) ppm.
^{13}C NMR (D_2O, 75 MHz)	: δ 62.1 (d), 62.2 (d), 78.1 (t) ppm.

(5*R*,6*R*,7*R*,7a*R*)-6,7-Bis(benzyloxy)-5-(benzyloxymethyl)tetrahydropyrrolo[1,2-c]oxazol-3(1*H*)-one (1.49)

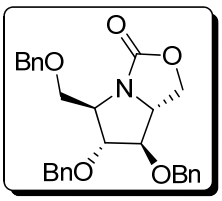

To a solution of DMDP **1.39** (1.7 g, 10.4 mmol) in 34 ml of 10% $NaHCO_3$ solution, triphosgene (3.4 g, 11.5 mmol) dissolved in 15 ml of toluene was added at rt. The biphasic mixture was stirred vigorously for 5 h. Aqueous layer was washed with (3 x 25 ml) toluene and concentrated under reduced pressure to dryness. The obtained thick yellow syrup (1.3 g, 66% yield) was dissolved in dry DMF and NaH (1.10 g, 27.5 mmol) was added in portions at 0 °C and stirred at rt for 1 h. To this BnBr (4.06 ml, 34.4 mmol) was added drop wise over a period of 10 min at 0 °C and stirred at rt overnight. The reaction mixture was poured into water and extracted with ethyl acetate. The organic layer was dried with sodium sulphate and concentrated under reduced pressure. The product was purified by column chromatography on silica gel (2:l hexane/ethyl acetate) to afford **1.49** (2.60 g, 82%) as a colorless syrup.

Mol. Formula	: $C_{28}H_{29}NO_5$
$[\alpha]_D$	: +4.0 (*c* 1.0, $CHCl_3$)
IR ($CHCl_3$) $\tilde{\nu}$	: 3030, 2912, 2865, 1759, 1496, 1454, 1392, 1216 cm^{-1}.
^{1}H NMR ($CDCl_3$, 200 MHz)	: δ 3.57 (d, *J* = 5.3 Hz, 2H), 3.89 (d, *J* = 4.0 Hz, 1H), 3.96 (dd, *J* = 3.5, 22.4 Hz, 1H), 4.07–4.15 (m, 2H), 4.26 (t, *J* = 3.7 Hz, 1H), 4.33 (d, *J* = 7.8 Hz, 1H), 4.46 (dd, *J* = 5.8, 11.7 Hz, 2H), 4.54 (d, *J* = 2.8 Hz, 2H), 4.60 (dd, *J* = 2.8, 11.7 Hz, 2H), 7.22–7.35 (m, 15H) ppm.
^{13}C NMR ($CDCl_3$, 75 MHz)	: δ 61.6 (d), 62.0 (d), 66.6 (t), 69.3 (t), 71.3 (t), 71.9 (t), 72.7 (t), 85.3 (d), 87.7 (d), 127.1 (d, 3C), 127.2 (d, 2C), 127.3 (d, 2C), 127.4 (d, 2C), 127.5 (d), 127.8 (d), 127.9 (d, 3C), 128.0 (d), 137.1 (s), 137.2 (s), 137.5 (s), 160.2 (s) ppm.
ESI-MS (*m/z*)	: 482.5 $[M+Na]^+$.
Elemental Analysis	Calcd.: C, 73.18; H, 6.36; N, 3.05 Found: C, 73.12; H, 6.31; N, 3.00

((2*R*,3*R*,4*R*,5*R*)-3,4-Bis(benzyloxy)-5-(benzyloxymethyl)pyrrolidin-2-yl)methanol (1.50)

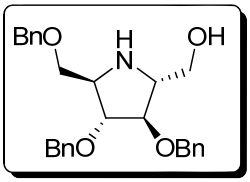

To a solution of **1.49** (1.5 g, 3.3 mmol) in EtOH:H_2O (3:1, 30 ml), NaOH (326 mg, 8.2 mmol) was added and refluxed for 6 h. Volatiles were evaporated under reduced pressure

and the crude was purified by column chromatography on silica gel (19:1 chloroform/methanol) to afford **1.50** (1.11 g, 78%) as a colorless thick liquid.

Mol. Formula	: $C_{27}H_{31}NO_4$
$[\alpha]_D$	: +32.4 (*c* 1.0, $CHCl_3$)
IR ($CHCl_3$) $\tilde{\nu}$	: 3400, 3018, 2400, 1496, 1454, 1094, 755 cm^{-1}.
^{1}H NMR ($CDCl_3$, 200 MHz)	: δ 2.46 (br s, 1H), 3.32 (dd, *J* = 5.6, 10.5 Hz, 2H), 3.43–3.45 (m, 1H), 3.50–3.58 (m, 3H), 3.80–3.88 (m, 1H), 3.90–3.95 (m, 1H), 4.46–4.54 (m, 6H), 7.20–7.35 (m, 15H) ppm.
^{13}C NMR ($CDCl_3$, 50 MHz)	: δ 61.2 (d), 61.9 (t), 63.1 (d), 69.5 (t), 71.7 (t, 2C), 72.9 (t), 85.2 (d), 85.6 (d), 127.4 (d, 4C), 127.5 (d, 3C), 127.6 (d, 2C), 128.1 (d, 2C), 128.2 (d, 4C), 137.7 (s), 137.8 (s, 2C) ppm.
ESI-MS (*m/z*)	: 456.6 $[M+Na]^+$.
Elemental Analysis	Calcd.: C, 74.80; H, 7.21; N, 3.23 Found: C, 74.76; H, 7.18; N, 3.19

(2*R*,3*R*,4*R*,5*R*)-Benzyl 3,4-bis(benzyloxy)-2-(benzyloxymethyl)-5-(hydroxymethyl)pyrrolidine-1-carboxylate (1.51)

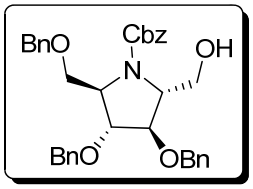

At 0 °C, a solution of aminol **1.50** (500mg, 1.15 mmol) in dioxan (10 ml), was treated with $NaHCO_3$ (193 mg, 2.3 mmol) followed by Cbz-Cl (0.23 ml, 1.38 mmol) and their mixture was stirred at the same temp for 4 h. Volatiles were evaporated under reduced pressure and the mixture was extracted with ethyl acetate, dried, concentrated and purified by column chromatography on silica gel (4:1 hexane/ethyl acetate) to afford **1.51** (600 mg, 91%) as a colorless thick liquid.

Mol. Formula	: $C_{35}H_{37}NO_6$
$[\alpha]_D$	: −35.3 (*c* 1.5, $CHCl_3$)
IR ($CHCl_3$) $\tilde{\nu}$	: 3451, 3031, 2928, 1701, 1496, 1453, 1411, 1349, 1213, 1095, 750 cm^{-1}.
^{1}H NMR ($CDCl_3$, 200 MHz)	Rotamers: δ 3.43–3.56 (m, 1H), 3.68–3.74 (m, 1H), 3.87 (br m, 2H), 3.94–4.08 (m, 2H), 4.14–4.21 (m, 2H), 4.37–4.68 (m, 6H), 5.02–5.21 (m, 2H), 7.21–7.33 (m, 20H) ppm.
^{13}C NMR	Major rotamer: δ 63.2 (d), 63.3 (t), 66.7 (d), 67.3 (t), 68.3 (t), 71.1

($CDCl_3$, 125 MHz)	(t), 71.3 (t), 73.0 (t), 81.6 (d), 84.0 (d), 127.5 (d, 3C), 127.8 (d, 3C), 128.1 (d, 3C), 128.3 (d, 3C), 128.4 (d, 5C), 128.5 (d, 3C), 136.1 (q), 137.3 (q, 2C), 138.0 (q), 155.5 (q) ppm. Minor rotamer: δ 61.8 (t), 63.4 (d), 65.3 (d), 67.2 (t), 67.5 (t), 71.2 (t, 2C), 73.0 (t), 80.5 (d), 85.2 (d), 127.5 (d, 3C), 127.6 (d, 2C), 127.7 (d, 2C), 127.8 (d, 2C), 127.9 (d, 2C), 128.0 (d, 2C), 128.1 (d, 4C), 128.3 (d, 3C), 136.2 (q), 136.9 (q), 137.2 (q), 138.3 (q),154.5 (q) ppm.
ESI-MS (*m/z*)	: 590.4 $[M+Na]^+$.
Elemental Analysis	Calcd.: C, 74.05; H, 6.57; N, 2.47 Found: C, 73.99; H, 6.52; N, 2.42

(2*R*,3*R*,4*R*,5*S*)-Benzyl 3,4-bis(benzyloxy)-2-(benzyloxymethyl)-5-formylpyrrolidine-1-carboxylate (1.37)

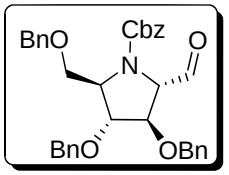

Trichloroisocyanuric acid (180 mg, 0.77 mmol) was added to a solution of the alcohol, **1.51** (400 mg, 0.70 mmol) in CH_2Cl_2 (20 ml) and the solution was stirred and maintained at 0 °C, followed by addition of TEMPO radical (1.1 mg, 0.007 mmol). Reaction mixture was stirred at 0 °C for 1 h and then was filtered on celite. Organic phase was washed with 15 ml of saturated solution of Na_2CO_3, followed by 1 N HCl and brine. The organic layer was dried (Na_2SO_4) and evaporated at reduced pressure to yield **1.37** which was used for the next step without any further purification.

Mol. Formula	: $C_{35}H_{37}NO_6$
^{1}H NMR ($CDCl_3$, 200 MHz)	: δ 3.57 (dd, *J* = 3.0, 9.0 Hz, 1/2H), 3.61 (dd, *J* = 3.0, 9.0 Hz, 1/2H), 3.73 (dd, *J* = 4.4, 9.0 Hz, 1/2H), 3.96 (dd, *J* = 4.5, 8.8 Hz, 1/2H), 4.05 (d, *J* = 3.8 Hz, 1H), 4.15 (br s, 1H), 4.18–4.69 (m, 8H), 5.03–5.29 (m, 2H), 7.15–7.33 (m, 20H), 9.34 (d, *J* = 1.9 Hz, 1/2H), 9.44 (d, *J* = 1.7 Hz, 1/2H) ppm.

(2*R*,3*R*,4*R*,5*R*)-Benzyl-3,4-bis(benzyloxy)-2-(benzyloxymethyl)-5-(1-hydroxypent-4-enyl)pyrrolidine-1-carboxylate (1.52a/1.52b)

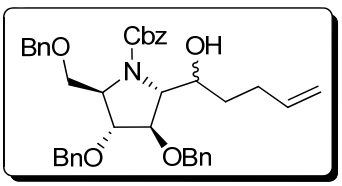

To a cooled solution of aldehyde **1.37** (200mg, 0.253 mmol) in dry THF (20 ml), was added freshly prepared solution of but-3-enylmagnesium bromide (10 ml solution in THF containing 1.77 mmol) slowly drop wise at −78 °C. The mixture was stirred for 2 h and the temperature was slowly raised to rt. Excess Grignard was quenched with careful addition of sat. NH_4Cl at 0 °C. The reaction mixture was diluted with ethyl acetate (20 ml) and water (20 ml). The organic phase was separated and the aqueous phase was in turn washed with ethyl acetate (2 X 20 ml). The combined organic extracts were dried over Na_2SO_4, filtered and concentrated and purified by column chromatography on silica gel (5:l hexane/ethyl acetate) to afford **1.52a/1.52b** (175 mg, 79%) as a colorless liquid.

Mol. Formula	: $C_{39}H_{43}NO_6$
IR ($CHCl_3$) $\tilde{\nu}$	: 3448, 3066, 3012, 2928, 1696, 1496, 1454, 1414, 1349, 1094, 756 cm^{-1}.
^{1}H NMR ($CDCl_3$, 200 MHz)	: δ 1.41–1.65 (m, 2H), 1.98–2.31 (m, 2H), 3.39–3.56 (m, 2H), 3.82–4.68 (m, 12H), 4.87–5.20 (m, 3H), 5.67–5.80 (m, 1H), 7.18–7.32 (m, 20H) ppm.
ESI-MS (*m/z*)	: 644.3 $[M+Na]^+$.
Elemental Analysis	Calcd.: C, 75.34; H, 6.97; N, 2.25. Found: C, 75.29; H, 7.01; N, 2.21.

(2*R*,3*R*,4*R*,5*R*)-Benzyl 3,4-bis(benzyloxy)-2-(benzyloxymethyl)-5-(1-hydroxypent-4-enyl)pyrrolidine-1-carboxylate (1.34)

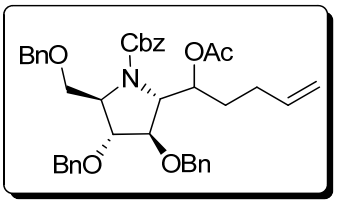

To a solution of (**1.52a/1.52b**) (200 mg, 0.32 mmol) in dry CH_2Cl_2 (10 ml) and TEA (67 mml, 0.48 mmol), acetic anhydride (49 mml, 0.48 mmol) was added slowly at 0 °C. The reaction mixture was stirred at 0 °C for 4 h. Volatiles were evaporated at reduced pressure and then crude was purified by flash column chromatography to get pure **1.34** (126 mg, 59% yield).

Mol. Formula	: $C_{41}H_{45}NO_7$
$[\alpha]_D$	: −36.6 (*c* 1.0, $CHCl_3$)
IR ($CHCl_3$) $\tilde{\nu}$	: 3019, 1735, 1697, 1521, 1454, 1415, 1349, 1096 cm^{-1}
^{1}H NMR (DMSO-d_6, 500	: δ 1.56 (q, *J* = 7.0 Hz, 2H), 1.79–1.88 (m, 1H), 1.92 (s, 3H) 1.90–1.98 (m, 1H), 3.46 (t, *J* = 9.3 Hz, 1H), 3.80 (br s, 1H),

MHz, 333 ^{o}K)	4.02–4.06 (m, 2H), 4.07 (s, 1H), 4.13 (s, 1H), 4.39–4.58 (m, 6H), 4.85–4.89 (m, 2H), 5.10 (s, 2H), 5.47 (br s, 1H), 5.60–5.68 (m, 1H), 7.25–7.36 (m, 20H), ppm.
^{13}C NMR ($CDCl_3$, 75 MHz)	: δ 20.8 (q), 29.2 (t), 29.9 (t), 67.1 (d), 67.6 (d), 67.6 (t, 2C), 71.0 (t), 71.1 (t), 71.4 (d), 73.0 (t), 83.0 (d, 2C), 114.7 (t), 127.4 (d, 3C), 127.6 (d, 3C), 127.7 (d, 3C), 128.1 (d, 1C), 128.3 (d, 4C), 128.4 (d, 3C), 128.5 (d, 3C), 137.6 (d), 137.7 (s, 4C), 154.5 (s), 170.0 (s) ppm.
ESI-MS (*m/z*)	: 686.5 $[M+Na]^+$.
Elemental Analysis	Calcd.: C, 74.18; H, 6.83; N, 2.11. Found: C, 74.23; H, 6.79; N, 2.07.

1,2:5,6-Di-*O*-isopropylidine-D-mannitol (1.54)

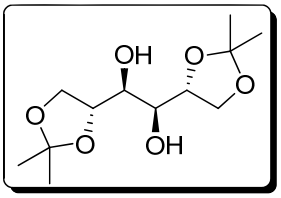

A suspension of powdered D-mannitol, **1.53** (60 g, 0.33 mol), PTSA (300 mg) and 2,2-dimethoxy propane (85.7 g, 0.82 mol) in dry DMSO (100 ml) was stirred at rt. under anhydrous nitrogen. Within one hour the suspended solid was dissolved and after 16 h the reaction mixture was poured into 3% aq. $NaHCO_3$ solution (300 ml). The mixture was extracted with ethyl acetate (4 x 500 ml) and the combined extract was washed with water (1 x 500 ml), dried over Na_2SO_4 and concentrated. The solid residue obtained was recrystallized (2:8, ethylacetate:pet ether) to give diacetonide **1.54** (52 g, 60%) as colorless solid.

Mol. Formula	: $C_{12}H_{22}O_6$
^{1}H NMR ($CDCl_3$, 500 MHz)	: δ 1.35 (s, 6H), 1.41 (s, 6H), 2.62 (br s, 2H), 3.72 (d, *J* = 6.4 Hz, 2H), 3.96 (dd, *J* = 8.5, 5.6 Hz, 2H), 4.10 (dd, *J* = 8.5, 6.5 Hz, 2H), 4.16 (q, *J* = 6.4 Hz, 2H) ppm.
^{13}C NMR ($CDCl_3$, 50 MHz)	: δ 24.4 (q, 2C), 25.8 (q, 2C), 65.9 (t, 2C), 69.5 (d, 2C), 74.0 (d, 2C), 107.5 (s, 2C) ppm.
ESI-MS (*m/z*)	: 285.6 $[M+Na]^+$.

Elemental Analysis	Calcd.: C, 54.95; H, 8.45. Found: C, 54.89; H, 8.39.

1,2 -*O*-isopropylidine-D-glyceraldehyde (1.36)

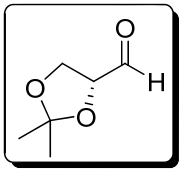

To a vigorously stirred suspension of silica gel-supported $NaIO_4$ (76 g) in CH_2Cl_2 (400 ml) was added a solution of diol **1.54** (10 g, 38 mmol) in CH_2Cl_2 (100 ml). The reaction was monitored by TLC until the disappearance of the starting material. The mixture was filtered through a sintered glass funnel and washed thoroughly with CH_2Cl_2 (400 ml). The filtrate was concentrated to give aldehyde **1.36** (9.3 g, 93%) as colorless oil, which was directly taken for the next step without further purification.

Mol. Formula	: $C_6H_{10}O_3$
^{1}H NMR ($CDCl_3$, 200 MHz)	: δ 1.39 (s, 3H), 1.45 (s, 3H), 4.05–4.08 (m, 1H), 4.12–4.15 (m, 1H), 4.33–4.35 (m, 1H), 9.68 (d, *J* = 2.0 Hz, 1H) ppm.
^{13}C NMR ($CDCl_3$, 50 MHz)	: δ 25.1 (q), 26.2 (q), 65.5 (t), 79.8 (d), 111.1 (s), 201.5 (d) ppm.
Elemental Analysis	Calcd.: C, 55.37; H, 7.74. Found: C, 55.23; H, 7.65.

(*S*)-Ethyl 3-(2,2-dimethyl-1,3-dioxolan-4-yl)acrylate (1.55a/1.55b)

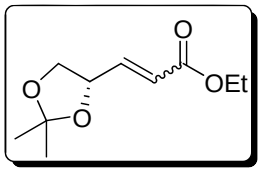

To a solution of *R*-glyceraldehyde **1.36** (2.0 g, 15.4 mmol) in CH_2Cl_2 (50 ml), solid carboethoxymethylene triphenylphosphorane (5.89 g, 16.9 mmol) was added at rt. After 3 h, TLC showed completion of reaction. Solvent was evaporated under reduced pressure and crude mass was purified by column chromatography using ethyl acetate/light petroleum ether (1:9) to afford 1.2:1 mixture of *E*/*Z* olefins (2.8 g, 91%).

Mol. Formula	: $C_{10}H_{16}O_4$
^{1}H NMR	: δ 1.25 (t, *J* = 8.0 Hz, 3H), 1.32 (s, 3H), 1.40 (s, 3H), 3.62 (t, *J* =

($CDCl_3$, 200 MHz), *E*-olefin	8.8 Hz, 1H), 4.15 (m, 3H), 4.64 (m, 1H), 6.08 (d, *J* = 16.0 Hz, 1H), 6.85 (dd, *J* = 6.5 and 16.0 Hz, 1H) ppm.
^{1}H NMR ($CDCl_3$, 200 MHz), *Z*-olefin	: δ 1.25 (t, *J* = 8.0 Hz, 3H), 1.38 (s, 3H), 1.45 (s, 3H), 3.65 (t, *J* = 8.2 Hz, 1H), 4.17 (q, *J* = 8.0 Hz, 2H), 4.36 (t, *J* = 8.0 Hz, 1H), 5.45 (m, 1H), 5.85 (d, *J* = 12.0 Hz, 1H), 6.35 (dd, *J* = 6.2, 12.0 Hz, 1H) ppm.
ESI-MS (*m/z*)	: 223.4 $[M+Na]^+$.
Elemental Analysis	Calcd.: C, 59.98; H, 8.05. Found: C, 56.05; H, 7.99.

(*S*)-Ethyl 3-(2,2-dimethyl-1,3-dioxolan-4-yl)propanoate (1.56)

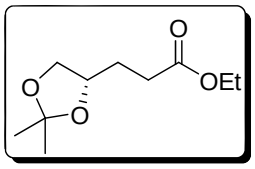

To a solution of *E/Z* mixture of olefins **1.55a/1.55b** (2.0 g, 10 mmol) in 20 ml of EtOAc and catalytic amount of 5% Pd/C (20 mg) was added and the resulting suspension was hydrogenated at balloon pressure (1 atm) for 2 h, then filtered trough celite pad and concentrated to produce 1.92 g, **1.56** (95%) as a colorless liquid.

Mol. Formula	: $C_{10}H_{18}O_4$
$[\alpha]_D$	: +2.0 (*c* 1.2, $CHCl_3$)
IR ($CHCl_3$) $\tilde{\nu}$	: 2988, 1730, 1372, 1216, 1074 cm^{-1}.
^{1}H NMR ($CDCl_3$, 200 MHz)	: δ 1.26 (t, *J* = 7.1 Hz, 3H), 1.33 (s, 3H), 1.39 (s, 3H), 1.80–1.92 (m, 2H), 2.37–2.46 (m, 2H), 3.53 (dd, *J* = 6.4, 7.4 Hz, 1H), 4.00–4.18 (m, 4H) ppm.
^{13}C NMR ($CDCl_3$, 75 MHz)	: δ 14.2 (q), 25.6 (q), 26.9 (q), 28.8 (t), 30.4 (t), 60.1 (t), 69.0 (t), 74.9 (d), 108.9 (s), 172.7 (s) ppm.
ESI-MS (*m/z*)	: 235.3 $[M+Na]^+$.
Elemental Analysis	Calcd.: C, 59.39; H, 8.97. Found: C, 59.42; H, 8.91.

(*S*)-3-(2,2-Dimethyl-1,3-dioxolan-4-yl)propanal (1.57)

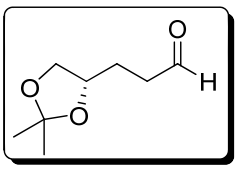

At –78 °C, a solution of **1.56** (606 mg, 3 mmol) in dry CH_2Cl_2 (20 ml) was treated with DIBAL-H (2.16 ml of 1.52 M solution in toluene, 3.30 mmol) and stirred for 1 h. To this saturated solution of sodium potassium tartrate (6 ml) was added and was vigorously stirred at rt for 6 h. The mixture was filtered through a pad of *celite* and it washed with CH_2Cl_2 (40 ml). The combine filtrate was concentrated and the crude aldehyde **1.57** (350 mg, 74%) was used for next step without any further purification.

(2-Tetrahydrofuranyl) diphenylphospine oxide (1.60)

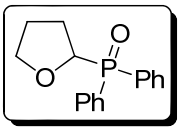

At 0 °C, to a cooled solution of 2,3-dihydrofuran (5.0 ml, 71.3 mmol) and TPP (18.71g, 71.3 mmol) in 50 ml of benzene, the HCl gas was passed for 30 min, and continued stirring for 6 h. The resulting white precipitate was filtered, yielding 22.64 g (86%) of (2-tetrahydrofuranyl)triphenylphosphonium chloride **1.59** as a low melting solid (MP–70 °C). The phosphonium salt was treated with aqueous NaOH (50 ml, 1N) at reflux for 2 h. The salt gradually dissolved and the resulting solution was extracted with CH_2Cl_2. The combine CH_2Cl_2 layer was dried (Na_2SO_4) and evaporated at reduced pressure to yield 14.5 g, **1.60** (87%) as a white free flowing solid.

Mol. Formula	: $C_{16}H_{17}O_2P$
M. P.	: 115 °C
IR ($CHCl_3$) $\tilde{\nu}$	: 3059, 2978, 2874, 1591, 1484, 1437, 1182, 1120, 1058, 696, 541 cm^{-1}.
^{1}H NMR ($CDCl_3$, 200 MHz)	: δ 1.70–1.87 (m, 2H), 2.12–2.31 (m, 2H), 3.68 (q, *J* = 7.1, 1H), 3.86 (q, *J* = 6.8, 1H), 4.71 (q, *J* = 7.8, 1H), 7.46–7.50 (m, 6 H), 7.84–7.92 (m, 4H) ppm.
^{13}C NMR ($CDCl_3$, 50 MHz)	: δ 25.6 (t, *J* = 4.7 Hz), 26.2 (t), 69.8 (t, *J* = 4.7 Hz), 75.8 (t, *J* = 90.4 Hz), 127.9 (d, *J* = 12.1 Hz, 4C), 130.7 (s, *J* = 96.6 Hz, 2C), 130.8 (d, *J* = 9.1 Hz, 2C), 131.4 (d, *J* = 1.8 Hz, 2C), 131.8 (d, *J* = 8.4 Hz, 2C) ppm.
ESI-MS (*m/z*)	: 295.3 $[M+Na]^+$.
Elemental Analysis	Calcd.: C, 70.58; H, 6.29. Found: C, 70.63; H, 6.32.

(5*R*,7*S*)-1,6-Dioxaspiro[4.5]decan-7-ylmethanol (1.63)

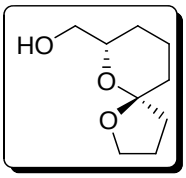

At –78 °C, a solution of aldehyde **1.57** (820 mg, 5.18 mmol) was treated with the ylide [prepared at –78 °C by treatment of phosphonate **1.60** (2.66 g, 9.81 mmol) in THF-Et_2O (3:1), with a freshly prepared LDA (10.79 mmol) solution. After stirring for 30 min, dark red color was developed indicating the formation of an anion.] Stirred for additional 3 h, to this water (40 ml) was introduced and warmed slowly to rt. Solid K_2CO_3 (3 g) was added and the organic layer was separated. The aq. Layer was extracted with ethylacetate; combined organic layer was dried (Na_2SO_4) and concentrated under reduced pressure to procure **1.61** in quantitative yield.

To complete Wittig-Horner reaction, the solution of potassium *tert* butoxide (1.14 g, 10.25 mmol) in 50 ml dry THF was added in one portion to a solution of adduct in 50 ml of THF. Slowly color change was observed from light red to dark blackish red for Stirring for 1 h at rt. Volatiles were evaporated at temperature not exceeding 40 °C, then CH_2Cl_2 (3 ml) was added, diluted with Et_2O and water which was extracted. The combined organic layer was dried (Na_2SO_4) and concentrated to give pale yellow enol ether.

Crude enol ether was dissolved in methanol and camphor sulfonic acid (5 mg) was added, and stirred at rt for 24 h, the crude was evaporated at reduced pressure and purified by column chromatography to yield **1.63** (315 mg, 38% overall yield).

Mol. Formula	: $C_9H_{16}O_3$
$[\alpha]_D$	: +84.7 (*c* 1.0, $CHCl_3$)
IR ($CHCl_3$) $\tilde{\nu}$	: 3458, 3009, 2947, 1458, 1374, 1046, 1010 cm^{-1}.
^{1}H NMR ($CDCl_3$, 500 MHz)	: δ 1.20–1.29 (m, 1H), 1.42–1.46 (m, 1H), 1.57–1.66 (m, 4H), 1.76–1.84 (m, 1H), 1.85–1.91 (m, 1H), 1.93–2.01 (m, 1H), 2.25 (br s, 1H), 3.37–3.41 (m, 1H), 3.36–3.50 (m, 1H), 3.77–3.84 (m, 3H) ppm.
^{13}C NMR ($CDCl_3$, 125 MHz)	: δ 19.7 (t), 23.7 (t), 26.4 (t), 33.0 (t), 37.7 (t), 66.0 (t), 66.7 (t), 71.0 (d), 106.0 (s) ppm.
ESI-MS (*m/z*)	: 205.2 $[M+Na]^+$.

Elemental Analysis	Calcd.: C, 62.77; H, 9.36. Found: C, 62.81; H, 9.31.

(5*R*,7*S*)-7-Vinyl-1,6-dioxaspiro[4.5]decane (1.35)

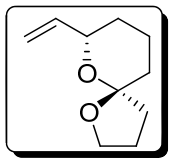

To a flame-dried 100 ml flask with oxalyl chloride (1.49 ml, 17.4 mmol) in 20 ml CH_2Cl_2, at −78 °C under Argon was added a solution of DMSO (1.85 ml, 26.1 mmol) in 5 ml CH_2Cl_2. The reaction was stirred 20 min. at −78 °C then treated with a solution of spiro alcohol **1.63** (1 g, 5.8 mmol) in CH_2Cl_2 (2 ml). Stirring was continued at –78 °C for additional 1 h and then Et_3N (4.84 ml, 34.9 mmol) was added.

The reaction mixture was slowly warmed to –0 °C and stirred at this temp for 20 min. The reaction was quenched with water (10 ml) and extracted with ethyl acetate, the organic layer was washed with aq. 1 M HCl (50 ml), $NaHCO_3$ (50 ml), brine (50 ml), dried (Na_2SO_4) and concentrated under reduced pressure to yield **1.64** (920 mg, 93%).

At 0 °C, a solution of aldehyde **1.64** (920 mg, 5.4 mmol) was treated with the ylide [prepared at 0 °C by treatment of methyltriphenylphosphonium bromide (5.79 g, 16.2 mmol) in THF, with a solution of *n*-BuLi (1.5 M, 9 ml, 13.5 mmol). After stirring for 30 min, orange color was developed indicating the formation of an anion.] Stirred for additional 1 h at rt, to this aq. NH_4Cl (10 ml) was introduced. The aq. layer was extracted with Et_2O; combined organic layer was dried (Na_2SO_4) and concentrated under reduced pressure to procure low boiling volatile **1.35** which was directly used for next step without any further purification.

(2*R*,3*R*,4*R*,5*R*)-Benzyl 2-((*R*)-1-acetoxy-5-((5*R*,7*S*)-1,6-dioxaspiro[4.5]decan-7-yl)pent-4-enyl)-3,4-bis(benzyloxy)-5-(benzyloxymethyl)pyrrolidine-1-carboxylate (1.65)

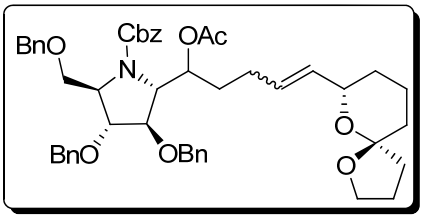

To a solution of chiral core subunit **1.34**, (40 mg, 0.06 mmol) and spiroketal side chain **1.35**, (50 mg, 0.30 mmol) in dry DCM (6 ml), Grubbs' I catalyst **1.4**, (10.6 mg, 0.012 mmol) was added and purged with argon. The contents were stirred at rt for 48 h with bubbling of argon gas. Volatiles were evaporated under reduced pressure. The residue obtained was purified by column chromatography (17:3 petroleum ether/ethyl

acetate) to afford inseparable mixture of *E* /*Z* isomers (**1.65**) (20 mg, 41%) as colorless oil, along with spiroketal side chain **1.66** (5 mg, 27%) as a pale yellow liquid.

Mol. Formula	: $C_{49}H_{57}NO_9$
$[\alpha]_D$	: −10.6 (*c* 1.3, MeOH)
IR ($CHCl_3$) $\tilde{\nu}$	: 3017, 2928, 2855, 1736, 1698, 1454, 1412, 1094 cm^{-1}.
^{1}H NMR (DMSO-d_6, 500 MHz, 343 ^oK)	: δ 1.48–1.66 (m, 9H), 1.73–1.85 (m, 5H), 1.92 (s, 3H), 1.93 (m, 2H), 3.48 (t, *J* = 9.4 Hz, 1H), 3.73–3.82 (m, 3H), 4.03–4.07 (m, 4H), 4.13 (br s, 1H), 4.41 (d, *J* = 12.4 Hz, 1H), 4.48–4.53 (m, 4H), 4.56 (d, *J* = 12.4 Hz, 1H), 5.10 (dd, *J* = 12.4, 17.9 Hz, 2H), 5.32 (dd, *J* = 5.5, 15.6 Hz, 1H), 5.41–5.46 (m, 2H), 7.26–7.36 (m, 20H) ppm.
^{13}C NMR (DMSO-d_6, 500 MHz, 333 ^oK)	: δ 19.6 (t), 20.2 (q), 23.2 (t), 27.6 (t), 28.6 (t), 30.5 (t), 32.4 (t), 37.3 (t), 63.4 (d), 65.7 (d), 66.0 (t), 66.2 (t), 69.8 (d), 70.4 (t), 70.5 (t), 70.7 (d), 72.2 (t), 82.5 (d), 82.6 (d), 105.2 (s), 127.1 (d, 3C), 127.1 (d, 2C), 127.17 (d, 3C), 127.22 (d, 2C), 127.3 (d), 127.5 (d), 127.6 (d), 127.9 (d, 3C), 128.0 (d, 2C), 128.1 (d, 2C), 128.5 (d), 132.0 (d), 136.3 (s), 137.5 (s, 2C), 138.0 (s), 153.6 (s), 169.2 (s) ppm.
ESI-MS (*m/z*)	: 826.1 $[M+Na]^+$.
Elemental Analysis	Calcd.: C, 73.20; H, 7.15; N, 1.74. Found: C, 73.17; H, 7.11; N, 1.69.

1-((5R,7S)-1,6-Dioxaspiro[4.5]decan-7-yl)-2-((R)-1,6-dioxaspiro[4.5]decan-7-yl)ethene (1.66)

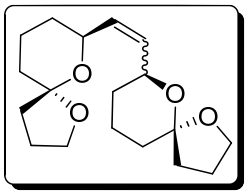

Mol. Formula	: $C_{18}H_{28}O_4$
^{1}H NMR ($CDCl_3$, 200 MHz)	: δ 1.53–1.64 (m, 12H), 1.82–1.98 (m, 8H), 3.81 (t, *J* = 6.6 Hz, 4H), 4.16 (d, *J* = 12.0 Hz, 2H), 5.53–5.54 (m, 2H) ppm.
ESI-MS (*m/z*)	: 331.6 $[M+Na]^+$.

(5*R*,6*R*,7*R*,7a*R*)-6,7-bis(benzyloxy)-5-(benzyloxymethyl)-1-(but-3-enyl)tetrahydropyrrolo[1,2-c]oxazol-3(1*H*)-one (1.69a/1.69b)

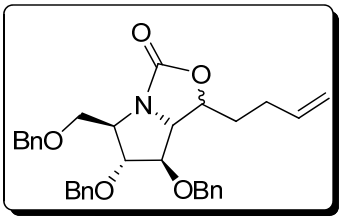

To a suspension of NaH (9.1 mg, 0.3 mmol) in THF, solution of alcohols **1.52a/1.52b** (120 mg, 0.19 mmol) was added at 0 °C. Then it was slowly allowed warm to rt and stirring continued for additional 30 min. Excess of hydride was quenched by addition of ice cooled water (2 ml) at 0 °C. The reaction mixture was further diluted with water (20 ml) and extracted with EtOAc. The combined extract was dried on Na_2SO_4 and evaporated under reduced pressure. The residue was purified by column chromatography (15:3 petroleum ether/ethyl acetate) to afford bicyclic mixture **1.69a/1.69b** (54 mg, 54%) in ratio (1:2.2) as colorless oil.

Mol. Formula	: $C_{32}H_{35}NO_5$
IR ($CHCl_3$) $\tilde{\nu}$	: 3015, 2927, 1755, 1671, 1454, 1365, 1216, 1111, 1027, 755 cm^{-1}.
^{1}H NMR ($CDCl_3$, 500 MHz)	: δ 1.63–1.82 (m, 2H), 2.08–2.27 (m, 2H), 3.52–3.54 (m, 2H), 3.82–3.88 (m, 1H), 3.97–4.00 (m, 1/2H), 4.10–4.14 (m, 1H), 4.20–4.22 (m, 1H), 4.23–4.25 (m, 1/2H), 4.38–4.46 (m, 2H), 4.50–4.60 (m, 5H), 4.98–5.04 (m, 2H), 5.67–5.78 (m, 1H), 7.21–7.32 (m, 15H) ppm.
^{13}C NMR ($CDCl_3$, 500 MHz)	: Major δ 28.7 (t), 34.5 (t), 62.3 (d), 67.4 (d), 69.7 (t), 71.9 (t), 72.5 (t), 73.3 (t), 79.2 (d), 85.4 (d), 87.9 (d), 115.9 (t), 127.6 (d, 2C), 127.8 (d, 2C), 128.0 (d, 2C), 128.4 (d, 7C), 128.6 (d, 2C), 136.6 (d), 137.4 (s), 137.5 (s), 137.8 (s), 160.3 (s) ppm. Minor δ 29.4 (t), 29.9 (t), 62.4 (d), 64.6 (d), 70.4 (t), 72.0 (t), 72.1 (t), 73.4 (t), 75.6 (d), 82.3 (d), 86.4 (d), 115.9 (t), 127.9 (d, 2C), 127.73 (d, 2C), 127.9 (d, 2C), 128.0 (d), 128.07 (d, 2C), 128.12 (d, 2C), 128.2 (d, 2C), 128.4 (d, 2C), 136.7 (d), 137.1 (s), 137.5 (s), 137.7 (s), 160.4 (s) ppm.
ESI-MS (*m/z*)	: 536.6 $[M+Na]^+$.

(5*R*,6*R*,7*R*,7a*R*)-1-(4-((5*R*,7*S*)-1,6-dioxaspiro[4.5]decan-7-yl)but-3-enyl)-6,7-bis(benzyloxy)-5-(benzyloxymethyl)tetrahydropyrrolo[1,2-c]oxazol-3(1*H*)-one (1.70a/1.70b)

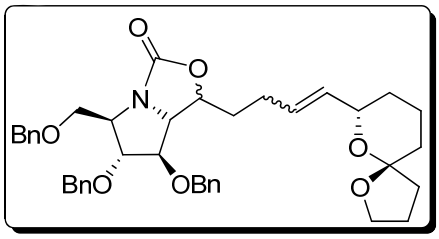

To a solution of oxazolidinones **1.69a/1.69b**, (50 mg, 0.097 mmol) and spiroketal side chain **1.35**, (82 mg, 0.486 mmol) in dry DCM (10 ml), Grubbs' I catalyst **1.4**, (16 mg, 0.020 mmol) was added and purged with argon. The contents were stirred at rt for 48 h with bubbling of argon gas. Volatiles were evaporated under reduced pressure. The residue obtained was purified by column chromatography (17:3; petether/ethyl acetate) to afford inseparable mixture of *E* /*Z* isomers **1.70a/1.70b** (24 mg, 38%) as colorless oil.

Mol. Formula	: $C_{40}H_{47}NO_7$
IR ($CHCl_3$) $\tilde{\nu}$	: 3019, 1749, 1645, 1427, 1215, 1046, 756, 669 cm^{-1}.
^{1}H NMR ($CDCl_3$, 300 MHz)	: δ 1.40–1.65 (m, 8H), 1.77–2.23 (m, 6H), 3.47 (d, *J* = 6.0 Hz, 2H), 3.78–3.81 (m, 2H), 4.04–4.15 (m, 4H), 4.36–4.53 (m, 8H), 5.35–5.56 (m, 2H), 7.14–7.23 (m, 15H) ppm.
^{13}C NMR ($CDCl_3$, 300 MHz)	: Major δ 20.2 (t), 23.8 (t), 27.3 (t), 29.6 (t), 31.0 (t), 32.9 (t), 38.0 (t), 62.4 (d), 66.9 (t), 67.4 (d), 69.7 (t), 70.7 (d), 72.0 (t), 72.5 (t), 73.3 (t), 79.4 (d), 85.7 (d), 88.0 (d), 106.0 (s), 127.7 (d, 3C), 127.9 (d, 3C), 128.0 (d, 2C), 128.2 (d), 128.3 (d, 4C), 128.6 (d, 2C), 128.9 (d), 133.0 (d), 137.4 (s), 137.5 (s), 137.9.0 (s), 160.4 (s) ppm.
ESI-MS (*m/z*)	: 654.5 $[M+Na]^+$.
Elemental Analysis	Calcd.: C, 73.48; H, 7.25; N, 2.14. Found: C, 73.41; H, 7.19; N, 2.09.

(1*S*,5*R*,6*R*,7*R*,7a*S*)-1-(4-((5*R*,7*R*)-1,6-Dioxaspiro[4.5]decan-7-yl)butyl)-6,7-dihydroxy-5-(hydroxymethyl)tetrahydropyrrolo[1,2-c]oxazol-3(1*H*)-one (1.71)

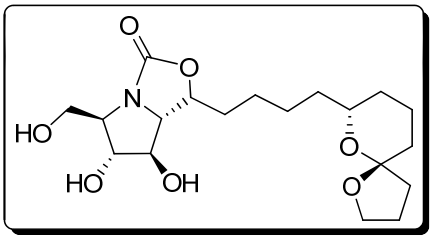

To a solution of *E* /*Z* isomers **1.70a/1.70b** (24 mg, 0.036 mmol) in MeOH (5 ml), $Pd(OH)_2$ (1 mg) was added and stirred under hydrogen atmosphere (ballon) for 6 h. The

reaction mixture was filtered through a pad of celite and concentrated. The residue was purified by preparative TLC using MeOH:$CHCl_3$ (1:19) as solvent system, which resulted **1.71** (10 mg, 70%) as a colorless liquid.

Mol. Formula	: $C_{19}H_{31}NO_7$
$[\alpha]_D$	: +7.9 (*c* 1.2, MeOH)
IR ($CHCl_3$) $\tilde{\nu}$	: 3458, 3009, 2947, 2923, 1747, 1462, 1376, 1149, 1046, 1010, 722 cm^{-1}.
^{1}H NMR (Acetone-d_6, 500 MHz)	: δ 1.11–1.16 (m, 1H), 1.30–1.43 (m, 6H), 1.46–1.64 (m, 6H), 1.75–1.84 (m, 4H), 1.92–2.01 (m, 1H), 3.43–3.61 (m, 2H), 3.63–3.73 (m, 2H), 3.77–3.92 (m, 2H), 4.10–4.20 (m, 1H), 4.41–4.48 (m, 1H), 4.58–4.87 (m, 2H) ppm.
^{13}C NMR (Acetone-d_6, 500 MHz)	: δ 21.1 (t), 24.3 (t), 25.2 (t), 26.0 (t), 31.8 (t), 33.6 (t), 36.2 (t), 36.7 (t), 38.4 (t), 62.7 (t), 65.5 (d), 67.0 (t), 67.7 (d), 69.1 (d), 70.4 (d), 77.3 (d), 80.1 (d), 81.1 (d), 106.2 (s), 161.6 (s) ppm.
ESI-MS (*m/z*)	: 408.3 $[M+Na]^+$.
Elemental Analysis	Calcd.: C, 59.20; H, 8.11; N, 3.63. Found: C, 59.15; H, 8.09; N, 3.58

(+)-Broussonetine G (1.28)

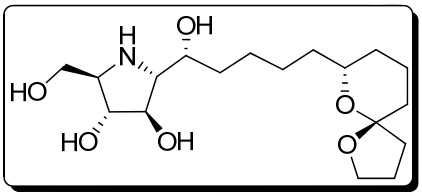

To a cooled solution of **1.71** (10 mg, 0.026 mmol) in EtOH:H_2O (3:1), solid NaOH (2.6 mg, 0.064 mmol) was added at 0 °C. Reaction mixture was allowed to warm to rt, stirred for 2 h. TLC in solvent system MeOH:$CHCl_3$:NH_4OH (1:19:0.5) showed the completion of reaction. Ethanol was evaporated at reduced pressure. The residue was purified by preparative TLC using MeOH:$CHCl_3$:NH_4OH (1:19:0.3) as solvent system, which resulted **1.28** (7 mg, 75%) as a light white film.

Mol. Formula	: $C_{18}H_{33}NO_6$
$[\alpha]_D$	: +20.8 (*c* 1.0, MeOH) (lit +19.3 (*c* 0.74, MeOH))
IR ($CHCl_3$) $\tilde{\nu}$	: 3352, 3019, 2939, 1641, 1428, 1385, 1215, 1071, 754, 669 cm^{-1}.
^{1}H NMR (Pyridine-d_5, 500	: δ 1.10–1.13 (m, 1H), 1.38–1.41 (m, 4H), 1.59–1.64 (m, 7H), 1.86–1.94 (m, 6H), 3.52–3.57 (m, 1H), 3.80–3.85 (m, 4H),

MHz)	3.99–4.04 (m, 1H), 4.21–4.23 (m, 1H), 4.32 (dd, *J* = 2.9, 10.8 Hz, 1H), 4.72 (d, *J* = 5.9 Hz, 1H), 5.05 (d, *J* = 5.9 Hz, 1H), 5.19 (br s, 1H, -OH), 8.55 (br s, 1H, -OH) ppm.
^{13}C NMR (Pyridine-d_5, 500 MHz)	: δ 21.1 (t), 24.2 (t), 26.4 (t), 26.8 (t), 31.3 (t), 33.4 (t), 35.4 (t), 36.6 (t), 38.2 (t), 64.8 (t), 65.9 (d), 66.8 (t), 67.6 (d), 70.2 (d), 74.0 (d), 80.6 (d), 81.9 (d), 105.9 (s) ppm.
ESI-MS (*m/z*)	: 360.2 $[M+Na]^+$.
Elemental Analysis	Calcd.: C, 60.14; H, 9.25; N, 3.90. Found: C, 60.09; H, 9.19; N, 3.84.

(2*R*,3*R*,4*R*,5*R*)-Benzyl 3,4-bis(benzyloxy)-2-(benzyloxymethyl)-5-vinylpyrrolidine-1-carboxylate (1.33)

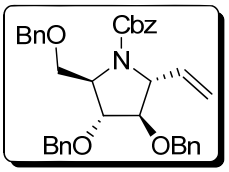

To a suspension of methyltriphenylphosphonium bromide (6.32 g, 17.68 mmol) in (30 + 10 ml) THF and ether, $NaNH_2$ (620 mg, 15.91 mmol) was added and stirred overnight. A thick yellow color indicated the formation of anion, which was cannulated dropwise to a solution of aldehyde **1.37** (1 g, 1.77 mmol) in THF (20 ml) at 0 °C and stirring was continued for 1 h at rt. The reaction was quenched by addition of saturated NH_4Cl solution (10 ml), diluted with EtOAc (50 ml) and H_2O (15 ml). The aqueous layer was washed with (2 x 50 ml) EtOAc, the organic layers combined, washed with brine; dried over $NaSO_4$ and was evaporated at reduced pressure yielding thick syrup which was purified by column chromatography (4:21 EtOAc/hexane) to yield **1.33** (220 mg, 22%).

Mol. Formula	: $C_{36}H_{37}NO_5$
$[\alpha]_D$	: −7.6 (*c* 1.0, $CHCl_3$)
IR ($CHCl_3$) $\tilde{\nu}$	: 3087, 3064, 3030, 2926, 2862, 1701, 1496, 1454, 1407, 1350, 1215, 1096, 753 cm^{-1}.
^{1}H NMR (DMSO-d_6, 500 MHz, 343 ^oK)	: δ 3.48 (t, *J* = 9.5 Hz, 1H), 3.82 (br s, 1H), 3.94 (s, 1H), 4.10 (dd, *J* = 3.8, 9.8 Hz, 1H), 4.15 (s, 1H), 4.36 (d, *J* = 7.8 Hz, 1H), 4.41 (br s, 1H), 4.47–4.56 (m, 5H), 5.01–5.14 (m, 4H), 5.80 (ddd, *J* = 7.8, 10.0, 17.3 Hz, 1H), 7.24–7.35 (m, 20H) ppm.
^{13}C NMR (DMSO-d_6, 125 MHz, 343 °K)	: δ 63.1 (d), 66.2 (t), 66.4 (t), 67.8 (d), 70.4 (t), 70.8 (t), 72.3 (t), 82.0 (d), 85.6 (d), 115.9 (t), 127.3 (d, 3C), 127.4 (d, 4C), 127.48 (d), 127.5 (d), 127.7 (d), 128.1 (d, 3C), 128.14 (d, 3C), 128.2 (d,

4C), 136.5 (d), 136.6 (s), 137.6 (s), 137.8 (s), 138.2 (s), 154.0 (s) ppm.

ESI-MS (*m/z*) : 586.6 $[M+Na]^+$.

Elemental Analysis Calcd.: C, 76.71; H, 6.62; N, 2.48. Found: C, 76.68; H, 6.57; N, 2.43.

Dec-9-enal (1.73)

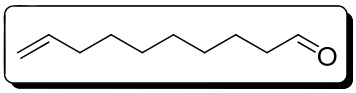

To a solution of IBX (13.44 g, 48 mmol) in 45 ml DMSO, commercially available 9-Decene-ol (**1.72**, 3 g, 19.2 mmol) was added at 0 °C. Reaction mixture was slowly allowed to rise to rt and stirred for additional 1 h. To this (20 ml) water was added and stirred vigorously which resulted in white precipitation To it 50 ml of ether was added and the resulting suspension was filtered through a pad of celite. The organic layer was dried (Na_2SO_4) and crude was purified by column chromatography (1:9 EtOAc/hexane) to yield **1.73** (2.7 g, 91%).

Mol. Formula : $C_{10}H_{18}O$

IR ($CHCl_3$) $\tilde{\nu}$: 3019, 2930, 2976, 2400, 1708, 1638, 1612, 1514, 1424, 1216, 1084, 1045, 928, 669 cm^{-1}.

^{1}H NMR ($CDCl_3$, 200 MHz) : δ 1.32 (br s, 8H), 1.61 (q, *J* = 7.2 Hz, 2H), 2.02 (q, *J* = 6.8 Hz, 2H), 2.36 (t, *J* = 7.2 Hz, 2H), 4.88–5.05 (m, 2H), 5.69–5.86 (m, 1H), 9.93 (br s, 1H) ppm.

^{13}C NMR ($CDCl_3$, 50 MHz) : δ 24.5 (t), 28.7 (t), 28.7 (t), 28.8 (t), 28.9 (t), 33.6 (t), 33.9 (t), 114.1 (t), 138.6 (d), 179.7 (s) ppm.

ESI-MS (*m/z*) : 155.3 $[M+1]^+$.

Elemental Analysis Calcd.: C, 77.87; H, 11.76. Found: C, 77.92; H, 11.71.

1-(Benzyloxy)tridec-12-en-4-ol (1.74)

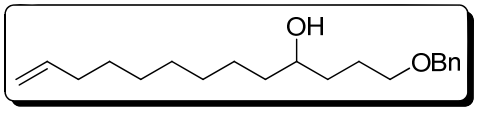

At 0 °C, a solution of aldehyde **1.73** (4.09 g, 26.52 mmol) in THF was treated with 3-(benzyloxy)-propylmagnesium bromide [prepared from ((3-bromopropoxy)methyl)benzene (9.1 g, 79.55 mmol) and Mg (1.93 g, 79.55 mmol)] in ether (100 ml) and the contents were stirred for 2 h at rt. The reaction mixture was quenched with sat. NH_4Cl (10 ml) and extracted with EtOAc (3 x 25 ml). The combined

organic extract was dried, concentrated and the crude was purified by column chromatography (3:17 EtOAc/hexane) to yield **1.74** (6.64 g, 82%).

Mol. Formula	: $C_{20}H_{32}O_2$
IR ($CHCl_3$) $\tilde{\nu}$	: 3448, 3019, 2930, 2976, 2400, 1638, 1612, 1514, 1424, 1216, 928, 669cm^{-1}.
^{1}H NMR ($CDCl_3$, 200 MHz)	: δ 1.30 (br s, 8H), 1.38–1.48 (m, 5H), 1.54–1.63 (m, 1H), 1.67–1.76 (m, 2H), 2.03 (q, *J* = 6.95 Hz, 2H), 3.50 (t, *J* = 3.81 Hz, 2H), 3.56–3.64 (m, 1H), 4.51 (s, 2H), 4.86–5.03 (m, 2H), 5.69–5.89 (m, 1H), 7.29–7.33 (m, 5H) ppm.
^{13}C NMR ($CDCl_3$, 50 MHz)	: δ 25.4 (t), 25.7 (t), 28.6 (t), 28.8 (t), 29.2 (t), 29.4 (t), 33.5 (t), 34.0 (t), 37.1 (t), 70.1 (t), 70.8 (d), 72.5 (t), 113.9 (t), 127.1 (d), 127.2 (d, 2C), 127.9 (d, 2C), 137.9 (s), 138.6 (d) ppm.
ESI-MS (*m/z*)	: 305.4 $[M+1]^+$.
Elemental Analysis	Calcd.: C, 78.90; H, 10.59. Found: C, 78.84; H, 10.54.

1-(Benzyloxy)tridec-12-en-4-one (1.40)

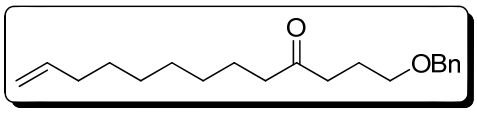

To a solution of IBX (4.6 g, 16.4 mmol) in 15 ml DMSO, **1.74** (3 g, 19.2 mmol) in THF (10 ml) was added at 0 °C. Reaction mixture was slowly allowed to rise to rt and stirred for additional 1 h. To this (20 ml) water was added and stirred vigorously which resulted in white precipitation. To it 50 ml of ether was added and the resulting suspension was filtered through a pad of celite. The organic layer was dried (Na_2SO_4) and crude was purified by column chromatography (1:9 EtOAc/hexane) to yield **1.40** (1.55 g, 78 %).

Mol. Formula	: $C_{20}H_{30}O_2$
IR ($CHCl_3$) $\tilde{\nu}$	: 3017, 2930, 2976, 1710, 1639, 1612, 1514, 1424, 1216, 1096, 1045, 928, 669 cm^{-1}.
^{1}H NMR ($CDCl_3$, 200 MHz)	: δ 1.26–1.28 (m, 8H), 1.51–1.61 (m, 2H), 1.81–1.94 (m, 2H), 1.97–2.07 (m, 2H), 2.37 (t, *J* = 7.4 Hz, 2H), 2.50 (t, *J* = 7.1 Hz, 2H), 3.46 (t, *J* = 6.1 Hz, 2H), 4.46 (s, 2H), 4.88–5.03 (m, 2H), 5.71–5.88 (m, 1H), 7.25–7.34 (m, 5H) ppm.
^{13}C NMR ($CDCl_3$, 50 MHz)	: δ 23.5 (t), 23.6 (t), 28.6 (t), 28.7 (t), 28.9 (t), 29.0 (t), 33.5 (t), 38.9 (t), 42.5 (t), 69.0 (t), 72.5 (t), 114.0 (t), 127.2 (d), 127.3 (d,

2C), 128.0 (d, 2C), 138.2 (s), 138.6 (d), 209.8 (s) ppm.

ESI-MS (*m/z*)	: 303.6 $[M+1]^+$.
Elemental Analysis	Calcd.: C, 79.42; H, 10.00. Found: C, 79.37; H, 9.93.

2-(3-(Benzyloxy)propyl)-2-(non-8-enyl)-1,3-dioxane (1.75)

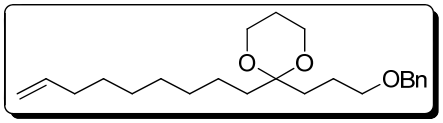

A solution of **1.40** (600 mg, 1.98 mmol), 1,3 propane diol (0.71 ml, 9.92 mmol) and PTSA (10 mg) in 30 ml benzene was refluxed for 24 h. The water formed in the reaction was azotropically removed using deanstork apparatus. The reaction mixture was concentrated at reduced pressure and the residue was purified by column chromatography (2:23 EtOAc/hexane) to yield 13-C side chain **1.75** (395 mg, 55%).

Mol. Formula	: $C_{23}H_{36}O_3$
IR ($CHCl_3$) $\tilde{\nu}$	: 3017, 2929, 2857, 1640, 1454, 1363, 1215, 1098, 914, 668 cm^{-1}.
^{1}H NMR ($CDCl_3$, 200 MHz)	: δ 1.29 (br s, 10H), 1.60–1.79 (m, 8H), 1.98–2.08 (m, 2H), 3.48 (t, *J* = 6.0 Hz, 2H), 3.86 (t, *J* = 5.6 Hz, 4H), 4.50 (s, 2H), 4.87–5.03 (m, 2H), 5.69–5.89 (m, 1H), 7.24–7.34 (m, 5H) ppm.
^{13}C NMR ($CDCl_3$, 50 MHz)	: δ 23.1 (t), 23.6 (t), 25.4 (t), 28.8 (t), 29.0 (t), 29.4 (t), 29.9 (t), 30.5 (t), 33.7 (t), 34.0 (t), 59.1 (t, 2C), 70.4 (t), 72.6 (t), 100.2 (t), 114.2 (t), 127.3 (d), 127.4 (d, 2C), 128.2 (d, 2C), 138.6 (s), 138.9 (d) ppm.
ESI-MS (*m/z*)	: 361.3 $[M+1]^+$.
Elemental Analysis	Calcd.: C, 76.62; H, 10.06. Found: C, 76.57; H, 10.02.

1,16-bis(2-(3-(Benzyloxy)propyl)-1,3-dioxan-2-yl)hexadec-8-ene (1.76)

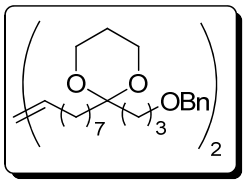

To a solution of olefinic subunit **1.33**, (35 mg, 0.062 mmol) and C-13 side chain **1.75**, (111 mg, 0.310 mmol) in dry DCM (10 ml), Grubbs' II catalyst **1.5**, (10.2 mg, 0.012 mmol) was added and purged with argon. The contents were stirred at rt for 24 h with bubbling of argon gas. Volatiles were evaporated under reduced pressure. The residue obtained was purified by column chromatography (18:2 petroleum ether/ethyl acetate) to

afford side chain dimmer (**1.76**) (30 mg, 69%) as colorless oil, ketal deprotected dimmer **1.77** (9 mg, 25%) as a colorless liquid along with ketal deprotected side chain **1.40** (21 mg).

Mol. Formula	: $C_{44}H_{68}O_6$
IR ($CHCl_3$) $\tilde{\nu}$	: 3017, 2857, 1639, 1453, 1359, 1216, 1097, 667 cm^{-1}.
^{1}H NMR ($CDCl_3$, 200 MHz)	: δ 1.26–1.28 (m, 16H), 1.50–1.67 (m, 8H), 1.79–2.05 (m, 8H), 2.37 (t, *J* = 7.2 Hz, 2H), 2.50 (t, *J* = 7.2 Hz, 2H), 3.47–3.51 (m, 4H), 3.80–3.88 (m, 4H), 4.46–4.50 (m, 4H), 5.32–5.37 (m, 2H), 7.24–7.33 (m, 10H) ppm.
ESI-MS (*m/z*)	: 693.5 $[M+1]^+$.
Elemental Analysis	Calcd.: C, 76.26; H, 9.89. Found: C, 76.19; H, 9.85.

1,24-bis(Benzyloxy)tetracos-12-ene-4,21-dione (1.77)

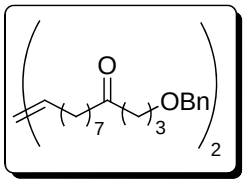

Mol. Formula	: $C_{38}H_{56}O_4$
IR ($CHCl_3$) $\tilde{\nu}$	: 3067, 3026, 2926, 2854, 1713, 1495, 1454, 1362, 1216, 1028, 968, 755 cm^{-1}.
^{1}H NMR ($CDCl_3$, 200 MHz)	: δ 1.26 (br s, 16H), 1.51–1.58 (m, 4H), 1.82–1.96 (m, 8H), 2.38 (t, *J* = 7.4 Hz, 4H), 2.51 (t, *J* = 7.2 Hz, 4H), 3.47 (t, *J* = 6.1 Hz, 4H), 4.48 (s, 4H), 5.36–5.39 (m, 2H), 7.29–7.35 (m, 10H) ppm.
^{13}C NMR ($CDCl_3$, 50 MHz)	: δ 23.1 (t, 2C), 23.3 (t, 2C), 28.4 (t, 2C), 28.6 (t, 2C), 28.7 (t, 2C), 28.9 (t, 2C), 32.0 (t, 2C), 38.5 (t, 2C), 42.0 (t, 2C), 68.7 (t, 2C), 72.0 (t, 2C), 126.7 (d, 2C), 126.8 (d, 4C), 127.6 (d, 4C), 129.6 (d, 2C), 138.0 (s, 2C), 209.0 (s, 2C) ppm.
ESI-MS (*m/z*)	: 577.8 $[M+1]^+$.
Elemental Analysis	Calcd.: C, 79.12; H, 9.78. Found: C, 79.07; H, 9.73.

(2*R*,3*R*,4*R*,5*R*)-Benzyl 3,4-bis(benzyloxy)-2-(13-(benzyloxy)-10-oxotridec-1-enyl)-5-(benzyloxymethyl)pyrrolidine-1-carboxylate (1.78)

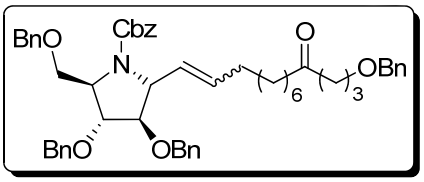

To a solution of olefin derivative **1.33** (42 mg, 0.074 mmol) and keto side chain **1.40** (113 mg, 0.372 mmol) in dry DCM (10 ml), Grubbs' II catalyst **1.5**, (12.3 mg, 0.015 mmol) was added and purged with argon. The reaction mixture was refluxed at 40 °C for 10 h under argon gas atmosphere. Volatiles were evaporated under reduced pressure and the residue obtained was purified by column chromatography (18:2 petroleum ether/ethyl acetate) to afford cross metathesis product **1.78** (17 mg, 27%) as colorless oil, keto side chain dimmer **1.77** (46 mg) along with unreacted chiral core subunit **1.33** (23 mg).

Mol. Formula : $C_{54}H_{63}NO_7$

$[\alpha]_D$: –13.5 (*c* 0.5, $CHCl_3$)

IR ($CHCl_3$) $\tilde{\nu}$: 3017, 2929, 2858, 1734, 1699, 1585, 1497, 1454, 1410, 1351, 1216, 1098, 756 cm^{-1}.

^{1}H NMR ($CDCl_3$, 500 MHz) : δ 1.26 (br s, 10H), 1.53–1.55 (m, 2H), 1.88 (qui, *J* = 6.6 Hz, 2H), 2.36 (t, *J* = 7.5 Hz, 2H), 2.49–2.52 (m, 2H), 3.47 (t, *J* = 6.0 Hz, 2H), 3.50–3.53 (m, 1H), 3.70–4.02 (m, 2H), 4.17 (s, 1H), 4.28–4.64 (m, 10H), 5.01 (d, *J* = 12.4 Hz, 1H), 5.11–5.17 (m, 1H), 5.37–5.50 (m, 2H), 7.19–7.33 (m, 25H) ppm.

^{13}C NMR ($CDCl_3$, 125 MHz) : Major δ 22.7 (t), 23.9 (t), 29.0 (t), 29.3 (t), 29.7 (t, 2C), 31.9 (t), 39.3 (t), 42.8 (t), 63.1 (d), 66.6 (d), 66.8 (t), 69.3 (t, 2C), 71.3 (t), 72.8 (t, 2C), 73.0 (t), 81.6 (d), 87.0 (d), 127.51 (d, 3C), 127.54 (d, 3C), 127.58 (d, 5C), 127.6 (d, 2C), 127.7 (d), 127.9 (d), 128.1 (d), 128.27 (d, 3C), 128.3 (d, 4C), 128.4 (d, 3C), 133.0 (d), 136.7 (s), 137.6 (s), 137.9 (s), 138.4 (s), 138.5 (s), 155.0 (s), 210.5 (s) ppm.

: Minor δ 22.7 (t), 23.8 (t), 28.9 (t), 29.2 (t), 29.4 (t), 29.6 (t), 32.0 (t), 39.3 (t), 42.8 (t), 62.7 (d), 66.5 (d), 67.9 (t), 68.8 (t, 2C), 70.9 (t), 72.8 (t, 2C), 73.0 (t), 82.9 (d), 86.0 (d), 127.51 (d, 3C), 127.54 (d, 3C), 127.58 (d, 5C), 127.6 (d, 2C), 127.7 (d), 127.9 (d), 128.1 (d), 128.27 (d, 3C), 128.3 (d, 4C), 128.4 (d, 3C), 133.0 (d), 136.7 (s), 137.6 (s), 137.9 (s), 138.4 (s), 138.5 (s), 155.0 (s), 210.5 (s) ppm.

ESI-MS (*m/z*)	: 839.9 $[M+1]^+$.
Elemental Analysis	Calcd.: C, 77.39; H, 7.58; N, 1.67. Found: C, 77.43; H, 7.53; N, 1.62.

(2*R*,3*R*,4*R*,5*R*)-*tert*-Butyl 3,4-bis(benzyloxy)-2-(benzyloxymethyl)-5-(hydroxymethyl)pyrrolidine-1-carboxylate (1.80)

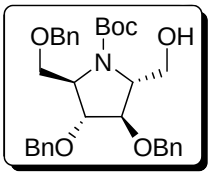

To a solution of aminol **1.50** (2 g, 4.61 mmol) in CH_2Cl_2 (25 ml), TEA (1.9 ml, 13.84 mmol) was added followed by $(Boc)_2O$ (1.3 ml, 5.54 mmol) at 0 °C. The reaction mixture was stirred at rt for 5 h. Methanol (1 ml) was added and stirred for 10 min. Volatiles were evaporated under reduced pressure and the mixture was extracted with ethyl acetate, dried, concentrated and purified by column chromatography on silica gel (4:1 hexane/ethyl acetate) to afford **1.80** (2.07 g, 84%) as a colorless liquid.

Mol. Formula	: $C_{32}H_{39}NO_6$
$[\alpha]_D$	: –40.0 (*c* 0.7, $CHCl_3$)
IR ($CHCl_3$) $\tilde{\nu}$	: 3453, 3064, 3031, 2927, 1759, 1693, 1496, 1454, 1392, 1366, 1172, 1096, 1028, 750, 697 cm^{-1}.
^{1}H NMR ($CDCl_3$, 200 MHz)	: δ 1.26–1.47 (m, 9H), 3.40–3.57 (m, 1H), 3.72–3.82 (m, 3H), 3.94–4.30 (m, 4H), 4.38–4.68 (m, 6H), 7.30 (br s, 15H) ppm.
^{13}C NMR ($CDCl_3$, 50 MHz)	: δ 28.4 (q, 3C), 63.4 (d), 64.3 (t), 66.4 (d), 68.3 (t), 71.3 (t, 2C), 73.1 (t), 80.6 (d), 81.8 (d), 84.1 (s), 127.6 (d, 4C), 127.8 (d, 3C), 127.8 (d), 128.3 (d), 128.4 (d, 2C), 128.5 (d, 3C), 129.7 (d), 137.4 (s, 3C), 155.4 (s) ppm.
ESI-MS (*m/z*)	: 534.7 $[M+1]^+$.
Elemental Analysis	Calcd.: C, 72.02; H, 7.37; N, 2.62. Found: C, 71.97; H, 7.32; N, 2.57.

(2*R*,3*R*,4*R*,5*R*)-*tert*-Butyl 3,4-bis(benzyloxy)-2-(benzyloxymethyl)-5-vinylpyrrolidine-1-carboxylate (1.81)

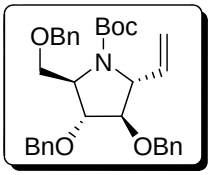

Trichloroisocyanuric acid (479 mg, 2.06 mmol) was added to a solution of the alcohol **1.80** (1 g, 1.87 mmol) in CH_2Cl_2 (20 ml) and the solution was stirred and maintained at 0

°C, followed by addition of TEMPO radical (3 mg, 0.018 mmol). Reaction mixture was stirred at 0 °C for 1 h and then was filtered on celite. Organic phase was washed with saturated solution of Na_2CO_3 (15 ml), followed by 1 N HCl and brine. The organic layer was dried (Na_2SO_4) and evaporated at reduced pressure to yield **1.38** (760 mg, 76%) which was used for the next step without any further purification.

At 0 °C, a solution of aldehyde **1.38** (760 mg, 1.43 mmol) was treated with 1-C-wittig ylide [prepared from methyltriphenylphosphonium bromide (5.11 g, 14.30 mmol) and $NaNH_2$ (502 mg, 12.87 mmol)] in (3:1; THF:ether) and the contents were stirred for 1 h at rt. The reaction mixture was quenched with sat. NH_4Cl (10 ml) and extracted with EtOAc (3 x 25 ml). The combined organic extract was dried, concentrated and the crude was purified by column chromatography (1:4 EtOAc/hexane) to yield **1.81** (296 mg, 39%).

Mol. Formula	: $C_{33}H_{39}NO_5$
$[\alpha]_D$	: −12.2 (*c* 1.3, MeOH)
IR ($CHCl_3$) $\tilde{\nu}$	: 3019, 2964, 1770, 1719, 1642, 1584, 1452, 1409, 1370, 1215, 1159, 758, 668 cm^{-1}.
^{1}H NMR (DMSO-d_6, 500 MHz, 343 ^{o}K)	: δ 1.35 (s, 9H), 3.44 (t, *J* = 9.5 Hz, 1H), 3.78 (br s, 1H), 3.90 (s, 1H), 3.99 (d, *J* = 7.0 Hz, 1H), 4.12 (s, 1H), 4.22 (d, *J* = 7.5 Hz, 1H), 4.43–4.59 (m, 6H), 5.06 (d, *J* = 10.3 Hz, 1H), 5.11 (d, *J* = 17.3 Hz, 1H), 5.79 (ddd, *J* = 8.3, 10.0, 17.6 Hz, 1H), 7.24–7.35 (m, 15H) ppm.
^{13}C NMR (DMSO-d_6, 500 MHz, 343 ^{o}K)	: δ 28.0 (q, 3C), 62.7 (t), 66.3 (d), 68.0 (d), 70.3 (t), 70.7 (t), 72.2 (t), 78.9 (s), 81.7 (d), 85.7 (d), 115.5 (t), 127.3 (d, 3C), 127.4 (d, 5C), 127.5 (d), 128.1 (d, 2C), 128.12 (d, 2C), 128.2 (d, 2C), 136.8 (d), 137.7 (s), 137.8 (s), 138.3 (s), 153.2 (s) ppm.
ESI-MS (*m/z*)	: 530.2 $[M+1]^+$.
Elemental Analysis	Calcd.: C, 74.83; H, 7.42; N, 2.64. Found: C, 74.79; H, 7.39; N, 2.59.

tert-butyl 2-(benzyloxymethyl)-5-vinyl-1*H*-pyrrole-1-carboxylate (1.82)

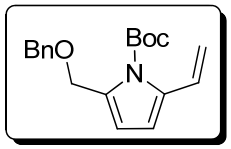

At 0 °C, a solution of aldehyde **1.38** (760 mg, 1.43 mmol) was treated with 1-C-wittig ylide [prepared from methyltriphenylphosphonium bromide (6.72 g, 18.82 mmol) and potassium *ter*-butoxide (2.11 g, 18.82 mmol)] in THF (30 ml) and the contents were

stirred for 8 h at rt. The reaction mixture was quenched with sat. NH_4Cl (10 ml) and extracted with EtOAc (3 x 25 ml). The combined organic extract was dried, concentrated and the crude was purified by column chromatography (1:19 EtOAc/hexane) to yield **1.82** (361 mg, 36%).

Mol. Formula	: $C_{19}H_{23}NO_3$
^{1}H NMR ($CDCl_3$, 400 MHz)	: δ 1.58 (s, 9H), 4.50 (s, 2H), 4.66 (s, 2H), 5.06 (dd, *J* = 1.5, 11.0 Hz, 1H), 5.46 (dd, *J* = 1.5, 17.6 Hz, 1H), 6.16 (d, *J* = 3.3 Hz, 1H), 6.30 (d, *J* = 3.3 Hz, 1H), 7.00 (dd, *J* = 11.0, 17.6 Hz, 1H), 7.30–7.31 (m, 5H) ppm.
^{13}C NMR ($CDCl_3$, 50 MHz)	: δ 28.0 (q, 3C), 60.1 (t), 71.7 (t), 84.2 (s), 109.3 (d), 113.1 (t), 113.2 (d), 127.5 (d), 127.7 (d, 2C), 128.3 (d, 2C), 128.6 (d), 132.4 (s), 136.0 (s), 138.4 (s), 149.7 (s) ppm.
ESI-MS (*m/z*)	: 314.4 $[M+1]^+$.
Elemental Analysis	Calcd.: C, 72.82; H, 7.40; N, 4.47. Found: C, 72.77; H, 7.35; N, 4.43.

(2*R*,3*R*,4*R*,5*R*)-*tert*-butyl 3,4-bis(benzyloxy)-2-(13-(benzyloxy)-10-oxotridec-1-enyl)-5-(benzyloxymethyl)pyrrolidine-1-carboxylate (1.83)

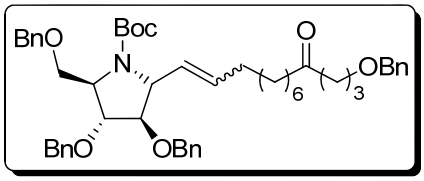

To a solution of chiral core subunit **1.81** (100 mg, 0.188 mmol) and keto side chain **1.40** (171 mg, 0.566 mmol) in dry DCM (15 ml), Grubbs' II catalyst **1.5** (31 mg, 0.037 mmol) was added and purged with argon. The reaction mixture was refluxed at 40 °C for 24 h under argon gas atmosphere. Volatiles were evaporated under reduced pressure and the residue obtained was purified by column chromatography (18:2 petroleum ether/ethyl acetate) to afford cross metathesis product **1.83** (35 mg, 22%) as colorless oil, keto side chain dimmer **1.77** (55 mg) along with unreacted chiral core subunit **1.81** (39 mg).

Mol. Formula	: $C_{51}H_{65}NO_7$
$[\alpha]_D$	: –19.3 (*c* 0.7, MeOH)
IR ($CHCl_3$) $\tilde{\nu}$	: 3016, 2930, 2860, 1737, 1699, 1585, 1497, 1454, 1410, 1351, 1216, 1098, 756 cm^{-1}.
^{1}H NMR	: δ 1.19–1.28 (m, 8H), 1.34 (s, 9H), 1.43 (qui, *J* = 6.8 Hz, 2H),

(DMSO-d_6, 500 MHz, 343 ^oK)	1.74 (qui, *J* = 6.8 Hz, 2H), 1.90–1.95 (m, 2H), 2.33 (t, *J* = 7.3 Hz, 2H), 2.43 (t, *J* = 7.3 Hz, 2H), 3.40 (t, *J* = 6.3 Hz, 2H), 3.41–3.43 (m, 1H), 3.77 (d, *J* = 9.8 Hz, 1H), 3.85 (s, 1H), 3.99 (d, *J* = 6.8 Hz, 1H), 4.09 (s, 1H), 4.17 (d, *J* = 7.8 Hz, 1H), 4.41 (s, 2H), 4.44–4.55 (m, 6H), 5.30–5.54 (m, 2H), 7.23–7.34 (m, 20H) ppm.
^{13}C NMR (DMSO-d_6, 500 MHz, 343 ^oK)	: δ 23.3 (t), 23.7 (t), 28.0 (q, 3C), 28.2 (t), 28.4 (t), 28.5 (t), 28.6 (t), 31.3 (t), 38.6 (t), 41.9 (t), 62.8 (d), 65.8 (d), 69.1 (t, 2C), 70.4 (t), 70.7 (t), 71.9 (t), 72.3 (t), 78.8 (s), 82.0 (d), 86.0 (d), 127.2 (d), 127.3 (d, 2C), 127.4 (d, 2C), 127.43 (d, 2C), 127.48 (d, 2C), 127.5 (d), 128.1 (d, 2C), 128.17 (d, 3C), 128.2 (d, 2C), 128.5 (d), 128.6 (d), 129.1 (d), 129.4 (d), 131.6 (d), 137.8 (s), 137.9 (s), 138.4 (s), 138.7 (s), 155.0 (s), 210.1 (s) ppm.
ESI-MS (*m/z*)	: 804.5 $[M+1]^+$.
Elemental Analysis	Calcd.: C, 76.18; H, 8.15; N, 1.74. Found: C, 76.23; H, 8.10; N, 1.69.

1.5 NMR Spectral Data

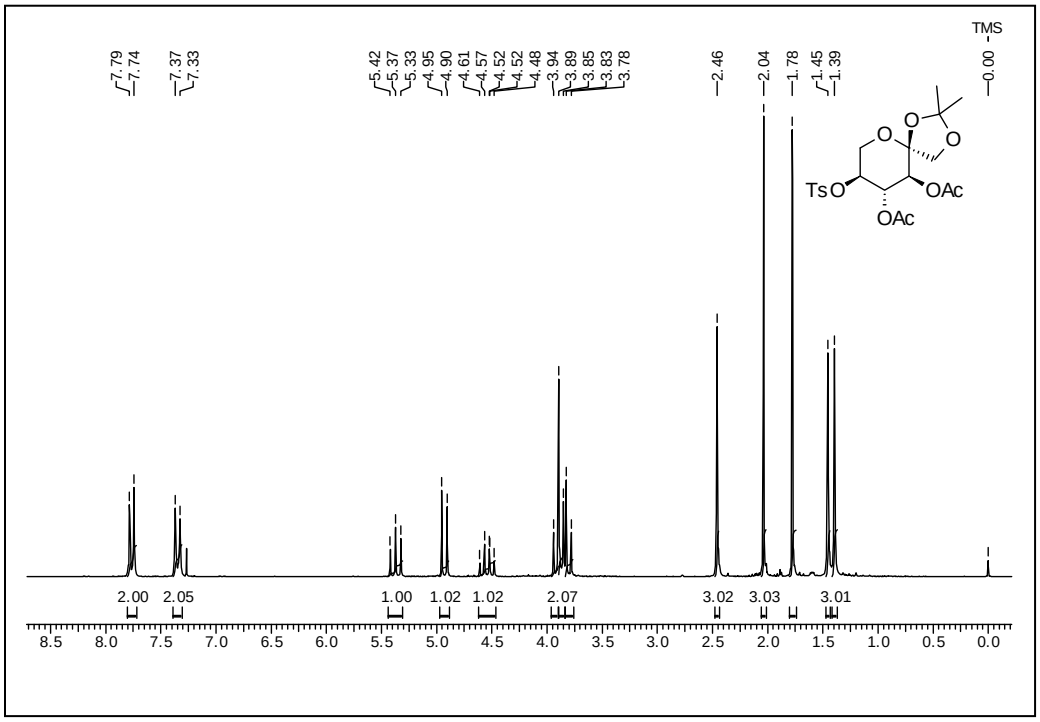

^{1}H NMR Spectrum of 1.44 in $CDCl_3$

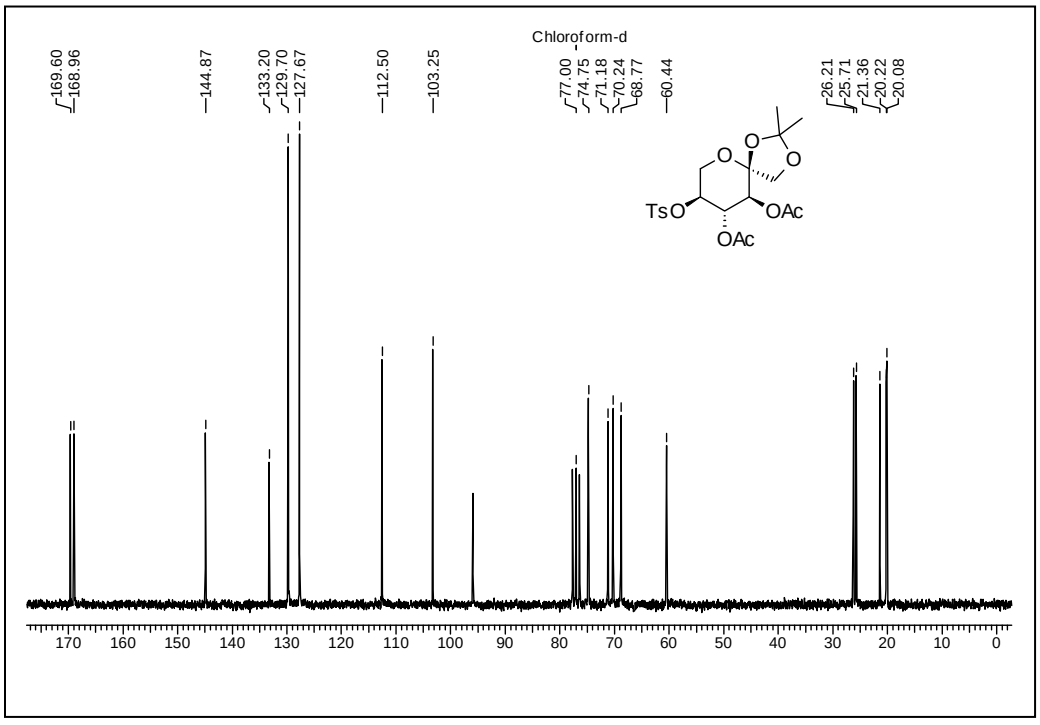

^{13}C NMR Spectrum of 1.44 in $CDCl_3$

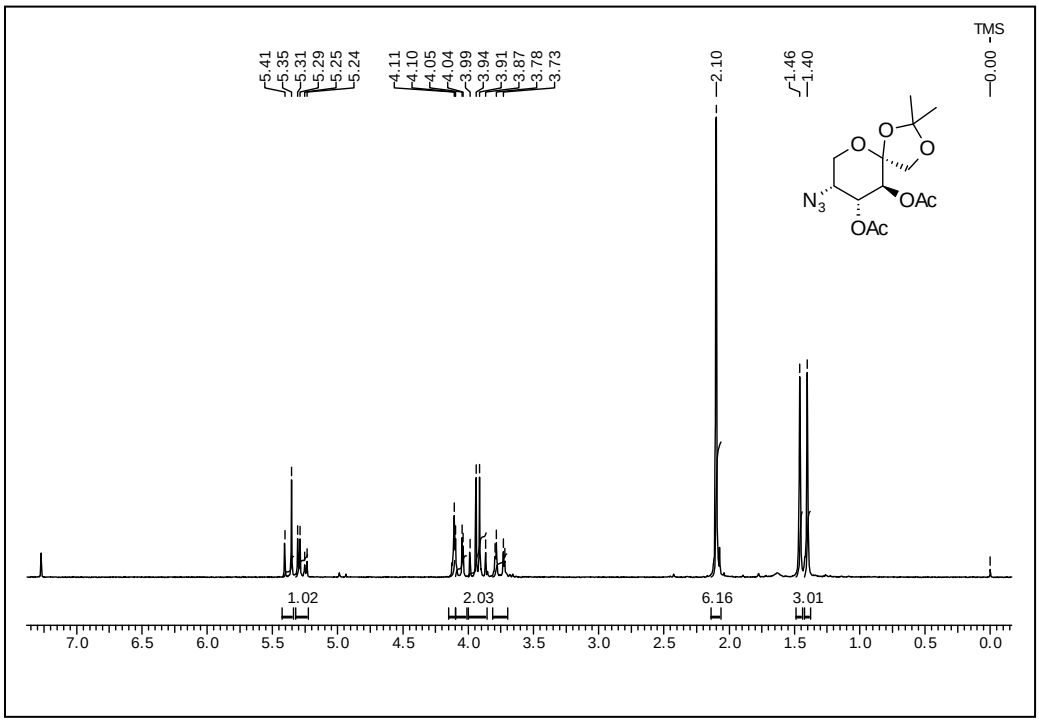

^{1}H NMR Spectrum of 1.145 in $CDCl_3$

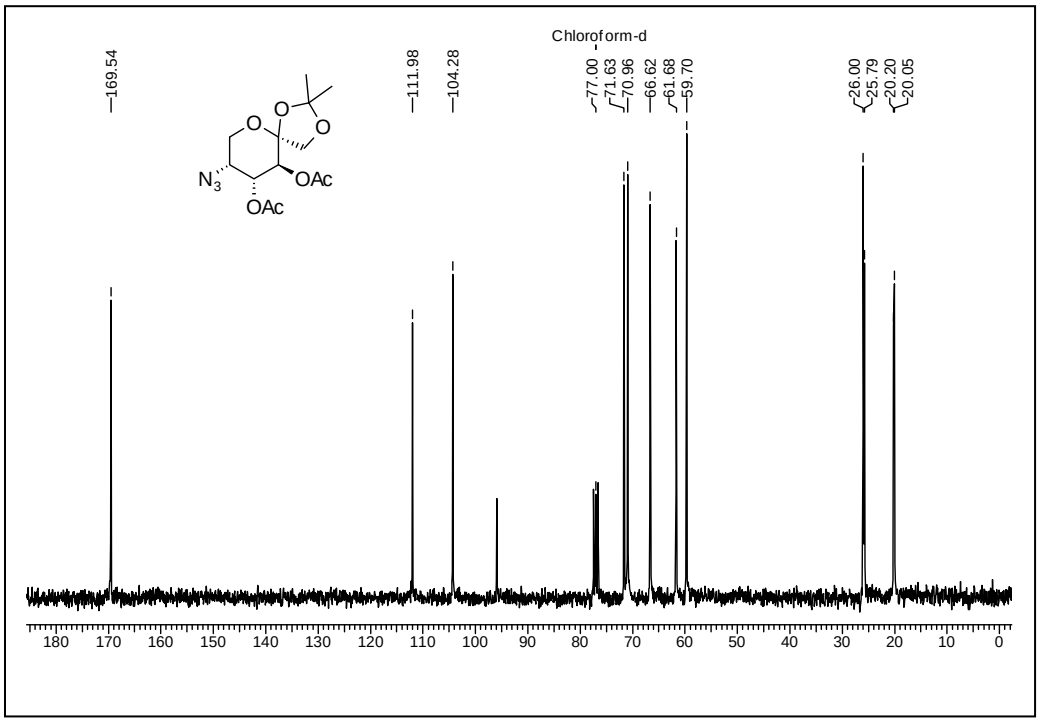

^{13}C NMR Spectrum of 1.145 in $CDCl_3$

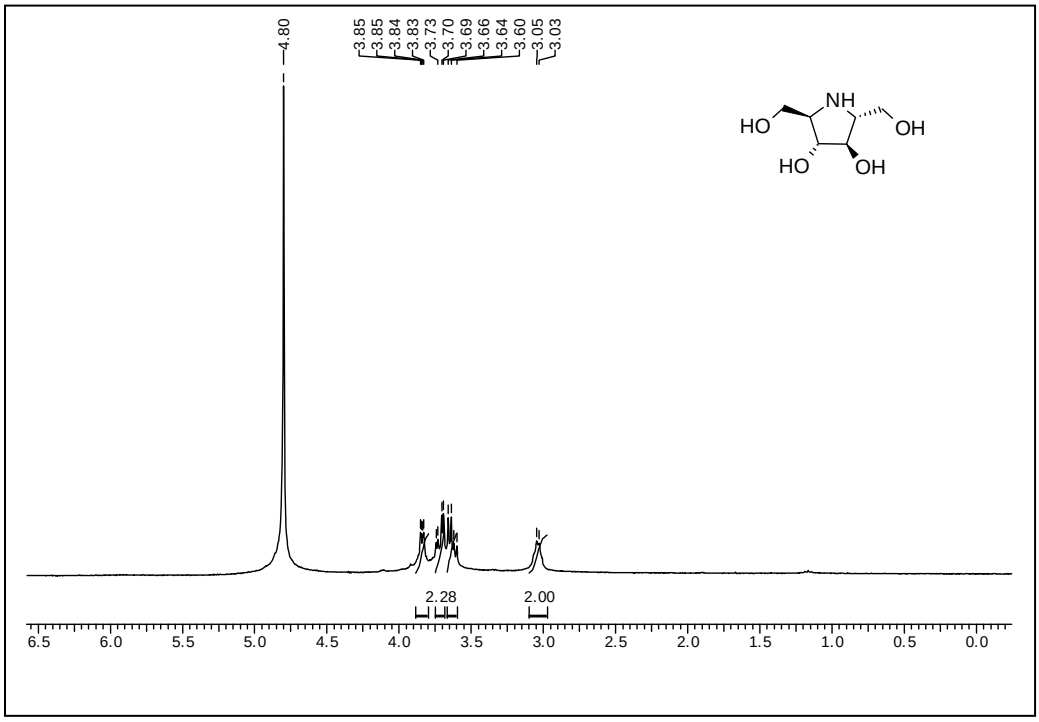

^{1}H NMR Spectrum of 1.39 in D_2O

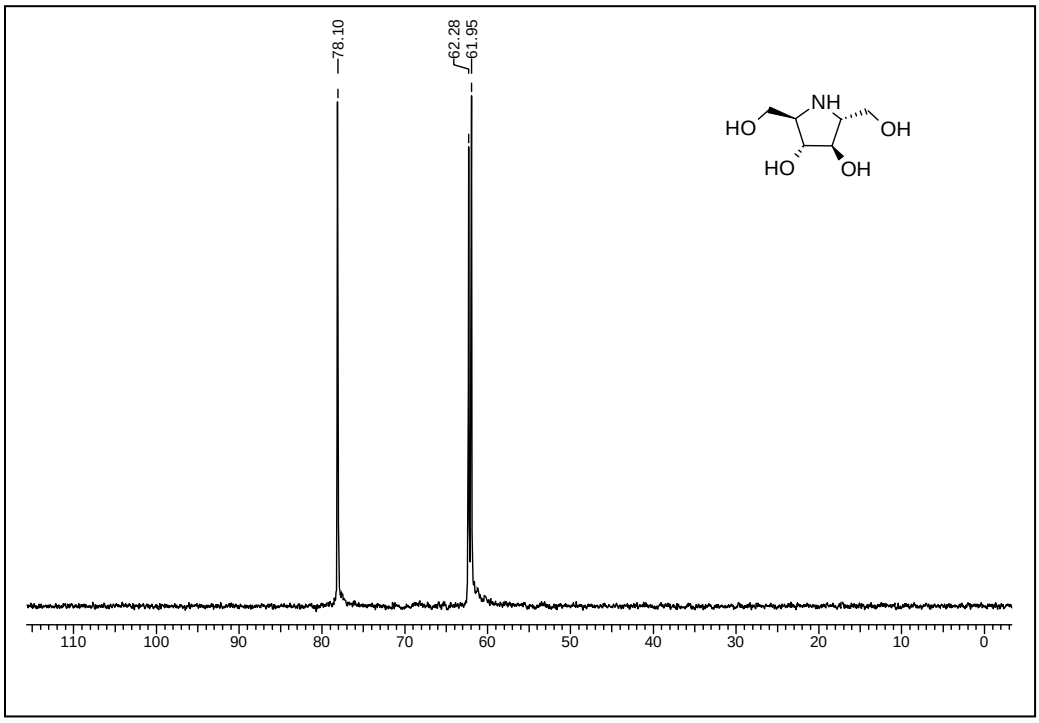

^{13}C NMR Spectrum of 39 in D_2O

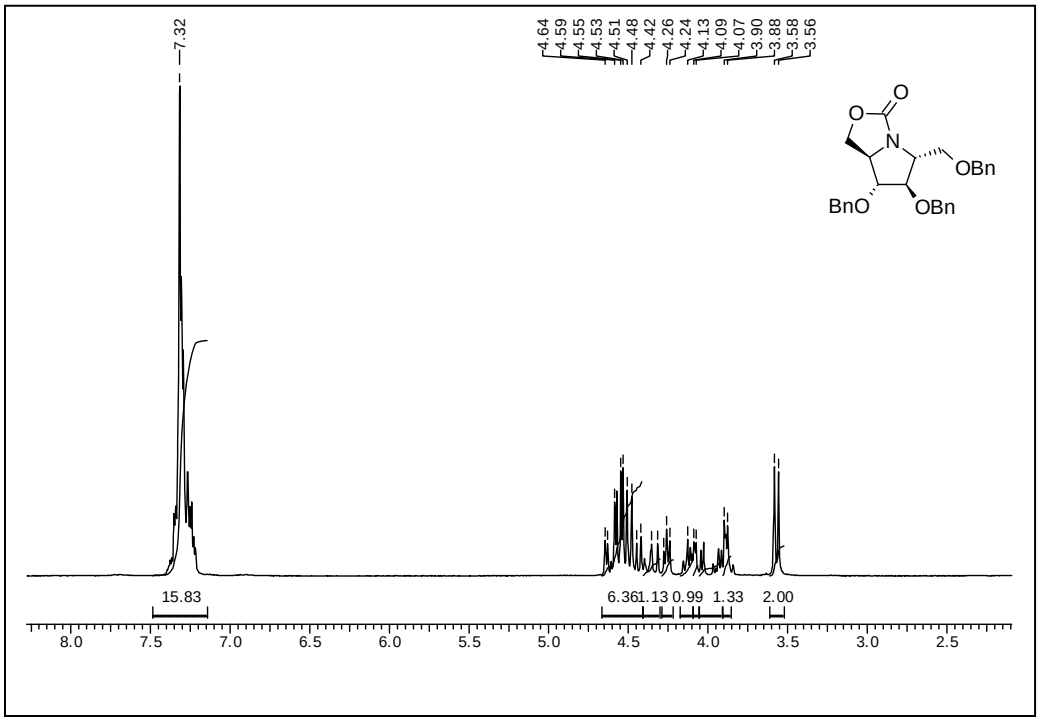

^{1}H NMR Spectrum of 1.49 in $CDCl_3$

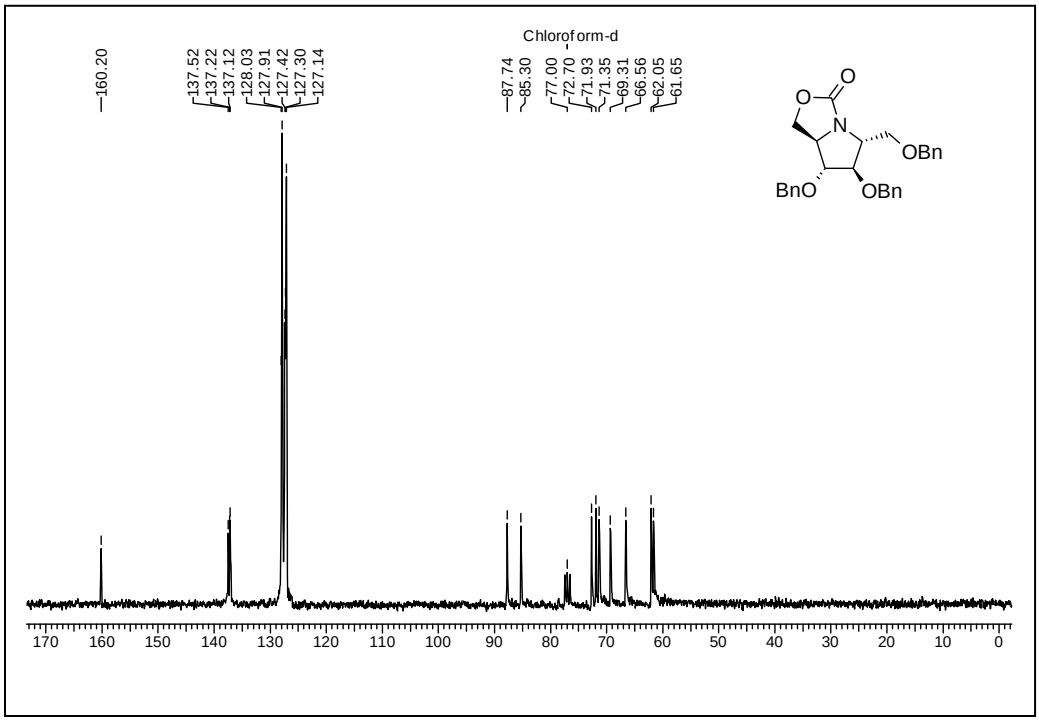

^{13}C NMR Spectrum of 1.49 in $CDCl_3$

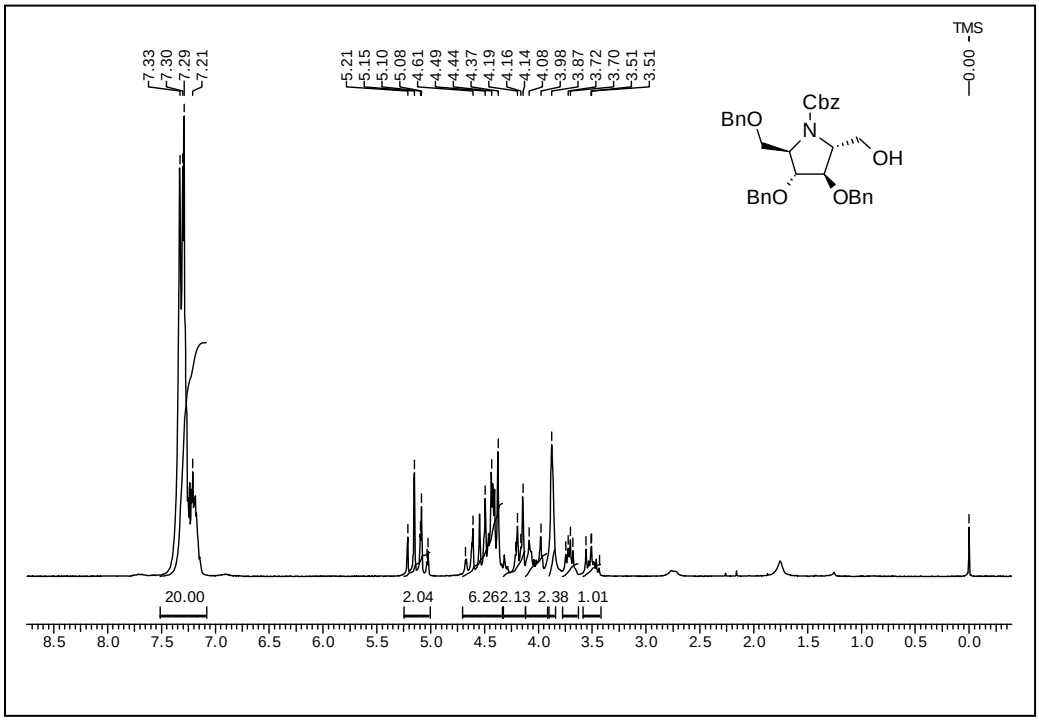

^{1}H NMR Spectrum of 1.51 in $CDCl_3$

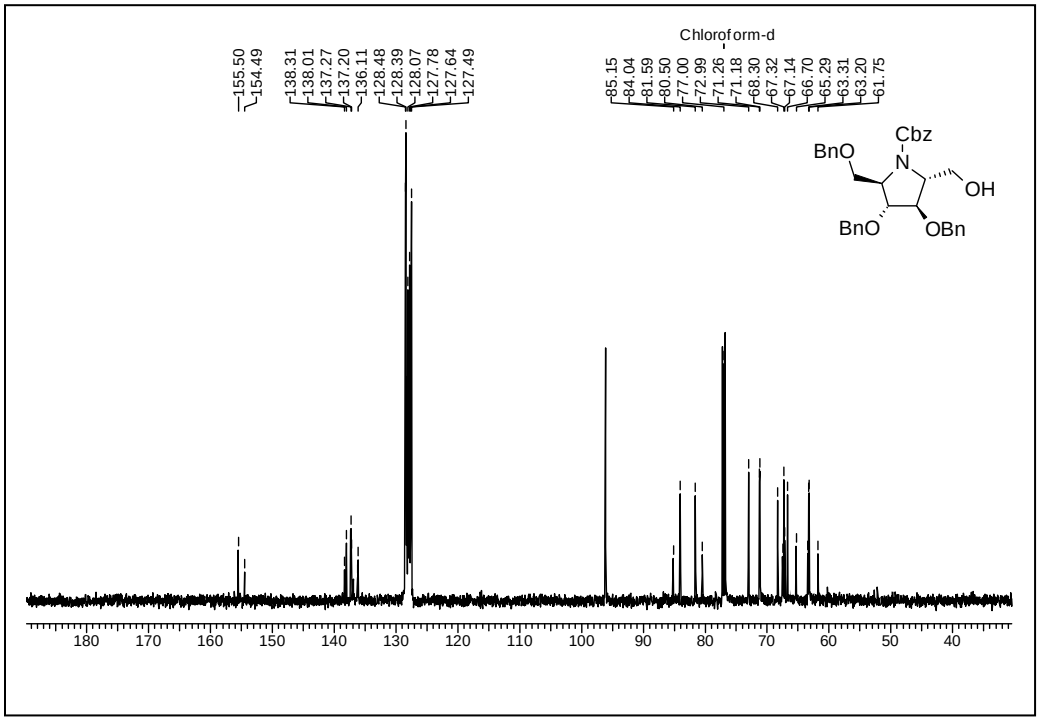

^{13}C NMR Spectrum of 1.51 in $CDCl_3$

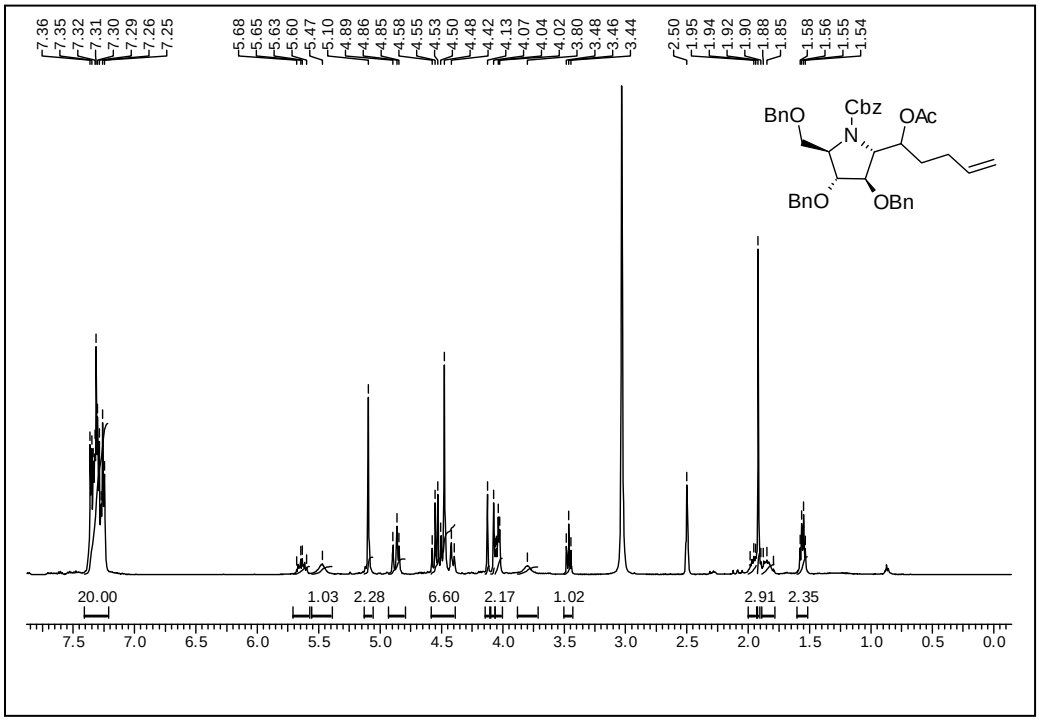

^{1}H NMR Spectrum of 1.34 in DMSO-d_6 at 333 °K

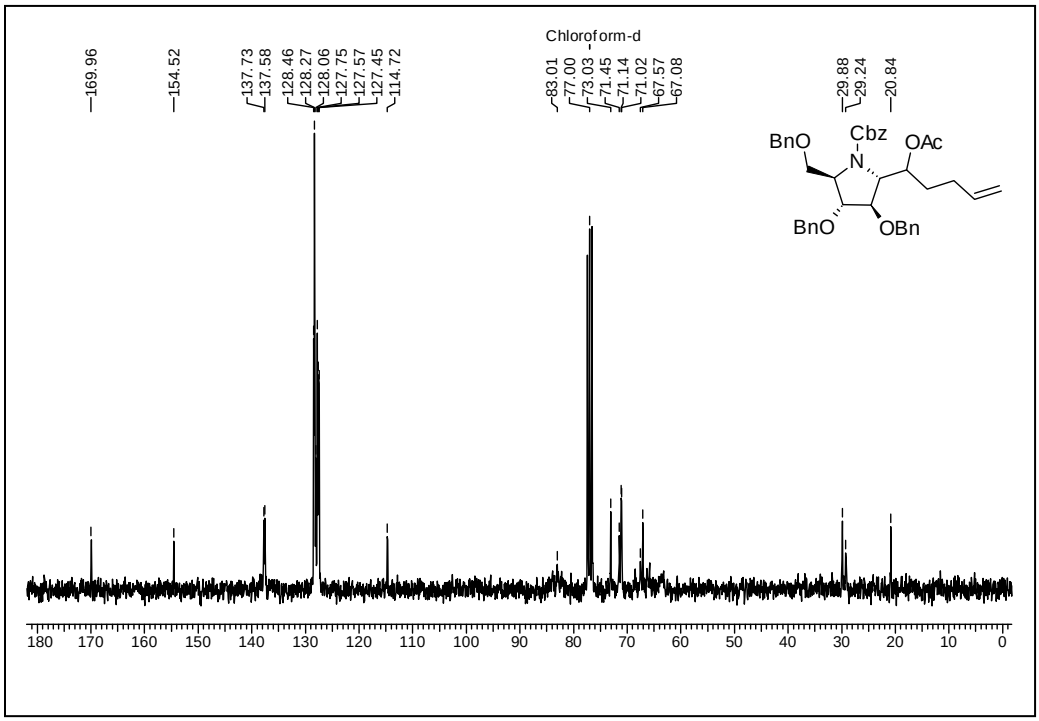

^{13}C NMR Spectrum of 1.34 in $CDCl_3$

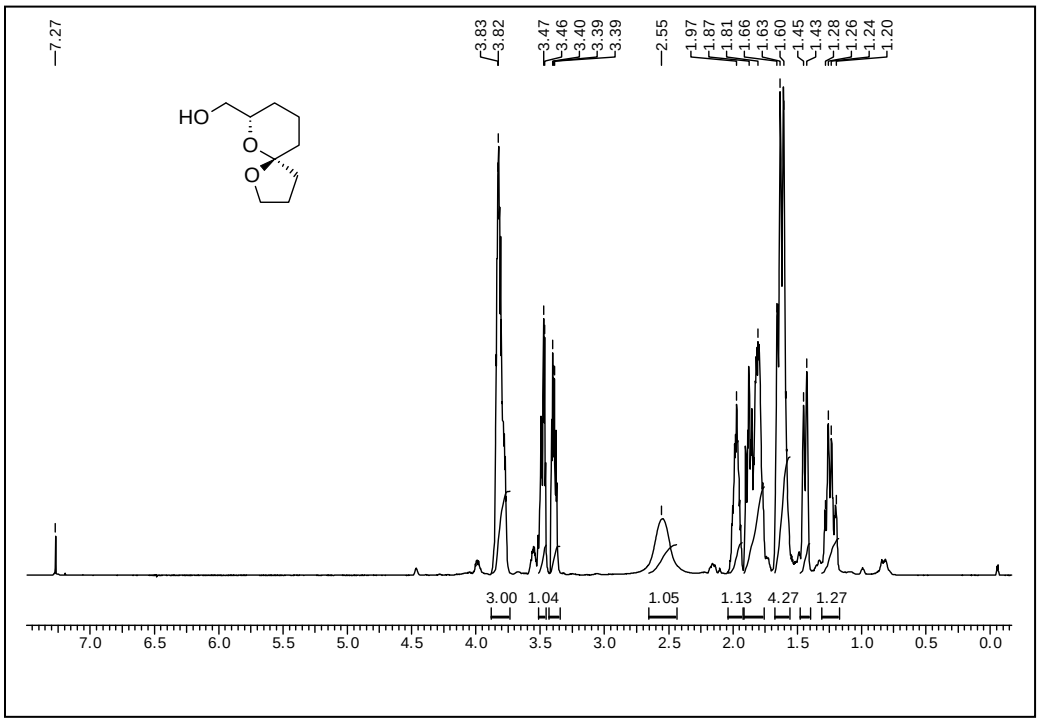

^{1}H NMR Spectrum of 1.63 in $CDCl_3$

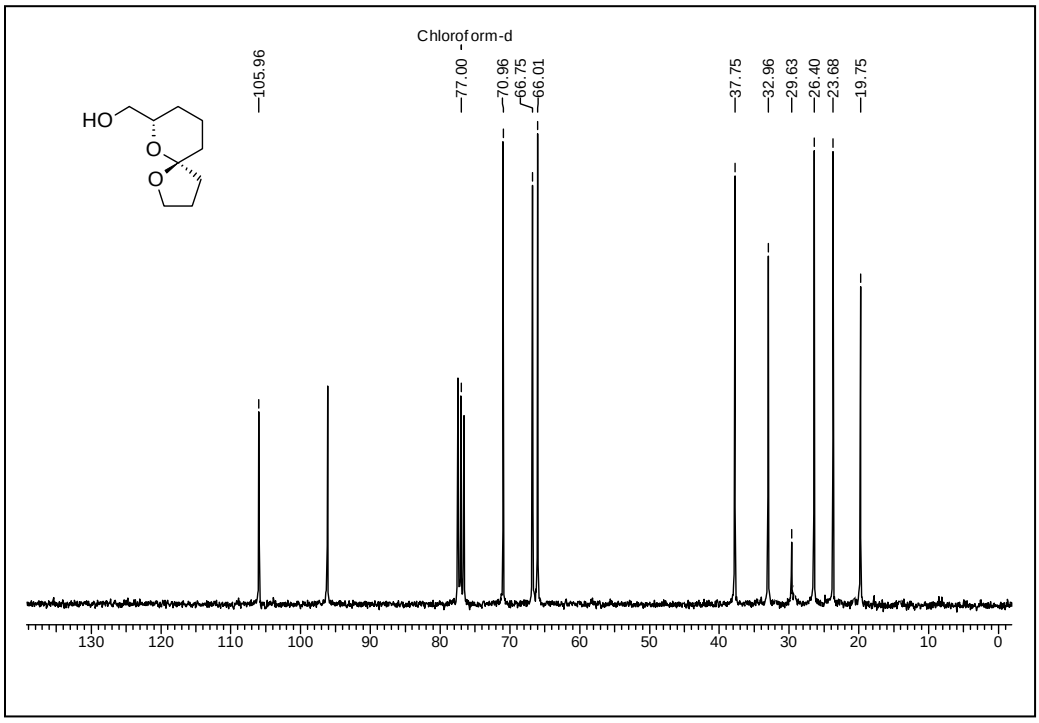

^{13}C NMR Spectrum of 1.63 in $CDCl_3$

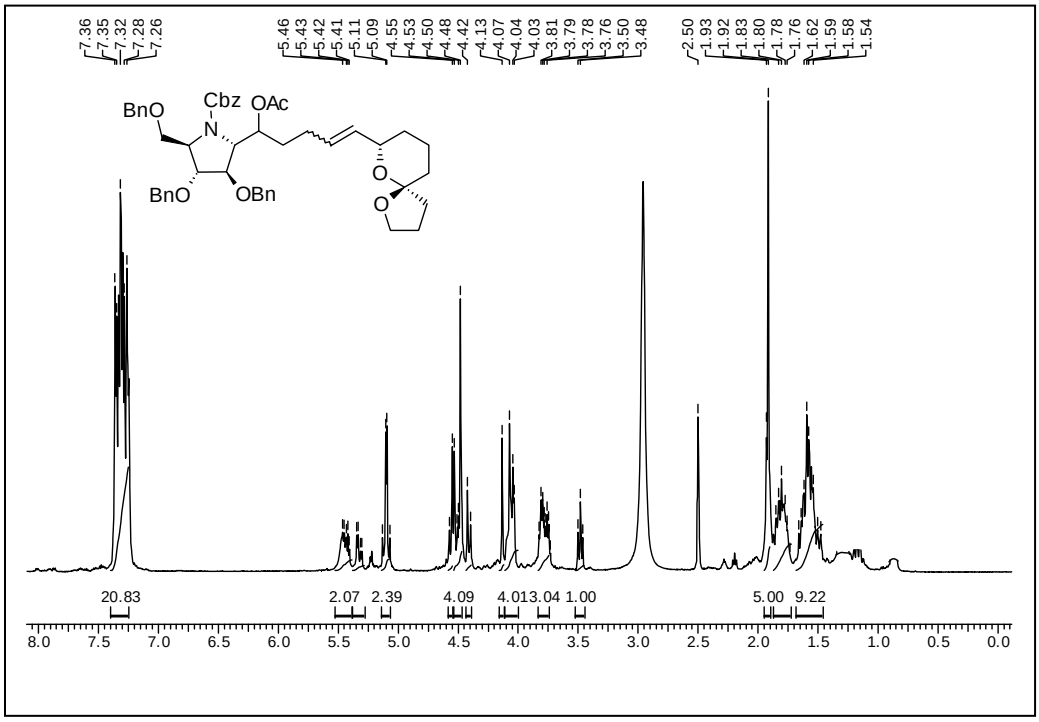

^{1}H NMR Spectrum of 1.65 in DMSO-d_6 at 343 °K

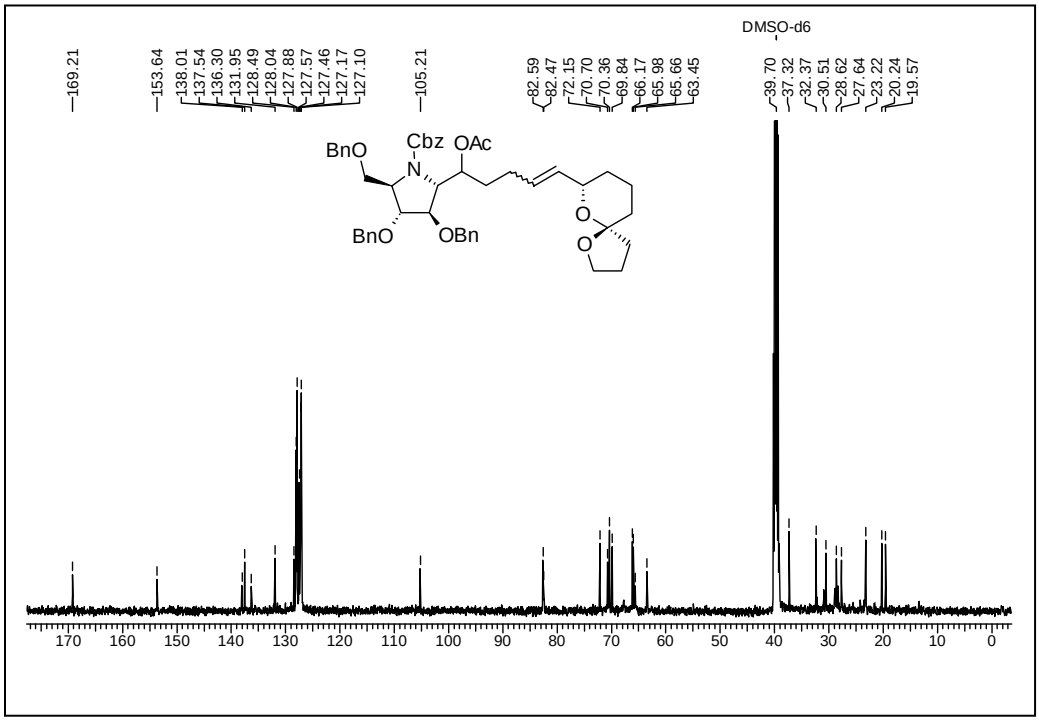

^{13}C NMR Spectrum of 1.65 in DMSO-d_6 at 333 °K

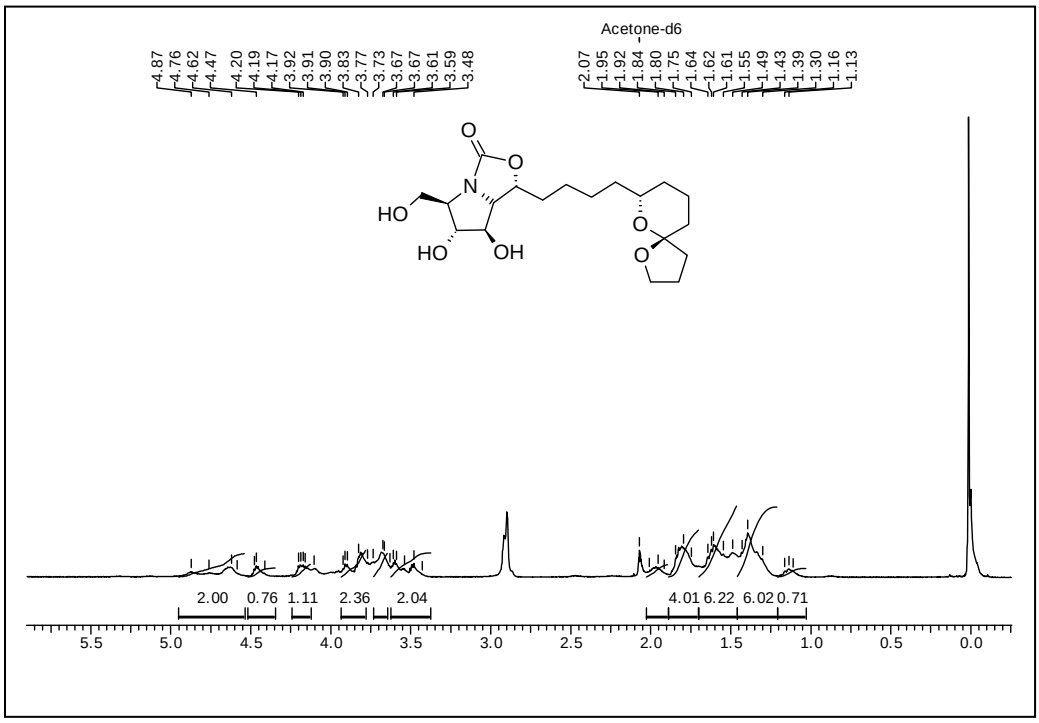

^{1}H NMR Spectrum of 1.71 in Acetone-d_6

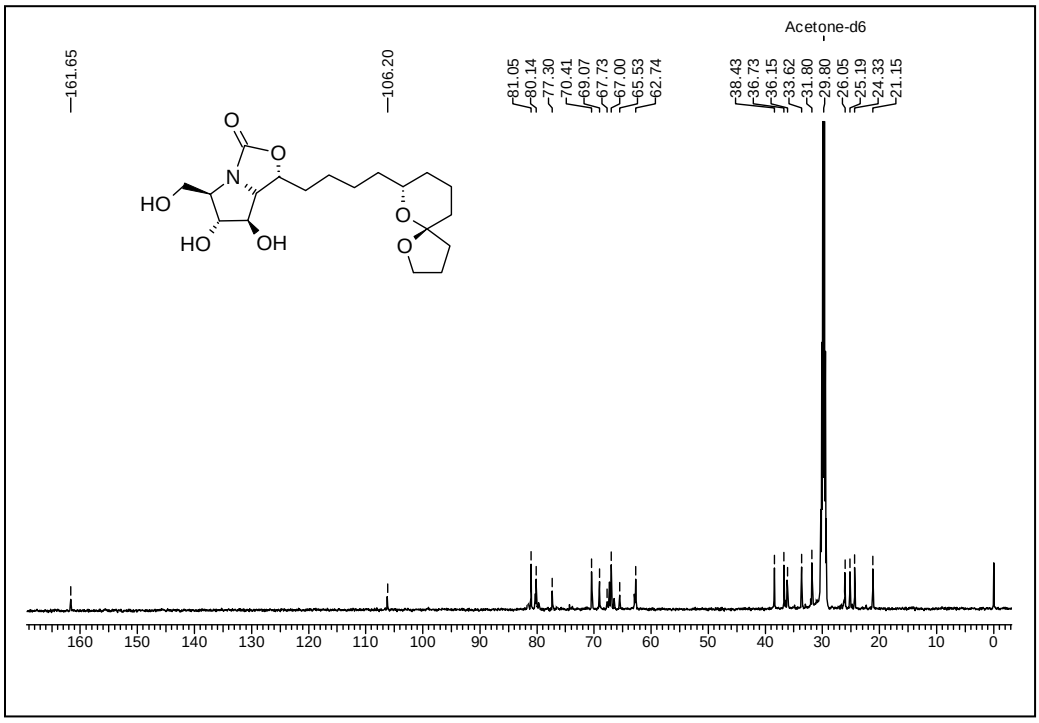

^{13}C NMR Spectrum of 1.71 in Acetone-d_6

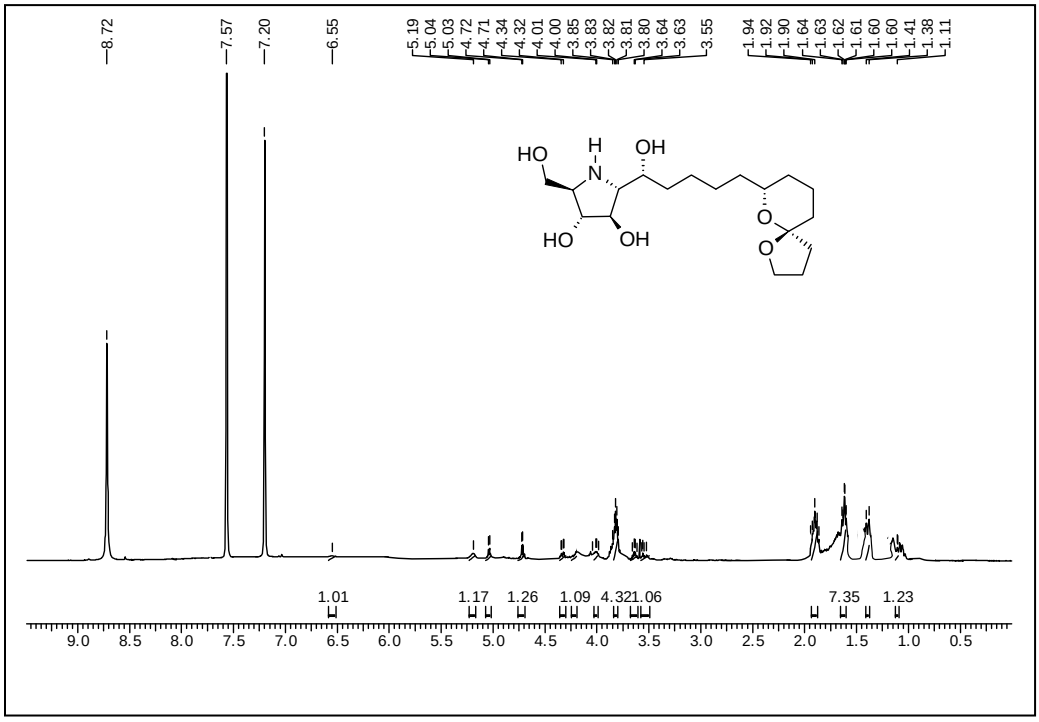

^{1}H NMR Spectrum of 1.28 in Pyridine-d_5

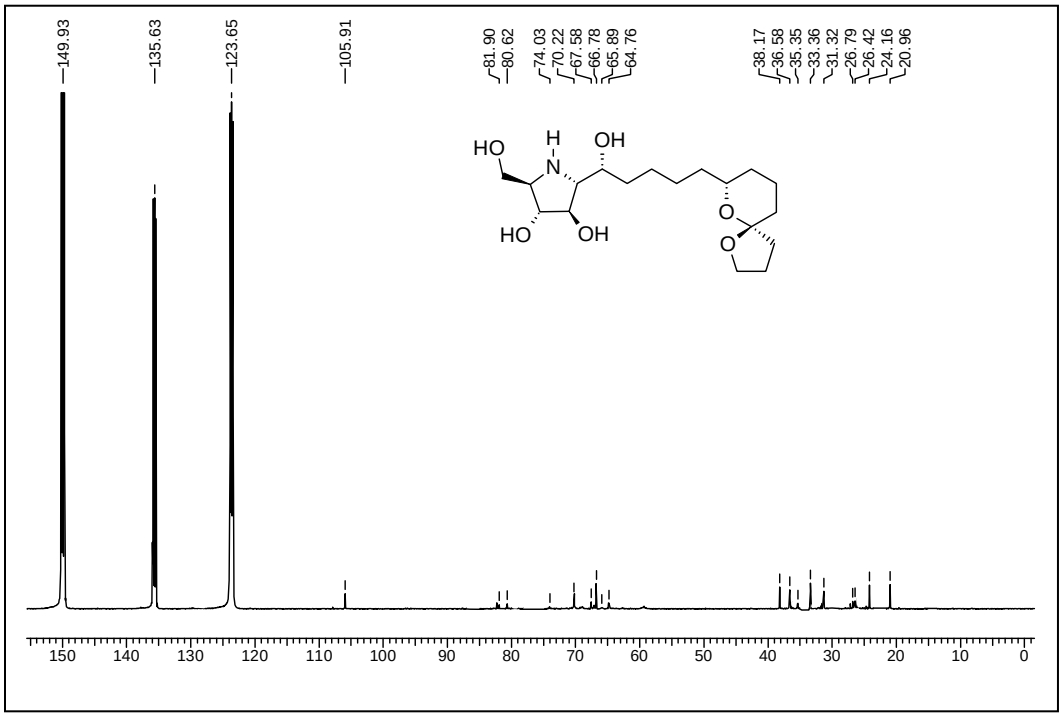

^{13}C NMR Spectrum of 1.28 in Pyridine-d_5

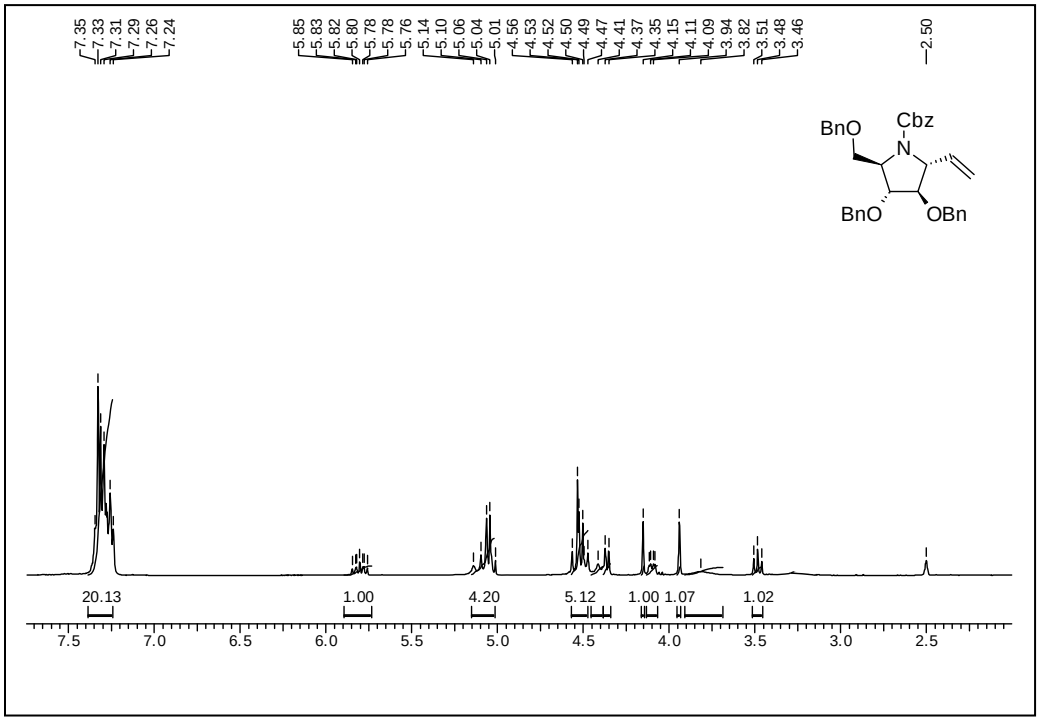

^{1}H NMR Spectrum of 1.33 in DMSO-d_6 at 333 °K

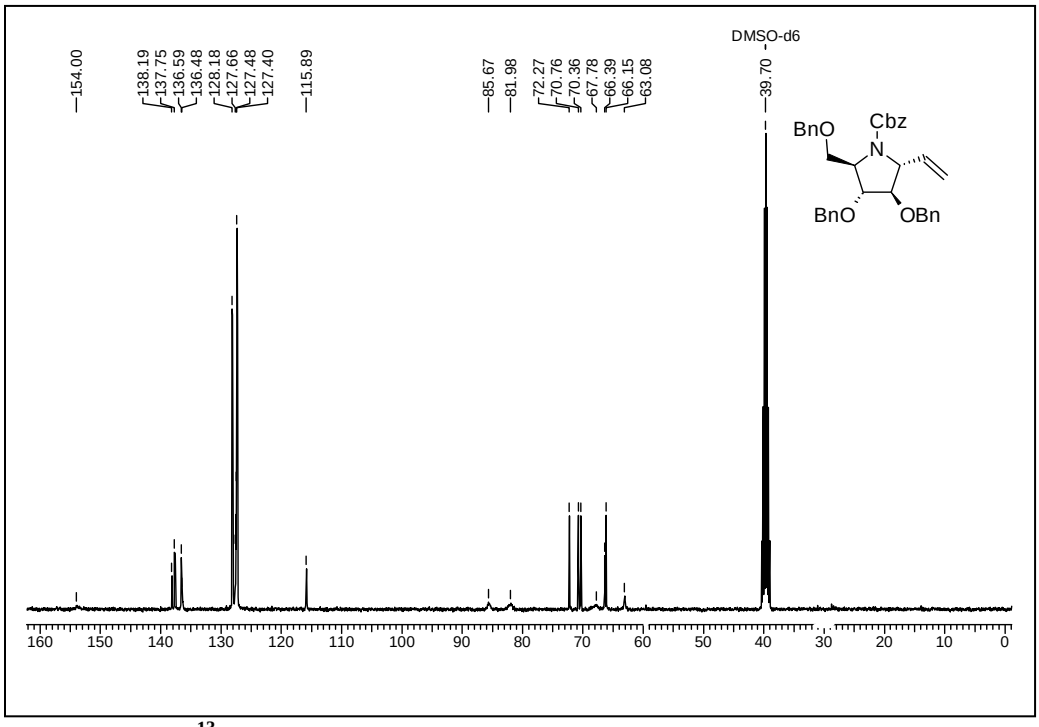

^{13}C NMR Spectrum of 1.33 in DMSO-d_6 at 333 °K

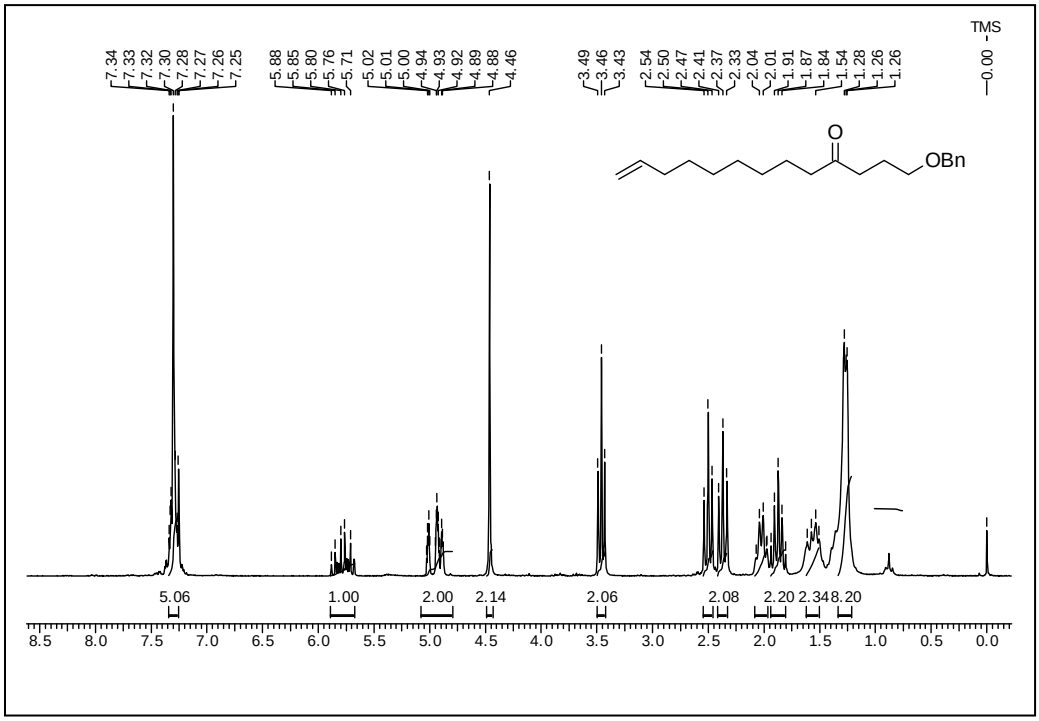

^{1}H NMR Spectrum of 1.40 in $CDCl_3$

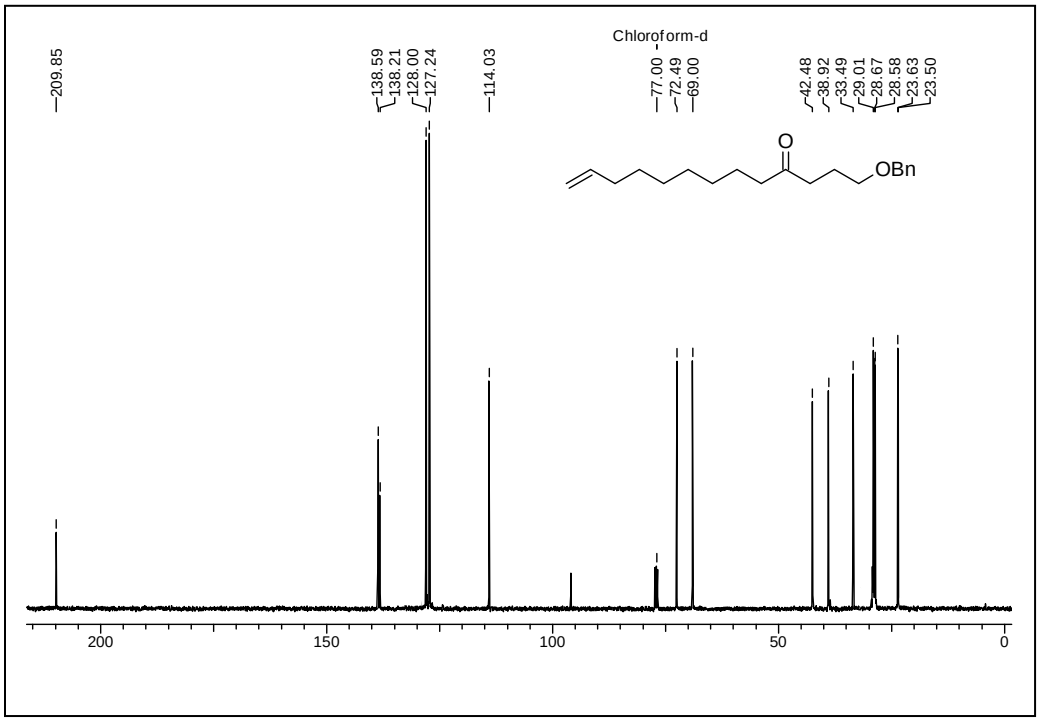

^{13}C NMR Spectrum of 1.40 in $CDCl_3$

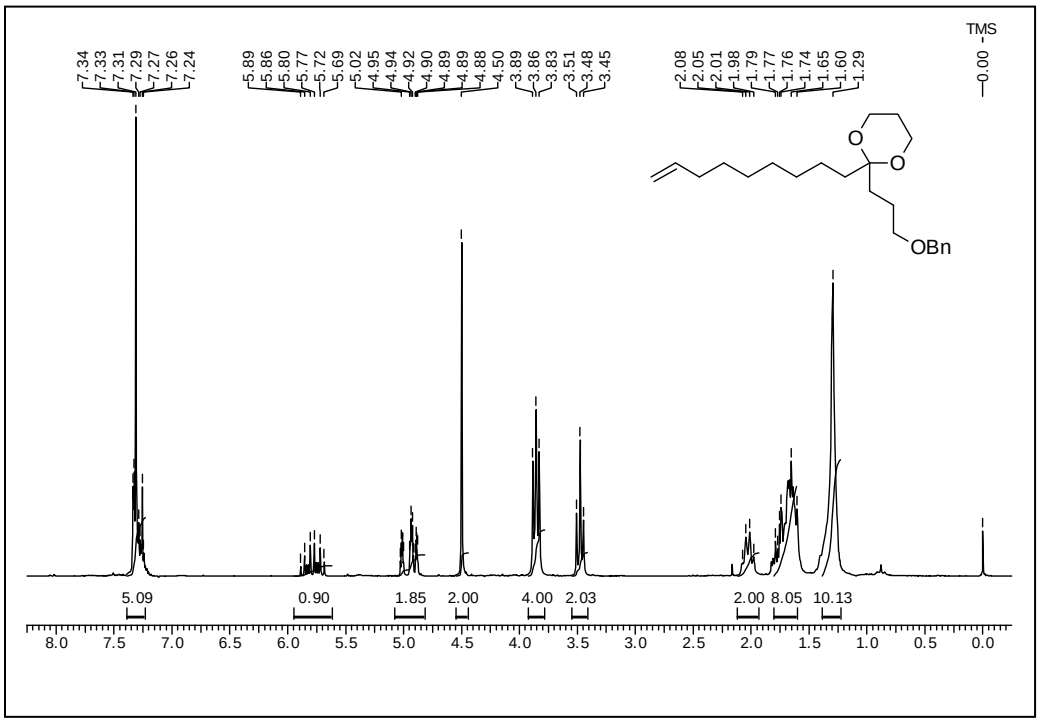

^{1}H NMR Spectrum of 1.75 in $CDCl_3$

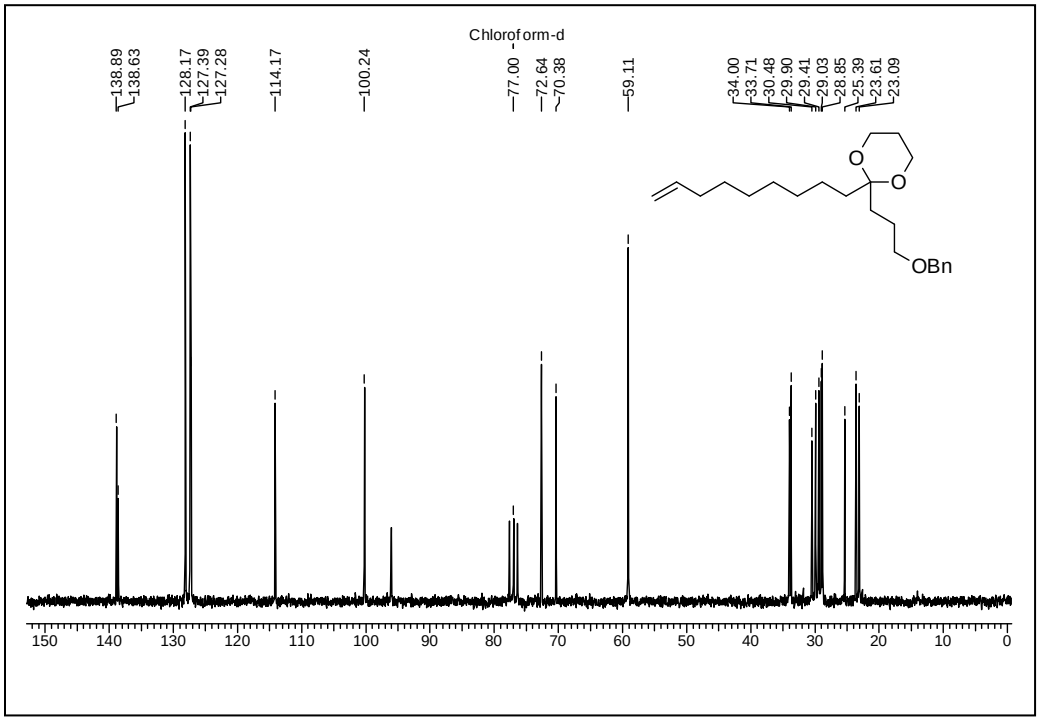

^{13}C NMR Spectrum of 1.75 in $CDCl_3$

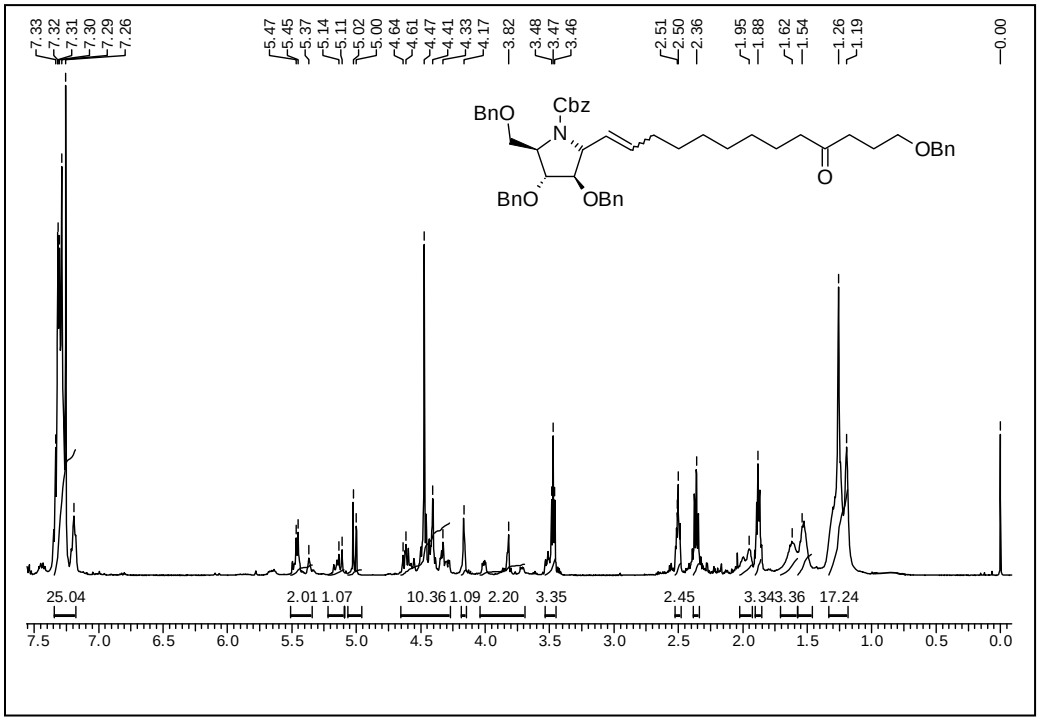

^{1}H NMR Spectrum of 1.78 in $CDCl_3$

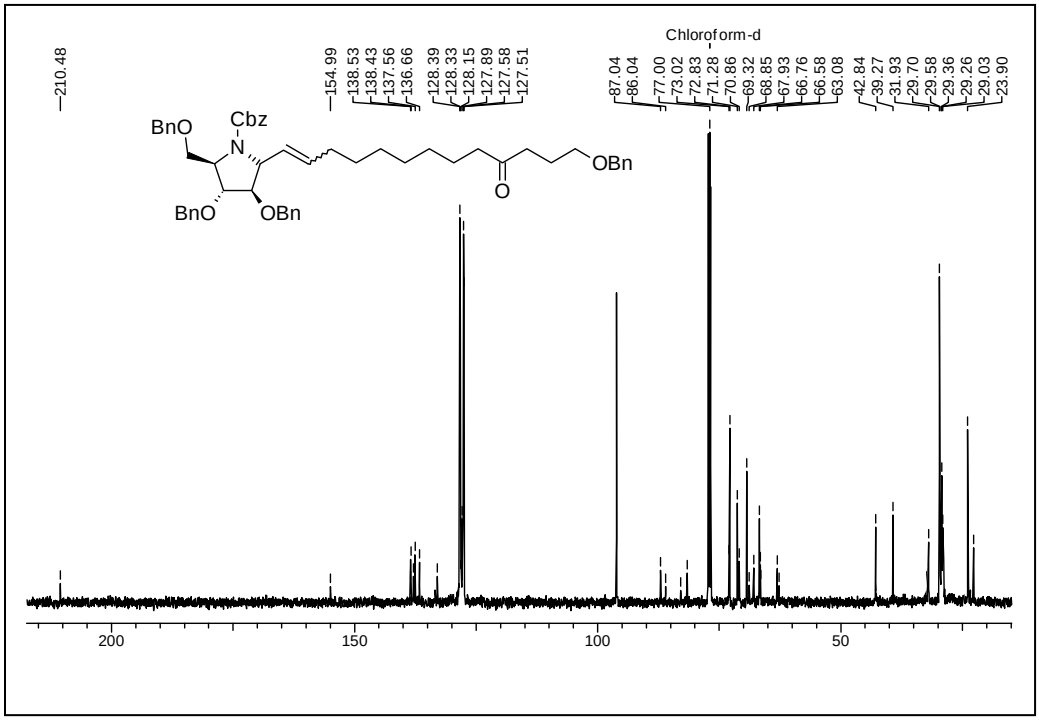

^{13}C NMR Spectrum of 1.78 in $CDCl_3$

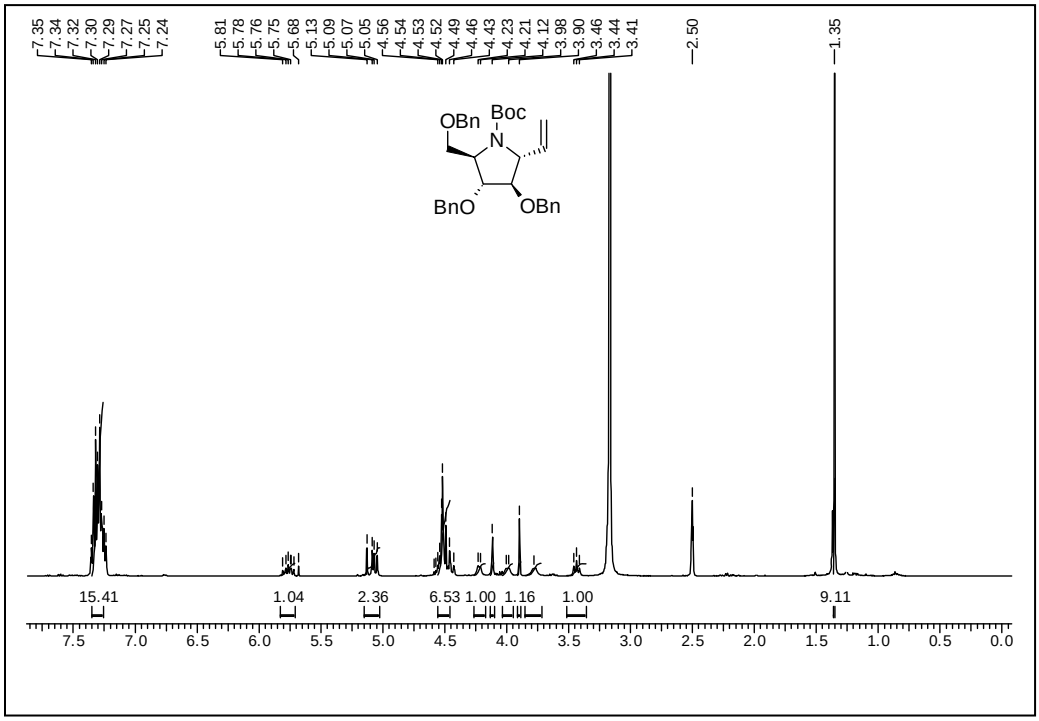

^{1}H NMR Spectrum of 1.81 in DMSO-d_6 at 343 °K

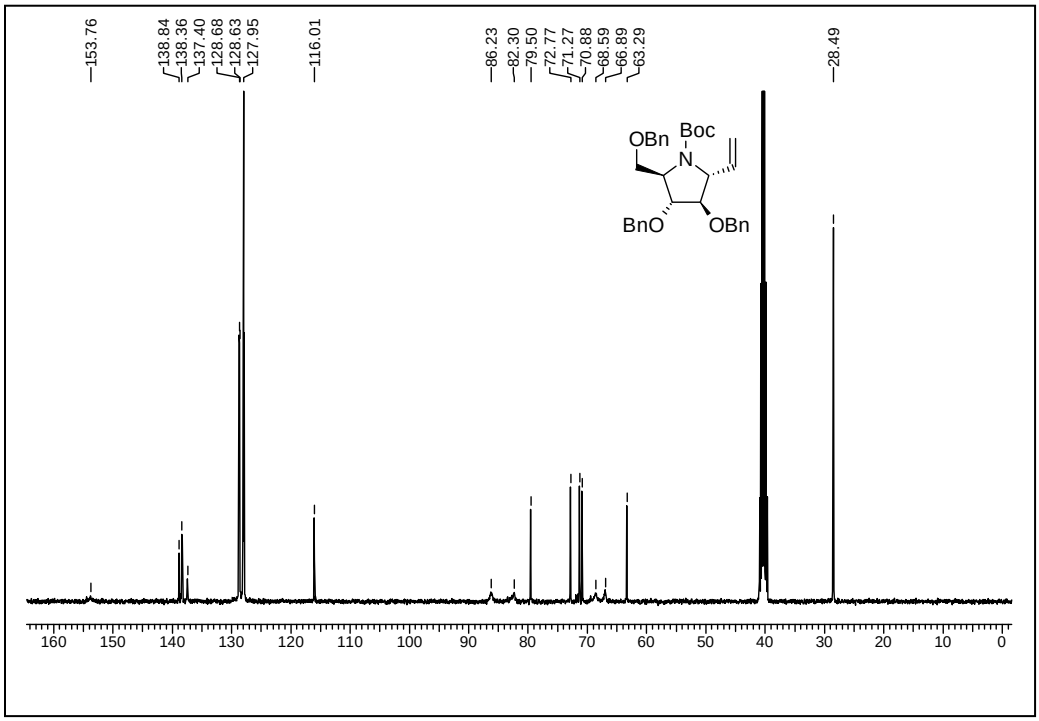

^{13}C NMR Spectrum of 1.81 in DMSO-d_6 at 343 °K

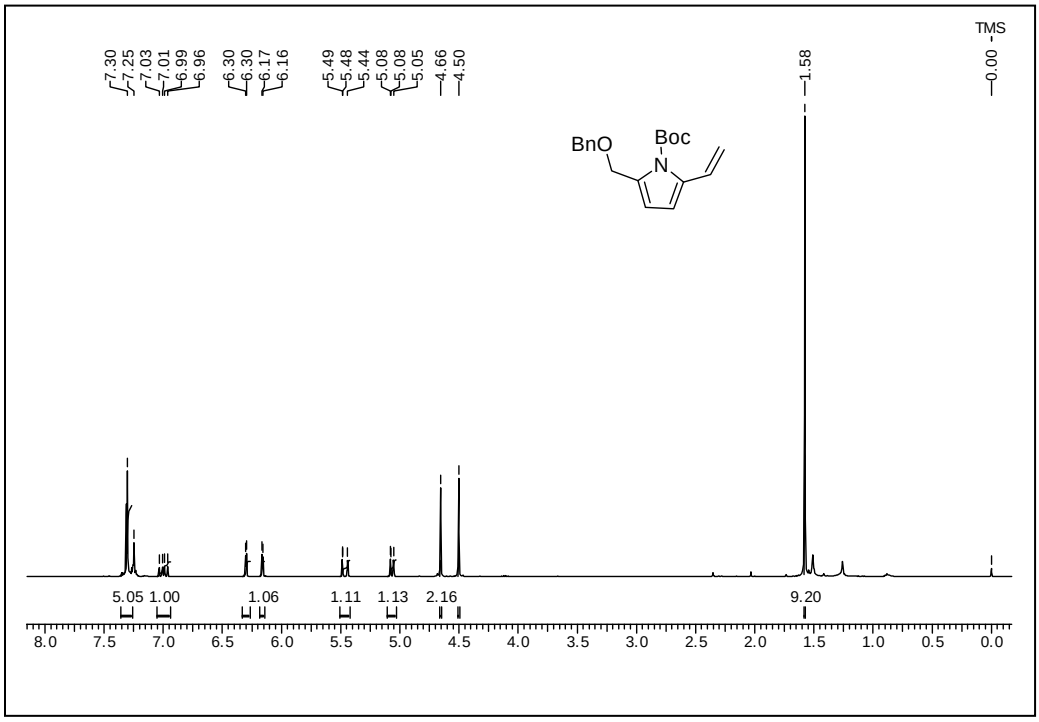

^{1}H NMR Spectrum of 1.82 in $CDCl_3$

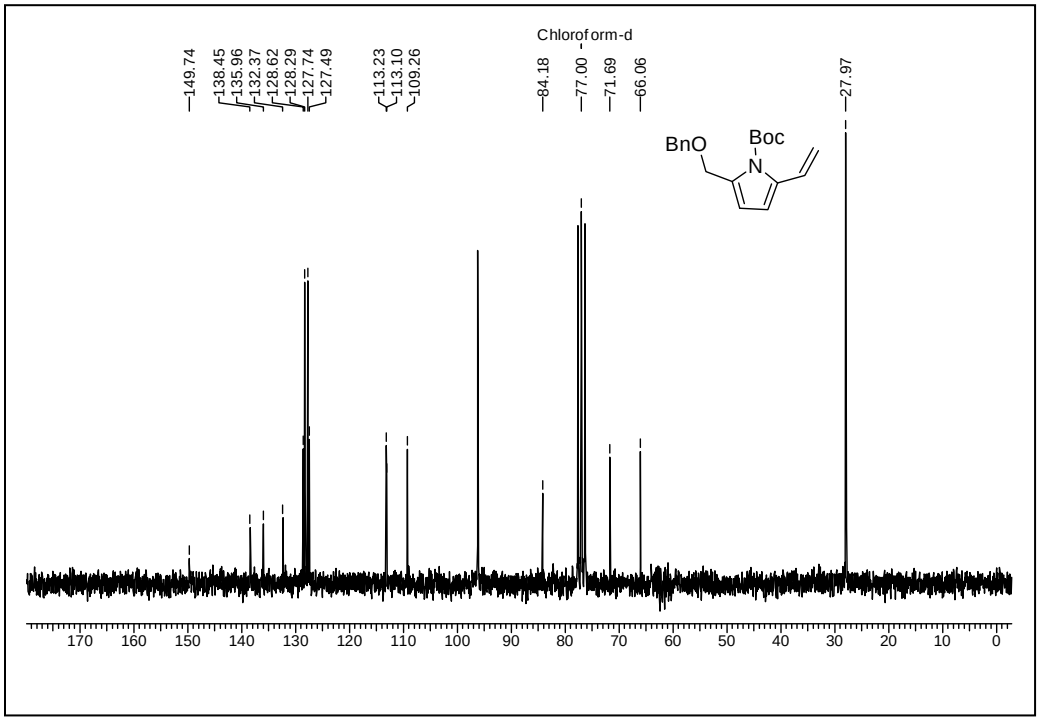

^{13}C NMR Spectrum of 1.82 in $CDCl_3$

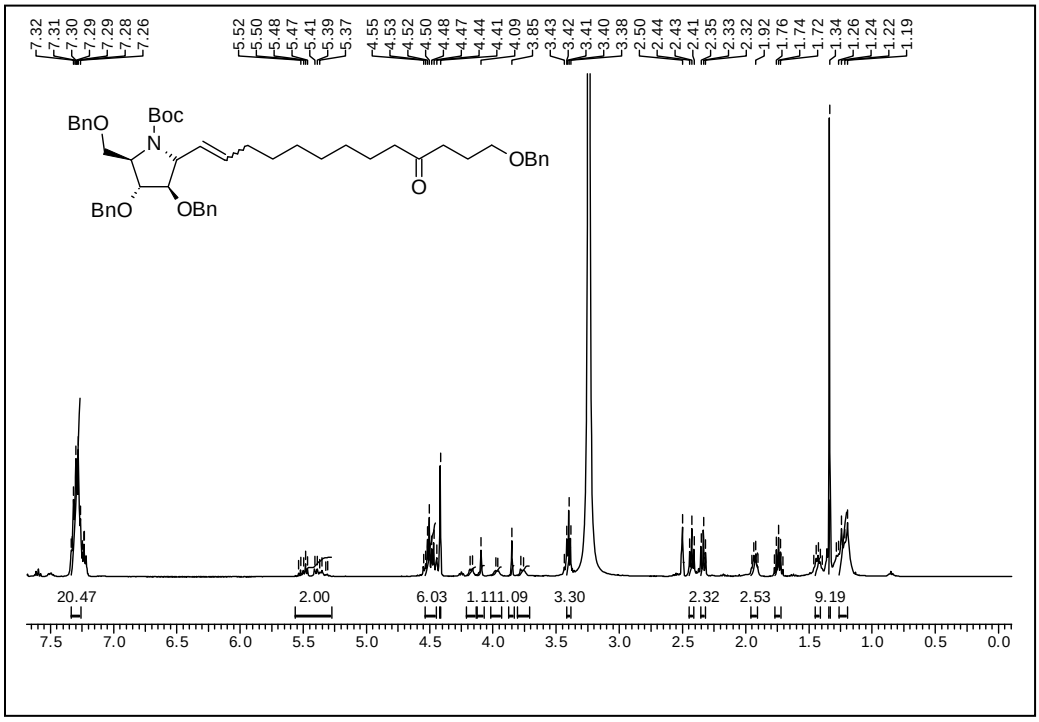

^{1}H NMR Spectrum of 1.83 in DMSO-d_6 at 343 °K

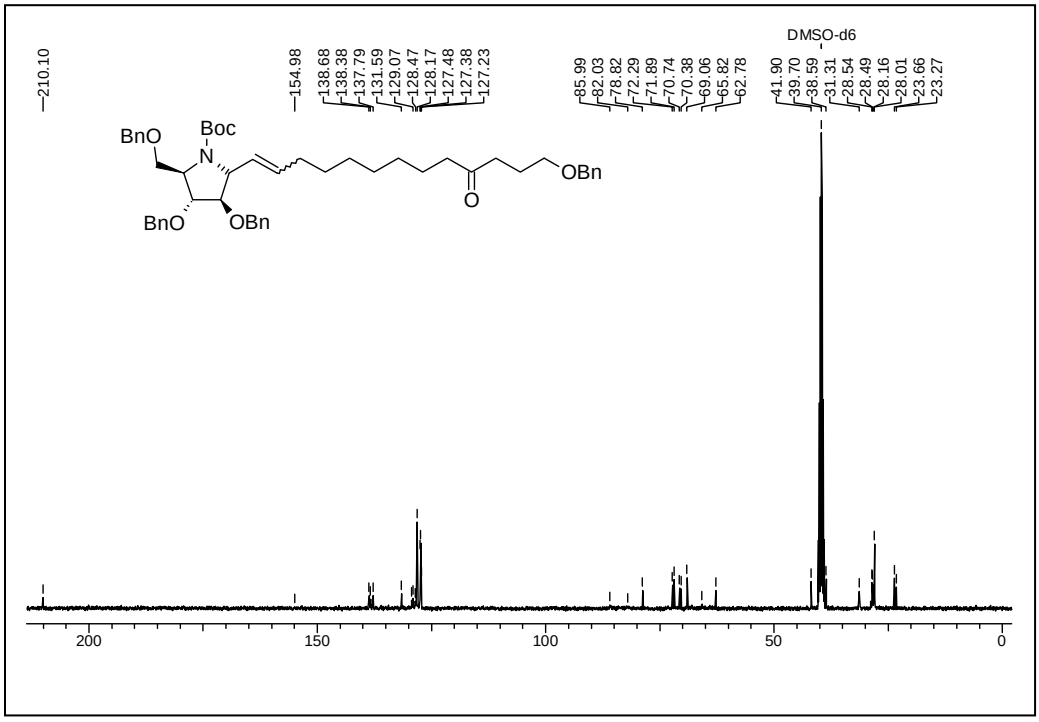

^{13}C NMR Spectrum of 1.83 in DMSO-d_6 at 343 °K

1.6 References

1. a) Hoveyda, A. H.; Zhugralin, A. R. *Nature* **2007**, *450*, 243–251; b) Clavier, H.; Grela, K.; Kirschning, A.; Mauduit, M.; Nolan, S. P. *Angew. Chem. Int. Ed*. **2007**, *46*, 6786–6801; c) Nicolaou, K. C.; Bulger, P. G.; Sarlah, D. *Angew. Chem. Int. Ed*. **2005**, *44*, 4490–4527; d) Grubbs, R. H. *Tetrahedron* **2004**, *60*, 7117–7140; e) Martin, W. H. C.; Blechert, S. *Current Topics in Medicinal Chemistry* **2005**, *5*, 1521–1540; f) Schrock, R. R.; Hoveyda, A. H. *Angew. Chem. Int. Ed*. **2003**, *42*, 4592–4633; g) T. M. Trnka,; R. H. Grubbs. *Acc. Chem. Res*. **2001**, *34*, 18–29; h) Roy, R.; Das, S. K. *Chem. Comm*. **2000**, 519–529; i) Jørgensen, M.; Hadwiger, P.; Madsen, R.; Stütz, A. E.; Wrodnigg, T. M. *Current Organic Chemistry* **2000**, *4*, 565–588; j) Fürstner, A. *Angew. Chem. Int. Ed*. **2000**, *39*, 3013–3043; k) Grubbs, R. H.; Chang, S. *Tetrahedron* **1998**, *54*, 4413–4450.
2. a) Brik, A. *Advanced Synthesis and Catalysis* **2008**, *350*, 1161–675; b) Prunet, J. *Current Topics in Medicinal Chemistry* **2005**, *5*, 1559–1577; c) Connon, S. J.; Blechert, S. *Angew. Chem. Int. Ed*. **2003**, *42*, 1900–1923; d) Grubbs, R. H.; Chang, S. *Tetrahedron* **1998**, *54*, 4413–4450; e) Alkene Metathesis in Organic Synthesis (Ed.: Fürstner, A.), Springer, Berlin, **1998**.
3. a) Freitas, E. R.; Gum, C. R. *Chem. Eng. Prog.* **1979**, *75*, 73–76; b) Shell International Chemical Company, SHOP—Linear Alpha Olefins (Company publication), **1982**.
4. Phillips Petroleum Company, Hydrocarbon Process **1967**, *46*, 232.
5. a) Tsuji, J.; Hashiguchi, S. *Tetrahedron Lett.* **1980**, *21*, 2955–2958; b) Tsuji, J.; Hashiguchi, S. *J. Organomet. Chem.* **1981**, *218*, 69–73; c) Plugge, M. F.; Mol, J. C. *Synlett.* **1991**, *7*, 507–508.
6. Nugent, W. A.; Feldman, J.; Calabrese, J. C. *J. Am. Chem. Soc.* **1995**, *117*, 8992–8998.
7. a) Descotes, G.; Ramja, J.; Basset, J.–M.; Pagano, S. *Tetrahedon Lett.* **1994**, *35*, 7379–7382. b) Couturier, J.–L.; Tanaka, K.; Leconte, M.; Basset, J.–M.; Ollivier, J. *Angew. Chem. Int. Ed.* **1993**, *32*, 112–115.
8. Bazan, G. C.; Oskam, J. H.; Cho, H.–N.; Park, L. Y.; Schrock, R. R. *J. Am. Chem. Soc.* **1991**, *113*, 6899–6907.

9. a) Schwab, P.; France, M. B.; Ziller, J. W.; Grubbs, R. H. *Angew. Chem. Int. Ed*. **1995**, *34*, 2039–2041.
10. Lynn, D. M.; Mohr, B.; Grubbs, R. H. *J. Am. Chem. Soc.* **1998**, *120*, 1627–1628.
11. Wakamatsu, H.; Blechert, S. *Angew. Chem. Int. Ed*. **2002**, *41*, 2403–2405.
12. HQrisson, J. L.; Chauvin, Y. *Makromol. Chem*. **1970**, *141*, 161–176.
13. Dominique, R.; Liu, B.; Das, S. K.; Roy, R. *Synthesis* **2000**, *6*, 862–868.
14. Gan, Z.; Roy, R. *Tetrahedron* **2000**, *56*, 1423–428.
15. Hu Y. J.; Roy, R. *Tetrahedron Lett.* **1999**, *40*, 3305–3308.
16. Brüchner, P.; Koch, D.; Voigtmann, U.; Blechert, S. *Syn. Comm*. **2007**, *37*, 2757–2769.
17. Wan, Q.; Cho, Y.–S.; Lambert, T. H.; Danishefsky, S. J. *J. Carboh. Chem.* **2005**, *24*, 425–440.
18. Dondoni, A.; Giovannini, P. P.; Marra, A. *J. Chem. Soc. Perkin Trans*. **2001**, *1*, 2380–2388.
19. Dondoni, A.; Giovannini, P. P.; Perrone, D. *J. Org. Chem*. **2005**, *70*, 5508–5518.
20. Bernardes, G. J. L.; Chalker, J. M.; Errey, J. C.; Davis, B. G. *J. Am. Chem. Soc.* **2008,** *130*, 5052–5053.
21. Verbicky, C. A.; Zercher, C. K.; *Tetrahedron Lett*. **2000**, *41*, 8723–8727.
22. Grubbs, R. H.; Blackwell, H. E.; Chatterjee, A. K.; O'Leary, D. J.; Washenfelder, R. A.; Bussmann, D. A. *J. Am. Chem. Soc.* **2000**, *122*, 58–71.
23. Barrett, A. G. M.; Kasdorf, K. *J. Am. Chem. Soc.* **1996**, *118*, 11030–11037.
24. Passiniemi, M.; Koskinen, A. M. P. *Tetrahedron Lett*. **2008**, *49*, 980–983.
25. Cossy, J.; Willis, C.; Bellosta, V. *Synlett.* **2001**, *10*, 1578–1580.
26. Radha Krishna, P.; Dayaker, G. *Tetrahedron Lett.* **2007**, *48*, 7279–7282.
27. Xu, S.; Arimoto, H.; Uemura, D. *Angew. Chem. Int. Ed.* **2007**, *46*, 5746–5749.
28. Ying, Y.; Taori, K.; Kim, H.; Hong, J.; Luesch, H. *J. Am. Chem. Soc.* **2008**, *130*, 8455–8459.
29. Oguri, H.; Sasaki, S. Y.; Oishi, T.; Hirama, M. *Tetrahedron Lett.* **1999**, *40*, 5405–5408.
30. McDonald, F. E.; Wei, X. *Org. Lett.* **2002**, *4*, 593–595.
31. Ghosh, A. K.; Gong, G. *J. Am. Chem. Soc.* **2004**, *126*, 3704–3705.
32. Xiong, Z.; Corey, E. J. *J. Am. Chem. Soc*. **2000**, *122*, 4831–4832.
33. Diver, S. T.; Schreiber, S. L. *J. Am. Chem. Soc*. **1997**, *119*, 5106–5109.
34. Buncel, E.; Bradley, P. R. *Can. J. Chem.* **1967**, *45*, 515.

35. Sinnott, M. L. *Chem. Rev.* **1990**, *90*, 1171–1202.

36. Asano, N. *Glycobiology* **2003**, *13*, 93R–104R.

37. Inoue, S.; Tsuroka, T.; Niida, T. *J. Antibiot.* **1966**, *19*, 288–296.

38. Niwa, T.; Inoue, S.; Tsuruoka, T.; Koaze, Y; Niida, T. *Agric. Biol. Chem.* **1970**, *34*, 966– 968.

39. Kornfeld, R.; Kornfeld, S. *Annu. Rev. Biochem.* **1985**, *54*, 631–664.

40. a) Karpas, A; Fleet, G. W. J.; Dwek, R. A; Petursson, S.; Namgoong, S. K.; Ramsden, N. G.; Jacob, G. S.; Rademacher, T. W. *Proc. Natl. Acad. Sci. U.* S. *A.* **1988**, *85*, 9229–9233. b) Fu, Y. K.; Hart, T. K.; Jonak, Z. L.; Bugelski, P. *J. Virol.* **1993**, *67*, 3818–3825. c) Fischer, P. B.; Karlsson, G. B.; Dwek, R. A.; Platt, F. M. *J. Virol.* **1996**, *70*, 7153–7160. d) Taylor, D. L.; Sunkara, P. S.; Liu, P. S.; Kang, M. S.; Bowlin, T. L.; Tyms, A. S. *AIDS* **1991**, *5*, 693–696.

41. Sunkara, P. S.; Taylor, D. L.; Kang, M. S.; Bowlin, T. L.; Liu, P. S.; Tyms, A. S. *Lancet* **1989**, 1206–1207.

42 Cook, C. S.; Karabatsos, P. J.; Schoenhard, G. L.; Karim, A. *Pharm. Res.* **1995**, *12*, 1158–1164.

43. "Basic Diabetes Information" American Diabetes Association http://www.diabetes.org/info/diabetesinfo.jsp (5 November 2003).

44. Junge, B.; Matzke, M.; Stltefuss, J. In *Handbook of Experimental Pharmacology;* Kuhlmann, J. and Puls, W., Eds.; Springer–Verlag: Berlin, Heidelberg, New York, 1996; Vol. 119.

45 Stutz, A. E., Ed. *Irninosugars as Glycosidase Inhibitors: Nojirimycin and Beyond;* Wiley-VCR: Weinheim, 1999.

46. a) Cipolla, L.; La Feria, B.; Nicotra, F. *Curr. Top. Med. Chem.* **2003**, *3*, 485–511. b) Berecibar, A.; Grandjean, C.; Siriwardena, A. *Chem. Rev.* **1999**, *99*, 779–844. c) El Nemr, A. *Tetrahedron* **2000**, *56*, 8579–8629. d) Casiraghi, G.; Zanardi, F.; Rassu, G.; Spanu, P. *Chem. Rev.* **1995**, *95*, 1677–1716.

47. Wrodnigg, T.M. *Monatsh. Chem.* **2002**, *133*, 393–426.

48. Weintraub, P. M.; Sabol, J. S.; Kane, J. A.; Borcherding, D. R. *Tetrahedron* **2003**, *59*, 2953–2989.

49. For a recent review of the isolation, biology, and chemistry of broussonetines, see: Shibano, M.; Tsukamoto, D.; Kusano, G. *Heterocycles* **2002**, *57*, 1539–1553.

50. a) Saul, R.; Chambers, J. P.; Molyneux, R. J.; Elbein, A. D. *Arch. Biochem. Biophys.* **1983**, *221*, 593–597. b) Saul, R.; Chambers, J. P.; Molyneux, R. J.;

Elbein, A. D. *Arch. Biochem. Biophys.* **1984**, *230*, 668–675. c) Winchester, B.; Fleet, G. W. J. *J. Carbohydr. Chem.* **2000**, *19*, 471–483.

51. Yoda, H.; Shimojo, T.; Takabe, K. *Tetrahedron Lett.* **1999**, *40*, 1335–1336.
52. Perlmutter, P.; Vounatsos, F. *J. Carbohydr. Chem.* **2003**, *22*, 719–732.
53. Brimble, M. A.; Park, I. H.; Taylor, D. L. *Tetrahedron* **2003**, *59*, 5861–5868.
54. Trost, B. M.; Horne, D. B.; Woltering, M. J. *Angew. Chem. Int. Ed.* **2003**, *42*, 5987–5990.
55. Chmielewski, M.; Whistler, R. L. *J. Org. Chem.* **1975**, *40*, 639–643.
56. Card, P. J.; Hitz, W. D. *J. Org. Chem.***, 1985**, *50***,** 891–893.
57. Kierstead, R. W.; Faraone, A.; mennona, F.; Mullin, J.; Guthrie, R. W.; Crowley, H.; Sinko, B.; Blabber, L. C. *J. Med. Chem*. **1983**, *26*, 1561–1569.
58. Zhong, Y.; Shing, T. K. M. *J. Org. Chem*. **1997**, *62*, 2622–2624.

CHAPTER-I

Section II: Synthesis of *C*-glycosides of dodecanoic acid employing cross metathesis and their application as new capping/reducing agents for silver nanoparticles synthesis.

1.7 Introduction

1.7.1 Introduction to Nanotechnology

Nanoscience deals with the study of the objects and systems in which at least one dimension is within 1–100 nm range and can be considered as the science and technology that enable us to prepare and understand the various aspects of materials between the molecular and bulk regimes. It embraces many different fields including biology, chemistry, physics, engineering and medicine etc. A nanometer, a billionth of a meter, is about the size of six carbon atoms in a row. The term "nano" is taken from a Greek word "nanos", which means "little old man" or "dwarf".

Figure 1.14 *A picture representing the relative sizes of various natural & man-made objects*

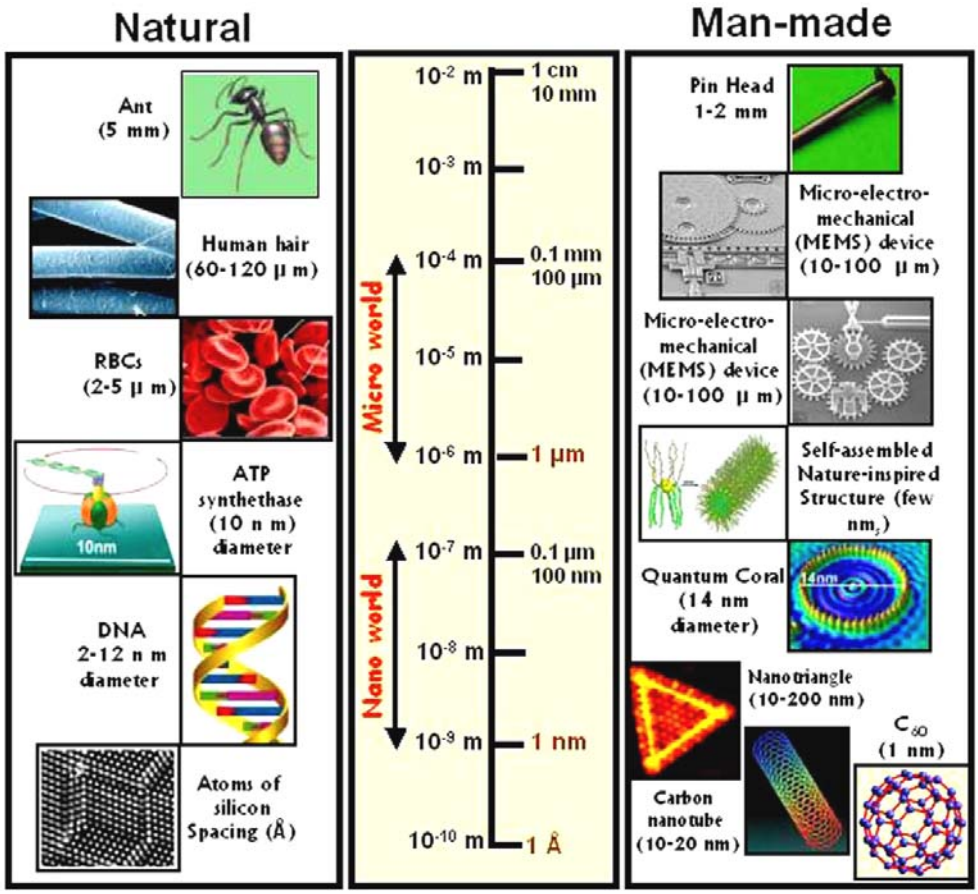

1.7.2 Properties of Nanomaterials

At the nanoscale dimensions, the material properties change significantly differing completely from their bulk counterparts. Nanomaterials display new phenomenon associated with the quantized effects and with the preponderance of surfaces and interfaces. The quantization effect arises in nanometer regime because the overall dimensions of objects are comparable to the characteristic wavelength of fundamental excitations in materials.

As the size of material decreases, the percentage of surface atoms increases, thus increasing the reactivity and making them highly reactive catalysts.[1] For example, iron nanoparticles of sizes 3 nm, 10 nm and 30 nm will have 50%, 10% and 5% of atoms on surface. Among the surface atoms, atoms sitting on the edges and corners are more reactive than those in planes. Also, the percentage of atoms at the edges and corners increases with decrease in the particle size and therefore, smaller metal particles are preferred for catalysis. A schematic representation is shown in figure 1.15.

Figure 1.15 *Schematic representation of increasing surface area with decrease in size*

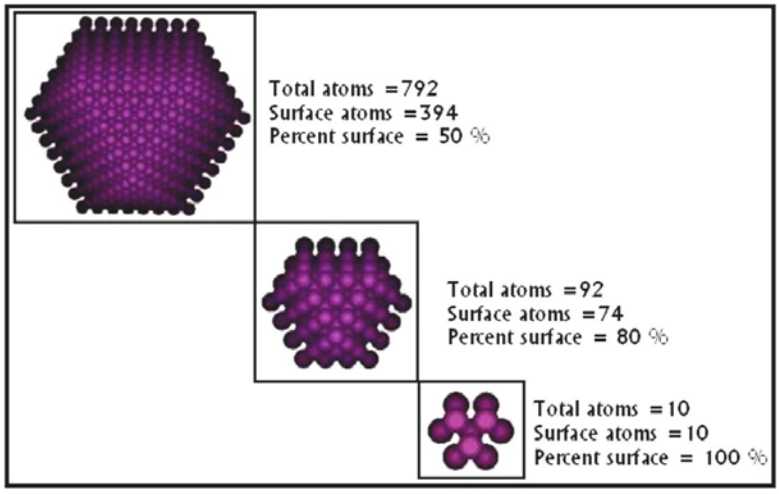

An interesting feature of metal and semiconductor nanoparticles is their optical property. These nanomaterials exhibit interesting shape and size dependent optical properties due to quantum confinement. However, in a bulk crystal, the properties of material depend on chemical composition and not on size. Due to the decrease in size of a crystal towards nanometer regime, the electronic structure is altered from continuous electronic bands to discrete or quantized electronic levels. Therefore, the continuous

optical transitions between the electronic bands become discrete and the properties of nanomaterial become size dependent. [2]

Metal nanoparticle (Au, Ag and Cu) dispersions exhibit colors due to the surface plasmon resonance (SPR) phenomenon, which is caused by the coherent oscillation of conduction band electrons when they interact with electromagnetic field.[3] During SPR, polarization of the electrons with respect to the much heavier ionic core is induced by the electric field of an interacting light wave. This creates a net charge difference at nanoparticle surface, which acts as a restoring force. Thus, a dipolar oscillation of all the electrons with the same phase is created (Figure 1.16). The so observed color originates from the strong absorption by the metal nanoparticles when the frequency of electromagnetic field becomes resonant with the coherent oscillation of electron motion.[4] The frequency and width of SPR depends on the metal nanoparticle size, shape, dielectric constant of the metal itself and the surrounding medium. Similarly, other important properties such as electronic properties,[5] magnetic properties,[6] melting point[7] and catalytic properties[8] of the nanomaterials depending on their shape, size, composition and surrounding medium have been studied in great detail.

Figure 1.16 *Illustration of the excitation of the dipole surface plasmon oscillation. A dipolar oscillation of the electrons is created with period T*

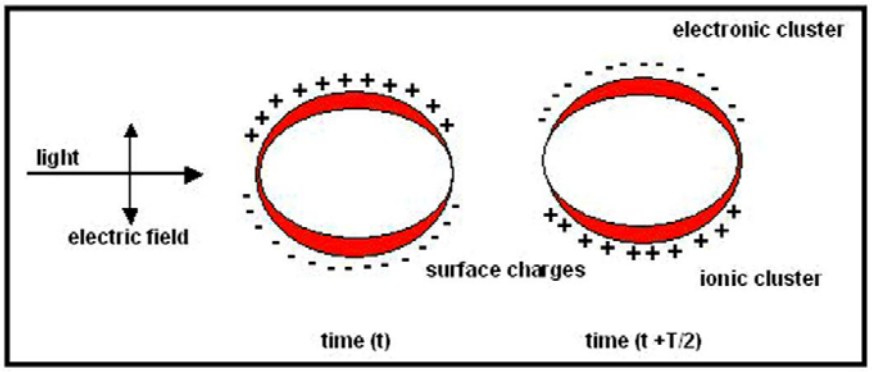

Another most important property of nanomaterials, especially semiconductor nanoparticles, is to exhibit photocatalytic behavior. Size dependent properties (quantization) of semiconductors (such as TiO_2 and ZnO etc.) and quantized charging effects in metal nanoparticles provide the basis for developing new and effective systems.[9] These nanostructures provide innovative strategies for designing next generation energy conversion devices.[10] In a semiconductor, the energy difference between the valence band and the conduction band is known as the "Band Gap". When it

absorbs radiation from sunlight or illuminated light source (fluorescent lamp), it generates pair of electron and hole. This stage is known as the semiconductors "photo-excitation state." The recombination of electron-hole pair may result in light emission with appropriate further reactions. These semiconductors behave as photocatalysts. (Figure 1.17)

Figure 1.17 *Schematic representation of photocatalytic degradation of an organic compound through light mediated excitation of electron across the band gap*

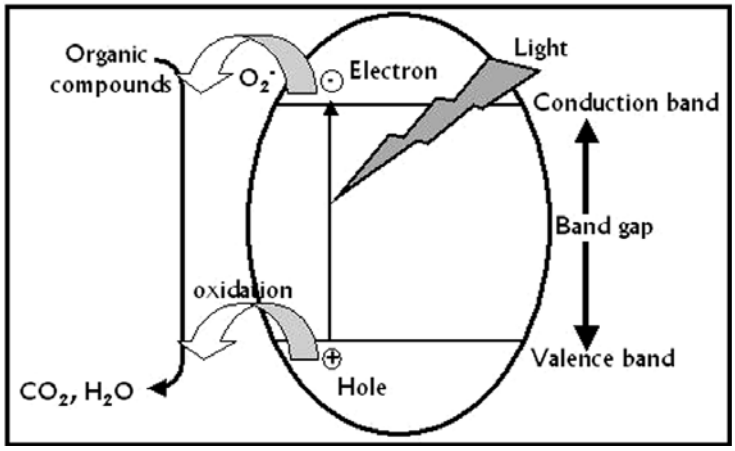

Nanotechnology has created a kind of revolution as this new area encompasses physics, chemistry, materials science and engineering and also biology and medicine. Several applications are envisaged from these interesting materials in the field of sensors,[11] catalysis,[12] diagnostic tools,[13] therapeutic agents,[14] drug/gene delivery vehicles,[15] solar cells,[16] plasmonics devices,[17] cosmetics,[18] coating materials,[19] cell imaging,[20] fuel cells,[21] photonic band gap materials,[22] single electron transistors,[23] non-linear optics devices[24] and surface enhanced raman spectroscopy.[25]

1.7.3 Synthesis of Nanomaterials

The most challenging part of research in the field of nanotechnology is the cost effective and environmentally safe procedures for nanomaterials synthesis. The approach towards nanomaterials synthesis could be broadly divided into two groups following the principle of either "top down approach" or "bottom up approach" (Figure 1.18). The top down approach seeks to fabricate nanodevices on silicon (or other semiconductors) chips directly using electron beam or X-ray lithography. In the bottom-up approach, nanostructures are synthesized from atoms or molecules. In the latter, the synthesis protocols can be further divided into physical methods, chemical methods and

biological/bio-inspired methods. A flow chart indicating the different synthetic methods for nanomaterials has been shown in Figure 1.19. Various physical methods have been successfully employed for nanomaterial synthesis such as vapor deposition,[26] thermal decomposition,[27] spray pyrolysis,[28] photoirradiation,[29] laser ablation,[30] ultrasonication,[31] radiolysis[32] and solvated metal atom dispersion.[33]

Figure 1.18 *Examples that depict the fabrication (complexicity) of materials at different length scales by 'Top-down' and 'Bottom-up' approaches*

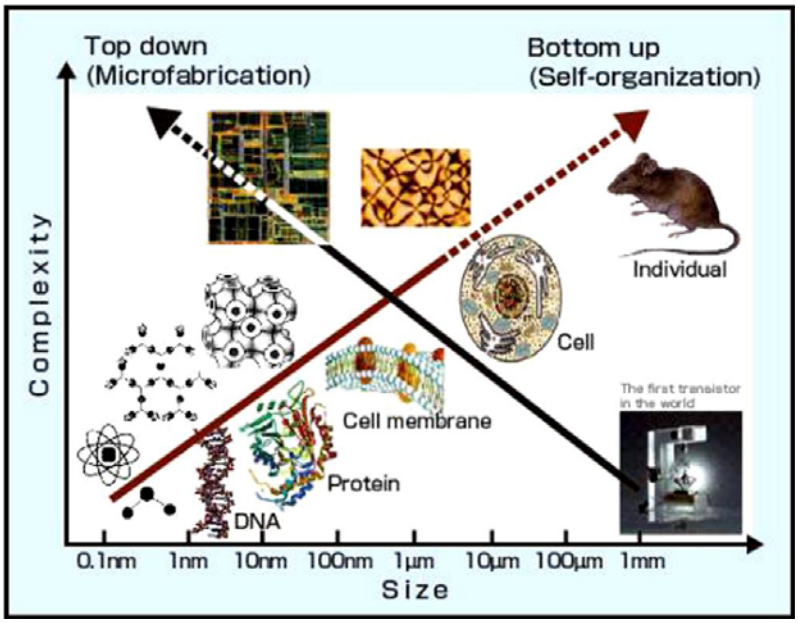

However, chemical methods have had several advantages over physical methods; therefore chemical methods are widely accepted for nanomaterials synthesis. Nanomaterials such as metals, metal oxides and semiconductor nanoparticles can be synthesized by chemical methods by reduction or oxidation of metal ions or by precipitation of the desired composites (by carrying out appropriate chemical reaction).

Chemical methods may require a capping agent to restrict the growth of particles in the nanometer dimension. The use of capping molecules results in better shape and size control, stability and assembly of nanomaterials. Different capping agents starting from simple ions to various biomolecules have been employed for nanomaterial stability.[34] Following chemical methods nanomaterials can be synthesized in aqueous medium as well as in organic medium too, depending on their intended applications. Aqueous dispersed chemically synthesized metal nanoparticles can be easily phase transferred to organic medium.[35] Although, above mentioned synthetic procedures result in good

control over shape, size and crystallinity, they very often involve the use of hazardous reagents, volatile solvents and intense physico-chemical conditions. Therefore, currently researchers are more interested towards development of environmentally benign procedures for nanoparticle synthesis.

Biological methods for nanomaterials synthesis involve either bio-organisms or biomolecules derived from bio-organisms. Among the bio-organisms bacteria[36] and yeasts[37] are well known for detoxification processes that involve reduction of metal ions or the formation of insoluble complexes with the metal ion in the form of nanoparticles.

Figure 1.19 *Schematic outlines of the various approaches for the synthesis of nanoparticles*

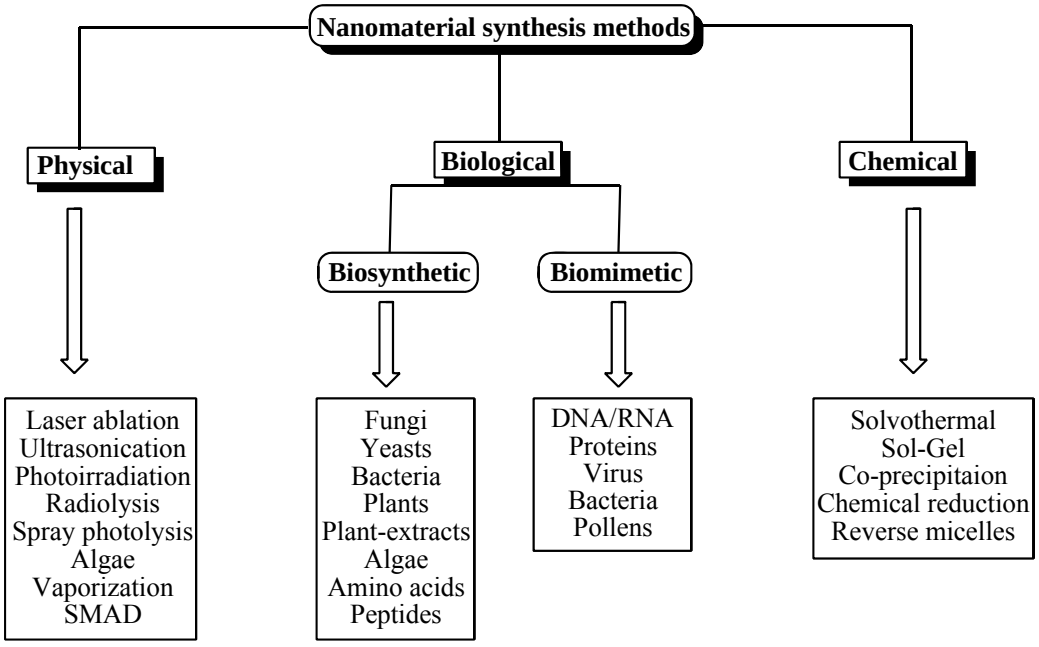

1.7.4 Glyconanoparticles

Carbohydrates are, together with nucleic acids and proteins, important molecules for life. Much is already known about the structure, interactions and function of nucleic acids and proteins, however, the role of carbohydrates in the cell is less clear. The surface of mammalian cells is covered by a dense coating of carbohydrates named glycocalyx.[39] In the glycocalyx, carbohydrates appear mainly conjugated to proteins and lipids (glycoproteins, glycolipids and proteoglycans) and it is as glycoconjugates that they develop their biological function. Now, it is known that these complex oligosaccharides or monosaccharides are involved in the control of many normal and pathological processes.[40,41]

A characteristic feature of the biological interactions where carbohydrates are involved is their extreme low affinity that has to be compensated by multivalent presentation of the ligands. For this reason, Penadés and coworkers developed a new integrated approach based on the use of nanoparticles that they have named as Glyconanotechnology[38] to understand the carbohydrate-carbohydrate and the carbohydrate-protein interactions. Nanoparticles conjugated with carbohydrates are known as glyconanoparticles.

Several research groups have developed different strategies to prepare and apply nanoparticles functionalized with biologically relevant oligosaccharides to study carbohydrate interactions or to intervene in carbohydrate mediated biological processes. So now there are enough results to state that carbohydrates are joining proteins, peptides and DNA as biological partners of inorganic nanomaterials to intervene in biological processes.

These nanomaterial-biomolecules multifunctional systems could be used as useful tool to mimic the behavior of biomolecules in cells and therefore could be helpful to explain the mechanism of complex biological processes with a several potential applications. Glycolipid-nanoparticles conjugates are recently being developed that are expected to have many applications.

Glyconanoparticles have unusual physical properties due to its quantum size effect,[42] which can be used for the detection and evaluation of interactions. Several biotechnological and biomedicinal such as anti-adhesive property[43] of nanoparticle-carbohydrate systems have already been reported. Other applications such as carbohydrate interactions,[44] carbohydrate-protein interaction,[45] as biolabels[46] and some applications in the field of materials science[47] have also been published recently. The possible applications of glyconanoparticles in various fields of science have been shown in figure 1.20.

Three important properties of glyconanoparticles make them suitable model systems for different applications.

1. They are of similar size to many biomolecules and therefore can reproduce or mimic the carbohydrate presentation in glycoproteins etc.
2. They provide a glycocalyx-like surface thus presenting the carbohydrates in a globular and polyvalent configuration on their surfaces.
3. The glyconanoparticles would exhibit unusual physical properties due to their quantum size effect which could be used for the detection and evaluation of interactions.

Figure 1.20 *Schematic representations explaining the potential application of glyconanoparticles in the field of Glycobiology, Biotechnology and Material science*

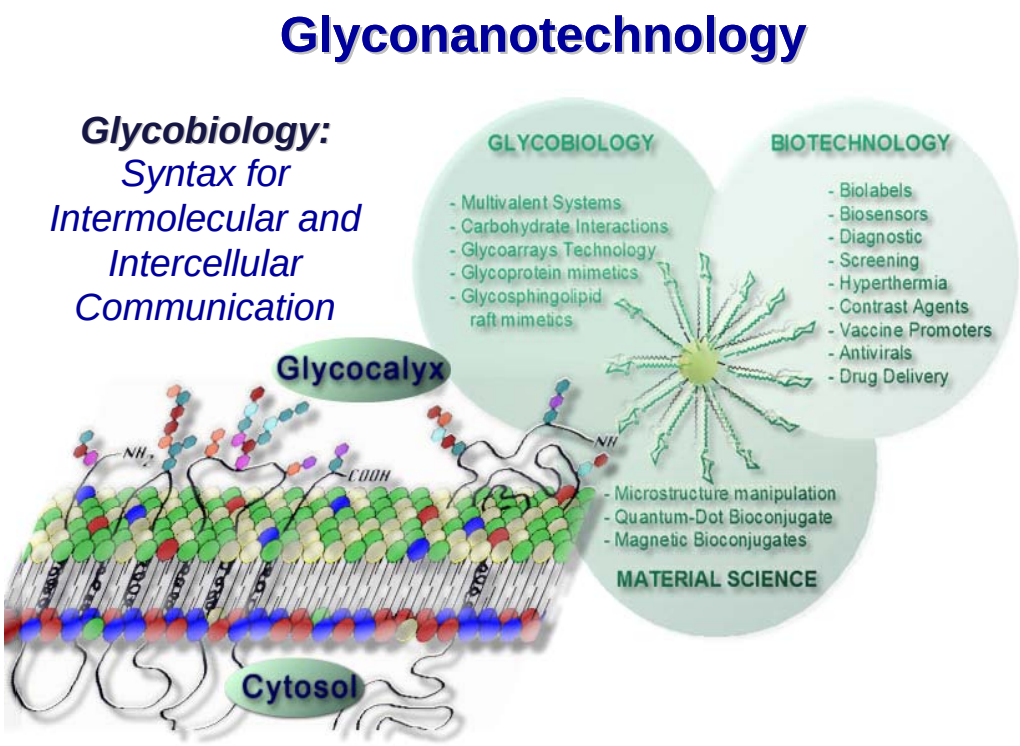

1.7.5 Types and synthesis of glyconanoparticles

Three different types of glyconanoparticles have been reported so far including gold and silver glyconanoparticles,[48] glyco-quantum dots[49] and magnetic glyconanoparticles.[50]

1.7.5.1 Gold and silver glyconanoparticles

Gold nanoparticles are the most stable metal nanoparticles, and present interesting properties which include a wide array of assembling model and unexpected size-related electronic, magnetic and optical properties (quantum size effect). They already have a number of applications in catalysis and biology. Therefore, their promises are in these fields as well as in the bottom-up approach of nanotechnology, and they will be key materials and building blocks in the 21st century.

While numerous routes exist for the production of colloidal gold nanoparticles, the method described by Brust *et al.*[51] and its variation[52] are the most popular synthetic schemes in the field. But there are very few systems reported involving carbohydrates. On

the other hand functionalization with modified saccharide system is receiving great attention these days.

Scheme 1.53 *Synthesis of Le^x, Le^y, glucose, lactose and maltose gold glyconanoparticles by Penades' methodology*

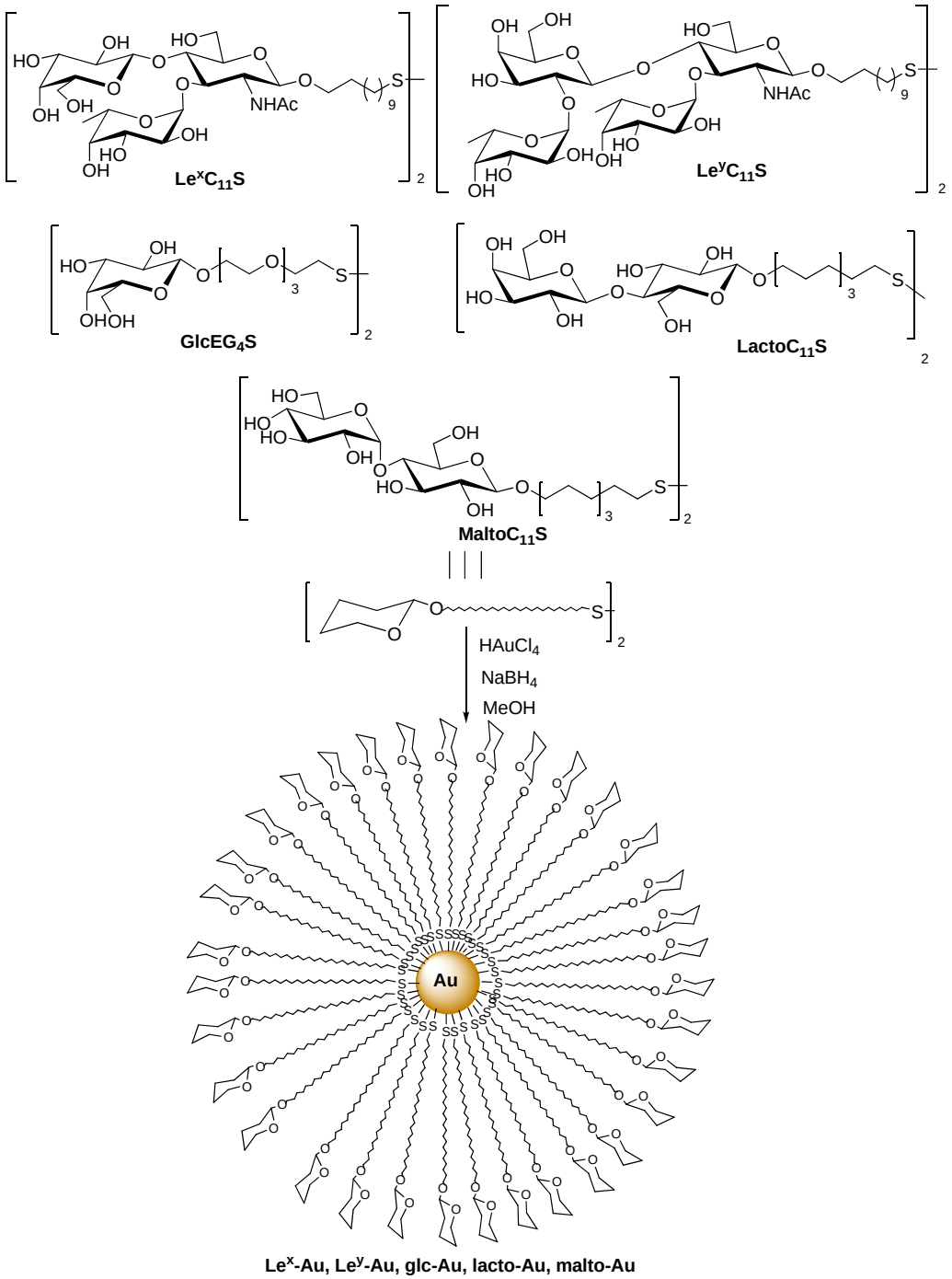

Penadés and coworkers first reported the synthesis of glyconanoparticles by the addition of methanolic solution of a neoglycoconjugate functionlized with a thiol group, to an aqueous solution of tetrachloroauric acid ($HAuCl_4$) and its subsequent reduction by $NaBH_4$.[53] (Scheme 1.53)

This method was further used for the synthesis of different glyconanoparticles functionalized with tetrasaccharide,[54] trisaccharide, diasaccharides lactose and maltose or monosaccharide glucose.[55] Different linkers of hydrophobic (alkanes) and hydrophilic (polyethylene glycol derivatives) nature were used to bind the carbohydrate to the gold core. The glyconanoparticles prepared in this way are water soluble, stable in solution for years, non-cytotoxic and exceptionally small (less 2 nm). This small size confers them unusual properties as a permanent magnetism even at room temperature.

Lin *et al.*[56] have also used the same synthetic protocol to prepare gold nanoparticles functionalized with glucose, mannose, galactose and mannosides. Further, Gervay-Hague *et al.*[57] have shown the same with glucose and galactose. A three-step procedure has also been used by Lakowicz *et al*.[58] to prepare hybrid silver glyconanoparticles. Recently, Panacek *et al.*[59] have synthesized silver nanoparticles capped with different saccharides, which showed high antibacterial activity against different bacterial species including highly multiresistant strains.

All the above mentioned methods provide water soluble nanoparticles of reduced dispersion and controlled size. These nanoparticles are stable, and self-aggregation has not been observed in any case.

1.7.5.2 Glyco-quantum dots

Nanocrystals of semiconducting materials, otherwise included in the term quantum dots (QDs), have fascinated physicists, chemists, and electronic engineers since the 1970s. The most striking feature of these materials is that their chemical and physical properties differ markedly from those of the bulk solid. Since their quantum size effects are understood, fundamental and applied research on these systems has become increasingly popular. One of the most interesting applications is the use of nanocrystals as luminescent labels for biological systems.[60] QDs have several advantages over conventional fluorescent dyes: they emit light at a variety of precise wavelengths depending on their size and have long fluorescent lifetimes. There are several approaches for the coupling of biomolecules to semiconductor QDs.[61]

Glyco-conjugated semiconductor nanoparticles (quantum dots) have been synthesized by several groups and different approaches have been followed.[62] Most commonly, QDs are first prepared at high temperature in presence of capping agents to avoid aggregation. Further, in second step, the biomolecules were conjugated with so synthesized QDs. Thiol capped QDs have been bio-conjugated with different biomolecules such as peptides and proteins, antibodies, DNA and other molecules too. However, there are only few examples of QDs conjugated to carbohydrate antigens for specific cell targeting.

The first example of QDs protected with polysaccharides was reported in 2003 by Rosenzweig *et al*.[63] This group prepared CdSe-ZnS quantum dots protected with carboxymethyldextran and polylysine, and they proved the high affinity of the QDs toward the glucose binding protein-Concanavalin A (Con A).

Scheme 1.54 *Preparation of glyco-QDs*

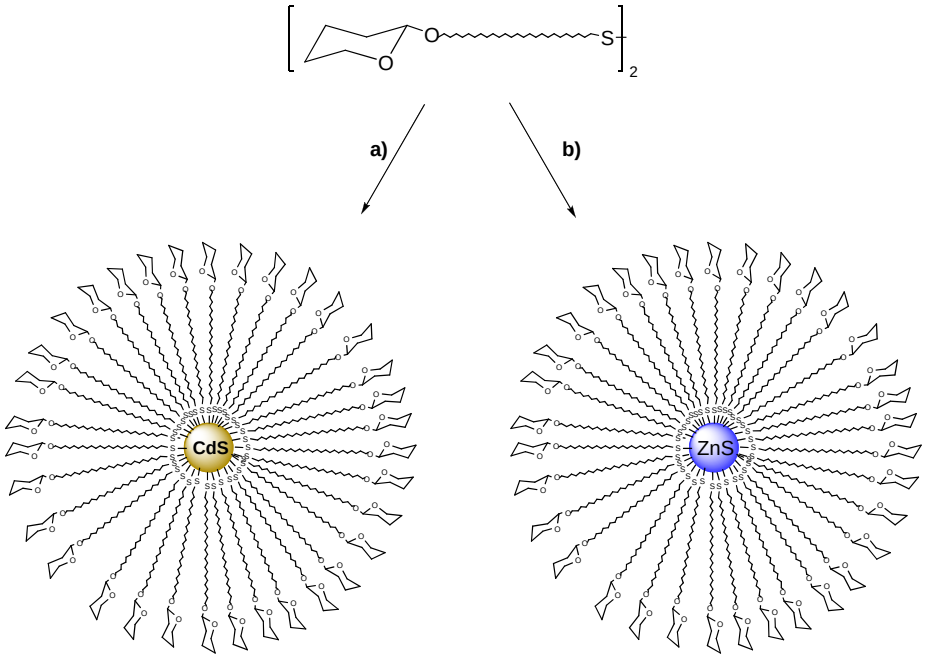

(a) $Cd(NO_3)_2 \cdot 4H_2O$, Na_2S, pH 10; (b) $Zn(NO_3)_2\ 6H_2O$, Na_2S, pH 10.

Chaikof *et al*. reported in 2004 the coupling of commercially available QDs-streptavidin with a biotin end-terminated lactose glycopolymer.[64] Confocal microscopy confirmed fluorescent staining of Ricinus communis agglutinin (RCA120)-immobilized agarose beads due to the glycopolymer-lectin interaction. Penadés and coworkers have reported the preparation of water soluble nanoclusters of cadmium sulphide and zinc

sulphide covalently bound to biologically significant neoglycoconjugates by a single step solution procedure (Scheme 1.54).[65] The synthesis of Lex and maltose protected CdS and Zns nanocrystals were carried out. The procedure was also used for the synthesis of tiopronin and tiopronin-Tat functionalized QDs which where able to label the nucleus of human fibroblasts. Fang *et al*. have recently reported the functionalization with β-N-acetylglucosamine of CdSe/ZnS core-shell QDs previously encapsulated with pyridine. The pyridine-encapsulated QDs were treated with a disulphide derivative of N-acetylglucosamine and $NaBH_4$ in aqueous solution to give water soluble glyco-QDs.[66]

1.7.5.3 Magnetic glyconanoparticles

Magnetic nanoparticles offer exciting new opportunities including the improvement of the quality of magnetic resonance imaging (MRI), hyperthermic treatment for malignant cells, site-specific drug delivery and also the recent research interest of manipulating cell membranes (Scheme 1.55).[67,68] Previously reported iron oxide superparamagnetic nanoparticles prepared by different surface chemistry have been widely used for numerous in vivo applications. The biological applications of these nanomaterials require these nanoparticles to have high magnetization values, size smaller than 20 nm, narrow particle size distribution and a special surface coating for both avoiding toxicity and allowing the coupling of biomolecules. Most commonly, iron oxide nanoparticles are prepared by coprecipitation of ferrous and ferric salts solution and stabilized using biocompatible molecules as dextran or oleic acid. In a second step, the biomolecules are attached by covalent or electrostatic coupling to the protected nanoparticle. Bioconjugated magnetic nanoparticles to peptides, proteins and antibodies have been developed and tested as biological markers or in hyperthermia treatments. There are very few examples of magnetic glyconanoparticle synthesis. Pendes prepared gold-iron nanoparticles functionalized with glucose, maltose and lactose by adding an iron salt to the aqueous $AuCl_4^-$solution.[69] The so produced nanoparticles are water soluble, stable and exceptionally small. The properties of these nanoparticles are particularly interesting as a result of their quantum size.

Scheme 1.55 *Potential applications of magnetic glyconanoparticles*

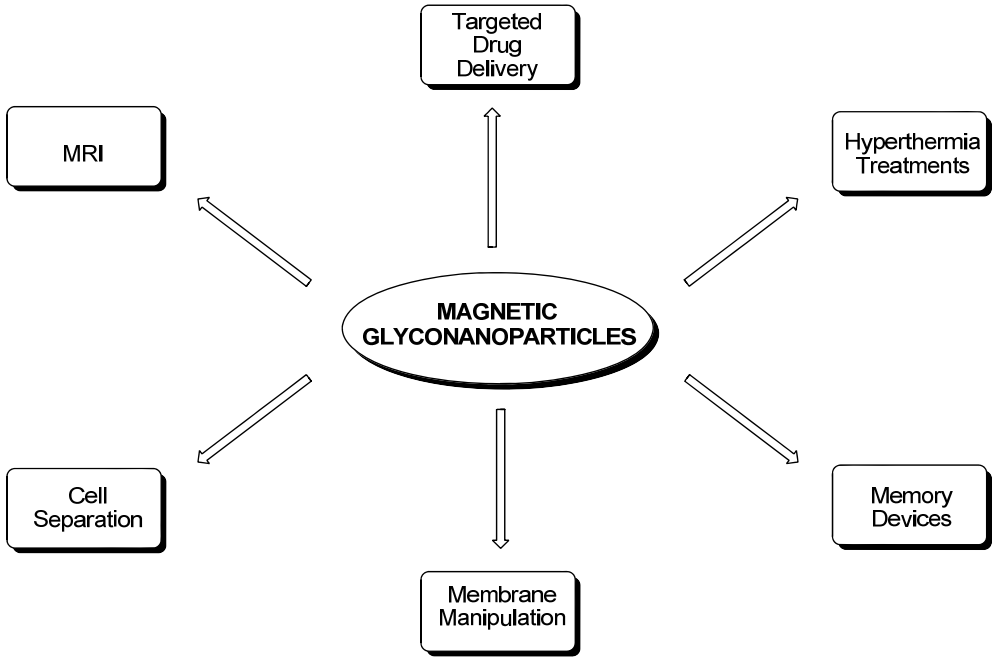

1.8 Present Work

Over the last decade, the potential of noble metal nanoparticles has been explored in various fields such as optics, microelectronics, sensors, catalysis, and so on.[11-25] The mutually advantageous conjugation of metal nanoparticles with biomolecules or biologically relevant ligands has gained much impetus because of their promising biomedicinal and bioanalytical applications in addition to hydrophilic rendition to surfaces and biocompatiblity.[38,53] In this context, *glyconanoparticles* (GNPs), derived from the surface modification of metal nanoparticles by connecting with sugar residues through *O*-glycoside linkages, have been recognized as novel tools to investigate carbohydrate recognition processes.[39-47]

Figure 1.21 *C-Glycosides of dodecanoic acid: new capping/reducing agents for glyconanoparticle synthesis*

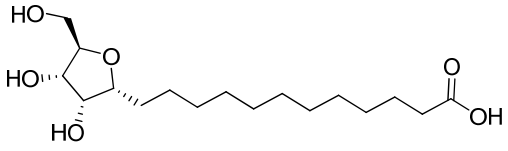

1.101; 12–α-*C*-ribo- furanosyl-dodecanoic acid

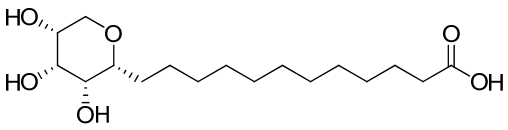

1.102; 12–α-*C*-ribo-pyranosyl-dodecanoic acid

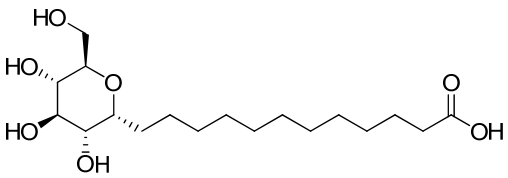

1.103; 12–α-*C*-gluco-pyranosyl-dodecanoic acid

An important issue regarding the *in vivo* application of glyconanoparticles is their susceptibility for enzymatic degradation. A viable alternative in this regard are *C*-glycosides, which have served as potential carbohydrate analogues resistant to metabolic processes. *C*-Glycosides, which entail methylene substitution for the anomeric oxygen, are isosteric mimics of their *O*-glycoside counterparts and offer a great deal of stability without substantial conformational amendment.[70] Though the application of *C*-

glycosylated long chain alkanes has been explored in liquid crystals and as surfactants,[71] their use in glyconanoparticle synthesis has been not yet documented. We have initiated a program on the synthesis of *C*-glycosyl long chain acids (Figure 1.21) and their use as capping/reducing agents for various metal nanoparticles.

1.8.2 Retrosynthesis

Considering the fact that the simple monosaccharides in biological systems can exist either in furanose or pyranose form, three compounds **1.101**–**1.103** were slected as representatives of pentoaldofurnaose (D-*ribo*), pentoaldopyranose (D-*ribo*) and hexoaldopyranose (D-*gluco*) respectively. The intended retrosynthetic strategy for the *C*-glycosyl acids **1.101**–**1.103** is based upon the cross metathesis of the corresponding peracetylated *C*-allyl glycosides **1.107**, **1.114** and **1.124** with 10-undecene-1-ol (**1.104**) followed by oxidation and deprotection. (Figure 1.22)

Figure 1.22 *Selected 12-C-glycosylated dodecanoic acids **1 .101–1.103** and the retrosynthetic strategy*

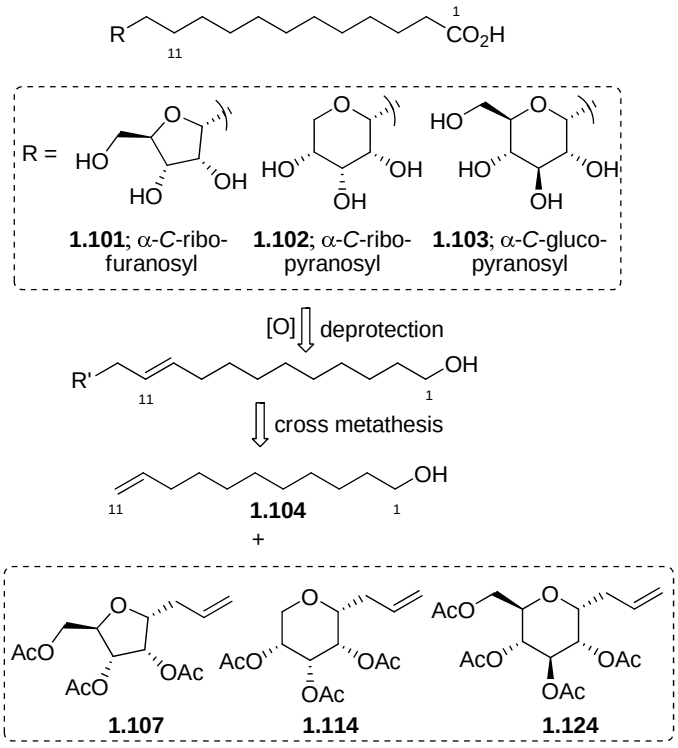

1.8.3 Synthesis of 12-α-*C*-ribo- furanosyl-dodecanoic acid (1.101)

One of the advanced intermediate we identified for the targeted synthesis is α-*C*-allylribofuranoside which was well reported in the literature.[72] As allylation of tetraacetyl ribofuranoside was documented to be nonspecific,[73d] methyl 2,3,5-tri-*O*-acetyl-α-ribofuranoside (**1.106**) was subjected to allylation to afford a 11:1 anomeric mixture, α-anomer **1.107** being the major product.

Scheme 1.56 *Synthesis of the protected α-C-allylribofuranoside* (***1.107***)

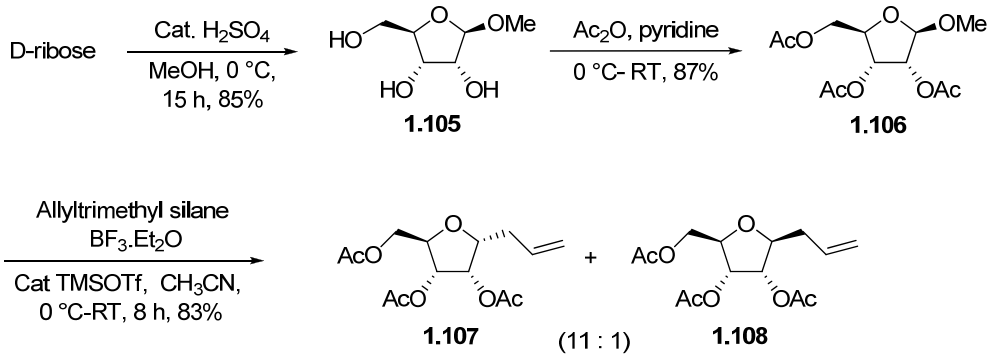

As shown in scheme 1.56, the synthetic sequences started with commercially available D-ribose, which upon treatment with cat. sulphuric acid in dry methanol at 0 °C, yielded methyl-α-ribofuranoside (**1.105**) in 85% yield. The free hydroxy were acetylated using acetic anhydride and pyridine resulting **1.106** in good yields. The ^{1}H NMR spectrum showed resonance of anomeric proton H-1 at δ 4.86, whereas H-5, H-4, H-5' resonated at δ 4.07 (dd, *J* = 5.3, 11.1 Hz, 1H), 4.24 (dt, *J* = 3.6, 6.3 Hz, 1H), 4.32 (dd, *J* = 3.6, 11.2 Hz, 1H) and H-2, H-3 resonated downfield at δ 5.17 (dd, *J* = 0.8, 4.9 Hz, 1H), 5.29 (dd, *J* = 4.9, 6.3 Hz, 1H) ppm. The pressence of three acetate groups was indicated by singlets at δ 2.03, 2.07, 2.09 and methyl ether was represented by singlet at δ 3.35 ppm. The ^{13}C NMR spectrum showed the acetate functionality; carbonyl carbons at δ 168.8, 168.9 and 169.7 ppm.

C-allylation was carried out using allyltrimethyl silane and cat. TMSOTf in pressence of lewis acid $BF_3.Et_2O$ in acetonitrile solvent yielding **1.107** and **1.108** (11:1 ratio) in 83% yield. The spectral data of compound **1.107** was in good agreement with the reported data. The ^{1}H NMR spectrum showed resonance of H-1 at δ 4.22, whereas H-4 resonated at δ 4.23 ppm and olefinic peaks were observed at δ 5.07–5.09, 5.72. The ^{13}C

NMR spectrum showed the olefin peaks at 117.3 (t), 132.9 (d) and allyl CH_2 at 33.6 ppm along with acetate functionality; carbonyl carbons at δ 169.1, 169.2, 170.0. Further mass spectrum shows m/z at 323.1 $[M+Na]^+$. Rest of the analytical data was in full agreement with the assigned structure.

The α-*C*-allylribofuranoside derivative **1.107** underwent cross metathesis with 10-undecene-1-ol (**1.104**) using Grubbs' I catalyst **1.4** (20 mol%) to afford inseparable mixture of *E/Z* olefin **1.109** [2.7:1 ratio], along with the 10-undecene-1-ol dimer (**1.110**). The yield of the reaction increased from 55% to 81% by switching to Grubbs' II catalyst. (Scheme 1.57)

Scheme 1.57 *Cross metathesis approach for **1.109***

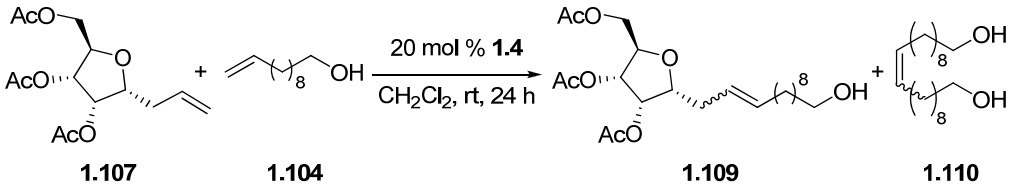

1.107 **1.104** **1.109** **1.110**

In ^1H & ^{13}C NMR spectrum of **1.109** have the characteristic signals of both the fragments along with olefinic peaks resonated at δ 123.8 (d) and 134.1 (d) ppm. ^1H NMR spectrum revealed resonance of peaks at δ 1.27 (m, 10H), 1.4–1.57 (m, 4H), 1.94 (dd, *J* = 6.6, 13.1 Hz, 2H) indicative of methelene's in long aliphatic chain, peaks at δ 3.61 (t, *J* = 6.6 Hz, 2H) indicates the pressence of O-CH_2 of aliphatic chain. Sugar fragment peaks resonated at δ 4.06 (dd, *J* = 4.6, 11.2 Hz, 1H), 4.10–4.21 (m, 2H), 4.26 (dd, *J* = 2.7, 11.2 Hz, 1H), 5.22 (dd, *J* = 4.5, 7.8 Hz, 1H), 5.39 (dd, *J* = 3.4, 4.5 Hz, 2H) ppm, and the olefinic peaks resonated at δ 5.24 (ddd, *J* = 6.8, 11.5, 14.7 Hz, 1H), 5.42–5.53 (m, 1H) ppm. Further ^{13}C NMR spectral data supported the formation of **1.109**. Mass spectra shows {(*m/z*) at 465.2 $[M+Na]^+$} and other analytical data were in agreement with the assigned structure.

After synthesizing cross metathesis product **1.109**, the stage was ready for transfer hydrogenation, functional group manipulation and removal of acetate moieties to yield the 12-α-*C*-ribo-furanosyl-dodecanoic acid (**1.101**).

Scheme 1.58 *Synthesis of 12-α-C-ribo-furanosyl-dodecanoic acid:* (***1.101***)

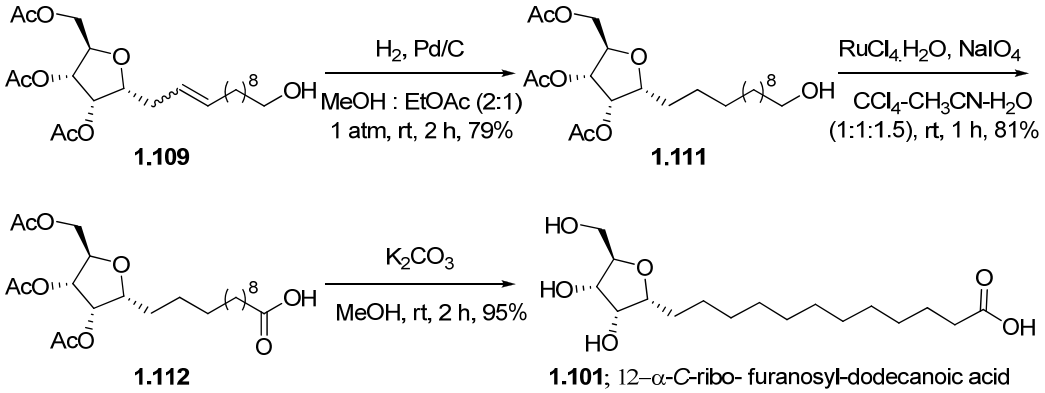

The olefinic *E/Z* mixture **1.109** was hydrogenated with 5 mol% of Pd/C in methanol:ethyl acetate (1:2) to yield saturated alcohol **1.111**. Absence of olefinic peaks in ^{13}C NMR indicates the completion of hydrogenation. Rest of the peaks were in accordance with the assigned structure. Oxidation of the free hydroxyl group with $RuCl_4.H_2O$ and $NaIO_4$ was carried out at rt to yield **1.112** in 81% yield. (Scheme 1.58) The characteristic acid carbonyl resonated at δ 178.7 ppm in ^{13}C NMR spectrum. Further mass spectra shows (*m/z*) at 481.1 $[M+Na]^+$ confirmed it's assigned structure. Deacetylation with K_2CO_3 in MeOH completed the synthesis of 12-α-*C*-ribo-furanosyl-dodecanoic acid **1.101** in an overall yield of 49%.

1.8.4 Synthesis of 12-α-*C*-ribo-pyranosyl-dodecanoic acid (1.102)

Scheme 1.59 *Synthesis of the protected α-C-allylribofuranoside* (***1.114***)

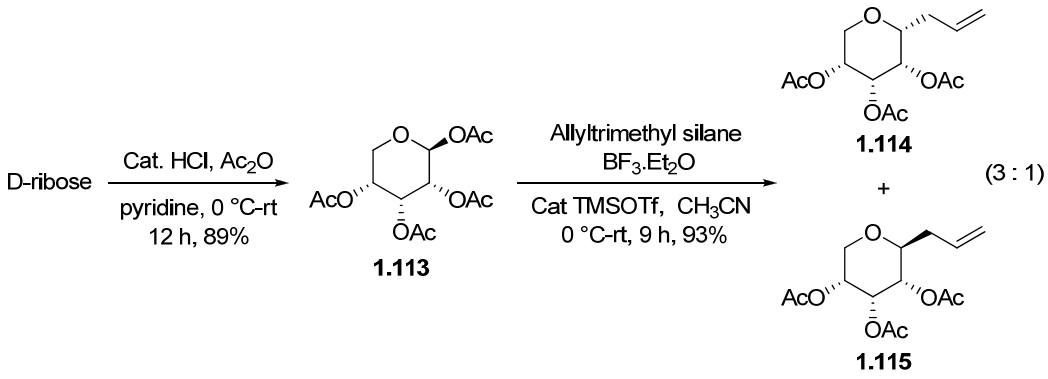

After successful synthesis of **1.101**, utilising *C*-allylation, cross metathesis as the key steps, we have utilised same strategy for the synthesis of 12-α-*C*-ribo-pyranosyl-

dodecanoic acid (**1.102**). Thus 2,3,4,5-tetra-*O*-acetyl-β-ribopyranoside (**1.110**)[73] was prepared accordingly and subjected to allylation to afford a 3:1 anomeric mixture, the α-anomer **1.114** being the major product.

C-allylation of **1.113** was carried out using allyltrimethyl silane and cat. TMSOTf in pressence of $BF_3.Et_2O$ in acetonitrile yielding **1.114** and **1.115** (3:1 ratio) in 93% yield. (Scheme 1.59) The ^{1}H NMR spectrum of **1.114** showed resonance of H-1, H-2, H-3 and H-4 at δ 3.55 (ddd, *J* = 1.2, 6.4, 7.6 Hz, 1H), 5.18 (dd, *J* = 1.2, 3.7 Hz, 1H), 5.23 (dt, *J* = 1.2, 3.7 Hz, 1H), 5.11 (dd, *J* = 1.5, 3.7 Hz, 1H) ppm respectively, and the olefinic peaks appeared at δ 5.07–5.09 (m, 2H), 5.73–5.81 (m, 1H). The ^{13}C NMR spectrum showed the olefin peaks at 117.8 (t), 132.7 (d) and allyl CH_2 at 35.1 ppm along with acetate functionality; carbonyl carbons at δ 169.4, 170.0, 170.03. Further mass spectrum shows m/z at 323.4 $[M+Na]^+$. Rest of the analytical data is in full agreement with the assigned structure.

However, as the data of compound **1.114** was found to match with that reported for the corresponding β-*C*-allylribofuranoside,[73d] we carried out single crystal X-ray structural analysis of **1.114** (Figure 1.23), which confirmed our assignments beyond the doubt.

Figure 1.23 *The molecular structure of compound **1.114***

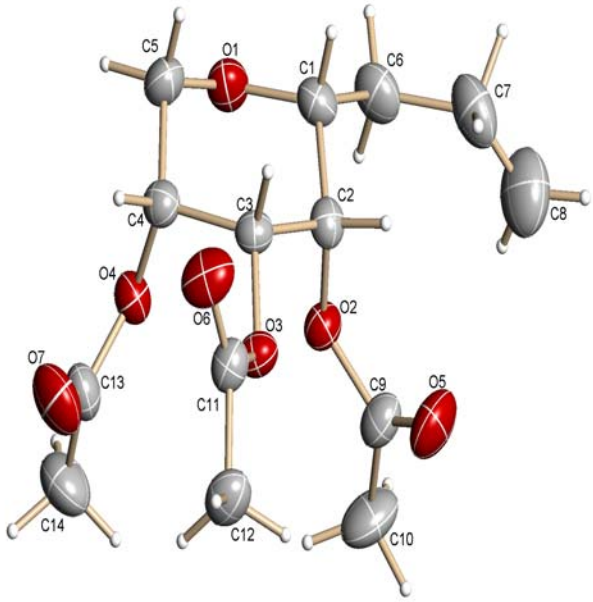

The α-*C*-allylribopyranoside derivative **1.114** underwent cross metathesis with 10-undecene-1-ol (**1.104**) using Grubbs' I catalyst **1.4** (20 mol%) to afford inseparable mixture of *E/Z* olefin **1.116** [6:1 ratio], along with the 10-undecene-1-ol dimer (**1.110**). (Scheme 1.60) The yield of the reaction increased from 41% to 79% by switching to Grubbs' II catalyst.

Scheme 1.60 *Cross metathesis approach for **1.116***

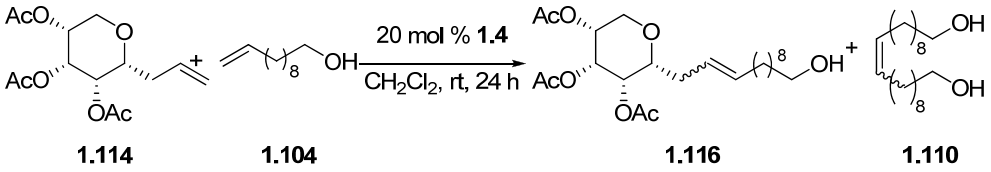

1.114 **1.104** **1.116** **1.110**

^{1}H & ^{13}C NMR spectra of **1.116** have the characteristic peaks of both fragment and the olefinic peaks resonating at δ 123.4 (d), 134.4 (d) ppm. ^{1}H NMR spectrum revealed resonance of peaks at δ 1.25 (m, 14H), 1.48–1.65 (m, 4H) indicative of methelene's in long aliphatic chain, peaks at δ 3.62 (t, *J* = 6.5 Hz, 2H) indicated the pressence of O-CH_2 of aliphatic chain. Sugar fragment peaks resonated at δ 3.47 (dt, *J* = 1.2, 6.9 Hz, 1H), 3.71 (d, *J* = 1.6 Hz, 1H), 4.11 (dd, *J* = 1.6, 13.0 Hz, 1H), 5.03 (t, *J* = 3.8 Hz, 1H), 5.14–5.21 (m, 2H), and the olefinic peaks appeared at δ 5.29–5.53 (m, 2H) ppm. Further ^{13}C NMR spectral data, mass spectra {(*m/z*) at 465.2 $[M+Na]^+$} and other analytical data were in agreement with the assigned structure.

Scheme 1.61 *Cross metathesis approach using **1.117***

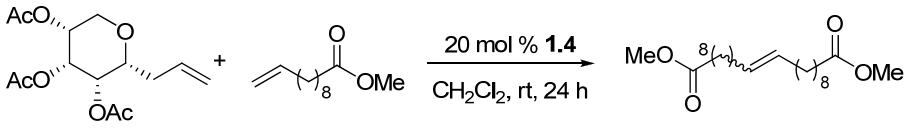

1.114 **1.117** **1.118**

In order to increase overall yield of the reaction sequence cross metathesis was attempted betweeen α-C-allylribopyranoside derivative **1.114** and methyl undec-10-enoate (**1.117**) using Grubbs' I catalyst **1.4** (20 mol%) in CH_2Cl_2 at reflux condition for 6 h. which afforded ester dimer **1.118**, along with unreacted **1.114**. (Scheme 1.61) The rate of formation of ester dimer was much faster than the cross coupling reaction.

After having an easy access to **1.116**, the stage set for the synthesis of 12-α-*C*-ribo-pyranosyl-dodecanoic acid (**1.102**), following established 3 step sequence.

Scheme 1.62 *Synthesis of 12-α-C-ribo-pyranosyl-dodecanoic acid:* (***1.102***)

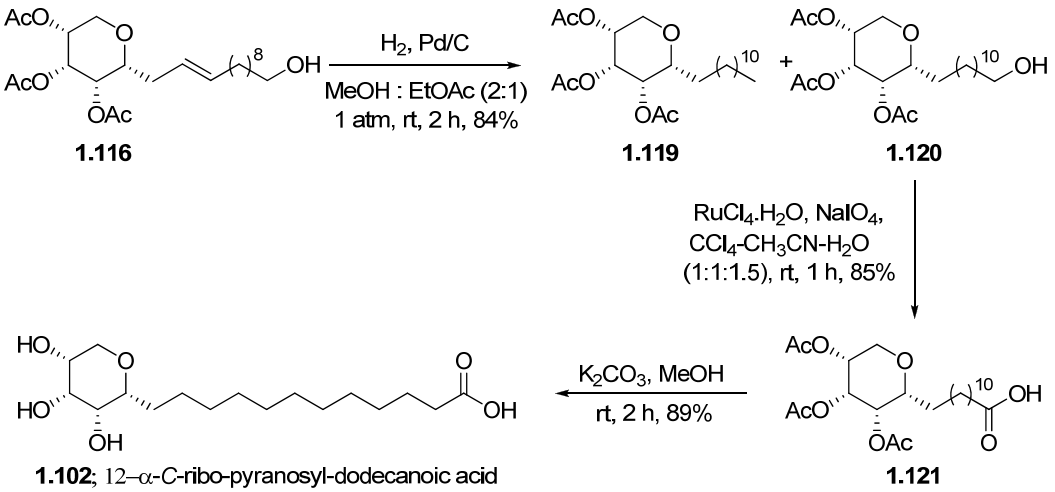

The olefinic *E/Z* mixture **1.116** was hydrogenated with 5 mol% of Pd/C in methanol:ethyl acetate (2:1) to yield the saturated alcohol **1.120** along with trace amount of deoxygenated product **1.119**. Absence of olefinic peaks in ^{13}C NMR indicates the completion of hydrogenation. Rest of the peaks were in accordance with the assigned structure. Oxidation of the free hydroxyl group in **1.120** with $RuCl_4.H_2O$ and $NaIO_4$ was carried out at rt to yield **1.121** in 85% yield. (Scheme 1.62) The characteristic acid carbonyl resonated at δ 179.1 ppm in ^{13}C NMR spectrum. Further mass spectra shows (*m/z*) at 481.3 $[M+Na]^+$ confirmed it's assigned structure **1.121**. Deacetylation with K_2CO_3 in MeOH completed the synthesis of 12-α-*C*-ribo-pyranosyl-dodecanoic acid **1.102** in an overall yield of 50%.

1.8.5 Synthesis of 12-α-*C*-gluco-pyraranosyl-dodecanoic acid (1.103)

After successful synthesis of **1.101** and **1.102**, utilising *C*-allylation, cross metathesis as a key steps, we have employed the same strategy for the synthesis of 12-α-*C*-gluco-pyranosyl-dodecanoic acid (**1.103**). Thus per acylated-β-glucopyranoside (**1.122**) was prepared according to the literature precedence and was subjected to allylation to afford exclusive α-anomer **1.123**.[74]

Scheme 1.63 *Synthesis of the protected α-C-allylglucopyranoside* (***1.123***)

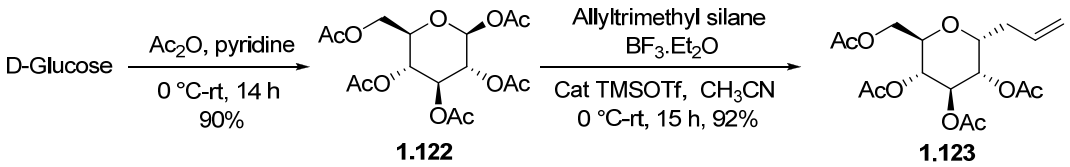

C-allylation was carried out using allyltrimethyl silane and cat. TMSOTf in pressence of lewis acid $BF_3.Et_2O$ in acetonitrile solvent yielding **1.123** in 92% yield. (Scheme 1.63). Analytical data of **1.123** was full agreement with the reported data.[74b]

Cross metathesis reaction of α-*C*-allylglucopyranoside derivative **1.123** with 10-undecene-1-ol (**1.104**) was facile with using Grubbs' I catalyst **1.4** (20 mol%) along with the 10-undecene-1-ol dimer (**1.110**). (Scheme 1.64) The yield of the reaction increased from 37% to 75% by switching to Grubbs' II catalyst.

Scheme 1.64 *Cross metathesis approach for* ***1.124***

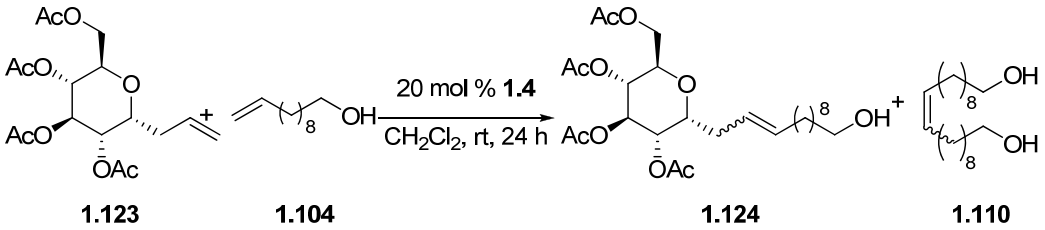

^{1}H & ^{13}C NMR spectrum of **1.124** have characteristic peaks of both fragment along with the olefinic peaks resonated at δ 123.8 (d) and 133.7 (d) ppm. ^{1}H NMR spectrum revealed resonance of peaks at δ 1.20–1.40 (m, 12H), 1.50–1.65 (m, 4H) indicative of methelene's in long aliphatic chain, peaks at δ 3.63 (t, *J* = 6.6 Hz, 2H) indicates the pressence of O-CH_2 of aliphatic chain. Sugar fragment peaks resonated at δ 3.75–3.87 (m, 1H), 3.99–4.09 (m, 1H), 4.15–4.27 (m, 2H), 4.93–5.11 (m, 2H), 5.45–5.61 (m, 1H). Whereas olefinic peaks resonated at δ 5.31 (dt, *J* = 3.4, 9.0 Hz, 2H) ppm. Further ^{13}C NMR spectral data supported the formation of **1.124**. Further mass spectra shows (*m/z*) at 537.6 $[M+Na]^+$. Other analytical data was in agreement with the assigned structure.

The olefinic *E/Z* mixture **1.124** was hydrogenated with 5 mol% of Pd/C in methanol:ethyl acetate (1:2) to yield saturated alcohol **1.125**. Absence of olefinic peaks in ^{13}C NMR indicates the completion of hydrogenation. Rest of the peaks were in

accordance with the assigned structure. Oxidation of the free hydroxyl group with $RuCl_4.H_2O$ and $NaIO_4$ was carried out at rt to yield **1.126** in 88% yield. The characteristic acid carbonyl resonated at δ 179.3 ppm in ^{13}C NMR spectrum. Further mass spectra shows (*m/z*) at 553.3 $[M+Na]^+$ confirmed it's assigned structure. Deacetylation with K_2CO_3 in MeOH completed the synthesis of 12-α-*C*-gluco-furanosyl-dodecanoic acid **1.103** in an overall yield of 47%.

Scheme 1.65 *Synthesis of 12-α-C-gluco-pyranosyl-dodecanoic acid:* (***1.103***)

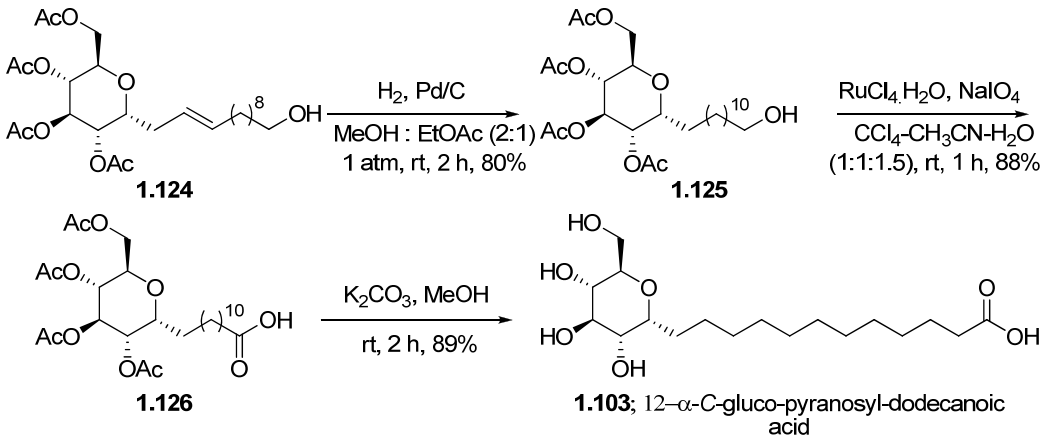

1.8.4 Glyconanoparticle synthesis

After synthesizing the requisite *C*-glycosyl acids **1.101–1.103**, the next objective was to use them as capping agents for metal nanoparticles. Our initial experiments with Co-metal nanoparticle synthesis employing **1.101–1.103** as the capping agents under established procedures[75] resulted in aggregation of the nanoparticles. This may be attributed to the lack of an olefinic moiety in these molecules which seems to impart stability to metal nanoparticle systems such as Co and Ni.

After a substantial optimization of the experimental parameters, a reductive synthesis of desired *C*-glycoside capped silver nano particles (Ag NPs) was concluded successfully by heating equimolar quantities silver nitrate and *C*-glycoside **1.101** or **1.102** in dilute alkaline solution (10^{-4} M). The reduction was instantaneous and the Ag NPs could be isolated as stable powders by simple centrifugation. With *C*-glucoside **1.103**, aggregation of the initially formed Ag NPs occured. Figures A and C (Inset, Figure 1.24) show UV-Vis spectra and recorded from alkaline solutions of silver nitrate and acids **1.101** and

1.102, respectively. The strong absorption at *ca.* 410 nm clearly indicates the formation of Ag NPs. This absorption is due to excitation of the surface plasmons present in the nanoparticles. Transmission electron microscope (Figures B and D) images of synthesized Ag NPs revealed the average particle size to be ~15 nm.

Figure 1.24 *Figures A and C showing the UV-vis spectra of AgNPs synthesized from 1.101 and 1.102 respectively. Figure B and D showing TEM image of AgNPs synthesized from 1.101 and 1.102 respectively. Insets (A) and (C) shows the colors of the AgNPs synthesized from 1.101 and 1.102 respectively.*

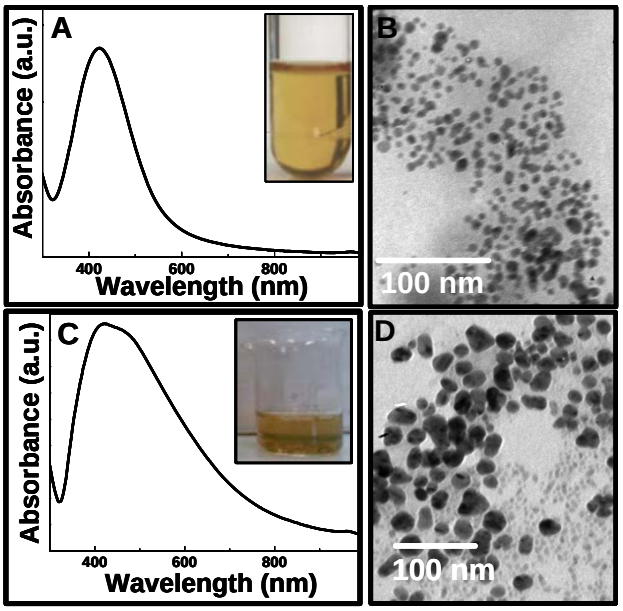

1.4.4 Conclusion

A concise synthesis of 12-*C*-glycosylated dodecanoic acids employing an olefin cross metathesis reaction is developed. Examination of these acids as capping agents for the synthesis of metal nanoparticles reveal that they do not cap the Co-metal nanoparticles synthesized in aqueous phase, but that two of them can reduce and cap the Ag nanoparticles in water without any aggregation.

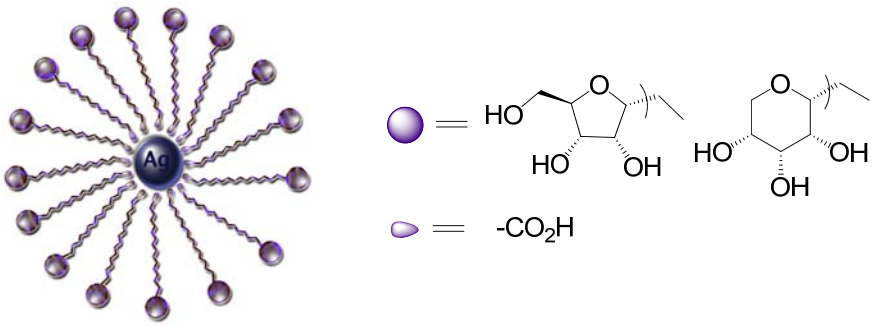

1.9 Experimental

Methyl 2,3,5-tri-*O*-acetyl-β-D-ribofuranoside (1.106)

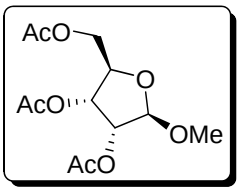

Conc. H_2SO_4 (0.5 ml) was added to an ice cooled clear solution of D-Ribose (5 g, 33.3 mmol) in 30 ml methanol. Stirred at 0 °C for 15 h and then neutralized with solid K_2CO_3. Reaction mixture was filtered through celite; volatiles were evaporated at reduced pressure to yield mix of methyl-α/β-D-ribofuranoside, which was dissolved in 30 ml of pyridine and acetic anhydride (14.8 ml, 133 mmol) was added at rt. Continued stirring for 6 h and tlc showed the completion of reaction. Pyridine was evaporated at reduced pressure and extracted with ethyl acetate. The residue obtained was purified by column chromatography (3:1 petroleum ether/ethyl acetate) to afford pure **1.106** (7.2 g, 74%) as colorless oil.

Mol. Formula	: $C_{12}H_{18}O_8$
$[\alpha]_D$	: −15.8 (*c* 1.0, $CHCl_3$)
IR ($CHCl_3$) $\tilde{\nu}$	: 3023, 2938, 1751, 1442, 1235, 1094, 1057, 667 cm^{-1}.
^{1}H NMR ($CDCl_3$, 200 MHz)	: δ 2.03 (s, 3H), 2.07 (s, 3H), 2.09 (s, 3H), 3.35 (s, 3H), 4.07 (dd, *J* = 5.3, 11.1 Hz, 1H), 4.24 (dt, *J* = 3.6, 6.3 Hz, 1H), 4.32 (dd, *J* = 3.6, 11.2 Hz, 1H), 4.86 (d, *J* = 0.8, Hz, 1H), 5.17 (dd, *J* = 0.8, 4.9 Hz, 1H), 5.29 (dd, *J* = 4.9, 6.3 Hz, 1H) ppm.
^{13}C NMR ($CDCl_3$, 50 MHz)	: δ 19.7 (q), 19.8 (q), 20.0 (q), 54.4 (q), 63.7 (t), 70.9 (d), 74.0 (d), 78.0 (d), 105.6 (d), 168.8 (s), 168.9 (s), 169.7 (s) ppm.
ESI-MS (*m/z*)	: 313.1 $[M+Na]^+$.
Elemental Analysis	Calcd.: C, 49.65; H, 6.25. Found: C, 49.59; H, 6.21.

3-(2,3,5-Tri-*O*-acetyl-α-D̃-ribofuranosyl)-l-propene (1.107)

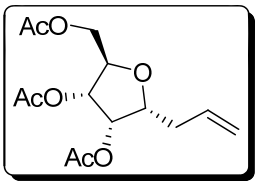

At 0 °C, solution of **1.106** (3.550 g, 12.23 mmol), $BF_3.OEt_2$ (4.06 ml, 24.46 mmol) and TMSOTf (0.45 ml, 2.44 mmol) in dry acetonitrile (30 ml) was treated with allyl trimethyl silane (3.9 ml, 24.46 mmol) and the contents were stirred at rt for 15 h. Saturated aq. NH_4Cl (5 ml) solution was added and volatiles were evaporated at reduced pressure. The residue obtained was purified by flash column chromatography (5:1 petroleum ether/ethyl acetate) to afford **1.107** and **1.108** in 11:1 ratio. (3.05 g, 83%).

Mol. Formula : $C_{14}H_{20}O_7$

$[\alpha]_D$: +51.7 (*c* 1.2, $CHCl_3$)

IR ($CHCl_3$) $\tilde{\nu}$: 3021, 2981, 1751, 1432, 1374, 1235, 1046, 1021 cm^{-1}.

^{1}H NMR ($CDCl_3$, 500 MHz) : δ 2.04 (s, 3H), 2.10 (s, 3H), 2.14 (s, 3H), 2.37 (dtt, *J* = 1.4, 7.1, 14.3 Hz, 1H), 2.45 (dtt, *J* = 1.4, 7.1, 14.3 Hz, 1H), 4.11 (dd, *J* = 5.0, 12.0 Hz, 1H), 4.22 (ddd, *J* = 1.7, 3.3, 8.0 Hz, 1H), 4.23 (dd, *J* = 3.5, 7.6 Hz, 1H), 4.30 (dd, *J* = 3.0, 12.0 Hz, 1H), 5.07–5.13 (m, 2H), 5.27 (dd, *J* = 4.6, 8.0 Hz, 1H), 5.45 (dd, *J* = 3.5, 4.6 Hz, 1H), 5.72 (ddt, *J* = 6.9, 10.2, 17.0 Hz, 1H) ppm.

^{13}C NMR ($CDCl_3$, 50 MHz) : δ 20.0 (q), 20.1 (q), 20.3 (q), 33.6 (t), 63.4 (t), 71.8 (d), 72.0 (d), 76.4 (d), 78.5 (d), 117.3 (t), 132.9 (d), 169.1 (s), 169.2 (s), 170.0 (s) ppm.

ESI-MS (*m/z*) : 323.1 $[M+Na]^+$.

Elemental Analysis Calcd.: C, 55.99; H, 6.71.
Found: C, 56.03; H, 6.73

1-(2,3,5-Tri-*O*-acetyl-α-D-ribofuranosyl)-12-hydroxydodec-2-ene (1.109)

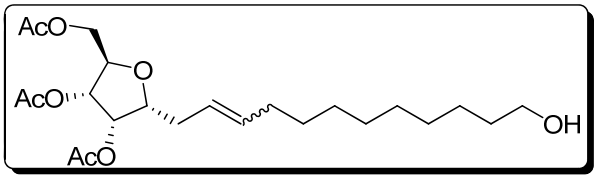

A solution of *C*-allyl derivative **1.107** (200 mg, 0.665 mmol), 10-undec-1-ol (567 mg, 3.33 mmol), Grubbs' I generation catalyst **1.4** (26 mg, 0.032 mmol) was degassed with argon and heated at 40 °C (oil bath temperature) for 24 h, under inert atmosphere in dry DCM (15 ml). The reaction mixture was cooled to room temperature and

concentrated under reduced pressure. The residue was purified by column chromatography (4:1 petroleum ether/ethyl acetate) to afford inseparable mixture of *E/Z* isomers **1.109** [2.7:1ratio] (110 mg, 37%) as colorless oil, 10-undec-1-ol dimers **1.110** (115 mg, 55%) as a white amorphous solid.

Mol. Formula	: $C_{23}H_{38}O_8$
IR ($CHCl_3$) $\tilde{\nu}$	: 3482, 3018, 2929, 2855, 1750, 1437, 1374, 1326,756 cm^{-1}
^{1}H NMR ($CDCl_3$, 200 MHz)	: δ 1.27 (m, 10H), 1.4–1.57 (m, 4H), 1.94 (dd, *J* = 6.6, 13.1 Hz, 2H), 2.02 (s, 3H), 2.08 (s, 3H), 2.12 (s, 3H), 2.31 (dd, *J* = 6.7, 13.6 Hz, 2H), 3.61 (t, *J* = 6.6 Hz, 2H), 4.06 (dd, *J* = 4.6, 11.2 Hz, 1H), 4.10–4.21 (m, 2H), 4.26 (dd, *J* = 2.7, 11.2 Hz, 1H), 5.22 (dd, *J* = 4.5, 7.8 Hz, 1H), 5.24 (ddd, *J* = 6.8, 11.5, 14.7 Hz, 1H), 5.39 (dd, *J* = 3.4, 4.5 Hz, 2H), 5.42–5.53 (m, 1H) ppm.
^{13}C NMR ($CDCl_3$, 50 MHz)	: δ 20.3 (q), 20.4 (q), 20.6 (q), 25.6 (t), 27.2 (t), 27.3 (t), 28.9 (t), 29.1 (t), 29.3 (t), 29.4 (t), 32.4 (t), 32.6 (t), 62.6 (t), 63.6 (t), 72.0 (d), 76.5 (d), 79.1 (d), 79.3 (d), 123.8 (d), 134.1 (d), 169.5 (s), 169.6 (s), 170.4 (s) ppm.
ESI-MS (*m/z*)	: 465.2 $[M+Na]^+$.
Elemental Analysis	Calcd.: C, 62.42; H, 8.65. Found: C, 62.39; H, 8.60.

Icos-10-ene-1,20-diol (1.110)

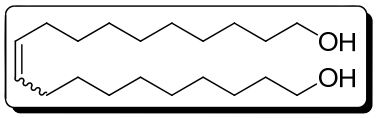

Mol. Formula	: $C_{20}H_{40}O_2$
M. P.	: 76.1 °C (EtOAc)
IR ($CHCl_3$) $\tilde{\nu}$	: 3418, 3018, 2928, 2856, 1455, 1373, 1046, 668 cm^{-1}.
^{1}H NMR ($CDCl_3$, 200 MHz)	: δ 1.27 (s, 22H), 1.48–1.57 (m, 6H), 1.90–1.99 (m, 4H), 3.61 (t, *J* = 6.5 Hz, 4H), 5.34 (ddd, *J* = 1.5, 3.6, 5.2 Hz, 2H) ppm.
^{13}C NMR ($CDCl_3$, 50 MHz)	: δ 25.7 (t, 2C), 27.0 (t, 2C), 29.0 (t, 2C), 29.3 (t, 4C), 29.5 (t, 2C), 32.4 (t, 2C), 32.6 (t, 2C), 62.6 (t, 2C), 130.2 (d, 2C) ppm.
ESI-MS (*m/z*)	: 335.5 $[M+Na]^+$.
Elemental Analysis	Calcd.: C, 76.86; H, 12.90. Found: C, 76.91; H, 12.89.

12-(2,3,5-Tri-*O*-acetyl-α-D-ribofuranosyl)-dodecane (1.111)

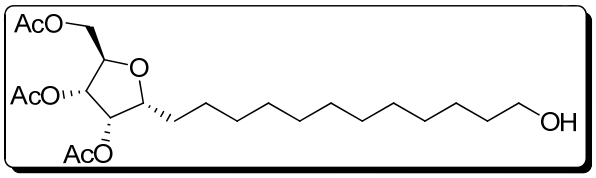

To a solution of alcohols **1.109** (200 mg, 0.45 mmol) in MeOH:EtOAc (1:2), 5% Pd-C (10 mg) was added. The solution was stirred under a hydrogen atmosphere at room temperature for 2 h. Reaction mixture was filtered through a short pad of celite and washed with ethyl acetate. The combined filtrate was concentrated and the crude residue was purified by column chromatography (4:1 petroleum ether/acetone) to furnish the alcohol **1.111** (159 mg, 79%) as a colorless liquid.

Mol. Formula	: $C_{23}H_{40}O_8$
$[\alpha]_D$	: +32.0 (*c* 1.0, $CHCl_3$)
IR ($CHCl_3$) $\tilde{\nu}$	: 3404, 3019, 2928, 2855, 1745, 1216, 1046, 757, 668 cm^{-1}.
^{1}H NMR ($CDCl_3$, 200 MHz)	: δ 1.24 (s, 18H), 1.45–1.60 (m, 4H), 2.02 (s, 3H), 2.08 (s, 3H), 2.12 (s, 3H), 3.61 (t, *J* = 6.5 Hz, 2H), 4.06 (dd, *J* = 4.8, 10.9 Hz, 1H), 4.11 (dd, *J* = 1.8, 3.3 Hz, 1H), 4.15 (dd, *J* = 4.5, 7.6 Hz, 1H), 4.26 (dd, *J* = 2.3, 10.9 Hz, 1H), 5.22 (dd, *J* = 4.5, 7.6 Hz, 1H), 5.39 (dd, *J* = 3.3, 4.5 Hz, 1H) ppm.
^{13}C NMR ($CDCl_3$, 50 MHz)	: δ 20.2 (q), 20.3 (q), 20.6 (q), 25.3 (t), 25.6 (t), 29.0 (t), 29.2 (t), 29.3 (t), 29.3 (t), 29.3 (t), 29.4 (t), 29.4 (t), 32.6 (t), 62.5 (t), 63.6 (t), 72.2 (d), 72.3 (d), 76.2 (d), 79.4 (d), 169.4 (s), 169.7 (s), 170.3 (s) ppm.
ESI-MS (*m/z*)	: 467.2 $[M+Na]^+$.
Elemental Analysis	Calcd.: C, 62.14; H, 9.07.
	Found: C, 62.19; H, 9.11.

1-(2,3,5-Tri-*O*-acetyl-α-D-ribofuranosyl)-12-dodecanoic acid (1.112)

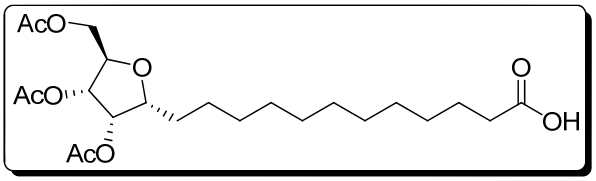

To a solution of alcohol **1.111** (150 mg, 0.337 mmol) in CCl_4 (2 ml)-CH_3CN (2 ml)-H_2O (3 ml), were added $NaIO_4$ (288 mg, 1.35 mmol) and $RuCl_4.H_2O$ (1.76 mg, 0.0067 mmol). The biphasic suspension was stirred vigorously for 1 h. The color was changed from wine red to pale brown. Reaction mixture was extracted with DCM (3 x 25 ml). The combined organic layer was dried, (Na_2SO_4) filtered and concentrated. To it

diethyl ether (20 ml) was added, filtered through a celite pad to remove metal impurities, the filtrate was concentrated at reduced pressure and purified by column chromatography (3:1 petroleum ether/acetone) to furnish the triacetate acid **1.112** (126 mg, 81%) as a colorless liquid.

Mol. Formula	: $C_{23}H_{38}O_9$
$[\alpha]_D$	: +21.1 (*c* 1.0, $CHCl_3$)
IR ($CHCl_3$) $\tilde{\nu}$	: 3400, 3020, 2929, 1744, 1711, 1215, 1046, 668cm^{-1}.
^{1}H NMR ($CDCl_3$, 200 MHz)	: δ 1.25 (s, 16H), 1.49–1.70 (m, 4H), 2.03 (s, 3H), 2.08 (s, 3H), 2.12 (s, 3H), 2.32 (t, *J* = 7.4 Hz, 2H), 4.04–4.19 (m, 3H), 4.26 (dd, *J* = 2.3, 11.1 Hz, 1H), 5.22 (dd, *J* = 4.5, 7.6 Hz, 1H), 5.39 (dd, *J* = 3.3, 4.5, Hz, 1H) ppm.
^{13}C NMR ($CDCl_3$, 50 MHz)	: δ 20.1 (q), 20.2 (q), 20.4 (q), 24.4 (t), 25.3 (t), 28.8 (t), 28.9 (t), 29.0 (t), 29.1 (t), 29.2 (t), 29.2 (t), 33.7 (t), 63.5 (t), 72.2 (d), 72.2 (d), 76.2 (d), 79.3 (d), 169.4 (s), 169.6 (s), 170.3 (s), 178.7 (s) ppm.
ESI-MS (*m/z*)	: 481.1 $[M+Na]^+$.
Elemental Analysis	Calcd.: C, 60.24; H, 8.35.
	Found: C, 60.30; H, 8.39.

1-(α-D-Ribofuranosyl)-12-dodecanoic acid (1.101)

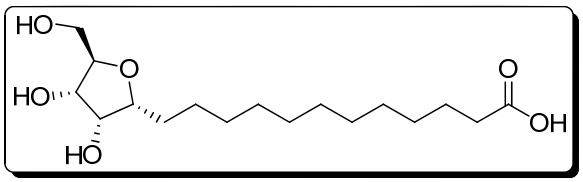

To a solution of acid **1.112** (100 mg, 0.218 mmol) in 5 ml of dry methanol, K_2CO_3 (90 mg, 0.654 mmol) was added. The suspension was stirred at room temperature for 1 h. The reaction mixture was filtered through a celite pad, washed with methanol and combined filtrate was concentrated at reduced pressure. Crude mass was purified by column chromatography (8:1:1 $CHCl_3$/MeOH/AcOH) to furnish the *C*-glycosyl acid **1.101** (69 mg, 95%) as a white hygroscopic solid.

Mol. Formula	: $C_{17}H_{32}O_6$
M. P.	: 130.8 °C
$[\alpha]_D$	: +9.0 (*c* 1.0, MeOH)
IR (nujol) $\tilde{\nu}$	: 3439, 3258, 2923, 2852, 1709, 1462, 1377 cm^{-1}.
^{1}H NMR	: δ 1.32 (s, 16H), 1.59–1.71 (m, 4H), 2.26 (t, *J* = 7.3 Hz, 2H),

(CD_3OD, 400 MHz)	3.58 (dd, *J* = 4.8, 11.8 Hz, 1H), 3.74 (dd, *J* = 2.8, 11.8 Hz, 1H), 3.79 (ddd, *J* = 2.8, 4.5, 7.5 Hz, 1H), 3.91 (dt, *J* = 2.8, 6.8 Hz, 1H), 3.96 (dd, *J* = 3.0, 4.3 Hz, 1H), 4.11 (dd, *J* = 4.5, 8.0 Hz, 1H) ppm.
^{13}C NMR	: δ 26.4 (t), 27.0 (t), 30.4 (t), 30.5 (t), 30.6 (t), 30.7 (t), 30.8 (t),
(CD_3OD, 100 MHz)	31.0 (t), 35.8 (t), 63.5 (t), 73.8 (d), 74.0 (d), 82.6 (d), 82.9 (d), 178.8 (s) ppm.
ESI-MS (*m/z*)	: 355.1 $[M+Na]^+$.
Elemental Analysis	Calcd.: C, 61.42; H, 9.70.
	Found: C, 61.46; H, 9.73.

3-(2,3,4-Tri-*O*-acetyl-α-D–ribopyranosyl)-l-propene (1.114)

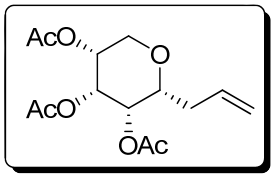

A solution of D-Ribose (5 g, 33.3 mmol), acetic anhydride (20 ml) in dry pyridine (40 ml) was stirred vigorously at rt for 12 h. Volatiles were evaporated at reduced pressure, the residue obtained was purified by column chromatography (4:1 petroleum ether/ethyl acetate) to afford **1.113** as a colorless oil. At 0 °C, solution of **1.113** (3.550 g, 12.23 mmol), $BF_3.OEt_2$ (4.06 ml, 24.46 mmol) and TMSOTf (0.45 ml, 2.44 mmol) in dry acetonitrile (30 ml) was treated with allyl trimethyl silane (3.9 ml, 24.46 mmol) and the contents were stirred at rt for 9 h. Saturated aq. NH_4Cl (5 ml) solution was added and volatiles were evaporated at reduced pressure. The residue obtained was purified by flash column chromatography (5:1 petroleum ether/ethyl acetate) to afford **1.114** and **1.115** in 3:1 ratio. (3.05 g, 83%).

Crystal data: X-ray intensity data was collected on a Bruker SMART APEX CCD diffractometer with omega and phi scan mode, $\lambda_{MoK\alpha}$ = 0.71073 Å at T = 297(2) K. All the data were corrected for Lorentzian, polarisation and absorption effects using Bruker's SAINT and SADABS programs. The crystal structures were solved by direct method using SHELXS-97 and the refinement was performed by full matrix least squares of F^2 using SHELXL-97 (G. M. Sheldrick, SHELX-97 program for crystal structure solution and refinement, University of Göttingen, Göttingen, Germany, 1997). Hydrogen atoms were included in the refinement as per the riding model. *Crystal data for* **1.114**

($C_{14}H_{20}O_7$): M = 301.31, crystal dimensions 0.53 x 0.28 x 0.27 mm^3, Orthorhombic, space group $P2_12_12_1$, a = 8.7430(4), b = 13.2602(6), c = 13.4236(6) Å, V = 1556.25(12) $Å^3$, Z = 4; ρ_{calcd} = 1.286 gcm^{-3}, μ (Mo–K_α) = 0.103 mm^{-1}, *F(000)* = 644, $2\theta_{max}$ = 50.00°, 11275 reflections collected, 7086 unique, 2732 observed ($I > 2\sigma(I)$) reflections, 2633 refined parameters, R value 0.0341, $wR2$ = 0.0902 (all data R = 0.0328, $wR2$ = 0.0888), S = 1.082, minimum and maximum transmission 0.9473 and 0.9727 respectively, maximum and minimum residual electron densities +0.165 and –0.277 e $Å^{-3}$.

Mol. Formula	: $C_{14}H_{20}O_7$
M. P.	: 86.7 °C
$[\alpha]_D$	: +2.0 (*c* 1.0, $CHCl_3$)
IR ($CHCl_3$) $\tilde{\nu}$	: 3019, 1743, 1262, 1228, 668 cm^{-1}.
^{1}H NMR ($CDCl_3$, 500 MHz)	: δ 2.00 (s, 3H), 2.16 (s, 3H), 2.17 (s, 3H), 2.21–2.26 (m, 1H), 2.42–2.48 (m, 1H), 3.55 (ddd, J = 1.2, 6.4, 7.6 Hz, 1H), 3.71 (dd, J = 1.5, 13.3 Hz, 1H), 4.13 (dd, J = 1.8, 13.3 Hz, 1H), 5.07–5.09 (m, 2H), 5.11 (dd, J = 1.5, 3.7 Hz, 1H), 5.18 (dd, J = 1.2, 3.7 Hz, 1H), 5.23 (dt, J = 1.2, 3.7 Hz, 1H), 5.73–5.81 (m, 1H) ppm.
^{13}C NMR ($CDCl_3$, 50 MHz)	: δ 20.3 (q), 20.4 (q), 20.7 (q), 35.1 (t), 66.3 (d), 67.5 (d), 68.0 (d), 68.6 (t), 77.1 (d), 117.8 (t), 132.7 (d), 169.4 (s), 170.0 (s), 170.03 (s) ppm.
ESI-MS (*m/z*)	: 323.4 $[M+Na]^+$.
Elemental Analysis	Calcd.: C, 55.99; H, 6.71. Found: C, 56.02; H, 6.74.

3-(2,3,4-Tri-*O*-acetyl-β-D-ribopyranosyl)-l-propene (1.115)

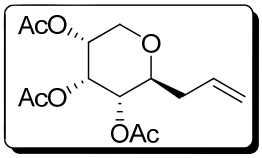

Mol. Formula	: $C_{14}H_{20}O_7$
$[\alpha]_D$	: –9.8 (*c* 1.5, $CHCl_3$)
IR ($CHCl_3$) $\tilde{\nu}$	: 3079, 3022, 2981, 2882, 1747, 1372, 1108, 667 cm^{-1}.
^{1}H NMR ($CDCl_3$, 400 MHz)	: δ 2.01 (s, 3H), 2.01 (s, 3H), 2.16 (s, 3H), 2.13–2.20 (m, 1H), 2.32–2.37 (m, 1H), 3.63 (t, J = 10.8 Hz, 1H), 3.73 (ddd, J = 3.5, 7.8, 10.8 Hz, 1H), 3.85 (ddd, J = 0.5, 5.3, 10.5 Hz, 1H),

	4.73 (dd, *J* = 2.8, 10.0 Hz, 1H), 4.98 (ddd, *J* = 3.0, 5.5, 10.8 Hz, 1H), 5.06–5.11 (m, 2H), 5.63 (t, *J* = 2.5 Hz, 1H), 5.78–5.89 (m, 1H) ppm.
^{13}C NMR ($CDCl_3$, 50 MHz)	: δ 20.4 (q), 20.5 (q), 35.5 (t), 63.2 (t), 66.5 (d), 67.8 (d), 69.5 (d), 72.7 (d), 117.3 (t), 133.2 (d), 169.1 (s), 169.2 (s), 169.8 (s) ppm.
ESI-MS (*m/z*)	: 323.6 $[M+Na]^+$.
Elemental Analysis	Calcd.: C, 55.99; H, 6.71.
	Found: C, 56.04; H, 6.74.

1-(2,3,4-Tri-*O*-acetyl-α-D-ribopyranosyl)-12-hydroxydodec-2-ene (1.116)

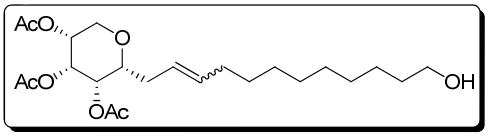

A solution of *C*-allyl derivative **1.114** (100 mg, 0.33 mmol), 10-undec-1-ol (283 mg, 1.66 mmol), Grubbs' I generation catalyst, **1.4** (13 mg, 0.016 mmol) was degassed with argon and heated at 40 °C (oil bath temperature) for 24 h, under inert atmosphere in dry DCM (10 ml). The reaction mixture was cooled to room temperature and concentrated under reduced pressure. The residue was purified by column chromatography (4:1 petroleum ether/ethyl acetate) to afford inseparable mixture of *E/Z* isomers **1.116** [6:1 ratio] (61 mg, 41%) as colorless oil, 10-undec-1-ol dimers **1.110** (51 mg, 49%) as a white amorphous solid.

Mol. Formula	: $C_{23}H_{38}O_8$
$[\alpha]_D$	: −12.2 (*c* 1.0, $CHCl_3$)
IR ($CHCl_3$) $\tilde{\nu}$	: 3450, 3019, 2929, 2856, 1742, 1263, 1261, 756, 668 cm^{-1}.
^{1}H NMR ($CDCl_3$, 200 MHz)	: δ 1.25 (m, 14H), 1.48–1.65 (m, 4H), 1.98 (s, 3H), 2.13 (s, 3H), 2.15 (s, 3H), 3.47 (dt, *J* = 1.2, 6.9 Hz, 1H), 3.62 (t, *J* = 6.5 Hz, 2H), 3.71 (d, *J* = 1.6 Hz, 1H), 4.11 (dd, *J* = 1.6, 13.0 Hz, 1H), 5.03 (t, *J* = 3.8 Hz, 1H), 5.14–5.21 (m, 2H), 5.29–5.53 (m, 2H) ppm.
^{13}C NMR ($CDCl_3$, 50 MHz)	: δ 20.2 (q), 20.4 (q), 20.7 (q), 25.4 (t), 28.7 (t), 28.8 (t), 29.0 (t), 29.1 (t), 29.2 (t), 32.2 (t), 32.4 (t), 33.9 (t), 62.3 (t), 66.4 (d), 67.3 (d), 68.1 (d), 68.6 (t), 77.6 (d), 123.4 (d), 134.4 (d), 169.5 (s), 170.0 (s), 170.1 (s) ppm.

ESI-MS (*m/z*) : 465.2 $[M+Na]^+$.

Elemental Analysis Calcd.: C, 62.42; H, 8.65.
Found: C, 62.39; H, 8.60.

Methyl undec-10-enoate (1.117)

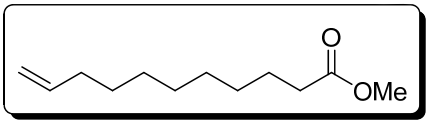

Mol. Formula : $C_{12}H_{22}O_2$

IR ($CHCl_3$) $\tilde{\nu}$: 3018, 2929, 2855, 1747, 1437, 1374, 1326, 756 cm^{-1}.

^{1}H NMR ($CDCl_3$, 200 MHz) : δ 1.28 (s, 10H), 1.57–1.64 (m, 2H), 1.97–2.07 (m, 2H), 2.28 (t, *J* = 7.4 Hz, 2H), 3.65 (s, 3H), 4.90 (ddd, *J* = 1.1, 3.3, 10.1 Hz, 1H), 4.95 (ddd, *J* = 1.5, 3.7, 17.1 Hz, 1H), 5.77 (ddt, *J* = 6.7, 10.1, 17.1 Hz, 1H) ppm.

^{13}C NMR ($CDCl_3$, 50 MHz) : δ 24.7 (t), 28.6 (t), 28.8 (t), 28.9 (t), 29.0 (t), 29.1 (t), 33.5 (t), 33.7 (t), 50.9 (q), 113.9 (t), 138.6 (d), 173.5 (s) ppm.

ESI-MS (*m/z*) : 220.2 $[M+Na]^+$.

Elemental Analysis Calcd.: C, 72.68; H, 11.18.
Found: C, 72.70; H, 11.20.

Dimethyl icos-10-enedioate (1.118)

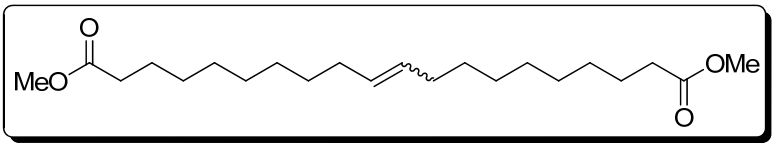

Mol. Formula : $C_{22}H_{40}O_4$

IR ($CHCl_3$) $\tilde{\nu}$: 3020, 2928, 2856, 1749, 1436, 1374, 1325, 756 cm^{-1}.

^{1}H NMR ($CDCl_3$, 200 MHz) : δ 1.28 (s, 20H), 1.61 (dt, *J* = 7.1, 14.2 Hz, 4H), 1.90–2.04 (m, 4H), 2.29 (t, *J* = 7.4 Hz, 4H), 3.66 (s, 6H), 5.32–5.37 (m, 2H) ppm.

^{13}C NMR ($CDCl_3$, 50 MHz) : δ 24.8 (t), 27.0 (t), 28.9 (t), 29.0 (t), 29.1 (t), 29.2 (t), 29.2 (t), 29.5 (t), 29.6 (t), 32.4 (t), 33.9 (t), 51.1 (q), 129.6 (d), 130.1 (d), 173.8 (s) ppm.

ESI-MS (*m/z*) : 390.5 $[M+Na]^+$.

Elemental Analysis Calcd.: C, 71.70; H, 10.94.
Found: C, 71.91; H, 11.01.

1-(2,3,4-Tri-*O*-acetyl-α-D-ribopyranosyl)-12-hydroxydodecane (1.120)

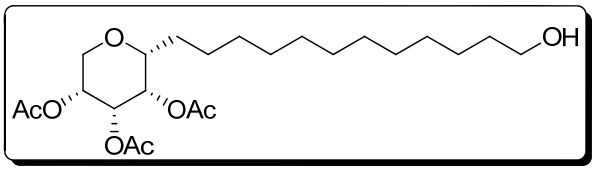

To a solution of unsaturated alcohols **1.116** (200 mg, 0.45 mmol) in methanol: ethyl acetate (2:1), 5% Pd-C (10 mg) was added. The solution was stirred under a hydrogen atmosphere at room temperature for 2 h. Reaction mixture was filtered through a short pad of celite and washed thoroughly with ethyl acetate, concentrated and the crude residue was purified by column chromatography (4:1 petroleum ether/acetone) to furnish saturated alcohol **1.120**(169 mg, 84%) as a white low melting solid along with deoxygenated product **1.119** (10 mg) as a colorless liquid.

Mol. Formula : $C_{23}H_{40}O_8$

M. P. : 43–44°C

$[\alpha]_D$: −6.2 (*c* 1.5, $CHCl_3$)

IR ($CHCl_3$) $\tilde{\nu}$: 3474, 3018, 2928, 2855, 1741, 1263, 1229, 755, 667 cm^{-1}.

^{1}H NMR ($CDCl_3$, 200 MHz) : δ 1.24 (s, 18H), 1.47–1.66 (m, 4H), 1.98 (s, 3H), 2.13 (s, 3H), 2.14 (s, 3H), 3.44 (dd, *J* = 2.8, 7.9 Hz, 1H), 3.61 (t, *J* = 6.5 Hz, 2H), 3.66 (dd, *J* = 1.5, 13.4 Hz, 1H), 4.10 (dd, *J* = 1.70, 13.3 Hz, 1H), 5.04 (t, *J* = 3.8 Hz, 1H), 5.13–5.18 (m, 2H) ppm.

^{13}C NMR ($CDCl_3$, 50 MHz) : δ 20.3 (q), 20.5 (q), 20.8 (q), 25.0 (t), 25.6 (t), 29.1 (t), 29.2 (t), 29.2 (t, 2C), 29.3 (t, 2C), 29.4 (t), 30.6 (t), 32.5 (t), 62.4 (t), 66.6 (d), 68.1 (d), 68.2 (d), 68.6 (t), 77.5 (d), 169.4 (s), 170.0 (s), 170.2 (s) ppm.

ESI-MS (*m/z*) : 467.5 $[M+Na]^+$.

Elemental Analysis Calcd.: C, 62.14; H, 9.07.
Found: C, 62.19; H, 9.10.

1-(2,3,4-Tri-*O*-acetyl-α-D-ribopyranosyl)-dodecane 1.119

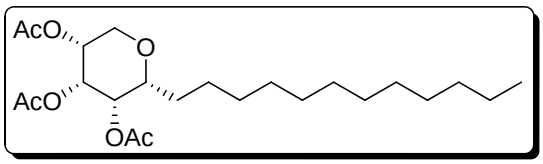

Mol. Formula : $C_{23}H_{40}O_7$

$[\alpha]_D$: −3.0 (*c* 1.0, $CHCl_3$)

IR ($CHCl_3$) $\tilde{\nu}$: 2926, 1744, 1466, 1377, 1365, 1115, 667 cm^{-1}.

^{1}H NMR : δ 0.88 (t, *J* = 6.4 Hz, 3H), 1.25 (s, 18H), 1.43 (br s, 2H),

($CDCl_3$, 200 MHz)	1.59–1.67 (m, 2H), 2.00 (s, 3H), 2.15 (s, 3H), 2.16 (s, 3H), 3.46 (dd, *J* = 3.0, 8.2 Hz, 1H), 3.68 (dd, *J* = 1.4, 13.3 Hz, 1H), 4.11 (dd, *J* = 1.8, 13.3 Hz, 1H), 5.06 (t, *J* = 3.7 Hz, 1H), 5.15–5.20 (m, 2H) ppm.
^{13}C NMR ($CDCl_3$, 50 MHz)	: δ 13.9 (q), 20.3 (q), 20.5 (q), 20.8 (q), 22.5 (t), 25.1 (t), 29.2 (t), 29.2 (t), 29.2 (t), 29.3 (t), 29.4 (t), 30.7 (t), 31.7 (t), 66.6 (d), 68.2 (d), 68.2 (d), 68.7 (t), 77.6 (d), 169.3 (s), 169.9 (s), 170.1 (s) ppm.
ESI-MS (*m/z*)	: 451.5 $[M+Na]^+$.
Elemental Analysis	Calcd.: C, 64.46; H, 9.41. Found: C, 64.41; H, 9.39.

1-(2,3,4-Tri-*O*-acetyl-α-D-ribopyranosyl)-12-dodecanoic acid (1.121)

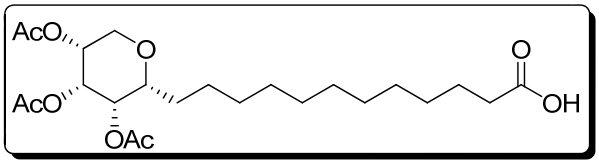

To a solution of alcohol **1.120** (160 mg, 0.36 mmol) in CCl_4 (2 ml)-CH_3CN (2 ml)-H_2O (3 ml), were added $NaIO_4$ (315 mg, 1.44 mmol) and $RuCl_4.H_2O$ (1.88 mg, 0.0072 mmol). The biphasic suspension was stirred vigorously for 1 h. The color was changed from wine red to pale brown. Reaction mixture was extracted with DCM (3 x 25 ml). The combined organic layer was dried, (Na_2SO_4) filtered and concentrated. To it diethyl ether (20 ml) was added, filtered through a celite pad to remove metal impurities, the filtrate was concentrated at reduced pressure and purified by column chromatography (3:1 petroleum ether/acetone) to furnish the triacetate acid **1.121** (141 mg, 85%) as a colorless liquid.

Mol. Formula	: $C_{23}H_{38}O_9$
$[\alpha]_D$	: −2.9 (*c* 1.1, $CHCl_3$)
IR ($CHCl_3$) $\tilde{\nu}$	: 3338, 3019, 2928, 1743, 1706, 1263, 1228, 667cm^{-1}.
^{1}H NMR ($CDCl_3$, 200 MHz)	: δ 1.24 (m, 18H), 1.61 (t, *J* = 7.1 Hz, 2H), 1.99 (s, 3H), 2.13 (s, 3H), 2.15 (s, 3H), 2.32 (t, *J* = 7.4 Hz, 2H), 3.45 (dd, *J* = 2.7, 8.0 Hz, 1H), 3.67 (dd, *J* = 1.4, 13.3 Hz, 1H), 4.10 (ddd, *J* = 3.0, 7.1, 13.3 Hz, 1H), 5.05 (t, *J* = 3.8 Hz, 1H), 5.13–5.18 (m, 2H) ppm.
^{13}C NMR	: δ 20.4 (q), 20.5 (q), 20.8 (q), 24.5 (t), 25.0 (t), 28.9 (t), 29.1

($CDCl_3$, 50 MHz)	(t), 29.2 (t), 29.2 (t, 2C), 29.3 (t), 29.3 (t), 30.7 (t), 33.8 (t), 66.7 (d), 68.2 (d), 68.3 (d), 68.7 (t), 77.6 (d), 169.5 (s), 170.2 (s), 170.3 (s), 179.1 (s) ppm.
ESI-MS (*m/z*)	: 481.3 $[M+Na]^+$.
Elemental Analysis	Calcd.: C, 60.24 H, 8.35
	Found: C, 60.31; H, 8.39.

1-(α-D-Ribopyranosyl)-12-dodecanoic acid (1.102)

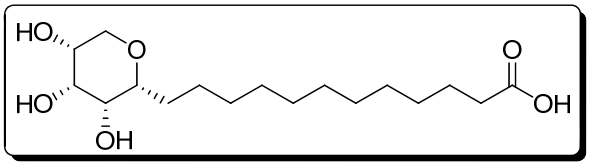

To a solution of acid **1.121** (100 mg, 0.218 mmol) in 5 ml of dry methanol, K_2CO_3 (91 mg, 0.654 mmol) was added. The suspension was stirred at room temperature for 1 h. Reaction mixture was filtered through a celite pad, washed with methanol & the filtrate was concentrated and purified by column chromatography (8:1:1 $CHCl_3$/MeOH/AcOH) to furnish *C*-glycosyl acid **1.102** (65 mg, 89%) as white amorphous solid.

Mol. Formula	: $C_{17}H_{32}O_6$
M. P.	: 115–116 °C
$[\alpha]_D$	: −15.3 (*c* 0.5, MeOH)
IR (nujol) $\tilde{\nu}$	: 3364, 3019, 2928, 1701, 1461, 1376, 1102, 722 cm^{-1}.
^{1}H NMR	: δ 1.31 (s, 18H), 1.57–1.69 (m, 2H), 2.20 (t, *J* = 7.3 Hz, 2H),
(CD_3OD, 200 MHz)	3.26 (dd, *J* = 5.3, 8.3 Hz, 1H), 3.51 (d, J = 12.4 Hz, 1H), 3.60 (t, *J* = 3.3 Hz, 1H), 3.66 (br s, 1H), 3.79 (br s, 1H), 3.94 (dd, *J* = 2.0, 12.4 Hz, 1H) ppm.
^{13}C NMR	: δ 26.4 (t), 26.7 (t), 30.4 (t), 30.5 (t), 30.7 (t), 30.8 (t), 30.8 (t,
(CD_3OD, 50 MHz)	4C), 32.4 (t), 70.5 (d), 71.3 (d), 72.3 (t), 73.2 (d), 80.8 (d) ppm.
ESI-MS (*m/z*)	: 354.8 $[M+Na]^+$.
Elemental Analysis	Calcd.: C, 61.42; H, 9.70.
	Found: C, 61.39; H, 9.66.

3-(2,3,4,6-Tetra-*O*-acetyl-α-D–glucopyranosyl)-l-propene (1.123)

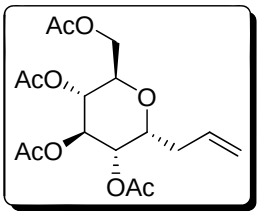

D-Glucose (5 g, 33.3 mmol) was added to a vigorously stirred solution of dry pyridine (60 ml) and acetic anhydride (25 ml) at 0 °C then stirred at rt for 12 h. volatiles were evaporated at reduced pressure to yield **1.122** as colorless oil. To a cooled solution of **1.122** (3.550 g, 12.23 mmol), $BF_3.OEt_2$ (4.06 ml, 24.46 mmol) and TMSOTf (0.45 ml, 2.44 mmol) in dry acetonitrile (30 ml), allyl trimethyl silane (3.9 ml, 24.46 mmol) was added slowly at 0 °C. Reaction mixture was allowed to warm at rt and stirred for 15 h. Saturated aq. NH_4Cl solution was added and volatiles were evaporated at reduced pressure. The residue obtained was purified by flash column chromatography (5:1 petroleum ether/ethyl acetate) to afford **1.123** (3.05 g, 83%).

Mol. Formula : $C_{17}H_{24}O_9$

IR ($CHCl_3$) $\tilde{\nu}$: 3018, 1744, 1261, 1227, 668 cm^{-1}.

^{1}H NMR ($CDCl_3$, 500 MHz) : δ 2.04 (s, 3H), 2.05 (s, 3H), 2.05 (s, 3H), 2.08 (s, 3H), 2.32–2.37 (m, 1H), 2.53–2.59 (m, 1H), 3.86 (ddd, *J* = 2.6, 5.3, 9.4 Hz, 1H), 4.09 (dd, *J* = 2.6, 12.2 Hz, 1H), 4.21 (dd, *J* = 5.3, 12.2 Hz, 1H), 4.29 (dt, *J* = 4.7, 11.2 Hz, 1H), 4.99 (t, *J* = 9.1 Hz, 1H), 5.09 (dd, *J* = 5.7, 9.4 Hz, 1H), 5.12–5.18 (m, 2H), 5.34 (t, *J* = 9.1 Hz, 1H), 5.71–5.79 (m, 1H) ppm.

^{13}C NMR ($CDCl_3$, 100 MHz) : δ 20.6 (q), 20.7 (q, 3C), 30.5 (t), 62.2 (t), 68.7 (d, 2C), 70.2 (d), 70.3 (d), 71.8 (d), 117.8 (t), 132.9 (d), 169.5 (s), 169.6 (s), 170.1 (s), 170.6 (s) ppm.

ESI-MS (*m/z*) : 394.6 $[M+Na]^+$.

Elemental Analysis Calcd.: C, 54.83; H, 6.50.
Found: C, 54.90; H, 6.59

1-(2,3,4,6-Tetra-*O*-acetyl-α-D-glucopyranosyl)-12-hydroxydodec-2-ene (1.124)

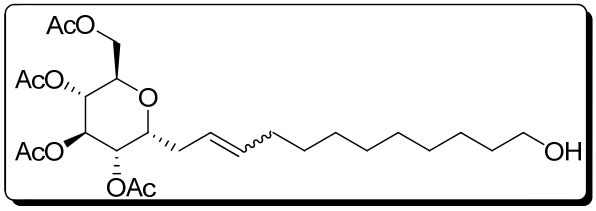

A solution of *C*-allyl derivative **1.123** (100 mg, 0.268 mmol), 10-undec-1-ol (228 mg, 1.34 mmol), Grubbs' I generation catalyst **1.4** (11 mg, 0.013 mmol) was degassed with argon and heated at 40 °C (oil bath temperature) for 24 h, under inert atmosphere in dry DCM (15 ml). The reaction mixture was cooled to room temperature and concentrated under reduced pressure. The residue was purified by column chromatography (4:1 petroleum ether/ethyl acetate) to afford inseparable mixture of *E/Z* isomers **1.124** [2:1 ratio] (52 mg, 37%) as colorless oil, 10-undec-1-ol dimers **1.110** (51 mg, 61%) as a white amorphous solid.

Mol. Formula	: $C_{26}H_{42}O_{10}$
IR ($CHCl_3$) $\tilde{\nu}$	: 3410, 3020, 2929, 1743, 1750, 1215, 1034, 758, 668 cm^{-1}.
^{1}H NMR ($CDCl_3$, 200 MHz)	: δ 1.20–1.40 (m, 12H), 1.50–1.65 (m, 4H), 2.03 (s, 3H), 2.04 (s, 3H), 2.05 (s, 3H), 2.09 (s, 3H), 2.21–2.37 (m, 1H), 2.41–2.60 (m, 1H), 3.63 (t, *J* = 6.6 Hz, 2H), 3.75–3.87 (m, 1H), 3.99–4.09 (m, 1H), 4.15–4.27 (m, 2H), 4.93–5.11 (m, 2H), 5.31 (dt, *J* = 3.4, 9.0 Hz, 2H), 5.45–5.61 (m, 1H) ppm.
^{13}C NMR ($CDCl_3$, 50 MHz)	: δ 20.3 (q), 20.4 (q), 23.8 (t), 25.5 (t), 27.3 (t), 28.8 (t), 29.0 (t), 29.1 (t), 29.2 (t), 29.3 (t), 32.4 (t), 32.5 (t), 61.9 (t), 62.3 (t), 68.3 (d), 68.5 (d), 68.6 d), 70.0 (d), 70.1 (d), 72.0 (d), 72.2 (d), 123.3 (d), 123.8 (d), 132.4 (d), 133.7 (d), 169.1 (s), 169.2 (s), 169.7 (s), 169.8 (s), 170.2 (s) ppm.
ESI-MS (*m/z*)	: 537.6 $[M+Na]^+$.
Elemental Analysis	Calcd.: C, 62.42; H, 8.65. Found: C, 62.39; H, 8.60.

1-(2,3,4,6-Tetra-*O*-acetyl-α-D-glucopyranosyl)-12-hydroxydodecane (1.125)

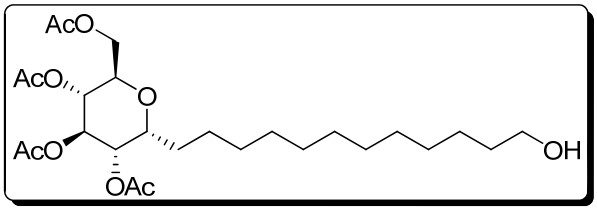

To a solution of alcohol **1.124** (200 mg, 0.388 mmol) in methanol: ethyl acetate (1:2), 5% Pd-C (10 mg) was added. The solution was stirred under a hydrogen atmosphere at room temperature for 2 h. Reaction mixture was filtered through a short pad of celite and washed thoroughly with ethyl acetate, concentrated and the crude residue was purified by column chromatography (4:1 petroleum ether/acetone) to furnish saturated alcohol **1.125** (161 mg, 80%) as colorless liquid.

Mol. Formula	: $C_{26}H_{44}O_{10}$
$[\alpha]_D$	: +15.2 (*c* 1.2, $CHCl_3$)
IR ($CHCl_3$) $\tilde{\nu}$	: 3482, 3021, 2929, 1749, 1369, 1216, 1034, 757, 668 cm^{-1}.
^{1}H NMR ($CDCl_3$, 200 MHz)	: δ 1.24 (br s, 18H), 1.53–1.90 (m, 4H), 2.03 (s, 3H), 2.03 (s, 3H), 2.05 (s, 3H), 2.09 (s, 3H), 3.63 (t, *J* = 6.5 Hz, 1H), 3.79 (ddd, *J* = 2.3, 5.1, 9.2 Hz, 1H), 4.06 (dd, *J* = 2.6, 12.0 Hz, 2H), 4.22 (dd, *J* = 5.1, 12.0 Hz, 2H), 4.96 (dd, *J* = 9.1, 9.4 Hz, 1H), 5.05 (dd, *J* = 5.8, 9.6 Hz, 1H), 5.29 (dd, *J* = 9.1. 9.4 Hz, 1H) ppm.
^{13}C NMR ($CDCl_3$, 50 MHz)	: δ 20.4 (br q, 2C), 20.5 (br q, 2C), 24.8 (t), 25.0 (t), 25.6 (t), 29.1 (t), 29.3 (t), 29.4 (t, 4C), 29.4 (t), 32.6 (t), 62.2 (t), 62.6 (t), 68.3 (d), 68.8 (d), 70.4 (d), 72.4 (d), 169.3 (s), 169.3 (s), 169.9 (s), 170.3 (s) ppm.
ESI-MS (*m/z*)	: 539.6 $[M+Na]^+$.
Elemental Analysis	Calcd.: C, 60.45; H, 8.58. Found: C, 60.39; H, 8.54.

1-(2,3,4,6-Tetra-*O*-acetyl-α-D-glucopyranosyl)-12-dodecanoic acid (1.126)

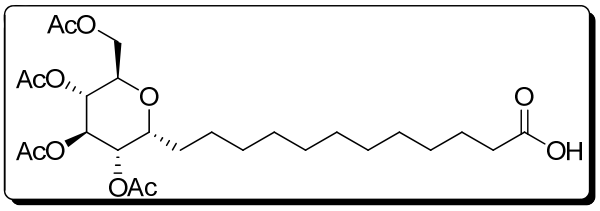

To a solution of alcohol **1.125** (160 mg, 0.309 mmol) in CCl_4 (2 ml)-CH_3CN (2 ml)-H_2O (3 ml), were added $NaIO_4$ (266 mg, 1.24 mmol) and $RuCl_4.H_2O$ (1.6 mg, 0.0061 mmol). The biphasic suspension was stirred vigorously for 1 h. The color was changed from wine red to pale brown. Reaction mixture was extracted with DCM (3 x 25 ml). The combined organic layer was dried, (Na_2SO_4) filtered and concentrated. To it diethyl ether (20 ml) was added, filtered through a celite pad to remove metal impurities, the filtrate was concentrated at reduced pressure and purified by column chromatography (3:1 petroleum ether/acetone) to furnish the triacetate acid **1.126** (146 mg, 88%) as a colorless liquid.

Mol. Formula	: $C_{26}H_{42}O_{11}$
$[\alpha]_D$	: +54.4 (*c* 1.1, $CHCl_3$)
IR ($CHCl_3$) $\tilde{\nu}$	: 3401, 2929, 1748, 1710, 1368, 1216, 1034, 756 cm^{-1}.

^{1}H NMR (CDCl$_3$, 400 MHz) : δ 1.27 (br s, 15H), 1.45–1.51 (m, 2H), 1.63 (qui, *J* = 7.3, 14.5 Hz, 2H), 1.73–1.81 (m, 1H), 2.03 (s, 3H), 2.04 (s, 3H), 2.05 (s, 3H), 2.09 (s, 3H), 2.35 (t, *J* = 7.5 Hz, 2H), 3.81 (ddd, *J* = 2.2, 5.3, 8.8 Hz, 1H), 4.09 (dd, *J* = 2.3, 12.0 Hz, 1H), 4.16 (ddd, *J* = 2.2, 5.3, 8.8 Hz, 1H), 4.23 (dd, *J* = 5.3, 12.0 Hz, 1H), 4.98 (dd, *J* = 9.1. 9.3 Hz, 1H), 5.07 (dd, *J* = 5.8, 9.5 Hz, 1H), 5.33 (dd, *J* = 9.1. 9.3 Hz, 1H) ppm.

^{13}C NMR (CDCl$_3$, 100 MHz) : δ 20.5 (q), 20.6 (q, 3C), 24.6 (t), 24.8 (t), 25.1 (t), 28.9 (t), 29.1 (t), 29.1 (t), 29.2 (t), 29.4 (t), 29.4 (t, 2C), 29.5 (t), 62.3 (t), 68.4 (d), 68.9 (d), 70.4 (d, 2C), 72.5 (d), 169.5 (s), 169.6 (s), 170.2 (s), 170.6 (s), 179.3 (s) ppm.

ESI-MS (*m/z*) : 553.3 $[M+Na]^+$.

Elemental Analysis Calcd.: C, 58.85; H, 7.98.
Found: C, 58.80; H, 8.02.

1-(α-D-Glucopyranosyl)-12-dodecanoic acid (1.103)

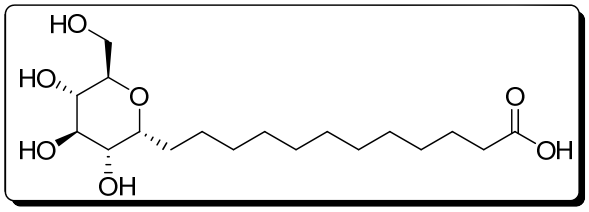

To a solution of acid **1.126** (100 mg, 0.188 mmol) in 5 ml of dry methanol, K_2CO_3 (78 mg, 0.565 mmol) was added. The suspension was stirred at room temperature for 1 h. Reaction mixture was filtered through a celite pad, washed with methanol & the filtrate was concentrated and purified by column chromatography (8:1:1 $CHCl_3$/MeOH/AcOH) to furnish *C*-glycosyl acid **1.103** (61 mg, 89 %) as a colorless liquid.

Mol. Formula : $C_{18}H_{34}O_7$

$[\alpha]_D$: +46.5 (*c* 4.0, MeOH)

IR (nujoll) $\tilde{\nu}$: 3365, 2853, 1709, 1569, 1455, 1377, 1032, 721 cm^{-1}.

^{1}H NMR (CD$_3$OD, 400 MHz) : δ 1.30 (br s, 16H), 1.59–1.65 (m, 4H), 2.22 (t, *J* = 7.3 Hz, 2H), 3.25 (dd, *J* = 8.5, 9.3 Hz, 1H), 3.39 (ddd, *J* = 2.2, 5.3, 8.0 Hz, 1H), 3.52 (t, *J* = 8.8 Hz, 1H), 3.6 (dd, *J* = 5.5, 9.5 Hz, 1H), 3.63 (dd, *J* = 5.3, 11.5 Hz, 1H), 3.77 (dd, *J* = 2.5, 11.8 Hz, 1H), 3.80 (dt, *J* = 5.0, 10.0 Hz, 1H) ppm.

^{13}C NMR : δ 25.4 (t), 26.7 (t), 27.0 (t), 30.6 (t), 30.6 (t), 30.7 (t), 30.7 (t,

(CD_3OD, 100 MHz)	5C), 63.1 (t), 72.4 (d), 73.1 (d), 74.3 (d), 75.3 (d), 77.3 (d) ppm.
ESI-MS (*m/z*)	: 385.4 $[M+Na]^+$.
Elemental Analysis	Calcd.: C, 59.65; H, 9.45.
	Found: C, 59.69; H, 9.49.

General procedure for the preparation of Ag NPs

Typical expermental procedure for Synthesis of *C*-glycoside of dodecanoic acid-reduced Ag NPs **:** To a boiling solution of *C*-glycoside of dodecanoic acid **1.101** (33 mg, 100 μM) and silver nitrate (17 mg, 100 μM) in MilliQ H_2O (100 mL), 1 mL of 0.1M KOH solution (pH ~10) was added and allowed to boil for 5 minutes. The colorless solution turned yellow, which indicated the formation of Ag NPs. The obtained Ag NPs were centrifuged at 8000 rpm for 20 min for removal of excess of *C*-glycoside of dodecanoic acid and KOH. The yellow pellet obtained was redispersed in MilliQ water (10 mL) and again centrifuged. The pellet was dried under ambient conditions to obtain a yellow powder. The purified sample was used for further characterizations. The yellow powder was found to be redispersible in water without any aggregation by mild sonication.

In order to prove that the reduction occurred only at alkaline pH, a control experiment was set up in which the above reaction was carried out without the addition of KOH. It was observed that silver nanoparticle formation did not occur under neutral and acidic conditions. In another control experiment the above reaction was performed with silver nitrate and KOH without the addition of *C*-glycoside of dodecanoic acid **1.101** and it was observed that even after prolonged boiling there was no formation of Ag NPs. This clearly indicates the crucial role of *C*-glycoside of dodecanoic acid as a pH dependent reducing agent for the synthesis of Ag NPs.

1.10 Spectra

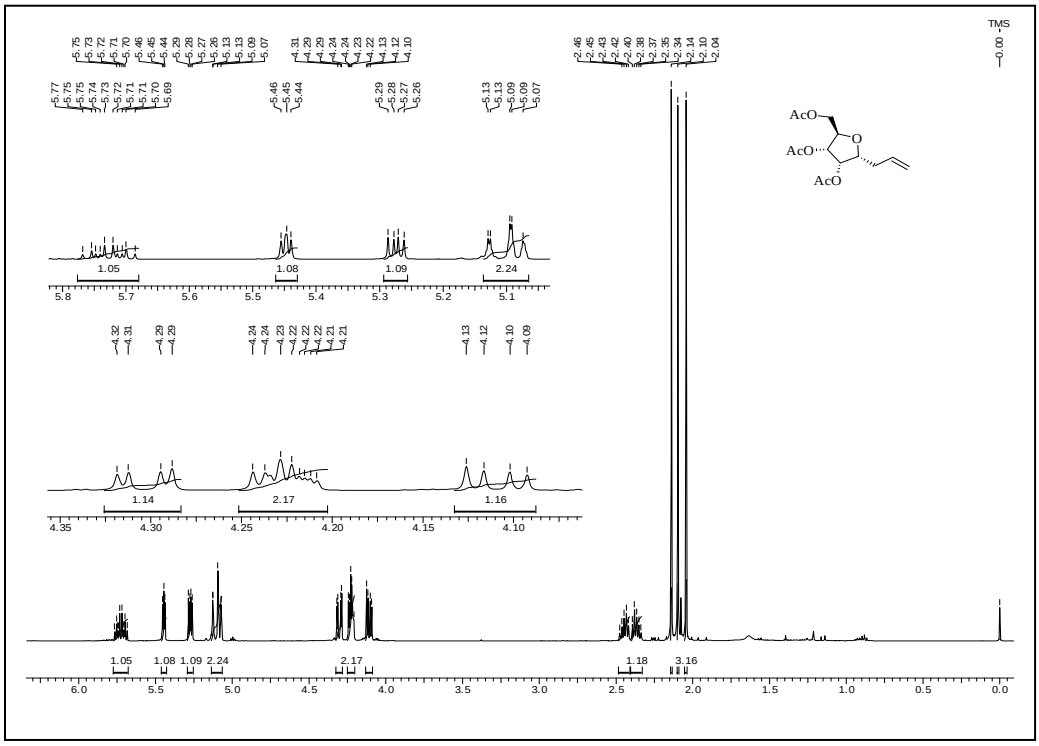

^{1}H NMR Spectrum of 1.106 in $CDCl_3$

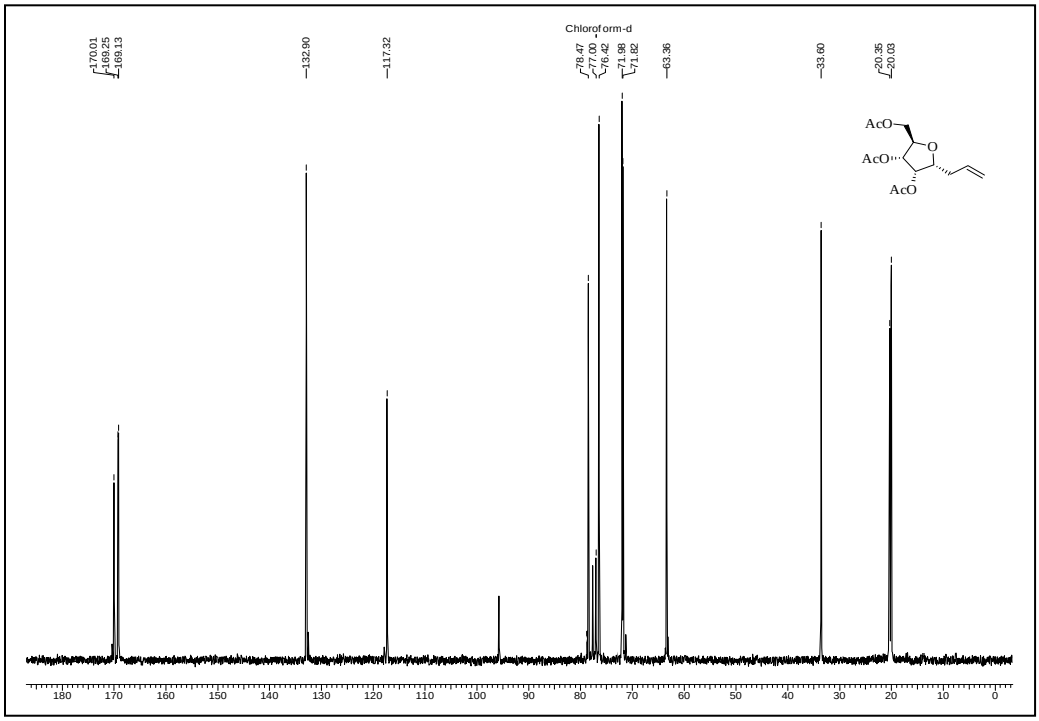

^{13}C NMR Spectrum of 1.106 in $CDCl_3$

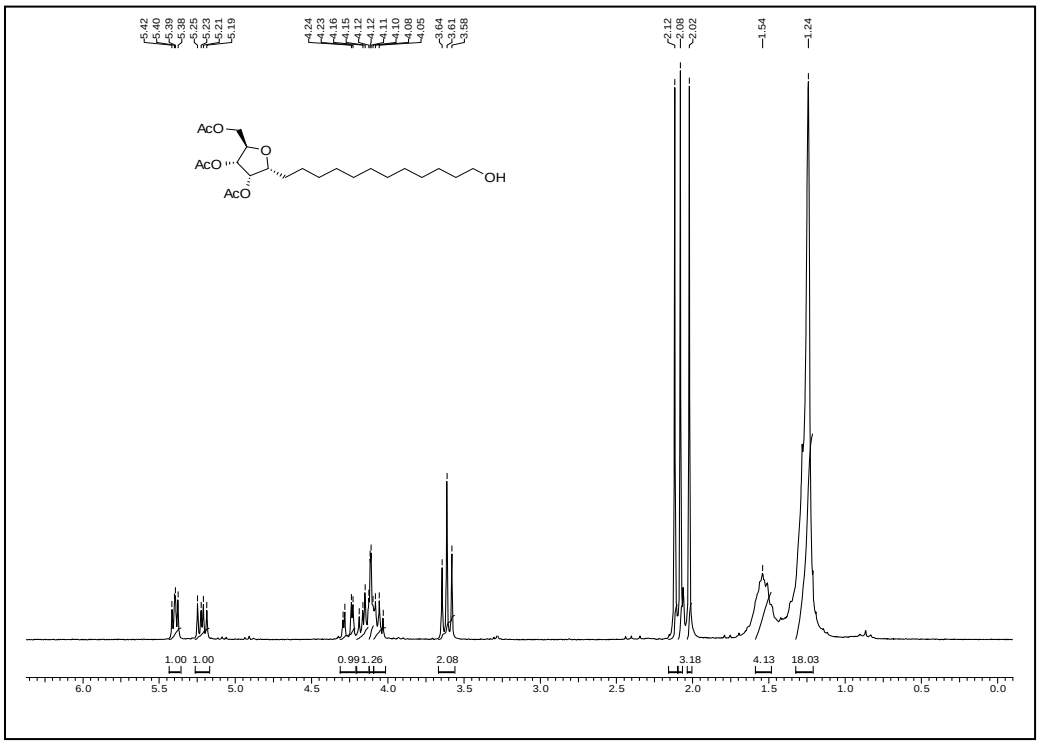

^{1}H NMR Spectrum of 1.111 in $CDCl_3$

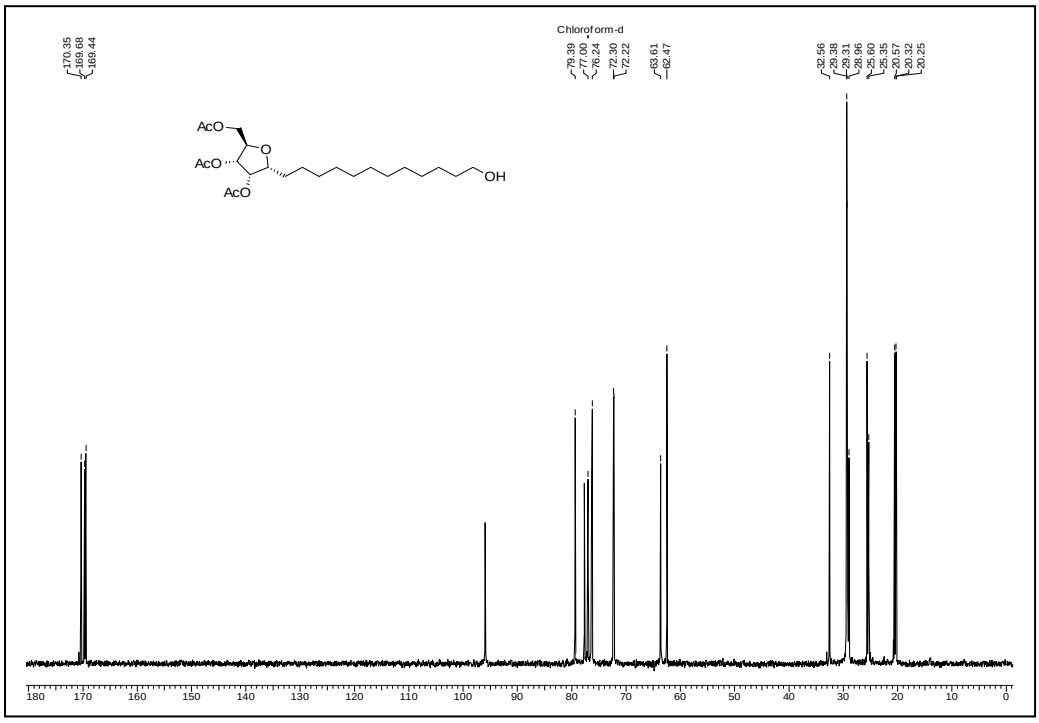

^{13}C NMR Spectrum of 1.111 in $CDCl_3$

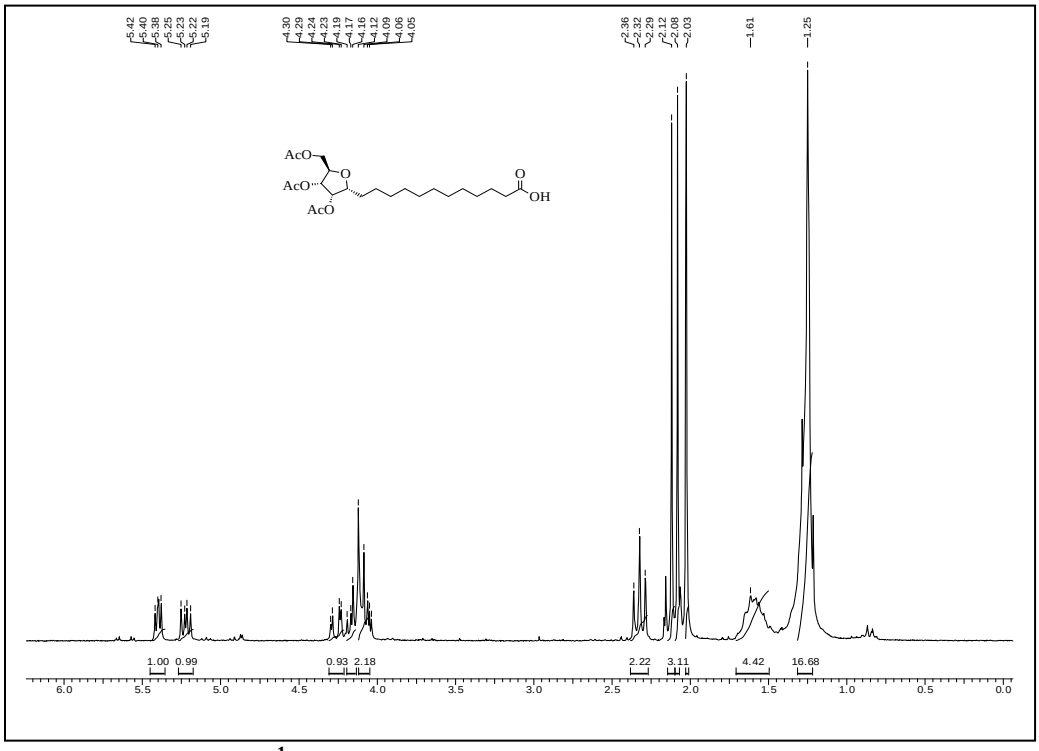

^{1}H NMR Spectrum of 1.112 in $CDCl_3$

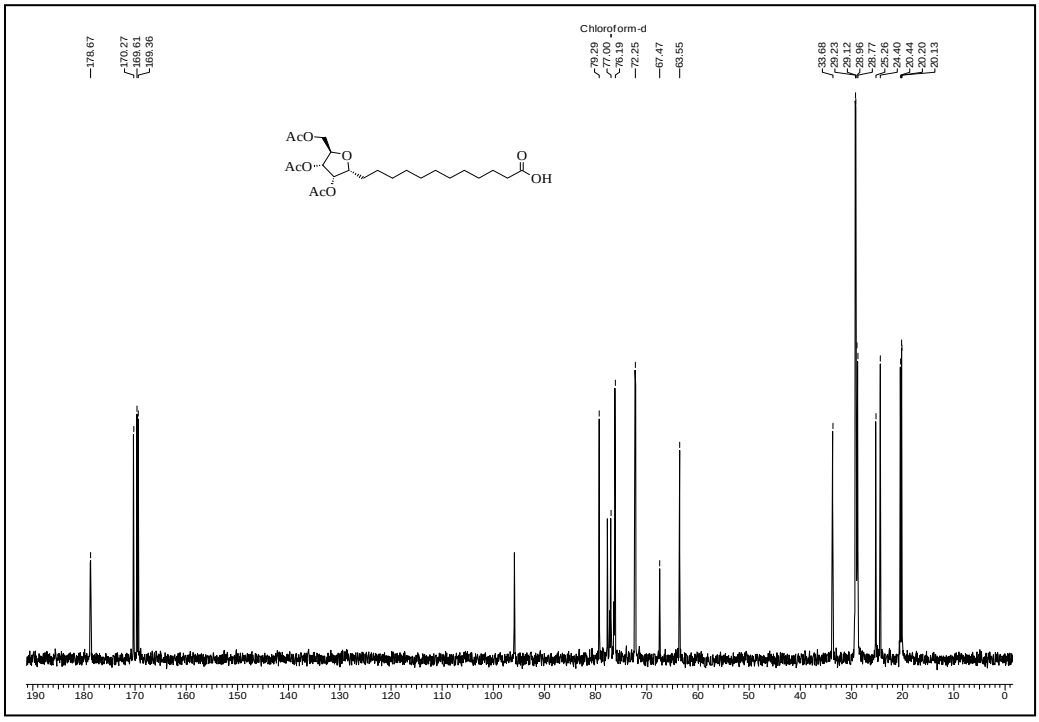

^{13}C NMR Spectrum of 1.112 in $CDCl_3$

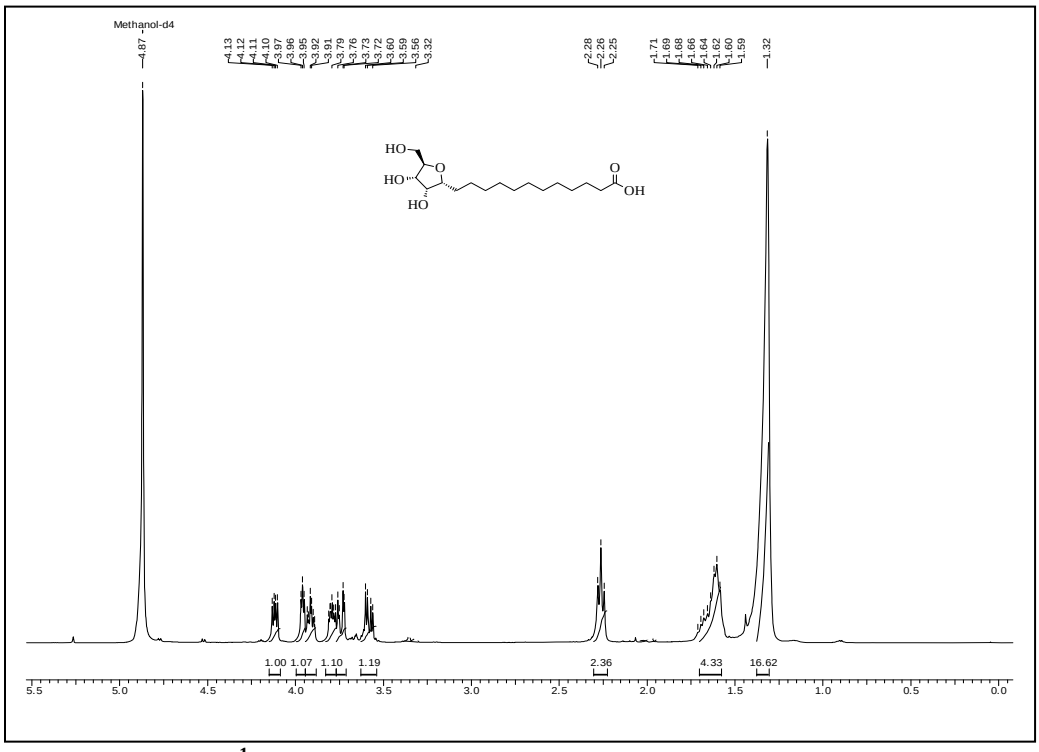

^{1}H NMR Spectrum of 1.101 in Methanol-d$_4$

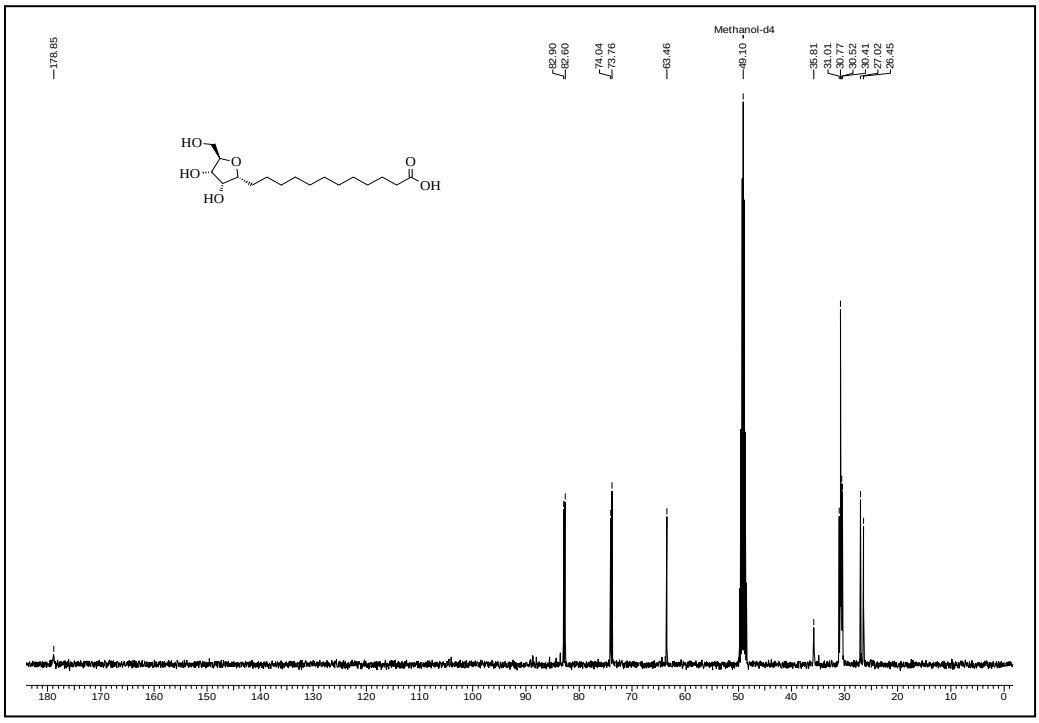

^{13}C NMR Spectrum of 1.101 in Methanol-d$_4$

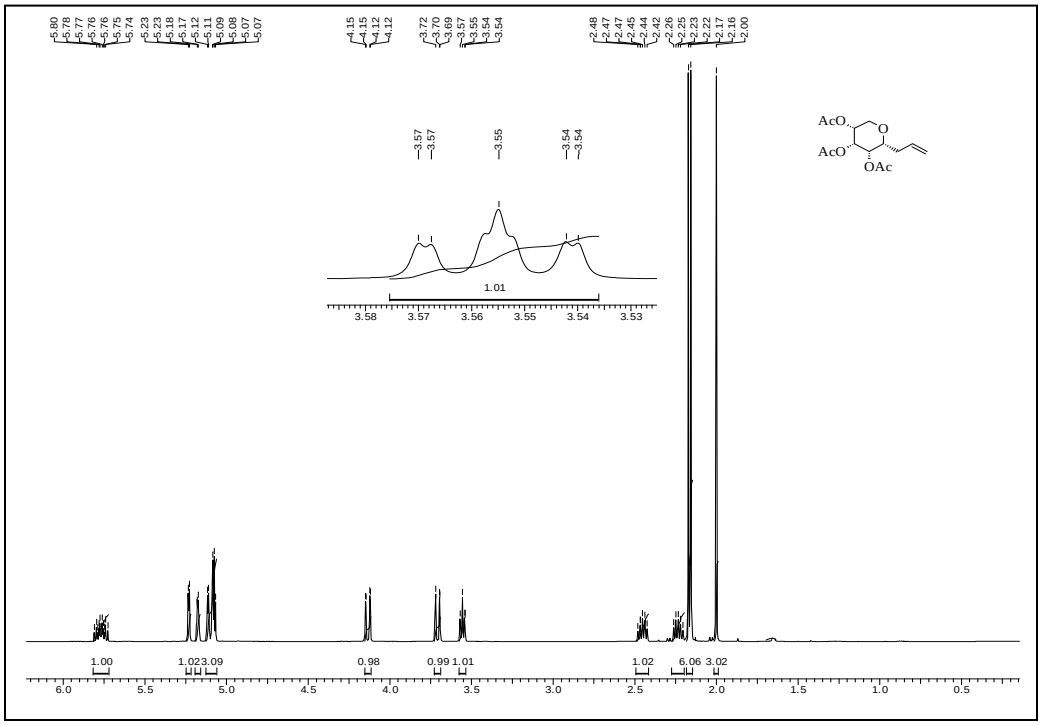

^{1}H NMR Spectrum of 1.114 in $CDCl_3$

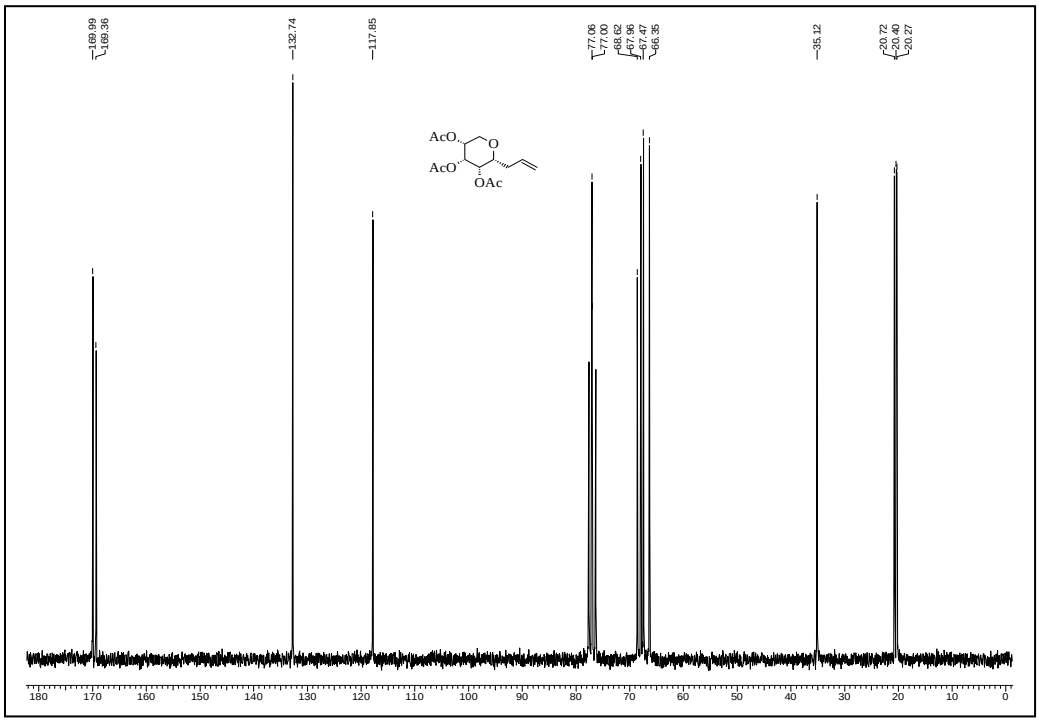

^{13}C NMR Spectrum of 1.114 in $CDCl_3$

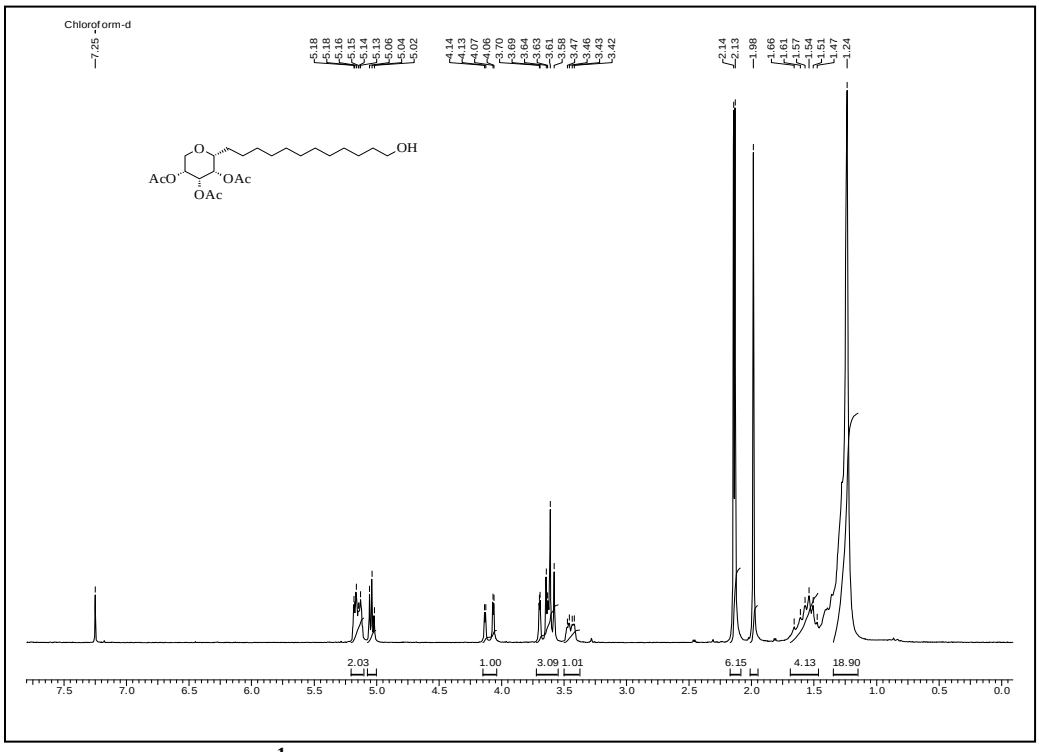

^{1}H NMR Spectrum of 1.120 in $CDCl_3$

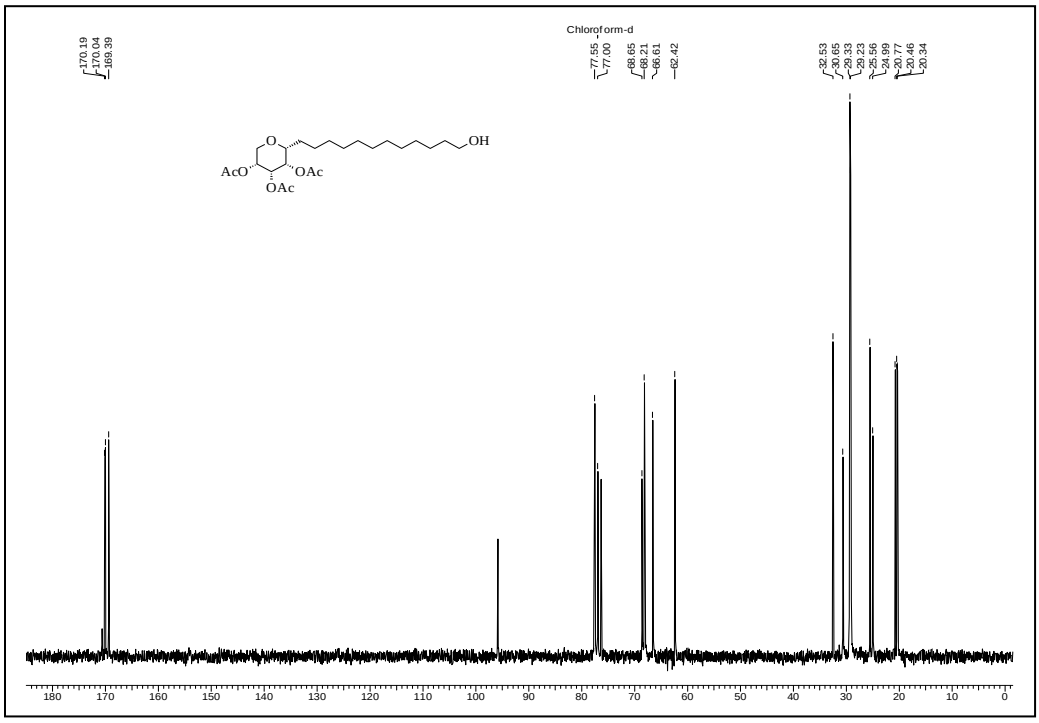

^{13}C NMR Spectrum of 1.120 in $CDCl_3$

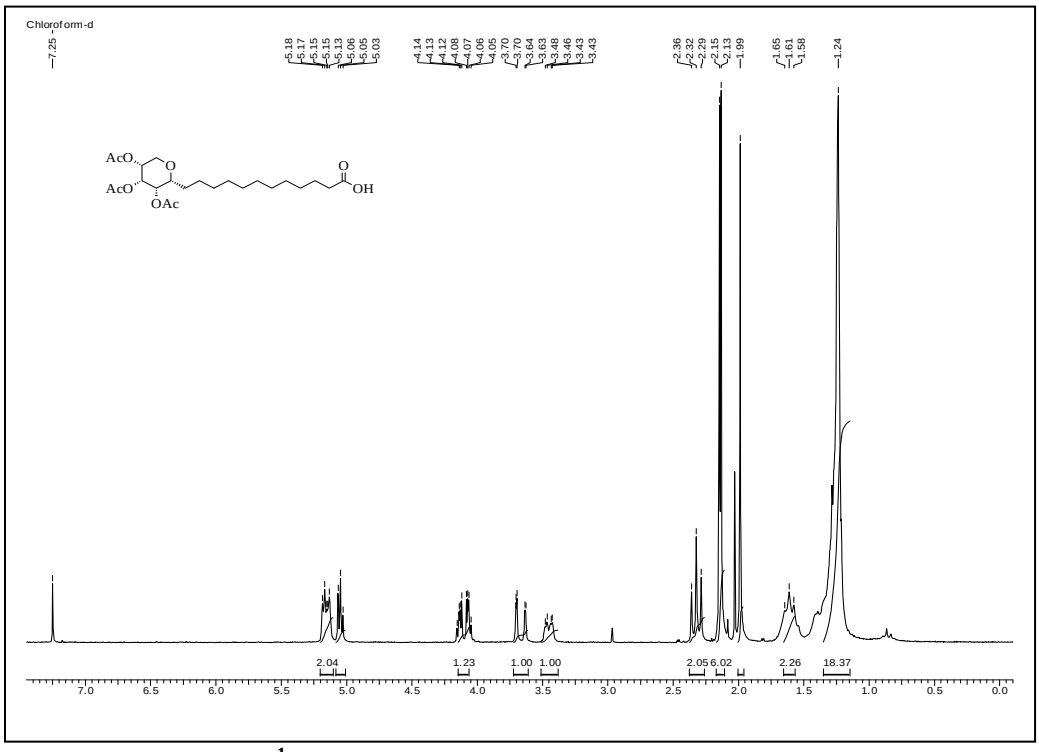

^{1}H NMR Spectrum of 1.121 in $CDCl_3$

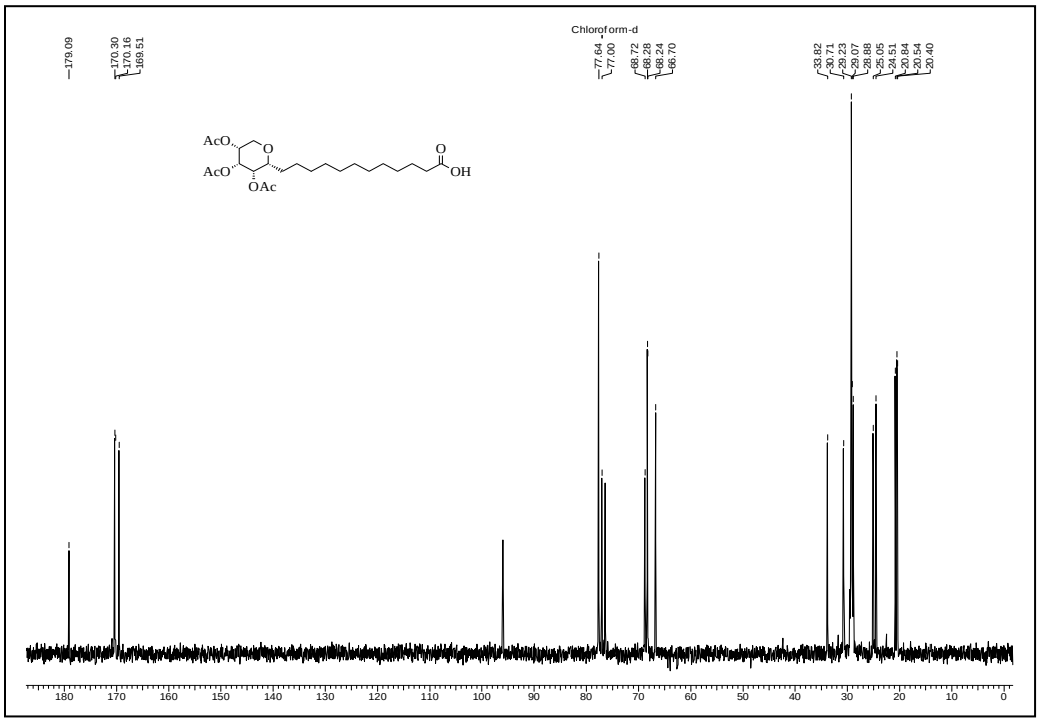

^{13}C NMR Spectrum of 1.121 in $CDCl_3$

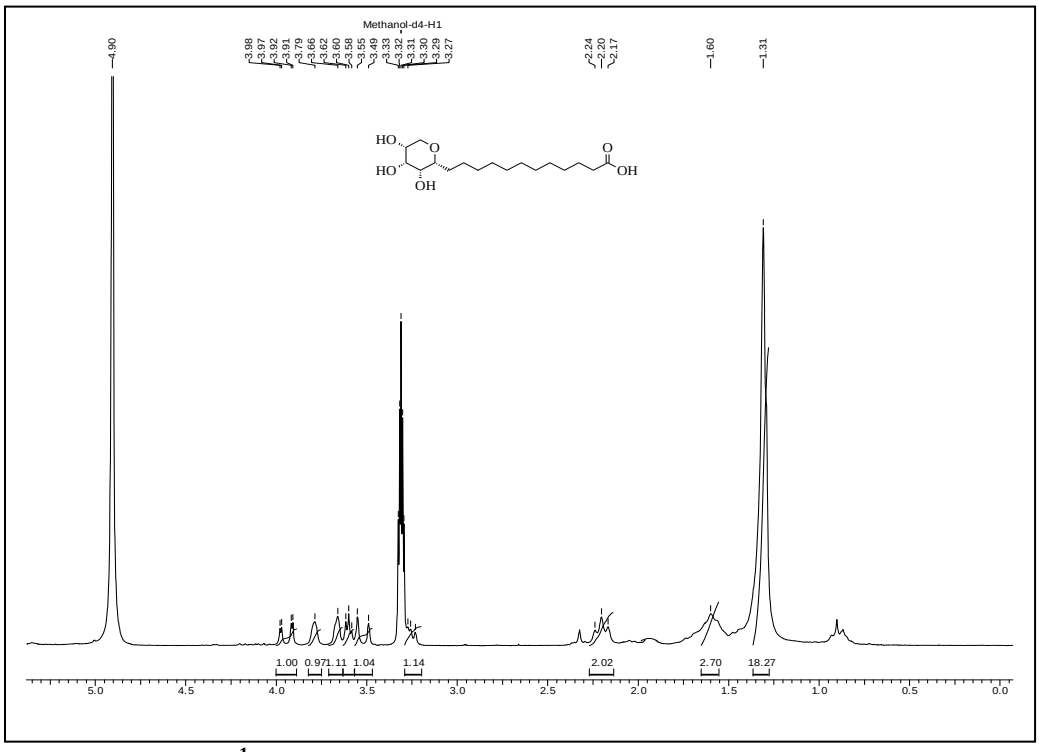

^{1}H NMR Spectrum of 1.102 in Methanol-d_4

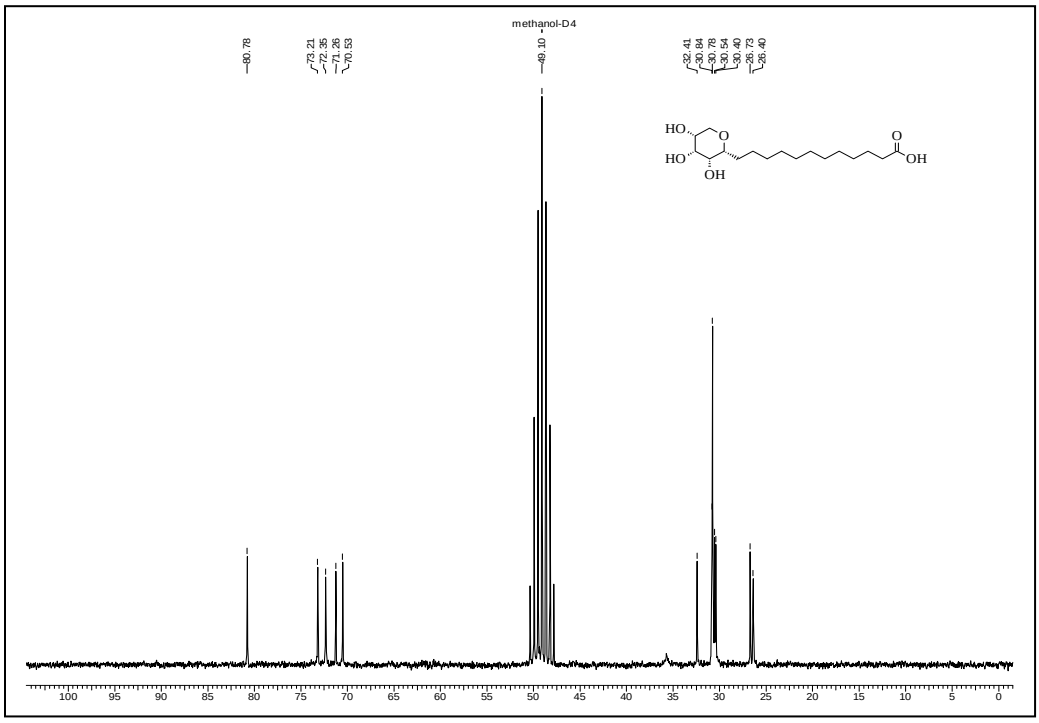

^{13}C NMR Spectrum of 1.102 in Methanol-d_4

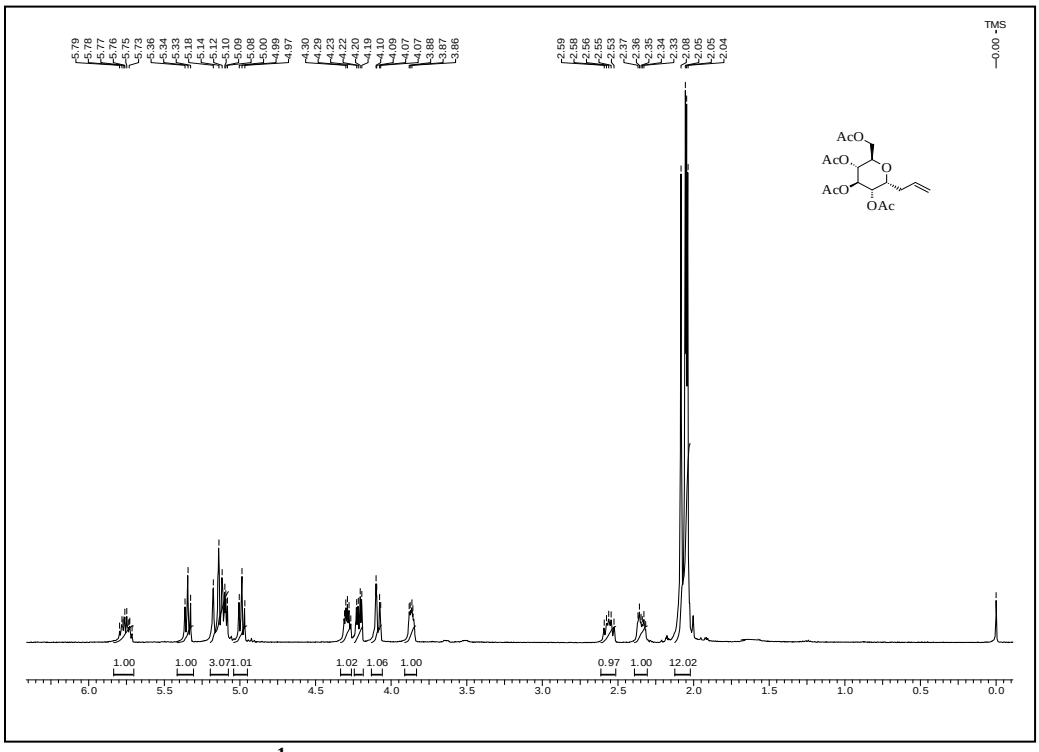

^{1}H NMR Spectrum of 1.123 in $CDCl_3$

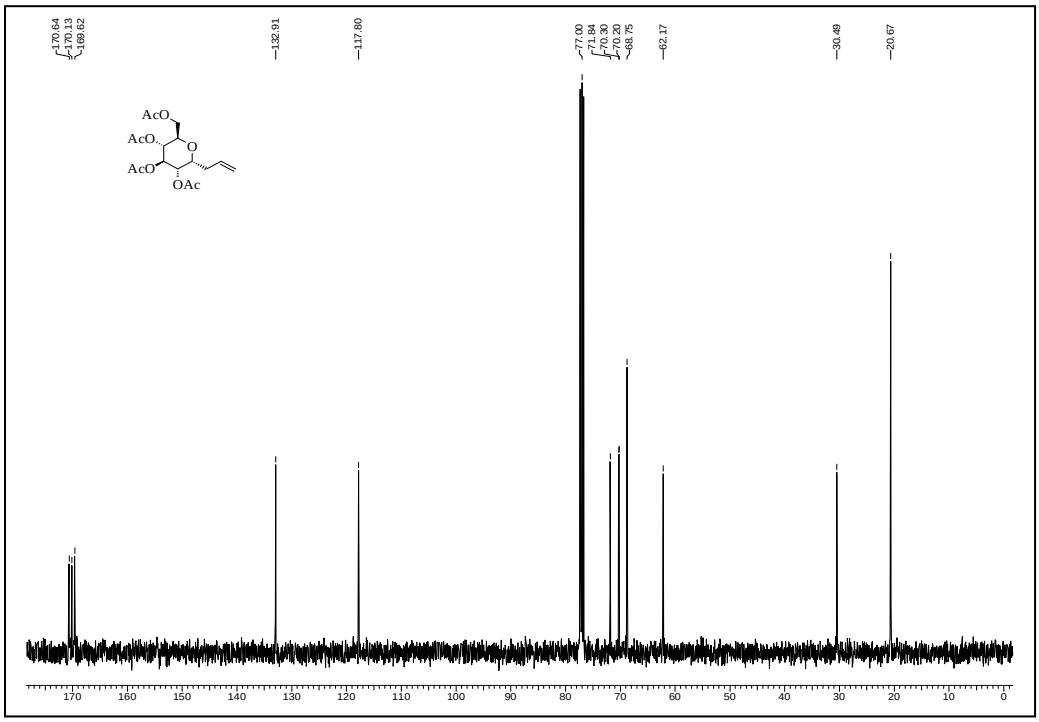

^{13}C NMR Spectrum of 1.123 in $CDCl_3$

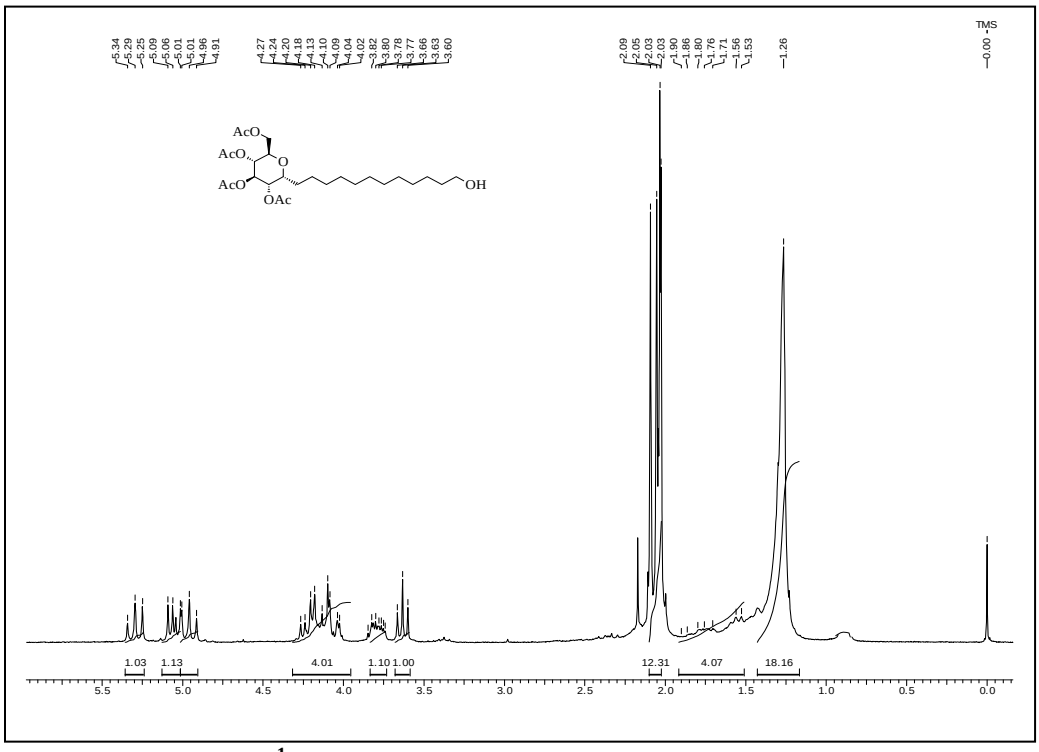

^{1}H NMR Spectrum of 1.125 in $CDCl_3$

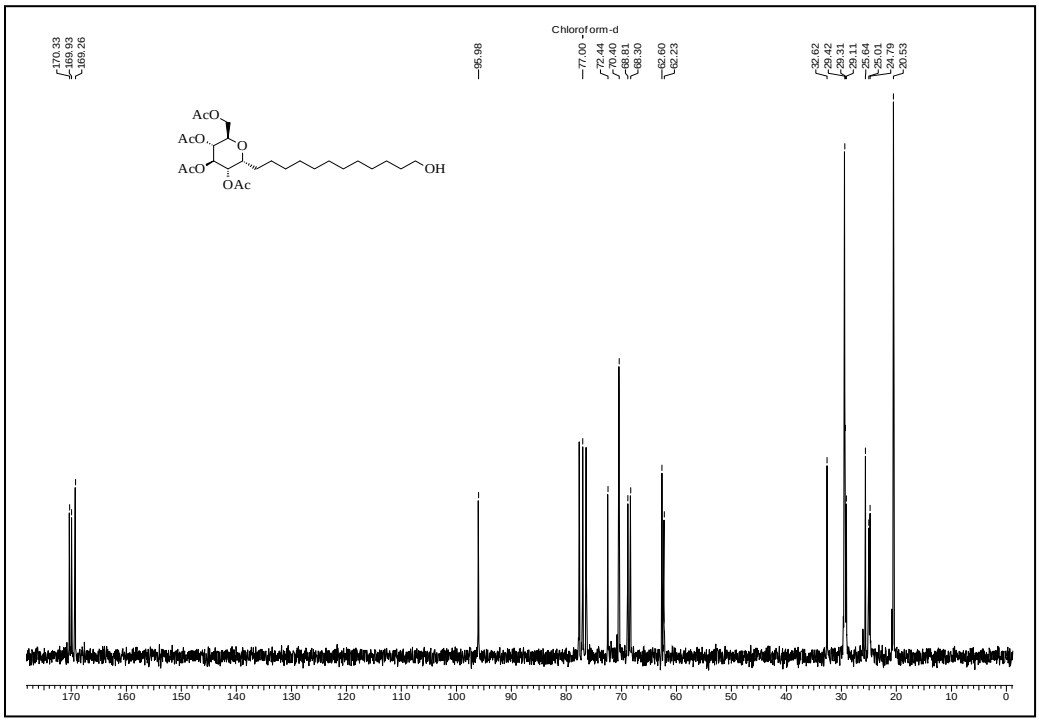

^{13}C NMR Spectrum of 1.125 in $CDCl_3$

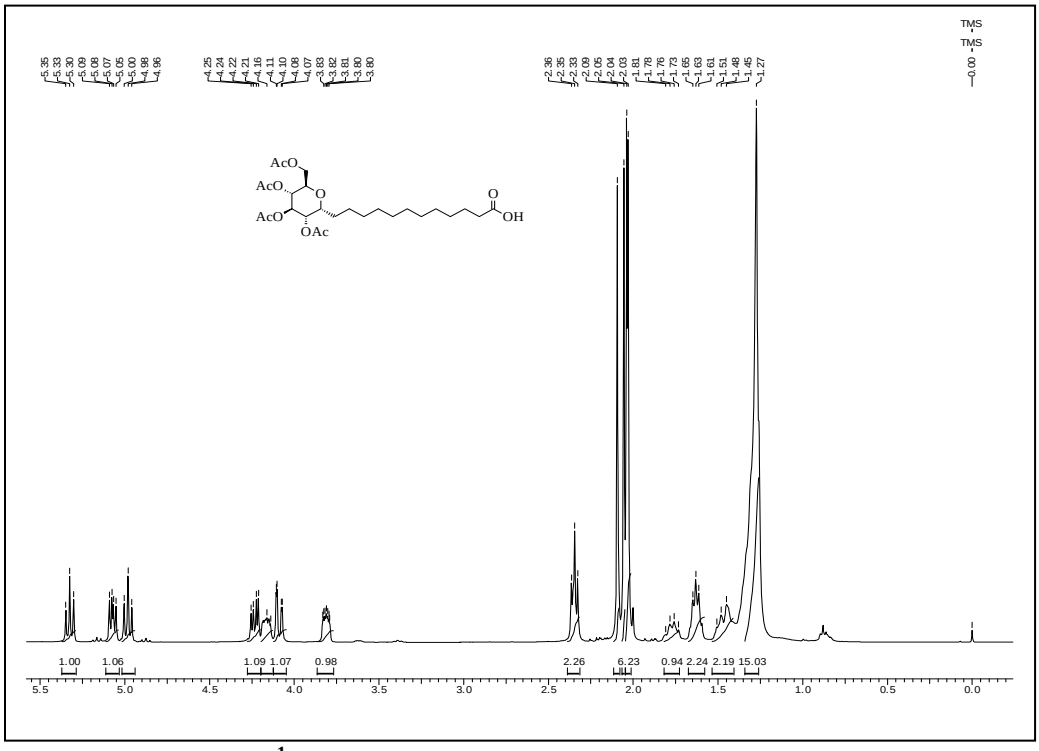

^{1}H NMR Spectrum of 1.126 in $CDCl_3$

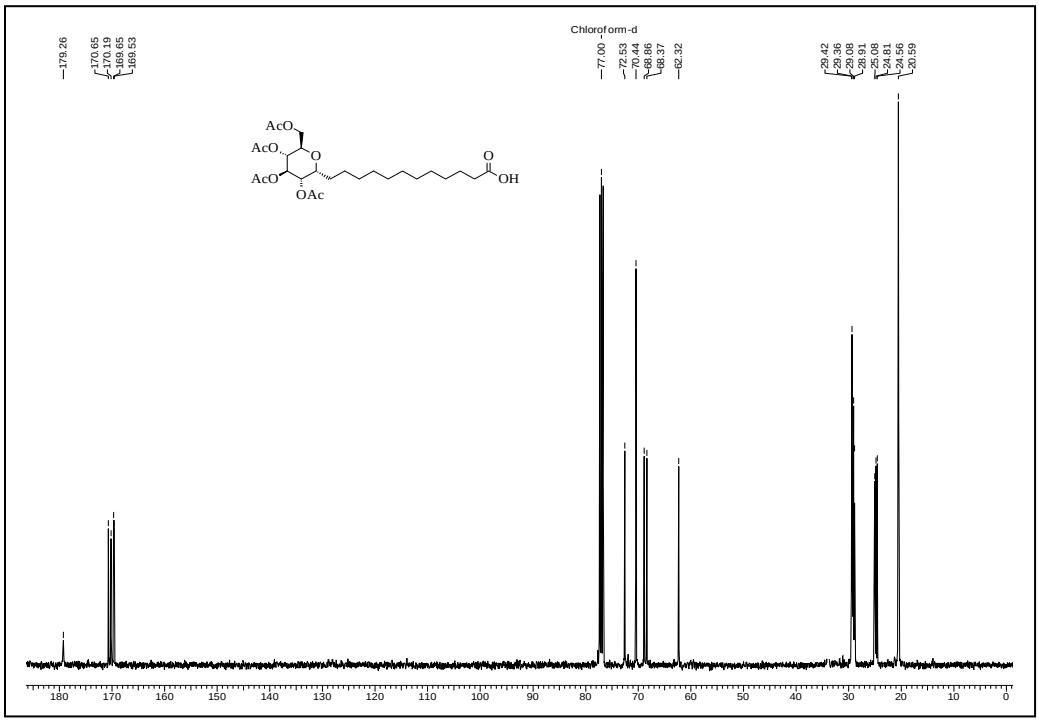

^{13}C NMR Spectrum of 1.126 in $CDCl_3$

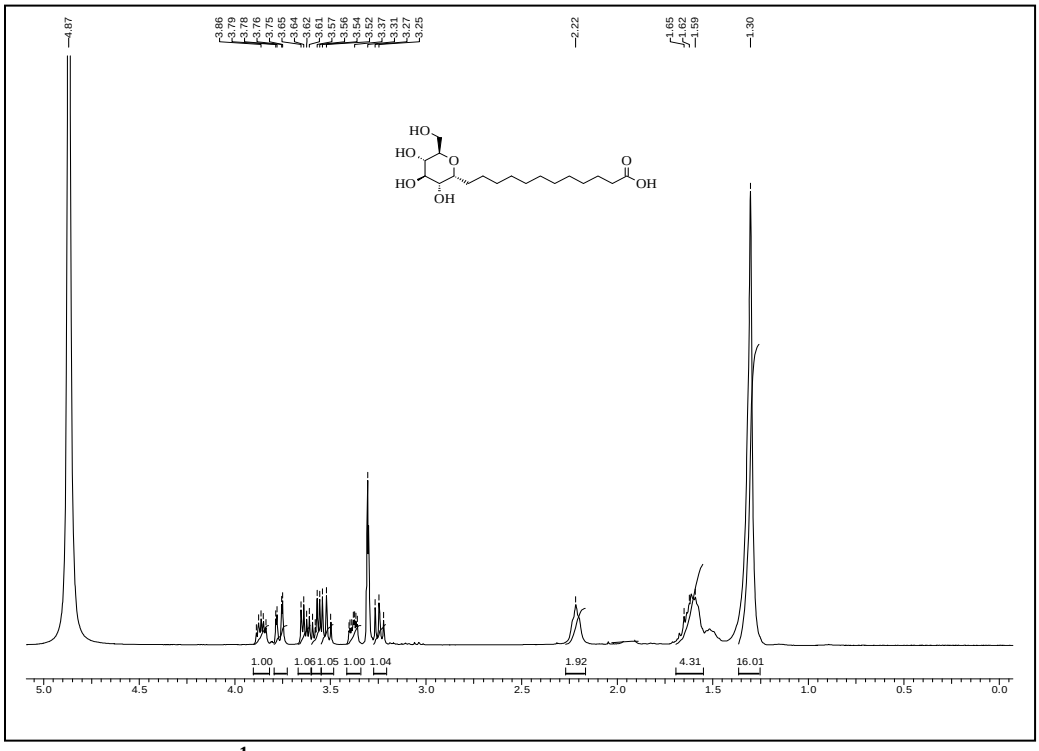

^{1}H NMR Spectrum of 1.103 in Methanol-d$_4$

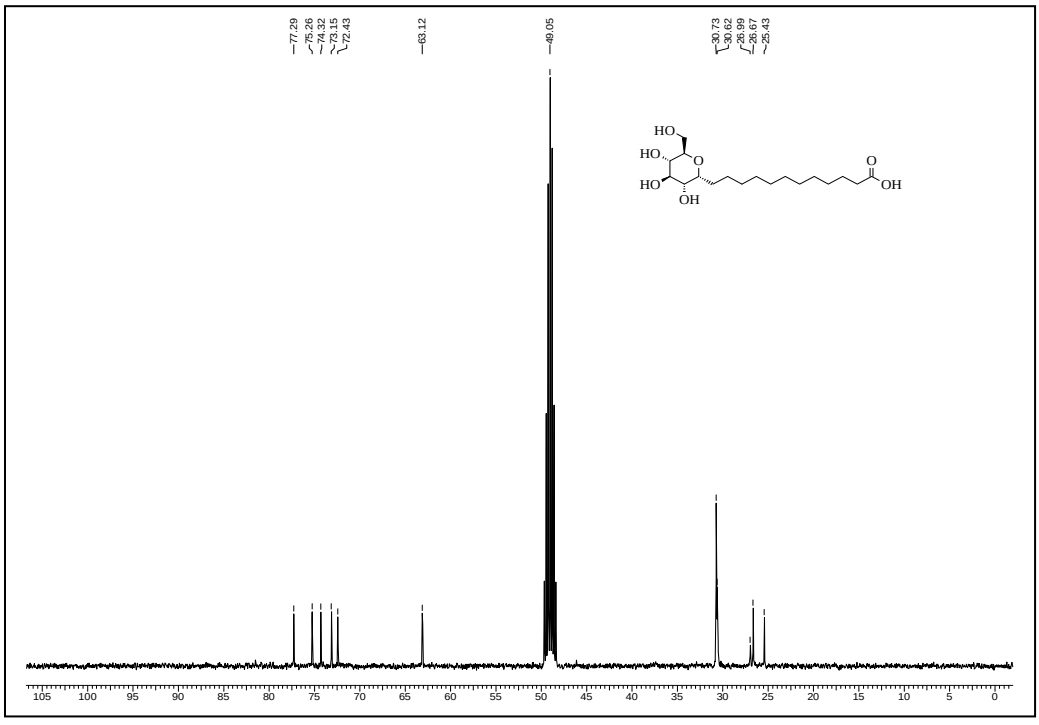

^{13}C NMR Spectrum of 1.103 in Methanol-d$_4$

1.11 References

1. Klabunde, K. J. "*Nanoscale Materials in Chemistry"* (Ed.), **2000**, John Wiley, New York, pp. 18–22.
2. a) Brus, L. E. *Appl*. *Phys*. *A* **1991**, *53*, 465–474. b) Alivisatos, A. P. *Science* **1996**, *271*, 933–937.
3. a) Link, S.; El-Sayed, M. A. *Int*. *Rev*. *Phys*. *Chem*. **2000**, *19*, 409–453. b) Link, S.; El-Sayed, M. A. *Annu*. *Rev*. *Phys*. *Chem*. **2003**, *54*, 331–366.
4. Burda, C.; Chen, X.; Narayanan, R.; El-Sayed, M. A. *Chem*. *Rev*. **2005,** *105*, 1025–1102.
5. a) Andersen, N. A.; Lian, T. *Ann*. *Rev*. *Phy*. *Chem*. **2005**, *56*, 491–519. b) Kamat, P. V. *J*. *Phys*. *Chem*. *B* **2002**, *106*, 7729–7744.
6. Liu, S. M. *Chem*. *Commun*. **2004**, *10*, 2726–2730.
7. Qu, J. R.; Hu, M. A.; Chen, J. Z.; Han, W. *J*. *China Univ*. *Geosci*. **2005**, *30*, 195–209.
8. Saponjic, Z. V. *et al*. *Adv*. *Mater*. **2005**, *17*, 965–971.
9. a) Henglein, A. *Chem*. *Rev*. **1989**, *89*, 1861–1873. b) Steigerwald, M. L.; Brus, L. E. *Acc*. *Chem*. *Res*. **1990**, 23, 183–188. c) Weller, H. *Adv*. *Mater*. **1993**, *5*, 88–95.
10. a) Thomas, G. K.; Kamat, P. V. *Acc*. *Chem*. *Res*. **2003**, *36*, 888–898. b) Willner, I.; Kaganer, E.; Joselevich, E.; Durr, H.; David, E.; Gunter, M. J.; Johnston, M. R. *Coord*. *Chem*. *Rev*. **1998**, *171*, 261–288. c) Ward, M. D. *Chem*. *Soc*. *Rev*. **199**7, *5*, 365–376.
11 Haes, A. J.; Van Duyne, R. P. *Anal*. *Bioanal*. *Chem*. **2004**, *379*, 920–930.
12. (a) Roucoux, A.; Schulz, J.; Patin, H. *Chem*. *Rev*. **2002**, *102,* 3757–3778. (b) Lewis, L. N. *Chem*. *Rev*. **1993**, *93*, 2693–2730.
13. Rosi, N. L.; Mirkin, C. A. *Chem*. *Rev*. **2005**, *105*, 1547–1562.
14. Liu, C. *et al*., *Neuroscience Lett*. **2006**, *406*, 189–193.
15. Otsuka, H.; Nagasaki, Y.; Kataoka, K. *Adv*. *Drug Delivery Rev*. **2003**, *55*, 403–419.
16. Yae. S. *et al*., *Solar Energy Mater*. *Solar Cells* **2007**, *91*, 224–229.
17. Zou, S.; Schatz, G. C. *Phy*. *Rev*. *B* **2006**, *74*, 125111–125111-5.

18. Cengiz, E.; Wissing, S. A.; Muoller, R. H.; Yazan, Y. *Intl. J. Cosmetic Sci*. **2006**, *28*, 371–378.
19. a) Wang, Y. *et al., Nano Lett*. **2005**, *4*, 1689–1693. b) Sokolov, K. *et al., Cancer Res*. **2003**, *63*, 1999–2004.
20. Baglioni, P.; Giorgi, R. *Soft Matter* **2006**, *2*, 293–303.
21. Fichtner, M. *Adv. Engg. Mater*. **2005**, *7*, 443–455.
22. Moran, C. E.; Steele, J. M.; Halas, N. J. *Nano Lett*. **2004**, *4*, 1497–1500.
23. Simon, U. In *Nanoparticles: From Theory to Application*, Schmid, G., Ed. Wiley-VCH, Weinheim, **2004.**
24. Maier, S. A.; Brongersma, M. L.; Kik, P. G.; Atwater, H. A. *Phys. Rev. B*, **2002**, *65*, 193408–193408-4.
25. Li, X.; Xu, W.; Zhang, J.; Jia, H.; Yang, B.; Zhao, B.; Li, B.; Ozaki, Y. *Langmuir* **2004**, *20*, 1298–1304.
26. Wegner, K.; Walker, B.; Tsantilis, S.; Pratsinis, S. E. *Chem. Eng. Sci*. **2002**, *57*, 1753–1762.
27. Teng, X.; Black, D.; Watkins, N. J.; Gao, Y.; Yang, H. *Nano Lett*. **2003**, *3*, 261–264.
28. Suh, W. H.; Suslick, K. S. *J. Am. Chem. Soc*. **2005**, *127*, 12007–12010.
29. Sakamoto, M.; Tachikawa, T.; Fujitsuka, M.; Majima, T. *Langmuir* **2006**, *22,* 6361–6366.
30. Amendola, V.; Polizzi, S.; Meneghetti, M. *J. Phys. Chem. B* **2006**, *110,* 7232–7237.
31. Nemamcha, A.; Rehspringer, J.; Khatmi, D. *J. Phys. Chem. B* **2006**, *110,* 383–387.
32. Doudna, C. M.; Bertino, M. F.; Blum, F. D.; Tokuhiro, A. T.; Lahiri-Dey, D.; Chattopadhyay, S.; Terry, J. *J. Phys. Chem. B* **2003**, *107,* 2966–2970.
33. Stoeva, S.; Klabunde, K. J.; Sorensen, C. M.; Dragieva, I. *J. Am. Chem. Soc*. **2002**, *124*, 2305–2311.
34. Katz, E.; Willner, I. *Angew. Chem. Int. Ed*. **2004**, *43*, 6042–6108.
35. Sastry, M.; Kumar, A.; Mukherjee, P. *Colloids and Surf. A* **2001**,*181*, 255–259.
36. Stephen, J. R.; Maenaughton, S. J. *Curr. Opin. Biotechnol*. **1999**, *10*, 230–233.
37. Mehra, R. K.; Winge, D. R. *J Cell. Biochem*. **1991**, *45*, 30–40.
38. J.M. de la Fuente, S. Penadés, *Glycoconj. J*. **2004**, *21*, 149–163.
39. Frey, A.; Giannasca, K.T.; Weltzin, R.; Giannasca, P.J.; Reggio, H.;

Lencer, W.I.; Neutra, M.R. *J. Exp. Med.* **1996**, *184*,1045–1059.

40. Varki, A. *Glycobiology* **1993**, *3,* 97–130.
41. Dwek, R.A. Chem. Rev. **1996** *96,* 683–720.
42. Qi, L.; Xu, Z.; Jiang, X.; Li, Y.; Wang, M. *Bioorg. Med. Chem. Lett.* **2005**, *15,* 1397–1399.
43. Kim, T.H.; Park, I.K.; Nah, J.W.; Choi, Y.J.; Cho, C.S. *Biomaterials* **2004**, *25,* 3783–3792.
44. Tartaj, P.; Morales, M.P.; Veintemillas-Verdaguer, S.; Gonzalez-Carreño, T.; Serna, C.J.; *J. Phys., D, Appl. Phys.*; **2003**, *36,* R182–R197.
45. Templeton, A.C.; Chen, S.; Gross, S.M.; Murray, R.W. *Langmuir* **1999**, *15*, 66–76.
46. Lopez-Cartes, C.; Rojas, T.C.; Litran, R.; Martinez-Martinez, D.; de la Fuente, J.M.; Penades, S.; Fernandez, A. *J. Phys. Chem., B* **2005**, *109*, 8761–8766.
47. Crespo, P.; Litrán, R.; Rojas, T.C.; Multigner, M.; de la Fuente, J.M.; Sanchez-Lopez, J.C.; García, M.A.; Hernando, A.; Penadés, S.; Fernández, A. *Phys. Rev. Lett.* **2004**, *93*, 087204.
48. De la Fuente, J.M.; Barrientos, A.G.; Rojas, T.C.; Rojo, J.; Cañada, J.; Fernández, A.; Penadés, S. *Angew. Chem. Int. Ed.* **2001**, *40*, 2257–2261.
49. Schellenberger, E.A.; Reynolds, F.; Weissleder, R.; Josephson, L. *ChemBioChem* **2004**, *5,* 275–279.
50. Berry, C.C.; Wells, S.; Charles, S.; Aitchison, G.; Curtis, A.S.G. *Biomaterials* **2004**, *25*, 5405–5413.
51. Brust, M.; Walker, M.; Bethell, D.; Schiffrin, D.J.; Whyman, R. *J. Chem. Soc. Chem. Commun.* **1994**,801–802.
52. Collier, C.P.; Saykally, R.J.; Shiang, J.J.; Henrichs, S.E.; Heath, J.R. *Science* **1997**, *277*, 1978–1981.
53. De La Fuente, J. M.; Barrientos, Á. G.; Rojas, T. C.; Rojo, J.; Cañada, J.; Fernández, A.; Penadés, S. *Angew. Chem. Int. Ed.* **2001**, *40*, 2257–2261.
54. De Paz, J. L.; Ojeda, R.; Barrientos, A. G.; Penadés, S.; Martín-Lomas, M.; *Tetrahedron: Asymmetry* **2005**, *16*, 149–158.
55. Barrientos, A. G.; de la Fuente, J. M.; Rojas, T. C.; Fernández, A.; Penadés, S. *Chem.- Eur. J.* **2003**, *9*, 1909–1921.
56. Lin, C.-C.; Yeh, Y.-C.; Yang, C.-Y.; Chen, G.-F.; Chen, Y.-C.; Wu, Y.-C.; Chen, C.-C. *Chem. Commun.* **2003**, *23*, 2920–2921.

57. Nolting, B.; Yu, J.-J.; Liu, G.-Y.; Cho, S.-J.; Kauzlarich, S.; Gervay-Hague, J. *Langmuir* **2003**, *19*, 6465–6473.

58. Zhang, J.; Geddes, C. D.; Lakowicz, J. R. *Anal. Biochem.* **2004**, *332*, 253–260.

59. Panacek, A.L. Kvıtek, R. Prucek, M. Kolar, R. Vecerova, N. Pizurova, Virender K. Sharma,Tatjana Nevecna, R Zboril *J. Phys. Chem. B* 2006, *110*, 16248-16253.

60. Bruchez, M.; Moronne, M.; Gin, P.; Weiss, S.; Alivisatos, A.P. *Science* **1998**, *281*, 2013–2016.

61. Sutherland, A.J. *Curr. Opin. Solid State Mater. Sci.* **2002**, *6*3, 65–370.

62. Hou, Y.; Kondoh, H.; Kogure, T.; Ohta, T. *Chem. Mater.* **2004**, *16,* 5149–5152.

63. Chen, Y.; Ji, T.; Rosenzweig, Z. *Nano Lett.* **2003**, *3*, 581–584.

64. Sun, X.-L.; Cui, W.; Haller, C.; Chaikof, E.L. *ChemBio- Chem* **2004**, *5*, 1593–1596.

65. De la Fuente, J.M.; Penadés, S. *Tetrahedron Asymmetry* **2005**, *16*, 387–391.

66. Robinson, A.; Fang, J.-M.; Chou, P.T.; Liao, K.W.; Chu, R.M.; Lee, S.-J. *ChemBioChem* **2005**, *6*, 1899–1905.

67. Berry, C.C.; Curtis, A.S.G. *J. Phys., D, Appl. Phys.* **2003**, *36*, R198–R206.

68. Pankhurst, Q.A.; Connolly, J.; Jones, S.K.; Dobson, J. *J. Phys., D, Appl. Phys.* **2003**, *36*, R167–R181.

69. Penades, S.; Martin-Lomas, M.; De la Fuente, J.M.; Rademacher, T.W. WO 2004/108165 A2

70. a) Levy, D. E.; Tang, C. In *The Chemistry of C–Glycosides*, 1995. b) Witczak, Z. J.; Nieforth, K. A. In *Carbohydrates in Drug Design*, 1997. c) Du, Y.; Linhardt, R. J.; Vlahov, I. R. *Tetrahedron* **1998**, *54*, 9913–9959. d) Beau, J.-M.; Vauzeilles, B.; Skrydstrup, T. In *Glycoscience: Chemistry and Chemical Biology*, **2001**; Vol. 3; pp. 2679–2724.

71. a) Harenbrock, M.; Matzeit, A.; Schaefer, H. J. *Liebigs Annalen* **1996**, 55–62. b) Schwabisch, D.; Wille, S.; Hein, M.; Meithchen, R. *Liquid Crystals* **2004**, *31*, 1143–1150.

72. a) Cupps, T. L.; Wise, D. S.; Townsend, L. B. *J. Org. Chem.* **1982**, *47*, 5115–5120. b) Kozikowski, A. P.; Sorgi, K. L.; Wang, B. C.; Xu, Z.-B. *Tetrahedron Lett.* **1983**, *24*, 1563–1566. c) Araki, Y.; Kobayashi, N.; Ishido, Y.; Nagasawa, J. *Carbohydr. Res.* **1987**, *171*, 125–139. d) Bennek, J. A.; Gray, G. R. *J. Org. Chem.* **1987**, *52*, 892-897. e) McDevitt, J. P.; Lansbury Jr, P. T. *J. Am. Chem. Soc.* **1996**,

118, 3818–3828. f) Larsen, C. H.; Ridgway, B. H.; Shaw, J. T.; Smith, D. M.; Woerpel, K. A. *J. Am. Chem. Soc.* **2005**, *127*, 10879–10884.

73. Durette, P.L., Horton, D. *J. Org. Chem.* **1971**, *36*, 2658–2669.

74. a) Giannis, A.; Sandhoff, K. *Tetrahedron Lett.* **1985**, *26*, 1479–1482. b) Horton, D.; Miyake, T. *Carbohydr. Res.* **1988**, *184*, 221–239.

75. Kasture, M.; Singh, S.; Patel, P.; Joy, P. A.; Prabhune, A. A.; Ramana, C. V.; Prasad, B. L. V. *Langmuir* **2007**, *23*, 11409–11412.

CHAPTER-II

Section I: "Cu(I) promoted one–pot "S_NAr–Click reaction" of fluoronitrobenzenes"

2.1 Introduction

2.1.1 "Click Chemistry"

Following nature's lead, Sharpless and coworkers[1] endeavor to generate substances by joining small units together with heteroatom links (C-X-C). The goal is to develop an expanding set of powerful, selective, and modular "blocks" that work reliably in both small and large scale applications. They have termed the foundation of this approach as "Click Chemistry", and have defined a set of stringent criteria that a process must meet to be useful in this context. Carbon-heteroatom bond forming reactions comprise the most common examples, including the following classes of chemical transformations. (Figure 2.1)

Figure 2.1 *Carbon-heteroatom bond forming reactions*

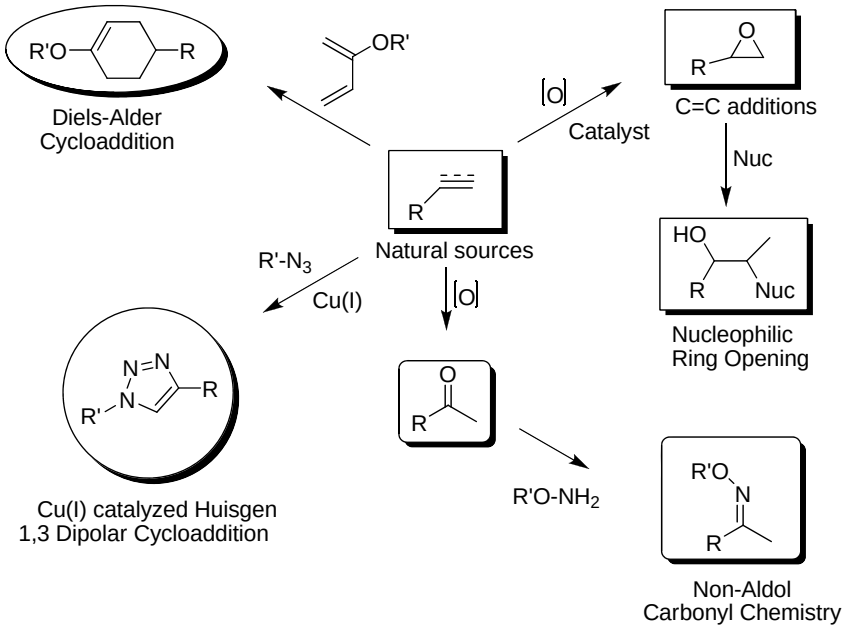

- Cycloadditions of unsaturated species, especially 1,3-dipolar cycloaddition reactions, but also Diels-Alder family of transformations.
- Neucleophilic substitution chemistry, particularly ring opening reactions of strained heterocyclic electrophiles such as epoxides, aziridines, aziridinium ions, and episulfonium ions.
- Carbonyl chemistry of the "non-aldol" type, such as formation of ureas, thioureas, aromatic heterocycles, oxime ethers, hydrazones & amides.

- Additions to carbon-carbon multiple bonds, especially oxidative cases such as epoxidation, dihydroxylation, aziridination, and sulfonylhalide addition, but also Michael additions to Nu-H reactants.

Of all the reactions which achieve "click status" the Hüisgen 1,3-dipolar cycloaddiotion[2] of alkynes and azides to yield 1,2,3-triazoles is undoubtedly the premier example of a click reaction. The each of synthesis of alkyne and azide functionalities, coupled with their kinetic stability and tolerence to a wide variety of functional groups and reaction conditions, make these complementary coupling partners particularly attractive. However, it was the recent discovery of the dramatic rate acceleration of the azide-alkyne coupling event,[3,4] under copper(I) catalysis and the beneficial effects of water that have placed this reaction at the 'center stage' of click chemistry. This new reaction process requires no protecting groups, and proceeds with almost complete conversion and selectivity for the 1,4-disubstituted 1,2,3-triazole (*anti*-1,2,3-triazole). No purification is generally required. This 'near perfect' reaction has become synonymous with click chemistry, and is often referred as 'The Click Reaction'.[5] (Figure 2.2)

Figure 2.2 *The1,3-dipolar cycloaddition between azides and alkynes*

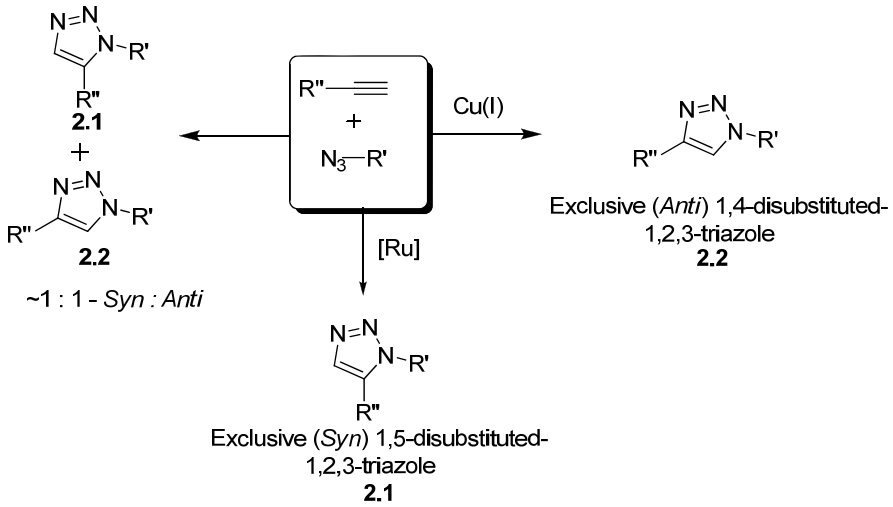

Around 110 years ago, O. Dimoth discovered the formation of triazoles by addition of organic azides to acetylenes. Of greater mechanistic interest is the closely related reaction of phenyl azide with bicyclo-[2,2,1]hept-2-ene and its derivatives, described by Alder and Stein in 1931.[6]

Scheme 2.1

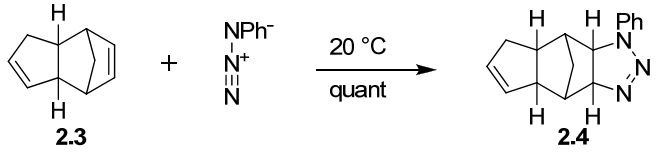

Hüisgen[7] in early 60's described the plausible mechanism involved in the reaction between azides and carbon-carbon double bond. Phenyl azide has two mesomeric structures with electron octets on all atoms, and both are dipolar in character. Three more canonical forms each having one electron sextet contribute to somewhat less extent. On the basis of all octet structures phenyl azide is a linear tripole: the middle nitrogen holds the formal positive charge while the negative charges shared between the end nitrogen atoms.

In addition of phenyl azide to double bond, three mechanisms are conceivable. (Figure 2.3, A) The positive end of the dipole may initiate the attack and the negative pole complete the addition; or (B) the negative center may be attached first, and then the positive end; (C) both the charge centers may add at the same time.

Figure 2.3

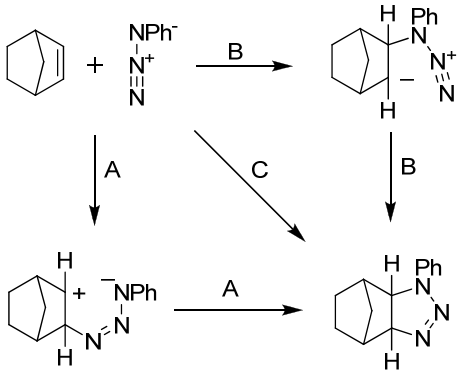

Doubts concerning mechanisms A and B are immediately raised because the sluggish organic azide displays neither strong electrophilic nor nucleophilic character. The concerted process C is immune to such objections. Here a synchronous shift of electrons result in the formation of two new σ-bonds and allow all three nitrogen atoms to achieve stable octets without having to bear a formal charge.

Azides are essentially inert to most biological and organic conditions, including highly functionalized biological molecules, molecular oxygen, water and majority of

common reaction conditions in organic synthesis.[4,8] For the formation of 1,2,3-triazole using Cu(I) as catalyst where azides can react with acetylene 10^7 times faster than the previously described methods. Till date this is probably the most powerful discovery of click reaction.

Despite the thermodynamic favorability of azide decomposition, kinetic factors allow aliphatic azides to remain nearly invisible until presented with a good dipolarophile. This kinetic stability of alkynes and azides is directly responsible for their slow cycloaddition, which generally requires elevated temperatures and long reaction times.[9,10] Good regioselectivity in the uncatalyzed Hüisgen type cycloaddition is observed for coupling reactions involving highly electron deficient terminal alkynes,[11] but reactions with other terminal alkynes usually afford mixtures of 1,4- and 1,5-regioisomers.[12]

Thus only following the recent discovery of the advantages of Cu(I) catalyzed azide-alkyne coupling, did the main benefits to this cycloaddition, become clear. Cu(I) catalysis dramatically improves the regioselectivity to afford the 1,4-regioisomer exclusively and increases the reaction rate upto 10^7 times,[13] eliminating the need for elevated temperatures. This high yielding reaction tolerates a variety of functional groups and affords the 1,2,3-triazole product with minimal work up and purification, as an ideal click reaction.

Click chemistry was postulated initially as a specific organic reaction but by time it became a very important tool in different fields of chemistry. The major improvement was seen in materials chemistry.[14] In 2004, Hawker, Fokin, Sharpless, and coworkers have reported the first illustration on this field. Afterwards, the popularity of click chemistry within the materials science grew considerably by the influential works of Hawker, Fréchet, Finn, Hawker, Fokin, Sharpless and coworkers.

2.1.2 Click Chemistry and Multicomponent Reactions

The potential of click reactions can be further amplified by combining it with multicomponent reactions. Multicomponent reactions (MCRs) are reactions where three or more substrates combine in one step to give a product that contains essential parts of all of them. The combination of a classical multicomponent reaction with a classical organic transformation has been shown by many to be a powerful strategy to yield complex structures in few synthetic steps.

The idea of using a MCR followed by a Hüisgen copper catalyzed reaction was first presented by Barbas and coworkers.[15] In this paper, a multicomponent reaction between a phosphorane (**2.5**), a spirolactone (**2.6**), an aryl aldehyde (**2.7**) and aryl azide using an L-proline catalyst, gave various functionalized dispirolactones (**2.8**) through a domino Wittig/Knoevenagel/Diels-Alder/Cu catalyzed Hüisgen cycloaddition reaction. Dispirolactones have been shown to possess antioxidant and free radical scavenger activities. The combined organo-catalysis and CuAAC approach (termed by the authors ‘‘organo-click’’), would appear promising for the generation of diverse chemical libraries. (Scheme 2.2)

Scheme 2.2 *Four component multicatalytic one pot reaction, where X=C, N or O*

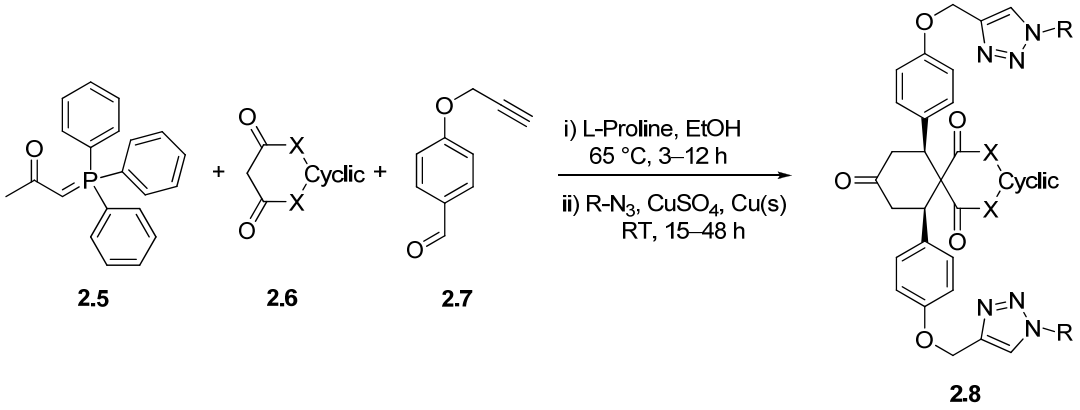

Scheme 2.3 *Six component multicatalytic one pot reaction*

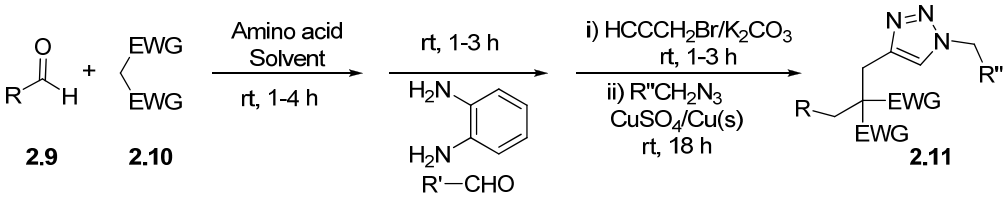

This work has also been further developed by Ramachary and Reddy,[16] in which a six component multicatalytic reaction using Knoevenagel condensation, hydrogenation, alkylation, and click chemistry was utilized to afford the product (**2.11**) in a 90% yield (Scheme 2.3).

Akritopoulou-Zanze *et al.* demonstrated that the combination of the Ugi multicomponent reaction with the intramolecular azide-alkyne cyclization provides access to unique fused triazole ring systems.[17] (Scheme 2.4)

Scheme 2.4 *synthesis of fused triazolo derivatives by sequential Ugi/alkyne-azide cycloaddition reactions*

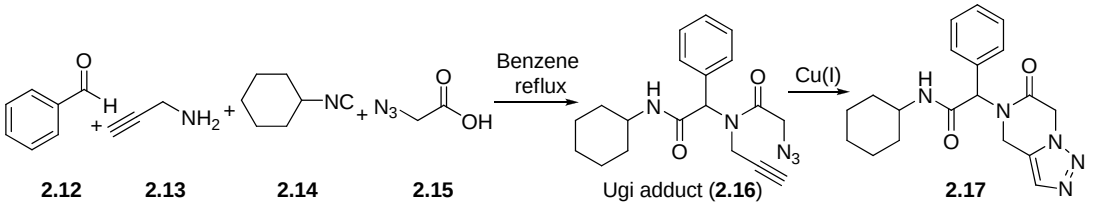

Chandrasekhar *et al.*[18] demonstrated that acetylated Baylis-Hillman adducts (**2.18**) undergo smooth three component coupling with sodium azide and terminal alkynes in one pot to furnish the diverse multifunctional 1,4-disubstituted triazoles. (Scheme 2.5)

Scheme 2.5 *One pot synthesis of 1,4-disubstituted-1,2,3-triazoles using Baylis-Hillmann adducts*

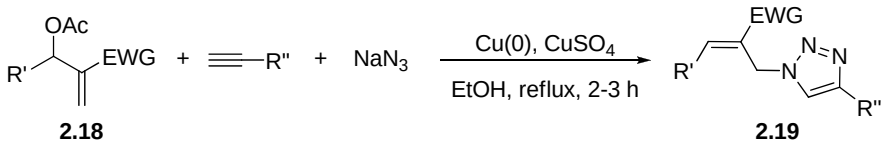

Smietana *et al.* developed one pot procedure for the conversion of a variety of aldehydes into 1,2,3-triazole-bridged conjugates through a sequential Seyferth-Gilbert/CuAAC combination.[19] The method is very useful for the synthesis of glyco-, peptido and nucleosido-bioconjugates, and is tolerant to a wide range of functional groups. Moreover, the first preparation of fluorescent triazolylaryl boronates from commercially available formyl boronic acid (**2.20**) was reported. These compounds could be of interest as fluorescent sensors for the carbohydrates. (Scheme 2.6)

Scheme 2.6 *One pot synthesis of 1,2,3-triazoles from aldehydes via in situ generated alkynes*

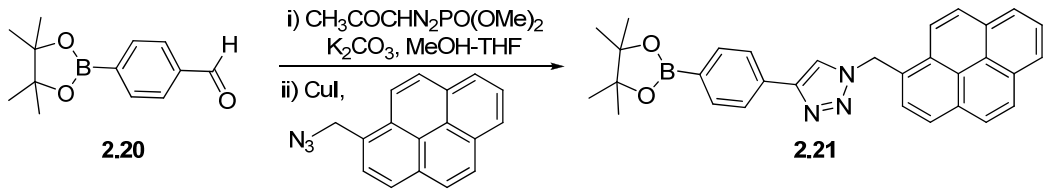

Fletcher and coworkers developed regioselective formation of 1-substituted-1,2,3-triazoles using a two step one pot TMS deprotection/click synthetic approach.[20] (Scheme 2.7)

Scheme 2.7 *Two step one pot deprotection/click additions of trimethylsilylacetylene*

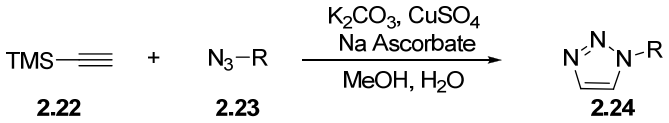

2.22 **2.23** **2.24**

Yadav *et al.* have described a direct and efficient protocol for the preparation of β-hydroxytriazoles via a three component reaction of an epoxide (**2.15**), sodium azide and an alkyne.[21] (Scheme 2.8)

Scheme 2.8 *One pot synthesis of β-hydroxytriazoles from epoxides via 'click reactions*

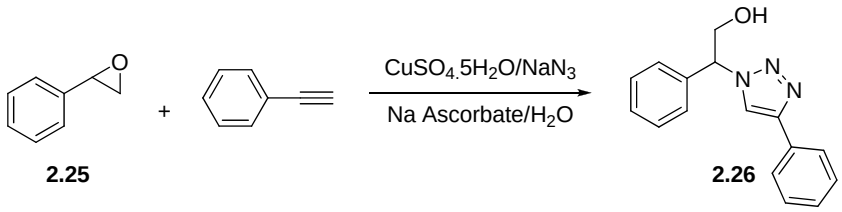

2.25 **2.26**

Moses *et al.* developed a simple and highly efficient procedure for the conversion of aromatic amines (**2.27**) into their corresponding azides, (**2.28**) under very mild conditions, and Cu(I)-catalyzed azide-alkyne 1,3-dipolar cycloaddition ("click reaction") in one pot.[22] (Scheme 2.9)

Scheme 2.9 *Efficient conversion of aromatic amines into azides: A one pot synthesis of triazole linkages*

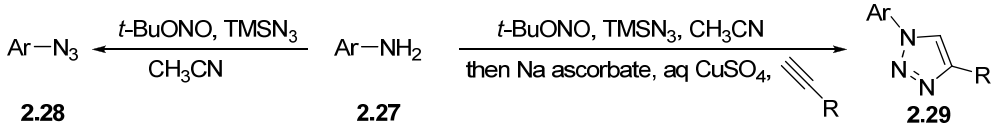

2.28 **2.27** **2.29**

Wittmann *et al.* at developed sequential one pot procedures for diazo transfer and azide alkyne cycloaddition giving access to triazoles commencing with amines being commercially available in a great variety.[23] (Scheme 2.10)

Scheme 2.10 *Sequential one pot procedure in toluene, isopropyl alcohol, and water*

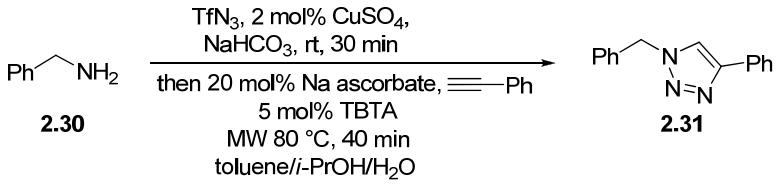

Microwave enhanced, fast, and efficient three component reaction for generation of 1,4-disubstituted- 1,2,3-triazoles in a completely regioselective manner has been developed by Fokin *et al.*[24] The method avoids isolation and handling of potentially unstable small organic azides and provides triazole products in pure form. (Scheme 2.11) Microwave irradiation dramatically decreases reaction time from hours to minutes. 1,2,3-Triazole products often crystallize from the reaction mixture and do not require any purification, rendering the process an ideal multicomponent click reaction.

Scheme 2.11 *Microwave assisted three component synthesis of 1,4-disubstituted 1,2,3-triazoles*

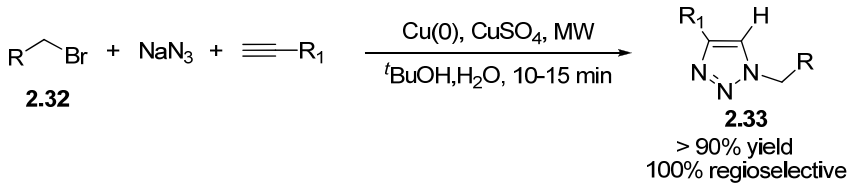

Scheme 2.12 One pot synthesis of 1,2,3-triazoles from alkyl/aryl/vinyl iodides, NaN_3, and alkynes

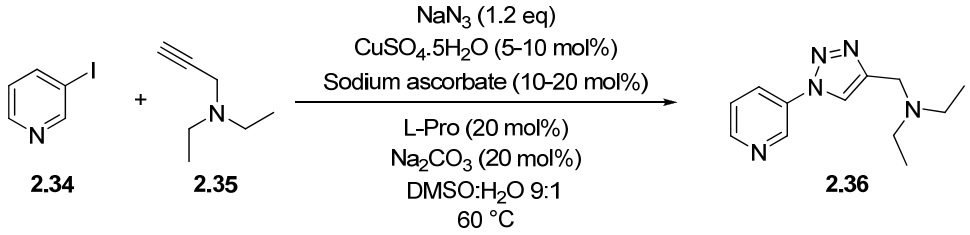

Further screening a variety of copper sources, ligands, and solvent combinations, Fokin *et al.* arrived at the experimentally simple and safe general procedure for one pot two step process.[25] Under the optimized conditions, the triazole products are obtained in

good yields, and formation of the undesired N-H triazole byproducts is suppressed. The regioselectivity of the reaction is maintained even at the elevated temperatures. (Scheme 2.12)

Recently Ackermann *et al.* developed inexpensive copper catalysts enabled modular one pot multicomponent syntheses of fully decorated triazoles through a sustainable "click" reaction/direct arylation sequence.[26] (Scheme 2.13)

Scheme 2.13 *Sequential copper catalyzed four component synthesis*

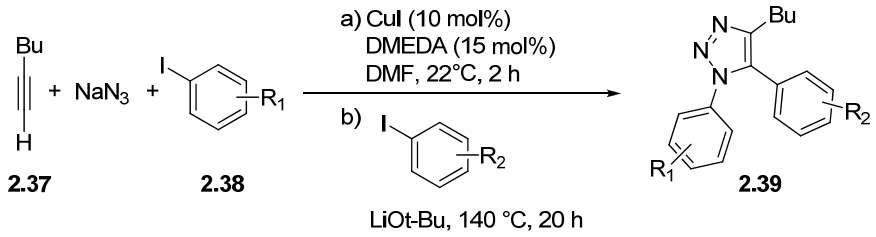

2.2 PRESENT WORK

The nucleophilic substitution reaction (S_NAr) of activated aryl halides is an important transformation for C−C and C−hetero atom bond formation with aryl rings.[27] These reactions are facilitated by the presence of –M groups like a nitro or a carbonyl ortho or para to the leaving group in general and with meta isomers in some rare cases.[28] Various carbon and hetero atom nucleophiles have been employed in this context.[29] Reports concerning the azide as a nucleophile in S_NAr were mainly limited to the mechanistic investigations.[30]

Multicomponent reactions (MCRs) are reactions where three or more substrates combine in one step to give a product that contains essential parts of all of them. The combination of a classical multicomponent reaction with a classical organic transformation has been shown by many to be a powerful strategy to yield complex structures in few synthetic steps. The potential of click reactions can be further amplified by combining it with multicomponent reactions.

Inspired with the broad spectrum application of Cu(I)-catalyzed 1,3-cycloaddition between an azide and an alkyne in the discovery of drugs and materials, and less reports concerning the azide as a nucleophile in S_NAr reaction, we have initiated a program to design a methodology in which these two reactions occur in one pot.

Initially, the S_NAr of 2-, 3- and 4-nitrofluorobenzenes (**2.40**–**2.42**) with NaN_3 and phenyl acetylene (**2.43**) as the dipolarophile was attempted in absence of any additives. DMSO has been selected as a solvent considering the dependence of rate of S_NAr reactions on the solvent employed. Parker and Cox have studied the effects of solvent transfer on free energies, enthalpies, and entropies of activation of an aromatic nucleophilic substitution (S_NAr) reaction. Authors found that hexamethylphosphoramide (HMPA) and DMSO are the excellent solvents for S_NAr reactions.[31]

Recently Jorgensen *et al.* have investigated the nucleophilic aromatic substitution (S_NAr) reaction between azide ion and 4-fluoronitrobenzene using QM/MM and DFT/PCM calculations in protic and dipolar aprotic solvents. They found that large rate increases in proceeding from protic to dipolar aprotic solvents is only reproduced by the QM/MM methodology.[32]

Scheme 2.14 *Optimization of one-pot S_NAR with azide and azide-alkyne cycloaddition of isomeric nitrofluorobenzenes*

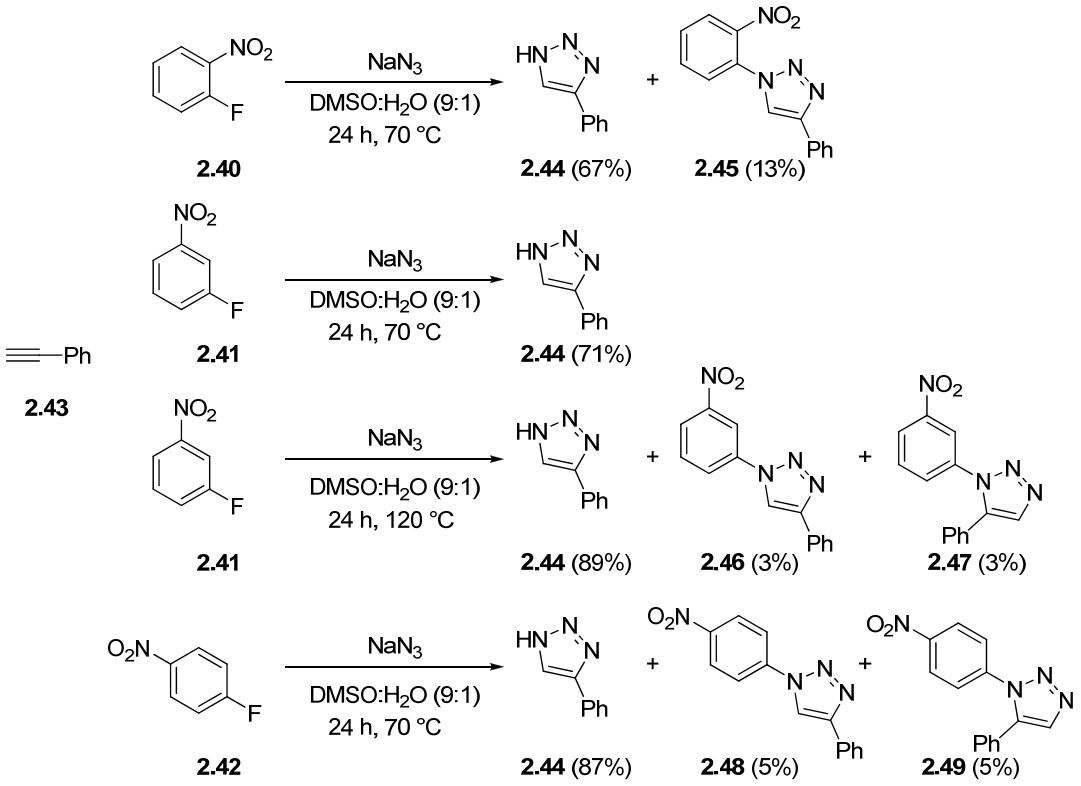

The reactions (Scheme 2.14) were sluggish (heated at 70 ^oC for 24 h) and resulted in products with poor yields. The major product isolated was cycloadduct of phenyl acetylene with sodium azide (4-phenyl-1*H*-1,2,3-triazole, **2.44**). The ^1H NMR spectrum of it revealed the aromatic N-H proton resonated at δ 12.4 ppm whereas the proton in triazole ring resonated as a singlet at δ 8.0. ppm Further mass spectra shows (*m/z*) at 168.3 $[M+Na]^+$ which confirms its structure. In case of 2-nitrofluorobenzene (**2.40**) we could isolate 1,4-diaryltriazole (**2.45**) in only 13% yield. The ^1H NMR spectrum of it revealed the proton in triazole ring resonated as a singlet at δ 9.2 ppm. ^{13}C NMR spectrum shows most deshielded peak at 147.1 ppm indicating carbon attached with nitro group. It also showed peaks at 129.8, 131.3, 144.0 indicating quarternary carbons accordingly to the assigned structure.

The S_NAr of *m*-isomer **2.41**, gave exclusively **2.44** when the reaction was conducted at 70 ^oC, and when heated at 120 ^oC, a 1:1 mixture of 1,4- and 1,5-diaryl

triazoles **2.46** and **2.47** was isolated in 6% yield. The ^{1}H NMR spectrum of **2.46** revealed the proton in triazole ring resonated as a singlet at δ 8.32 ppm. Whereas ^{1}H NMR spectrum of 1,5-diaryl triazoles (**2.47**) revealed the proton in triazole ring resonated as a singlet at δ 7.87 ppm. The constitution of 1-(3-nitrophenyl)-5-phenyl-1*H*-1,2,3-triazole (**2.47**) was further confirmed by single crystal X-ray structural analysis (Figure 2.4).

Figure 2.4 *The molecular structure of compound **2.47** (displacement ellipsoids are drawn at the 50% probability level)*

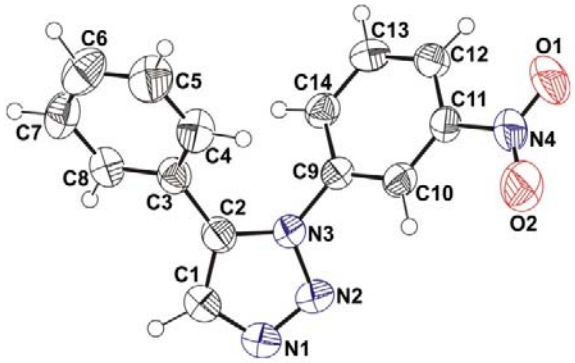

In case of 4-nitrofluorobenzene (**2.42**), after 2 days at 70 ^{o}C, a 1:1 mixture of 1,4-disubstituted-triazole **2.48** and 1,5-disubstituted-triazole **2.49** in 10% yield was obtained. The ^{1}H NMR spectrum of **2.48** revealed the proton in triazole ring resonated as a singlet at δ 9.48 ppm as most deshielded peak. Whereas ^{1}H NMR spectrum of 1,5-diaryl triazoles (**2.49**) revealed the proton in triazole ring resonated as a singlet at δ 7.86 ppm.

The yields and the regioselectivity dramatically improved when the reactions were carried out under standard "Click Reaction" conditions.[25] In case of 1-fluoro-2-nitrobenzene (**2.40**) the yield increased from 13% to 79%. The substrate 1-fluoro-3-nitrobenzene (**2.41**) was difficult to substitute even under harsh conditions and yielded regioselectively 1-(3-nitrophenyl)-4-phenyl-1*H*-1,2,3-triazole (**2.46**) in 11% yield. The one-pot "S_NAr-click reaction" of 1-fluoro-4-nitrobenzene (**2.42**) was slow and took nearly 2 days for completion and gave exclusively 1,4-isomer **2.48** in 75% yield. (Scheme 2.15)

Scheme 2.15 *One-pot S_NAr with azide and azide-alkyne cycloaddition of isomeric nitrofluorobenzenes*

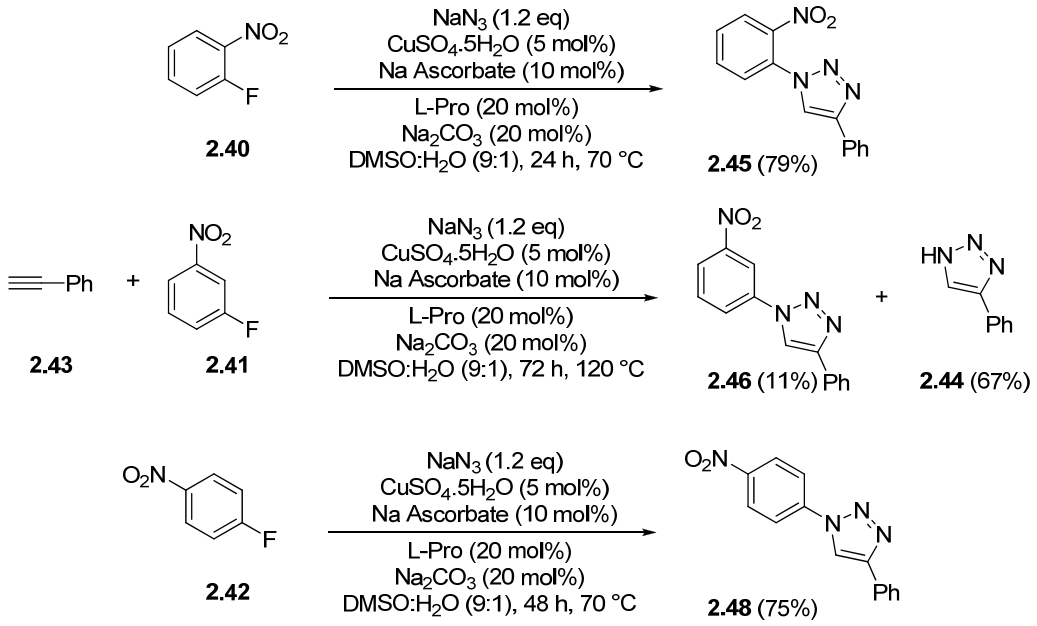

Scheme 2.16 *Control experiments to determine reaction pathway*

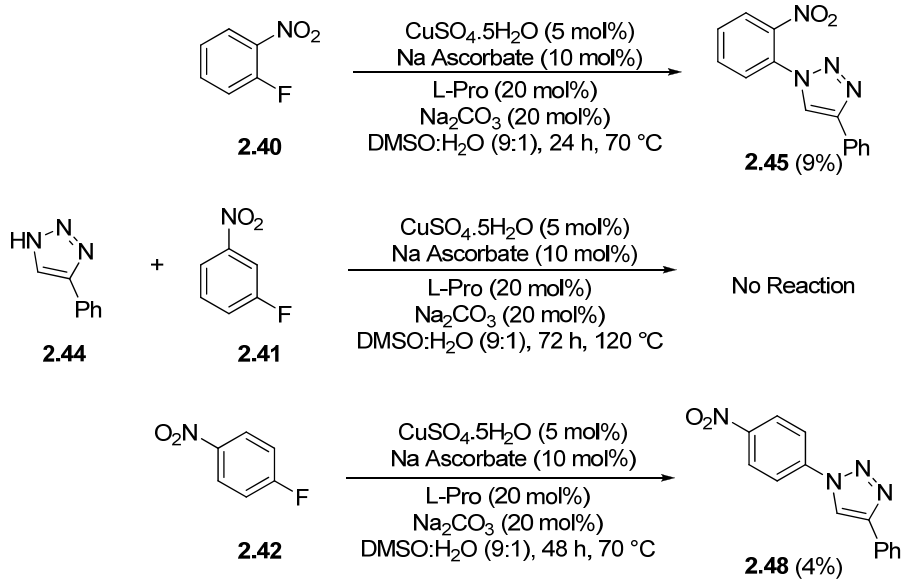

As a control, the S_NAr of fluoronitrobenzenes **2.40**–**2.42** were carried out with the triazole **2.44** (Scheme 2.16) under the similar conditions. The reactions in general were

sluggish and resulted in poor yields revealing the activation of S_NAr by Cu(I) catalyst and also that the sequence of reactions as S_NAr followed by cycloaddition.

To obtain more information about the role of Cu(I) catalyst on S_NAr, the azide displacement reactions of **2.40**–**2.42** were carried out under click conditions at room temperatures. The reactions were smooth and took 6 h (**2.40**) and 12 h (**2.42**) and provided the corresponding azido benzenes (**2.50** & **2.51**) in 79% and 91% respectively. With **2.41**, starting compound remained unchanged even at 60 °C. (Scheme 2.17)

Scheme 2.17 *Cu(I) catalysed azidation of isomeric nitrofluorobenzenes at RT*

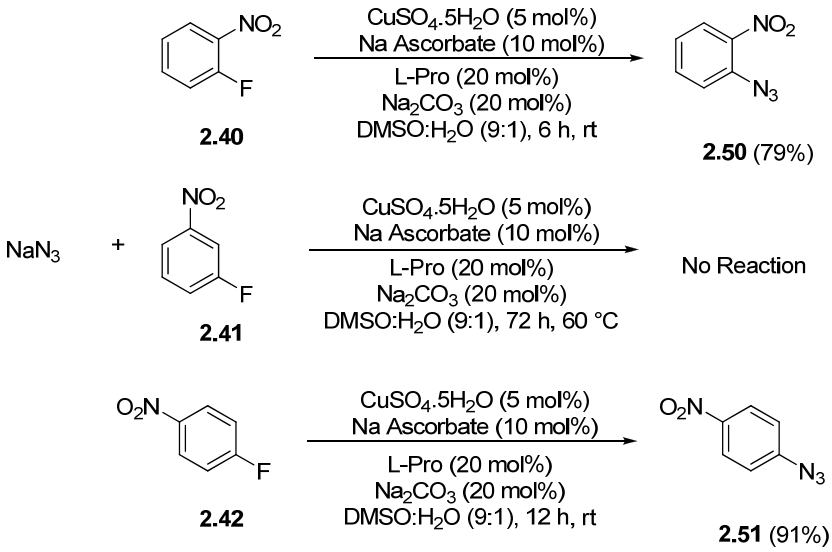

Scheme 2.18 *Uncatalysed azidation of isomeric nitrofluorobenzenes at 60 °C*

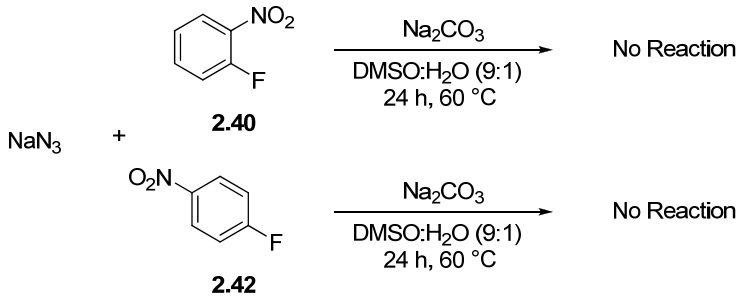

As expected, the azide displacement reactions of **2.40** and **2.42** without any additives were not facile and starting compounds remain unchanged even after prolonged heating, Thus, the room temperature azido displacements of **2.40** and **2.42** under click

reaction conditions revealed a significant role of Cu(I) catalyst over these reactions. (Scheme 2.18)

The reaction is even applicable for chloro displacement, as in case of 1-chloro-2-nitrobenzene (**2.52**). The spectral and analytical data was identical with the earlier synthesised **2.45**. With the less activated 2-fluorobenzaldehyde (**2.53**), the S_NAr reaction was sluggish and the corresponding 1,4-diaryltriazole **2.54** was obtained in poor yield.

Scheme 2.19 *Compatibility of other leaving groups in one-pot "S_NAr-click reaction"*

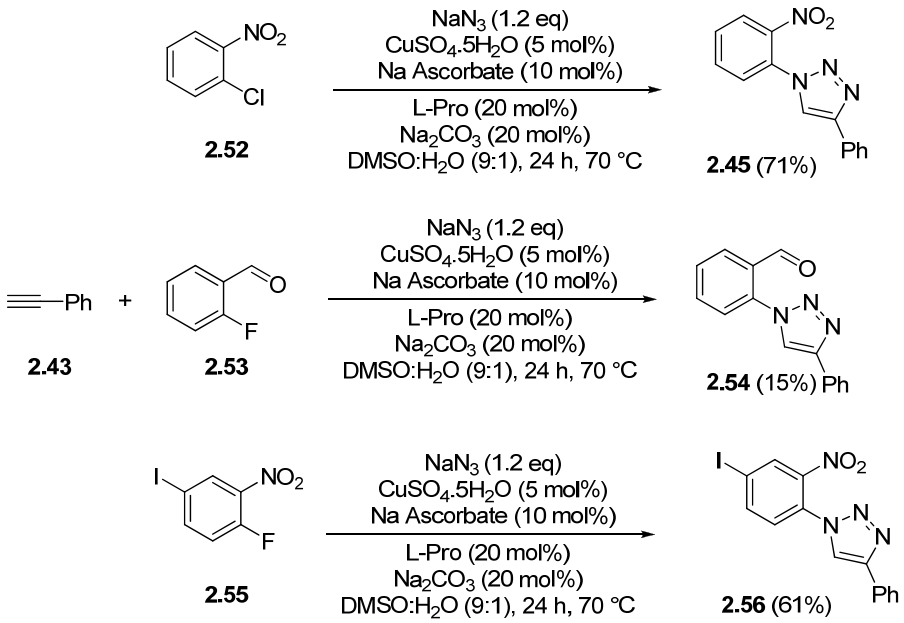

The 1-fluoro-4-iodo-2-nitrobenzene (**2.55**) has been employed as a substrate to find out the compatibility of other leaving groups and found that fluorine was displaced selectively leaving the iodo group intact yielding triazoles **2.56** in 61% yield. (Scheme 2.19) The ^1H NMR spectrum of **2.56** revealed the proton in triazole ring resonated as a singlet at δ 8.80 whereas the proton ortho to nitro group attached resonated at δ 8.33 ppm. ^{13}C NMR spectrum shows peaks at 93.6, 127.4, 128.2, 142.5, 146.0 indicating quarternary carbons accordingly to the assigned structure. The structures of **2.56** was further confirmed by single crystal X-ray structural analysis (Figure 2.5)

The one-pot "S_NAr-click reaction" of 2-nitrofluorobenzene (**2.40**) have been generalized by employing various functionalized terminal alkynes which include the nitroaryl alkynes such as **2.57**, **2.58**, isomeric bromoaryl alkynes such as **2.59–2.61**,

heteroaryl alkyne (**2.62**). The reactions are smooth and resulted exclusively with 1,4-disubstituted-1,2,3-triazoles **2.69–2.74** in 57–71% yield. (Table 2.1)

Figure 2.5 *The molecular structure of compound* ***2.56***

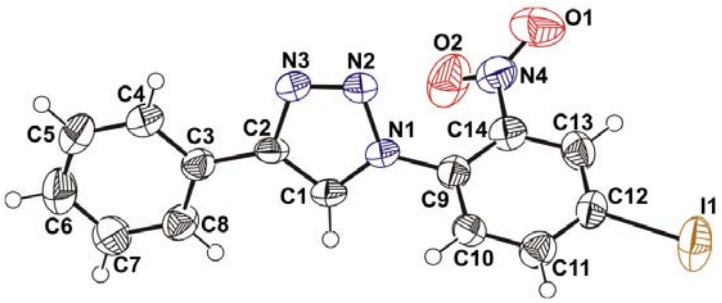

In the ^{1}H NMR spectrum of **2.69** triazole-H ring resonated as a singlet at δ 9.15 ppm. The structure of **2.69** was further confirmed by ESI-MS (*m/z*) peaks at 312.20 $(M+H)^{+}$, 334.17 $(M+Na)^{+}$. In case of isomeric bromo nitro triazoles **2.70–2.72** the proton in triazole ring resonated as a singlet at δ 9.45, 8.56 and 8.04 ppm respectively in ^{1}H NMR spectrum. ^{13}C NMR spectrum showed five quaternary carbons in all the three isomeric triazoles. Further mass spectra confirmed the assigned structures. In case of heteroaryl triazoles **2.73** the proton in triazole ring resonated as a singlet at δ 8.68 and methylene CH_2 resonated at 4.95 (2H) ppm in ^{1}H NMR spectrum. Further ^{13}C NMR spectrum showed peaks of both coupling partners i.e. nitro group containing aromatic ring, heteroaromatic ring along with triazoles ring.

Other various functionalized terminal alkynes such as aliphatic alkynes (**2.63**, **2.64**), long chain aliphatic alkyne[33] (**2.65**) and various sugar derived alkynes (**2.66–2.68**) have been utilized for one-pot "S_NAr-click reaction" of 2-nitrofluorobenzene (**2.40**). The reactions are smooth and resulted exclusively with 1,4-disubstituted-1,2,3-triazoles **2.75–2.82** in 65–78% yield. (Table 2.2)

Table 2.1 *One pot "S_NAr-click reaction" of* ***2.40*** *employing functionalized alkynes* ***2.57–2.62***

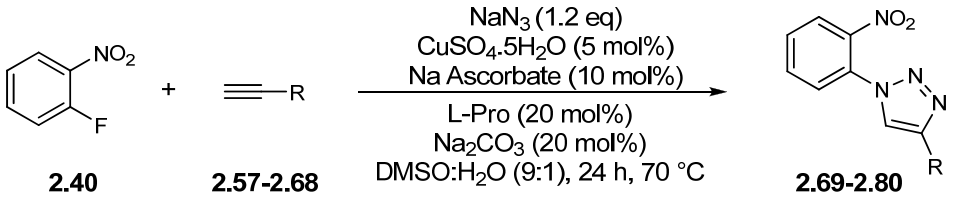

2.40 **2.57-2.68** **2.69-2.80**

Entry	Alkyne	Product	Yield
1	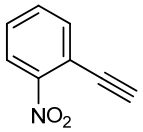 **2.57**	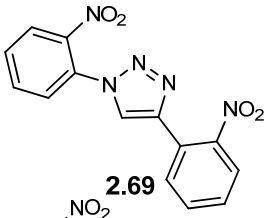 **2.69**	61%
2	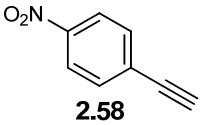 **2.58**	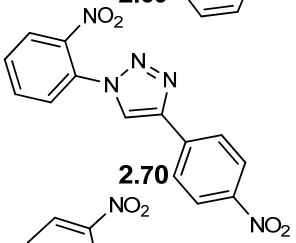 **2.70**	64%
3	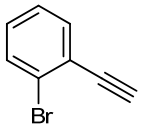 **2.59**	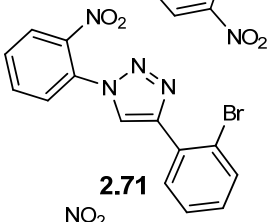 **2.71**	65%
4	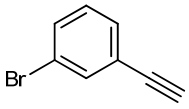 **2.60**	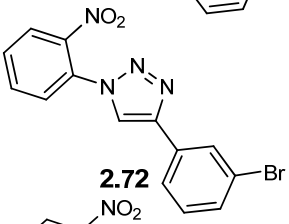 **2.72**	71%
5	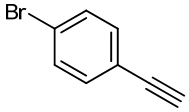 **2.61**	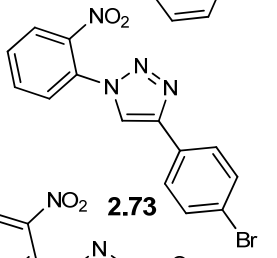 **2.73**	57%
6	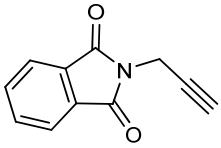 **2.62**	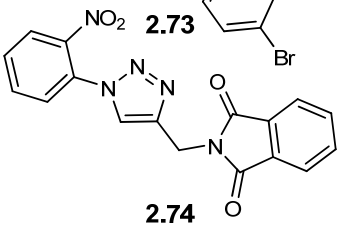 **2.74**	68%

Table 2.2 *One pot "S_NAr-click reaction" of* ***2.40*** *employing functionalized alkynes* ***2.63–2.68***

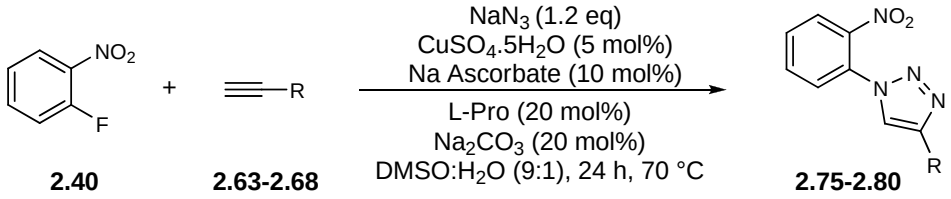

2.40 **2.63-2.68** **2.75-2.80**

Entry	Alkyne	Product	Yield
1	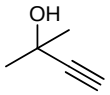 **2.63**	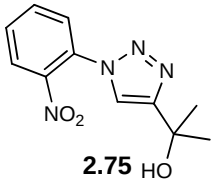 **2.75**	73%
2	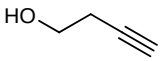 **2.64**	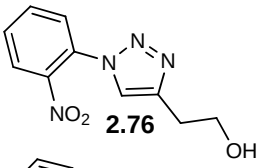 **2.76**	71%
3	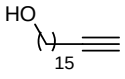 **2.65**	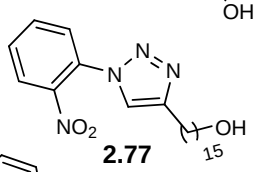 **2.77**	79%
4	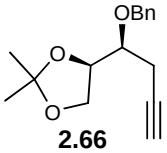 **2.66**	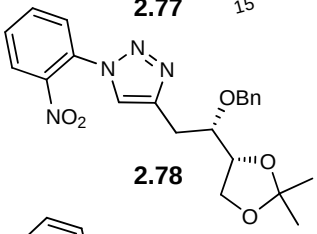 **2.78**	65%
5	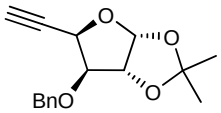 **2.67**	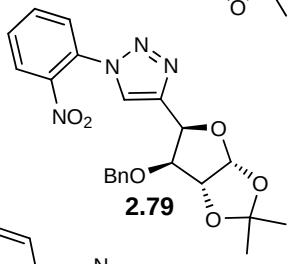 **2.79**	71%
6	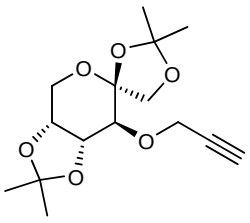 **2.68**	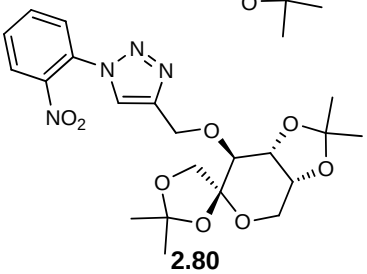 **2.80**	78%

The ^{1}H NMR spectrum of **2.75** revealed the proton in triazole ring resonated as a singlet at δ 8.45 ppm. ^{13}C NMR spectrum showed peaks at 67.2, 129.4, 144.2, 156.8 ppm indicating pressence of four quarternary carbons and peaks at 121.9, 125.5, 127.2, 130.8, 134.3 ppm indicates pressence of five C-H carbons, 30.7 (2C) indicated pressence of two methyl groups, according to the assigned structure. The structure was further confirmed by ESI-MS (*m/z*) peaks at 249.21 $(M+H)^+$, 271.20 $(M+Na)^+$. In case of other aliphatic alkyne (**2.64**) the resulted 1,4 triazole (**2.76**), the proton in triazole ring resonated as a singlet at δ 8.43, the two methylenes resonated at 2.88 (t, *J* = 6.9 Hz, 2H), 3.67–3.75 (m, 2H) ppm respectively in ^{1}H NMR spectrum. ^{13}C NMR spectrum showed peaks at 129.4, 144.2, 145.7 ppm indicating pressence of three quarternary carbons and peaks at 123.8, 125.5, 127.2, 130.9, 134.3 ppm indicates pressence of five methylidine carbons, whereas peaks at 29.1, 60.3 indicated pressence of two CH_2 groups, according to the assigned structure. The structure was further confirmed by ESI-MS (*m/z*) peaks at 235.20 $(M+H)^+$, 257.19 $(M+Na)^+$. In case of long aliphatic chain triazole **2.77** the proton in triazole ring resonated as a singlet at δ 8.42 ppm in ^{1}H NMR spectrum. Further ^{13}C NMR spectrum showed peaks of both coupling partners i.e. nitro group containing aromatic ring, aliphatic long chain along with triazoles ring.

The spectral and analytical data was consistent with the sugar derived 1,4 triazoles. Mannitol derived alkyne **2.66** yielded regioselectively 1,4 triazole **2.78** in 65%. The ^{1}H NMR spectrum of it revealed the proton of triazole ring resonated as a singlet at δ 7.65 ppm. ^{13}C NMR spectrum show peaks at 129.6, 137.7, 143.9, 144.2 ppm indicating pressence of four quarternary carbons according to the assigned structure. The structure was further confirmed by ESI-MS (*m/z*) peaks at 425.6 $(M+H)^+$, 447.6 $(M+Na)^+$. In case of glucose derive alkyne **2.67** yield of it's 1,4 triazole derivative **2.79** was 71%. In ^{1}H NMR spectrum, proton of triazole ring resonated as a singlet at δ 7.96 ppm. ^{13}C NMR spectrum showed five quaternary carbons and further mass spectra confirmed the assigned structure. Similarly the assigned structure of fructose derived triazole **2.80** was confirmed by spectral and analytical data.

The one-pot "S_NAr-click reaction" of 4-nitrofluorobenzene (**2.42**) have also been generalized by employing various functionalized terminal alkynes such as isomeric bromoaryl alkynes such as **2.59–2.61**, heteroaryl alkyne (**2.62**). The reactions are smooth

and resulted exclusively with 1,4-disubstituted-1,2,3-triazoles **2.69–2.74** in 61–81% yield. (Table 2.3)

Table 2.3 *One pot "S_NAr-click reaction" of **2.42** employing functionalized alkynes*

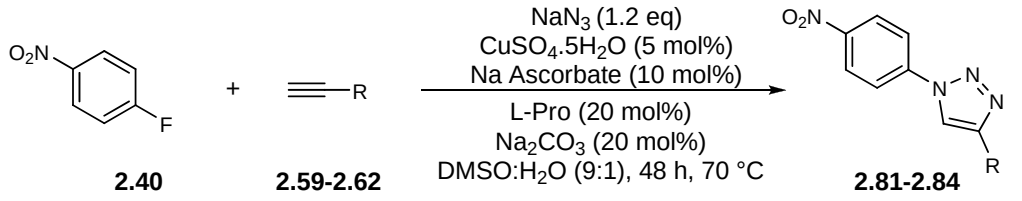

2.40 **2.59-2.62** **2.81-2.84**

Entry	Alkyne	Product	Yield
1	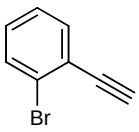 **2.59**	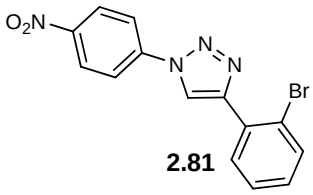 **2.81**	83%
2	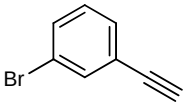 **2.60**	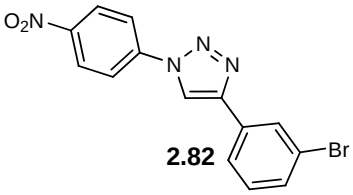 **2.82**	81%
3	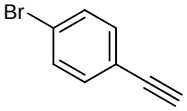 **2.61**	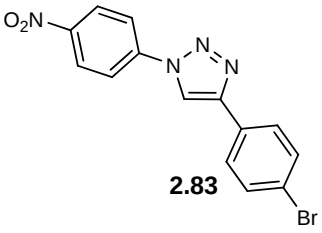 **2.83**	81%
4	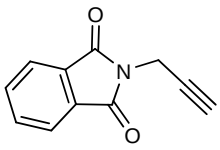 **2.62**	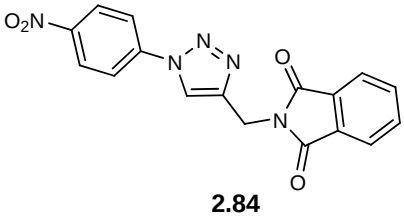 **2.84**	61%

^{1}H NMR spectrum of isomeric bromo nitro triazoles **2.81–2.84** the proton in triazole ring resonated as a singlet at δ 8.79, 9.47 and 8.48 ppm respectively. ^{13}C NMR spectrum showed five quaternary carbons in all the three isomeric triazoles. Further mass spectra confirmed the assigned structures. In case of heteroaryl triazoles **2.85** the proton in triazole ring resonated as a singlet at δ 9.00 and methylene CH_2 resonated at 4.95 (2H)

ppm in ^{1}H NMR spectrum. Further ^{13}C NMR spectrum showed peaks of both coupling partners i.e. nitro group containing aromatic ring, heteroaromatic ring along with triazoles ring.

Table 2.4 *One pot "S_NAr-click reaction" of* ***2.42*** *employing functionalized alkynes*

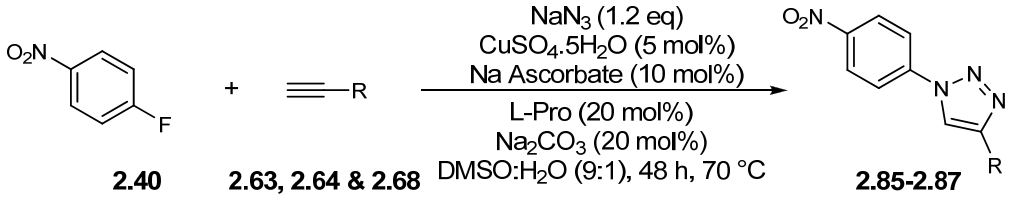

2.40 **2.63, 2.64 & 2.68** **2.85-2.87**

Entry	Alkyne	Product	Yield
5	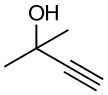 **2.63**	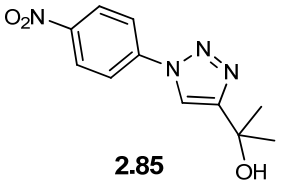 **2.85**	63%
6	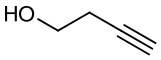 **2.64**	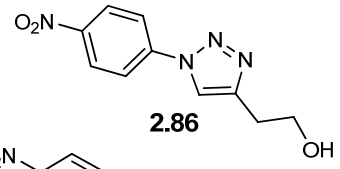 **2.86**	61%
7	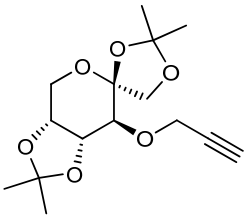 **2.68**	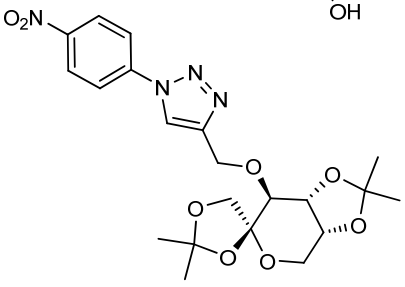 **2.87**	71%

Functionalized terminal alkynes such as aliphatic alkynes (**2.63**, **2.64**) and sugar derived alkyne (**2.68**) have been also utilized for one-pot "S_NAr-click reaction" with 4-nitrofluorobenzene (**2.42**). The reactions are smooth and resulted exclusively with 1,4-disubstituted-1,2,3-triazoles **2.85–2.87** in 61–71% yield. (Table 2.4)

The structures of **2.85** was further confirmed by single crystal X-ray structural analysis (Figure 2.6)

Figure 2.6 *The molecular structure of compound* ***2.85*** *(displacement ellipsoids are drawn at the 50% probability level)*

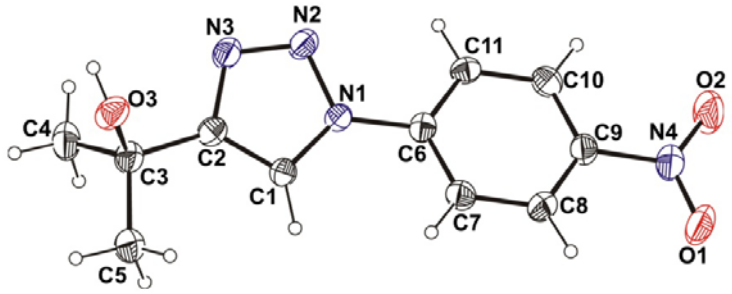

To conclude, a three component one-pot "S_NAr-click reaction" has been explored by employing *o*- and *p*-nitrofluorobenezenes and a diverse set of alkynes. Control experiments reveal the course of the reaction as S_NAr with azide nucleophile followed by the cycloaddition of the resulting nitroazidobenzene intermediate and both the reactions being catalyzed by Cu(I). The reactions are generally regioselective and various commonly employed protecting groups are found to be compatible with the conditions employed.

2.3 Experimental

2.3.1 General Procedure A (products precipitate from the reaction mixture)

Fluoronitrobenzene (100 mg, 0.71 mmol) was mixed with phenyl acetylene (72 mg, 0.71 mmol) in 9:1 DMSO:H_2O (10 ml). To the mixture were added L–Proline (16 mg, 0.142 mmol), Na_2CO_3 (15 mg, 0.142 mmol), NaN_3 (55 mg, 0.852 mmol), sodium ascorbate (14 mg, 0.071 mmol), and $CuSO_4.5H_2O$ (9 mg, 0.036 mmol). The mixture was stirred for 24–48 h at 70 °C (bath temperature) and then the mixture was poured into 30 ml of ice–cold water. The solid residue was filtered and crystallized from appropriate solvent systems to procure white to yellow crystalline solids in (57–83%) yield.

2.3.2 General Procedure B (**2.45**, **2.47**, **2.49**, **2.71**, **2.76**, **2.78**, **2.79**, **2.80, 2.81, 2.87: products purified by column chromatography)**

The reactions were carried out as described above and after completion, the contents were poured into 30 ml of water and combined water layer was thoroughly extracted with ethyl acetate (3 x 25 ml). Organic layer was dried over sodium sulphate and concentrated under reduced pressure. The crude solid was purified by column chromatography over 60–120 silica gel using ethyl acetate–light petroleum (1:4) to obtain white to yellow solids (65–77%).

1-(2-Nitrophenyl)-4-phenyl-1*H*-1,2,3-triazole[34] (2.45)

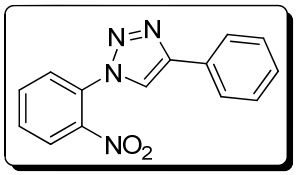

Mol. Formula	: $C_{14}H_{10}N_4O_2$
M. P.	: 140–141 °C (lit. 144–145 °C).
IR (Nujol) $\tilde{\nu}$	: 3143, 2725, 1641, 1605 1526, 1507, 1462, 1376, 1356, 1227 cm^{-1}.
^{1}H NMR (DMSO-d_6, 500 MHz)	: δ 7.40 (tt, *J* = 1.2, 7.3 Hz, 1H), 7.49–7.53 (m, 2H), 7.87 (ddd, *J* = 2.2, 7.1, 9.1 Hz, 1H), 7.94–7.97 (m, 2H), 7.98–8.02 (m, 2H), 7.87 (dd, *J* = 1.0, 8.1 Hz, 1H), 9.20 (s, 1H) ppm.
^{13}C NMR (DMSO-d_6, 125	: δ 120.7 (d), 125.4 (d, 2C), 125.6 (d), 127.4 (d), 128.5 (d), 129.1 (d, 3C), 129.8 (s), 131.3 (s), 134.5 (d), 144.0 (s), 147.1

MHz)	(s) ppm.
ESI-MS (*m/z*)	: 267.15 $(M+H)^+$, 289.14 $(M+Na)^+$.
Elemental Analysis	Calcd.: C, 63.15; H, 3.79.
	Found: C, 63.18; H, 3.80.

1-(3-Nitrophenyl)-4-phenyl-1*H*-1,2,3-triazole[35] (2.46)

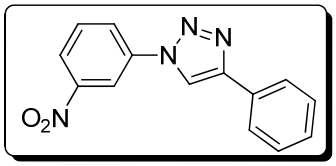

Mol. Formula	: $C_{14}H_{10}N_4O_2$
M. P.	: 204–205 °C (lit. 198–200 °C).
^{1}H NMR ($CDCl_3$, 200 MHz)	: δ 7.41–7.54 (m, 3H), 7.78 (t, *J* = 8.21 Hz, 1H), 7.91–7.96 (m, 2H), 8.25–8.36 (m, 2H), 8.32 (s, 1H), 8.66 (t, *J* = 2.15 Hz, 1H) ppm.
^{13}C NMR (DMSO-d_6, 50 MHz)	: δ 115.0 (d), 120.4 (d), 123.5 (d), 125.8 (d, 2C), 126.3 (d), 128.9 (d), 129.5 (d, 2C), 130.2 (s), 132.0 (d), 137.5 (s), 148.1 (s), 148.9 (s) ppm.
ESI–MS (*m/z*)	: 289.3 $(M+Na)^+$.
Elemental Analysis	Calcd.: C, 63.15; H, 3.79; N, 21.04.
	Found: C, 63.11; H, 3.73; N, 20.97.

1-(3-Nitrophenyl)-5-phenyl-1*H*-1,2,3-triazole[36] (2.47)

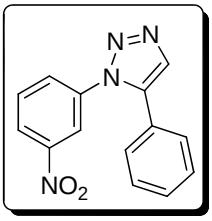

Crystal data: X–ray intensity data was collected on a Bruker SMART APEX CCD diffractometer with omega and phi scan mode, $\lambda_{MoK\alpha}$ = 0.71073 Å at T = 297(2) K. All the data were corrected for Lorentzian, polarisation and absorption effects using Bruker's SAINT and SADABS programs. The crystal structures were solved by direct method using SHELXS–97 and the refinement was performed by full matrix least squares of F^2 using SHELXL–97 (G. M. Sheldrick, SHELX–97 program for crystal structure solution and refinement, Unversity of Göttingen, Göttingen, Germany, 1997). Hydrogen atoms were included in the refinement as per the riding model. *Crystal data for* **4ba**

($C_{14}H_{10}N_4O_2$): M = 266.26, crystal dimensions 0.62 x 0.23 x 0.01 mm^3, Monoclinic, space group $P2_1/n$, a = 7.533(11), b = 18.94(3), c = 9.546(14) Å, β = 98.37(3)°, V = 1347(3) $Å^3$, Z = 4; ρ_{calcd} = 1.313 gcm^{-3}, μ (Mo-K_α) = 0.092 mm^{-1}, *F(000)* = 552, T = 297(2) K, $2\theta_{max}$ = 50.00°, 6348 reflections collected, 2346 unique, 1322 observed ($I > 2\sigma(I)$) reflections, 221 refined parameters, R value 0.0542, $wR2$ = 0.1111 (all data R = 0.1090, $wR2$ = 0.1366), S = 1.002, minimum and maximum transmission 0.9450 and 0.9991 respectively, maximum and minimum residual electron densities +0.216and –0.169 e $Å^{-3}$.

Mol. Formula	: $C_{14}H_{10}N_4O_2$
M. P.	: 133–134 °C.
^{1}H NMR ($CDCl_3$, 200 MHz)	: δ 7.21–7.26 (m, 2H), 7.37–7.43 (m, 3H), 7.58–7.66 (m, 1H), 7.71 (td, J = 1.8, 8.2 Hz, 1H), 7.87 (s, 1H), 8.28–8.32 (m, 2H) ppm.
^{13}C NMR ($CDCl_3$, 125 MHz)	: δ 120.1 (d), 123.7 (d), 126.1 (d), 128.8 (d, 2C), 129.3 (d, 2C), 130.0 (d), 130.3 (d), 130.4 (d), 133.9 (s), 137.6 (s), 137.9 (s), 148.7 (s) ppm.
ESI–MS (*m/z*)	: 289.3 $(M+Na)^+$.
Elemental Analysis	Calcd.: C, 63.15; H, 3.79; N, 21.04. Found: C, 63.21; H, 3.75; N, 20.97.

1-(4-Nitrophenyl)-4-phenyl-1*H*-1,2,3-triazole[37] (2.48)

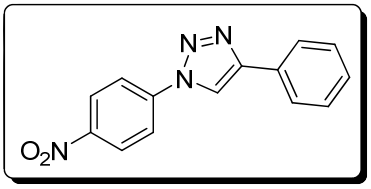

Mol. Formula	: $C_{14}H_{10}N_4O_2$
M. P.	: 236–238 °C.
IR ($CHCl_3$) $\tilde{\nu}$	: 3018, 2925, 2855, 1598, 1521, 1348, 1215, 855, 759 cm^{-1}.
^{1}H NMR (DMSO-d_6, 200 MHz)	: δ 7.41–7.56 (m, 3H), 7.93–7.98 (m, 2H), 8.23–8.28 (m, 2H), 8.47–8.51 (m, 2H), 9.48 (s, 1H) ppm.
^{13}C NMR (DMSO-d_6, 125 MHz)	: δ 120.1 (d), 120.6 (d, 2C), 125.5 (d, 2C), 125.7 (d, 2C), 128.7 (d), 129.2 (d, 2C), 129.8 (s), 140.9 (s), 146.8 (s), 148.0 (s) ppm.

ESI–MS (*m/z*) : 267.14 $(M+H)^+$.

Elemental Analysis Calcd.: C, 63.15; H, 3.79; N, 21.04.
Found: C, 63.31; H, 3.53; N, 20.91.

1-(4-Nitrophenyl)-5-phenyl-1*H*-1,2,3-triazole[38] (2.49)

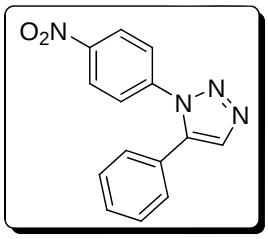

Mol. Formula : $C_{14}H_{10}N_4O_2$

M. P. : 165–166 °C.

IR ($CHCl_3$) $\tilde{\nu}$: 3018, 2925, 2855, 1598, 1521, 1348, 1215, 855, 759 cm^{-1}.

^{1}H NMR ($CDCl_3$, 200 MHz) : δ 7.21–7.26 (m, 2H), 7.36–7.46 (m, 3H), 7.54–7.61 (m, 2H), 7.86 (s, 1H), 8.26–8.34 (m, 2H) ppm.

^{13}C NMR (DMSO-d_6, 50 MHz) : δ 126.0 (d), 126.1 (d), 127.5 (d, 2C), 127.8 (d, 2C), 128.3 (d, 2C), 130.1 (d, 2C), 130.1 (s), 140.9 (s), 144.7 (s), 146.2 (s) ppm.

ESI–MS (*m/z*) : 267.4 $(M+H)^+$.

Elemental Analysis Calcd.: C, 63.15; H, 3.79; N, 21.04.
Found: C, 63.11; H, 3.73; N, 20.97.

2-(4-Phenyl-1*H*-1,2,3-triazol-1-yl)benzaldehyde (2.54)

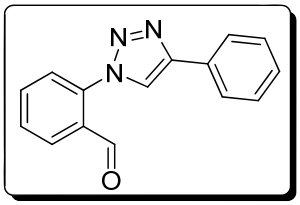

Mol. Formula : $C_{15}H_{11}N_3O$

IR (Nujol) $\tilde{\nu}$: 3017, 1696, 1601, 1456, 1216, 1024, 694, 667 cm^{-1}.

^{1}H NMR ($CDCl_3$, 500 MHz) : δ 7.39–7.49 (m, 3H), 7.58 (dd, *J* = 1.4, 7.8 Hz, 1H), 7.66–7.70 (m, 1H), 7.75–7.82 (m, 2H), 7.92–7.94 (m, 1H), 8.13 (dd, *J* = 1.6, 7.7 Hz, 1H), 8.19 (s, 1H), 9.99 (s, 1H) ppm.

^{13}C NMR ($CDCl_3$, 125 MHz) : δ 121.5 (d), 125.3 (d), 125.9 (d, 2C), 128.7 (d), 129.0 (d, 2C), 129.5 (s), 129.6 (d), 130.1 (d), 130.4 (s), 134.7 (d), 138.3 (s),

	148.5 (s), 188.5 (d) ppm.
ESI–MS (*m/z*)	: 250.18 $(M+H)^+$.
Elemental Analysis	Calcd.: C, 72.28; H, 4.45; N, 16.86.
	Found: C, 72.31; H, 4.49; N, 16.80.

1-(4-Iodo-2-nitrophenyl)-4-phenyl-1*H*-1,2,3-triazole (2.56)

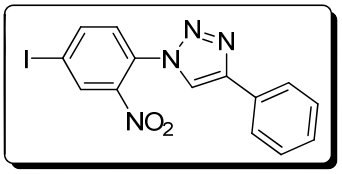

Crystal data for **3fa** ($C_{14}H_9IN_4O_2$): M = 392.15, Crystal dimensions 0.68 x 0.15 x 0.05 mm^3, Monoclinic, space group $P2_1/c$, a = 5.5301(12), b = 17.085(4), c = 15.094(3) Å, β = 93.124(4)°, V = 1424.0(5) $Å^3$, Z = 4; ρ_{calcd} = 1.829 gcm^{-3}, μ (Mo-K_α) = 2.258 mm^{-1}, *F(000)* = 760, T = 297(2) K, $2\theta_{max}$ = 50.00°, 7072 reflections collected, 2501 unique, 1831 observed ($I > 2\sigma(I)$) reflections, 190 refined parameters, R value 0.0548, $wR2$ = 0.1245 (all data R = 0.0762, $wR2$ = 0.1362), S = 1.094, minimum and maximum transmission 0.3089 and 0.8955 respectively, maximum and minimum residual electron densities +1.454 and –0.679 e $Å^{-3}$.

Mol. Formula	: $C_{14}H_9IN_4O_2$
M. P.	: 199–201 °C.
IR (Nujol) $\tilde{\nu}$	: 2926, 2854, 146, 1377, 1215, 764, 669 cm^{-1}.
^{1}H NMR (DMSO-d_6, 200 MHz)	: δ 7.27–7.40 (m, 3H), 7.57 (d, J = 8.1 Hz, 1H), 7.81–7.91 (m, 2H), 8.16 (d, J = 7.3 Hz, 1H), 8.33 (s, 1H), 8.80 (s, 1H) ppm.
^{13}C NMR ($CDCl_3$+DMSO-d_6, 100 MHz)	: δ 93.6 (s), 120.3 (d), 124.0 (d, 2C), 126.7 (d), 126.9 (d), 127.2 (d, 2C), 127.4 (s), 128.2 (s), 132.0 (d), 141.2 (d), 142.5 (s), 146.0 (s) ppm.
ESI–MS (*m/z*)	: 393.10 $(M+H)^+$.
Elemental Analysis	Calcd.: C, 42.88; H, 2.31; N, 14.29.
	Found: C, 42.93; H, 2.27; N, 14.24.

1,4-Bis(2-nitrophenyl)-1*H*-1,2,3-triazole (2.69)

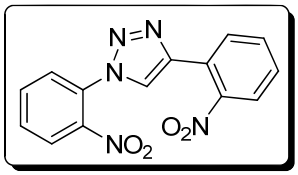

Mol. Formula	: $C_{14}H_9N_5O_4$
M. P.	: 215–216 °C.
IR (Nujol) $\tilde{\nu}$	: 2924, 2854, 1377, 761 cm^{-1}.
^{1}H NMR (DMSO-d_6, 500 MHz)	: δ 7.69 (t, *J* = 7.3 Hz, 1H), 7.83 (t, *J* = 7.5 Hz, 1H), 7.87–7.91 (m, 2H), 7.96–8.02 (m, 3H), 8.27 (d, *J* = 7.8 Hz, 1H), 9.15 (s, 1H) ppm.
^{13}C NMR (DMSO-d_6, 125 MHz)	: δ 122.7 (s), 124.3 (d), 125.0 (d), 125.7 (d), 127.7 (d), 128.8 (s), 130.0 (d), 130.6 (d), 131.6 (d), 132.8 (d), 134.6 (d), 142.6 (s), 144.0 (s), 148.2 (s) ppm.
ESI–MS (*m/z*)	: 312.20 $(M+H)^+$, 334.17 $(M+Na)^+$.
Elemental Analysis	Calcd.: C, 54.02; H, 2.91; N, 22.50. Found: C, 53.98; H, 2.88; N, 22.46.

1-(2-Nitrophenyl)-4-(4-nitrophenyl)-1*H*-1,2,3-triazole (2.70)

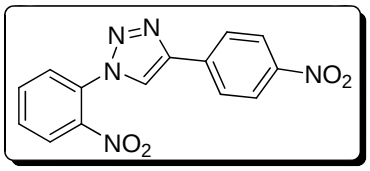

Mol. Formula	: $C_{14}H_9N_5O_4$
M. P.	: 290–292 °C.
IR (Nujol) $\tilde{\nu}$	: 3147, 1604, 1534, 1511, 1459, 1339, 1108, 1024, 854, 756 cm^{-1}.
^{1}H NMR (DMSO-d_6, 400 MHz)	: δ 7.88–7.92 (m, 1H), 7.99–8.05 (m, 2H), 7.21 (d, *J* = 8.5 Hz, 2H), 8.28 (d, *J* = 8.0 Hz, 1H), 8.39 (d, *J* = 8.8 Hz, 2H), 9.45 (s, 1H) ppm.
^{13}C NMR (DMSO-d_6, 125 MHz)	: δ 124.6 (d, 2C), 124.9 (d), 125.8 (d), 126.3 (d, 2C), 127.6 (d), 128.9 (s), 131.6 (d), 134.7 (d), 136.2 (s), 144.0 (s), 145.2 (s), 147.0 (s) ppm.
ESI–MS (*m/z*)	: 312.18 $(M+H)^+$, 334.11 $(M+Na)^+$.
Elemental Analysis	Calcd.: C, 54.02; H, 2.91; N, 22.50. Found: C, 54.10; H, 2.87; N, 22.44.

4-(2-Bromophenyl)-1-(2-nitrophenyl)-1*H*-1,2,3-triazole (2.71)

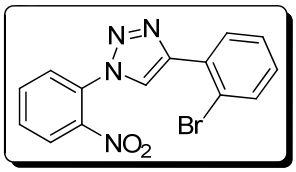

Mol. Formula	: $C_{14}H_9BrN_4O_2$
M. P.	: 125 °C.
^{1}H NMR ($CDCl_3$, 400 MHz)	: δ 7.24 (dt, *J* = 1.7, 7.8 Hz, 1H), 7.46 (dt, *J* = 1.2, 7.8 Hz, 1H), 7.68 (dd, *J* = 1.0, 8.1 Hz, 1H), 7.73 (br. s, 1H), 7.75 (br. s, 1H), 7.83 (dt, *J* = 1.6, 8.1 Hz, 1H), 8.12 (dd, *J* = 1.5, 8.2 Hz, 1H), 8.24 (dd, *J* = 1.8, 7.8 Hz, 1H), 8.56 (s, 1H) ppm.
^{13}C NMR ($CDCl_3$, 100 MHz)	: δ 121.3 (s), 124.3 (d), 125.7 (d, 2C), 127.4 (s), 127.8 (d), 128.1 (s), 129.7 (d), 130.7 (d), 130.9 (d), 133.7 (d, 2C), 142.0 (s), 145.9 (s) ppm.
Elemental Analysis	Calcd.: C, 48.72; H, 2.63; Br, 23.15; N, 16.23. Found: C, 48.98; H, 2.39; Br, 23.19; N, 16.51.

4-(3-Bromophenyl)-1-(2-nitrophenyl)-1*H*-1,2,3-triazole (2.72)

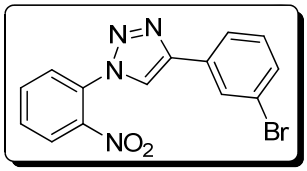

Mol. Formula	: $C_{14}H_9BrN_4O_2$
M. P.	: 101 °C.
^{1}H NMR ($CDCl_3$, 400 MHz)	: δ 7.02–7.44 (m, 3H), 7.58–7.82 (m, 4H), 7.94–8.04 (m, 2H) ppm.
^{13}C NMR ($CDCl_3$, 100 MHz)	: δ 121.4 (d), 123.1 (s), 124.5 (d), 125.7 (d), 126.9 (d), 127.90 (d), 129.0 (d), 130.5 (d), 130.8 (d), 131.5 (d), 131.8 (s), 133.8 (s), 144.4 (s), 146.9 (s) ppm.
Elemental Analysis	Calcd.: C, 48.72; H, 2.63; Br, 23.15; N, 16.23. Found: C, 48.76; H, 2.52; Br, 23.42; N, 16.11.

4-(4-Bromophenyl)-1-(2-nitrophenyl)-1*H*-1,2,3-triazole (2.73)

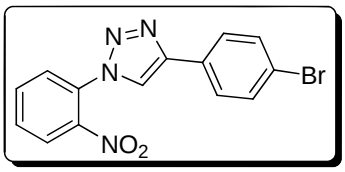

Mol. Formula : $C_{14}H_9BrN_4O_2$

M. P. : 136–137 °C.

^{1}H NMR ($CDCl_3$, 400 MHz) : δ 7.40–7.50 (m, 1H), 7.57 (dt, *J* = 2.2, 8.7 Hz, 1H), 7.65–7.88 (m, 5H), 8.06 (s, 1H), 8.06–8.22 (m, 1H) ppm.

^{13}C NMR ($CDCl_3$, 100 MHz) : δ 121.0 (d), 122.7 (s), 125.6 (d), 127.5 (d, 2C), 127.9 (d), 129.8 (s), 130.8 (d), 132.2 (d, 2C), 132.4 (s), 133.8 (d), 144.4 (s), 147.4 (s) ppm.

Elemental Analysis Calcd.: C, 48.72; H, 2.63; Br, 23.15; N, 16.23.
Found: C, 48.44; H, 2.40; Br, 23.11; N, 16.41.

2-((1-(2-Nitrophenyl)-1*H*-1,2,3-triazol-4-yl)methyl)isoindoline-1,3-dione (2.74)

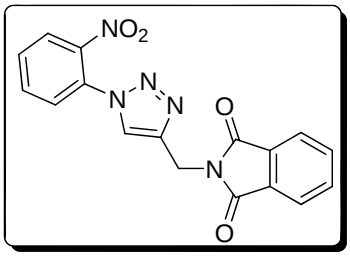

Mol. Formula : $C_{17}H_{11}N_5O_4$

M. P. : 213–214 °C.

IR (Nujol) $\tilde{\nu}$: 2921, 2724, 1765, 1717, 1586, 1604, 1528, 1463, 1376, 1312, 1041, 934, 714 cm^{-1}.

^{1}H NMR (DMSO-d_6, 200 MHz) : δ 4.95 (s, 2H), 7.77–7.96 (m, 7H), 8.16–8.21 (m, 1H), 8.68 (s, 1H) ppm.

^{13}C NMR (DMSO-d_6, 100 MHz) : δ 32.9 (t), 123.4 (d, 2C), 124.7 (d), 125.6 (d), 127.6 (d), 129.1 (s), 131.3 (d), 131.7 (s), 134.5 (d), 134.8 (d, 2C), 143.4 (s, 2C), 144.1 (s), 167.5 (s, 2C) ppm.

ESI–MS (*m/z*) : m/z: 350.34 $(M+H)^+$, 372.32 $(M+Na)^+$.

Elemental Analysis Calcd.: C, 58.45; H, 3.17; N, 20.05.
Found: C, 58.50; H, 3.20; N, 20.10.

2-(1-(2-Nitrophenyl)-1*H*-1,2,3-triazol-4-yl)propan-2-ol (2.75)

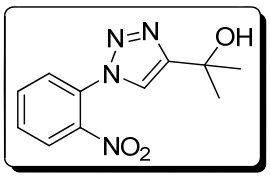

Mol. Formula	: $C_{11}H_{12}N_4O_3$
M. P.	: 111–113 °C.
IR (Nujol) $\tilde{\nu}$	: 3349, 3149, 2924, 1607, 1538, 1506, 1462, 1376, 1362, 1234 cm^{-1}.
^{1}H NMR (DMSO-d_6, 200 MHz)	: δ 1.53 (s, 6H), 5.34 (s, 1H), 7.76–7.82 (m, 1H), 7.84–7.85 (m, 1H), 7.89–7.98 (m, 1H), 8.18 (dd, J = 1.4, 8.1 Hz, 1H), 8.45 (s, 1H) ppm.
^{13}C NMR (DMSO-d_6, 50 MHz)	: δ 30.7 (q, 2C), 67.2 (s), 121.9 (d), 125.5 (d), 127.2 (d), 129.4 (s), 130.8 (d), 134.3 (d), 144.2 (s), 156.8 (s) ppm.
ESI–MS (*m/z*)	: m/z: 249.21 $(M+H)^+$, 271.20 $(M+Na)^+$.
Elemental Analysis	Calcd.: C, 53.22; H, 4.87; N, 22.57. Found: C, 53.18; H, 4.82; N, 22.52.

2-(1-(2-Nitrophenyl)-1*H*-1,2,3-triazol-4-yl)ethanol (2.76)

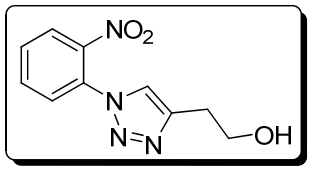

Mol. Formula	: $C_{10}H_{10}N_4O_3$
M. P.	: 92–93 °C.
IR (Nujol) $\tilde{\nu}$	: 3326, 3137, 2724, 1605, 1536, 1503, 1460, 1376, 1365, 1241 cm^{-1}.
^{1}H NMR (DMSO-d_6, 200 MHz)	: δ 2.88 (t, J = 6.9 Hz, 2H), 3.67–3.75 (m, 2H), 4.83 (t, J = 5.1 Hz, 1H) 7.76–7.81 (m, 1H), 7.84 (d, J = 0.8 Hz, 1H), 7.89–7.98 (m, 1H), 8.15–8.20 (m, 1H), 8.43 (s, 1H) ppm.
^{13}C NMR (DMSO-d_6, 50 MHz)	: δ 29.1 (t), 60.3 (t), 123.8 (d), 125.5 (d), 127.2 (d), 129.4 (s), 130.9 (d), 134.3 (d), 144.2 (s), 145.7 (s) ppm.
ESI–MS (*m/z*)	: m/z: 235.20 $(M+H)^+$, 257.19 $(M+Na)^+$.
Elemental Analysis	Calcd.: C, 51.28; H, 4.30; N, 23.92. Found: C, 51.34; H, 4.35; N, 23.84.

15-(1-(2-Nitrophenyl)-1*H*-1,2,3-triazol-4-yl)pentadecan-1-ol (2.77)

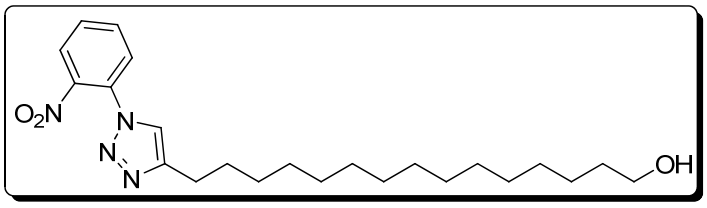

Mol. Formula	: $C_{23}H_{36}N_4O_3$
M. P.	: 95–96 °C.
IR ($CHCl_3$) $\tilde{\nu}$	: 3420, 3019, 2928, 2855, 2400, 1610, 1538, 1505, 1466, 1354, 1215, 1042, 7557, 668, cm^{-1}.
^{1}H NMR (DMSO-d_6, 500 MHz)	: δ 1.22 (s, 18H), 1.31–1.34 (m, 4H), 1.38 (q, *J* = 6.6 Hz, 2H), 1.65 (q, *J* = 7.3 Hz, 2H), 2.70 (t, *J* = 7.4 Hz, 2H), 3.35 (dd, *J* = 6.2, 11.8 Hz, 2H), 4.35 (t, *J* = 4.9 Hz, 1H), 7.79–7.84 (m, 2H), 7.93 (t, *J* = 7.7 Hz, 1H), 8.17 (d, *J* = 7.8 Hz, 1H), 8.42 (s, 1H) ppm.
^{13}C NMR (DMSO-d_6, 125 MHz)	: δ 24.8 (t), 25.5 (t), 28.5 (t), 28.7 (t), 28.8 (t), 29.0 (t, 2C), 29.1 (t, 4C), 29.1 (t, 2C), 32.6 (t), 60.8 (t), 123.1 (d), 125.4 (d), 127.1 (d), 129.3 (s), 130.8 (d), 134.2 (d), 144.1 (s), 147.9 (s) ppm.
ESI–MS (*m/z*)	: 417.6 $(M+H)^+$, 439.6 $(M+Na)^+$.
Elemental Analysis	Calcd.: C, 66.32; H, 8.71; N, 13.45. Found: C, 66.26; H, 8.77; N, 13.49.

4,5-*O*-Isopropylidene-3-*O*-benzyl-1-deoxy-1-*C*-ethynyl - D-erythritol[39] (2.66)

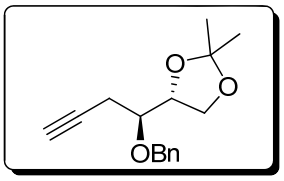

Mol. Formula	: $C_{16}H_{20}O_3$
$[\alpha]_D$	: +67.1 (*c* 0.2, $CHCl_3$)
IR ($CHCl_3$) $\tilde{\nu}$	: 3293, 2988, 2883, 1955, 1455, 1371, 1255, 1212, 1074 cm^{-1}.
^{1}H NMR ($CDCl_3$, 200 MHz)	: δ 1.34 (s, 3H), 1.38 (s, 3H), 2.00 (t, *J* = 2.7 Hz, 1H), 2.52 (dd, *J* = 2.6, 5.2 Hz, 1H), 2.58 (dd, *J* = 2.7, 4.6 Hz, 1H), 3.54 (dd, *J* = 4.9, 11.7 Hz, 1H), 3.87 (dd, *J* = 5.6, 8.3 Hz, 1H), 4.05 (dd, *J* = 6.3, 8.3 Hz, 1H), 4.15 (dd, *J* = 5.6, 6.8 Hz, 1H), 4.77 (d, *J* =

11.5 Hz, 1H), 4.88 (d, *J* = 11.5 Hz, 1H), 7.25–7.35 (m, 5H) ppm.

^{13}C NMR ($CDCl_3$, 50 MHz) : δ 20.8 (t), 25.1 (q), 26.5 (q), 66.3 (t), 70.3 (d), 72.0 (t), 76.2 (d), 77.3 (d), 80.3 (s), 109.0 (s), 127.5 (d), 127.6 (d, 2C), 128.1 (d, 2C), 137.8 (s) ppm.

Elemental Analysis Calcd.: C, 73.82; H, 7.74.
Found: C, 73.78; H, 7.70.

4,5-*O*-Isopropylidene-3-*O*-benzyl-1-deoxy-1-*C*-[(1-(2-nitrophenyl)-1*H*-1,2,3-triazol-4-yl)]-D-erythritol (2.78)

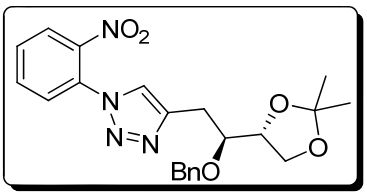

Mol. Formula : $C_{22}H_{24}N_4O_5$

$[\alpha]_D$: +7.0 (*c* 3.5, $CHCl_3$)

IR ($CHCl_3$) $\tilde{\nu}$: 3144, 2987, 2885, 1720, 1609, 1588, 1537, 1506, 1454, 1355, 1214, 1071, 852, 748, 699 cm^{-1}.

^{1}H NMR ($CDCl_3$, 200 MHz) : δ 1.36 (s, 3H), 1.45 (s, 3H), 3.06 (dd, *J* = 6.7, 15.2 Hz, 1H), 3.26 (dd, *J* = 4.1, 15.2 Hz, 1H), 3.86–3.94 (m, 2H), 4.02–4.17 (m, 2H), 4.61 (s, 2H), 7.24–7.31 (m, 5H), 7.54 (dd, *J* = 1.6, 7.6 Hz, 1H), 7.65 (s, 1H), 7.67 (dt, *J* = 1.7, 7.7 Hz, 1H), 7.77 (dt, *J* = 1.8, 7.7 Hz, 1H), 8.06 (dd, *J* = 1.7, 7.8 Hz, 1H) ppm.

^{13}C NMR ($CDCl_3$, 50 MHz) : δ 24.8 (q), 26.2 (q), 27.0 (t), 65.9 (t), 72.2 (t), 76.5 (d), 78.2 (d), 108.8 (s), 123.5 (d), 125.0 (d), 127.0 (d), 127.2 (d), 127.4 (d, 2C), 127.9 (d, 2C), 129.6 (s), 130.2 (d), 133.4 (d), 137.7 (s), 143.9 (s), 144.2 (s) ppm.

ESI–MS (*m/z*) : 425.6 $(M+H)^+$, 447.6 $(M+Na)^+$.

Elemental Analysis Calcd.: C, 62.25; H, 5.70; N, 13.20
Found: C, 62.19; H, 5.67; N, 13.18

(4*R*) 1,2-*O*-Isopropylidene-3-*O*-benzyl-4-*C*-ethynyl - L –threofuranose[40] (2.67)

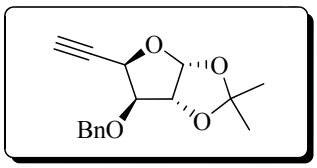

Mol. Formula	: $C_{16}H_{18}O_4$
$[\alpha]_D$	: +3.1 (*c* 1.05, $CHCl_3$)
IR ($CHCl_3$) $\tilde{\nu}$	: 3089, 3063, 2985, 2864, 1954, 1497, 1455, 1383, 1360, 1248, 1217, 1162, 1078, 1027, 885, 862, 735, 796, 667 cm^{-1}.
^{1}H NMR ($CDCl_3$, 200 MHz)	: δ 1.29 (s, 3H), 1.46 (s, 3H), 2.61 (d, *J* = 2.27 Hz, 1H), 3.99 (d, *J* = 3.0 Hz, 1H), 4.58 (d, *J* = 3.7 Hz, 1H), 4.77 (d, *J* = 4.5 Hz, 2H), 4.83 (t, *J* = 2.7 Hz, 1H), 5.96 (d, *J* = 3.7 Hz, 1H), 7.28–7.41 (m, 5H) ppm.
^{13}C NMR ($CDCl_3$, 100 MHz)	: δ 26.1 (q), 26.7 (q), 70.6 (d), 72.5 (t), 76.4 (s), 77.5 (s), 82.4 (d), 82.8 (d), 104.7 (d), 111.9 (d), 127.7 (d, 2C), 127.9 (d), 128.4 (d, 2C), 137.3 (s) ppm.
Elemental Analysis	Calcd.: C, 70.06; H, 6.61. Found: C, 70.11; H, 6.66.

(4*R*) 1,2-*O*-Isopropylidene-3-*O*-benzyl-4-*C*-[(1-(2-nitro-phenyl)-1*H*-1,2,3-triazol-4-yl)]-L-threofuranose (2.79)

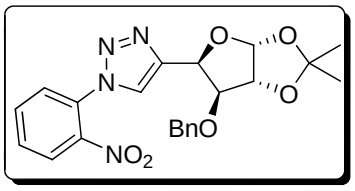

Mol. Formula	: $C_{22}H_{22}N_4O_6$
$[\alpha]_D$	: +5.6 (*c* 1.2, $CHCl_3$)
IR ($CHCl_3$) $\tilde{\nu}$	: 3018, 2923, 1725, 1609, 1539, 1508, 1454, 1355, 1076, 1026, 753, 666 cm^{-1}.
^{1}H NMR ($CDCl_3$, 200 MHz)	: δ 1.37 (s, 3H), 1.58 (s, 3H), 4.23 (d, *J* = 3.0 Hz, 1H), 4.46 (dd, *J* = 12.0, 19.2 Hz, 2H), 4.75 (d, *J* = 3.7 Hz, 1H), 5.64 (d, *J* = 3.0 Hz, 1H), 6.06 (d, *J* = 3.7 Hz, 1H), 7.14–7.19 (m, 2H), 7.24–7.30 (m, 3H), 7.46–7.51 (m, 1H), 7.65–7.81 (m, 2H), 7.96 (s, 1H), 8.07–8.11 (m, 1H) ppm.
^{13}C NMR ($CDCl_3$, 50 MHz)	: δ 26.2 (q), 26.7 (q), 72.5 (t), 76.1 (d), 82.4 (d), 83.0 (d), 104.6 (d), 112.1 (s), 125.3 (d), 125.5 (d), 127.5 (d, 2C), 127.8 (d), 128.4 (d, 2C), 129.6 (d), 130.1 (s), 130.7 (d), 133.7 (d), 137.1 (s), 144.2 (s), 144.4 (s) ppm.
ESI–MS (*m/z*)	: 439.3 $(M+H)^+$, 461.3 $(M+Na)^+$.

Elemental Analysis Calcd.: C, 60.27; H, 5.06; N, 12.78.
Found: C, 60.31; H, 5.12; N, 12.74.

1,2:4,5-Di-*O*-isopropylidene-3-*O*-(prop-2-ynyloxy)-D-fructopyranose[41] (2.68)

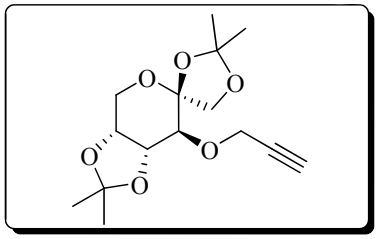

Mol. Formula : $C_{15}H_{22}O_6$

$[\alpha]_D$: +43.23 (*c* 1.3, $CHCl_3$)

IR ($CHCl_3$) $\tilde{\nu}$: 3089, 3063, 2985, 2864, 1954, 1497, 1455, 1383, 1360, 1248, 1217, 1162, 1078, 1027, 885, 862, 735, 796, 667 cm^{-1}.

^{1}H NMR ($CDCl_3$, 200 MHz) : δ 1.34 (s, 3H), 1.39 (s, 3H), 1.47 (s, 3H), 1.56 (s, 3H), 2.39 (t, *J* = 2.3 Hz, 1H), 3.71 (d, *J* = 7.5 Hz, 1H), 3.89–4.30 (m, 6H), 4.40 (dd, *J* = 2.4, 16.0 Hz, 1H), 4.53 (dd, *J* = 2.3, 16.0 Hz, 1H) ppm.

^{13}C NMR ($CDCl_3$, 50 MHz) : δ 26.0 (q), 26.3 (q), 26.7 (q), 28.1 (q), 58.1 (t), 60.0 (t), 71.7 (t), 73.9 (d), 74.0 (d), 74.9 (d), 77.6 (d), 79.6 (s), 104.2 (s), 109.0 (s), 111.9 (s) ppm.

Elemental Analysis Calcd.: C, 60.39; H, 7.43.
Found: C, 60.44; H, 7.39.

1,2:4,5-Di-*O*-isopropylidene-3-*O*-[(1-(2-nitrophenyl)-1*H*-1,2,3-triazol-4-yl)methyl]-D-fructopyranose (2.80)

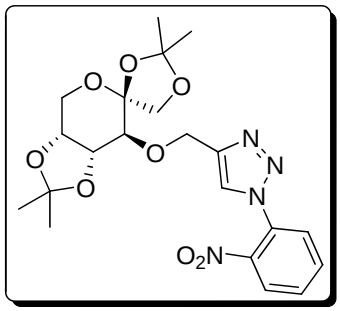

Mol. Formula : $C_{21}H_{26}N_4O_8$

$[\alpha]_D$: –62.2 (*c* 1.0, $CHCl_3$)

IR ($CHCl_3$) $\tilde{\nu}$: 3018, 2935, 2400, 1734, 1609, 1541, 1508, 1457, 1382, 1218, 1117, 1082, 1017, 882, 768, 668 cm^{-1}.

^{1}H NMR : δ 1.39 (s, 6H), 1.49 (s, 3H), 1.59 (s, 3H), 3.62 (d, *J* = 7.3 Hz,

(CDCl$_3$, 200 MHz) 1H), 3.92 (d, *J* = 8.59 Hz, 1H), 4.05–4.14 (m, 3H), 4.23 (dd, *J* = 1.9, 5.6 Hz, 1H), 4.39 (dd, *J* = 5.9, 7.2 Hz, 1H), 4.94 (d, *J* = 12.7 Hz, 1H), 5.17 (d, *J* = 12.7 Hz, 1H), 7.62 (dd, *J* = 1.4, 7.6 Hz, 1H), 7.72 (dd, *J* = 1.6, 7.8 Hz, 1H), 7.78 (dd, *J* = 1.7, 7.5 Hz, 1H), 7.86 (s, 1H), 8.08 (dd, *J* = 1.6, 7.8 Hz, 1H) ppm.

^{13}C NMR : δ 25.5 (q), 25.8 (q), 26.4 (q), 27.8 (q), 59.7 (t), 64.2 (t), 71.3 (CDCl$_3$, 50 MHz) (t), 73.4 (d), 76.2 (d), 77.0 (d), 103.8 (s), 108.7 (s), 111.6 (s), 123.8 (d), 125.1 (d), 127.2 (d), 129.5 (s), 130.5 (d), 133.6 (d), 144.0 (s), 145.4 (s) ppm.

ESI–MS (*m/z*) : 463.7 $(M+H)^+$, 485.6 $(M+Na)^+$.

Elemental Analysis Calcd.: C, 60.39; H, 7.43.
Found: C, 60.44; H, 7.39.

4-(2-Bromophenyl)-1-(4-nitrophenyl)-1*H*-1,2,3-triazole (2.81)

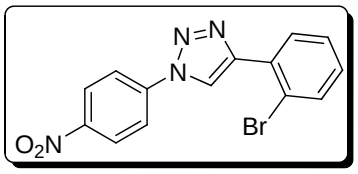

Mol. Formula : $C_{14}H_9BrN_4O_2$

M. P. : 170–171 °C.

^{1}H NMR : δ 7.26 (ddd, *J* = 1.8, 7.4, 9.2 Hz, 1H), 7.47 (dt, *J* = 1.2, 7.8 (CDCl$_3$, 400 MHz) Hz, 1H), 7.69 (dd, *J* = 1.2, 7.9 Hz, 1H), 8.04 (t, *J* = 2.6 Hz, 1H), 8.09 (t, *J* = 2.6 Hz, 1H), 8.2 (dd, *J* = 1.6, 7.8 Hz, 1H), 8.42 (t, *J* = 2.6 Hz, 1H), 8.47 (t, *J* = 2.6 Hz, 1H), 8.79 (s, 1H) ppm.

^{13}C NMR : δ 120.5 (d), 121.3 (s), 124.1 (d), 124.9 (d), 125.6 (d), 127.9 (CDCl$_3$, 100 MHz) (d), 130.0 (d), 130.2 (d), 130.8 (d), 131.9 (s), 133.8 (d), 141.1 (s), 146.7 (s), 147.3 (s) ppm.

Elemental Analysis Calcd.: C, 48.72; H, 2.63; Br, 23.15; N, 16.23.
Found: C, 48.57; H, 2.90; Br, 22.89; N, 16.12.

4-(3-Bromophenyl)-1-(4-nitrophenyl)-1*H*-1,2,3-triazole (2.82)

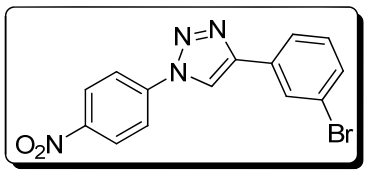

Mol. Formula	: $C_{14}H_9BrN_4O_2$
M. P.	: 217–218 °C.
^{1}H NMR (DMSO-d_6, 400 MHz)	: δ 7.36–7.54 (m, 2H), 7.96 (dt, *J* = 1.8, 7.6 Hz, 1H), 8.14 (t, *J* = 1.6 Hz, 1H), 8.26, 8.31, 8.45, 8.51 (4br. m, 4H), 9.47 (s, 1H) ppm.
^{13}C NMR (DMSO-d_6, 100 MHz)	: δ 118.6 (d, 2C), 120.8 (d), 122.6 (s), 123.8 (d), 124.1 (d), 126.5 (d), 127.4 (d), 129.1 (d), 129.4 (d), 130.5 (s), 139.3 (s), 145.0 (s), 145.1 (s) ppm.
Elemental Analysis	Calcd.: C, 48.72; H, 2.63; Br, 23.15; N, 16.23. Found: C, 48.63; H, 2.88; Br, 23.29; N, 16.48.

4-(4-Bromophenyl)-1-(4-nitrophenyl)-1*H*-1,2,3-triazole (2.83)

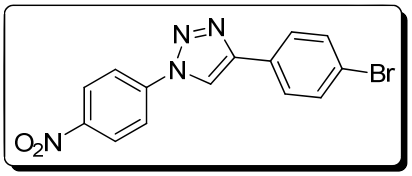

Mol. Formula	: $C_{14}H_9BrN_4O_2$
M. P.	: 149–150 °C.
^{1}H NMR (DMSO-d_6, 400 MHz)	: δ 7.59 (t, *J* = 2.2 Hz, 1H), 7.64 (t, *J* = 2.2 Hz, 1H), 7.77 (t, *J* = 2.2 Hz, 1H), 7.82 (t, *J*=2.2 Hz, 1H), 8.01 (t, *J* = 2.2 Hz, 1H), 8.06 (t, *J* = 2.2 Hz, 1H), 8.28 (t, *J* = 2.2 Hz, 1H), 8.44 (t, *J* = 2.2 Hz, 1H), 8.48 (t, *J* = 2.2 Hz, 1H) ppm.
^{13}C NMR (DMSO-d_6, 100 MHz)	: δ 118.2 (d), 118.5 (d, 2C), 119.9 (s), 123.7 (d, 2C), 125.5 (d, 2C), 127.3 (s), 130.1 (d, 2C), 139.1 (s), 144.9 (s), 145.2 (s) ppm.
Elemental Analysis	Calcd.: C, 48.72; H, 2.63; Br, 23.15; N, 16.23. Found: C, 48.70; H, 2.40; Br, 23.43; N, 16.01.

2-((1-(4-Nitrophenyl)-1H-1,2,3-triazol-4-yl)methyl)isoindoline-1,3-dione (2.84)

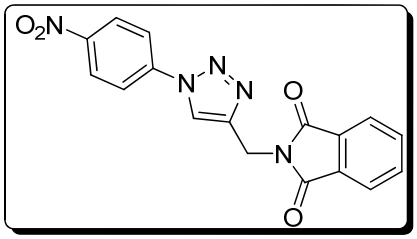

Mol. Formula	: $C_{17}H_{11}N_5O_4$
M. P.	: 266–268 °C.
IR ($CHCl_3$) $\tilde{\nu}$	: 3129, 2725, 1764, 1717, 1594, 1520, 1503, 1455, 1338, 1246, 1043, 935, 857, 773, 718 cm^{-1}.
^{1}H NMR (DMSO-d_6, 500 MHz)	: δ 4.95 (s, 2H), 7.86–7.93 (m, 4H), 8.18 (d, J = 9.1 Hz, 2H), 8.42 (d, J = 9.1 Hz, 2H), 9.00 (s, 1H) ppm.
^{13}C NMR (DMSO-d_6, 125 MHz)	: δ 32.9 (t), 120.6 (d, 2C), 121.8 (d), 123.3 (d, 2C), 125.6 (d, 2C), 131.7 (s, 2C), 134.6 (d, 2C), 140.8 (s), 144.4 (s), 146.7 (s), 167.4 (s, 2C) ppm.
ESI–MS (*m/z*)	: 372.3 $(M+Na)^+$.
Elemental Analysis	Calcd.: C, 58.45; H, 3.17; N, 20.05. Found: C, 58.51; H, 3.21; N, 19.99.

2-(1-(4-Nitrophenyl)-1*H*-1,2,3-triazol-4-yl)propan-2-ol (2.85)

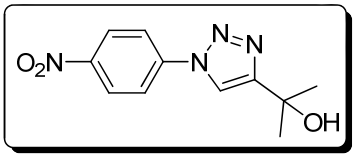

Crystal data for **2.85** ($C_{11}H_{12}N_4O_3$): M = 248.25, crystal dimensions 0.30 x 0.12 x 0.06 mm^3, Monoclinic, space group $P2_1/c$, a = 13.948(4), b = 12.875(4), c = 6.5711(18) Å, β = 93.463(5)°, V = 1177.9(6) $Å^3$, Z = 4; ρ_{calcd} = 1.400 gcm^{-3}, μ (Mo-K_α) = 0.105 mm^{-1}, *F(000)* = 520, T = 133(2) K, $2\theta_{max}$ = 51.00°, 8641 reflections collected, 2183 unique, 1969 observed ($I > 2\sigma(I)$) reflections, 211 refined parameters, R value 0.0599, $wR2$ = 0.1505 (all data R = 0.0651, $wR2$ = 0.1526), S = 1.155, minimum and maximum transmission 0.9691 and 0.9937 respectively, maximum and minimum residual electron densities +0.353 and -0.224 e $Å^{-3}$.

Mol. Formula	: $C_{11}H_{12}N_4O_3$
M. P.	: 121–122 °C.
IR ($CHCl_3$) $\tilde{\nu}$	: 3401, 3019, 2982, 1599, 1530, 1507, 1344, 1235, 1215, 1036, 855, 757, 668 cm^{-1}.
^{1}H NMR (DMSO-d_6, 500 MHz)	: δ 1.54 (s, 6H), 5.34 (s, 1H), 8.23 (dd, J = 2.2, 7.1 Hz, 2H), 8.41 (dd, J = 2.2, 7.1 Hz, 2H), 8.81 (s, 1H) ppm.
^{13}C NMR	: δ 30.5 (q, 2C), 67.0 (s), 119.3 (d), 120.3 (d, 2C), 125.5 (d,

(DMSO-d_6, 125 MHz)	2C), 141.1 (s), 146.5 (s), 157.6 (s) ppm.
ESI–MS (*m/z*)	: 249.3 $(M+H)^+$, 271.3 $(M+Na)^+$.
Elemental Analysis	Calcd.: C, 53.22; H, 4.87; N, 22.57. Found: C, 53.29; H, 4.93; N, 22.61.

2-(1-(4-Nitrophenyl)-1*H*-1,2,3-triazol-4-yl)ethanol[42] (2.86)

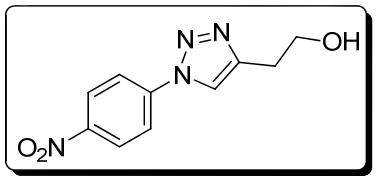

Mol. Formula	: $C_{10}H_{10}N_4O_3$
M. P.	: 148–150 °C.
IR ($CHCl_3$) $\tilde{\nu}$	: 3311, 1596, 1528, 1502, 1462, 1376, 1340, 1242, 1045, 853 cm^{-1}.
^{1}H NMR (DMSO-d_6, 500 MHz)	: δ 2.87 (t, *J* = 6.8 Hz, 2H), 3.70–3.74 (m, 2H), 4.81 (t, *J* = 5.4 Hz, 1H) 7.14–7.18 (m, 2H), 8.38–8.41 (m, 2H), 8.75 (s, 1H) ppm.
^{13}C NMR (DMSO-d_6, 125 MHz)	: δ 29.1 (t), 60.1 (t), 120.2 (d, 2C), 121.2 (d), 125.6 (d, 2C), 141.0 (s), 146.4 (s), 146.5 (s) ppm.
ESI–MS (*m/z*)	: 235.3 $(M+H)^+$, 257.3 $(M+Na)^+$.
Elemental Analysis	Calcd.: C, 51.28; H, 4.30; N, 23.92. Found: C, 51.34; H, 4.26; N, 23.87.

1,2:4,5-Di-*O*-isopropylidene-3-*O*-(1-(4-nitrophenyl)-1*H*-1,2,3-triazol-4-yl)methyl]- D-fructopyranose (2.87)

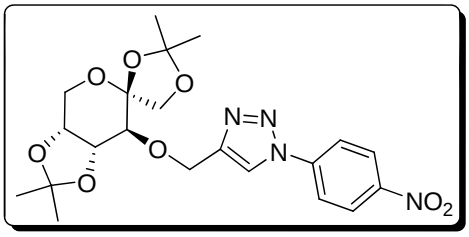

Mol. Formula	: $C_{21}H_{26}N_4O_8$
M. P.	: 135–137 °C.
IR ($CHCl_3$) $\tilde{\nu}$	: 3400, 2990, 2935, 1599, 1528, 1508, 1382, 1342, 1218, 1118, 1082, 854, 751cm^{-1}.

^{1}H NMR ($CDCl_3$, 500 MHz)	: δ 1.39 (s, 3H), 1.41 (s, 3H), 1.50 (s, 3H), 1.57 (s, 3H), 3.63 (d, *J* = 7.6 Hz, 1H), 3.96 (d, *J* = 8.6 Hz, 1H), 4.04 (d, *J* = 13.4 Hz, 1H), 4.12–4.17 (m, 2H), 4.25 (dd, *J* = 2.2, 5.6 Hz, 1H), 4.39 (dd, *J* = 5.6, 7.1 Hz, 1H), 4.92 (d, *J* = 12.5 Hz, 1H), 5.17 (d, *J* = 12.7 Hz, 1H), 7.98 (dd, *J* = 2.0, 7.1 Hz, 2H), 8.14 (s, 1H), 8.42–8.45 (m, 2H) ppm.
^{13}C NMR ($CDCl_3$, 125 MHz)	: δ 26.1 (q), 26.2 (q), 26.6 (q), 28.2 (q), 60.2 (t), 65.1 (t), 71.9 (t), 73.8 (d), 77.3 (d), 77.4 (d), 104.2 (s), 109.2 (s), 112.1 (s), 120.3 (d, 2C), 120.4 (d), 125.5 (d, 2C), 141.1 (s), 147.1 (s), 147.2 (s) ppm.
ESI–MS (*m/z*)	: 463.4 $(M+H)^+$, 485.3 $(M+Na)^+$.
Elemental Analysis	Calcd.: C, 54.54; H, 5.67; N, 12.12. Found: C, 54.60; H, 5.71; N, 12.18.

2.4 Spectra

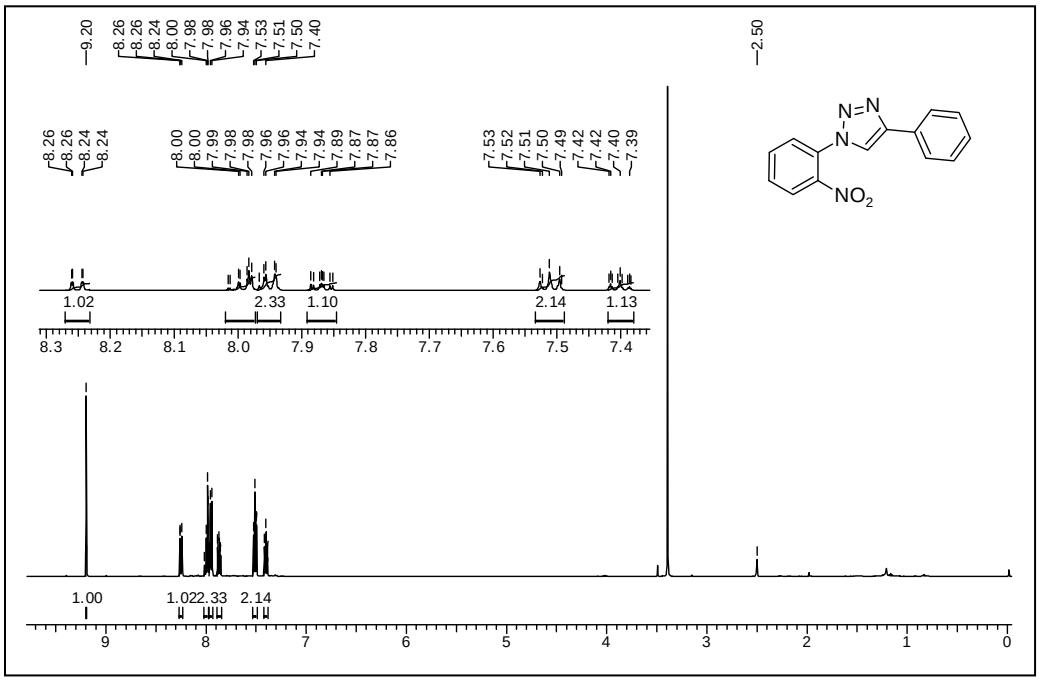

^{1}H NMR Spectrum of 2.45 in DMSO-d_6

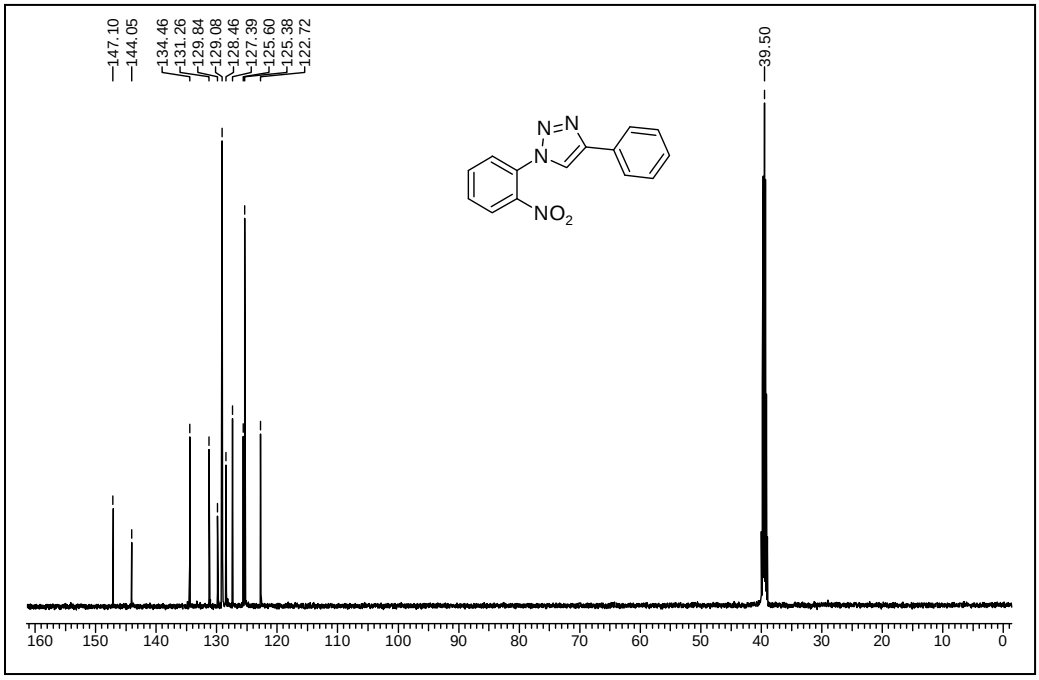

^{13}C NMR Spectrum of 2.45 in DMSO-d_6

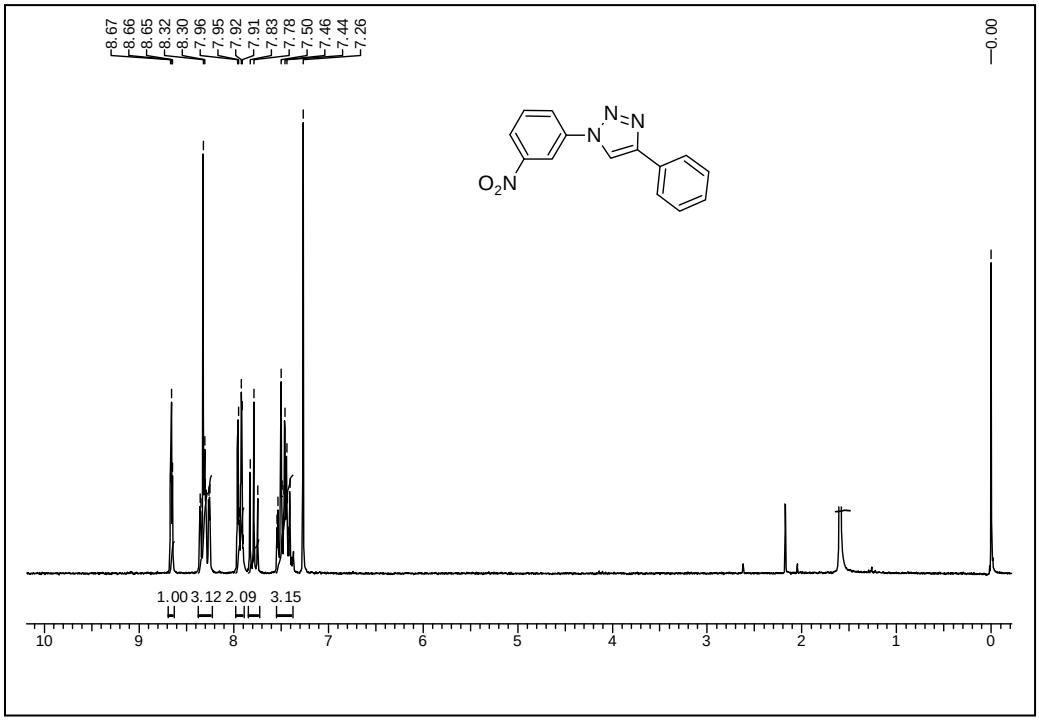

^{1}H NMR Spectrum of 2.46 in $CDCl_3$

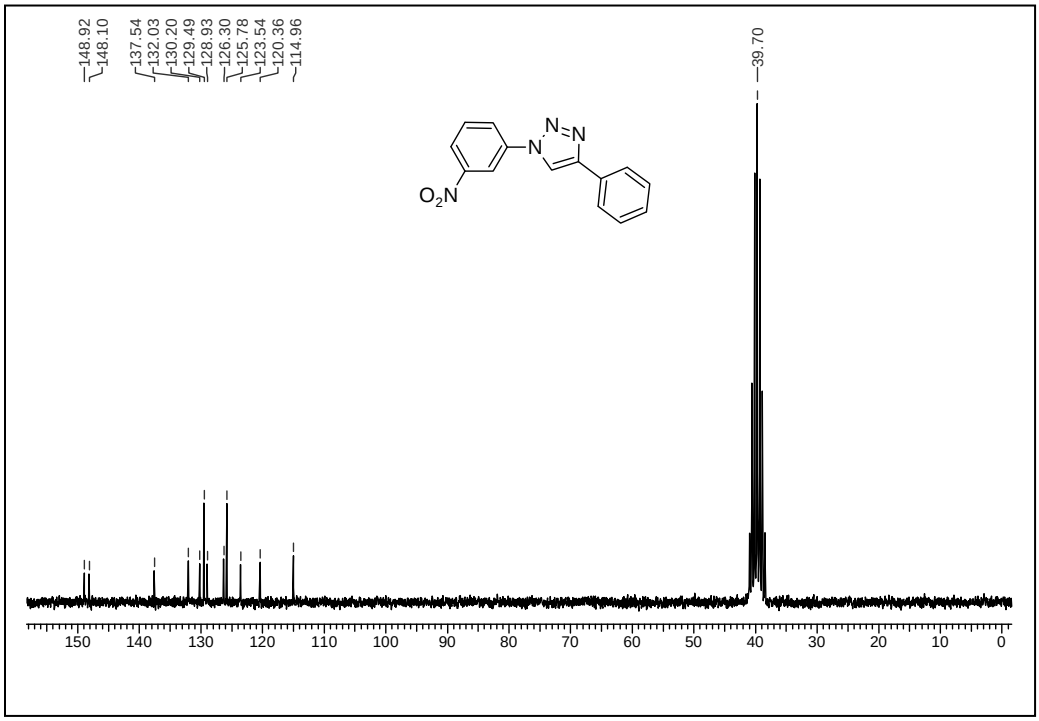

^{13}C NMR Spectrum of 2.46 in DMSO-d_6

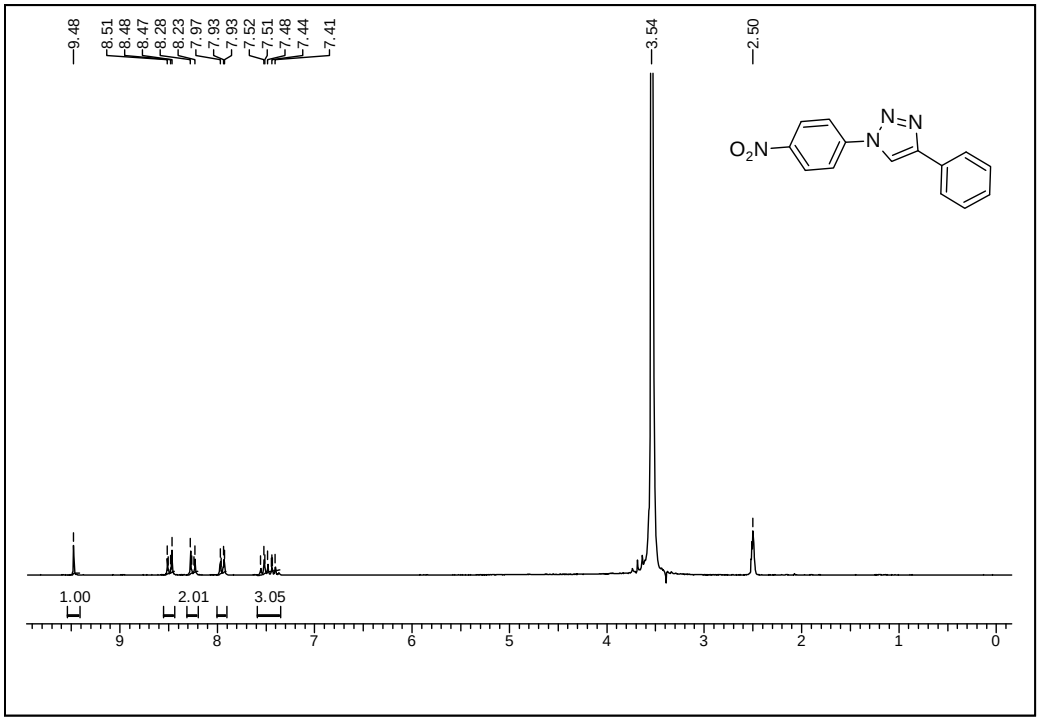

^{1}H NMR Spectrum of 2.48 in DMSO-d_6

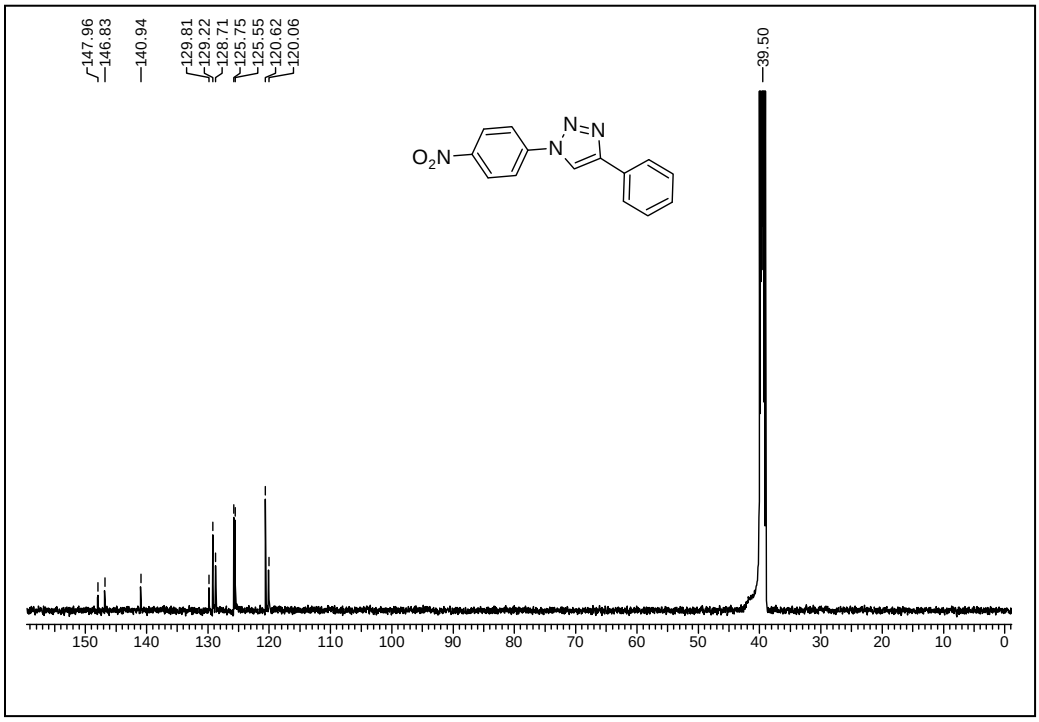

^{13}C NMR Spectrum of 2.48 in DMSO-d_6

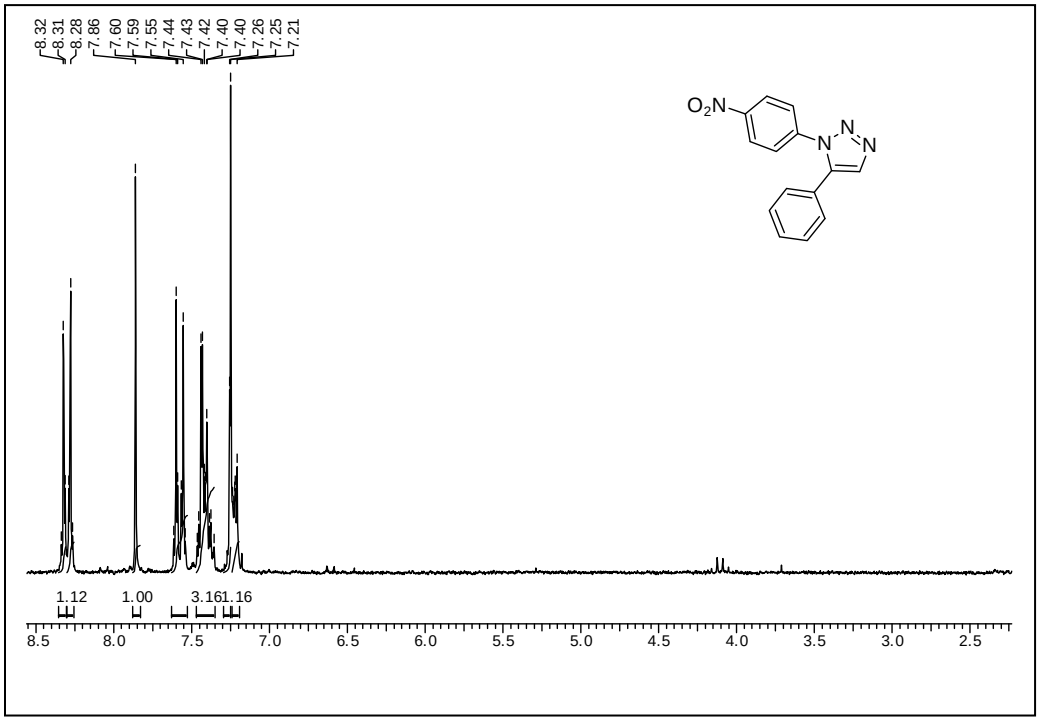

^{1}H NMR Spectrum of 2.49 in $CDCl_3$

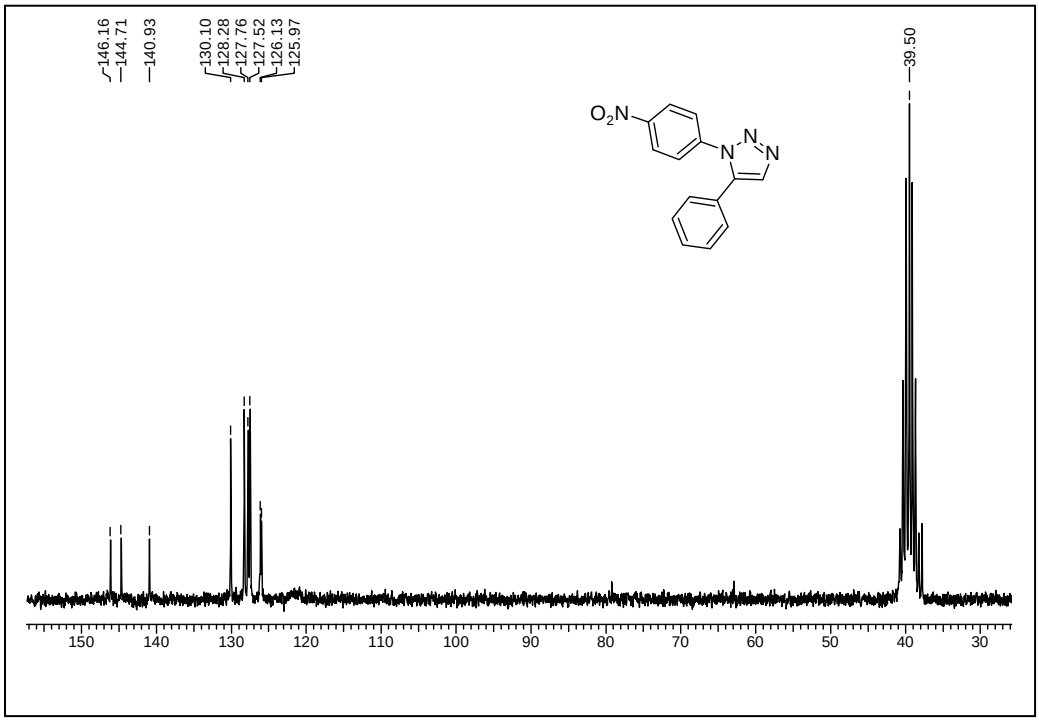

^{13}C NMR Spectrum of 2.49 in DMSO-d_6

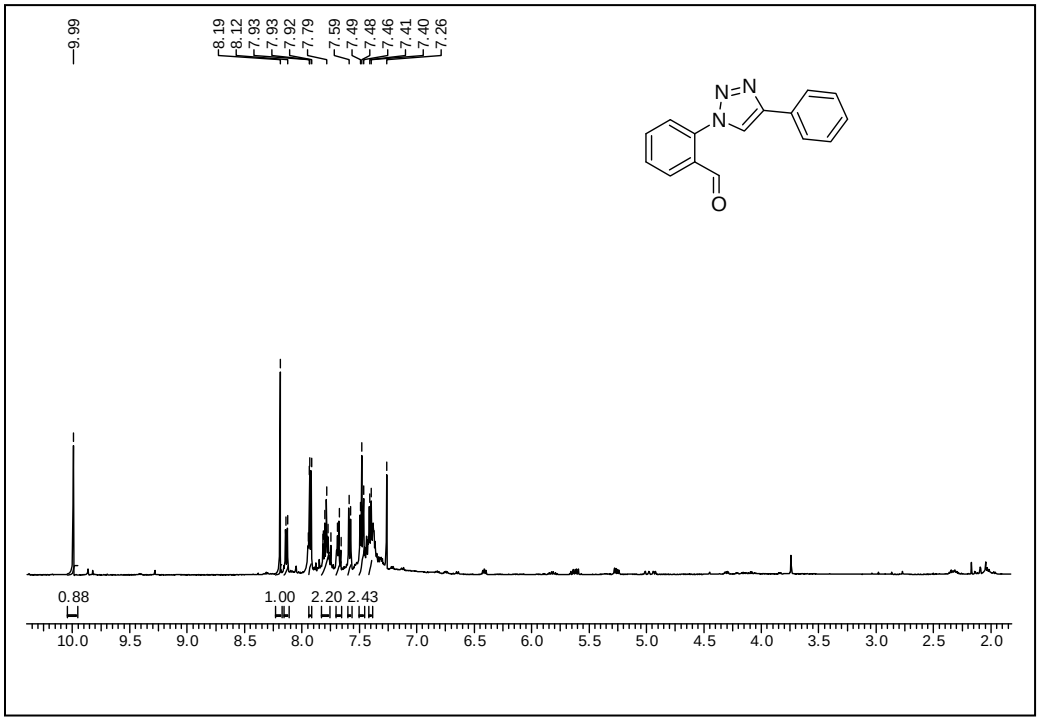

^{1}H NMR Spectrum of 2.54 in $CDCl_3$

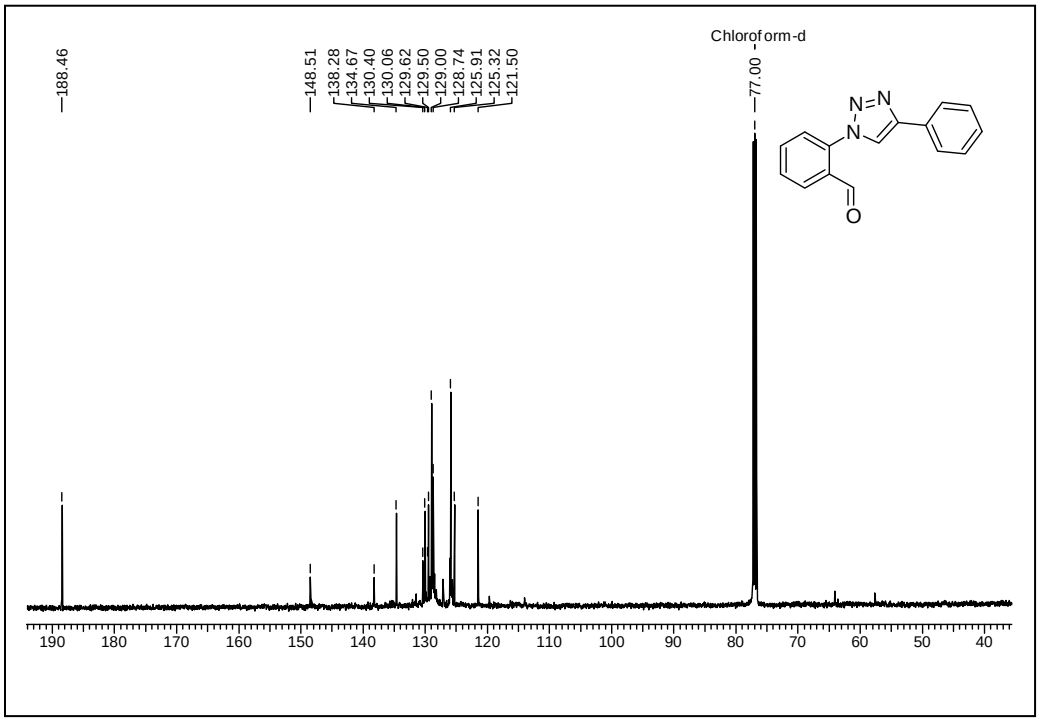

^{13}C NMR Spectrum of 2.54 in $CDCl_3$

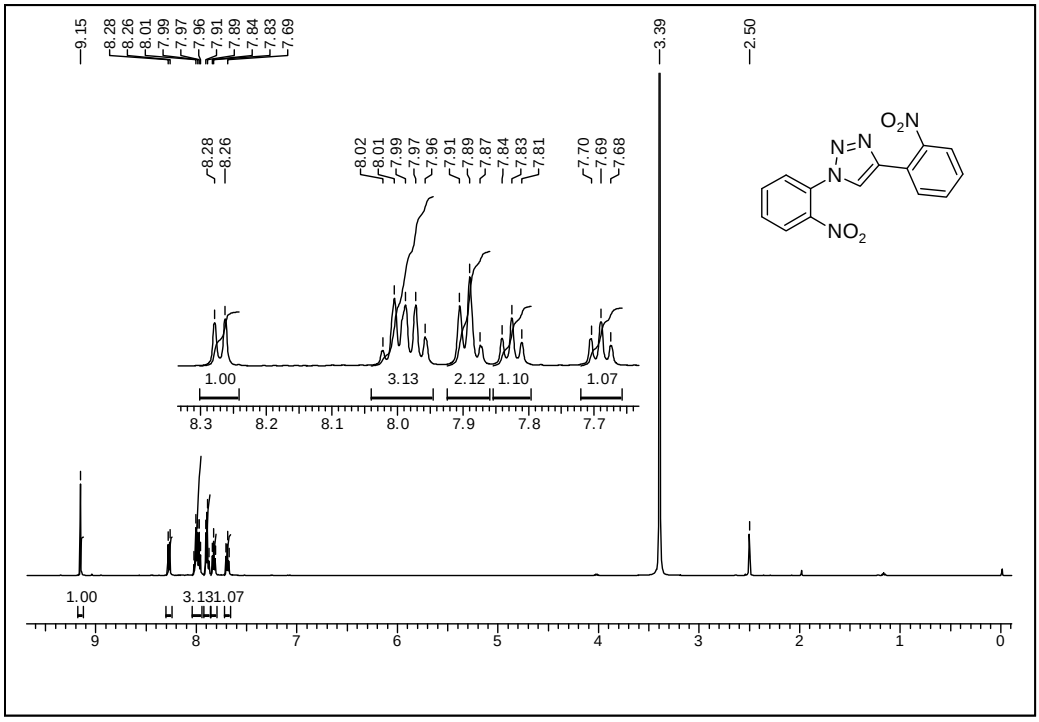

^{1}H NMR Spectrum of 2.69 in DMSO-d_6

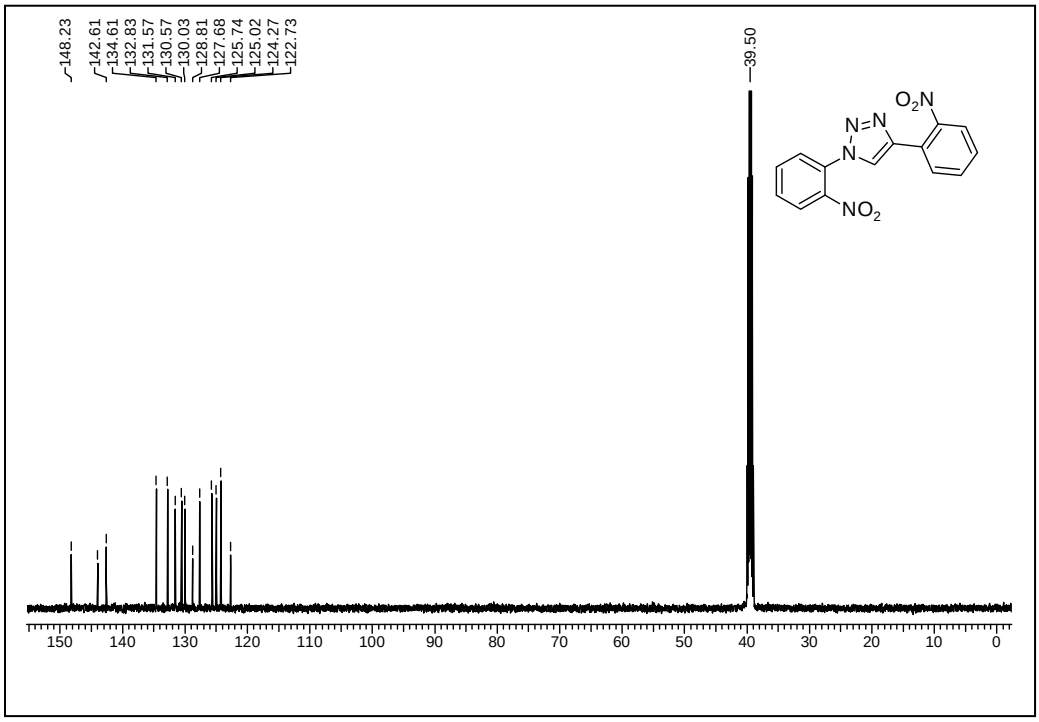

^{13}C NMR Spectrum of 2.69 in DMSO-d_6

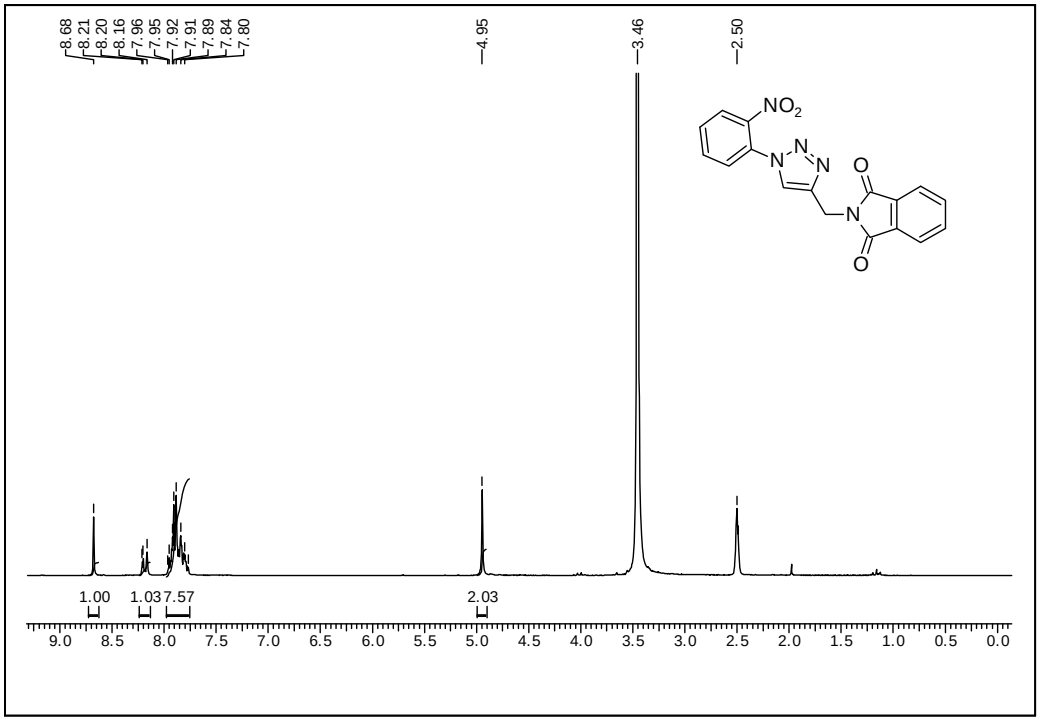

^{1}H NMR Spectrum of 2.74 in DMSO-d_6

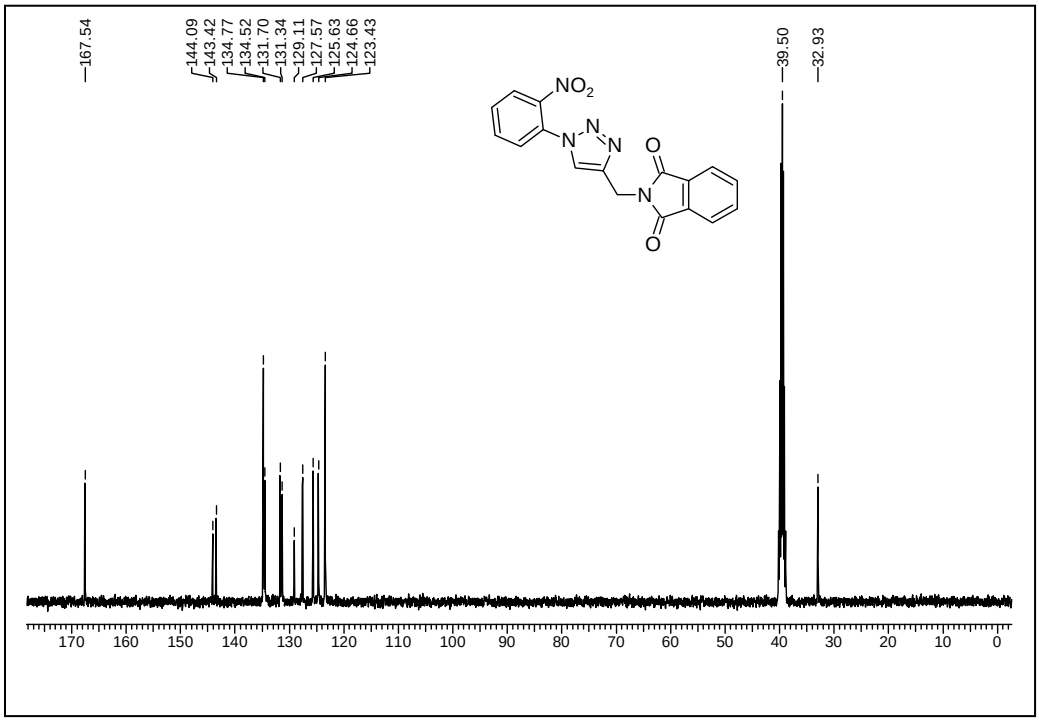

^{13}C NMR Spectrum of 2.74 in DMSO-d_6

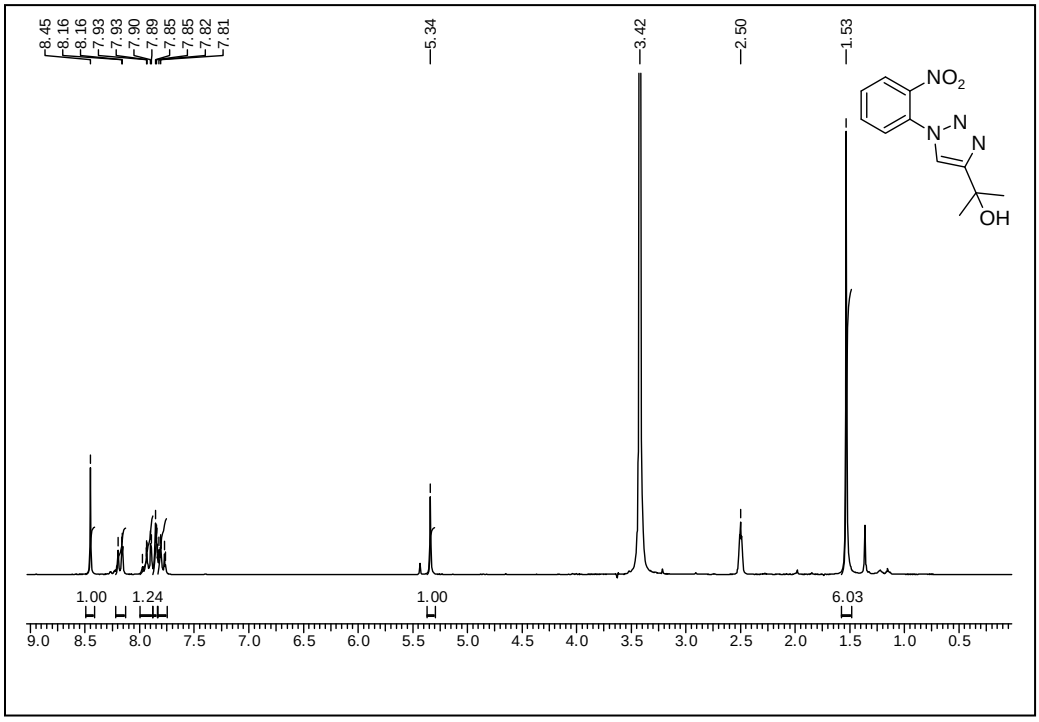

^{1}H NMR Spectrum of 2.75 in DMSO-d_6

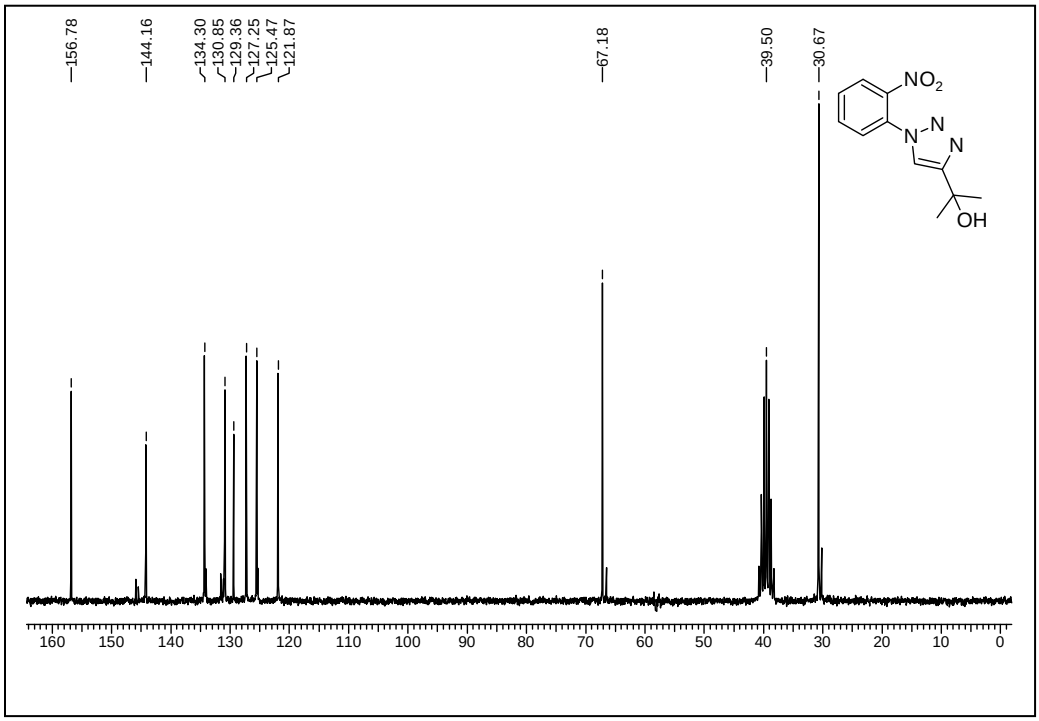

^{13}C NMR Spectrum of 2.75 in DMSO-d_6

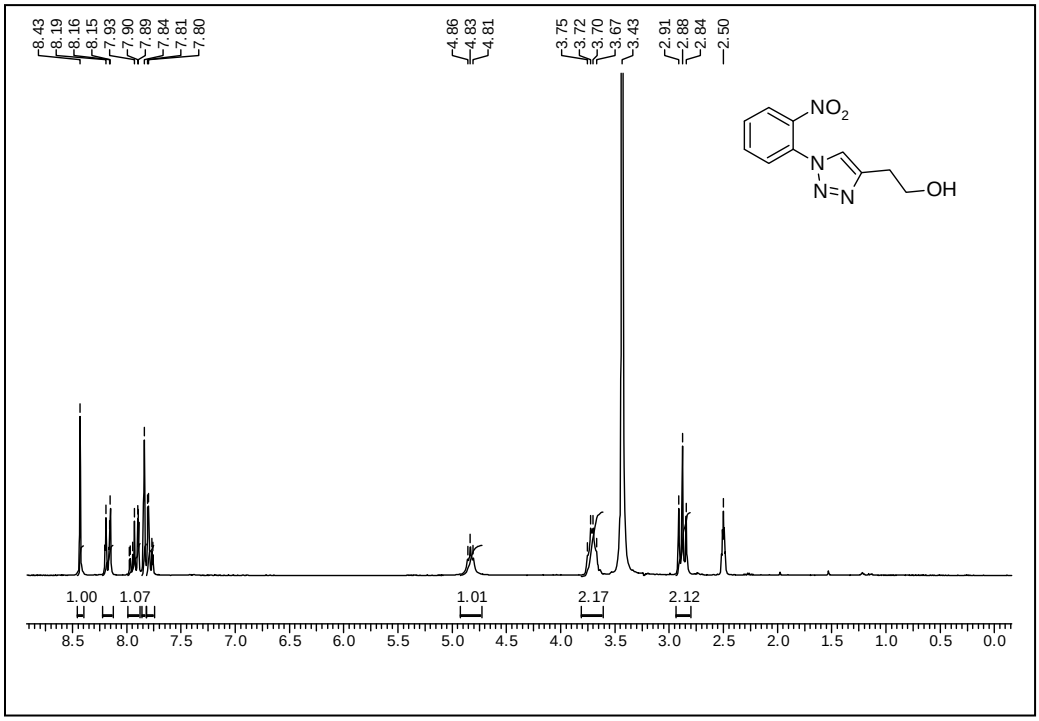

^{1}H NMR Spectrum of 2.76 in DMSO-d_6

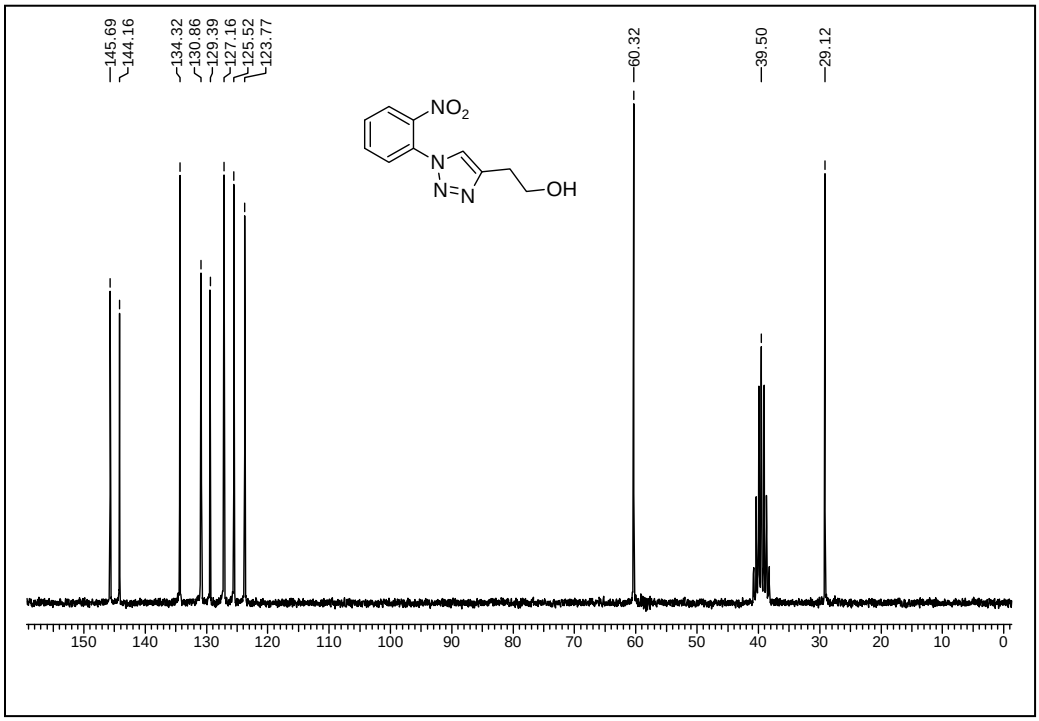

^{13}C NMR Spectrum of 2.76 in DMSO-d_6

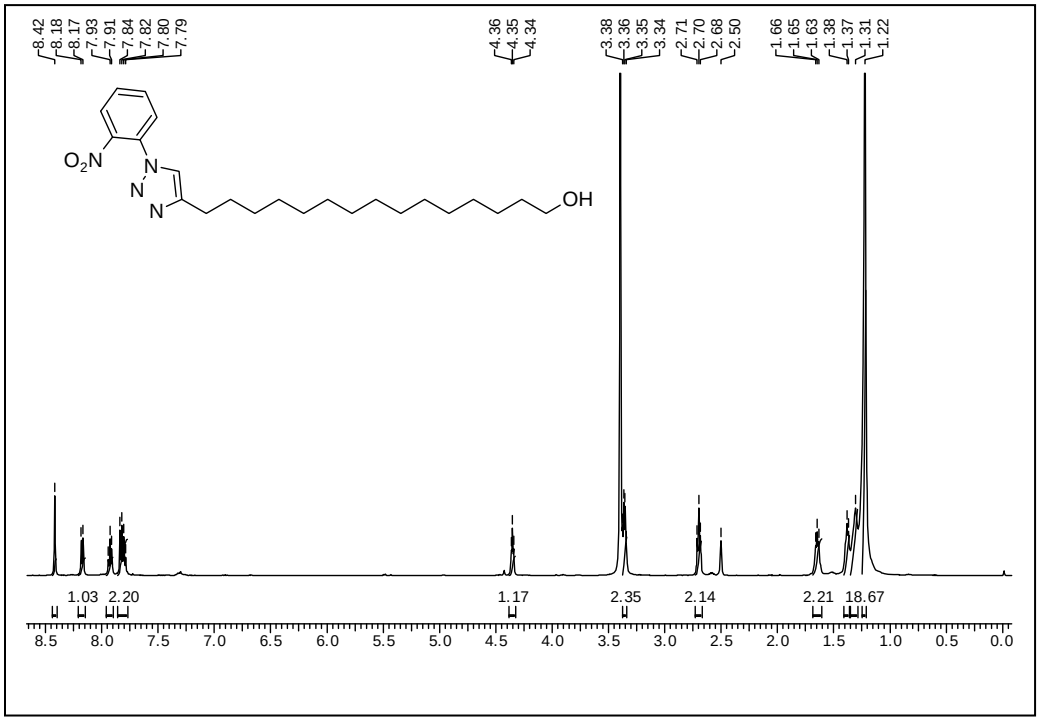

^{1}H NMR Spectrum of 2.77 in DMSO-d_6

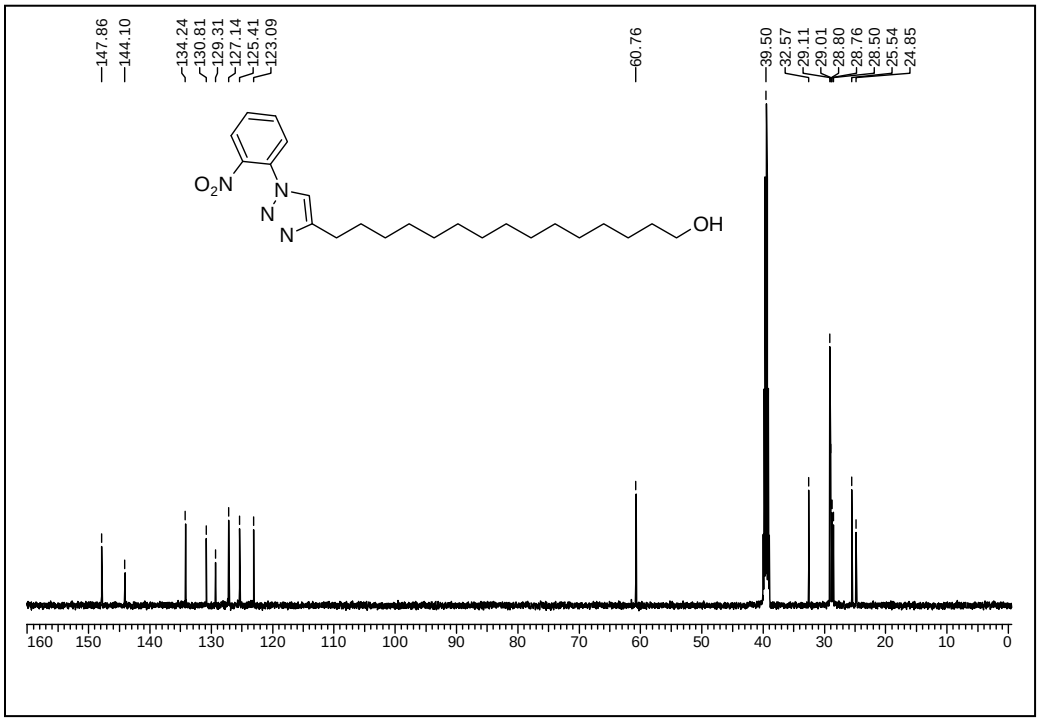

^{13}C NMR Spectrum of 2.77 in DMSO-d_6

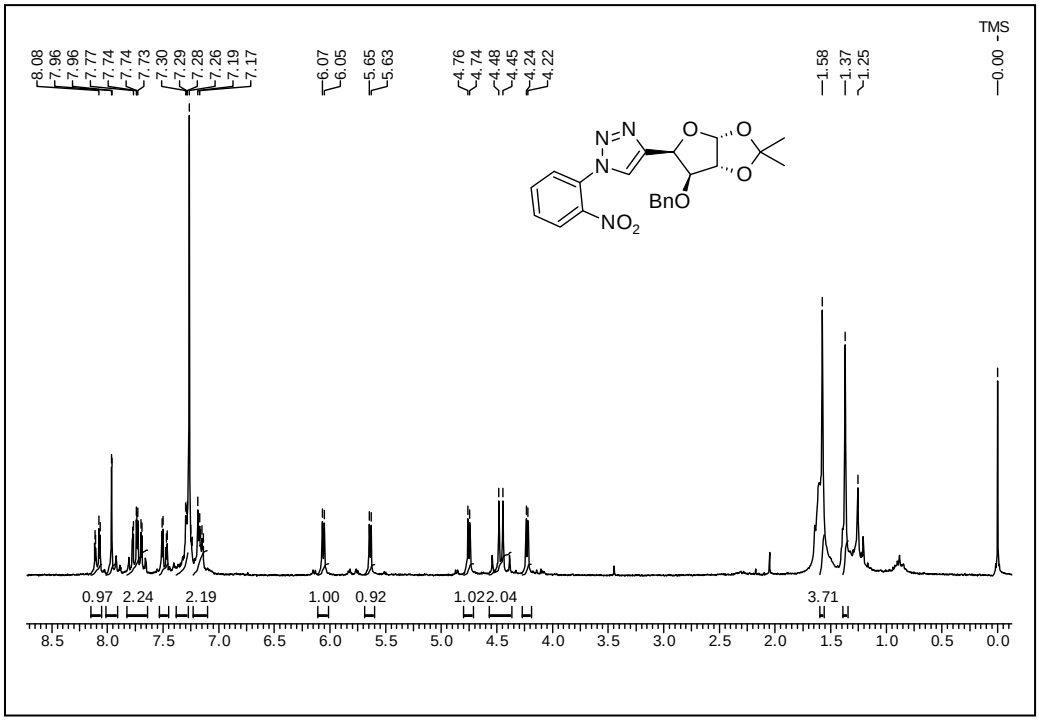

^{1}H NMR Spectrum of 2.79 in $CDCl_3$

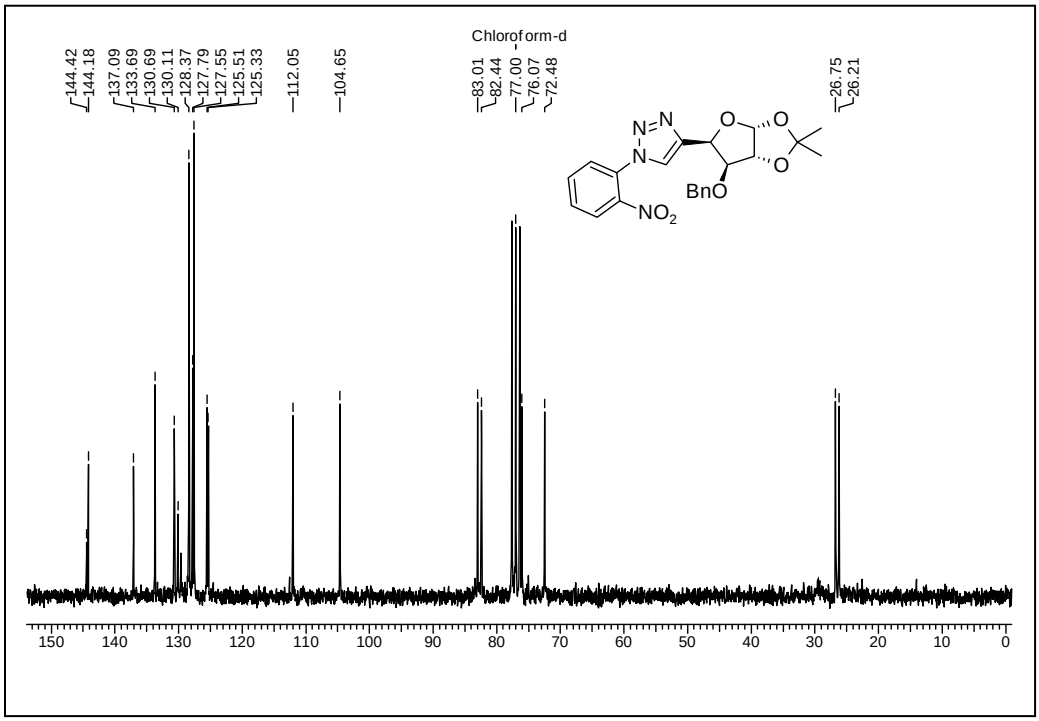

^{13}C NMR Spectrum of 2.79 in $CDCl_3$

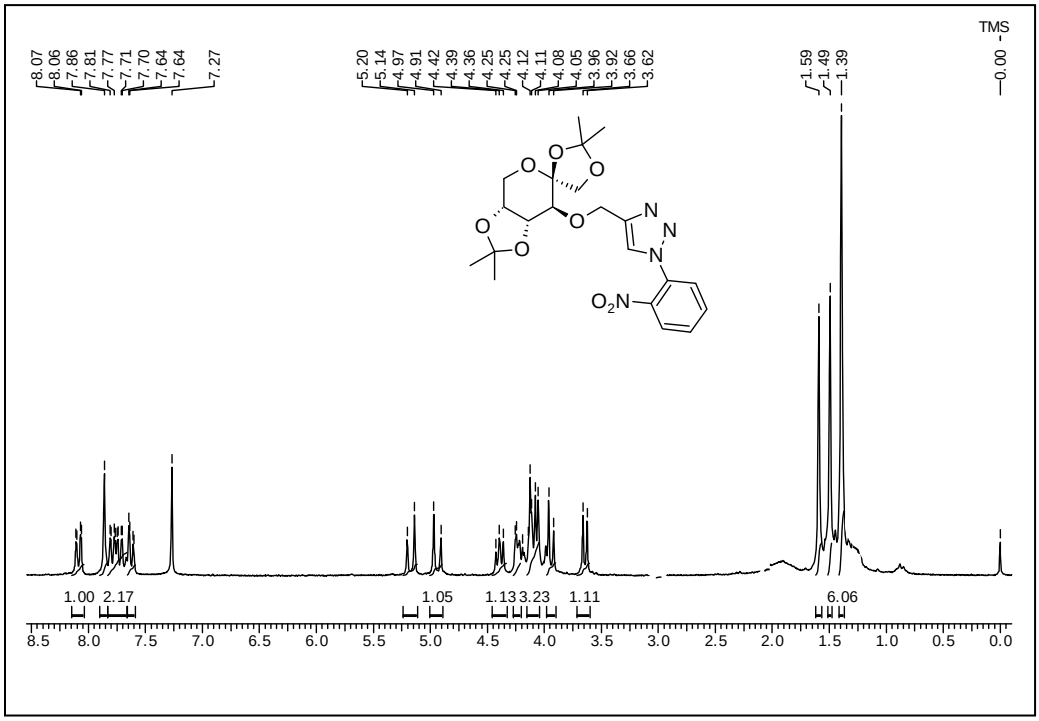

^{1}H NMR Spectrum of 2.80 in $CDCl_3$

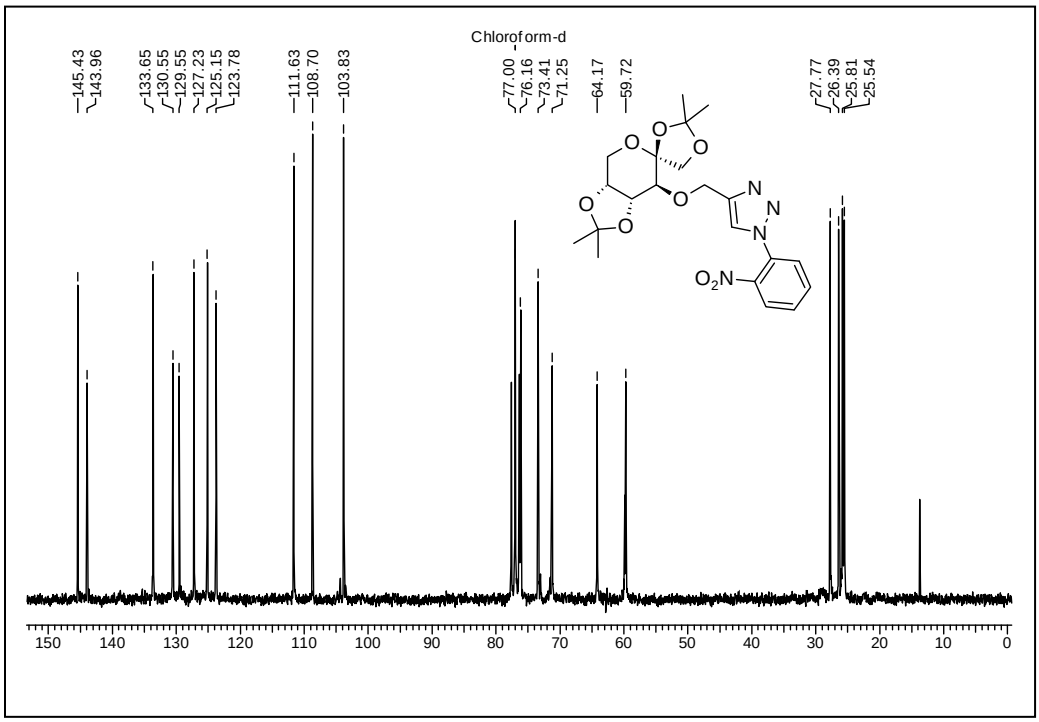

^{13}C NMR Spectrum of 2.80 in $CDCl_3$

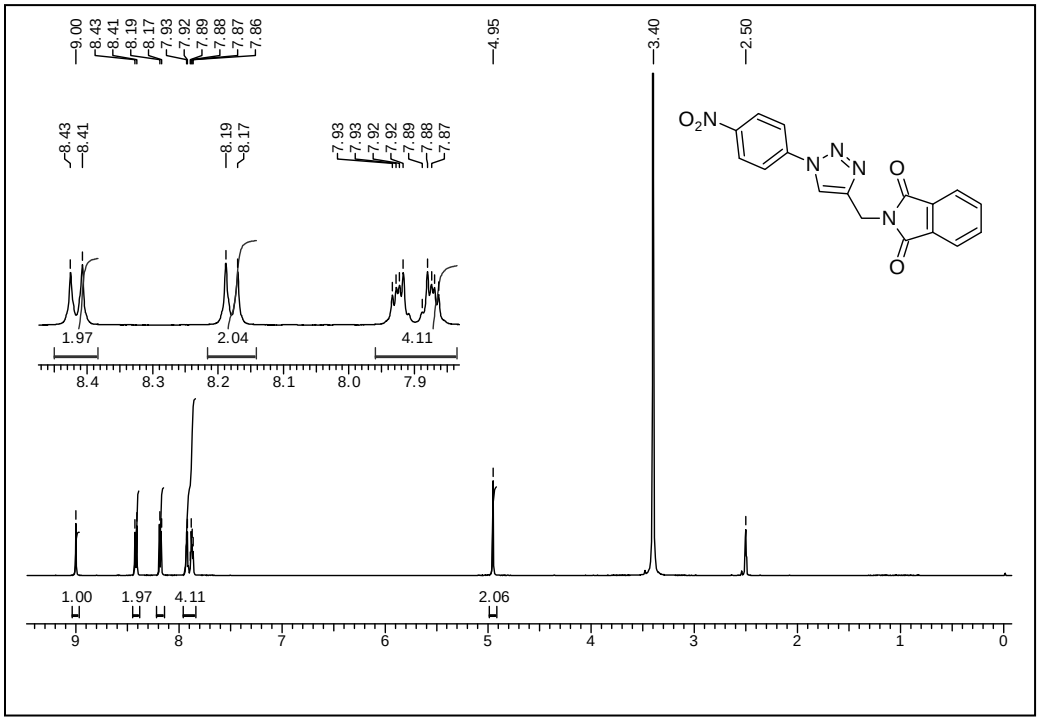

^{1}H NMR Spectrum of 2.84 in DMSO-d_6

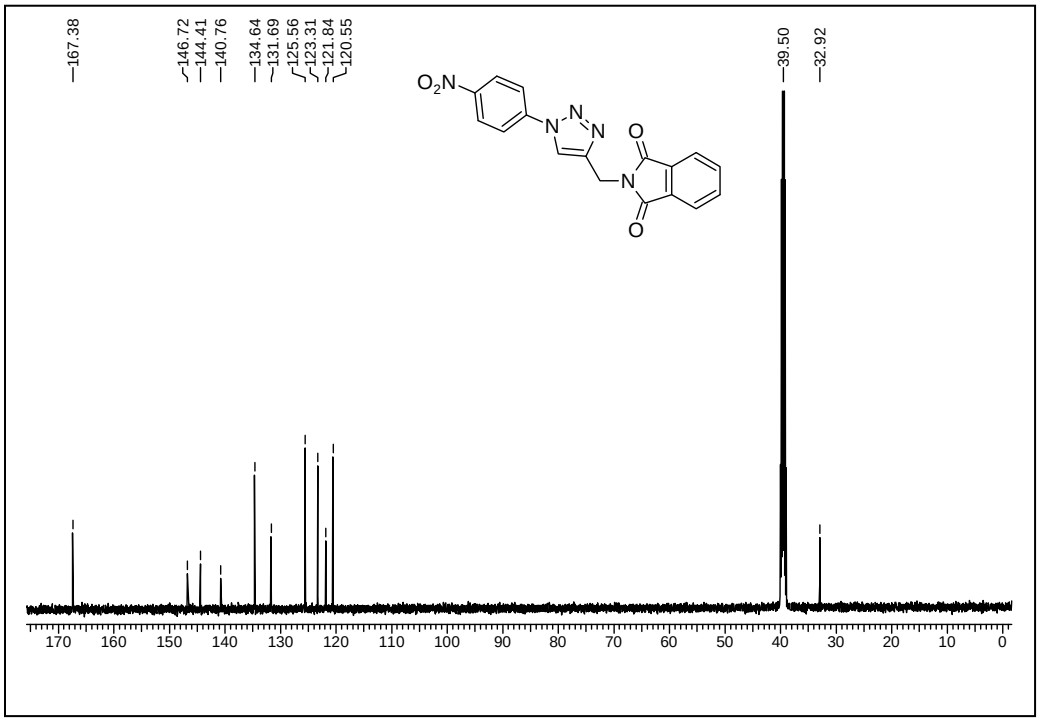

^{13}C NMR Spectrum of 2.84 in DMSO-d_6

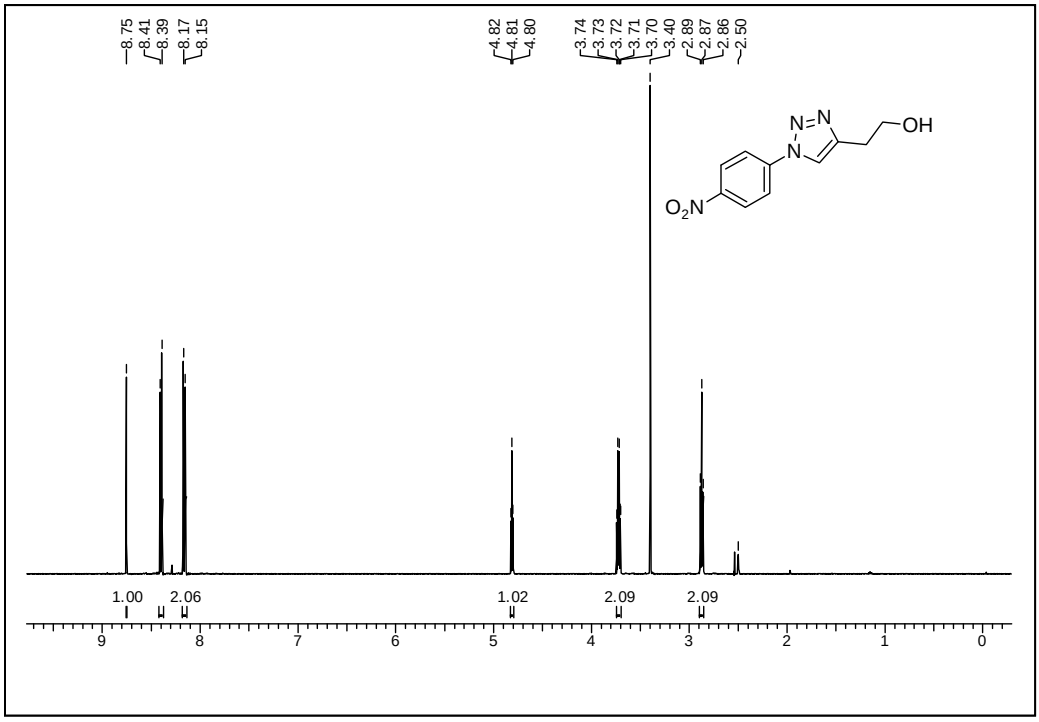

^{1}H NMR Spectrum of 2.86 in DMSO-d_6

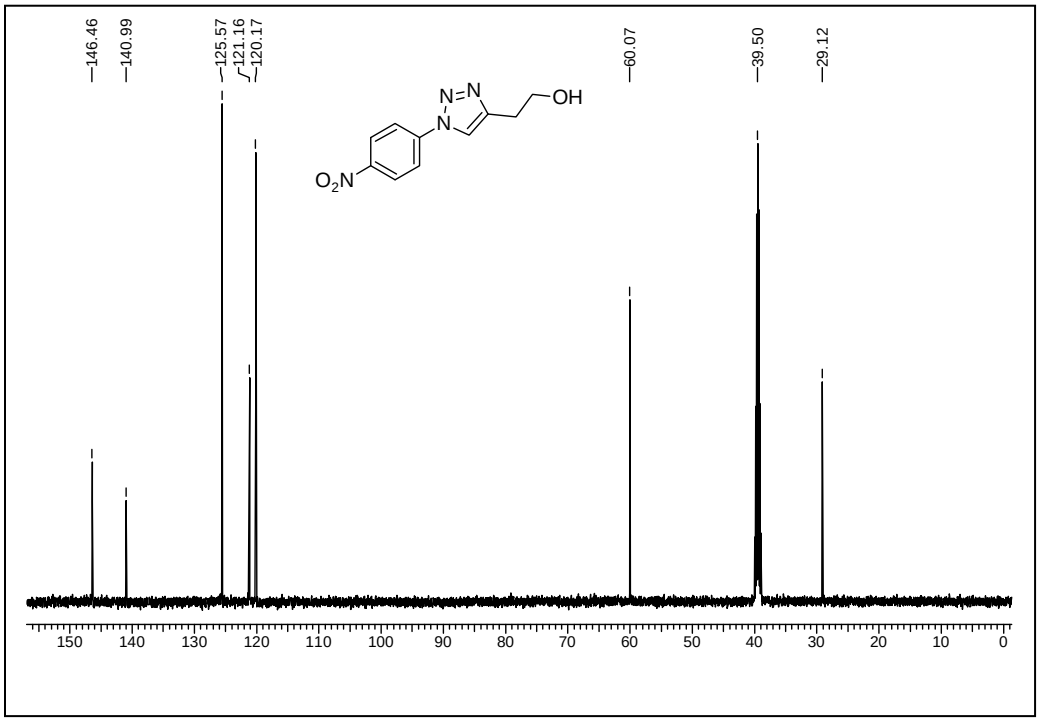

^{13}C NMR Spectrum of 2.86 in DMSO-d_6

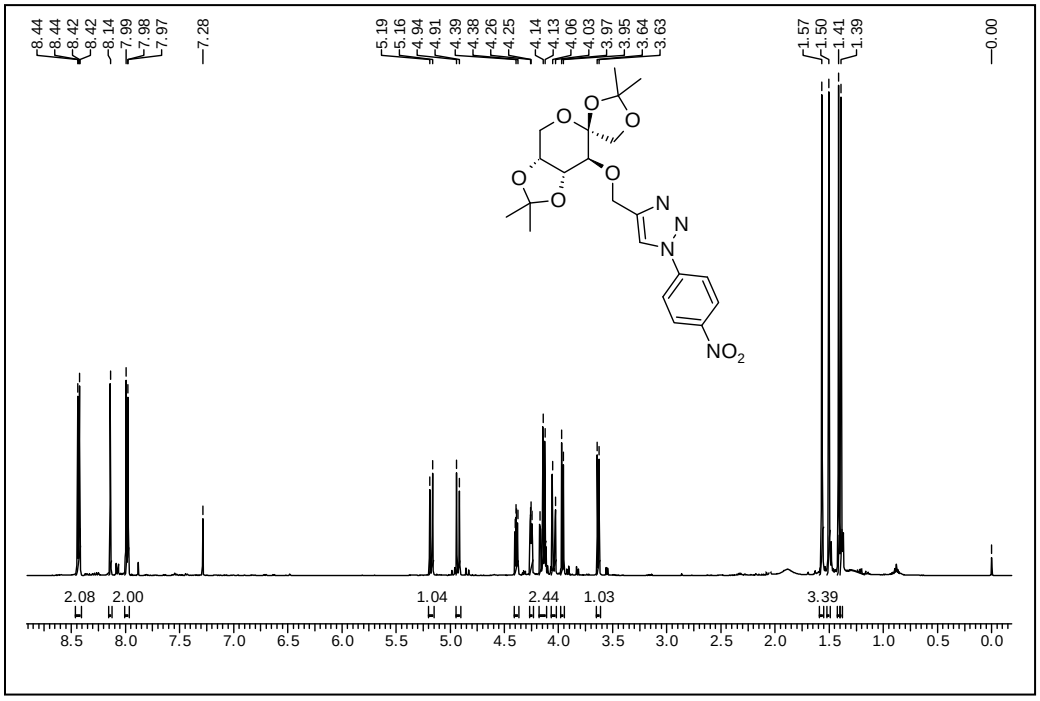

^{1}H NMR Spectrum of 2.87 in $CDCl_3$

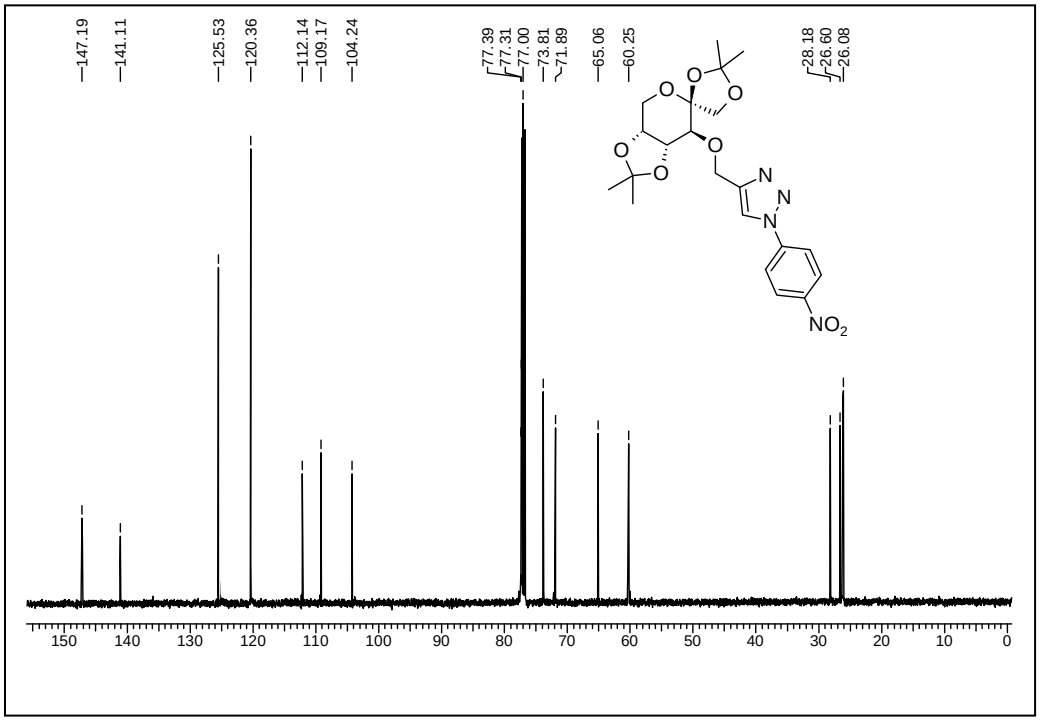

^{13}C NMR Spectrum of 2.87 in $CDCl_3$

2.5 References

1. a) Kolb, H. C.; Finn, M. G.; Sharpless, K. B. *Angew. Chem. Int. Ed.* **2001**, *40*, 2005–2021. b) Kolb, H. C.; Sharpless, K. B. *Drug Discovery Today* **2003**, *8*, 1128–1137. c) Binder, W. H.; Sachsenhofer, R. *Macromol. Rapid Commun.* **2007**, *28*, 15–54. d) Gil, M. V.; Arevalo, M. J.; Lopez, O. *Synthesis* **2007**, 1589–1620. e) Evans, R. A. *Aust. J. Chem.* **2007**, *60*, 384–395. f) Wolfbeis, O. S. *Angew. Chem. Int. Ed.* **2007**, *46*, 2980–2982.
2. Hüisgen, R. *1,3-Dipolar Cycloaddition Chemistry* (Ed.: A. Padwa), Wiley, New York. **1984**.
3. Tornøy, C. W.; Christensen, C.; Mendal, M. *J. Org. Chem*. **2002**, *67*, 3057–3064.
4. Rostovtsev, V. V.; Green, L. G., Fokin, V. V.; Sharpless, K. B. *Angew. Chem. Int. Ed*. **2002**, *41*, 2596.
5. Bock, V. D.; Hiemstra, H.; van Maarseveen, J. H. *Eur. J. Org. Chem*. **2006**, *1*, 51–68.
6. Alder, K.; Stein, T.; Finzenhagen, M. *Annalen* **1931**, *485*, 211–216.
7. Hüisgen, R. *Proceedings of the Chemical Society*, Centinary Lecture, **1961**, 357.
8. Saxon, A.; Bertozzi, C. R. *Science* **2000**, *287*, 2007–2010.
9. a) Gothelf, K. V.; Jorgensen, K. A. *Chem. Rev*. **1998**, *98*, 863–910. b) Mulzer, J. *Org. Synth. Highlights* **1991**, 77–95.
10. Katritzky, A. R.; Singh, S. K. *J. Org. Chem*. **2002**, *67*, 9077–9079.
11. Clarke, D.; Mares, R. W.; Mc Nab, H. *J. Chem. Soc. Perkin Trans. 1* **1997**, 1799–1804.
12. Reddy, K. R.; Rajgopal, K.; Kantam, M. L. *Synlett* **2006**, *6*, 957–960.
13. Appukkuttan, P.; Dehaen, W.; Fokin, V. V.; Van der Eycken, E. *Org. Lett.* **2004**, *6*, 4223– 4225.
14. Lutz, J. - F. *Angew. Chem. Int. Ed*. **2007**, *46*, 1018 and references therein.
15. Ramachary, D. B.; Barbas, C. F. *Chem. Eur. J.* **2004**, *10*, 5323–5331.
16. Ramachary, D. B.; Kishor, M.; Reddy, Y. V. *Eur. J. Org. Chem.* **2008**, 975–993.
17. Akritopoulou-Zanze, I.; Djuric, S. W. *Tetrahedron Lett.* **2004**, *45*, 8439–8441.
18. Chandrasekhar, S.; Rambabu, C. *Tetrahedron Lett.* **2006**, *47*, 3059–3063.
19. Luvino, D.; Amalric, C.; Vasseur, J.-J. *Synlett* **2007**, *19*, 3037–3041.
20. Fletcher, J. T.; Keeney, M. E. *Tetrahedron Lett.* **2008**, *49*, 7030–7032.

21. Yadav, J. S.; Reddy, B. V. S. *Tetrahedron Lett.* **2007**, *48*, 8773–8776.
22. Barral, K.; Moorhouse, A. D.; Moses, J. E. *Org. Lett.* **2007**, *9*, 1809–1811.
23. Beckmann, H. S. G.; Wittmann, V. *Org. Lett.* **2007**, *9*, 1–4.
24. Fokin, V. V.; Appukkuttan, P.; Dehaen, W. *Org. Lett.* **2004**, *6*, 4223– 4225.
25. Feldman, A. K.; Colasson, B.; Fokin, V. V. *Org. Lett.* **2004**, *6*, 3897–3899.
26. Ackermann, L.; Potukuchi, H. K.; Landsberg, D. *Org. Lett.* **2008**, *10*, 3081– 3084.
27. (a) Smith, M. B.; March, J. *Advanced Organic Chemistry*, Wiley-Interscience, New York, 2001, 5th edn, ch. 13, p. 850. (b) Terrier, F. (1991) *Nucleophilic Aromatic Displacement*, VCH Publishers, New York. (c) Paradisi, C. *Comprehensive Organic Synthesis*, Pergamon Press, Oxford, 1991, vol. 4, pp. 423–450. (d) Buncel, E.; Dust, J. M.; Terrier, F. *Chem. Rev.*, **1995**, *95*, 2261–2280. (e) Zoltewics, J. A. *Top. Curr. Chem.* **1975**, *59*, 33–64. (f) Bunnett, J. F.; Zahler, R. E. *Chem. Rev.* **1951**, *49*, 273–412.
28. (a) Shen, H. C.; Ding, F.-X.; Colletti, S. L. *Org. Lett.* **2006**, *8*, 1447–1450. (b) Li, F.; Meng, Q.; Chen, H.; Li, Z.; Wang, Q.; Tao, F. *Synthesis* **2005**, 1305–1313. (c) Chung, I. S.; Kim, S. Y. *J. Am. Chem. Soc.* **2001**, *123*, 11071–11072. (d) F. Terrier, In *Nucleophilic Aromatic Displacement: The Influence of the Nitro Group*; VCH Publishers: New York, 1991.
29. (a) Qu, G.-R.; Xia, R.; Yang, X.-N.; Li, J.-G.; Wang, D.-C.; Guo, H.-M. *J. Org. Chem.* **2008**, *73*, 2416–2419. (b) Lee, J.-K.; Fuchter, M. J.; Williamson, R. M.; Leeke, G. A.; Bush, E. J.; McConvey, I. F.; Saubern, S.; Ryan, J. H.; Holmes, A. B. *Chem. Commun.* **2008**, 4780–4782. (c) Krchňák, V.; Moellmann, U.; Dahse, H.-M.; Miller, M. J. *J. Combi. Chem.* **2008**, *10*, 104–111. (d) El Akkaoui, A.; Koubachi, J.; El Kazzouli, S.; Berteina-Raboin, S.; Mouaddib, A.; Guillaumet, G. *Tetrahedron Lett.* **2008**, *49*, 2472–2475. (e) D'Anna, F.; Marullo, S.; Noto, R. *J. Org. Chem.* **2008**, *73*, 6224–6228. (f) Coelho, P. J.; Carvalho, L. M. *Dyes and Pigments* **2008**, *78*, 173–176
30. (a) Miller, J.; Parker, A. J. *J. Am. Chem. Soc.* **1961**, *83*, 117–123. (b) Hill, D. L.; Ho, K. C.; Miller, J. *J. Chem.Soc. B.* **1966**, 299–309. (c) Landini, D.; Maia, A.; Montanari, F. *J. Chem. Soc., Perkin Trans. 2* **1983**, 461–466 (d) Danikiewicz, W.; Bieńkowski, T.; Kozłowska, D.; Zimnicka, M. *J. Am. Soc. Mass Spec.* **2007**, *18*, 1351–1363.
31. Cox, B. G.; Parker, A. J. *J. Am. Chem. Soc.* **1973**, *95*, 408–410.
32. Acevedo, O.; Jorgensen, W. L. *Org. Lett.* **2004,** *6*, 2881–2884.
33. Ramana, C. V.; Induvadana, B. *Tetrahedron Lett.* **2009**, *50*, 271–273.
34. Saha, B.; Sharma, S.; Sawant, D.; Kundu, B. *Synlett* **2007**, 1591–1594.

35. Wang, Z.-X.; Qin, H.-L. *Chem. Commun.* **2003**, *9*, 2450–2451.
36. Messori, V.; Baldi, L.; Bianchetti, G. *Chimica e l'Industria* **1977**, *59.*
37. Huisgen, R.; Moebius, L.; Szeimies, G. *Chem. Ber.* **1965**, *98*, 1138–1152.
38. Krasinski, A.; Fokin, V. V.; Sharpless, K. B. *Org. Lett.* **2004**, *6*, 1237–1240.
39. Trost, B. M.; Rhee, Y. H. *Org. Lett.* **2004**, *6*, 4311–4313.
40. Ramana, C. V.; Giri, A. G.; Suryawanshi S. B.; Gonnade, R. G. *Tetrahedron Lett.* **2007**, *48*, 265–268.
41. Hausherr, A.; Orschel, B.; Scherer, S.; Reissig, H.-U. *Synthesis* **2001**, 1377–1385.
42. Trost, B. M.; Rhee, Y. H. *Org. Lett.* **2004**, *6*, 4311–4313.

CHAPTER-II

Section II: "Click" synthesis of isomeric compounds for assessing the efficiency of bifurcated Cl···NO_2 synthon.

2.6 INTRODUCTION

2.6.1 Crystal Engineering

The term crystal engineering can be explained as the understanding of intermolecular interactions in the context of crystal packing and in utilization of such understanding in the design of new solids with desired physical and chemical properties.[1] The importance of crystal engineering lies in the fact that the physical properties of a solid are dictated by the crystal packing of the compound, that is, how the modular components of a compound are oriented with respect to each other in three dimensions. To generate a stable, three-dimensional, predictable architecture, control of the assembly process is crucial and will only be realized by careful choice of suitable intermolecular 'connectors', as intermolecular interactions constitute the supramolecular 'glue'.

While applying crystal engineering into organic synthesis, different strategies will come into consideration where the molecules aggregate to form an assembly. In this aggregation some intermolecular linkers play a major role. In crystal engineering studies this linkers are named as *supramoleclar synthons*. The term *synthon* has been used in organic chemistry for many years. Corey's original definition of a *synthon* is "structural units within molecules which can be formed and/or assembled by known or conceivable synthetic operation."[2] The concept of *synthon* revolutionized organic synthesis as it is the basis of retrosynthetic analysis whereby some target molecule is broken down into successively simpler fragments until suitable starting materials are found. The *synthon* defines the connectivity between two fragments. Desiraju has applied this 'disconnection approach' to supramolecular chemistry.[3] Any supramolecular network can be broken into nodes (molecules) and node connectors (*synthons*). If molecules are built by connecting atoms together with covalent bonds, then supramolecular assemblies (crystals) are built by connecting molecules together with intermolecular forces.

Schmidt was the first person to coin the term 'crystal engineering' in a study of photochemical reactions of cinnamic acid derivatives in 1964.[4] Since then the field has greatly expanded to include areas as diverse as coordination polymers,[5] shape selective catalysis,[6] chemical sensors,[7] and non-linear optics.[8]

Although the main concern of crystal engineering is the bond connectivity but the nature of that connection especially in organic chemistry is very important. Organic

chemistry is defined in terms of covalent bonding between atoms. Supramolecular chemistry on the other hand is a relatively new scientific discipline and as such can not rely on a similar function. Like organic synthesis, supramolecular chemistry is concerned with connectivity. This connectivity, however, extended over a larger range and encompasses intermolecular forces rather than intramolecular bonds. In supramolecular chemistry, intermolecular forces link molecules together to form three-dimensional solids. Intermolecular forces comprise a number of different interactions including hydrogen bonds, van der Waals forces, dipole-dipole interactions and hydrophobic forces.

Figure 2.7 *Some supramolecular synthons used to generate infinite networks*

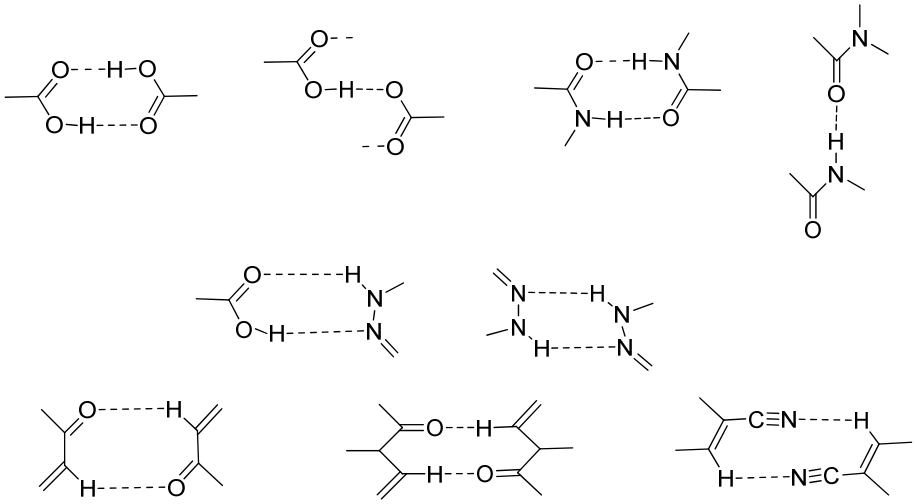

The fundamental objective of crystal engineering is to design organic solids that can find applications in material chemistry.[9] This needs to integrate our understanding about the interactions of various types and strengths that glue the molecules in the crystal structures, recognition events of complimentary functional groups, geometrical and topological constraints for intermolecular connectivity.[10] In this context identifying the interaction patterns[11] of supramolecular synthons[12] and understanding how these operate/exist across a set of related molecules that yield a set of related crystal structures are critical exercises to ensure three-dimensional structure control in molecular design for crystal engineering. Molecular design by employing conventional hydrogen bonding has been extensively practiced.[13] However, a number of weaker and softer interactions and respective synthons have been identified. The nature of these weak interactions in crystal structures can vary from passive to supportive (structure stabilization) to one that is

actually intrusive (structure destabilization).[14] Attempts to understand how these weak/soft interactions operate/exist across a set of related molecules has been limited to simple aromatic systems or to flexible biaryl systems containing stronger interactions too and this in general resulted with no similarities in the crystal structures of isomeric compounds.[15] For example, Glidewell and co-workers have examined the occurrence of I…NO_2 synthon employing diaryl compounds connected through a variety of polar functional groups and varying the I and NO_2 groups positions systematically. However, it led to the conclusion that the aggregation pattern for any one compound is not readily predictable from knowledge of the patterns in the other isomers. Apart from this, there are very few investigations that address predictability of weak synthons in isomeric compounds especially in absence of any strong non-covalent interactions.[16] Partly, this is because of the complexity involved in synthesizing the systems with architectural control and flexibility in the incorporation of functional groups and a deliberate suspicion about the crystallinity of the all isomers. In this context, developing simple and efficient protocols for generation of isomeric compound libraries (devoid of polar functional units) with sufficient flexibility in placing complimentary functional groups will be instrumental for crystal engineers to understand these weak non-covalent interactions, the topological constraints for intermolecular connectivity and to examine the predictability of corresponding weak synthons. To know about crystal engineering in details, all the major interactions associated with the crystal structures are to be discussed. Major interactions those affect/giude the crystal stuctures are divided into mainly two parts, 1) primary strong interactions 2) secondary weak interactions. It is observed that in major cases the stronger interactions guide the crystal orientation/packing but in absence of stronger interactions crystal structures are mainly guided by weaker interactions. Most interestingly, sometimes it is also seen that in presence of stronger interactions also srtuctural orientations are governed by the weaker interactions. So the role of all major interactions (stronger/weaker) are discussed here in brief.

2.6.2 Hydrogen Bonding

Amongst the various non-covalent interactions, hydrogen bonding is of major interest in crystal engineering. A formal definition of a hydrogen bond is difficult to express succinctly in words. For many years, hydrogen bonds were thought to obey the definition of Atkins[17] “a link formed by a hydrogen atom lying between two strongly

electrostatic atoms such as oxygen, nitrogen, fluorine". However, it is now widely accepted that a hydrogen atom attached to less electronegative atoms *e.g*. carbon, sulfur *etc*., can form a hydrogen bond with a variety of less electronegative acceptors *e.g*. S, Se, Cl, Br, I, π. It is primarily electrostatic in nature whereby a small finite positive charge is associated with hydrogen atom. The donor and acceptor atoms have a slightly negative charge associated with them, (at least relative to the hydrogen atom).

Figure 2.8 *Partial charges shown for donor and acceptor atoms in a hydrogen bond*

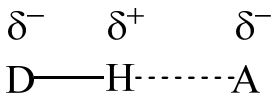

From the previous description of a hydrogen bond, it is evident that a great variety of donor and acceptor atoms of differing electronegativity can participate in a hydrogen bond. Therefore the strength of any one hydrogen bond can also vary greatly.

2.6.3 C-H…O/N interactions

In recent years, the weaker hydrogen bonds C-H…..O, X, N (where X= F, Cl, Br, I) have been recognized as viable intermolecular forces for constructing functional solids.[3] Even though inherently weaker than conventional D-H….A, (where D, A= O, N, F) weaker interactions used in sufficient numbers can generate predictable architectures. In particular, C-H…..O interaction has received significant attention both in terms of understanding their nature and as a directional force in crystal engineering.[18] Very often C-H…..O interactions occur in structures where stronger hydrogen bonds also exist. Obviously, stronger hydrogen bonds donors will compete more effectively for oxygen acceptor sites, relegating C-H…O interactions to a subservient role in architecture formation. However, there are many examples in the literature, where C-H…O interactions are primary structure forming agents.[19] In these cases stronger hydrogen bonds interactions are absent.

Desiraju[20] has recently published a comparative study of C-H…O, C-H…N, interactions involving similar hydrogen bonding patterns in the structures of 1,4-benzoquinone,[21] and 1,4-dicyanobenzene.[22] In all the structures the same one dimensional chain architectures are formed.

Figure 2.9 *Similar hydrogen bonded patterns are formed in (a) via C-H…O interactions and (b) via C-H…N interactions*

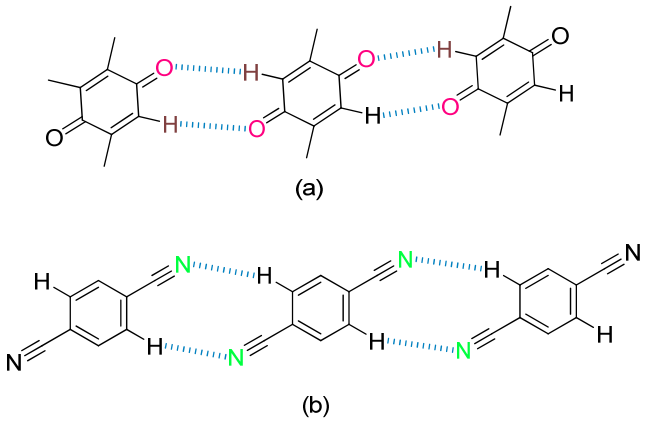

While discussing C-H…O interactions, it must be mentioned that in carboxylic acid structures two distinct motifs are displayed. First, the common acid-acid dimer motif in which each acid group links *via* hydrogen bonds through the carboxylic acid hydrogen to the carbonyl acceptor of the adjacent acid group. Frequently when the acid has a substituent in the *para* position, the dimers link together using C-H…O interactions to generate two-dimensional sheets.[23]

Figure 2.10 *C-H…O hydrogen bonding in para substituted aromatic compounds*

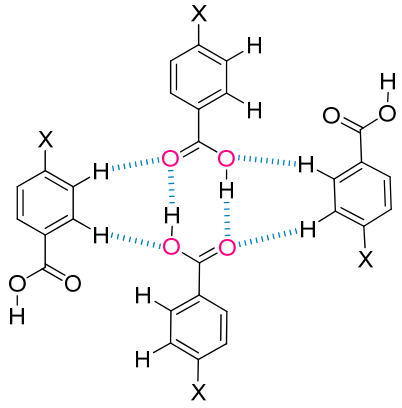

A much less common motif is the hydrogen-bonded catamer pattern. This produces a one-dimensional chain in which each carboxylic acid unit links to two others.

Figure 2.11 *Hydrogen-bonded pattern of a catamer motif*

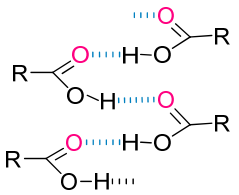

The study shows that weaker hydrogen bond interactions (C-H……O/N) possess directionality and robustness and hence can be used as structure-directing agents. Intermolecular interactions of the type C-H…X where X=F, have also received attention in the literature[24] as viable forces for crystal engineering, although for, X= Cl, Br, I, some questions remain as to whether they are robust enough.

2.6.4 Halogen ‑ Halogen interactions:

Speculation and debate has surrounded X…X interactions for many years. Their strength, nature, directionality are still poorly understood with little literature being published. Research was subdivided into two areas: (a) influence of X…X on molecular hydrogen-bonded crystals and (b) influence of X…X forces on ionic hydrogen-bonded networks.

Figure 2.12 *Short Cl…Cl contacts seen in the structure of 1,4-dichlorobenzene*

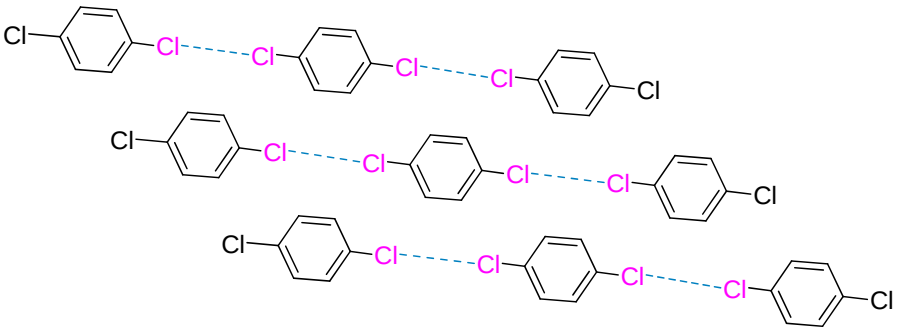

Supramolecular synthon must be robust enough to form in the presence of other intermolecular interactions such as C-H…O, C-H…X, π-π, hydrophobic forces, *etc*., if they are to be a structural tool in crystal engineering. The nature of halogen-halogen interactions are still under controversy. Many halogen-containing molecular crystals exhibit X…X contacts (where X = Cl, Br, I) that are significantly shorter than the sum of the van der Waals radii, (r_{Cl}=1.75 Å, r_{Br}=1.85 Å, r_{I}= 2.05 Å).[25]

These short distances are associated with certain angular geometric preferences defined by the angles θ and ϕ.

Figure 2.13 *(a) Type I contacts where θ = ϕ and (b) Type II contacts where θ = 180° and ϕ = 90°*

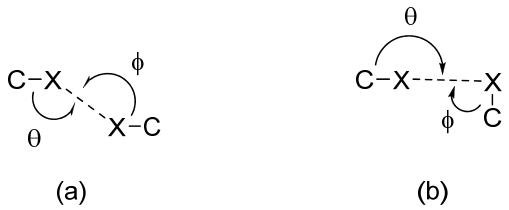

This observation is not new, but explanations of the nature of these contacts have only been postulated in recent years, with two different hypotheses being proposed. Using the crystallographic structure database (CSD), Desiraju *et al.*, have analyzed 794 crystal structures for short X…X contacts and found that as polarizability of the halogen atom increases, type II contacts become more significant than type I contacts.[26] They concluded that they are weak, attractive interactions due to induced polarization of the valence electron cloud of each atom.

Stone *et al.*, have proposed a different model where the inherent anisotropy of halogen atoms causes them to pack together in a least repulsive manner resulting in short X…X distances.[27] The debate has still not been resolved and indeed it has been noted that it is inherently difficult to distinguish between specific attractive forces *i.e*, increased attraction and nonspherical atoms packing closely together *i.e*, decreased repulsion.[28]

However, there is convincing evidence that short F…F contacts are unfavourable.[29] Theocharis *et al*., concluded that the small van der Waals radius for fluorine (1.47 Å) coupled with its high electronegativity, has a repulsive effect and causes adjacent molecules to pack in a manner so as to maximize non-bonded F…F distances.

2.6.5 Bifurcated halogen interactions:

This interaction is the extension of halogen-halogen interaction, the only difference here is another interacting atom which is other than halogen (mainly oxygen of nitro group). Bifurcated halogen bonds have attracted a great deal of interest in recent years because these weak three-center interactions play a crucial structural role in crystal architecture. Desiraju and co-workers first described the identification of the I…O mediated, iodo…nitro supramolecular synthon and its use in retrosynthetically guided

supramolecular synthesis as well as in the design of organic crystals with the property of second harmonic generation (SHG).[3,30] Allen *et al.*, examined the geometrical preferences of X(Cl, Br, I)…O(nitro) synthons and concluded that the C-X…O angles prone to linearity as the X…O shortens.[31] More recently Nangia and co-workers have reported that these soft and weak three-center interactions can be regarded as a 'discriminator synthon' even in the presence of strong N-H…O hydrogen bonds.[32] These X…O_2N contacts are of three types: a bifurcated contact where both the distances are equal ($D_1 \approx D_2$), a more unsymmetrical contact where D1> D2 and finally a contact where only one of the two nitro group O-atoms makes a contact with atom X. Generally the proportion of the first case decreases as one proceeds from Cl→Br→I. These trends have been generally noted in subsequent studies.

Figure 2.14 *Three types of halo…nitro interactions*

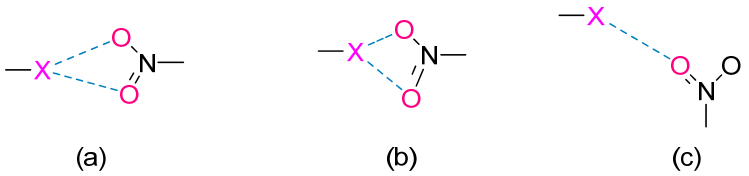

Out of many other types of chain patterns, infinite ribbons are formed using the I…O_2N synthon when 4-iodonittrobenzene crystallizes.

Figure 2.15 *Infinite chains of 4-iodonittrobenzene*

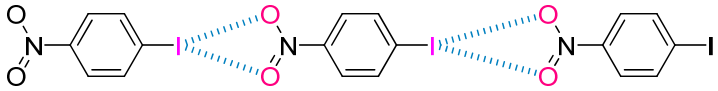

The bifurcated halo…nitro synthon, especially the iodo…nitro interaction has been a topic of extensive research in the recent years. Several groups have designated it as a robust synthon and as a predictable interaction that can be extended in the crystal engineering. However, on several occasions, the predictability correlate the interaction patterns intermolecularly between a series of compounds where the nitro-substituted aromatic ring is connected with a halo substituted aromatic ring through a suitable linker. But serious problems often arise in that no correspondence in molecular and crystal structure is easily perceived. This happens for several reasons, out of that the most difficult issue is the presence of polar connectors having stronger interactions, which

suppress the weaker interactions present in the molecules. Moreover, a little change in position or functionality in the system may cause a huge change in the intermolecular interactions.

Glidewell and co-workers[33] have tried with different linkers to find out the correlation but all the linkers were polar enough to dominate within the system.

Figure 2.16 *Series of isomeric compounds with different polar linkers*

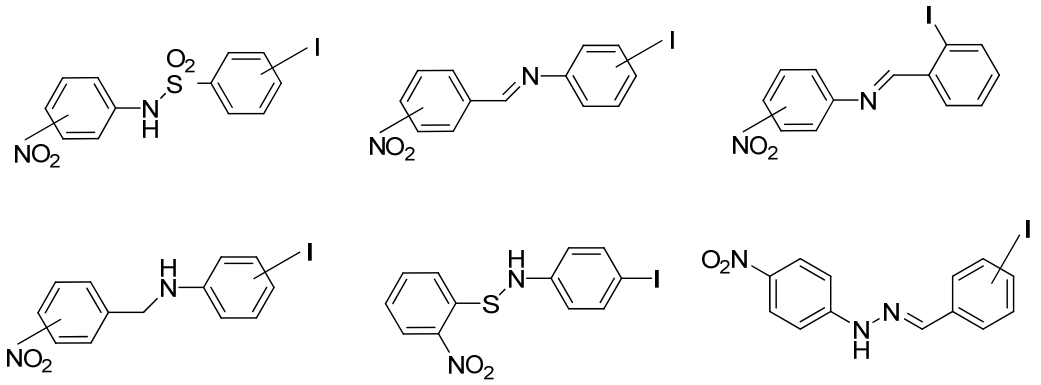

It is very important to note that, within each series of isomers, no two compounds manifest the same selection of direction-specific intermolecular interactions and, again within each series, no one structure is readily predictable from a knowledge of all the others. With the results obtained in mind they extended their studies towards more rigid isomeric systems N-(iodophenylnitrophthalimides) where polar linkers are excluded so that the hard hydrogen bonding interactions can be eliminated and the molecular frameworks have only a single degree of torsional freedom, about the N-aryl bond, so restraining somewhat the range of possible intermolecular interactions.[34]

Figure 2.17 *Isomeric compounds of somewhat rigid conformation*

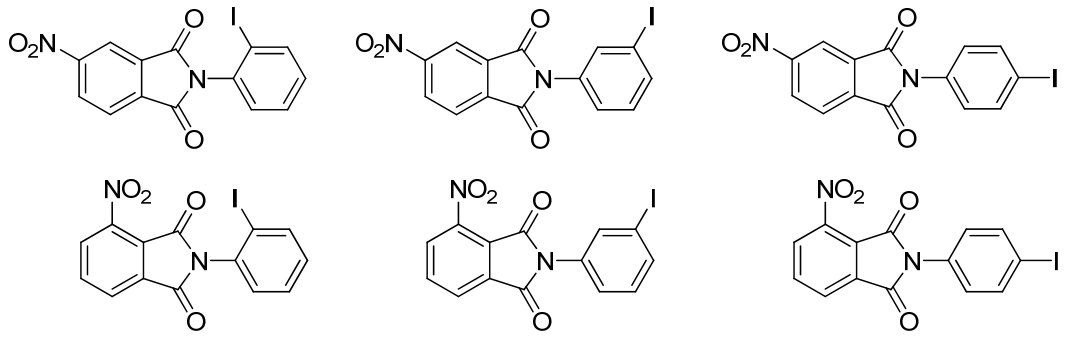

Although, here the polar linkers were removed and slight rigidity was brought into the system but still from thorough investigation of the different crystallographic data obtained from these isomeric compounds it is noteworthy to mention that, again it is difficult to discern any pattern in the intermolecular interactions which can provide a convincing interpretation of the conformational characteristics.

Recently Nangia and co-workers[35] also tried to find correlation between isomeric compounds with suitable disposition of nitro and halo group in unsymmetrical urea derivatives but the pattern similarity between the isomeric compounds was still not clearly understood.

Figure 2.18 *Chemical structures of unsymmetrical diaryl urea derivatives*

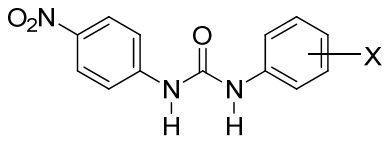

X = 4-F, 4-Cl, 4-Br, 4-I, 3-Br, 3-I

From the examples provided above that deal with the structural analyses of a group of isomeric compounds, it is evident that there is a need for a suitable soft linker with out any functional unit that can form the strong non-covalent interactions without any substantial conformational flexibility. One of fundamental requirement here is the flexibility and practicality in the incorporation of this linker. In this context, we have selected the currently coroneted "triazole-linker" in a variety of applications ranging from medicine, biology, to materials, as a soft linker and intended to introduce it in the area of crystal engineering.

2.6.6 "Click Chemistry" and the Triazole Linker

Click chemistry was postulated initially as a specific organic reaction but by time it became a very important tool in different fields of chemistry. The major improvement was seen in materials chemistry.[36] In 2004, Hawker, Fokin, Sharpless, and co-workers have reported the first illustration on this field. Afterwards, the popularity of click chemistry within the materials science grew considerably by the influential works of Hawker, Fréchet, and Finn. Hawker, Fokin, Sharpless, and co-workers explored first the CuAAC of various molecular building blocks for the convergent synthesis of dendrimers.

Overall, this method was found to be a straightforward strategy for the large-scale synthesis of triazole-based dendrimers. Shortly after, Finn and co-workers studied the click cycloaddition of azide- and alkyne-functionalized monomers for the preparation of either linear polymer chains or three-dimensional polymer networks. The latter was investigated as novel adhesives for copper surfaces, as triazole rings have a strong ability to coordinate transition metals.

Figure 2.19 *Examples of linear polymer structures*

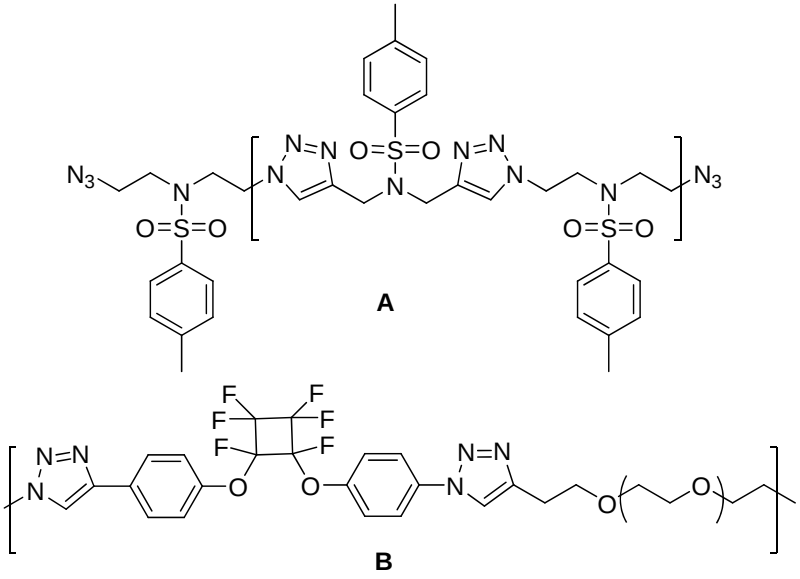

Figure 2.20 *Variations of simple theme: Examples of macromolecular architectures obtained by Click reaction*

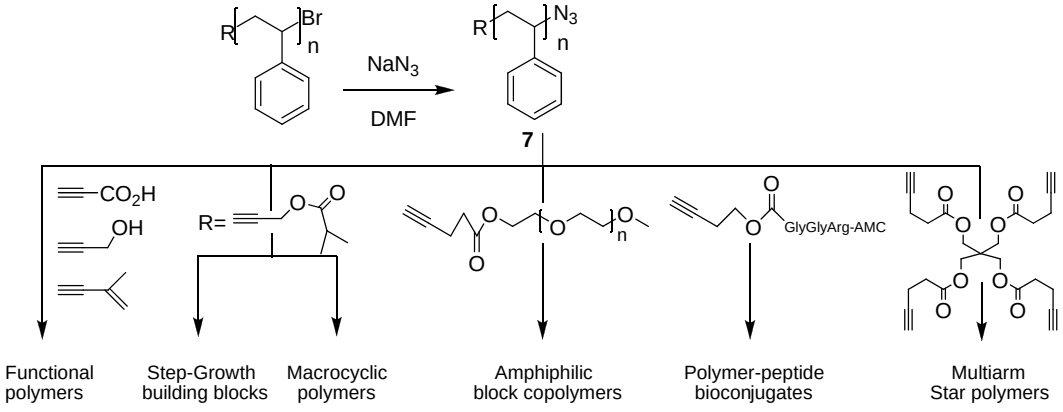

The first important application of CuAAC in polymer chemistry is undeniably the synthesis of functionalized polymers (either end-functionalized or side-functionalized). The post-functionalization of synthetic polymers is an important feature of macromolecular engineering, as many polymerization mechanisms are rather sensitive to bulky or functional groups.

Along with that, click reaction with CuAAC was investigated for modifying biological polymers such as nucleic acids or polysaccharides. Moreover, this is very useful for preparing polymer bioconjugates. Several reports indicated that sequence-defined oligopeptides can be linked to synthetic macromolecules using click ligation. More complex biological entities such as proteins, enzymes, viruses, bacteria, and cells may also be transformed using azide-alkyne chemistry.

It is apparent from the above discussion that "Click Reaction" in general and the triazole unit in particular has a great impact on several areas of research in the recent years. Encouraged by the simplicity of this "Click Reaction" and as described in the earlier part that detail the importance of soft linkers in addressing the predictability of a particular weak synthon like halo…nitro, we have initiated a program to employ this simple azide-alkyne "Click Reaction" for the synthesis of a collection of isomeric compounds with modular positioning of halo and NO_2 on a flexible tricyclic template and examination of the occurrence of the bifurcate X…NO_2 synthon with respect to their relative disposition. Apart from the projected X···NO_2 and competing X···X interactions, absence of any other stronger interactions in this system could provide the necessary criteria for existence of weak interactions like C–H···O, C–H···N, C–H···Cl and their influence on the overall molecular packing in crystals.

2.7 PRESENT WORK

The current resurgence of classical Hüisgen [3+2] cycloaddition by Sharpless-Finn-Kolb's "click reaction" has ascertained the triazole ring as an important heterocyclic pharmacophore in general and the overall process for affixation of ligands on to bio-polymers by post modification processes in particular. Herein, we describe the potential of azide-alkyne "click reaction" in crystal engineering to synthesize a collection of isomeric compounds with modular positioning of Cl and NO_2 on a flexible tricyclic template and reveal the occurrence and nature of chloro-nitro synthon with respect to their relative disposition.

As it expressed by Dunitz "the crystal is a supramolecule par excellence" that present how intermolecular links operate together. A detailed knowledge of intermolecular interactions and identifying respective molecular functionalities that form defined network structures will help to design the crystals for material applications. In this context, considering its similarity in action to *synthon*, the phrase 'supramolecular synthon' has been coined by Desiraju to describe a set of noncovalent interactions that form and modulate recognition patterns in the solid state. Various synthons comprising strong conventional hydrogen bonding to weak or unconventional (C-H …O, C-H …N, C-H …X and C-H …π) hydrogen bonding interactions have been identified. Homosynthons comprising conventional hydrogen bonding (COOH…COOH, OH…OH, $CONH_2$…$CONH_2$, X…X) were more reliably employed in crystal engineering because of their directionality and robustness. A recent trend in this regard is investigation of a set of isomeric compounds where the complimentary functional groups that control association are varied systematically on flexible templates, which indeed has provided valuable insight in crystal engineering. In this context, developing a simple synthetic tool that can deliver the medium size crystalline molecular systems with predictable architectural control and flexibility in the incorporation of functional group is warranted.

Inspired with the broad spectrum application of Cu(I)-catalyzed 1,3-dipolar cycloaddition between an azide and an alkyne in the discovery of drugs and materials, we have initiated a program to explore its potential in molecular design for crystal engineering. Surprised by the results shown by NO_2-Br heterosynthon[37] next we focused on the NO_2-Cl heterosynthon and to evaluate nature of this interaction in a group of

isomeric compounds where they are well separated through a flexible template and disposed with all possible and well defined geometries. As shown in figure 2.21, the tricyclic template comprising the 1,2,3-triazole unit as a linker (ring B) was designed with modular positioning of -Cl and -NO_2 groups on ring A and ring C, respectively. Apart from the projected NO_2…Cl and competing Cl…Cl interactions, absence of any other stronger interactions in this system should also provide the necessary criteria for existence of weak interactions like C-H…O, C-H…N, C-H…Cl and their interplay to influence the overall packing of the crystal.

Figure 2.21 *Key "Click chemistry" protocol, designed isomers and possible N-O…Cl synthon geometries*

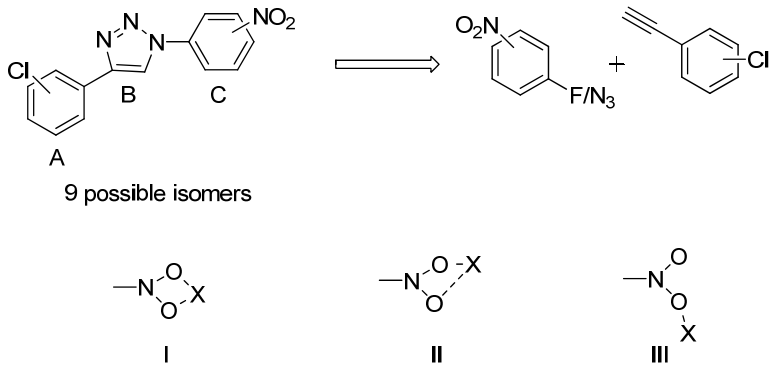

As discussed in earlier section we have explored a one-pot two-step sequence involving a nucleophilic aromatic substitution (S_NAr) of activated fluorobenzenes with azide nucleophile and *in situ* Huisgen cycloaddition of the resulting aryl azides with alkynes for a rapid access to 1,4-substituted triazoles. [38]

In a recent publication,[37] we have utilised the above mentioned strategy for synthesis of isomeric bromo nitro 1,4-diaryltriazoles.

Applying our in house methodology, synthesis commenced with isomeric nitrofluorobenzenes. In general, the reactions with 2-fluoronitrobenzene (**2.40**) are facile and with the 4-isomer (**2.42**), a prolonged heating is required. For preparing the 3-nitro isomer, 3-azidonitrobenzene (**2.95**) was employed under similar condition, as the displacement with 3-nitrofluorobenzene are sluggish. (Scheme 2.20-2.23) All these compounds were characterized by ^1H and ^{13}C NMR's as well as X-ray crystallography.

Scheme 2.20 *One-pot S_NAr-click reaction for synthesis of 2-nitro chloro triazoles*

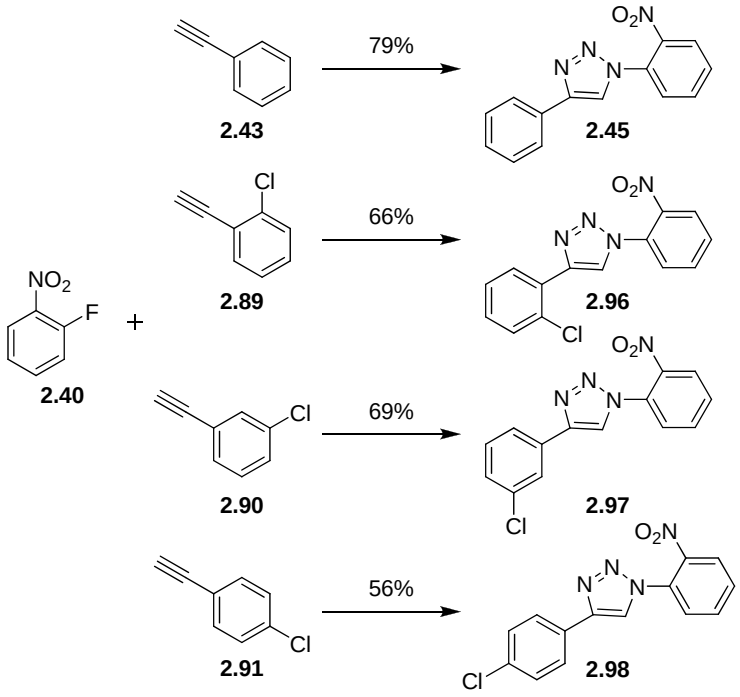

Reagents and conditions: L-Proline, Na_2CO_3, NaN_3, sodium ascorbate, $CuSO_4.5H_2O$, DMSO-H_2O (9:1), 70 °C, 24 h.

Scheme 2.21 *Attempted one-pot S_NAr-click reaction for 3-nitro chloro triazoles*

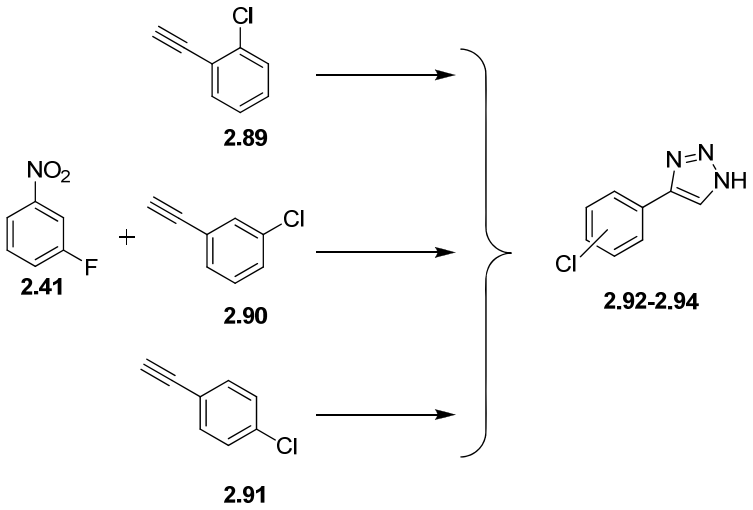

Reagents and conditions: L-Proline, Na_2CO_3, NaN_3, sodium ascorbate, $CuSO_4.5H_2O$, DMSO-H_2O (9:1), 70 °C, 48 h.

Scheme 2.22 *One-pot S_NAr-click reaction for synthesis of 3-nitro chloro triazoles*

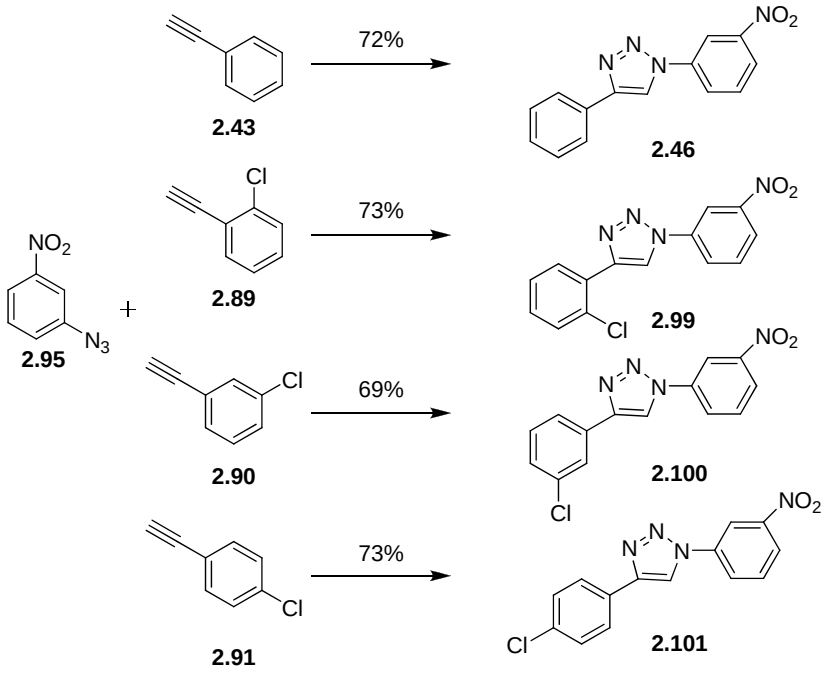

Reagents and conditions: L-Proline, Na_2CO_3, sodium ascorbate, $CuSO_4.5H_2O$, DMSO-H_2O (9:1), 70 °C, 24 h

Scheme 2.23 *One-pot S_NAr-click reaction for synthesis of 4-nitro chloro triazoles*

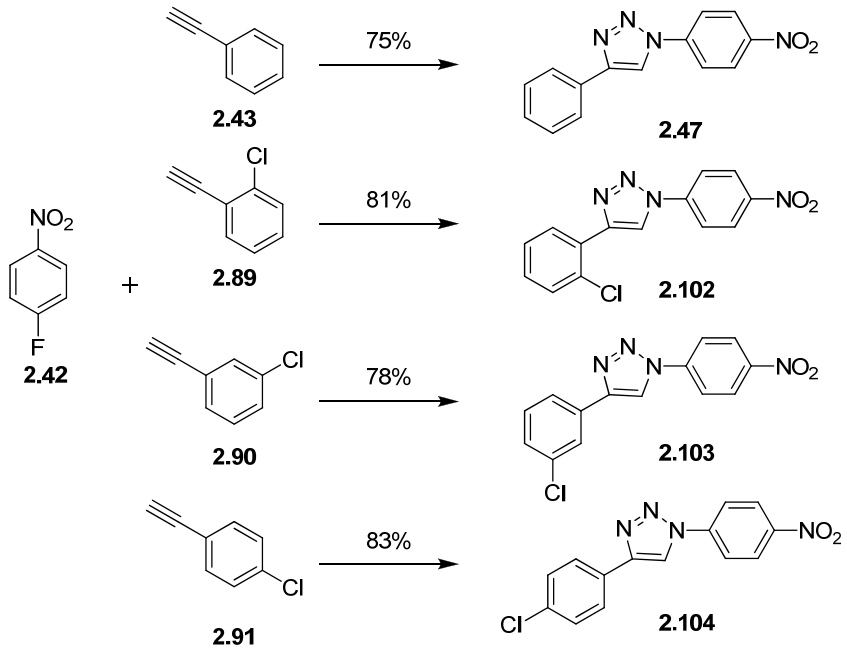

Reagents and conditions: L-Proline, Na_2CO_3, NaN_3, sodium ascorbate, $CuSO_4.5H_2O$, DMSO-H_2O (9:1), 70 °C, 48 h.

From the NMR studies, it has been found that for 1,4 disubstituted 1,2,3-triazole, the only proton present in triazole ring comes as most deshielded proton at above δ 8.5 in all the cases. These structures have further been confirmed by the X-ray studies. Detailed X-Ray crystallographic studies of available 12 compounds have been done and all the inherent structural features present in those 12 compounds are described below.

2-Nitro series:

The crystal structure of compound **2.45** contains one molecule for asymmetric unit. The aromatic ring is not coplanar with the triazole ring. The crystal structure is dominated by the C-H...O and/or C-H…N interactions. Molecules in compound **2.45** form isostructural helical assemblies along crystallographic 2_1-screw axis linked *via* C-H…O interaction involving C1-H1 group of triazole ring and oxygen O1 of nitro group. The neighbouring helices are bridged via centrosymmetric C-H…O interaction engaging nitro group phenyl ring. (Figure 2.22)

Figure 2.22 *Extended structure of* ***2.45***

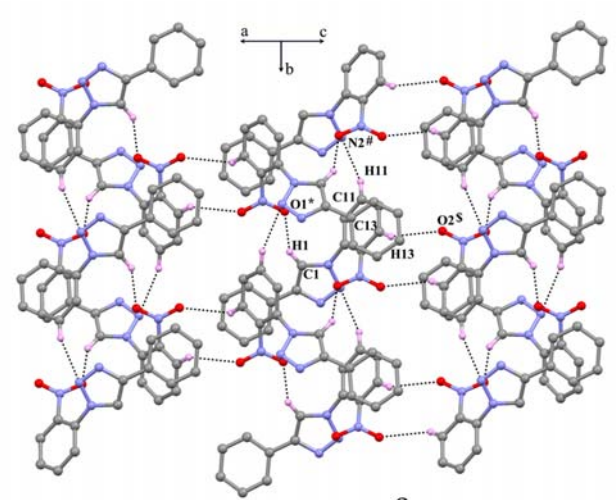

The crystal structures containing chloro substituted isomers **2.96**-**2.98**, the compound **2.96** belong to the monoclinic $P2_1/n$ system but interestingly other two compounds **2.97** and **2.98** resolved spontaneously in the crystalline state and belong to the chiral space group $P2_1$ (monoclinic system) and $P2_12_12_1$ (orthorhombic system) respectively. Crystal structures of the first two compounds (**2.96** and **2.97**) contain one molecule per asymmetric unit whereas that of compound **2.98** contains three independent

molecules in the asymmetric unit. In all the structures, aromatic ring bearing chlorine atom was somewhat in plane with the triazole ring (deviation from the plane of triazole ring in the range 2-19°). Whereas the nitrobenzene ring showed more divergence from the planarity of the triazole ring (range 47-65°). The three independent molecules in the asymmetric unit of **2.98** also revealed orientational difference of ~ 17° between molecules A and B and ~4° between molecules B and C due to free rotation along the C-N bond. The chlorobenzene ring orientation did not differ much in **2.96** and **2.98** but in **2.97**, it adopted almost opposite orientation with respect to other rings in **2.96** and **2.98**. The crystal structures of all the compounds in 2-nitro series in general are dominated by the C-H···O, C-H···N, C-H···Cl interactions and did not contain Cl···NO_2 contact in their crystals.

Molecules in compound **2.96** form helical assemblies along crystallographic 2_1-screw axis linked *via* C-H···O interaction involving C1-H1 of triazole ring and oxygen O1 of nitro group (Figure 2.23) similar to the previously reported Br and non-halo analogs. Along the helical assembly the unit-translated molecules are weakly associated *via* C5-H5···Cl1 contact. These neighbouring helices are bridged *via* centrosymmetric weak C-H···O interactions engaging nitro group phenyl ring.

Figure 2.23 *Extended structure of* ***2.96***

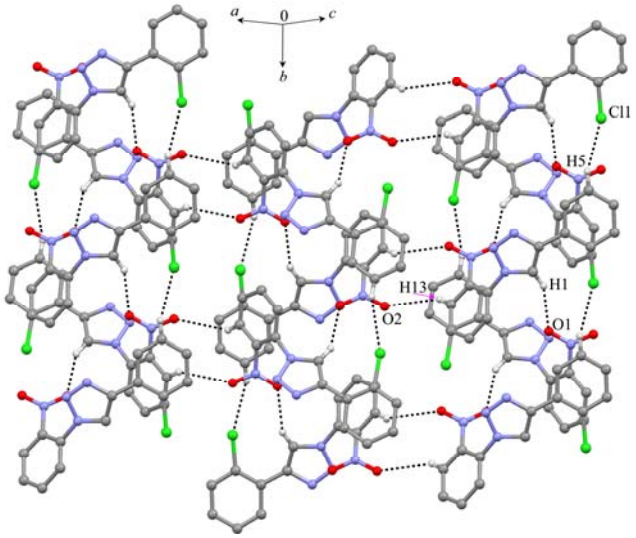

In **2.97**, the molecules also formed the helical architecture along the *b*-axis through C13-H13···N2 and offcentered C-H···π interaction between C-H of triazole ring and chlorobenzene ring. These helices are unit translated along the *c*-axis *via* C5-H5···O2 interactions producing overall zig-zag packing down the *a*-axis (Figure 2.24). The molecular packing viewed down the helical axis (*b*-axis) revealed a 2D layered structure containing tetrameric arrangement (Figure 2.25) of the unit translated molecules through C5-H5···O2 (along the *c*-axis) and C11-H11···N2 and C4-H4···Cl1 (along the *a*-axis).

Figure 2.24 *Extended structure of* ***2.97*** *along c-axis*

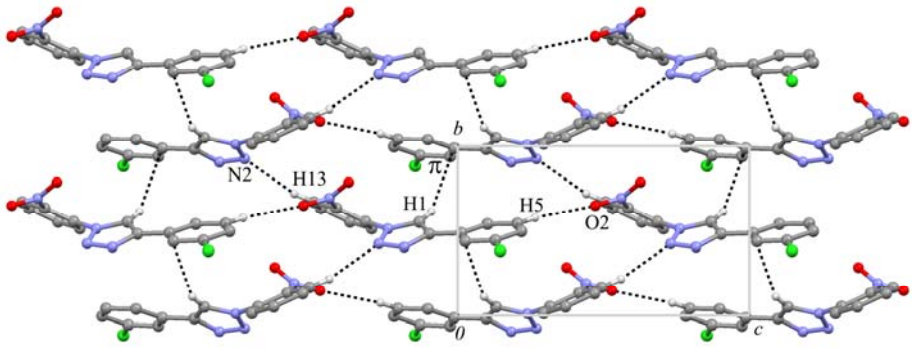

Figure 2.25 *Extended structure of* ***2.97*** *along b-axis*

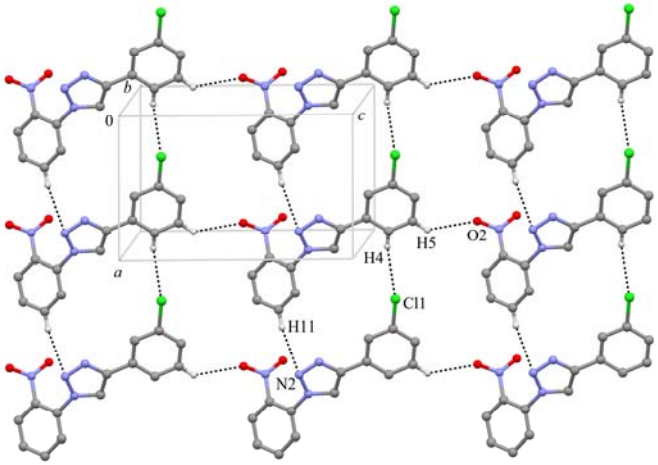

In compound **2.98**, the two symmetry independent molecules B and C together form composite helix where each molecule distributed alternately along the helix. The successive molecules B and C along the helix are linked *via* bifurcated C10C-

H10C···O2B, C1C-H1C···O2B and C1B-H1B···N2C, C1B-H1B···N3C interactions. The adjacent helix is of different chirality (complementary helix) and both these helices run in antiparallel fashion and are linked *via* C12B-H12B···O1C interactions. Interestingly, the third molecule A also forms helical architecture and is sandwiched between the complementary helical assemblies of molecules B and C along the *c*-axis (Figure 2.26) and are interacting *via* C5C-H5C···O1A, C5A-H5A···N2B contacts

Figure 2.26 *Extended structure of* ***2.98*** *along c-axis*

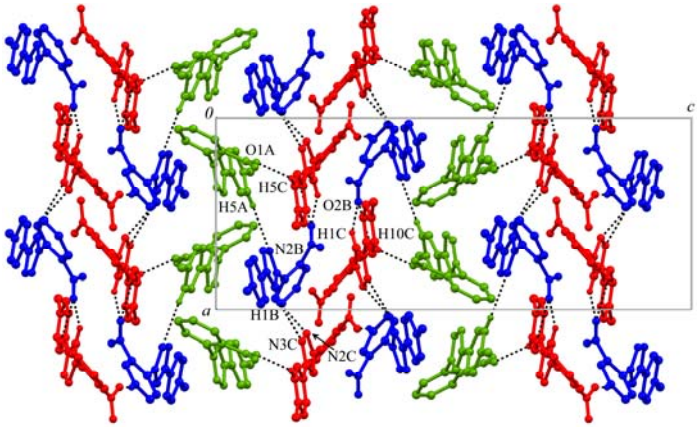

Figure 2.27 *Extended structure of* ***2.98***

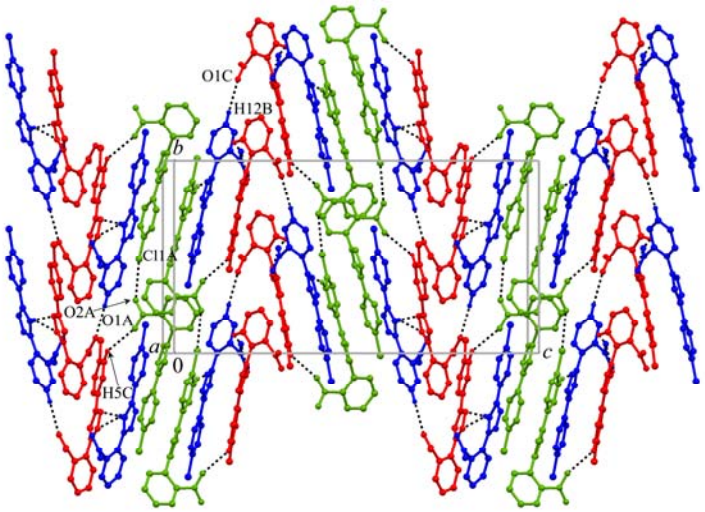

The molecular packing viewed down the helical axis revealed layered arrangement in which both molecules B and C constitute a layer of two strands linked *via* C12B-H12B···O1C along the *b*-axis. The molecule A also forms layered arrangement

sandwich between the two layers of molecules B and C. The molecules within the layer are linked *via* linear halogen bond involving Cl1A and O2A (Cl1A···O2A = 3.018 Å, ∠C6A- Cl1A···O2A = 172.6°) and are also interacting with neighboring layer *via* C5A-H5A···N2B and C5C-H5C···O1A interactions. (Figure 2.27)

3-Nitro series:

Crystal structures of **2.46** series are solely dominated by C-H…O interactions. In crystal structure, both aromatic rings are nearly coplanar with the triazole ring. Molecules forms a zero dimensional face-to-face centrosymmetric dimeric assembly *via* C-H…O interactions (Figure 2.28). The face-to-face dimers are connected *via* centrosymmetric C-H…N interaction forming a planar sheet diagonal to ab plane. These successive sheets along the c-axis are perpendicularly stitched through C-H…O interaction in **2.46** forming a square grid type network.

Figure 2.28 *Extended structure of* ***2.46***

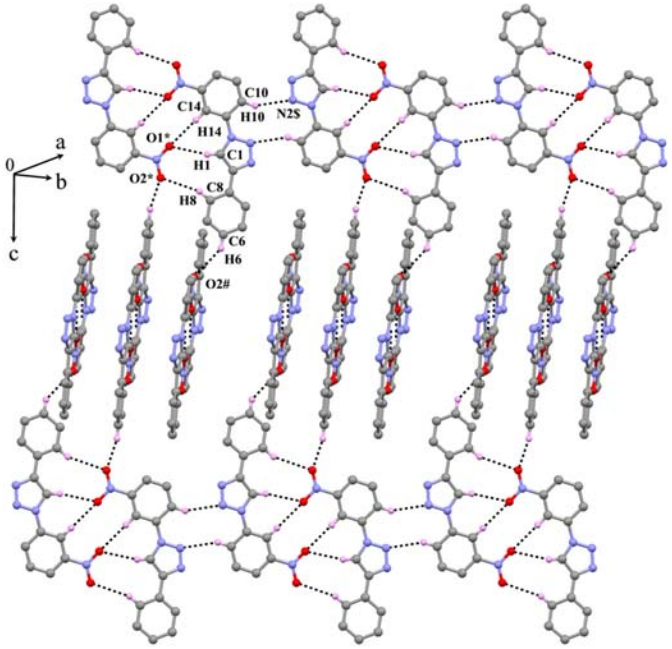

Crystal structures of the chloro derivatives of 3-NO_2 series belong to the centrosymmetric space group and contained only one molecule in asymmetric unit. In **2.99**, the nitrobenzene and chlorobenzene rings deviate slightly (15° and 24° respectively) from the planarity of the triazole moiety. In other two compounds, both the aromatic rings

are almost coplanar with the triazole ring. The crystal structures of all the structures in 3-nitro series in general are dominated by the C-H···O, C-H···N, C-H···Cl interactions and only in **2.101** molecule pack *via* Cl···NO_2 contact in their crystals.

Molecules in compound **2.99** form helical assemblies along crystallographic 2_1-screw axis (*b*-axis) linked *via* C-H···O interaction involving C1-H1 of triazole ring and oxygen O1 of nitro group (Figure 2.29) similar to **2.96**. The adjacent complementary helices are bridged *via* two *c*-glide related C-H···O interactions namely C6-H6···O1 and C7-H7···O2 engaging both the oxygens of nitro group. Thus oxygen O1 is involved in bifurcated C-H···O hydrogen boning interactions. Additionally, centrosymmetric π···π stacking interactions between the chlorobenzene rings also support the tight binding of the helices. It is interesting to note that the chlorobenzene rings have opposite orientation in π···π stacking geometry.

Figure 2.29 *Extended structure of* ***2.99***

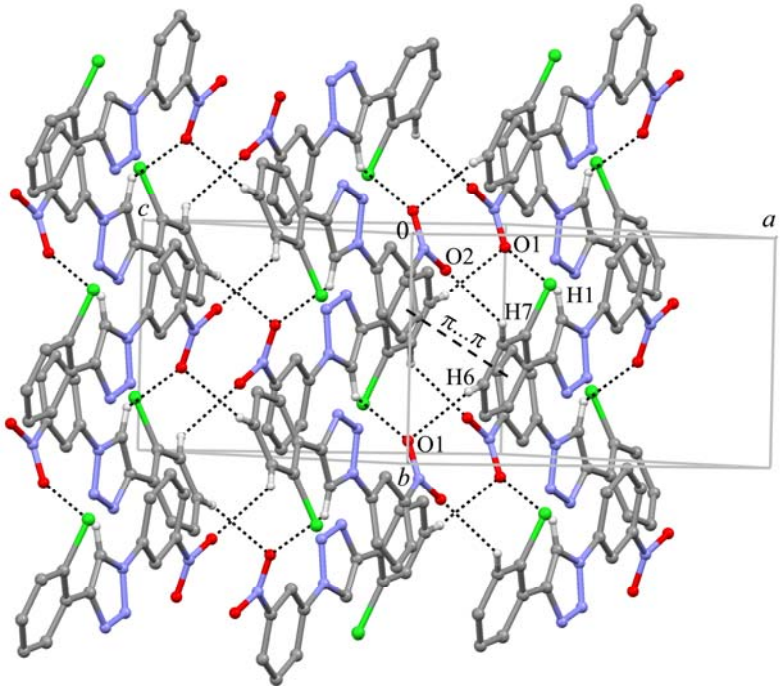

In **2.100**, the molecules form a 1D molecular string connecting the unit-translated molecules along the *b*-axis *via* bifurcated C-H···N and C-H···O interactions. The nitrogen atoms N2 and N3 of the triazole ring accept hydrogen H5 of the chlorobenzene ring of the

next unit translated molecule to from bifurcated C5-H5···N2 and C5-H5···N3 contacts. The former contact is shorter than the later but the later is more linear compared to the former. The oxygen O1 of the nitro group also accepts two H-atoms (H1 and H10) from the unit-translated molecule to form bifurcated C1-H1···O1 and C10-H10···O1 interactions. Although both the interactions have almost linear geometry, the former contact is very short whereas the later one is long. These 1D molecular chain are weaved centrosymmetrically *via* good C12-H12···O2 interaction to form a bilayer bringing the nitrobenzene group together with the chlorobenzene ring pointing away. These bilayers are in turn bridged together centrosymmetrically *via* weak C-H···Cl interaction engaging the aromatic hydrogen H6 and chlorine Cl1 to form a 2D molecular sheet. Along the third dimension these sheets are stacked one over the other in antiparallel fashion with interplanar spacing ~ 3.5 Å. (Figure 2.30)

Figure 2.30 *Extended structure of* ***2.100***

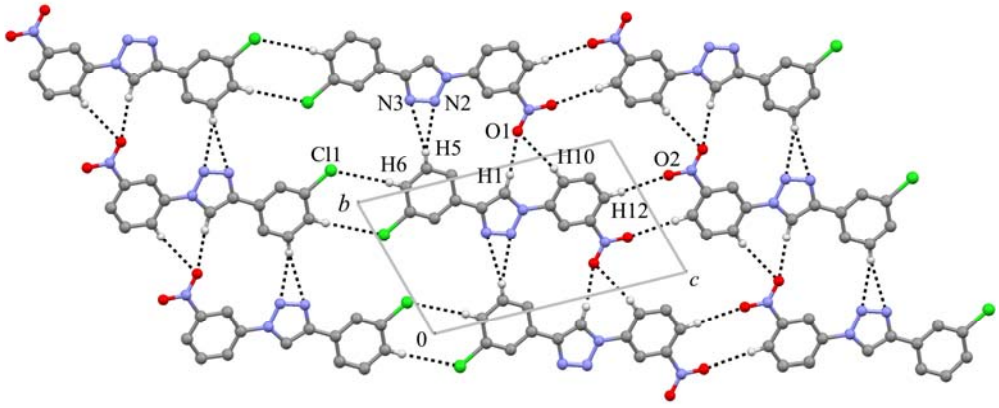

Crystal structures of **2.101** is isostructural with simple 3-NO_2 derivative and with the corresponding 4-Br derivative. Molecules form a zero dimensional face-to-face centrosymmetric dimeric assembly *via* C-H···O interactions (Figure 2.31). The centrosymmetric bifurcated C1-H1···O1, C14-H14···O1 and C8-H8···O2 stitched the adjacent molecule centrosymmetrically. The geometries of the bifurcated C-H···O interactions are better than the later. These face-to-face dimers are further connected centrosymmetrically *via* good C-H···N interactions involving C10-H10 and N2 atoms forming a planar sheet diagonal to *ab*-plane. These successive sheets along the c-axis are perpendicularly stitched through Cl···O_2N (C6-Cl1···O2) contact forming a square grid type network.

Figure 2.31 *Extended structure of* ***2.101***

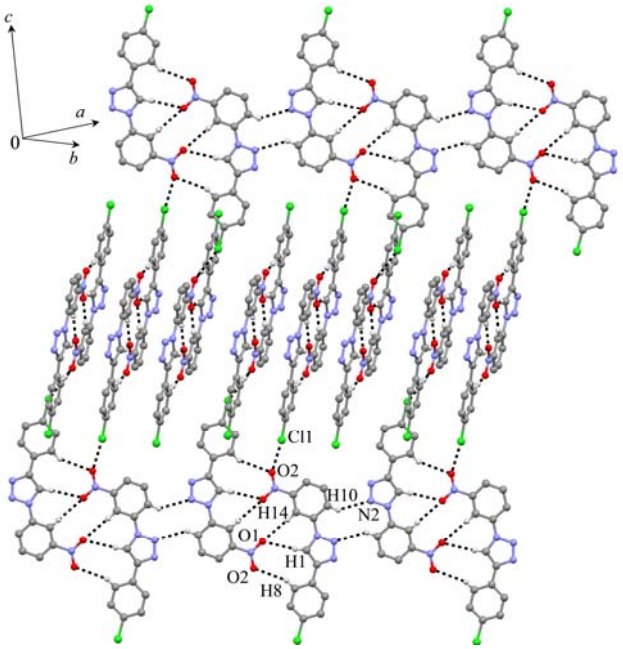

4-Nitro series:

In the crystal structure of **2.47** both aromatic rings are nearly coplanar with the central triazole ring. Molecules form a 2D sheet pattern linked *via* bifurcated C-H…O interactions. The spacing between the parallel sheets is about 3.9 Å. (Figure 2.32)

Figure 2.32 *Extended structure of* ***2.47***

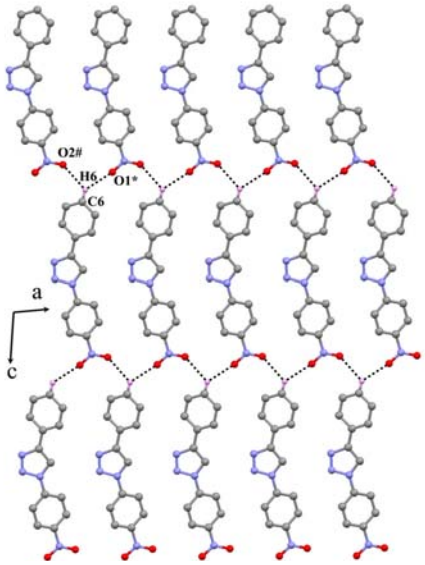

The crystal structures of chloroderivatives of this series belong to the centrosymmetric space groups and contain one molecule in asymmetric unit. The aromatic ring bearing chlorine atom is almost coplanar with the triazole ring whereas the nitrobenzene ring deviate by ~ 16°. The crystal structures of all the structures in 4-nitro series in general are dominated by the C-H···O, C-H···N, C-H···Cl interactions and only in **2.102** molecules pack *via* Cl···Cl contact. Crystal structures of all the compounds in this series displayed the 2D-sheet structure and molecular packing in **2.103** and **2.104** is almost isostructural.

In **2.102**, molecules form a 1D molecular string connecting the unit-translated molecules along the *b*-axis *via* C11-H11···N2, C14-H14···O2 and C5-H5···Cl1 interactions. The first two interactions have better geometry compared to the last one. These 1D molecular chains are stitched together along the *c*-axis *via* short and linear C6-H6···O2 interaction to form 2D molecular sheet. Along the third dimension these sheets are stacked one over the other in antiparallel fashion centrosymmetrically through short Cl1···Cl1 contact (3.482 Å) with interplanar spacing ~ 3.4 Å. (Figure 2.33)

Figure 2.33 *Extended structure of* **2.102**

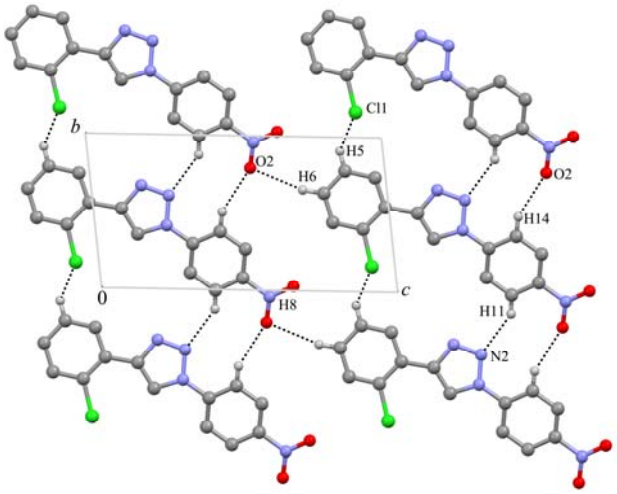

Figure 2.34 *Extended structure of* **2.103**

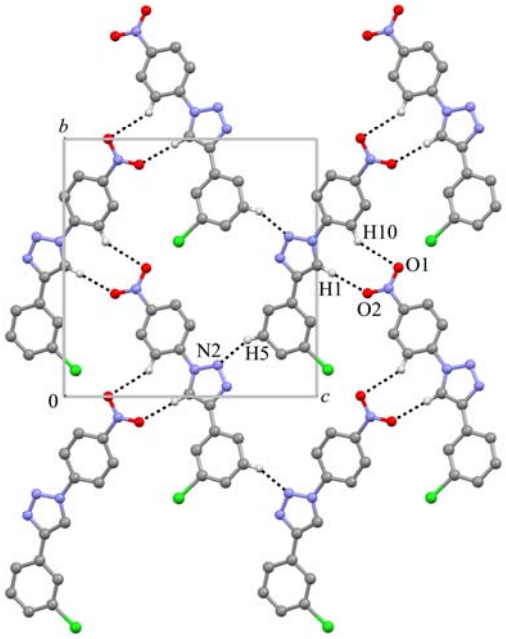

Figure 2.35 *Extended structure of* **2.104**

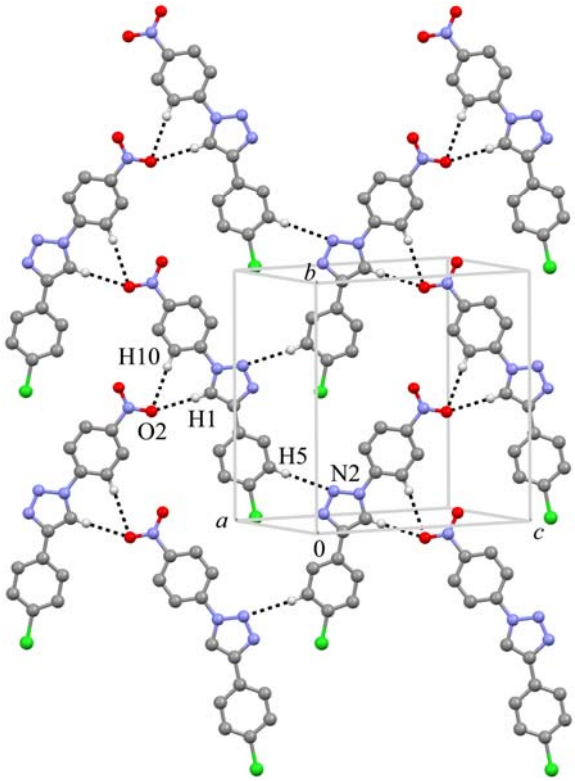

The structures of **2.103** and **2.104** revealed isostructural flat helical assembly around the crystallographic two-fold screw axis through two C-H···O contacts, C1-H1···O2 and C10-H10···O1 in **2.103** and C1-H1···O2 and C10-H10···O2 in **2.104**. In both the structures the former contacts are short and more linear when compared to the later. These flat helices are bridged along the *c*-axis *via* good C5-H5···N2 interactions forming 2D sheet structure (Figure 2.34-2.35). These sheets are stacked one over the other in antiparallel fashion with the interplanar spacing ~ 3.5 Å.

As indicated in the introduction, the prime objective of this investigation is to develop a simple protocol for the synthesis of a group of isomeric compounds having the orthogonal functional groups that form the weaker intermolecular interactions. The copper (I) catalyzed Hüisgen azide-alkyne cycloaddition (CuAAC) has been proven as highly relevant because of selectivity and its operational simplicity. The second objective is to examine the occurrence and geometrical preference of an identified Cl···NO_2 weak interaction. Apart from the projected Cl···NO_2 interaction, the absence of any strong and direction-specific intermolecular interactions in the present template gave an equal opportunity for the other weaker intermolecular interactions such as C-H···O, C-H···N, C-H···Cl, and, Cl···Cl short contacts to play their role in molecular aggregation. A comprehensive compilation of various weaker interactions observed in crystal structures of all the compounds revealed that out of nine compounds, molecules in two compounds (**2.98** and **2.101**) have Cl···NO_2 association, in one compounds Cl···Cl short contact (**2.102**) and in four compound (**2.96**, **2.97**, **2.100** and **2.102**) C-H···Cl electrostatic interaction were present.

A close look at the secondary structures of a set of isomeric compounds reveal substantial similarity in the patterns of supramolecular aggregation and the nature of the interactions involved. This is quite striking when compared with the earlier reports where complexity involved in extrapolating the aggregation patterns from one isomer to others, even in simple isomers is highlighting. The observed similarities in the 3 different groups of the present investigation is highly remarkable and demonstrates that it is not the weaker interactions that altered the intramolecular association, however, it is the relatively strong interactions which disturb the predictable weaker complimentary interaction patterns. It also indicates that structural analysis of weaker interactions in isolation and then examining the influence of strong interaction over them will give more valuable informations that can be used as the starting premise for crystal structure predictions in general and molecular design for material applications in particular.

In conclusion, the potential of Cu(I) caltalysed azide-alkyne “click reaction” as a simple synthetic tool for crystal engineering to build a collection of isomeric compounds with modular positioning of complimentary functional groups was demonstrated. The elegancy of this approach is that all the 9 compounds prepared through the [3+2]-azidoalkyne cycloaddition are crystalline. The investigation comprising the crystal structural analyses of closely related molecules demonstrate how weaker interactions like C-H···O and C-H···N could form self-complimentary motifs that are sufficiently strong enough to direct the crystal packing in general and also to block are fine tune the relatively stronger interactions like Cl···NO_2 and Cl···Cl. The helical assembly of molecules through C-H···O interactions in 2-nitro series, and the self complimentary patterns displayed in the crystal structures of 3-nitro series shows that one can design materials that require a reversible alternative for covalent bond by employing exclusively weak hydrogen bonding interactions like C-H···O/N to form either 2D sheets or 3D-helical networks and work in this direction is progressing in our lab.

2.8 Experimental

General experimental procedure for S_NAr reaction:

Fluoronitrobenzene (100 mg, 0.71 mmol) was mixed with chlorophenylacetylene (97 mg, 0.71 mmol) in 9:1 DMSO:H_2O (10 ml). To the mixture were added L–Proline (16 mg, 0.142 mmol), Na_2CO_3 (15 mg, 0.142 mmol), NaN_3 (55 mg, 0.852 mmol), sodium ascorbate (14 mg, 0.071 mmol), and $CuSO_4.5H_2O$ (9 mg, 0.036 mmol). The mixture was stirred for 24–48 h at 70 °C and then the mixture was poured into 30 ml of ice–cold water. The solid residue was filtered and crystallized in different solvent systems to procure white to yellow crystalline solid in 56–83% yield.

General procedure for cycloaddition reactions with 3-azidobenzene (2.95):

A mixture of 3-Azidonitrobenzene (116 mg, 0.71 mmol), chlorophenylactylene (97 mg, 0.71 mmol) was taken in 9:1 DMSO:H_2O (10 ml) in a round bottom flask and L–Proline (16 mg, 0.142 mmol), Na_2CO_3 (15 mg, 0.142 mmol), sodium ascorbate (14 mg, 0.071 mmol), and $CuSO_4.5H_2O$ (9 mg, 0.036 mmol) were added to that mixture and the complete reaction mixture was heated at 60 ºC (bath temperature) for 24 h with stirring. The reaction mixture was cooled to room temperature and diluted with 30 ml of water and combined water layer was thoroughly extracted with ethyl acetate (3 x 50 ml). Organic layer was dried over sodium sulphate and concentrated under vacuum. The crude solid was purified by column chromatography over 230–400 silica using ethyl acetate/light petroleum (1:4) to obtain white to yellow solids (63–79%). This solid was crystallized with different solvent systems.

1-(2-Nitrophenyl)-4-phenyl-1*H*-1,2,3-triazole (2.45)

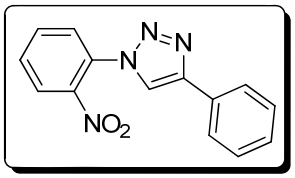

Figure 2.36 *The molecular structure of compound* ***2.45***

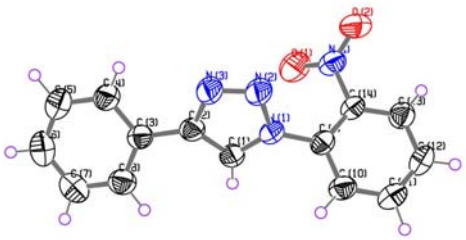

Bond length and bond angle in Å and º

O1…N4	1.214(4)	O2...N4	1.219(4)	N1...N2	1.358(3)
N1...C1	1.334(4)	N1...C9	1.426(3)	N2...N3	1.310(4)
N3...C2	1.360(4)	N4...C14	1.478(3)	C1…C2	1.367(4)
C2…C3	1.457(4)	C3…C4	1.406(4)	C3…C8	1.381(4)
C4…C5	1.377(5)	C5…C6	1.371(5)	C6…C7	1.384(5)
C7…C8	1.380(5)	C9…C10	1.387(3)	C9…C14	1.382(4)
C10…C11	1.379(4)	C11…C12	1.366(4)	C12…C13	1.392(4)
C13…C14	1.374(4)				

N2N1C1	110.7(2)	N2N1C9	119.5(2)	C1N1C9	129.8(2)
N1N2N3	106.4(2)	N2N3C2	109.8(2)	O1N4O2	124.2(2)
O1N4C14	117.3(2)	O2N4C14	118.5(2)	N1C1C2	105.7(2)
N3C2C1	107.4(2)	N3C2C3	122.6(2)	C1C2C3	129.9(2)
C2C3C4	120.4(2)	C2C3C8	121.6(2)	C4C3C8	117.9(2)
C3C4C5	120.8(3)	C4C5C6	120.0(3)	C5C6C7	120.1(3)
C6C7C8	119.8(3)	C3C8C7	121.2(3)	N1C9C10	119.9(2)
N1C9C14	121.2(2)	C10C9C14	118.9(2)	C9C10C11	119.3(2)
C10C11C12	121.2(3)	C11C12C13	120.3(3)	C12C13C14	118.2(3)
N4C14C9	120.7(2)	N4C14C13	117.1(2)	C9C14C13	122.1(2)

1-(3-Nitrophenyl)-4-phenyl-1*H*-1,2,3-triazole (2.46)

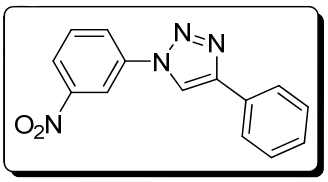

Figure 2.37 *The molecular structure of compound* ***2.46***

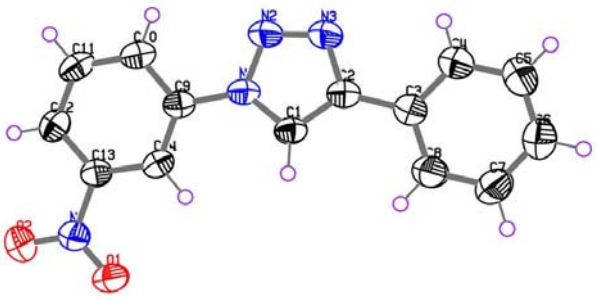

Bond length and bond angle in Å and º

O1..N4	1.227(3)	O2...N4	1.221(3)	N1...N2	1.357(3)
N1...C1	1.356(3)	N1...C9	1.427(3)	N2...N3	1.301(3)
N3...C2	1.373(3)	N4...C13	1.470(3)	C1...C2	1.375(3)
C2…C3	1.471(3)	C3…C4	1.391(3)	C3…C8	1.389(3)
C4…C5	1.374(4)	C5…C6	1.371(4)	C6…C7	1.380(4)
C7…C8	1.379(4)	C9…C10	1.399(3)	C9…C14	1.383(3)
C10…C11	1.375(3)	C11…C12	1.383(4)	C12…C13	1.384(3)

C13…C14	1.381(3)				
N2N1C1	110.3(2)	N2N1C9	119.8(2)	C1N1C9	129.9(2)
N1N2N3	107.4(2)	N2N3C2	109.7(2)	O1N4O2	122.9(2)
O1N4C13	118.3(2)	O2N4C13	118.8(2)	N1C1C2	105.2(2)
N3C2C1	107.5(2)	N3C2C3	122.0(2)	C1C2C3	130.5(2)
C2C3C4	120.7(2)	C2C3C8	121.5(2)	C4C3C8	117.9(2)
C3C4C5	121.2(2)	C4C5C6	120.3(3)	C5C6C7	119.6(3)
C6C7C8	120.3(3)	C3C8C7	120.8(2)	N1C9C10	119.1(2)
N1C9C14	120.4(2)	C10C9C14	120.5(2)	C9C10C11	119.4(2)
C10C11C12	121.4(2)	C11C12C13	117.8(2)	N4C13C12	119.0(2)
N4C13C14	118.3(2)	C12C13C14	122.7(2)	C9C14C13	118.2(2)

1-(4-Nitrophenyl)-4-phenyl-1*H*-1,2,3-triazole (2.47)

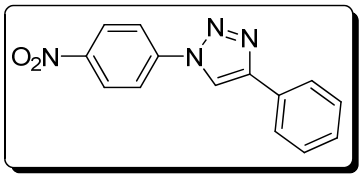

Figure 2.38 *The molecular structure of compound* ***2.47***

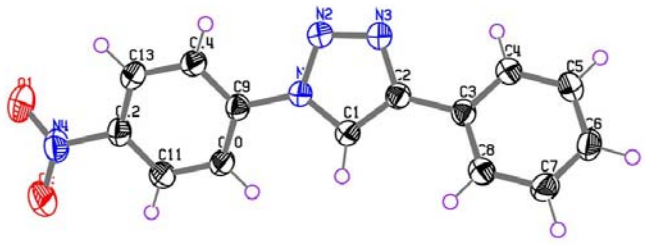

Bond length and bond angle in Å and º

O1...N4	1.220(2)	O2...N4	1.217(2)	N1...N2	1.354(2)
N1...C1	1.352(2)	N1...C9	1.422(1)	N2...N3	1.304(2)
N3...C2	1.368(2)	N4...C12	1.466(2)	C1...C2	1.363(2)
C2…C3	1.470(2)	C3…C4	1.392(2)	C3…C8	1.393(2)
C4…C5	1.383(2)	C5…C6	1.382(2)	C6…C7	1.380(2)
C7…C8	1.386(2)	C9…C10	1.386(2)	C9…C14	1.391(2)
C10…C11	1.380(2)	C11…C12	1.380(2)	C12…C13	1.380(2)
C13…C14	1.378(2)				
N2N1C1	110.5(1)	N2N1C9	120.0(1)	C1N1C9	129.4(1)
N1N2N3	107.0(1)	N2N3C2	109.3(1)	O1N4O2	123.9(1)
O1N4C12	118.1(1)	O2N4C12	117.9(1)	N1C1C2	105.0(1)
N3C2C1	108.1(1)	N3C2C3	122.1(1)	C1C2C3	129.7(1)
C2C3C4	120.2(1)	C2C3C8	120.8(1)	C4C3C8	118.9(1)
C3C4C5	120.4(1)	C4C5C6	120.3(1)	C5C6C7	119.8(1)
C6C7C8	120.3(1)	C3C8C7	120.3(1)	N1C9C10	119.4(1)

N1C9C14	119.1(1)	C10C9C14	121.5(1)	C9C10C11	119.1(1)
C10C11C12	118.7(1)	N4C12C11	118.0(1)	N4C12C13	119.1(1)
C11C12C13	122.9(1)	C12C13C14	118.3(1)	C9C14C13	119.5(1)

Table 2.5 *Crystal data of* ***2.96–2.98***

	2.45	**2.46**	**2.47**
Chemical formula	C14H10N4O2	C14H10N4O2	C14H10N4O2
M_r	266.26	266.26	300.70
Temperature/K	297(2)	297(2)	297(2)
Crystal size/mm	0.43×0.41×0.26	0.31x0.22x0.20	0.69x0.52x0.08
Crystal system	Monoclinic	Monoclinic	triclinic
Space group	P21/n	P21/c	P-1
a/Å	12.180(4)	8.502(3)	5.757(2)
b/Å	7.501(3)	8.051(9)	7.198(3)
c/Å	14.277(5)	14.256(15)	14.862(6)
α/°	90	90	101.081(6)
β/°	100.286(7)	100.286(7)	99.217(6)
γ/°	90	90	90.859(6)
V/Å^3	1293.5(8)	1240.1(7)	595.8(4)
Z	4	4	2
F(000)	522	552	276
D_{calc}/g cm^{-3}	1.378	1.426	1484
μ/mm^{-1}	0.097	0.100	0.104
Absorp.correction	Multi-scan	Multi-scan	Multi-scan
T min/max	0.9596 / 0.9753	0.9696/0.9802	0.9315/0.9917
Reflns collected	9605	5402	4652
Unique reflns	2513	2170	2296
Observed reflns	1661	1779	2006
h, k, l (min, max)	(-14,15),(-9,9), (-17,17)	(-10, 10),(-6, 6),(-32, 25)	(-7, 7),(-8, 8),(-16, 18)
R_{int}	0.0446	0.0364	0.0181
No. of parameters	221	181	221
R_1[I > 2σ(I)]	0.0619	0.0525	0.0363
wR_2[I > 2σ (I)]	0.1304	0.1260	0.0996
R_1_all data	0.0997	0.0655	0.0414
wR_2_all data	0.1475	0.1328	0.1042
GoF	1.098	1.038	1.060
$\Delta\rho_{max}$,$\Delta\rho_{min}$(eÅ^{-3})	0.162, -0.146	0.171, -0.147	0.195, -0.171
CCDC deposition no.	CCDC 679556	CCDC 679560	CCDC 679564

4-(2-Chlorophenyl)-1-(2-nitrophenyl)-1*H*-1,2,3-triazole (2.96)

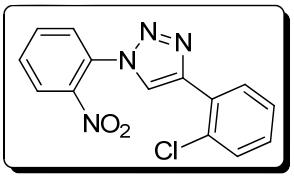

Mol. Formula	: $C_{14}H_9ClN_4O_2$
M. P.	: 168–169 ^oC
^{1}H NMR ($CDCl_3$, 500 MHz)	: δ 7.32 (dt, *J* = 1.6, 7.8 Hz, 1H), 7.41 (dt, *J* = 1.2, 7.7 Hz, 1H), 7.48 (dd, *J* = 0.8, 8.0 Hz, 1H), 7.69–7.73 (m, 2H), 7.82 (dt, *J* = 1.2, 7.8 Hz, 1H), 8.10 (dd, *J* = 1.2, 8.1 Hz, 1H), 8.32 (dd, *J* = 1.2, 7.8 Hz, 1H), 8.53 (s, 1H) ppm.
^{13}C NMR ($CDCl_3$, 125 MHz)	: δ 124.5 (d), 125.6 (d), 127.2 (d), 127.9 (d), 128.4 (s), 129.4 (d), 129.9 (d), 130.1 (s), 130.3 (d), 130.8 (d), 131.3 (s), 133.9 (d), 144.4 (s), 144.5 (s) ppm.
Elemental Analysis	Calcd.: C, 55.92; H, 3.02; Cl, 11.79; N, 18.63 Found: C, 55.87; H, 2.99; Cl, 11.75; N, 18.59

Figure 2.39 *The molecular structure of compound* ***2.96***

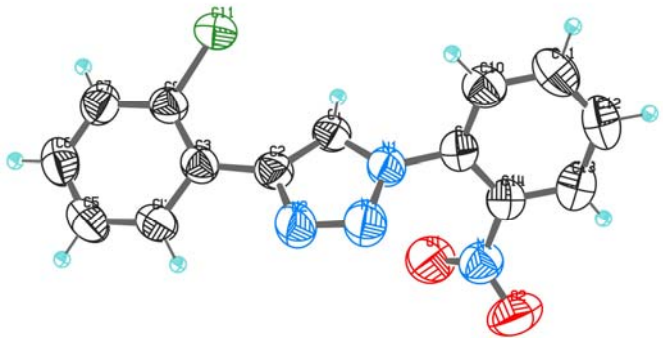

Bond length and bond angle in Å and °

Cl1…C8	1.738(2)	O1…N4	1.213(3)	O2…N4	1.214(3)
N1…N3	1.350(3)	N1…C1	1.337(3)	N1…C9	1.421(2)
N2...N3	1.307(3)	N2…C2	1.364(3)	N4…C14	1.468(2)
C1...C2	1.365(2)	C2…C3	1.472(3)	C3...C4	1.398(2)
C3…C8	1.393(3)	C4…C5	1.378(3)	C5…C6	1.367(4)
C6…C7	1.373(3)	C7...C8	1.385(3)	C9...C10	1.377(3)
C9...C14	1.389(3)	C10... C11	1.380(4)	C11...C12	1.372(4)
C12...C13	1.371(3)				

N3N1C1	110.6(2)	N3N1C9	119.7(2)	C1N1C9	129.7(2)
N3N2C2	109.9(2)	N1N3N2	106.6(2)	O1N4O2	123.7(2)
O1N4C14	117.9(2)	O2N4C14	118.4(2)	N1C1C2	105.9(2)
N2C2C1	107.0(2)	N2C2C3	119.2(2)	C1C2C3	133.7(2)
C2C3C4	118.4(2)	C2C3C8	124.9(2)	C4C3C8	116.6(2)
C3C4C5	121.4(2)	C4C5C6	120.6(2)	C5C6C7	119.6(2)

C6C7C8	120.0(2)	Cl1C8C3	121.0(1)	Cl1C8C7	117.3(1)
C3C8C7	121.7(2)	N1C9C10	119.7(2)	N1C9 C14	121.1(2)
C10C9 C14	119.0(2)	C9C10 C11	120.0(2)	C10C11C12	120.3(2)
C11C12C13	120.4(2)	C12C13C14	119.5(2)	N4C14C9	121.0(2)
N4C14 C13	118.1(2)	C9C14 C13	120.8(2)		

4-(3-Chlorophenyl)-1-(2-nitrophenyl)-1*H*-1,2,3-triazole (2.97)

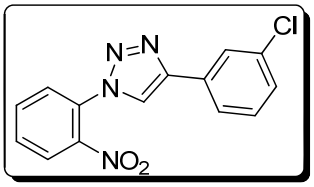

Mol. Formula	: $C_{14}H_9ClN_4O_2$
M. P.	: 129 °C
^{1}H NMR (DMSO-d_6, 400 MHz)	: δ 7.45 (ddd, *J* = 0.9, 1.9, 8.0 Hz, 1H), 7.53 (t, *J* = 7.8 Hz, 1H), 7.85–7.89 (m, 1H), 7.91 (d, *J* = 7.8 Hz, 1H), 7.93–8.01 (m, 3H), 8.24 (dd, *J* = 1.0, 8.3 Hz, 1H), 9.24 (s, 1H) ppm.
^{13}C NMR (DMSO-d_6, 100 MHz)	: δ 123.7 (d), 124.1 (d), 125.2 (d), 125.9 (d), 127.6 (d), 128.5 (d), 129.2 (s), 131.3 (d), 131.6 (d), 132.1 (s), 134.1 (s), 134.8 (d), 144.2 (s), 146.0 (s) ppm.
Elemental Analysis	Calcd.: C, 55.92; H, 3.02; Cl, 11.79; N, 18.63. Found: C, 55.97; H, 2.97; Cl, 11.72; N, 18.67.

Figure 2.40 *The molecular structure of compound* ***2.97***

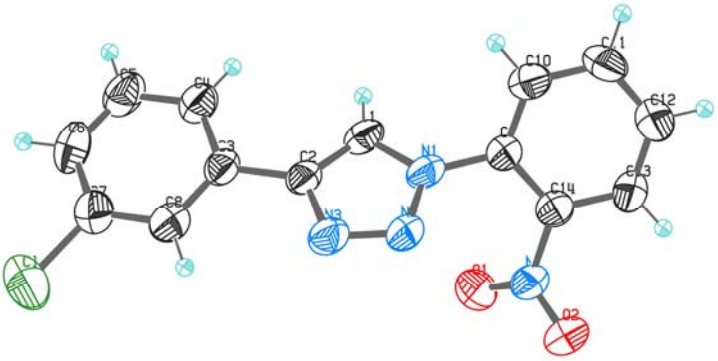

Bond length and bond angle in Å and °

Cl1...C7	1.735(7)	O1...N4	1.229(6)	O2...N4	1.230(6)
N1...N2	1.336(6)	N1...C1	1.360(6)	N1...C9	1.439(5)
N2…N3	1.322(6)	N3...C2	1.356(6)	N4…C14	1.444(7)

C1...C2	1.361(7)	C2…C3	1.495(6)	C3…C4	1.387(6)
C3…C8	1.380(7)	C4…C5	1.393(7)	C5…C6	1.368(9)
C6…C7	1.378(8)	C7…C8	1.398(8)	C9…C10	1.358(7)
C9…C14	1.396(6)	C10…C11	1.385(7)	C11…C12	1.392(8)
C12…C13	1.360(8)	C13…C14	1.394(7)	N2N1C1	110.6(3)
N2N1C9	120.9(3)	C1N1C9	128.4(3)	N1N2N3	107.7(4)
N2N3C2	108.1(4)	O1N4O2	122.7(4)	O1N4C14	119.9(4)
O2N4C14	117.4(4)	N1C1C2	104.3(4)	N3C2C1	109.4(4)
N3C2C3	121.3(4)	C1C2C3	129.3(4)	C2C3C4	120.5(4)
C2C3C8	119.9(4)	C4C3C8	119.6(4)	C3C4C5	120.1(4)
C4C5C6	120.6(5)	C5C6C7	119.3(5)	Cl1C7C6	119.6(4)
Cl1C7C8	119.4(4)	C6C7C8	120.9(5)	C3C8C7	119.5(5)
N1C9C10	121.1(4)	N1C9C14	119.6(4)	C10C9C14	119.4(4)
C9C10C11	121.2(5)	C10C11C12	119.2(5)	C11C12C13	120.6(5)
C12C13C14	119.7(5)	N4C14C9	121.7(4)	N4C14C13	118.2(4)
C9C14C13	120.0(4)				

4-(4-Chlorophenyl)-1-(2-nitrophenyl)-1*H*-1,2,3-triazole (2.98)

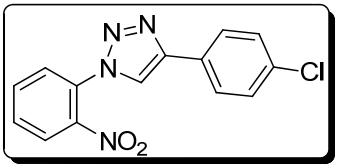

Mol. Formula	: $C_{14}H_9ClN_4O_2$
M. P.	: 136–138 ^oC
^{1}H NMR ($CDCl_3$, 500 MHz)	: δ 7.43 (d, *J* = 8.4 Hz, 2H), 7.67 (dd, *J* = 1.2, 7.7 Hz, 1H), 7.72 (dt, *J* = 1.2, 7.7 Hz, 1H), 7.80–7.84 (m, 3H), 8.08 (s, 1H), 8.10 (dd, *J* = 1.2, 8.1 Hz, 1H) ppm.
^{13}C NMR ($CDCl_3$, 125 MHz)	: δ 121.1 (d), 125.6 (d), 127.2 (d, 2C), 127.9 (d), 128.2 (s), 129.1 (d, 2C), 130.1 (s), 130.9 (d), 133.9 (d), 134.4 (s), 144.3 (s), 147.3 (s) ppm.
Elemental Analysis	Calcd.: C, 55.92; H, 3.02; Cl, 11.79; N, 18.63 Found: C, 55.94; H, 2.99; Cl, 11.74; N, 18.60

Figure 2.41 *The molecular structure of compound* ***2.98***

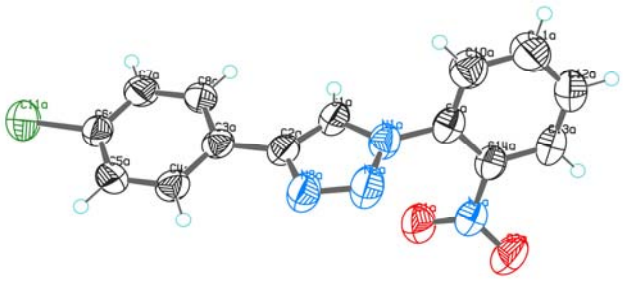

Bond length and bond angle in Å and º

Cl1A…C6A	1.739(3)	O1A…N4A	1.213(3)	O2A…N4A	1.208(3)
N1A…N2A	1.349(4)	N1A…C1A	1.341(3)	N1A…C9A	1.424(4)
N2A…N3A	1.320(3)	N3A…C2A	1.365(4)	N4A…C14A	1.468(4)
C1A…C2A	1.357(4)	C2A…C3A	1.468(4)	C3A…C4A	1.389(4)
C3A…C8A	1.384(4)	C4A…C5A	1.376(4)	C5A…C6A	1.362(4)
C6A…C7A	1.376(4)	C7A…C8A	1.379(4)	C9A…C10A	1.369(4)
C9A…C14A	1.387(4)	C10A…C11A	1.377(4)	C11A…C12A	1.374(4)
C12A…C13A	1.367(5)	C13A…C14A	1.381(4)	Cl1B…C6B	1.737(3)
O1B…N4B	1.208(4)	O2B…N4B	1.227(4)	N1B…N2B	1.355(3)
N1B…C1B	1.345(3)	N1B…C9B	1.420(3)	N2B…N3B	1.306(3)
N3B…C2B	1.373(4)	N4B…C14B	1.475(4)	C1B…C2B	1.362(4)
C2B…C3B	1.464(4)	C3B…C4B	1.384(4)	C3B…C8B	1.381(4)
C4B…C5B	1.380(4)	C5B…C6B	1.360(4)	C6B…C7B	1.369(4)
C7B…C8B	1.400(4)	C9B…C10B	1.364(4)	C9B…C14B	1.377(4)
C10B…C11B	1.384(4)	C11B…C12B	1.366(5)	C12B…C13B	1.377(5)
C13B…C14B	1.387(4)	Cl1C…C6C	1.737(3)	O1C...N4C	1.221(4)
O2C...N4C	1.218(5)	N1C...N2C	1.356(3)	N1C...C1C	1.341(4)
N1C...C9C	1.429(3)	N2C...N3C	1.309(3)	N3C...C2C	1.361(4)
N4C...C14C	1.475(4)	C1C...C2C	1.358(4)	C2C...C3C	1.470(4)
C3C...C4C	1.390(4)	C3C...C8C	1.383(5)	C4C…C5C	1.377(4)
C5C...C6C	1.372(5)	C6C...C7C	1.370(4)	C7C…C8C	1.385(4)
C9C...C10C	1.375(4)	C9C...C14C	1.385(4)	C10C…C11C	1.386(4)
C11C...C12C	1.380(6)	C12C...C13C	1.378(5)	C13C…C14C	1.380(4)

N2AN1AC1A	110.0(2)	N2AN1AC9A	122.1(2)	C1AN1AC9A	127.9(2)
N1AN2AN3A	107.0(2)	N2AN3AC2A	109.0(2)	O1AN4AO2A	122.8(3)
O1AN4AC14A	119.0(2)	O2AN4AC14A	118.1(2)	N1AC1AC2A	106.4(2)
N3AC2AC1A	107.5(2)	N3AC2AC3A	122.6(2)	C1AC2AC3A	129.8(3)
C2AC3AC4A	121.3(2)	C2AC3AC8A	120.4(3)	C4AC3AC8A	118.3(3)
C3AC4AC5A	120.4(3)	C4AC5AC6A	120.2(3)	Cl1AC6AC5A	120.2(2)
Cl1AC6AC7A	118.9(2)	C5AC6AC7A	120.9(3)	C6AC7AC8A	118.9(3)
C3AC8AC7A	121.3(3)	N1AC9AC10A	118.4(3)	N1AC9AC14A	122.5(3)
C10AC9AC14A	119.0(3)	C9AC10AC11A	120.3(3)	C10AC11AC12A	120.1(3)
C11AC12AC13A	120.6(3)	C12AC13AC14A	119.0(3)	N4AC14AC9A	121.6(3)
N4AC14AC13A	117.3(3)	C9AC14AC13A	120.9(3)	N2BN1BC1B	110.3(2)
N2BN1BC9B	119.6(2)	C1BN1BC9B	130.1(2)	N1BN2BN3B	106.9(2)
N2BN3BC2B	109.6(2)	O1BN4BO2B	125.0(3)	O1BN4BC14B	118.9(3)
O2BN4BC14B	116.1(3)	N1BC1BC2B	105.9(2)	N3BC2BC1B	107.2(2)
N3BC2BC3B	121.7(2)	C1BC2BC3B	131.0(3)	C2BC3BC4B	120.6(2)
C2BC3BC8B	120.9(2)	C4BC3BC8B	118.6(3)	C3BC4BC5B	120.8(3)
C4BC5BC6B	119.9(3)	Cl1BC6BC5B	119.2(2)	Cl1BC6BC7B	119.7(2)
C5BC6BC7B	121.1(3)	C6BC7BC8B	119.0(3)	C3BC8BC7B	120.6(3)
N1BC9BC10B	120.2(3)	N1BC9BC14B	120.7(3)	C10BC9BC14B	118.9(3)
C9BC10BC11B	120.3(3)	C10BC11BC12B	120.3(3)	C11BC12BC13B	120.4(3)
C12BC13BC14B	118.5(3)	N4BC14BC9B	121.1(3)	N4BC14BC13B	117.5(3)
C9BC14BC13B	121.4(3)	N2CN1CC1C	110.2(2)	N2CN1CC9C	119.0(2)
C1CN1CC9C	130.8(2)	N1CN2CN3C	107.0(2)	N2CN3CC2C	109.1(2)
O1CN4CO2C	124.7(3)	O1CN4CC14C	117.5(3)	O2CN4CC14C	117.7(3)

N1CC1CC2C 105.7(2)	N3CC2CC1C 108.0(3)	N3CC2CC3C 121.1(3)
C1CC2CC3C 130.8(3)	C2CC3CC4C 120.5(3)	C2CC3CC8C 122.1(3)
C4CC3CC8C 117.5(3)	C3CC4CC5C 121.4(3)	C4CC5CC6C 119.7(3)
Cl1CC6CC5C 119.3(2)	Cl1CC6CC7C 120.2(2)	C5CC6CC7C 120.5(3)
C6CC7CC8C 119.4(3)	C3CC8CC7C 121.6(3)	N1CC9CC10C120.3(3)
N1CC9CC14C120.7(3)	C10CC9CC14C119.0(3)	C9CC10CC11C120.0(3)
C10CC11CC12C120.3(3)	C11CC12CC13C120.2(3)	C12CC13CC14C118.9(3)
N4CC14CC9C120.8(3)	N4CC14CC13C117.6(3)	C9CC14CC13C121.5(3)

Table 2.6 *Crystal data of **2.96–2.98***

	2.96	**2.97**	**2.98**
Chemical formula	$C_{14}H_9ClN_4O_2$	$C_{14}H_9ClN_4O_2$	$C_{14}H_9ClN_4O_2$
M_r	300.70	300.70	300.70
Temperature/K	297(2)	297(2)	297(2)
Crystal size/mm	0.21 x 0.11 x 0.07	0.33 x 0.25 x 0.10	0.55 x 0.31 x 0.15
Crystal system	Monoclinic	Monoclinic	Orthorhombic
Space group	$P2_1/n$	$P21$	$P212121$
a/Å	12.340(3)	7.705(18)	10.8467(15)
b/Å	7.8967(15)	7.191(18)	14.129(2)
c/Å	14.187(3)	12.34(3)	26.790(4)
α/°	90	90	90
β/°	100.414(3)	92.39(7)	90
γ/°	90	90	90
V/Å^3	1359.7(5)	683(3)	4105.5(10)
Z	4	2	4
F(000)	616	308	1848
D_{calc}/g cm^{-3}	1.469	1.461	1.459
μ/mm^{-1}	0.291	0.289	0.289
Absorp.correction	Multi-scan	Multi-scan	Multi-scan
T min	0.9415	0.9106	0.8573
T max	0.9799	0.9717	0.9580
Reflns collected	12671	3964	27374
Unique reflns	2399	2311	7975
Observed reflns	1878	1804	5193
h, k, l (min, max)	(-14,14), (-9,9), (-16,16)	(-9,9), (-8,8), (-14,14)	(-13,13),(-17,17),(-32,33)
R_{int}	0.0344	0.0991	0.0466
No. of parameters	226	191	568
$R_1[I > 2\sigma(I)]$	0.0359	0.0697	0.0449
$wR_2[I > 2\sigma(I)]$	0.0887	0.1752	0.0761
R_1_all data	0.0488	0.0845	0.0859

wR_2_all data	0.0959	0.1845	0.0883
GoF	1.030	1.088	1.026
$\Delta\rho_{max},\Delta\rho_{min}(eÅ^{-3})$	0.185, -0.172	0.240, -0.241	0.155, -0.139

4-(2-Chlorophenyl)-1-(3-nitrophenyl)-1*H*-1,2,3-triazole (2.99)

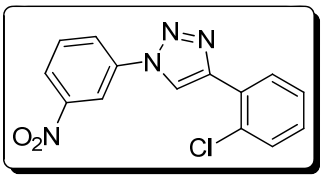

Mol. Formula : $C_{14}H_9ClN_4O_2$

M. P. : 149 ^oC

^{1}H NMR (CDCl$_3$, 500 MHz) : δ 7.35 (dt, *J* = 1.7, 7.6 Hz, 1H), 7.43 (dt, *J* = 1.2, 7.6 Hz, 1H), 7.48 (dd, *J* = 1.0, 8.1 Hz, 1H), 7.70 (t, *J* = 8.3, 1H), 8.26 (dd, *J* = 1.9, 8.1 Hz, 1H), 8.33 (dt, *J* = 1.7, 7.8 Hz, 2H), 8.69 (t, *J* = 2.2, 1H), 8.74 (s, 1H) ppm.

^{13}C NMR (CDCl$_3$, 125 MHz) : δ 115.3 (d), 120.9 (d), 123.3 (d), 126.0 (d), 127.3 (d), 128.3 (s), 129.7 (d), 130.0 (d), 130.4 (d), 131.0 (d), 131.4 (s), 137.7 (s), 145.3 (s), 149.0 (s) ppm.

Elemental Analysis
Calcd.: C, 55.92; H, 3.02; Cl, 11.79; N, 18.63
Found: C, 55.97; H, 2.97; Cl, 11.73; N, 18.60

Figure 2.42 *The molecular structure of compound* ***2.99***

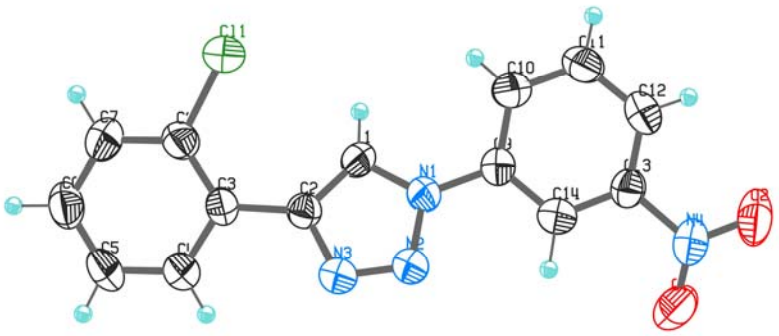

Bond length and bond angle in Å and °

Cl1…C8	1.745(4)	O1…N4	1.219(6)	O2…N4	1.219(5)
N1…N2	1.363(5)	N1…C1	1.351(6)	N1…C9	1.419(5)
N2…N3	1.295(5)	N3…C2	1.365(5)	N4…C13	1.481(5)
C1…C2	1.352(6)	C2…C3	1.477(5)	C3…C4	1.401(6)
C3…C8	1.386(6)	C4…C5	1.379(7)	C5…C6	1.361(8)
C6…C7	1.374(8)	C7…C8	1.373(6)	C9…C10	1.398(6)
C9…C14	1.378(6)	C10…C11	1.365(7)	C11…C12	1.385(7)
C12…C13	1.374(6)	C13…C14	1.370(6)		

N2N1C1	109.2(3)	N2N1C9	120.3(3)	C1N1C9	130.4(4)
N1N2N3	107.3(3)	N2N3C2	109.7(3)	O1N4O2	124.2(4)
O1N4C13	118.4(4)	O2N4C13	117.4(4)	N1C1C2	106.1(4)
N3C2C1	107.7(4)	N3C2C3	120.5(4)	C1C2C3	131.8(4)
C2C3C4	119.1(4)	C2C3C8	124.7(4)	C4C3C8	116.2(4)
C3C4C5	121.1(4)	C4C5C6	121.0(5)	C5C6C7	119.3(5)
C6C7C8	120.0(5)	Cl1C8C3	121.0(3)	Cl1C8C7	116.5(3)
C3C8C7	122.4(4)	N1C9C10	120.6(4)	N1C9C14	119.5(4)
C10C9C14	119.9(4)	C9C10C11	120.0(4)	C10C11C12	120.8(4)
C11C12C13	117.9(4)	N4C13 C12	119.5(4)	N4C13 C14	117.6(4)
C12C13C14	122.9(4)	C9C14 C13	118.5(4)		

4-(3-Chlorophenyl)-1-(3-nitrophenyl)-1*H*-1,2,3-triazole (2.100)

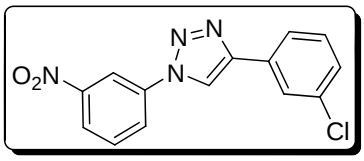

Mol. Formula	: $C_{14}H_9ClN_4O_2$
M. P.	: 186 °C
^{1}H NMR (DMSO-d_6, 500 MHz)	: δ 7.40 (dd, *J* = 1.0, 7.7 Hz, 1H), 3.50 (t, *J* = 7.9 Hz, 1H), 7.86–7.91 (m, 3H), 8.30 (dd, *J* = 1.6, 8.3 Hz, 1H), 8.37 (dd, *J* = 1.4, 8.0 Hz, 1H), 8.68 (t, *J* = 2.0 Hz, 1H), 9.57 (s, 1H) ppm.
^{13}C NMR (DMSO-d_6, 125 MHz)	: δ 114.6 (d), 120.8 (d), 123.4 (d), 124.0 (d), 125.2 (d), 125.9 (d), 128.4 (d), 131.2 (d), 131.8 (d), 132.1 (s), 134.0 (s), 137.2 (s), 146.5 (s), 148.7 (s) ppm.
Elemental Analysis	Calcd.: C, 55.92; H, 3.02; Cl, 11.79; N, 18.63 Found: C, 55.94; H, 2.99; Cl, 11.80; N, 18.67

Figure 2.43 *The molecular structure of compound* ***2.100***

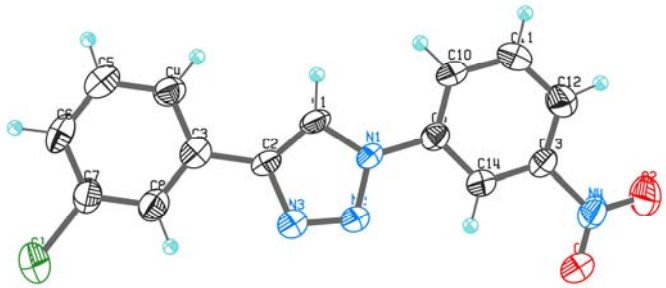

Bond length and bond angle in Å and °

Cl1…C7	1.741(4)	O1…N4	1.216(4)	O2…N4	1.225(6)
N1…N2	1.353(4)	N1…C1	1.355(6)	N1…C9	1.431(5)
N2…N3	1.304(6)	N3…C2	1.376(6)	N4…C13	1.484(7)
C1…C2	1.350(5)	C2…C3	1.473(7)	C3…C4	1.396(6)
C3…C8	1.379(5)	C4…C5	1.395(8)	C5…C6	1.373(7)
C6…C7	1.400(7)	C7…C8	1.367(7)	C9…C10	1.379(6)
C9…C14	1.386(7)	C10…C11	1.374(6)	C11…C12	1.374(8)
C12…C13	1.379(6)	C13…C14	1.373(6)		

N2N1C1	109.5(3)	N2N1C9	120.2(3)	C1N1C9	130.3(3)
N1N2N3	107.6(3)	N2N3C2	109.1(4)	O1N4O2	123.3(4)
O1N4C13	118.0(4)	O2N4C13	118.7(4)	N1C1C2	106.2(4)
N3C2C1	107.6(4)	N3C2C3	121.6(4)	C1C2C3	130.8(4)
C2C3C4	121.0(4)	C2C3C8	120.2(4)	C4C3C8	118.8(4)
C3C4C5	120.8(4)	C4C5C6	119.7(5)	C5C6C7	119.1(5)
Cl1C7C6	118.9(4)	Cl1C7C8	120.0(4)	C6C7C8	121.1(4)
C3C8C7	120.5(4)	N1C9C10	121.2(4)	N1C9C14	118.2(4)
C10C9C14	120.7(4)	C9C10C11	120.0(4)	C10C11C12	121.1(5)
C11C12C13	117.2(4)	N4C13C12	118.8(4)	N4C13C14	117.4(4)
C12C13C14	123.8(4)	C9C14C13	117.1(4)		

4-(4-Chlorophenyl)-1-(3-nitrophenyl)-1*H*-1,2,3-triazole(2.101)

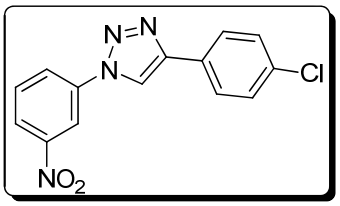

Mol. Formula : $C_{14}H_9ClN_4O_2$

M. P. : 223-224 °C

^{1}H NMR (DMSO-d_6, 200 MHz) : δ 7.37 (dd, *J* = 2.2, 8.5 Hz, 2H), 7.74–7.88 (m, 3H), 8.17 (dd, *J* = 1.6, 8.0 Hz, 1H), 8.31–8.36 (m, 1H), 8.72 (t, *J* = 2.1

	Hz, 1H), 9.37 (s, 1H) ppm.
^{13}C NMR (DMSO-d_6, 125 MHz)	: δ 113.2 (d), 118.1 (d), 121.3 (d), 124.1 (d), 125.6 (d, 2C), 127.4 (d, 2C), 127.5 (s), 129.7 (d), 132.1 (s), 136.2 (s), 145.7 (s), 147.3 (s) ppm.
Elemental Analysis	Calcd.: C, 55.92; H, 3.02; Cl, 11.79; N, 18.63 Found: C, 55.88; H, 2.99; Cl, 11.79; N, 18.69

Figure 2.44 *The molecular structure of compound* ***2.101***

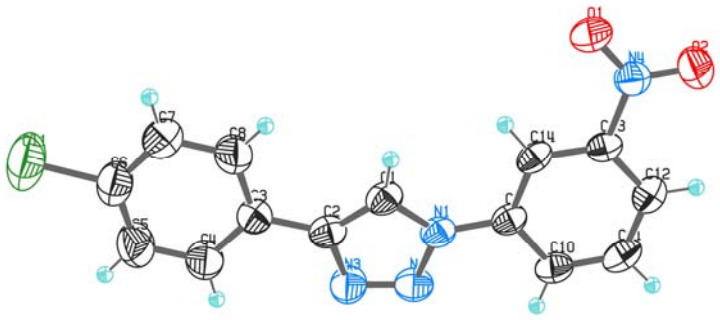

Bond length and bond angle in Å and °

Cl1...C6	1.730(4)	O1...N4	1.218(4)	O2...N4	1.216(4)
N1...N2	1.360(4)	N1...C1	1.351(5)	N1...C9	1.411(5)
N2...N3	1.299(5)	N3...C2	1.366(4)	N4...C13	1.470(4)
C1…C2	1.344(5)	C2…C3	1.459(5)	C3…C4	1.371(6)
C3…C8	1.383(6)	C4…C5	1.368(6)	C5…C6	1.361(7)
C6…C7	1.351(7)	C7…C8	1.378(6)	C9…C10	1.386(5)
C9…C14	1.383(5)	C10…C11	1.357(6)	C11…C12	1.381(5)
C12…C13	1.367(5)	C13…C14	1.365(5)		
N2N1C1	108.7(3)	N2N1C9	120.1(3)	C1N1C9	131.2(3)
N1N2N3	107.8(3)	N2N3C2	109.0(3)	O1N4O2	123.3(3)
O1N4C13	118.2(3)	O2N4C13	118.5(3)	N1C1C2	106.6(3)
N3C2C1	107.9(3)	N3C2C3	121.7(3)	C1C2C3	130.4(3)
C2C3C4	122.3(3)	C2C3C8	120.2(3)	C4C3C8	117.5(4)
C3C4C5	122.3(4)	C4C5C6	119.1(4)	Cl1C6C5	120.1(4)
Cl1C6C7	119.6(4)	C5C6C7	120.2(4)	C6C7C8	120.8(5)
C3C8C7	120.1(4)	N1C9C10	120.6(3)	N1C9C14	119.8(3)
C10C9C14	119.7(3)	C9C10C11	120.6(3)	C10C11C12	120.8(4)
C11C12C13	117.5(3)	N4C13C12	118.6(3)	N4C13C14	117.8(3)
C12C13C14	123.6(3)	C9C14C13	117.9(3)		

Table 2.7 *Crystal data of* ***2.99–2.101***

	2.99	**2.100**	**2.101**
Chemical formula	$C_{14}H_9ClN_4O_2$	$C_{14}H_9ClN_4O_2$	$C_{14}H_9ClN_4O_2$
M_r	300.70	300.70	300.70
Temperature/K	297(2)	297(2)	297(2)
Crystal size/mm	0.15 x 0.11 x 0.05	0.26 x 0.14 x 0.10	0.32 x 0.07 x 0.03
Crystal system	Monoclinic	Triclinic	Monoclinic
Space group	$P2_1/c$	*P-1*	*P21/n*
a/Å	12.448(4)	7.080(2)	8.550(5)
b/Å	6.992(2)	8.369(2)	5.256(3)
c/Å	15.083(4)	13.026(4)	29.749(18)
α/°	90	102.628(4)	90
β/°	95.273(6)	94.538(5)	96.543(10)
γ/°	90	114.741(4)	90
V/Å^3	1308.5(7)	671.2(3)	1328.1(14)
Z	4	2	4
F(000)	616	308	616
D_{calc}/g cm^{-3}	1.526	1.488	1.504
μ/mm^{-1}	0.302	0.294	0.298
Absorp.correction	Multi-scan	Multi-scan	Multi-scan
T min	0.9561	0.9274	0.9108
T max	0.9851	0.9712	0.9911
Reflns collected	9013	6261	6072
Unique reflns	2285	2348	2330
Observed reflns	1826	1794	1548
h, k, l (min, max)	(-14,13),(-8,8),(-17,17)	(-8,8), (-9,9), (-15,15)	(-10,108), (-6,6), (-35,19)
R_{int}	0.0546	0.0421	0.0618
No. of parameters	226	202	226
$R_1[I > 2\sigma(I)]$	0.0844	0.0821	0.0649
$wR_2[I > 2\sigma(I)]$	0.1507	0.1925	0.1399
R_1_all data	0.1069	0.1067	0.0993
wR_2_all data	0.1596	0.2050	0.1594
GoF	1.243	1.167	1.043
$\Delta\rho_{max},\Delta\rho_{min}$(eÅ^{-3})	0.214, -0.205	0.317, -0.300	0.232, -0.266

4-(2-Chlorophenyl)-1-(4-nitrophenyl)-1*H*-1,2,3-triazole(2.102)

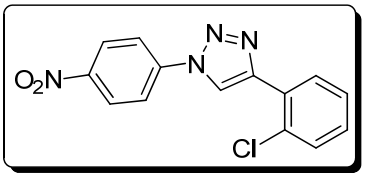

Mol. Formula	: $C_{14}H_9ClN_4O_2$
M. P.	: 214–216 °C
^{1}H NMR (DMSO-d_6, 400 MHz)	: δ 7.44–7.52 (m, 2H), 7.62 (d, *J* = 7.5 Hz, 1H), 8.08 (dd, *J* = 1.5, 7.5 Hz, 1H), 8.33 (d, *J* = 8.8, 2H), 8.45 (d, *J* = 9.0 Hz, 2H), 9.42 (s, 1H) ppm.
^{13}C NMR (DMSO-d_6, 100 MHz)	: δ 120.85 (d, 2C), 122.48 (d), 125.45 (d, 2C), 127.58 (d), 128.31 (s), 129.96 (d), 130.11 (d), 130.29 (d), 130.80 (s), 140.67 (s), 144.36 (s), 146.76 (s) ppm.
Elemental Analysis	Calcd.: C, 55.92; H, 3.02; Cl, 11.79; N, 18.63 Found: C, 55.97; H, 2.97; Cl, 11.77; N, 18.67

Figure 2.45 *The molecular structure of compound* ***2.102***

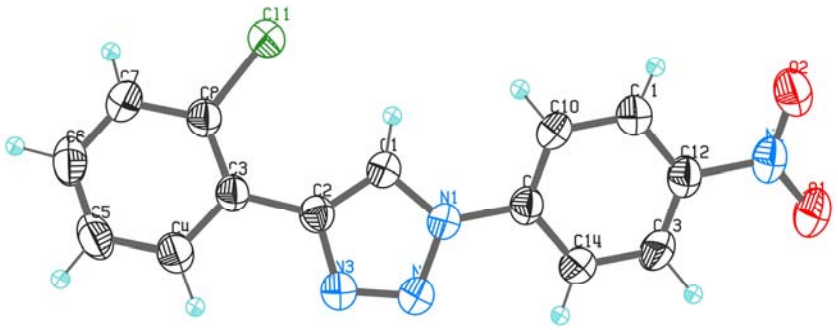

Bond length and bond angle in Å and °

Cl1…C8	1.734(3)	O1...N4	1.218(3)	O2...N4	1.222(4)
N1...N2	1.354(3)	N1...C1	1.352(3)	N1...C9	1.425(4)
N2...N3	1.309(3)	N3...C2	1.360(3)	N4...C12	1.473(4)
C1...C2	1.366(4)	C2...C3	1.478(4)	C3...C4	1.402(4)
C3...C8	1.391(3)	C4...C5	1.377(4)	C5...C6	1.374(4)
C6...C7	1.368(5)	C7...C8	1.387(4)	C9...C10	1.381(4)
C9...C14	1.390(4)	C10...C11	1.373(4)	C11…C12	1.388(4)
C12…C13	1.363(4)	C13…C14	1.381(4)		
N2N1C1	110.5(2)	N2N1C9	121.4(2)	C1N1C9	128.1(2)
N1N2N3	106.6(2)	N2N3C2	110.0(2)	O1N4O2	123.7(3)

O1N4C12	118.1(2)	O2N4C12	118.3(2)	N1C1C2	105.3(2)
N3C2C1	107.7(2)	N3C2C3	120.3(2)	C1C2C3	132.0(3)
C2C3C4	118.7(2)	C2C3C8	124.9(2)	C4C3C8	116.4(2)
C3C4C5	121.4(3)	C4C5C6	120.5(3)	C5C6C7	119.9(3)
C6C7C8	119.7(3)	Cl1C8C3	121.9(2)	Cl1C8C7	115.9(2)
C3C8C7	122.2(3)	N1C9C10	119.9(2)	N1C9C14	118.9(2)
C10C9C14	121.2(3)	C9C10C11	119.7(3)	C10C11C12	118.6(3)
N4C12C11	118.1(2)	N4C12C13	119.8(2)	C11C12C13	122.1(3)
C12C13C14	119.5(3)	C9C14C13	118.8(3)		

4-(3-Chlorophenyl)-1-(4-nitrophenyl)-1*H*-1,2,3-triazole (2.103)

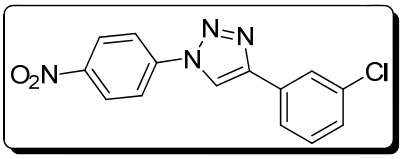

Mol. Formula	: $C_{14}H_9ClN_4O_2$
M. P.	: 222–223 ^oC
^{1}H NMR (DMSO-d_6, 400 MHz)	: δ 7.40 (dd, *J* = 0.9, 8.0 Hz, 1H), 7.48 (t, *J* = 8.0 Hz, 1H), 7.85 (d, *J* = 7.8 Hz, 1H), 7.90 (t, *J* = 1.9 Hz, 1H), 8.15 (d, *J* = 9.0 Hz, 2H), 8.41 (d, *J* = 9.0 Hz, 2H), 9.49 (s, 1H) ppm.
^{13}C NMR (DMSO-d_6, 100 MHz)	: δ 120.7 (d, 2C), 120.9 (d), 124.1 (d), 125.3 (d), 125.9 (d, 2C), 128.5 (d), 131.3 (d), 132.0 (s), 134.1 (s), 140.9 (s), 146.7 (s), 147.0 (s) ppm.
Elemental Analysis	Calcd.: C, 55.92; H, 3.02; Cl, 11.79; N, 18.63 Found: C, 55.87; H, 3.03; Cl, 11.73; N, 18.61

Figure 2.46 *The molecular structure of compound* ***2.103***

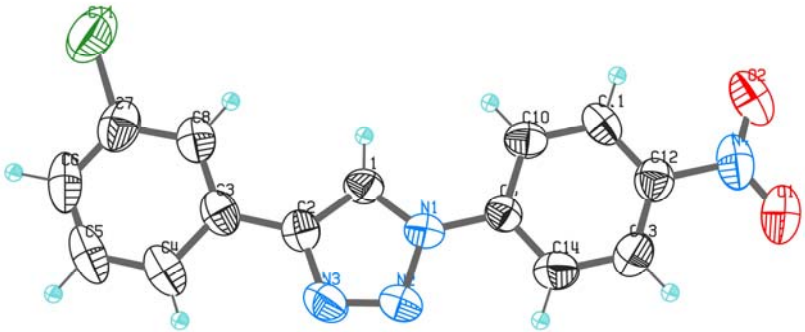

Bond length and bond angle in Å and º

Cl1...C7	1.746(7)	O1...N4	1.226(8)	O2...N4	1.215(8)
N1...N2	1.362(6)	N1...C1	1.345(7)	N1...C9	1.426(6)
N2...N3	1.307(7)	N3...C2	1.364(7)	N4…C12	1.478(8)
C1...C2	1.363(7)	C2…C3	1.462(8)	C3…C4	1.402(8)
C3…C8	1.396(8)	C4…C5	1.38(1)	C5…C6	1.37(1)
C6…C7	1.389(9)	C7…C8	1.394(8)	C9…C10	1.398(6)
C9…C14	1.369(7)	C10…C11	1.381(7)	C11…C12	1.366(8)
C12…C13	1.393(8)	C13…C14	1.388(8)		

N2N1C1	109.5(4)	N2N1C9	120.4(4)	C1N1C9	130.1(4)
N1N2N3	107.0(4)	N2N3C2	109.9(4)	O1N4O2	124.9(6)
O1N4C12	117.1(5)	O2N4C12	118.0(5)	N1C1C2	106.5(4)
N3C2C1	107.1(4)	N3C2C3	121.8(5)	C1C2C3	131.1(5)
C2C3C4	120.4(5)	C2C3C8	121.1(5)	C4C3C8	118.5(5)
C3C4C5	120.9(5)	C4C5C6	121.3(6)	C5C6C7	118.3(6)
Cl1C7C6	120.2(5)	Cl1C7C8	117.8(4)	C6C7C8	122.0(5)
C3C8C7	119.0(5)	N1C9C10	119.5(4)	N1C9C14	119.4(4)
C10C9C14	121.2(4)	C9C10C11	119.1(4)	C10C11C12	119.4(5)
N4C12C11	118.9(5)	N4C12C13	119.1(5)	C11C12C13	121.9(5)
C12C13C14	118.6(5)	C9C14C13	119.7(5)		

4-(4-Chlorophenyl)-1-(4-nitrophenyl)-1*H*-1,2,3-triazole (2.104)

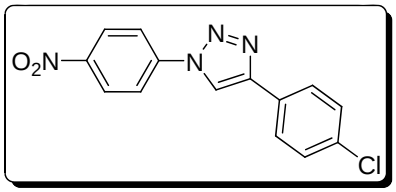

Mol. Formula	: $C_{14}H_9ClN_4O_2$
M. P.	: 246–248 ^oC
^{1}H NMR (DMSOd_6, 400 MHz)	: δ 7.58 (d, *J* = 5.6 Hz, 2H), 7.95 (d, *J* = 5.6 Hz, 2H), 8.23 (d, *J* = 7.0 Hz, 2H), 8.48 (d, *J* = 7.0 Hz, 2H), 9.53 (s, 1H) ppm.
^{13}C NMR (DMSOd_6, 100 MHz)	: δ 120.5 (d), 120.5 (s), 120.6 (d, 2C), 125.8 (d, 2C), 127.2 (d, 2C), 128.8 (s), 129.3 (d, 2C), 133.2 (s), 140.9 (s), 146.9 (s) ppm.
Elemental Analysis	Calcd.: C, 55.92; H, 3.02; Cl, 11.79; N, 18.63 Found: C, 55.87; H, 2.95; Cl, 11.72; N, 18.58

Figure 2.47 *The molecular structure of compound* ***2.104***

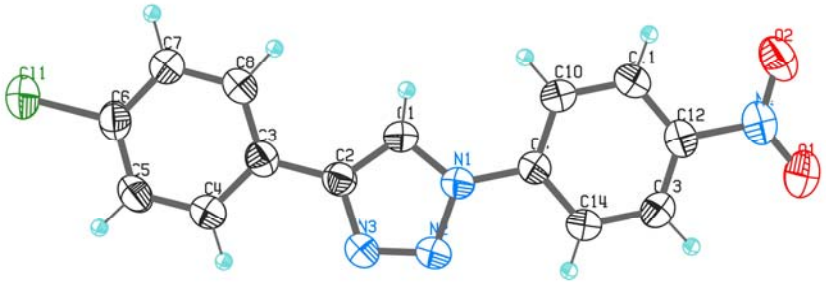

Bond length and bond angle in Å and º

Cl1...C6	1.747(3)	O1...N4	1.221(3)	O2...N4	1.229(3)
N1...N2	1.357(3)	N1...C1	1.348(3)	N1...C9	1.432(3)
N2...N3	1.306(3)	N3...C2	1.375(3)	N4…C12	1.476(3)
C1…C2	1.367(3)	C2…C3	1.469(3)	C3…C4	1.399(3)
C3…C8	1.394(3)	C4…C5	1.382(4)	C5…C6	1.391(3)
C6…C7	1.384(3)	C7…C8	1.383(3)	C9…C10	1.388(3)
C9…C14	1.389(3)	C10…C11	1.380(3)	C11…C12	1.381(3)
C12…C13	1.379(4)	C13…C14	1.379(3)		

N2N1C1	110.2(2)	N2N1C9	120.4(2)	C1N1C9	129.4(2)
N1N2N3	107.2(2)	N2N3C2	109.5(2)	O1N4O2	123.8(2)
O1N4C12	118.8(2)	O2N4C12	117.4(2)	N1C1C2	105.9(2)
N3C2C1	107.3(2)	N3C2C3	122.2(2)	C1C2C3	130.5(2)
C2C3C4	120.9(2)	C2C3C8	121.1(2)	C4C3C8	117.9(2)
C3C4C5	121.4(2)	C4C5C6	119.1(2)	Cl1C6C5	119.2(2)
Cl1C6C7	119.8(2)	C5C6C7	121.0(2)	C6C7C8	119.1(2)
C3C8C7	121.6(2)	N1C9C10	119.5(2)	N1C9C14	119.5(2)
C10C9C14	120.9(2)	C9C10C11	119.6(2)	C10C11C12	119.0(2)
N4C12C11	119.2(2)	N4C12C13	118.9(2)	C11C12C13	121.9(2)
C12C13C14	119.3(2)	C9C14C13	119.3(2)		

Table 2.8 *Crystal data of* ***2.102–2.104***

	2.102	**2.103**	**2.104**
Chemical formula	$C_{14}H_9ClN_4O_2$	$C_{14}H_9ClN_4O_2$	$C_{14}H_9ClN_4O_2$
M_r	300.70	300.70	300.70
Temperature/K	297(2)	297(2)	297(2)
Crystal size/mm	0.24 x 0.14 x 0.07	0.27 x 0.17 x 0.09	0.62 x 0.15 x 0.11
Crystal system	Triclinic	Monoclinic	Monoclinic
Space group	*P-1*	*P21/c*	*P21/c*
a/Å	7.013(4)	7.587(8)	7.954(7)
b/Å	7.312(4)	13.601(14)	13.263(11)
c/Å	13.309(7)	13.338(13)	12.684(11)
α/°	94.793(8)	90	90
β/°	96.114(8)	91.266(17)	94.559(14)
γ/°	107.261(8)	90	90
V/Å^3	643.2(6)	1376(2)	1334(2)
Z	2	4	4
F(000)	308	616	616
D_{calc}/g cm^{-3}	1.553	1.452	1.498
μ/mm^{-1}	0.307	0.287	0.296
Absorp.correction	Multi-scan	Multi-scan	Multi-scan
T min	0.9299	0.9265	0.8376
T max	0.9788	0.9746	0.9681
Reflns collected	5920	6269	9661
Unique reflns	2244	2422	2607
Observed reflns	1792	1560	2080
h, k, l (min, max)	(-8,8),(-8,8), (-15,15)	(-9,8),(-16,9), (-15,15)	(-9,9),(-16,16), (-15,15)
R_{int}	0.0496	0.0784	0.0364
No. of parameters	190	190	226
$R_1[I > 2\sigma(I)]$	0.0527	0.1000	0.0497
$wR_2[I > 2\sigma(I)]$	0.1434	0.2470	0.1148
R_1_all data	0.0634	0.1394	0.0637
wR_2_all data	0.1507	0.2781	0.1242
GoF	1.070	1.024	1.040
$\Delta\rho_{max},\Delta\rho_{min}$(eÅ^{-3})	0.221, -0.262	0.290, -0.302	0.307, -0.198

Table 2.9 Geometrical Parameters of Intermolecular Interactions

	D-H···A	D-H (Å)	H···A (Å)	D···A (Å)	D-H···A (°)	Symmetry codes
2.45	C1-H1···O1 C11-H11···N2 C13-H13···O2	0.94(3) 0.97(3) 0.97(3)	2.47(3) 2.71(3) 2.59(3)	3.270(3) 3.642(4) 3.334(4)	143(2) 162(2) 133(2)	1.5-x, -1/2+y, 1/2-z x, -1+y, z 1-x, -y, 1-z
2.46	C1-H1···O1 C14-H14···O1 C8-H8···O2 C6-H6···O2 C10-H10···N2	0.93 0.93 0.93 0.93 0.93	2.53 2.48 2.70 2.57 2.50	3.409(3) 3.408(3) 3.593(3) 3.372(3) 3.358(3)	158 176 160 144 154	-x, 2-y, 1-z -x, 2-y, 1-z -x, 2-y, 1-z x, 1.5-y, 1/2+z 1-x, -y, 1-z
2.47	C6-H6···O1 C6-H6···O2	0.956(17) 0.956(17)	2.575(17) 2.660(17)	3.342(2) 3.333(2)	137.3(13) 127.7(12)	x, 1+y, 1+z 1+x, 1+y, 1+z
2.96	C(1)-H(1)...O(1) C(13)-H(13)...O(2) C(5)-H(5)...Cl(1)	0.90(2) 0.88(2) 0.91(2)	2.58(2) 2.70(2) 2.89(2)	3.397(3) 3.385(3) 3.652(3)	150.4(16) 135.1(17) 142.0(18)	-x+1/2,y+1/2,-z+1/2 -x+1,-y+2,-z x,y-1,z
2.97	C(13)-H(13)...N(2) C(11)-H(11)...N(2) C(5)- H(5)...O(2) C(4)-H(4)...Cl(1)	0.93 0.93 0.93 0.93	2.66 2.68 2.64 2.92	3.573(9) 3.596(9) 3.379(10) 3.617(9)	168.3 168.6 136.3 132.7	-x+2,y+1/2,-z+1 x+1,y,z x,y,z+1 x+1,y,z
2.98	C(10C)-H(10C)...O(2B) C(1C)-H(1C)...O(2B) C(5C)-H(5C)...O(1A) C(1B)-H(1B)...N(3C) C(1B)-H(1B)...N(2C) C(12B)-H(12B)...O(1C) C(5A)-H(5A)...N(2B)	0.93 0.93 0.93 0.93 0.93 0.93 0.93	2.63 2.65 2.71 2.55 2.49 2.50 2.74	3.221(4) 3.416(4) 3.530(4) 3.445(4) 3.282(4) 3.413(4) 3.629(4)	122.0 140.3 146.8 162.8 142.7 168.5 160.4	-x+1,y-1/2,-z+1/2 -x+1,y-1/2,-z+1/2 -x+1,y-1/2,-z+1/2 -x+2,y+1/2,-z+1/2 -x+2,y+1/2,-z+1/2 x,y+1,z x,y,z
2.99	C(1)-H(1)...O(1) C(6)- H(6)...O(1) C(7)-H(7)...O(2)	0.91(3) 0.95(5) 0.94(4)	2.72(3) 2.66(6) 2.58(4)	3.252(6) 3.500(6) 3.328(6)	118(3) 147(4) 136(3)	-x+2,y-1/2,-z+3/2 x-1,-y+3/2,z-1/2 x-1,-y+1/2,z-1/2
2.100	C(5)-H(5)...N(2) C(12)-H(12)...O(2) C(1)-H(1)...O(1)	0.93(5) 0.94(2) 0.98(4)	2.60(5) 2.52(3) 2.26(4)	3.470(6) 3.418(6) 3.235(5)	157(4) 161(4) 171(3)	x,y+1,z -x+2,-y+1,-z+2 x,y+1,z
2.101	C(10)-H(10)...N(2) C(14)-H(14)...O(1) C(8)-H(8)...O(2) C(1)-H(1)...O(1)	0.88(3) 0.88(3) 0.89(3) 0.89(3)	2.59(3) 2.51(3) 2.64(4) 2.53(3)	3.338(5) 3.385(4) 3.460(5) 3.399(5)	143(3) 173(3) 154(3) 165(3)	-x+1,-y+2,-z+1 -x,-y,-z+1 -x,-y,-z+1 -x,-y,-z+1
2.102	C(6)-H(6)...O(2) C(14)-H(14)...O(2) C(5)-H(5)...Cl(1) C(11)-H(11)...N(2)	0.97(3) 0.93(3) 0.92(3) 0.91(3)	2.54(3) 2.51(3) 2.93(3) 2.57(3)	3.486(4) 3.377(4) 3.487(3) 3.367(4)	166(3) 155(2) 120(2) 147(2)	x,y+1,z-1 x,y+1,z x,y+1,z x,y-1,z
2.103	C(1)-H(1)...O(2) C(10)-H(10)...O(1) C(5)-H(5)...N(2)	0.93 0.93 0.93	2.36 2.63 2.58	3.283(7) 3.423(7) 3.438(7)	175.1 143.0 152.9	-x+1,y-1/2,-z+1/2 -x+1,y-1/2,-z+1/2 -x+2,y-1/2,-z-1/2
2.104	C(1)-H(1)...O(2) C(10)-H(10)...O(2) C(5)-H(5)...N(2)	0.86(2) 0.94(2) 0.92(3)	2.43(3) 2.62(3) 2.74(3)	3.288(3) 3.521(4) 3.622(4)	174(2) 162.1(18) 160.9(19)	-x+1,y-1/2,-z+3/2 -x+1,y-1/2,-z+3/2 -x,y-1/2,-z+5/2

2.9 REFERENCES

1. Desiraju, G. R. *Crystal Engineering: The Design of Organic Solids*. Elsevier, Amsterdam, **1989**.
2. Corey, E. J. *Pure Appl. Chem*. **1967**, *14*, 19–38.
3. Desiraju, G. R. *Angew. Chem. Int. Ed. Engl*. **1995**, *34*, 2311–2321.
4. Cohen, M. D.; Schmidt, G. M. *J. Chem. Soc*. **1964**, 1996–2000.
5. Janiak, C. *Angew. Chem. Int. Ed*. **1997**, *36*, 1431–1433.
6. Farrel, R. P. *Inorg. Chem*. **1995**, *34*, 757–758.
7. Beer, P. D. *Acc. Che. Res*. **1998**, *31*, 71–80.
8. Pecaut, J.; Levy, J. P. *J. Mater. Chem*. **1993**, *3*, 999–1003.
9. a) Schmidt, G. M. J. *Pure Appl. Chem.* **1971**, *27*, 647–678. b) Lehn, J. – M. *Pure Appl. Chem.* **1978**, *50*, 871–892. c) Lehn, J. – M. *Supramolecular Chemistry: Concepts and Perspectives*, VCH, Weinheim, **1995**. d) Aakeröy, C. B. *Acta Crystallogr. B* **1997**, *53*, 569–586. e) Lehn, J. – M. *Proc. Natl. Acad. Sci. USA* **2002**, *99*, 4763–4768. f) Whitesides, G. M.; Boncheva, M. *Proc. Natl. Acad. Sci. USA* **2002**, *99*, 4769–4774. g) Desiraju, G. R. *Crystal Design: Structure and Function*, Wiley: New York, **2003**. h) Desiraju, G. R. *J. Mol. Struct.* **2003**, *656*, 5–15. i) Bis, J. A.; Zaworotko, M. J. *Cryst. Growth Des*. **2005**, *5*, 1169–1197.
10. a) Kitaigorodsky, A. I. *Molecular Crystals and Molecules*, Academic Press, New York, London, **1973**, chap. 2. b) Dunitz, J. D. *X-Ray Analysis and the Structure of Organic Molecules*, Cornell University Press. Ithaca, London, **1979**, part 2. c) Lehn, J.–M. *Angew. Chem. Int. Ed. Engl.* **1990**, *29*, 1304–1319. d) Desiraju, G. R.; Steiner, T. *The Weak Hydrogen Bond in Structural Chemistry and Biology*, Oxford University Press, Oxford, **1999**. e) Steiner, T. *Angew. Chem. Int. Ed*. **2002**, *41*, 48–76. f) Meyer, E.A.; Castellano, R. K.; Diederich, F. *Angew. Chem. Int. Ed*. **2003**, *42*, 1210–1250. g) Dunitz, J. D.; Gavezzootti, A. *Angew. Chem. Int. Ed.* **2005**, *44*, 1766–1787.
11. a) Etter, M. C. *Acc. Chem. Res.* **1990**, *23*, 120–126. b) Etter, M. C. *J. Phys. Chem.* **1991**, *95*, 4601–4610. c) Bernstein, J. *Acta Crystallogr. B* **1991**, *47*, 1004–1007. d) Bernstein, J.; Davis, R. E.; Shimoni, L.; Chang, N. –L. *Angew. Chem. Int. Ed.* **1995**, *34*, 1555–1573.
12. a) Desiraju, G. R. *Angew. Chem. Int. Ed.* **1995**, *34*, 2311–2321. b) Nangia, A.; Desiraju, G. R. *Top. Curr. Chem.* **1998**, *198*, 57–95.

13. a) Taylor, R.; Kennard, O. *J. Am. Chem. Soc.* **1982**, *104*, 5063–5070. b) Aakeröy, C. B.; Seddon, K. R. *Chem. Soc. Rev.* **1993**, *22*, 397–407. c) Desiraju, G. R. *Curr. Opin. Solid State Mater. Sci.* **1997**, *2*, 451–454. d) Jeffrey, G. A. *An Introduction to Hydrogen Bonding*; Oxford University Press: New York, **1997**. e) Hollingsworth, M. D. *Science* **2002**, *295*, 2410–2413. f) Prins, L. J.; Hulst, R.; Timmerman, P.; Reinhoudt, D. N. *Chem. Eur. J.* **2002**, *8*, 2288–2310.
14. a) Desiraju, G. R. *Current Science* **2001**, *81*, 1038–1050. b) Moorthy, J. N.; Natarajan, R.; Mal, P.; Venugopalan, P. *J. Am. Chem. Soc.* **2002,** *124*, 6530–6531. c) Adams, H.; Cockroft, S. L.; Guardigli, C.; Hunter, C. A.; Lawson, K. R.; Perkins, J.; Spey, S. E.; Urch, C. J.; Ford, R. *Chem. Bio. Chem.* **2004**, *5*, 657–664. d) Nguyen, H. L.; Horton, P. N.; Hursthouse, M. B.; Legon, A. C.; Bruce, D. W. *J. Am. Chem. Soc.* **2004**, *126*, 16–17. e) Metrangolo, P.; Neukirch, H.; Pilati, T.; Resnati, G. *Acc. Chem. Res.* **2005**, *38*, 386–395. f) Paulini, R.; Müller, K.; Diederich, F. *Angew. Chem. Int. Ed.* **2005**, *44*, 1788–1805. g) Reddy, C. M.; Kirchner, M. T.; Gundakaram, R. C.; Padmanabhan, K. A.; Desiraju, G. R. *Chem. Eur. J.* **2006**, *12*, 2222–2234. h) Gonnade, R. G.; Sashidhar, M. S.; Bhadbhade, M. M. *J. Ind. Inst. Sci.* **2007**, *87*, 149–161. i) Politzer, P.; Lane, P.; Concha, M. C.; Ma, Y.; Murray, J. S. *J. Mol. Model.* **2007**, *13*, 305–311.
15. a) Maschiocchi, N.; Bergamo, M.; Sironi, A. *Chem. Commun.* **1998**, 1347–1349. b) Mossakowska, I.; Wojcik, G. *Acta. Crystallogr. C* **2007**, *63*, o123–o125. c) Custelcean, R. *Chem. Commun.* **2008**, 295–319.
16. Navon, O.; Bernstein, J.; Khodorkovsky, V. *Angew. Chem. Int. Ed.* **1997**, *36*, 601–603.
17. Atkins, P. W. *Physical Chemistry* 5th Ed. Oxford, **1995**.
18. Steiner, T. *J. Chem. Soc. Chem. Commun*. **1997**, 727–734.
19. Desiraju, G. R. *Acc. Chem. Res*. **1991**, 24, 290–296.
20. Desiraju, G. R. *J. Chem. Soc. Chem. Commun*. **1997**, 1475–1476.
21. Trotter, J. *Acta Crystallogr*. **1960**, *13*, 86–95.
22. Guth, H.; Heger, G.; Druck, U. *Z. Kristallog. Kristallg. Kristallp. Kristallch*. **1982**, *159*, 185–188.
23. Leiserowitz, L. *Acta Crystallogr. B* **1976**, *32*, 775–802.
24. Shimoni, L.; Glusker, J. P. *J. Am. Chem. Soc*. **1994**, *116*, 8162–8169.
25. Cerius Molecular Modeling Simulations, Version 2.1.
26. Pedireddi, V. R.; Desiraju, G. R. *J. Chem. Soc. Perkin Trans. 2*, **1994**, 2353–2354.

27. Price, S. L.; Stone, A. J. *J. Am. Chem. Soc*. **1994**, *116*, 4910–4918.

28. Williums, D. E.; Hsu, L. – Y. *Acta Crystallogr. A* **1985**, *41*, 296–301.

29. Desiraju, G. R.; Parthasarathy, R. *J. Am. Chem. Soc*. **1989**, *111*, 8725–8726.

30. a) Allen, F, H.; Goud, B. S.; Hoy, V. J.; Howard, J. A. K.; Desiraju, G. R. *J. Chem. Soc. Chem. Commun.* **1994**, 2729–2730. b) Thalladi, V. R.; Goud, B. S.; Hoy, V. J.; Allen, F. H.; Howard, J. A. K.; Desiraju, G. R. *Chem. Commun*. **1996**, 401–409. c) Sarma, J. A. R. P.; Allen, F. H.; Hoy, V. J.; Howard, J. A. K.; Thaimattam, R.; Birandha, K.; Desiraju, G. R. *Chem. Commun*. **1997**, 101–102. d) Thaimattam, R.; Sharma, C. V. K.; Clearfield, A.; Desiraju, G. R. *Cryst. Growth Des.* **2001**, *1*, 103–106.

31. Allen, F. H.; Lommerse, J. P. M.; Hoy, V. J.; Howard, J. A. K.; Desiraju, G. R. *Acta Crystallogr. B* **2001**, *53*, 1006–1016.

32. George, S.; Nangia, A.; Lam, C. – K.; Mak, T. C. W.; Nicoud, J. – F. *Chem. Commun*. **2004**, 1202–1203.

33. a) Garden, S. J.; da Cunha, F. R.; Wardell, J. L.; Skakle, J. M. S.; Low, J. N.; Glidewell, C. *Acta Crystallogr. C* **2002**, *58*, o463–o466. b) Garden, S. J.; Fontes, S. P.; Wardell, J. L.; Skakle, J. M. S.; Low, J. N.; Glidewell, C. *Acta Crystallogr. B* **2002**, *58*, 701–706. c) Kelly, C. J.; Skakle, J. M. S.; Wardell, J. L.; Wardell, S. M. S. V.; Low, J. N.; Glidewell, C. *Acta Crystallogr. B* **2002**, *58*, 94–108. d) Glidewell, C.; Low, J. N.; Skakle, J. M. S.; Wardell, S. M. S. V.; Wardell, J. L. *Acta. Crystallogr. B* **2004**, *60*, 472–479. e) Wardell, J. L.; Low, J. N.; Skakle, J. M. S.; Glidewell, C. *Acta Crystallogr. B* **2006**, *62*, 931–943.

34. Glidewell, C.; Low, J. N.; Skakle, J. M. S.; Wardell, S. M. S. V. Wardell, J. L. *Acta Crystallogr. B* **2005**, *61*, 227–237.

35. Reddy, L. S.; Chandran, S. K.; George, S.; Babu, N. J.; Nangia, A. *Cryst. Growth Des.* **2007**, *7*, 2675–2690.

36. Lutz, J. – F. *Angew. Chem. Int. Ed*. **2007**, *46*, 1018–1025 and references therein.

37. Ramana, C. V.; Chatterjee, S.; Durugkar, K. A.; Gonnade, R. G. *CrystEngComm* **2009**, *11*, 143-150.

38. Durugkar, K. A; Gonnade, R. G; Ramana, C. V. *Tetrahedron **2009***, (press).

LIST OF PUBLICATIONS

1. "Click" synthesis of isomeric compounds for assessing the efficiency of the bifurcated Br…NO_2 synthon C. V. Ramana, Soumitra Chatterjee, Kulbhushan A. Durugkar and Rajesh G. Gonnade *CrystEngComm*, **2009**, *11*, 143−150.
2. "Cu(I) Promoted One-pot "S_NAr–Click Reaction" of Fluoronitrobenzenes" Kulbhushan A. Durugkar, Rajesh G. Gonnade and C. V. Ramana *Tetrahedron* **2009** (*press*)**.**
3. "C-Glycosides of dodecanoic acid: new capping/reducing agents for glyconanoparticle synthesis " C. V. Ramana, Kulbhushan A. Durugkar, Vedavati G. Puranik, Sachin B. Narute and B.L.V. Prasad *Tetrahedron Letters* **2008**, *49*, 6227−6230.
4. "Efficient and selective cleavage of the tert-butoxycarbonyl (Boc) group under basic condition**"** Debendra K. Mohapatra and Kulbhushan A. Durugkar *Arkivoc* **2005**, *14*, 20−28.
5. "Studies towards the total synthesis of halicholactone and neohalicholactone: a stereoselctive synthesis of C1-C13 fragment" Debendra K. Mohapatra and Kulbhushan A. Durugkar *Arkivoc* **2004**, *1*, 146−155.
6. "Click Chemistry" Approach for Molecular Library Synthesis for Evaluating Synthon Robustness: A Case Study with Cl…NO_2 Synthon" C. V. Ramana, Kulbhushan A. Durugkar and Rajesh G. Gonnade (*communicated*).
7. "Total synthesis of (+)-broussonetine G & protected (+)-broussonetine C employing Cross Metathesis approach" C. V. Ramana and Kulbhushan A. Dururgkar (*communicated*).
8. "Glyconanoparticle synthesis employing α/β *C*-Glycosides of dodecanoic acid as new capping/reducing agents" C. V. Ramana, Kulbhushan A. Durugkar and B. L. V. Prasad (*to be communicated*).

Erratum